Study of the role of the Transmembrane Domain of Type IV Coupling Proteins

Biofisika Institute (UPV/EHU, CSIC)
Department of Biochemistry and Molecular Biology
Faculty of Science and Technology
University of the Basque Country (UPV/EHU)

Doctoral Thesis

Itxaso Alvarez Rodriguez

Leioa, 2020

Study of the role of the Transmembrane Domain of Type IV Coupling Proteins

Biofisika Institute (UPV/EHU, CSIC)
Department of Biochemistry and Molecular Biology
Faculty of Science and Technology
University of the Basque Country (UPV/EHU)

Doctoral Thesis

Itxaso Alvarez Rodriguez

Leioa, 2020

AURKIBIDEA

SUMMARY

The increase of multidrug-resistant bacteria has become one of the major health concerns in our society (World Health Organization, 2019). In this regard, it has been described that bacterial conjugation is one of the key mechanisms responsible for the spread of antibiotic resistance genes among bacteria (Bello-López et al., 2019). This process is performed through a type IV secretion system, a multiprotein complex machine that transfers the nucleoprotein substrate from a donor into a recipient bacterium (Waksman, 2019).

Type IV coupling proteins (T4CPs) are an essential element during the conjugative process, as they connect the substrates in the cytosol with the secretion machinery in the membrane (Gomis-Ruth et al., 2005). Additionally, they are an energy source during conjugation, have a role in signal transduction, and are postulated to act as molecular motors that pump the ssDNA substrate across the bacterial inner membrane (Llosa and Alkorta, 2017). They compose a broad protein family, showing different molecular architectures and being present in all the conjugative plasmids, in many plasmids related to pathogenic processes and in a few mobilizable plasmids (Smillie et al., 2010). Conjugative plasmid-related VirD4-type T4CPs are the most studied T4CP subfamily (Alvarez-Martinez and Christie, 2009). But even if they have been in-depth characterized for the last decades, as their nature as membrane proteins makes them challenging proteins to be studied, their characterization has been mostly accomplished using mutants that lack their transmembrane domain (TMD) (Larrea et al., 2017; Schroder and Lanka, 2003; Tato et al., 2007). However, several studies performed with $TrwB_{R388}$, the full-length T4CP of the conjugative plasmid R388, have proven that the TMD is more than a mere anchor to the membrane and that it has a role in protein activity, stability, oligomerization and subcellular localization (Hormaeche et al., 2002, 2004, 2006; Moncalián et al., 1999; Segura et al., 2013, 2014; Vecino et al., 2010, 2011).

The specific aims of this work have been to contribute to deciphering the role of the TMD in T4CPs and to assess if the features described for conjugative VirD4-type T4CPs can be extrapolated to the whole T4CP family. Once a better understanding of these proteins is achieved, different strategies to inhibit their activity can be developed, controlling in this manner the conjugative process and therefore reducing the spread of antibiotic resistance genes.

To better study the role of the TMD, a set of T4CP variants composed of native T4CPs, chimeric T4CPs with domains of different origins, and TMD-less mutants was obtained. Specifically, two chimeric proteins of $TrwB_{R388}$ were constructed: (i) $TMD_{TraJ}CD_{TrwB}$ composed of the TMD of $TraJ_{pKM101}$, the T4CP of plasmid pKM101, and the cytosolic domain of $TrwB_{R388}$ and (ii) $TMD_{TrwB}TraJ_{pIP501}$ composed of the TMD of $TrwB_{R388}$ and the T4CP of the $Gram^{+}$ pIP501 plasmid, $TraJ_{pIP501}$. Additionally a third chimeric protein was constructed with the small membrane protein $TraI_{pIP501}$ and $TraJ_{pIP501,}$ creating a complex that resembles the VirD4-type T4CPs. Also, the mobilizable plasmid related $MobB_{CloDF13}$ T4CP and its TMD-less mutant, MobBΔTMD, were obtained.

Firstly, the *in vivo* function and *in vivo* subcellular localization of these proteins was studied. Afterwards, they were purified and *in vitro* characterized using different biochemical

and biophysical techniques. In such a way their stability, DNA-binding capacity, oligomerization patterns, structure, and ATP hydrolase activity have been characterized. Finally, the experimental set-up to perform future single-GUV and TIRFM experiments has been optimized.

In accordance with published reports, we have described that T4CPs show polar location in the cell (Kumar and Das, 2002); additionally, we have observed that this tendency is increased in the presence of a secretion system. On the contrary, unlike what has been previously published for $TrwB_{R388}$ (Segura et al., 2014), our results here show that the presence of the TMD or a related membrane protein is not an essential element for the polar localization of the mobilizable plasmid-related T4CP $MobB_{CloDF13}$ and the TMD-less $TraJ_{pIP501}$ T4CP, respectively.

This thesis has shown that the $TMD_{TraJ}CD_{TrwB}$ chimeric protein is able to complement the conjugation of R388 in the abscencce of $TrwB_{R388}$, although with a lower transfer frequency. Moreover, it is capable of interacting with its both cognate systems (*i.e.*, R388 and pKM101), showing negative dominance in the presence of the native T4CPs $TrwB_{R388}$ or $TraJ_{pKM101}$. When comparing $TMD_{TraJ}CD_{TrwB}$ with $TrwB_{R388}$ it has been seen that the chimeric protein presents smaller stability against low ionic strength conditions, different oligomerization patterns, and smaller DNA-binding capacity, most likely due to the secondary structural differences observed in the cytosolic domain. These results suggest that the presence of a heterologous TMD affects the cytosolic domain and the processes related to it, such as substrate-binding and, therefore, *in vivo* activity.

On the contrary, the *in vitro* characterization of $MobB_{CloDF13}$ has shown that the presence of its TMD does not have any effect neither in the oligomerization pattern nor in the secondary structure of its cytosolic domain, even if it seems to affect its DNA-binding properties.

To sum up, the comparative study between the different T4CPs and their variants has underlined that the characteristics described for the conjugative plasmid related VirD4-type T4CPs and their TMDs should not be ascribed to the whole T4CP family. Specifically, it has been proven that TMD-less T4CPs and mobilizable plasmid-related VirD4-type T4CPs present different mechanisms of action.

ABBREVIATIONS / LABURDURAK

(v/v) / (b/b)	(volume/volume) / (bolumen/bolumen)
(w/v) / (p/b)	(weight/volume) / (pisu/bolumen)
(w/w) / (p/p)	(weight/weight) / (pisu/pisu)
5-IAF	5-iodoacetamide fluorescein / Fluoreszeina 5-iodoazetamida
AAD	All alpha domain / Alfa guztiko domeinua
ADP	Adenosine diphosphate / Adenosin difosfatoa
AFM	Atomic force microscopy / Indar atomikozko mikroskopioa
AmdiS	4-Acetamido-4'-Maleimidylstilbene-2,2'-Disulfonic Acid / Azido 4-azetamido-4'-maleimidilstilben-2 2'-disulfoniko
Amp	Ampicillin / Anpizilina
ARG	Antibiotic resistance genes / Antibiotikoen aurkako erresistentzia geneak
ATP	Adenosine triphosphate / Adenosin trifosfatoa
ATPase / ATPasa	ATP hidrolase / ATP hidrolasa
AUC	Analytical ultracentrifugation / Ultrazentrifugazio analitikoa
BB	Bio-Beads™
BCA	Bicinchoninic acid / Azido bizinkoninikoa
BIM	Bacterial inner membrane / Bakterioen barne mintza
BIMV	Bacterial inner membrane vesicle / Bakterioen barne mintzekin egindako besikulak
BN-PAGE	Blue native polyacrylamide gel electrophoresis / Poliakrilamidazko gel elektroforesi urdin-natiboa
BSA	Bovine Serum Albumin / Behi serumaren albumina
c(s)	Sedimentation coefficient distributions / Sedimentazio koefizienteen banaketa
Car	Carbenicillin / Karbenizilina
CD	Cytosolic domain / Domeinu zitosolikoa
Chl	Chloramphenicol / Kloranfenikola
CL	Cardiolipin / Kardiolipina
CMC	Critical micelle concentration / Kontzentrazio mizelar kritikoa
Cryo-EM	Cryo-electron microscopy / Mikroskopia krio-elektronikoa
cT4SS	Conjugative Type IV Secretion system / IV motako sekrezio sistema konjugatiboa
CTD	Carboxile terminal domain / Karboxilo muturreko domeinua
C-term / C-muturra	Carboxyl terminus in amino acid chain / Aminoazido katearen karboxilo muturra
Da	Dalton
DDM	n-dodecyl-β-D-maltopyranoside / n-dodezil-β-D-maltopiranosidoa
DiD	1,1'-Dioctadecyl-3,3,3',3'-Tetramethylindodicarbocyanine perchlorate /1,1'-Dioktadezil-3,3,3',3'-Tetrametilindodikarbozianin perkloratoa
DiO	3,3'-Dioctadecyloxacarbocyanine perchlorate / 3,3'-Dioktadeziloxakarbozianin perkloratoa
DMF	N, N-Dimethylformamide / N, N-Dimetilformamida
DNA	Deoxyribonucleic acid / Azido desoxirriboonukleikoa
DOPC	1,2-Dioleoyl-sn-glycero-3-phosphocholine / 1,2-Dioleoil-sn-glizero-3-fosfokolina
dsDNA	Double stranded DNA/ Kate bikoitzeko DNA
DTR	DNA transfer and replication / DNAren transferentzia eta bikoizketa
DTT	Dithiothreitol / Ditiotreitola
eGFP	Enhanced green fluorescent protein / Hobetutako proteina fluoreszente berdea
EMSA	Electroforetic shift mobility assay / Mugikortasun elektroforetikoaren aldaketaren entsegua
FCCS	Fluorescence cross correlation spectroscopy / Erlazio gurutzatutako fluoreszentzia mikroskopia
FRAP	Fluorescence recovery after photobleaching / Fotoamataketaren osteko fluoreszentziaren berreskurapena

FT-MLV	Freezed-thawn multilamellar vesicle / Izoztu-desizoztutako besikula multilamelarrak
G4-DNA	G-quadruplex DNA
Gram -	Gram negative /Gram negatibo
Gram +	Gram positive / Gram positibo
GUIMV	Giant unilamellar inner membrane vesicle / Barne mintzez eraturiko lamela bakarreko besikula erraldoiak
GUV	Giant unilamellar vesicle / Lamela-bakarreko besikula erraldoiak
HEPES	N-2-hydroxyethylpiperazine-N'-2-ethane sulfonic acid / N-2-hidroxietilpiperazin-N'-2-azido sulfo-etanikoa
HGT	Horizontal gene transfer / Gene transferentzia horizontala
HRP	Horseradish peroxidase / Errefau peroxidasa
ICE	Integrative and conjugative element / Elementu integratzaile eta konjugatiboa
ICH	Internal channel / Erdiko kanala
IM	Inner membrane / Barne mintza
IMAC	Immobilized metal affinity chromatography / Inmobilizaturiko metalen bidezko afinitate kromatografia
IMC	Inner membrane complex / Barne mintzeko konplexua
IMEs	Integrative and mobilizable elements / Elementu integratibo eta mugikorrak
Inc	Incompatibility group / Bateraezintasun taldea
IPTG	Isopropyl α-D-thiogalactopyranoside / Isopropil α-D-tiogalaktopiranosidoa
IRS	Infrared spectroscopy / Espektroskopia infragorria
IS	Insertion sequence / Txertaketa sekuentzia
ITO	Indium tin oxide / Indio tin oxidoa
Kan	Canamycin / Kanamizina
kb	Kilobase
LB	Luria Bertani Broth / Luria Bertani hazkuntza-medioa
LC-MS/MS	Liquid chromatography-tandem mass spectrometry / Kromatografia likido-tandem masa espektometria
LDAO	n-Dodecyl-N,N-Dimethylamine-N-Oxide / n-Dodezil-N,N-dimetilamina -N-Oxidoa
LDH	Lactate dehydrogenase / Laktato deshidrogenasa
LUV	Large unilamellar vesicle / Lamela-bakarreko besikula handiak
MDR	Multidrug resistant / Antibiotiko anitzen aurkako erresistentzia
MGE	Mobilizable genetic element/ Elementu genetiko mugikorra
Min	Minute / Minutu
MLV	Multilamellar large vesicles / Besikula multilamelar handiak
MOB	Mobility related genes / Mugikortasunarekin erlazionaturiko geneak
MP	Membrane protein / Mintz proteina
MPF	Mating pair formation related genes / Egitura parekatzailearen eraketarekin erlazionaturiko geneak
MWCO	Molecular weight cut off / Pisu molekularraren araberako iragazki tamaina
NAD	Nicotinamide adenine dinucleotide / Nikotinamida adenine dinukleotidoa
Nal	Nalidixic acid / Azido nalidixikoa
NBD	Nucleotide-binding domain / Nukleotidoen-atxikitze domeinua
NEM	N-Ethylmaleimide / N-etilmaleimida
NS-EM	Negative stain electron microscopy / Tindaketa negatibozko elektroi mikroskopia
nSLB	Native cellular membrane derived supported lipid bilayer / Zelula mintz natiboz osaturiko eutsitako bikapa lipidikoa
NTA	Nitriloacetic acid / Azido nitriloazetikoa
N-term / N-muturra	Free amine terminus in amino acid chains / Aminoazido katearen amino muturra
OD	Optical density / Dentsitate optikoa
OG	n-octyl-β-D-glucopyranoside / n-oktil-β-D-glukopiranosidoa
OM	Outter membrane / Kanpo mintza
OMCC	Outter membrane core complex / Kanpo mintzeko muin konplexua
OPPF-UK	Oxford Protein Production Facility UK
oriT	Origin of transfer sequence / Transferentziaren hasiera sekuentzia
P	Periplasm / Periplasma

PB	Power Broth
PBS	Phosphate buffer saline / Fosfato gatz indargetzailea
PC	Phosphatidylcholine / Fosfatidilkolina
PCR	Polymerase chain reaction / Polimerasaren kate erreakzioa
PDC	Protein-detergent complex / Proteina-detergente konplexua
PE	Phosphatidylethanolamine / Fosfatidiletanolamina
PEP	Phosphoenolpiruvate / Fosfoenolpirubatoa
PG	Phosphatidylglycerol / Fosfatidilglizerola
PG-hidrolasa	Peptidoglikano hidrolasa
PK	Pyrubate kinase / Pirubato kinasa
PMSF	Phenylmethanesulfonyl fluoride / Fenilmetanosulfonil fluoridoa
pT4SS	Pathogenic Type IV Secretion System / IV motako sekrezio sistema patogenikoa
RS	Regenerator system / Sistema birsortzailea
s	Sedimentation coefficient / Sedimentazio koefizientea
SDS	Sodium dodecyl sulphate / Sodio dodezil sulfatoa
SDS-PAGE	Sodium dodecyl sulphate polyacrylamide gel electrophoresis / Sodio dodezil sulfatozko poliakrilamidazko gel bidezko elekroforesia
SEC	Size exclusión chromatography / Gel iragazpeneko kromatografia
SEC-MALLS	Size exclusion chromatography-multi angle laser light scattering / Gel-iragazpeneko kromatografia bati akoplatutako angelu anitzeko laser argi dispertsioa
Seg	Second / Segundu
SLB	Supported lipid bilayer / Eutsitako bikapa lipidikoa
SOC	Super optimal broth with catabolite repressor / Katabolitoen errepresiodun hazkuntza medioa
Spc	Spectinomycin / Espektinomizina
ssDNA	Single stranded DNA / Kate bakarreko DNA
Str	Streptomycin / Estreptomizina
SUV	Small unilamellar vesicle / Lamela-bakarreko besikula txikiak
T4ASS	Type IV A secretion system / IV A motako sekrezio sistema
T4BSS	Type IV B secretion system / IV B motako sekrezio sistema
T4CP	Type IV Coupling Protein / IV motako proteina akoplatzailea
T4SS	Type IV secretion system / IV motako sekrezio sistema
TBONEX	Overnight Express™ Instant TB Medium
TCEP	Tris (2-carboxyethyl) phosphine / Tris (2-karboxietil) fosfina
TIRFM	Total internal reflection fluorescence microscopy / Barne isladapen osoko fluoreszentzia mikroskopia
T_m	Mid-point denaturation temperature / Erdiko desnaturalizazio tenperatura
TMD	Transmembrane domain / Transmintz domeinua
Tmp	Trimethoprim / Trimetoprima
Tn	Transposon / Transposoia
TrIP	Transfer DNA immunoprecipitation / Transferentzia DNAren immunoprezipitazioa
Tris	Tris (hydoxymethyl) aminomethane / Tris (hidoximetil) aminometanoa
TS	Translocation signal / Translokaziorako seinalea
UV	Ultraviolet light / Izpi ultramoreak
V_e	Elution volume / Eluzio-bolumena
WB	Western blotting / Western plapaketa
X-GAL	5-bromo-4-chloro-3-indolyl-β-D-galactopyranoside / 5-bromo-4-kloro-3-indolil-β-D-galactopiranosidoa
λ	Wavelength / Uhin luzera

1. KAPITULUA:

SARRERA

1. SARRERA

1.1. TESTUINGURUA

Antibiotikoak historiako iraultza mediko handiena izan dira aurkitu ziren momentu beretik, orain dela 70 urte baino gehiago. Tamalez, antibiotikoen erabilpena (medikuntza zein nekazaritza eta abeltzaintza praktiketan) eta bakterio erresistenteen agerpenaren artean erlazio zuzena ematen dela ikusi da. Antibiotikoen aurkako erresistentziaren ondorioz urtero Europan 33.000 pertsona hiltzen dira eta 1,5 bilioi euro gastatzen dira osasun arloan. Bestalde, aurresaten da 2050. urterako 10 milioi pertsonen bizitza arriskuan egongo dela arazo honen ondorioz, lehenago konponbiderik aurkitzen ez bada (Cassini et al., 2019).

Ospitaleetan antibiotiko anitzen aurkako erresistenteak (*Multidrug-Resistant*, MDR) diren bakterioek infekzioen %70a inguru eragiten dute. Hori dela eta, antibiotikoen aurkako erresistenzia giza-osasunaren aurkako mehatxu handia bilakatu da, non MDR bakterio patogenoen gorakadak arazo larriak eragiten dituen osasun eta gizarte mailan (World Health Organization, 2015, 2019). Gobernuak eta jendartea arazo honen inguruan sentsibilizatzeko asmoz, Giza Osasunaren Erakundeak (*World Health Organization*, WHO) antibiotikoen aurkako erresistentzia aurkezten duten mikroorganismo garrantzitsuenen zerrenda aurkeztu zuen, non *Acinetobacter baumannii*, *Pseudomonas aeruginosa* eta *Enterobactiaceae* espezieak nabarmentzen ziren (Tacconelli et al., 2017).

Nahiz eta medikuntzan egindako antibiotikoen erabileraren gehiegikeria arazo honen eragile nagusia izan, azken denboraldian ingurumenaren parte hartze garrantzitsua aldarrikatu egin da, antibiotikoen aurkako geneen (*Antibiotic Resistance Genes,* ARG) gordailu gisa jokatzen baitu. Akuifero, hondakin-ur, hiri, zein nekazaritza eta abeltzaintza inguruneetan erabiltzen diren antibiotikoek bakterioengan presioa eragiten dute, MDR bakterioen agerpena zein hedapena bultzaraziz, batez ere elementu mugikor genetikoen bidez (*Mobile Genetic Elements, MGE)* (Chan, 2015).

Zoritxarrez, egoera hau azken urteetan era kezkagarrian areagotu da, bakterioek eragindako infekzioen tratamendurako proposamen berrien agerpenaren urritasunagatik eta ikerketa arlo honetan egin diren baliabideen murrizketagatik (Högberg et al., 2010).

1.2. DNAren TRANSFERENTZIA HORIZONTALA

Bakterioen material genetikoen aldaketa hiru mekanismoen bidez eman daiteke: (i) DNA aldatzen duten mutazioak, (ii) berrantolaketa genetikoak, eta (iii) material genetiko berriaren harrera gene transferentzia horizontalaren bidez (*Horizontal Gene Transfer*, HGT). Genoma prokariotoak erkatuz ikusi zen bakterioen genomen ehuneko altu bat HGTari dagokiola, bere garrantzia azpimarratuz (Johnsborg et al., 2007; Thomas eta Nielsen, 2005). Literaturaren arabera, bakterioek DNA exogenoa mekanismo desberdinen bidez jaso dezakete: (i) transformazio naturala, (ii) konjugazioa eta (iii) transdukzioa, konjugazioa izanik hedatuena eta tesi honen aztergaia (Bello-López et al., 2019). Laugarren mekanismo bat ere badago,

DNAdun besikulen transferentzia, bakterioen artean askoz gutxiagotan ematen dena (Johnson eta Grossman, 2015)

1.2.1. ELEMENTU MUGIKOR GENETIKOAK

Transdukzioa eta konjugazioa MGE bidez gertatzen dira. MGEak bakterioen artean edota bakterioen barneko DNA molekula desberdinen artean geneen mugimenduak emateko beharrezko proteinak kodetzen dituzte (Frost et al., 2005). Ezagutzen den MGE kopurua handituz doa HGTa eragiten duten mekanismoen azterketa sakontzen den heinean. Hala ere, mekanismo hauen dinamismo eta erlazio konplexuek haien sailkapena sailtzen dute. Orokorrean MGEak bost talde desberdinetan sailkatu daitezke: (i) bakteriofagoak, (ii)plasmido transmitigarriak; (iii) uharte genomikoak; (iv) elementu transposagarriak eta (v) integroiak.

1. **Bakteriofago**ek DNAren segmentuak paketatu ahal dituzte ondoren bakterio ostalari berri batera igaroz. Bertan errekonbinazio bidez bakterioaren kromosomara batu daitezke eta hurrengo bakterio belaunaldietara igaro (Frost et al., 2005).

2. **Plasmido transmitigarriak** DNA molekula auto-erreplikagarri egonkorrak dira, konjugatibo edo mugikorrak izan daitezkeenak (1.2.3. atala ikusi). Kodetzen dituzten geneak ez dira funtzio zelularrak betetzeko funtsezkoak, baina baliogarriak suertatu daitezke baldintza gogorren aurka egiteko. Plasmido hauek bakterioen artean geneak mugi ahal dituzte makineria konjugatiboa erabiliz, IV motako sekrezio-sistemetako bat (*Type IV Secretion System,* T4SS, hurrengo atala ikusi).

3. **Uharte genomikoak** bakterioen kromosoman integratutako gene multzoak dira. Haien bidez bakterioek testuinguru jakinetan abantailatsuak izan daitezkeen funtzioak eskura ditzakete, besteak beste, infekzioso edota antibiotikoekiko erresistenteak izateko gaitasuna. Uharte genomikoak kromosomen bikoizketa, segregazio eta zelulen zatiketan zehar pasiboki hedatzen dira (Bellanger et al., 2014). Bi mota bereiz daitezke: alde batetik, Elementu Integratibo eta Konjugatiboak (*Integrative and Conjugative* Elements, ICEs), transposoi konjugatibo gisa ere izendatuak, berezko konjugazio sistema funtzionalak kodetzen dituztenak (Johnson eta Grossman, 2015); eta beste aldetik, Elementu Mugikor Integratzaileak (*Integrative Mobilizable Elements,* IMEs), haien erauzketa, birzirkularizazioa eta integrazioa burutzeko beharrezko sekuentziak kodetzen dituztenak. Hori dela eta, konjugazio bidez transferitzeko ICE edo plasmido konjugatibo baten makineria behar dute (Bellanger et al., 2014).

4. **Elementu transposagarriak** bakterio genomaren gune desberdinetara mugitzeko gai diren ADN sekuentziak dira. Hau jatorrizko gunetik erauziz eta gune berri batean txertatuz edo gune berri batera mugitzen den kopia berria sortuz burutzen dute. Talde honen barruan alde batetik transposoiak (*Transposons*, Tn) daude, transposiziorako beharrezkoak diren geneez gain beste gene batzuk kodetzen dituztenak ere. Beste aldetik, txertaketa sekuentziak (*Insertion Sequences*, IS) daude, haien transposiziorako beharrezkoak diren geneak soilik dauzkatenak (Siguier et al., 2014).

5. **Integroiek** introiaren barnean kodetutako integrasak erabiltzen dituzte errekonbinazio bidez gene kaseteak barneratzeko. Horretaz gain, sustatzaile bat daukate integroian dauden gene kaseteen transkripzio eta adierazpen egokia burutzeko. Integroiak haien zelula barneko eta zelula arteko mobilizazioa burutzeko gainerako MGEn barnean txertatu egiten dira (Gillings et al., 2008).

Gaur egunera arte plasmido konjugatiboak HGTaren eragile nagusitzat hartu dira, baina azken ikerketek IMEn hedapenaren garrantzia aldarrikatu dute (Guédon et al., 2017). Dena den, plasmido konjugatiboek haien transferentziarako beharrezkoak diren elementu guztiak kodetzen dituztenez aztertuagoak izan dira.

1.2.2. IV MOTAKO SEKREZIO SISTEMAK

T4SSak kate bakarreko DNA (*single stranded DNA*, ssDNA) edota proteinak ostalari ugarietara (zelula prokariotiko zein eukariotiko) garraiatzen dituzten sistema makromolekularrak dira, hainbat domeinuz eraikiak daudenak. T4SSen superfamilia funtzio eta egiturari dagokionez anitza da, bakterio Gram-negatibo ($Gram^-$) zein Gram-positiboetan ($Gram^+$) aurkitzen delarik (Christie et al., 2017). T4SSa gaur egun ezagutzen den domeinu/erreinu arteko garraio sistema bakarra da (Christie, 2016). Sistema hauen aniztasuna dela eta, hainbat irizpide desberdinetan oinarrituriko sailkapen desberdinak egin dira urteetan zehar (1.1. taula).

1.1. taula. Bibliografian aurkezten diren T4SSen sailkapen desberdinak.

	Sailkapen irizpidea	Azpifamiliak
Lawley et al., 2003	Pilus mota	F-mota, P-mota, I-mota
Garcillán-Barcia et al., 2009	Errelaxasa proteinaren filogenia	MOB(F), MOB(H), MOB(Q), MOB(C), MOB(P), MOB(V)
Alvarez-Martinez eta Christie, 2009	Substratua	Konjugazio sistemak (errelaxasa eta ssDNA), Efektoreen translokazio sistemak, DNA harrera eta askapen sistemak
Guglielmini et al., 2013	VirB4 proteinaren filogenia	MPF_I, MPF_C, MPF_G, MPF_T, MPF_F, MPF_B, MPF_{FATA}, MPF_{FA}

Nahiz eta zehaztasun eskasa izan eta zenbait kasu sailkapenetik kanpo utzi, bi sailkapenen erabilera nagusitu egin da. Lehenengoa prozesuaren izaeran oinarritzen da, bi T4SS mota bereiziz (de Paz et al., 2005): (i) konjugazioa burutzen dutenak (*conjugative type IV secretion system,* cT4SS) eta (ii) prozesu patogenikoetan parte hartzen dutenak (*pathogenic type IV secretion system*, pT4SS). Hala ere, zenbait sistemek, *Agrobacterium tumefaciens*-enak bezala, izaera duala aurkezten dute (Li eta Christie, 2018). Bigarren sailkapena proteina konposaketan oinarritzen da (Christie et al., 2017; Grohmann et al., 2018). Kasu honetan ere T4SSak bi taldetan banandu egiten dira: (i) *Type IV A* (T4ASS) eta (ii) *Type IV B* (T4BSS), zeinen sistema paradigmatikoak *A. tumefaciens*-ren VirB/VirD eta *Legionella pneumophila*-ren Dot/Icm sistemak diren, hurrenez hurren. T4ASSak 12 azpiunitate inguruz osatuak daude, *A.*

tumefaciens sistemaren 11 VirB eta VirD4 azpiunitateekin erlazionaturik daudenak (Christie et al., 2005). Talde honen barruan sartzen diren sistema guztien proteinei VirB1-11 izena ematen bazaie ere, joera bat sortarazi da VirB ordez TivB1-11 nomenklatura erabiltzearen alde, nahasmenak saihesteko (Thomas et al., 2017). T4BSSak, ordea, 25 azpiunitate baino gehiagoz osaturik daude, zeinetatik soilik batzuk VirB proteinen homologoak diren (Voth et al., 2012).

Tesi honetan aztertuko diren sistemak T4ASS taldearen barnean kokatzen dira (1.1. irudia). Hauek modulu funtzional desberdinez eraturiko egitura supramolekular gisa eboluzionatu zuten. Laburbilduz, zelula emaile barnean hiru talde funtzional nagusi bereiz daitezke. Lehenengoa energia-zentroa da, alde zitoplasmatikoan sekrezio kanalaren sarreran kokatzen dena eta hiru ATPasez eraturik dagoena: VirD4 proteina akoplatzailea (*Type IV coupling protein*, T4CP), VirB4 eta VirB11 (Ripoll-Rozada et al., 2013). Proteina hauek bigarren talde funtzionalarekin elkar eragiten dute, barne mintzeko konplexua deitua (*Inner membrane complex*, IMC) (Low et al., 2014). Azpiegitura hau, VirB3, VirB6 eta VirB8 proteinek eta VirB10en amino-muturrak (N-muturrak) eratzen dute eta barne mintzean (*Inner membrane*, IM) zehar substratuaren translokazioaz arduratzen da. IMC barnean energia zentroko VirB4 eta VirD4 proteinak sartu ohi dira baita. IMCa kanpo mintzeko muin konplexuarekin (*Outer membrane core complex*, OMCC) konektaturik dago, hirugarren modulua dena. Egitura hau VirB7, VirB9 proteinek eta VirB10 proteinaren karboxilo-muturrak (C-muturrak) eratzen dute eta periplasma eta kanpo mintzean (*Outer membrane*, OM) zehar substratuaren translokazioaz arduratzen da (Gordon et al., 2017).

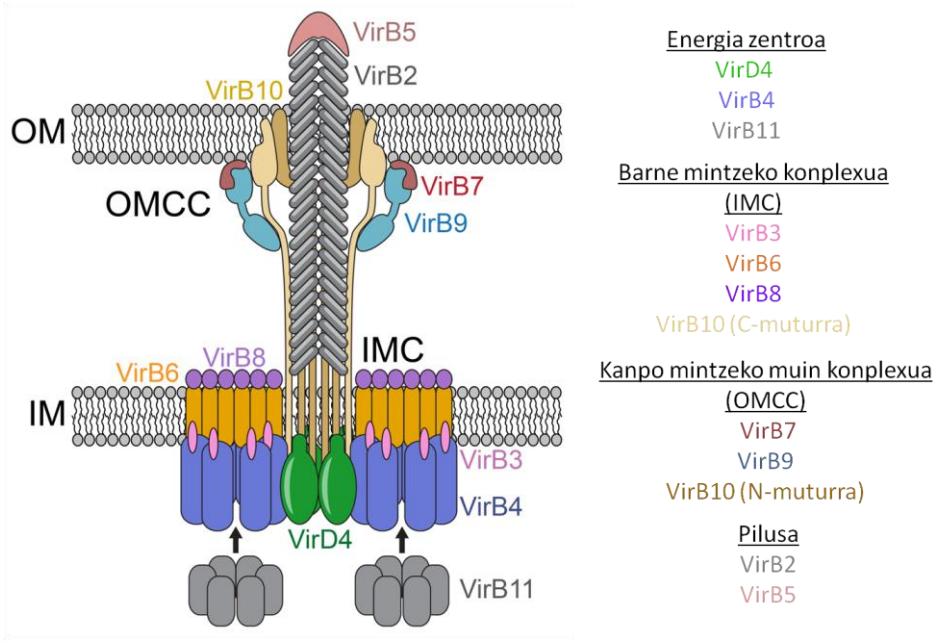

1.1. irudia. R388 sistema konjugatiboaren egitura molekularra. Irudikapen eskematikoa tindaketa negatibozko elektroi mikroskopiaz Redzej et al. (2017)-ek deskribaturiko egituran oinarriturik dago. Nahiz eta R388 sisteman proteinek TrwD →TrwN eta TrwB izenak jaso, VirB eta VirD4 nomenklaturarekin adierazi egin dira. Geziek prozesu konjugatiboan zehar VirB11 proteinen elkarrekintza dinamikoak adierazten dituzte. Irudia Waksman (2019)-tik egokitua izan da.

Horretaz gain T4ASSek zelula kanpoko egiturak eratzen dituzte, ala nola, pili konjugatiboak. Pilusa VirB2 azpiunitatez sortutako polimeroa da, bakterio emaile eta hartzailearen arteko kontaktu fisikoaz arduratzen dena (Lawley et al., 2003). Pilusaren muturrean VirB5 proteina kokatzen da. Pilus mota desberdinak bereizten dira: F-motako pilusak ingurune solido zein likidotan jardun dezaketen egitura luze, malgu eta dinamikoak dira; P-motako pilusak, ordea, ingurune solidoetan soilik burutzen dute bakterioen arteko kontatua; labur, lodi eta zurrunak izanik (Lawley et al., 2003; Schröder eta Lanka, 2005). Plasmido bakoitzak pilus mota bakarra kodetzen du, konjugazioa zein ingurunean gerta daitekeen mugatuz.

Aipatu beharra dago bakterio $Gram^+$-etan antolaketa funtzional hau desberdina dela. Izan ere, $Gram^-$-ek dituzten 11 proteinen ordez, sistema $Gram^+$-ek soilik sei VirB/VirD4 proteina dauzkate, ez baitute OMCCren beharrik. Are gehiago, ez dute pilus egiturarik sortzen, baizik eta adhesina moduko egituren bidez burutzen dute zelulen arteko ezagupena (Grohmann et al., 2017). Aipatu beharra dago azken ikerketetan ikusi egin dela $Gram^-$ T4ASS guztiek ez dutela beti bakterioen arteko kontaktuak pilusen bidez burutzen. Izan ere, deskribatu egin da pKM101 plasmidoak $Gram^+$ sistemen antzeko adhesinak erabiltzen dituela pilien ordez (González-Rivera et al., 2019).

1.2.3. PLASMIDO TRANSMITIGARRIAK

Plasmidoak bakterioetan aurki daitezkeen DNA molekula zirkularrak dira, 25 kb-ko batez besteko pisu molekularrarekin, kromosometatik banandurik daudenak eta erreplikazio independentea aurkezten dutenak. Normalean bakterioen zitoplasman aurkitzen dira eta mikroorganismoaren biziraupenerako abantailatsuak, baina ez beharrezkoak, diren ezaugarriak ematen dituzte, adibidez antibiotikoen aurkako erresistentzia. Plasmidoak bateraezintasun taldeen (*Incompatibility groups*, Inc) arabera sailkatzen dira. Honela, talde bereko bi plasmido ezin dira bakterio ostalari berdinean aurkitu une berean, konjugazio prozesua mugatuz. Inc talde batzuk (IncN, IncP eta IncW, kasu) ostalari talde anitzetan aurki daitezke; beste batzuk ordea (IncF eta IncI, kasu) bakterio espezie jakin batzuetan soilik manten daitezke era egonkorrean (Kittell eta Helinski, 1993). Naturan aurkitzen diren plasmidoen laurden bat inguru konjugatiboak dira eta beste laurden bat mugikorrak. Aurretik esan bezala, plasmido hauek konjugazioa burutzeko beharrezko gene guztiak (konjugatiboak) edo haietako batzuk (mugikorrak) kodetzen dituzte. Konjugazioan parte hartzen duten transferentzia geneak bi modulu espezializatutan banandu daitezke: Mugikortasunarekin erlazionaturiko geneak (*Mobility related genes,* MOB) eta zelula arteko transferentzia kanalarekin erlazionaturiko geneak (*Mating pair formation related genes,* MPF) (Smillie et al., 2010) (1.2. irudia).

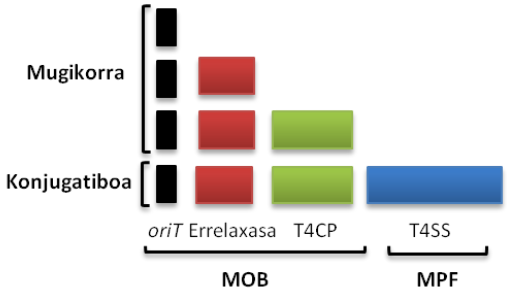

1.2. irudia. Konjugazio prozesuan parte hartzen duen material genetikoaren adierazpena. Konjugazioan parte hartzen duen material genetikoa bi taldetan banatzen da: MOB eta MPF. MOB geneak substratuaren prozesamendu eta harrerarekin erlazionaturik daude. Hiru elementu desberdin bereizten dira talde honen barruan: (i) transferentziaren hasiera sekuentzia (*oriT),* (ii) errelaxasa kodetzen duen genea (R) eta proteina akoplatzailea kodetzen duen genea (T4CP). MPF geneak IV motako sekrezio kanalarekin erlazionaturik daude. Plasmido konjugatiboek MOB eta MPF moduluak dauzkate; plasmido mugikorrek, ordea, MOB modulua soilik daukate, T4CPrekin edota T4CPrik gabe. Irudia Smillie et al. (2010)-tik egokitua izan da.

Plasmido konjugatiboek transferentziarako beharrezkoak diren bi moduluak kodetzen dituzte. Alde batetik, MOB moduluan (lehen *DNA Transfer and Replication*, DTR, gisa izenpetua) substratuaren prozesamendurako beharrezkoak diren hiru sekuentziak aurkitzen dira (Bhatty et al., 2013): (i) *oriT* sekuentzia (*origin of transfer*), DNAren prozesamendurako hasiera gunea ezartzen duena; (ii) errelaxasa proteina kodetzen duen sekuentzia. Proteina honek *oriT*a espezifikoki ezagutzen du eta plasmido transmitigarri guztietan kontserbaturiko proteina bakarra da; eta (iii) T4CPa kodetzen duen sekuentzia, errelaxosomaren ezagupena burutzen duena mintzeko sekrezio kanalarekin kontaktuan jarriz. Honetaz gain, MOB moduluaren barruan substratu prozesamenduan parte hartzen duten proteina laguntzaileak ager daitezke, sistemaren arabera aldatzen direnak. Bestalde, MPF moduluan sekrezio kanala osatzen duten proteinak aurkitzen dira (VirB1-11 T4ASS Gram$^-$ sistemen kasuan).

Plasmido mugikorrek MOB modulua kodetzen dute soilik, berezko *oriT* eta errelaxasa izanik. Hori dela eta, bakterio berean aurkitzen den plasmido konjugatibo batean kodeturiko T4SSaren beharra daukate transferituak izateko. T4CPari dagokionez, plasmido mugikor gehienek ez dute berezko T4CPrik eta plasmido konjugatiboarena erabili behar dute baita ere. Hala ere, plasmido mugikor batzuk haien berezko T4CPa kodetzen dute, esate baterako MOB_{C1} azpifamiliakoak, CloDF13 plasmidoa hauen prototipoa izanik (Garcillán-Barcia et al., 2009).

1.2.4. KONJUGAZIO PROZESUA

1946. urtean Joshua Lederberg eta Edward L. Tatum-ek bakterioen konjugazioa deskribatu zuten lehen aldiz, bakterioen arteko ugalketa sexual gisa (Lederberg eta Tatum, 1946). Gene transferentzia burutzeko mekanismo hau oso goiz agertu zen antzinako proteobakterioetan eta gero prokariotoen klado guztietara hedatu zen. Konjugazio bidez eskuratzen diren geneei esker, bakterio hartzaileak ezaugarri berriak irabazten ditu ingurune erronkatsuetan bizirauteko, hala nola antibiotikoen aurrean.

Konjugazioa bakterio arteko kontaktuen menpeko prozesua da, non substratua (ssDNA-errelaxasa konplexua) bakterio emailetik bakterio hartzailera garraiatzen den. Prozesua normalean hiru pausutan aurkezten da: (1) substratuaren prozesamendua, (2) substratuaren harrera sekrezio kanalera eta (3) substratuaren translokazioa bakterio hartzailera (Alvarez-Martinez eta Christie, 2009) (1.3. irudia).

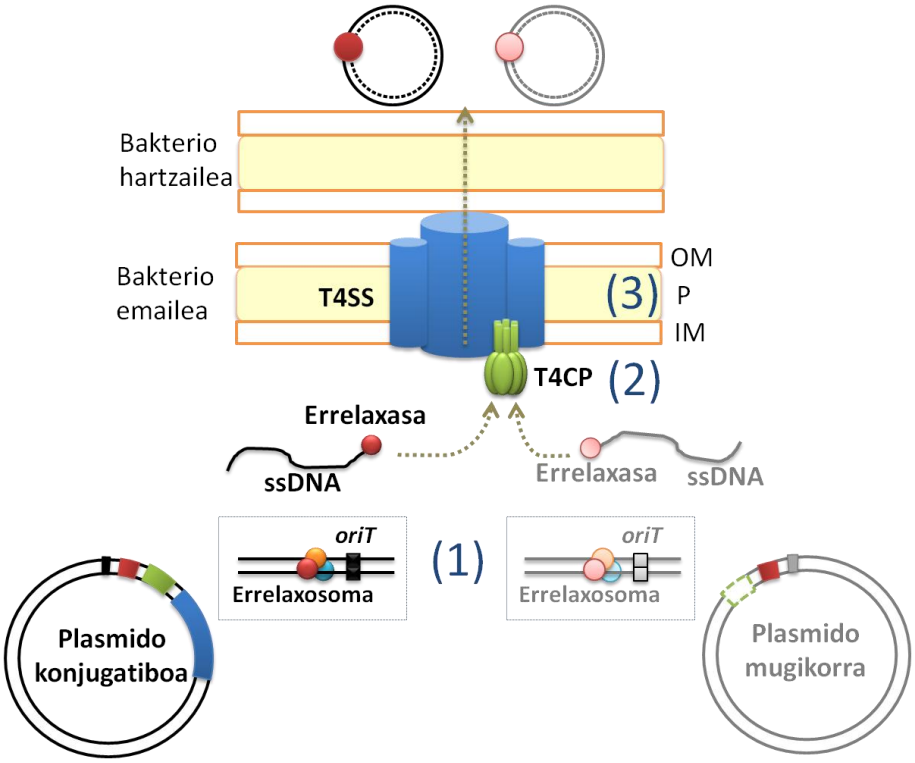

1.3. irudia. Plasmido konjugatibo eta mugikorren konjugazio prozesuaren irudikapen eskematikoa. Plasmido konjugatiboek (beltzez) prozesua burutzeko beharrezko elementu guztiak kodetzen dituzte, bere kabuz transferituak izateko gai izanik. Plasmido mugikorrek (grisez), ordea, plasmido konjugatiboek kodetutako T4SSa erabili behar dute, eta gehienetan T4CPa ere; plasmido mugikor gutxik kodetzen baitute berezko T4CPa (lerro etenez adierazia). Konjugazioa hiru pausu nagusitan banatu ohi da: (1) Substratuaren prozesamendua. Bertan errelaxasa bakoitzak bere jatorrizko plasmidoaren prozesamendua burutzen du *oriT*aren ezagupen espezifikoaren bidez. (2) Substratuaren harrera sekrezio sistemara. Plasmido konjugatiboek zein mugikorrek plasmido konjugatiboaren T4CPa erabili ohi dute, T4CP propioa duten plasmido mugikorrek salbu. (3) Substratuaren translokazioa zelula hartzailera beti plasmido konjugatiboak kodetutako T4SSaren bidez burutzen da. Bukatzeko, behin substratua zelula hartzailean egonda, ssDNAren birzikulazio eta bikoizketa burutzen da. Kolore kodea: *oriT*: beltza; *errelaxasa:* gorria; T4CP: berdea; T4SS: urdina.

Hala ere, azken ikerketek urrats gehiago proposatu dituzte. Alde batetik errelaxosomaren sorrera aurretik, sekrezio kanala eta pilusa sortu behar dira. Beste aldetik, transferentzian zehar, T4SS makineria proteina garraio modutik ssDNA garraio modura aldatu behar da (Waksman, 2019). Urrats hauek prozesu konjugatiboaren izaera konplexuaren isla dira, non hainbat jarduera aldi berean ematen diren. Horretarako energia gastu handia behar da, sisteman aurkitzen diren hiru ATPasen presentzia azaltzen duenak. Substratuen transferentzia energia gastu egokiarekin burutzeko, konjugazioa estuki erregulaturiko prozesua da. Gaur

egungo ezagumenduarekin tesi honetan prozesu konjugatiboa bost pausu nagusitan banandu egin da, ondoren azaldu bezala:

1. **T4SS kanalaren, pilus konjugatiboaren eta errelaxosomaren eraketa**: Sekrezio-kanala eratzeko seinale aktibatzaileen inguruan faktore ezezagun ugari daude. Adibidez, *A. tumefaciens* sistema kanonikoaren kasuan *virB* geneen adierazpena kanpo inguruneko faktoreen ezagumenduaren ondorioz ematen dela dirudi, beste sistemetan ere gerta litekeena (Li eta Christie, 2018). Horren ostean T4SSaren muntaia ematen da (Chandran Darbari eta Waksman, 2015) eta pilien eraketa. Azken prozesu hau sakonki berrikusi egin da literaturan (Lukaszczyk et al., 2019). Horretaz gain, errelaxosomaren eraketa ematen da, errelaxasa, DNA eta proteina laguntzailez osaturiko konplexua dena.

2. **Konjugazio-aurreko konplexuaren eraketa:** Behin pilusa, T4SSa eta errelaxosoma eraturik, haien artean elkarrekiten dute konjugazio-aurreko konplexua sortuz, konjugazioa hasi arte egoera ez-aktiboan mantentzen dena (Waksman, 2019). Konplexuaren eraketa emateko T4CPak errelaxosomaren harrera burutzen du elkarrekintza multzo baten bidez. Gaur egun elkarrekintza guzti hauen egitura oinarriak ez daude zehazki ebatzita eta oraindik ikerketa sakonagoak behar dira arlo honetan, batez ere T4CPari dagokionez. Interakzio indartsuenak T4CP eta transferitzen ez diren errelaxosomako proteina lagungarrien artean ematen dira (Llosa eta Alkorta, 2017). Horretaz gain, errelaxasek haien sekuentzian T4CPak ezagutzen dituen translokazio seinaleak (*Translocation signals*, TS) dauzkate (Christie, 2004). Hipotetizatu egin da elkarrekintza hauen ondorioz T4CPa homohexamero edota heterohexamero (VirB4 azpiunitateekin, ikusi 1.10. irudia) gisa oligomerizatzen duela T4SSra erantsita geratuz (Waksman, 2019). Era berean, badirudi azken elkarrekintza honek T4CPa eta VirB11-motako proteinek burutzen duten ATP-hidrolisia sustatzen duela. Azkenengoz, prozesu honek sekrezio kanala aktibatzen duen VirB10-motako proteinaren aldaketa konformazionala eragiten du (Cascales et al., 2013).

3. **Konjugazio prozesuaren aktibazioa:** Nahiz eta substratuaren transferentziarako DNAren batura eta ATParen hidrolisia eragindako seinaleak beharrezkoak izan, ez dira nahikoak; kanpo inguruneko seinale bat ere behar da. Seinale hori pilusa zelula hartzaile bat ezagutzen duenean sortzen da (Zechner et al., 2012). Behin kontaktua eginda, pilusa uzkurtu (F-mota) edota erori (P-mota) egiten da, bakterioen arteko elkarguneak sortuz (Lawley et al., 2003; Schröder eta Lanka, 2005). Iradokitzen da zelula arteko kontaktutik sortutako seinalea T4SStik zehar igorri egiten dela, VirB10-motako proteinaren bidez T4CPra helduz eta azkenengoz errelaxosoma aktibatuz (Llosa eta Alkorta, 2017). Honen ondorioz DNA substratuaren ebaketa ematen da, errelaxasa sortzen den 5’ muturrari kobalenteki lotuta geratuz. Orduan DNA substratuaren bikoizketa ematen da zirkulu biribilkari moduko erreplikazio bidez (*Rolling circle replication*, RCR) aske geratutako 3’ muturretik DNA katea luzatuz (Llosa et al., 2002).

4. **Substratuen garraioa T4SSan zehar:** Konjugazioaren substratua ssDNAri kobalenteki atxikitutako errelaxasa da. Bi osagai hain desberdinen (konposaketa kimiko zein egituraren aldetik) transferentzia egiteko badirudi T4SSak funtsezko aldaketak jasan behar dituela prozesuan zehar. Gai honen inguruan erantzun gabeko galdera ugari daude, hala nola zein osagai garraiatzen den lehenengoz edota nola destolesten eta garraiatzen den errelaxasa. Nahiz eta errelaxasaren transferentzia mekanismoa gaur egun ebatzirik ez egon, ikerketa desberdinak burutu dira substratu nukleikoaren inguruan. ssDNAk T4SS$_{A.\ tumefaciens}$-tik zehar burutzen duen ibilbidea *Transfer DNA Immunoprecipitation* (TrIP) izeneko entseguaren bidez ebatzi zen (Cascales eta Christie, 2004a). ssDNA T4CPtik VirB11ra igarotzen da, energia gasturik gabeko prozesuan. Hemendik VirB6 eta VirB8 proteinetara bideratzen da, prozesurako beharrezkoa den energia lortzeko sistemako hiru ATPasak modu aktiboan egotea ezinbestekoa delarik. Ondoren VirB8tik OMCCko VirB9 azpiunitatera igarotzen da eta azkenik bertatik piluseko VirB2ra. Hala ere, TrIP bidez ebatzitako substratuaren ibilbidea ez dator bat gaur egun dauden egitura ereduekin eta sakonago aztertu beharko lirateke (Waksman, 2019). Gaur egun hiru translokazio aukera posible proposatzen dira ssDNA substratuarentzat: (i) T4CP hexameroaren kanaletik T4SSra igarotzea, (ii) substratoaren harrera ostean hau VirB4 hexameroaren kanaletik translokatzea T4SSra, eta (iii) ATPasekin elkarreragin ostean substratua zuzenean IMCren azpiunitatez eraturiko kanaletik igarotzea. (Christie et al., 2017).

5. **Substratoaren harrera bakterio hartzailean eta konjugazioaren bukaera:** Nahiz eta T4SSan zeharreko garraioa nahiko aztertua egon, gaur egun ez dago ebatzirik nola zeharkatzen duen substratuak bakterio hartzailearen OM eta IMa. Behin hau gertatuta, errelaxasak ssDNA birzirkularizatzen du eta ziur asko kate osagarriaren sintesian parte hartzen du (Draper et al., 2005). Aurretik esan bezala, prozesu honi esker, hartzaileak plasmidoan kodeturiko ezaugarriak bereganatzen ditu. Modu horretan, jasotako plasmidoa konjugatiboa izanez gero, bakterio hartzaileak plasmidoa beste bakterioei pasatzeko ahalmena irabazten du.

Azpimarratu beharra dago aurkezten dituzten ezaugarri desberdinengatik konjugazioaren mekanismoa desberdina dela bakterio Gram$^-$ eta Gram$^+$-etan (Grohmann et al., 2018). Hemen azaldutako jarraibidea bakterio Gram$^-$-etan ematen den transferentziari dagokio.

Ikusi daitekeen moduan, konjugazioa prozesu konplexua da, hertsiki erregulatua, zeinetan erantzun gabeko galdera ugari geratzen diren oraindik. Alde batetik, nahiz eta substratu eta azpiunitateen arteko kontaktu sekuentzia definiturik egon, translokazio mekanismoa ez dago ondo ezarrita. Jatorriz pausu bateko edo bi pausutako translokazio ereduak aldarrikatu ohi dira. Lehenengoan ssDNA zuzenean T4SSra igarotzen zen. Bigarrenean ssDNA T4CParen kanaletik periplasmara igarotzen zen eta handik T4SSra (Llosa et al., 2002). Dena den azken eredu hau baztertu egin zen periplasman aurkitzen diren nukleasa kantitate altuagatik. Horren ordez, T4CPa T4SSren sarreran kokatzea proposatu zen, zuzenean substratua T4SSra igaroz (Christie, 2016).

1.3. PROTEINA AKOPLATZAILEAK

T4CPak ezinbestekoak dira T4SS gehienetan, sistema konjugatibo guztietan daudelarik, baita prozesu patogenikoekin erlazionaturiko efektoreen sistema translokatzaile askotan ere. Aurretik azaldu bezala plasmido transmitigarrien MOB moduluaren parte dira eta orokorrean errelaxasen ondoan kodeturik daude. Izan ere, haien filogeniak errelaxasen filogeniarekin antz handia erakusten du, substratuak eta hartzaileak elkarrekin eboluzionatu dutela iradokiz. Azpimarratu beharra dago, filogeniari dagokionez, T4CPak sistema konjugatiboen markatzaile onenak direla haien nonahikotasun eta tamaina handiaren ondorioz (Smillie et al., 2010). T4CP ikertuenak sistema $Gram^-$-ekin erlazionaturikoak dira (adibidez $VirD4_{A.\ tumefaciens}$, $TrwB_{R388}$ eta $TraD_F$), baina azken urteetan azterketak $Gram^+$-en T4CPtara (adibidez $PcFC_{pCF10}$ eta $TcpA_{pCW3}$) eta T4BSSen T4CPetara (adibidez $DotL_{L.\ pneumophila}$) hedatu dira.

Proteina hauen ikerketa helburu bikoitzarekin burutzen da. Alde batetik, konjugazioan daukaten garrantziaren ondorioz jomuga interesgarria dira prozesu honen aurkako inhibitzaileak garatzeko, T4SSen beste osagaiekin egin den bezala (Boudaher eta Shaffer, 2019; Shaffer et al., 2016). Izan ere, molekula zehatzen bidez T4CPen inhibizioa edota funtzioaren mugaketa burutzeak osasun eta ingurune arloan oso abantailatsua izango lirateke. cT4SSen kasuan, ARGen hedapena kontrolatu ahalko zen; eta pT4SSen kasuan, hainbat prozesu patogeniko oztopatu ahalko lirateke. Beste aldetik, T4CPek burutzen duten substratuaren garraio espezifikoak bioteknologiaren arloan aukera ugari eskaintzen ditu, hala nola aukeratutako molekulen garraio bideratua sistema heterologoen bidez (Guzmán-Herrador et al., 2017).

1.3.1. SAILKAPENA

T4CPak proteina familia heterogeneoa dira, sekuentzia zein domeinu arkitekturari dagokionez. Hala ere, orokorrean, filogenetikoki hurbilago dauden proteinek sekuentzia antzekotasun handiagoak aurkezten dituzte. Kontserbaturiko nukleotidoen-atxikitze domeinua (*Nucleotide-binding domain*, NBD) familiako kideak definitzen dituen domeinua da. Horretaz gain transmintz domeinu bat (*Transmembrane domain*, TMD) aurkeztu ohi dute N-muturrean, proteina bakterioen barne mintzera ainguratzen duena; alfa-guztiko domeinu bat (*All alpha domain*, AAD), zitoplasmaren alderantz; eta zenbait kasutan C-muturreko domeinu aldakor bat (*C-terminal domain*, CTD) (1.4. irudia).

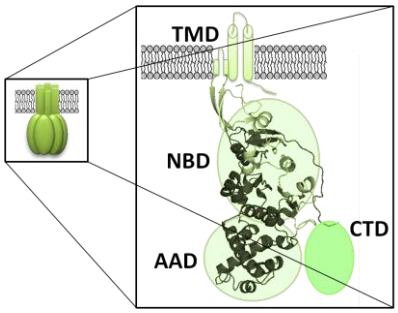

1.4. Irudia. T4CP domeinuen irudikapen eskematikoa. Lau domeinu desberdin bereizten dira: mintzean (i) TMDa eta zitosolean (ii) NBDa, (iii) AADa eta zenbait kasutan (iv) CTDa. TrwBΔN70ren egitura erabili da NBD eta AADa irudikatzeko **(**PDB: 19E6).

Domeinuen presentzia eta izaera irizpide gisa hartuz, T4CPak bost azpifamilia desberdinetan sailkatzen dira (Llosa eta Alkorta, 2017) (1.5. irudia).

1. **VirD4-motako T4CPak**: Azpifamilia honetako T4CPak deskribaturiko lehenak izan ziren eta gaur egunera arte ikertuenak dira (Christie, 2016). Haien izena *A. tumefaciens* T-plasmidoko T4CPtik, $VirD4_{A.tumefaciens}$, dator. Hala ere $TrwB_{R388}$ azpifamilia honen prototipoa da, sakonago aztertu delako eta bere egitura tridimentsionala ebatzita dagoelako (Christie, 2004; Gomis-Rüth et al., 2001). Proteina hauek 500-750 aminoazidoz osaturik daude eta N-muturrean gutxienez bi transmintz helize aurkezten dituzte. Horretaz gain, sekuentzia identitate baxua aurkezten dute haien artean (%15-20 inguru). Hala ere, ikusi egin da haietako batzuk *in vivo* elkar ordezkatu ahal direla plasmido mugikorren konjugazioa burutzerakoan (Cabezón et al., 1994; Llosa et al., 2003).

2. **TraG-J proteina bikoteak**: Azpifamilia honetako T4CPak VirD4-motakoen antzeko egitura aurkezten dute, 700 aminoazido inguru izanik, baina domeinu periplasmiko laburragoa. VirD4-motako T4CPak bezala, elkarren artean trukatu daitezke konjugazioa burutzeko; baina talde honetan T4CPen arteko sekuentzia antzekotasuna handiagoa da. Horretaz gain, haien funtzioa burutzeko mintz proteina (*Membrane protein,* MP) batekin (TraJ) elkarrekiten dute (Gunton et al., 2007). Azken hauek T4CP genearen ondoan kodeturik aurkitu ohi dira, 200 aminoazido inguru dauzkate eta bost transmintz helize arte izan ditzakete.

3. **TMDrik gabeko T4CPak**: Zenbait kasutan T4CPak ez dute TMDrik, nahiz eta hauek ezin bestekoak izan T4CP gehienen funtzionamendurako. Hala ere, badirudi talde honetako T4CP batzuek MP txikiekin elkarrekiten dutela (TraG-J bikotearen modura) VirD4-motako T4CPen antza duten konplexuak eratuz. Adibidez, hau $TraJ_{pIP501}$ T4CP (lehen $Orf10_{pIP501}$ moduan izenpetua) eta $TraI_{pIP501}$ (lehen $Orf9_{pIP501}$) MParen artean ematen dela dirudi (Grohmann et al., 2016).

4. **FtsK-motako T4CPak**: Deskribatu da T4CParen egiturak SpoIIIE/FtsK ssDNA translokasen egiturarekin antzekotasunak aurkezten dituela (Gomis-Rüth eta Coll,

2006). Antzekotasun hau FtsK-motako T4CPetan areagotu egiten da. T4CP hauek handiak dira (750 aminoazido baino gehiago) eta NBDtik lotura-sekuentzia luzeen bidez bananduriko TMD ugari aurkezten dituzte. Horretaz gain ez daukate AADrik, baina ATParen batura eta hidrolisian parte hartzen duen gainerako domeinu bat aurkezten dute (Parsons et al., 2007).

5. **Archaea-ko T4CPak**: NBDetan oinarrituriko sekuentzia iragarpenen bidez zenbait T4CP identifikatu dira Archaea erreinuan.

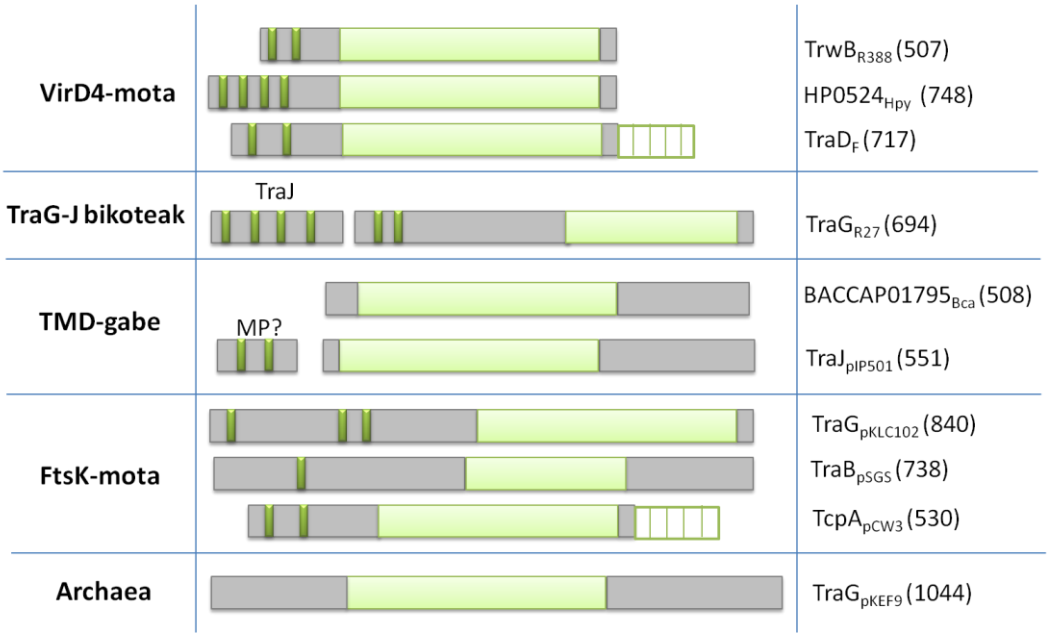

1.5. irudia. **T4CPen sailkapena domeinu arkitekturaren arabera.** Lerro bakoitzak bost azpifamilietako bat adierazten du. Bakoitzaren barnean adibide adierazgarriak erakusten dira bigarren (egitura molekularra) eta hirugarren (proteinaren izena eta aminoazido kopurua) zutabeetan. Berde iluna: transmintz helizeak; Berde argia: NBDa; Lauki marradunak: CTDa.

1.3.2. EGITURA

Aurreko atalean ikusi bezala, T4CP gehienak TMDaz eta domeinu zitosolikoaz (*Cytosolic domain*, CD) eraturik daude, azken honen barne NBDa, AADa eta CTDa (zenbait kasutan) aurkituz (1.4. irudia). Proteina hauen prototipoa TrwB$_{R388}$ da, zeinaren mutante solugarriaren egitura, TrwBΔN70, X-izpien bidez ebatzi zen (Gomis-Rüth et al., 2001).

1.3.2.1. DOMEINUAK

TRANSMINTZ DOMEINUA

VirD4-motako T4CPei dagokienez, TMDa ezinbestekoa da *in vivo* konjugazio prozesua burutzeko (Chen et al., 2008; Segura et al., 2013). Izan ere, domeinu honen bidez T4CPak VirB10 proteinarekin elkar eragiten du, T4SSan zehar substratuaren garraiorako beharrezkoa den seinaletako bat martxan jarriz (Llosa et al., 2003; Segura et al., 2013). Horretaz gain, oligomerizaziorako ezinbestekoa da, horretarako aminoazido gakoak bertan aurkituz (Redzej et

al., 2017). TMDan alfa-helizeez gain, periplasmako begiztak ere aurkitzen dira, T4SSrekiko elkarrekintzetan eta proteinaren funtzioan ezinbestekoak direnak (Gunton et al., 2005; Kumar eta Das, 2002).

TMDren inguruko ikerketa sakonenak $TrwB_{R388}$ proteinarekin burutu dira, hau baita purifikatu den mintz T4CP natibo bakarra. Deskribatu da TMDko elementuen galera progresiboa burutzerakoan konjugazioaren bidezko DNAren transferentzia maiztasuna murrizten doala, guztiz desagertu arte transmintz gabeko TrwBΔN70 mutantean (Segura et al., 2013). Era berean, infragorrien espektroskopia (*Infrared Spectroscopy*, IRS) saiakeren bidez TMDak proteinaren egonkortasun eta egituran daukan eragina deskribatu zen (Hormaeche et al., 2004; Vecino et al., 2011). Modu horretan ikustatu zen $TrwB_{R388}$ TrwBΔN70 baino egonkorragoa dela agente desnaturalizatzaileen aurrean (indar ioniko baxua, agente kaotropikoak eta tenperatura, kasu) eta TMDaren presentziak domeinu zitosolikoa era trinko eta ordenatuagoan tolestea eragiten duela. Bestaldetik deskribatu da TMDak nukleotidoen-atxikipenean eragina daukala ere, nahiz eta hau CDan gertatu. Hain zuzen ere, proteina natiboak nukleotido guztiekiko afinitate txikiagoa aurkezten du, baina espezifikotasun handiagoa nukleotido puriko trifosfatoentzat (Hormaeche et al., 2006). Are gehiago, deskribatu egin da nola TMDko elementuen galera progresiboa burutzerakoan afinitatearen handipen eta espezifikotasunaren murrizketa progresiboak ematen direla (Vecino et al., publikatu gabeko datuak). Badirudi TMDaren presentziak NBDko batura guneen eskuragarritasuna murrizten duela ATParekiko espezifikoagoak bihurtuz. Hala ere TrwBΔN70k proteina natiboan aurkitu ez den ATPasa aktibitatea aurkezten du, DNArekiko menpekoa dena eta $TrwA_{R388}$ proteinaz areagotua (Tato et al., 2007).

Datu guzti hauek TMDak domeinu zitosolikoarengan funtzio erregulatzailea daukala erasaten dute. Bukatzeko, proteina natiboa eta TMDa bakterio paretaren poloetan kokatzen diren bitartean, mutante solugarria zitoplasma osoan kokatzen da sistema konjugatiboaren gainerako proteinen absentzian. T4SSko proteinak daudenean, ordea, mintz osoan zehar kokatzen da (Segura et al., 2014). Honek adierazten du T4SSko proteinek T4CParen mintz kokapenean eragina daukatela CDarekin burutzen duten elkarrekintzen bidez; nahiz eta poloetako kokapenaren gidaria TMDa izan (Segura et al., 2014). Hain garrantzitsua izan arren, TMDa T4CPetan heterogeneotasun gehien aurkezten duen sekuentzia da.

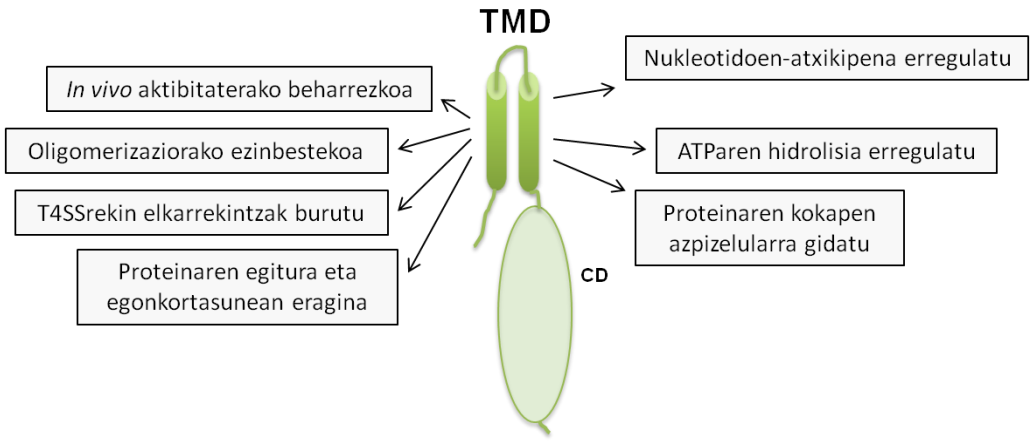

1.6. irudia. **TMDaren garrantzia VirD4-motako T4CPetan.** $TrwB_{R388}$ eta TrwBΔN70 proteinen azterketa konparatiboa burutuz Alkorta doktorearen laborategian ondorioztatutako TMDaren funtzio desberdinak adierazten dira.

VirD4-motako proteinen funtziorako ezinbestekoa bada ere (Chen et al., 2008; Segura et al., 2013), transferentzia burutzeko gai diren TMDrik gabeko T4CPak ere badaude. Are gehiago, FtsK-motako $TcpA_{pcW3}$ proteinaren TMDrik gabeko mutantea konjugazioa burutzeko gai da, baina jatorrizko proteina baino maiztasun baxuagoan (Parsons et al., 2007). Datu hauek zalantzan jartzen dute ea $TrwB_{R388}$ erabiliz, T4CPen prototipoa, ebatzi diren ezaugarri guztiak unibertsalki T4CP guztiei ezarri ahal diren ala ez. Zoritxarrez mintz proteinekin lan egitea astuna eta zaila denez, azterketa gehienak TMDrik gabeko proteina mutanteekin burutu dira, domeinu honen eragina baztertuz. Hori dela eta, sekuentzia osoko T4CPekin burututako ikerketa gehiagoren beharra dago.

DOMEINU ZITOSOLIKOA

CDa bi domeinu nagusietan banandu daiteke: NBDa eta AADa. Horretaz gain, zenbait kasuetan C-muturrean CTD domeinua ere ager daiteke.

NUKLEOTIDOEN ATXIKITZE DOMEINUA

Aldez aurretik esan bezala, NBDa T4CP guztietan kontserbaturiko domeinu bakarra da, mintzetik hurbil aurkitzen dena. Domeinu hau bi motiboz osatua dago. Alde batetik Walker A motiboa dago, *P-loop* gisa ere izendatua eta nukleotidoen β eta γ fosfatoak lotzen dituena (Walker et al., 1982). *P-loop*-a glizinan aberasturiko sekuentzia bat da, kontserbaturiko lisina batez jarraitua eta ostean serina edota treonina bat dituena; normalean G-x(4)-GK-[TS] moduan adierazten da, non x edozein aminoazido den. Motibo hau ATP edota GTPa lotzen duten proteina askotan agertzen da, hala nola ATP sintasen α eta β azpiunitateetan, miosinan, adenilato kinasan, ABC garraiatzaileen familian eta abar (Geourjon et al., 2001). NBDko bigarren motiboa Walker B motiboa da. Bere sekuentzia [RK]xxxGxxx-LhhhDE da, non x edozein aminoazido eta h aminoazido hidrofobiko bat diren (Hanson eta Whiteheart, 2005; Walker et al., 1982). Topologikoki NBDa mintzetik hurbil kokatzen da eta estrukturalki biraturiko β-orri batez eratua dago, α-helizez inguraturik dagoena (Gomis-Rüth eta Coll, 2006). Konformazio hau FtsK proteinaren β-domeinuaren antza aurkezten du. FtsK mintz proteina bat

da, zelula bikoizketan mintzean zehar DNAren garraioa burutzen duena (Aussel et al., 2002). Antzekotasun honek T4CParen *in vivo* funtzioa iradoki dezake, hau da, konjugazioan zehar DNA garraiatzea.

Funtzioari dagokionez NBDak ezinbestekoak dira T4CPen *in vivo* aktibitaterako. Izan ere, Walker A domeinuko mutanteak ez dira gai konjugazio prozesua burutzeko (Gunton et al., 2005; Kumar eta Das, 2002; Moncalián et al., 1999). Badirudi inhibizio hau ATParen hidrolisiarekin erlazionaturik dagoela, TrwBΔN70(K136T) mutanteak ez baitu ATPasa aktibitaterik aurkezten (Tato et al., 2005). Dena den, mutante hauetako batzuk proteina natiboen hainbat ezaugarri erakusten dituzte; hala nola, kokapen azpizelularra, nukleotidoen atxikitze afinitateak eta substratuekiko elkarrekintzak (Chen et al., 2008; Moncalián et al., 1999). Honek adierazten du Walker A motiboaren ezinbesteko funtzioa nukleotido eta substratuarekiko elkarrekintzen ostean ematen dela.

ALFA-GUZTIKO DOMEINUA

AADa zitoplasmarantz kokaturik aurkitzen da eta tamaina, sekuentzia eta α-helize tolesdura aldakorrak erakusten ditu. Domeinu hau aldez aurretik aipatutako RecA familiako proteina askok daukate (Gomis-Rüth et al., 2001). Izan ere, $TrwB_{R388}$ren AADa XerD errekombinasaren N-muturrarekiko antzekotasun estrukturalak aurkezten ditu. XerD aldez aurretik aipatutako FtsK proteinarekin elkarrekiten du bikoizketaren ostean DNAn sortutako korapiloak askatzen. XerD-ren N-muturreko domeinua NBDaren gainean kokatzen da, DNAren batura oztopatuz. Honek adierazten du konformazio berrantolaketa bat eman behar dela substratuarekiko elkarrekintza emateko; T4CPetan ere gerta daitekeena. T4CPen kasuan AADak NBDaren sarrera oztopatuko luke, konformazio aldaketa baten ostean DNArekiko elkarrekintzan parte hartuz eta NBDa libre utziz. Horretaz gain, $TrwB_{R388}$ren 40 aminoazido inguruz osaturiko AADko 3 alfa-helizek antzekotasun topologikoak erakusten dituzte $TraM_F$ proteinaren DNA-batura domeinuarekin. $TraM_F$ F plasmidoko errelaxosomaren osagaia da, $TraD_F$ T4CParekin elkarrekiten duena. R388 plasmidoan ez dagoenez $TraM_F$ren homologorik, badirudi $TrwB_{R388}$k DNArekiko elkarrekintza domeinu hori bere egituran barneratu duela.

Whitaker eta lankideek (2015) AADaren funtzioa sakonki ikertu zuten, konjugaziorako ezinbestekoa dela ikusiz. $VirD4_{A.\ tumefaciens}$ren AADak funtzio bikoitza burutzen du, alde batetik sekrezio kanalaren aktibazioan parte hartuz eta beste aldetik substratu espezifikoen ezagupena burutuz. Honi dagokionez, AADak DNAarekin batura ez-espezifikoa eratzen du baina espezifikoa errelaxosoma (TS sekuentzien ezagupenaren bidez) eta proteina laguntzaileekin. Plasmido mugikorrak, ordea, AADaren espezifikotasun giltza gainditzeko gai dira, ziur aski hau izanik hainbat T4SStik transferitzeko daukaten gaitasunaren arrazoia (Lee et al., 2012; Whitaker et al., 2015).

C-MUTURREKO DOMEINUA

Zenbait T4CPk C-muturrean egitura motibo edota domeinu berriak eskuratu dituztela dirudi (Alvarez-Martinez eta Christie, 2009). Hauek VirD4-motako (adibidez $VirD4_{A.\ tumefaciens}$), FtsK-motako (adibidez $TcpA_{pCW3}$) eta Archaea-motako (adibidez $TraG_{pKEF9}$) T4CPetan aurkitu

ahal diren α-helizedun domeinuak dira. Sekuentzia eta tamaina heterogeneotasuna aurkeztu arren, glutamato eta aspartato aminoazidoetan aberatsak dira.

CTDen ikerketa sistema desberdinetan burutu da, funtzio desberdinak ikusi direlarik. Deskribaturik dago hainbat proteinek buztan azidiko hauek aurkezten dituztela DNA eta proteinekin elkarrekintzak burutzeko (Basu et al., 2020; Harrison et al., 2016; Lee eta Thomas, 2000; Wang et al., 2007); eta badirudi hau ere izan daitekeela haien funtzio orokorra T4CPetan. Adibidez F plasmidoko $TraD_F$ T4CParen kasuan, CTDaren bidez errelaxosomako $TraM_F$ proteina lagungarriarekiko elkarrekintza ematen da (Lu eta Frost, 2005; Lu et al., 2008). Kasu honetan CTDa ezinbestekoa da plasmidoaren ezagupen eta transferentziarako, espezifikotasun kontrol gisa jardunez eta substratu heterologoen bazterketa burutuz. Antzeko eran, $TcpA_{pCW3}$ T4CPan CTDaren presentziak konjugazio maiztasuna 3 magnitude ordenetan bultzatzen du eta gainera T4SSko proteinekin elkarrekintzak burutzen ditu (Steen et al., 2009).

Sistema patogenikoekin erlazionaturiko zenbait T4CPek ere CTD sekuentziak dauzkate. Alde batetik, Whitaker eta lankideek (2016) egindako ikerketan ikusi zen nola $VirD4_{A.\ tumefaciens}$ CTDaren eragina substratuaren arabera aldatzen zela, zenbait kasutan funtziorik gabea edota antagonikoa izanik. Baita CTD hau efektore errepertorioa handitzeko eta T4SSra efektoreen aurkezpen espazio-tenporala erregulatzeko eboluzionatu zela ondorioztatu zuten. Bestaldetik deskribatu da $DotL_{L.\ pneumophila}$ T4CPak 200 aminoazido inguruko mutur azidikoa daukala; zeinaren bidez IcmSW sistemako proteina efektoreen harrera burutzen duen (Meir et al., 2018; Sutherland et al., 2012). Izan ere $DotL_{L.\ pneumophila}$ CTDaren egitura efektoreen garraiorako ezinbestekoak diren bi elkarrekintza desberdin burutzerakoan ebatzi da: IcmSW sistemarekin eta DotN proteinarekin (Kwak et al., 2017).

1.3.2.2. $TrwB_{R388}$ren EGITURA

Orain arte, T4CPekin erlazionaturiko bi kristal egitura baino ez dira ebatzi. Alde batetik, $TrwB_{R388}$ren mutante solugarriaren, TrwBΔN70, egitura (Gomis-Rüth et al., 2001); eta bestetik, $DotL_{L.\ pneumophila}$ T4CParen CTDa, Dot/Icm konplexuaren barnean (Kwak et al., 2017). $TrwB_{R388}$ T4CP aztertuena izan denez, proteina familia honen arketipotzat jotzen da.

TrwBΔN70 ligandorik gabe, zein nukleotido eta sulfato ioiekin lotua kristalizatu da (Gomis-Rüth et al., 2001, 2002a). Ebatzitako egiturak aldez aurretik literaturan deskribaturiko proteina familien antza aurkezten zuen (aurreko ataletan aipatutako AAA+ ATPasak, RNA eta DNA helikasak eta FtsK/SpoIIIE familiako proteinak). Bere egitura 110 X 90 Å-eko homohexamero globularra da, hexameroa zeharkatzen duen erdiko kanal bat izanik (*Internal channel*, ICH). Kanal honek 22 Å dauzka mintzeko alderantz, zitosoleko aldean 7 Å soilik izanik. Estutze honek substratuaren garraiorako konformazio aldaketak eman behar direla iradokitzen du (Schröder eta Lanka, 2005). Horretaz gain, deskribatu da ICHaren barnean hiru gune elektrostatiko bereizten direla: alde zitosolikoan eskualde hidrofobiko labur bat, elektronegatibitate altuko erdiko segmentu batez jarraitua eta proteinaren bigarren erdi elektropositiboa. Bertako aminoazidoen ikerketak ICHko bi muturretako aminoazidoek kanalaren ireki-itxiera mekanismoa kontrolatzen dutela erakutsi du, erdiko aminoazidoek substratuaren translokaziorako bidea ezartzen duten bitartean (Larrea et al., 2017). AAD domeinua egituraren aldetik zitoplasmarantz zuzendutako zazpi alfa-helizez osatua dago, eta

$TrwK_{R388}$ (R388 sistemaren VirB4ren homologoa) egituraren antza aurkezten du (Walldén et al., 2012). Honek VirD4-motako T4CP eta VirB4 proteinen arteko homologia estrukturala azpimarratzen du, bien arteko erlazio filogenetikoa aldarrikatuz nahiz eta sekuentzia antzekotasun txikia izan (Guglielmini et al., 2013; Walldén et al., 2012).

Egitura primarioari dagokionez (1.7. irudia, A), lehenengo aminoazidoak (M_1-etik K_8-ra) eskualde zitosoliko txiki batekin erlazionaturik daude, TMDaz jarraitua (V_9-etik V_{69}-ra). Eskualde hau *in silico* modelatu egin da, bi α-helize lortuz monomero bakoitzeko (1.7. irudia, B). Hauen artean gune periplasmatikoa egongo lirateke, α-helize batez jarraitutako begizta batez eratua. Begizta hauek T4SSarekin elkarreragiteaz gain, alboko azpiunitateko begiztekin elkarrekiten dutela proposatu da, erroska hexameriko bat eratuz. NBDa TMDaren ostean dagoen eskualdean hasten da, L_{71}tik K_{183}ra eta D_{298}tik I_{507}ra; lehenengo gunean Walker A motiboa egonik eta bigarrenean Walker B. Bi motibo hauen artean AAD domeinuaren sekuentzia (G_{184} eta G_{297}) aurkitzen da. R_{437}-T_{444} eta T_{450}-E_{455} aminoazidoen arteko eskualdea, β9 eta β10 harizpien mintz-ertz proximalarekin erlazionatutarik dagoena, ez zen kristalezko egituran ebatzi; ziur asko TMDarekin elkarrekiten duelako (Moncalián et al., 1999). Eskualde honen *in silico* modelizazioa burutuz TMDaren α-helizez ainguraturiko β-orriak ikusi ziren, estaldura hidrofobiko bat eratuz; kanalean zeharreko DNAren garraioa ematekotan oso garrantzitsua izango liratekena (1.7. irudia, C, grisez).

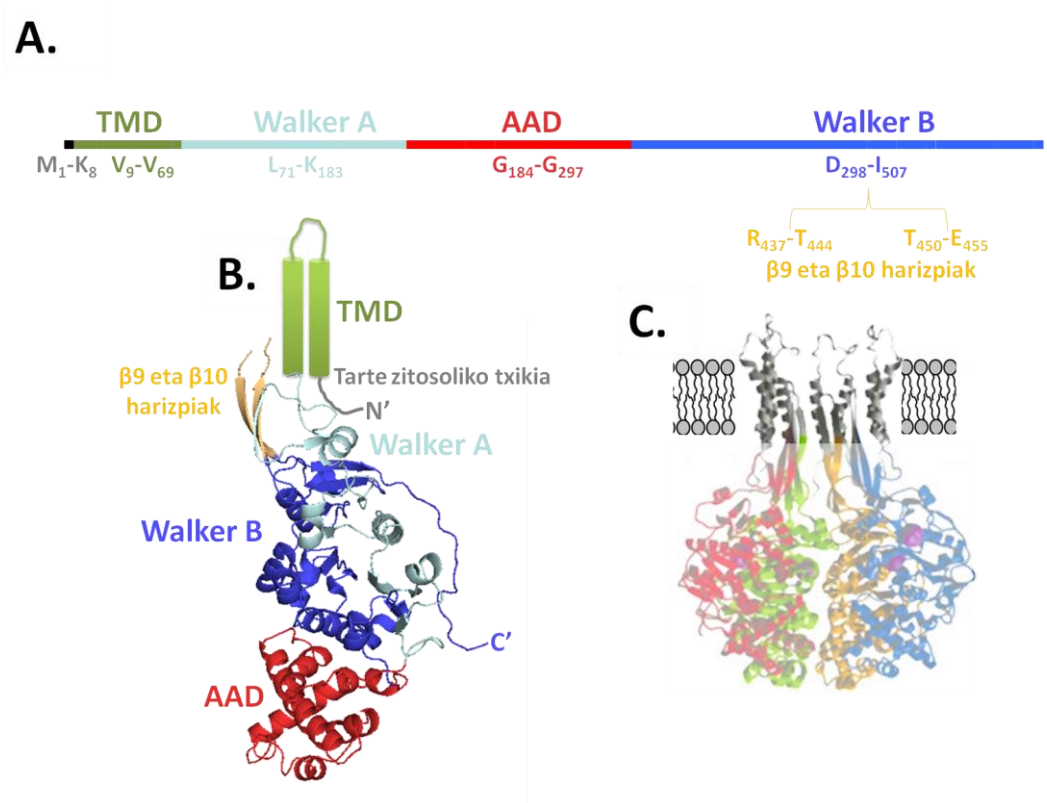

1.7. irudia. $TrwB_{R388}$ren egitura. A) Egitura primarioaren irudikapen eskematikoa. Sekuentzia primarioan domeinu desberdinen kokapena adierazten da. **B)** TrwBΔN70 monomero baten diagrama. Domeinu desberdinak A-n erabilitako kolore kodearekin irudikatu dira. TMDa (berdez) kristalezko egituran ebatzi ez zenez bi zilindro gisa irudikatu egin da. β9 eta β10 harizpiei dagokienez (laranjaz), soilik kristalezko egituran ebatzitako tarteak erakusten dira.

PDB: 19E6 **C)** Lau monomeroren adierazpena (monomero bakoitza kolore batez), X-izpien bidez ebatzitako egiturari *in silico* modelaturiko TMDa, β9 eta β10 harizpiak gehituz (grisez). C irudia Gomis-Rüth et al., 2002b-tik egokitua izan da.

TrwBΔN70ren azpiunitate bakoitza laranja zati forma dauka eta aurretik aipaturiko NBD eta AAD domeinuetan banatzen da (1.7. irudia, B). Nukleotidoen atxikitze poltsikoak bi azpiunitateen arteko azaleko kontaktu guneetan daude. Elkar ondoan dauden bi monomeroen arteko kontaktu guneak bakoitzaren gainazalaren %25a hartzen du; beraz, hexameroan, azpiunitate bakoitzaren %50a alboko azpiunitateekin kontaktuan aurkitzen da. Nukleotidoen presentzian ebatzitako egituren azterketak gune aktiboan ematen diren mugimendu konformazionalak erakusten ditu, ICH guztitik hedatzen direnak. Honek hautematera ematen du nukleotidoen batura edota hidrolisia T4CP osoan ematen den egitura aldaketaren eragilea dela, substratuarekiko elkarrekintza erraztuz (Gomis-Rüth et al., 2002a).

Gaur egunera arte lorturiko T4CP oso baten irudi bakarra Hormaeche et al. (2002)-en argitaratu zen. Hauek tindaketa negatibozko mikroskopia elektroniko (*Negative stain electron microscopy*, NS-EM) bidez lortu ziren eta bertan TrwBΔN70ren antzeko egitura ikusi zen (laranja modukoa, erdiko kanal batekin), baita zitosoleko domeinuan ez zegoen 25 Å-eko eranskina, TMDa izan litekeena (1.8. irudia).

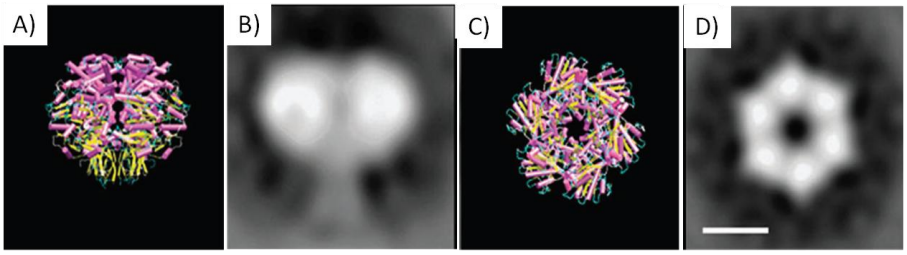

1.8. irudia. NS-EM bidez lortutako TrwB$_{R388}$ren irudiak. A eta C) X-izpien difrakzioz ebatzitako TrwBΔN70ren egitura tridimentsionalaren alboko eta goiko ikuspegiaren irudikapenak, hurrenez hurren. **B eta D)** TrwB$_{R388}$ren alboko eta goiko ikuspegiaren batez-besteko irudiak, hurrenez hurren. Irudi guztiak eskala beran erakusten dira. Eskala: 50 Å. Irudia Hormaeche et al. (2002)-tik egokitua izan da.

Honetaz gain, Redzej et al. (2017), NS-EM bidez ere, TrwB$_{R388}$ren bistaratzea burutu zuten T4SS$_{R388}$ konplexuarekin batera (1.9. irudia). Ikusi egin zen nola bi TrwB$_{R388}$ dimero bi TrwK$_{R388}$ hexameroen artean kokatzen zirela. Aipatu beharra dago, bai NS-EM zein kristalografia bidez lortutako egiturek, T4CPen jarduera dinamiko guztien une zehatz bat soilik erakusten dutela. Ordea, konjugazio prozesuak izaera dinamikoa dauka eta badirudi substratu eta T4SSaren arteko elkarrekintzak konplexuak eta aldakorrak direla substratuaren transferentzian zehar. Hau guztia dela eta, arlo honen inguruko azken lanek zalantzan jartzen dute TrwBΔN70ren egitura hexamerikoa *in vivo* ematen den egoera oligomeriko eta funtzionalaren islapen zehatza izatea (Li et al., 2019).

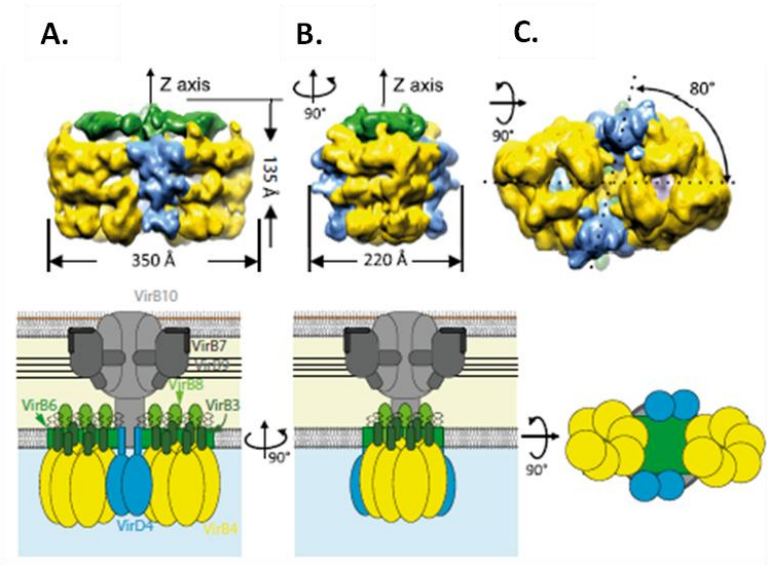

1.9. irudia. NS-EM bidez ebatzitako T4SS konplexuak. Purifikaturiko $T4SS_{VirB3\text{-}10+D4}$ konplexua aurreko **(A)**, alboko **(B)** eta beheko **(C)** bistetatik. Goikaldean NS-EM bidez ebatzitako dentsitateak erakusten dira eta bekaldean adierazpen eskematikoa. Konplexu osoaren neurriak Å-etan adierazita daude eta beheko bistan $TrwK_{R388}$ eta $TrwB_{R388}$ ardatzen arteko angelua adierazten da. IMCko arkuko egiturak, $TrwK_{R388}$ kupelak eta $TrwB_{R388}$ berdez, horiz eta urdinez adierazita daude, hurrenez hurren. Irudiak Redzej et al. (2017)-tik egokituak izan dira.

1.3.2.3. OLIGOMERIZAZIOA

Gaur egunera arte T4CPen egitura funtzionala homohexameroak direla aldarrikatu da, monomeroen alde zitoplasmatikoen arteko kontaktu gune zabalekin. Hala ere, aurreko atalean esan bezala, Redzej eta lankideek (2017) argitaratutako lanean *in vivo* ematen den egoera-funtzionala dinamikoa dela iradokitzen da, dimeroetatik hexameroetara igaroz. Are gehiago, gerta liteke T4CPen egoera aktiboa VirB4-motako proteinekin heterohexameroak sortuz izatea (1.10. irudia) (Waksman, 2019). Horretaz gain elektroi-kriotomografia bidez, sekrezio sistemen egitura aztertzeko gero eta gehiago erabiltzen ari den teknika (Oikonomou eta Jensen, 2019), $DotL_{L.\ pneumophila}$ eta $Cag\beta_{Helicobacter\ pylori}$ T4CPen dentsitateen lehenengo irudiak lortu dira (Chetrit et al., 2018; Hu et al., 2019; Li et al., 2019). Egitura hauek, Dot/Icm_{T4SS} eta Cag_{T4SS} sistema patogenikokoak, hurrenez hurren, desadostasun nabarmenak erakusten dituzte T4CP konjugatiboen *in vivo* egoera ereduekin, arlo honetan sakontzeko beharra azpimarratuz.

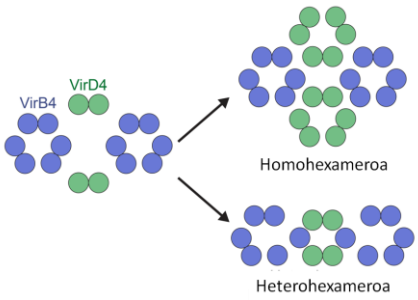

1.10. irudia. T4CPen egoera oligomeriko funtzional posibleen irudikapen eskematikoa. Deskribatu da T4CPak dimero gisa elkarrekiten dutela T4SSarekin (Redzej et al., 2017). Haien

egoera aktiboa hexameroa izanik, haien funtzioa burutzeko bi modelo proposatu egin dira: (i) T4CP sei monomeroz sortutako homohexamero gisa; eta (ii) T4CP lau monomeroz eta VirB4 bi monomeroz sortutako heterohexamero gisa.

Oligomerizaziorako ematen den TMDaren beharra hainbat ikerketetan ikusi da (Hormaeche et al., 2002; Mihajlovic et al., 2009; Schroder eta Lanka, 2003). Deskribatu egin da $TrwB_{R388}$ren TMDa oligomerizazioa emateko ezinbesteko elementua dela (Segura et al., 2013). Are gehiago, badirudi oligomerizaziorako beharrezko elkarrekintzak TMDaren bigarren helizean dauden aminoazido gakoen bidez ematen direla; izan ere GXXXXG motiboa bertan aurkitzen da, hainbat MPen oligomerizazioan parte hartzen duena (Teese eta Langosch, 2015). TMDrik gabeko mutanteei dagokionez, kontutan hartu behar da TrwBΔN70 soilik monomero gisa purifikatzen dela, $TrwB_{R388}$ monomero zein hexamero gisa lortzen den heinean (Hormaeche et al., 2002, 2004). Honen inguruan, *in vitro* saiakeren bidez ikusi zen TrwBΔN70k oligomerizatzeko, G-kuadruplex egiturak sortzen dituen DNArekin (G4-DNA) elkarrekin behar duela (Matilla et al., 2010), proteina natiboetan beharrezkoa ez dena.

Haft et al., (2007) $TraD_F$ proteinarentzako *in vivo* oligomerizazio modelo bat deskribatu zuten, non domeinu guztiek parte hartzen zuten DNArekiko batura beharrezkoa ez izanik (Haft et al., 2007). $TraD_F$ren oligomerizazio modeloaren arabera T4CPa monomero gisa mintzean txertatzen da, TMDen artean hasierako kontaktuaz ezarriz eta jarraian C-muturreko domeinuen artean homodimeroak eratuz. Horren ostean, F plasmidoan kodeturiko proteina laguntzaile batzuk dimeroen N-muturreko sekuentziak ezagutzen dituzte eta dimeroen trimero eraketa bultzatzen dute, mintzean egonkorrak diren hexameroak lortuz. Gainera, TMDaren papera azpimarratzeko, ikusi zen zitosoleko domeinuak ez zutela elkar eragiten TMDaren absentzian. Dena den, zitosolean ematen diren elkarrekintzak garrantzitsuak dira baita ere, nahiz eta oligomerizazioaren gidariak ez izan.

TMDrik gabeko T4CP natiboetan ematen den oligomerizazio mekanismoa ezezaguna da, haien dimerizazioaren hainbat froga egon arren, gaur egunera arte ez baita T4CP hauen hexamerorik deskribatu (Abajy et al., 2007).

1.3.3. KOKAPEN AZPIZELULARRA

T4SS eta T4CPen inguruan gehien aztertutako ezaugarrietako bat kokapen azpizelularra da, konjugazio prozesua emateko ezinbestekoa baita (Chen et al., 2008; Leonetti et al., 2015). T4SSen sorkuntza zelulen poloetan ematen dela dirudi, baina ez dago argi bertan mantentzen diren ala ez, mintzean zehar sakabanatutako fokoetan lokalizatu egin baitira ere (Aguilar et al., 2010; Chandran Darbari eta Waksman, 2015). T4SSen osagai desberdinen kokapena sakonki ikertu egin da azken urteetan. Kanalaren azpiegiturei dagokienez, deskribatu egin da $VirB10_{A.\ tumefaciens}$ eta $VirB9_{A.\ tumefaciens}$ gainerako osagaien absentzian ausaz kokatzen direla mintzean zehar, T-DNAren presentzian gune zehatzetan taldekaturik kokatzen diren heinean (Kumar et al., 2000). Era berean, $VirB3_{A.\ tumefaciens}$ gainerako proteina konjugatiboen presentzian mintz poloetan kokatzen da (Mossey et al., 2010), eta $ConE_{ICEBs1}$, $VirB4_{A.\ tumefaciens}$ren homologoa, zitosolean kokatzen da T4SS ezan, baina poloetan bere presentzian (Leonetti et al., 2015). Emaitza hauek iradokitzera ematen dute T4SS kanala eratzen duten proteinek mintzean kokatzen direla, orokorrean poloetan, gainerako T4SS osagaien

presentziaren menpean. MOB eskualdearen osagaiei dagokienez, $PcfG_{pCF10}$ eta $PcfF_{pCF10}$ proteinek, pCF10 plasmidoko errelaxasa eta proteina laguntzailea, hurrenez hurren, nahiz eta solugarriak izan zelula periferian kokatzen direla ikusi egin da (Chen et al., 2008).

Argi dago T4CPak haien funtzio akoplatzailea burutzeko T4SSren ondoan kokatu behar direla. Hau kolokalizazio saiakera baten bidez frogatu zen, zeinetan $VirD4_{A.\ tumefaciens}$ eta $VirB6_{A.\ tumefaciens}$ proteinak zelulen poloetan kokatzen ziren batera (Jakubowski et al., 2004). T4CP desberdinen kokapen azpizelularraren inguruan egindako ikerketek ez dute patroi zehatzik erakutsi. Honek iradokitzera ematen du kokapena sistema bakoitzaren araberakoa dela. Honen inguruan aztertutako T4CP guztiak mintzean kokatzen ziren haien egoera natiboan, bai mintz periferian, foku jakinetan, edo poloetan. $TrwB_{R388}$ eta $VirD4_{A.\ tumefaciens}$ poloetan kokatzen ziren gainerako konjugazio elementuen presentzia zein absentzian (Kumar eta Das, 2002; Segura et al., 2014). $VirD4_{pLS20}$, ordea, zitosolerantz jotzen zuen sekrezio sistemaren ezan, nahiz eta MP bat izan (Bauer et al., 2011). Dena den, $VirD4_{A.\ tumefaciens}$ bi poloetan kokatzen zen, $TrwB_{R388}$ polo bakarrean egiten zuen heinean. $TraG_{R27}$, ordea, mintzean zeharreko foku jakinetan kokatzen zen; $TrhC_{R27}$ren antzera, bere VirB4 homologoa (Gunton et al., 2005). Patroi berdin hau sistema $Gram^+$-ko $PcfC_{pCF10}$ T4CPan deskribatu zen ere (Chen et al., 2008).

Kokapenean domeinu bakoitzaren garrantzia ere aztertu da. TMDaren garrantzia prozesu honetan onarturik dago (Chen et al., 2008; Kumar eta Das, 2002; Segura et al., 2014), baina emaitza eztabaidagarriak lortu dira NBDari dagokionez. Alde batetik, ikusi egin da $TrwB_{R388}$ren TMDa (TrwBTM proteina) mintz poloetan kokatzen zela bere kabuz, $TrwB\Delta N70$ zitosolean kokatzen zen heinean T4SSaren absentzian, baina mintz periferian T4SSaren presentzian (Segura et al., 2014). Emaitza honek iradokitzera ematen du TMDa kokapenaren gidaria izanik, domeinu zitosolikoaren eta T4SSaren artean ematen diren elkarrekintzek T4CPa mintzera erakarri egiten dutela ere. Beste aldetik, deskribatu zen $VirD4_{A.\ tumefaciens}$ren periplasmako begizta ezinbestekoa zela proteinaren kokapen polarra emateko (Kumar eta Das, 2002), baina Walker A domeinuko mutazio batek kokapen hori eragozten zuela. Beraz, badirudi kasu horretan TMDaren presentzia soilik ez zela nahikoa proteina natiboa mintz poloetan kokatzeko.

Bukatzeko ikusi da $Gram^+$ pLS20 plasmidoko T4CPa zelula fase desberdinetan poloetara batu eta ondoren berriro banandu egiten dela (Bauer et al., 2011). Gerta liteke T4SS konplexuaren fase zelularraren menpeko kokapenak konjugazio prozesua erregulatzea, pLS20 plasmidoa soilik hasierako fase esponentzialetan transferitzen baita (Itaya et al., 2006).

1.3.4. ELKARREKINTZA MOLEKULARRAK

T4CPak elkarrekintzen sare konplexua eratzen du bai T4SSko azpiunitateekin zein substratuarekin. Badirudi elkarrekintza hauek dinamikoak direla, konjugazio prozesuan zehar aldatuz, ziur aski seinale desberdinen menpean (Christie, 2016; Redzej et al., 2017). Aurreko ataletan azaldu bezala, T4CPen domeinu bakoitza elkarrekintza desberdinez arduratzen da.

Alde batetik errelaxosomarekiko elkarrekintzak daude, substratu zein proteina laguntzaileekin ematen direnak zitosoleko domeinuaren bidez (ikusi 1.3.2.1. atala). Nahiz eta errelaxasarekin ematen den elkarrekintza espezifikoa izan, proteina laguntzaile edota txaperona molekularrekin ematen direnak indartsuagoak dira (Hamilton et al., 2000; Llosa et

al., 2003; Sastre et al., 1998). Errelaxosomako proteinez gain, hainbat kasutan T4CP eta DNAren arteko elkarrekintzak ere deskribatu dira, bai *in vivo* zein *in vitro*. Elkarrekintza hauek DNAren sekuentziarekiko ez-menpekoak dira (Abajy et al., 2007; Moncalián et al., 1999), baina badirudi *in vivo* DNAren prozesamenduaren eta MOB proteinen aktibitatearen menpekoak direla (Cascales eta Christie, 2004b; Chen et al., 2008). DNAren egiturak, ordea, elkarrekintzaren espezifikotasunean eragina dauka, TrwBΔN70k afinitate handiagoa aurkezten baitu G4-DNA molekulekiko (Matilla et al., 2010). Honetaz gain, ikusi da ATP, ADP eta Mg^{2+} molekulek *in vivo* $TraG_{RP4}$ eta DNArekiko elkarrekintza inhibitzen dutela (Schroder eta Lanka, 2003).

Beste aldetik T4SSarekin elkarrekintzak ematen dira, zitoplasmako zein transmintz domeinuen bidez. T4CPak zitoplasma aldetik energia-zentroa eratzen duten gainerako ATPasekin (VirB4 eta VirB11-motako proteinekin) elkarrekiten du (Llosa eta Alkorta, 2017) eta TMDtik VirB10-motako kanaleko azpiunitatekin (Segura et al., 2013). Azken kasu honetan ikusi da periplasmako begiztak ezinbestekoak direla eta elkarrekintza hau sistemarekiko ez-espezifikoa dela (Gunton et al., 2005; Llosa et al., 2003). T4CPak T4SS heterologoekin elkarrekiteko gai dira, konjugazio eta efektore translokatzaileen arteko sistema kimerikoak eratzeko aukera eskainiz, bioteknologiari dagokionez oso interesgarria izan daitekeena (de Paz et al., 2005). $Gram^{+}$-en konjugazio sistemetan T4CPak kanaleko hainbat azpiunitatekin elkarrekiten dute, baita bakterio $Gram^{-}$-etan ez dauden peptidoglikano hidrolasekin ere (Alvarez-Martinez eta Christie, 2009).

T4BSSekin erlazionaturiko T4CPek substratu talde konplexuagoa aurkezten dute proteina efektoreen garraioa dela eta. $DotL_{L.\ pneumophila}$ren kasuan deskribatu da nola CTDaren bidez DotM, DotN, IcmSW eta LvgA proteina eta konplexuekin elkarrekiten duela. Honek T4CPa egonkortu egiten du substratuen harrerarako prestatuz (Kwak et al., 2017). T4CP hauetan DNA molekulekiko batura ere deskribatu da, nahiz eta soilik proteina efektoreen garraioarekin erlazionaturik egon (Schroder et al., 2002).

1.3.5. FUNTZIOA

T4CPek konjugazio prozesuan zehar dituzten eginkizunak ez daude guztiz adosturik. Egitura ebatzi zenean substratu eta T4SSaren arteko akoplatzailea izateaz gain, motore molekular eta DNA injektore gisa funtzionatzen zutela proposatu zen ere (Gomis-Rüth et al., 2001). Gaur egun lau funtzio posible aldarrikatzen dira: (i) substratuaren harrera T4SSra, (ii) konjugaziorako energi iturria, (iii) seinaleen transferentzia eta (iv) substratuaren translokazioa. Argi dago T4CPak ezinbestekoak direla konjugazioa emateko. Are gehiago, domeinu bakoitzak bere garrantzia dauka eta haien absentzia edota mutazioak konjugazio maiztasunean eragina dauka (Cascales et al., 2013; De Paz et al., 2010; Whitaker et al., 2015). Aldez aurretik azaldu bezala, TMDrik gabeko eta NBD domeinuetako mutanteek ez dira konjugazio prozesua aurrera eramateko gai. Honek TMDaren (kokapenean, erregulazioan, T4SSrekiko elkarrekintzan) eta ATPasa aktibitatearen garrantzia azpimarratzen du (Chen et al., 2008; Gunton et al., 2005; Kumar eta Das, 2002; Lang eta Zechner, 2012; Moncalián et al., 1999). Izan ere frogatu egin da T4CPen ATPasa aktibitatea konjugazioa emateko ezinbestekoa dela (Cascales et al., 2013). Are gehiago, Walker A motiboan burututako mutazioek ATPasa aktibitatea eta ondorioz konjugazioa galarazi egiten dute (Tato et al., 2005). Dena den, gaur egun, ez da ATPasa

aktibitaterik deskribatu T4CP natiboetan, ziur asko *in vivo* ematen den seinaleztapen sare konplexuaren ondorioz, proteina osagarri zein lipidoekin ematen diren elkarrekintzen edota zelula barne zein kanpo seinaleen bidez burutzen dena (Cascales et al., 2013).

Prozesu konjugatiboaren urrats desberdinak aldez aurretik azaldu direnez (ikusi 1.2.4. atala), atal honetan substratuen transferentzian T4CPen ezinbesteko funtzioak soilik azpimarratuko dira. Alde batetik, frogatu da T4CPen ATPasa aktibitatea ezinbestekoa dela errelaxasaren transferentziarako, DNAren garraio ezan (Draper et al., 2005; De Paz et al., 2010). Beste aldetik, TrIP saiakeraren bidez frogatu da T4CPa ssDNA substratuarekin elkarrekiten duen lehenengo proteina dela, substratua VirB11-motako proteinara igaroz jarraian (Cascales eta Christie, 2004b).

Azkenengoz, T4CPek, DNA translokatzen duten beste proteinekin duten homologia estrukturala kontutan hartuz, ssDNA ponpatzen duten motor gisa jarduten dutela iradoki da. Garraio hau ICHtik zehar burutuko lirateke haien ATPasa jardueratik lortutako energia erabiliz (Cabezon eta de la Cruz, 2006). Hala ere, ICHaren azterketan ez dira garraio honetarako aminoazido gakorik identifikatu (Larrea et al., 2017).

1.4. IKERGAI SISTEMAK: R388, pKM101, pIP501 ETA ClоDF13

Tesi honen helburuetako bat jatorri desberdinetako T4CPen azterketa burutzea da. Horretarako R388, pKM101, pIP501 eta CloDF13 sistemak aukeratu ziren.

1.4.1. R388

R388 33 kilobasetako (kb) plasmido konjugatiboa da, IncW bateraezintasun taldearen barruan sailkaturik dagoena, non plasmido konjugatibo txikienak aurkitzen diren. *E. coli*-ren andui klinikoetan aurkitua izan arren (Datta eta Hedges, 1972) bakterio Gram$^-$-en ostalari sorta zabal batera transmititu ahal da. 1988. urtean genetikoki karakterizatua izan zen (Avila eta de la Cruz, 1988) eta handik aurrera bere transferentzia eskualdeko (TRA_W) funtzionamendu, osagai eta ezaugarriak sakonki ikertuak izan dira (Arechaga et al., 2008; Fernández-González et al., 2011, 2016; García-Cazorla et al., 2018; González-Prieto et al., 2017; Guynet et al., 2011; Machon et al., 2002; Yanagida et al., 2016). Plasmido konjugatibo bat izanik, transferentzia genetan MOB_W eta MPF_W taldeak bereizten dira. MOB_W barnean *oriT,* $TrwC_{R388}$ errelaxasa, $TrwA_{R388}$ proteina laguntzailea eta $TrwB_{R388}$ T4CPa kodeturik daude. MPF_Wn T4SSa eratzen duten VirB proteinen homologoez gain (TrwD → TrwN proteinak) *eex* gainazalaren bazterketaz arduratzen den genea eta *korA*, *korB* y *orf34* gene erregulatzaileak daude (Bolland et al., 1990; de Paz et al., 2005).

$TrwB_{R388}$ plasmido honen T4CPa da, aurretik aipatu bezala T4CPen prototipotzat hartzen dena. 507 aminoazido eta 56,3 kDa-eko VirD4-motako MPa da. Aurreko ataletan azaldu bezala, egitura zein funtzio aldetik oso aztertua izan da, batez ere mutante solugarri eta proteina natiboaren ikerketa konparatiboen bidez (Cabezón et al., 1997; Gomis-Rüth et al., 2001; Hormaeche et al., 2002, 2004, 2006; Larrea et al., 2013; Llosa et al., 2003; Moncalián et al., 1999; de Paz et al., 2010; Segura et al., 2014, 2013; Tato et al., 2005, 2007; Vecino et al.,

2010, 2011, 2012). Modu honetan T4CPen aktibitatearen erregulazioan TMDaren garrantzia aldarrikatu da (1.6. irudia). Hala ere, proteina familia honetan dagoen heterogeneotasunaren ondorioz, oso arriskutsua izango lirateke $TrwB_{R388}$ prototipoan deskribaturiko ezaugarriak gainerako T4CPei esleitzea. Hori dela eta beste sistemetako proteinekin antzeko azterketak burutu behar dira, ezaugarri unibertsalen ebazpena burutzeko.

1.4.2. pKM101

pKM101 35,4 kb-tako eta IncN bateraezintasun taldeko plasmidoa da, K. Mortelmans-ek isolatu zuen Stocker laborategian hirurogeita hamarreko hamarkadan (Mortelmans eta Stocker, 1979). pKM101 delezio bidez R46 plasmidotik eratorria izan zen, erresistentzien transferentzia faktore gisa deskribaturik zegoena. Izan ere, jatorrizko R46 plasmidoak anpizilina, estreptomizina, sulfonamida eta tetraziklina antibiotikoen aurkako erresistentzia geneak kodetzen ditu. pKM101ren organizazio funtzionalaren azterketa Walker-en laborategian burutu zen, konjugazio sisteman sakonduz (Langer et al., 1981; Winans eta Walker, 1985). Lan horietan oinarrituz *tra* eskualdearen azterketak egin ziren, MOB geneek antzekotasun handia aurkezten zutela R388 plasmidoko geneekin ikusiz (Paterson et al., 1999; Pohlman et al., 1994).

pKM101 plasmidoko konjugazio sistema literaturan zehar oso ikertua izan da, bai egitura zein funtzioaren arloan (Casu et al., 2016, 2017, 2018; Durand et al., 2011; Fronzes et al., 2009; González-Rivera et al., 2019; Whitaker et al., 2016). $TraJ_{pKM101}$ plasmido honen T4CPa da, VirD4-motako MPa, 509 aminoazido eta 57,76 kDa-eko pisu molekularra izanik. Ikerketa filogenetikoen bidez ikusi da $TrwB_{R388}$tik filogenetikoki hurbilen aurkitzen den proteina dela (Alvarez-Martinez eta Christie, 2009) eta horregatik tesi honetarako aukeratua izan zen. Izan ere, ikusi zen pKM101 eta R388ren T4SSak sistema heterologoaren T4CParekin elkarrekiteko gai zirela (Llosa et al., 2003).

1.4.3. pIP501

pIP501 plasmidoa *Streptococcus agalactiae*-n andui kliniko batean aurkitua izan zen lehenengo aldiz (Horodniceanu et al., 1976). 30 kb dauzka eta kloranfenikol eta eritromizina antibiotikoen aurreko erresistentziarako geneak kodetzen ditu. Inc18 bateraezintasun taldearen barnean sailkatzen da, ostalari $Gram^-$ zein $Gram^+$ talde zabal batera transferitzeko gaitasuna izanik (Grohmann et al., 2017). Bere transferentzia eskualdearen inguruan azterketa desberdinak burutu egin dira, 15 transferentzia gene identifikatuz errelaxasaren bidezko erregulazioz adierazten direnak (Kurenbach et al., 2002, 2003, 2006; Wang eta Macrina, 1995). Proteina hauen banakako ikerketez gain (Arends et al., 2013; Fercher et al., 2016; Goessweiner-Mohr et al., 2014a, 2014b; Grohmann et al., 2016; Kohler et al., 2018) haien arteko elkarrekintzen mapa burutu egin da ere (Abajy et al., 2007). Aipatu beharra dago proteina hauen izena aldatu egin zela; jatorriz Orf1 → Orf15 taldea izanik, gaur egun TraA → TraO moduan izendatzen dira.

$TraJ_{pIP501}$ (lehen $Orf10_{pIP501}$) pIP501 sistemako T4CPa da, 559 aminoazido eta 64,1 kDa-eko pisu molekularrarekin. TMDrik gabeko T4CP solugarrien talde urriaren barruan sartzen da, T4CPen arteko ikerketa konparatiborako oso interesgarria bihurtzen duena. Badirudi proteina

honek bere funtzioa burutzeko mintzeko $TraI_{pIP501}$ (lehen $Orf9_{pIP501}$) proteinarekin elkarrekiten duela, VirD4-motako T4CPen antzeko egitura bat sortuz (Grohmann et al., 2016). Dena den, legamiaren hibrido bikoitzeko sistemaren bidez $TraJ_{pIP501}$ren elkarrekintzak soilik $TraA_{pIP501}$ (errelaxasa), $TraF_{pIP501}$ (mintzeko proteina) eta $TraG_{pIP501}$ (peptidoglikano hidrolasa) proteinekin deskribatu ziren (Abajy et al., 2007), baina ez $TraI_{pIP501}$rekin.

1.4.4. CloDF13

Aurretik aurkeztutako sistemak ez bezala, CloDF13 plasmido mugikorra da, hau da, ez du sekrezio kanalik kodetzen eta beraz bakterio berean aurkitzen den plasmido konjugatibo baten beharra dauka transferitua izateko. *Enterobacter cloacae* bakterioen jatorrizko 9,9 kb-tako plasmidoa da 70eko hamarkadan isolatu zena (Veltkamp eta Nijkamp, 1973), nahiz eta bere sekuentzia 1986. urtera arte ez ebatzi (Nijkamp et al., 1986). Plasmido hau oso ikertua izan zen bere izaera bakteriozinogenikoaren ondorioz (van den Elzen et al., 1980; Luirink et al., 1986; Oudega et al., 1982; Van Tiel-Menkvled et al., 1979), baina baita bere izaera mugikorragatik ere (Cabezón et al., 1997; Christie et al., 2005; Escudero et al., 2003; Lang et al., 2014). Transferentzia eskualdeak plasmido osoaren %30a inguru hartzen du, mugikortasunarekin erlazionaturiko bi proteina kodetuz, B eta C proteinak (van Putten et al., 1987). Aurrerago bi proteina hauek $MobB_{CloDF13}$ eta $MobC_{CloDF13}$ gisa izendatuak izan ziren, hurrenez hurren (Núñez eta de La Cruz, 2001). $MobC_{CloDF13}$k 243 aminoazido ditu eta errelaxasen funtzioak betetzen ditu, nahiz eta haiekin sekuentzia antzekotasunik ez izan.

$MobB_{CloDF13}$ sistema honen T4CPa da. Aurretik azaldu bezala, plasmido mugikor gehienek ez dute T4CPrik eta konjugazio sistema egoiliarrarena erabiltzen dute. Honek $MobB_{CloDF13}$ ikerketa xede interesgarria bihurtzen du. Proteina hau 653 aminoazidoz eraturik dago, 73,8 kDa-eko pisu molekularra eta iragarritako hiru transmintz helize izanik. Are gehiago, T4CP berezi bat da *in vivo oriT* sekuentziaren mozketarako beharrezkoa delako, gainerako sistemetan gertatzen ez den moduan, non soilik errelaxasek hartzen duten parte. Transferentzia eskualdeko bi proteinen berezitasunen ondorioz CloDF13 elementu mugikorren beste klase berri bat izatea proposatu zen (Núñez eta De La Cruz, 2001).

1.5. IKERKETA HONEN GARRANTZIA

Sarrera honetan T4CPek konjugazio prozesuan daukaten garrantzia azpimarratu egin da, substratu zein kanalarekin burutzen dituzten elkarrekintzengatik. Ala ere, nahiz eta konjugazioan ezinbesteko proteinak izan, haien funtzio eta paperaren inguruan galdera ugari geratzen dira erantzun gabe; ziur asko haien MP izaera dela eta, ikerketak burutzea eragozten duena.

Tesi lan honetan galdera horietako batzuei erantzuna eman nahi zaie, T4CPen azterketa biokimiko eta biofisikoak burutuz. Guzti hau T4CP familia hobeto ezagutzearen helburuarekin. T4CP desberdinen ikerketaren bidez haien arteko ezaugarri komunak ezagutu daitezke, honetan oinarrituz haien funtzio biologikoa kontrolatu ahal izateko. Behin hau lortuta, bakterioen arteko ARGen hedapena balaztatu ahalko zen MDR bakterioek gizartean sortzen duten arazo larriari konponbide berri bat eskainiz.

HELBURUAK

HELBURUAK

HELBURU OROKORRAK

1. Jatorri desberdineko proteina akoplatzaileen transmintz domeinuaren papera aztertzea.
2. VirD4-motako proteina akoplatzaile azpifamiliarekin deskribaturiko ezaugarriak proteina akoplatzaileen familia osoari egokitzen diren aztertzea.

HELBURU ESPEZIFIKOAK

1. Jatorri desberdineko proteina akoplatzaile eta transmintz domeinuarekin erlazionaturiko mutanteen lorpena biologia molekularreko tekniken bidez.
2. Lortutako proteina akoplatzaile mutante eta kimera sortaren *in vivo* funtzionalitatearen azterketa konjugazio entseguen bidez.
3. Kokapen azpizelularrean jatorri desberdineko proteina akoplatzaileen transmintz domeinuaren eraginaren azterketa mikroskopia konfokala erabiliz.
4. Lortutako proteina akoplatzaile mutante eta kimera sortaren *in vitro* karakterizazioa, haien egonkortasuna, egitura, oligomerizatzeko joera, DNArekiko elkarrekintza eta ATParen hidrolisi aktibitatea aztertuz.
5. Molekula-bakarreko tekniken bidez proteina akoplatzaileen azterketa burutzeko protokoloen ebazpena.

2. KAPITULUA:

MATERIAL ETA TEKNIKA ESPERIMENTALAK

2. MATERIAL ETA TEKNIKA ESPERIMENTALAK

Atal honetan aurkeztutako proteina guztiek (TrwBΔN70k izan ezik) sei edota zortzi histidinako katea aurkezten dute C-muturrean, nomenklatura errazteagatik proteinen izendapenean adierazi ez dena. Halaber, TraJ proteina azpi-indizerik gabe aurkezten denean pKM101 plasmidoko T4CPari dagokio, pIP501 plasmidoko T4CPari dagokionean $TraJ_{pIP501}$ moduan adierazten den heinean. eGFP fusio-proteina guztiak GFP gisa izendatu dira nomenklatura errazteagatik.

Tesi honetan erabilitako material, erreaktibo eta aparatu guztiak eranskineko A.1. taulan laburbilduta agertzen dira, etxe komertzialen arabera sailkatuak. Era berean indargetzaileak eta disoluzio guztiak eranskineko A.2. taulan laburbilduta daude.

2.1. ERABILITAKO ANDUI ETA PLASMIDOAK ETA HAIEN BILTEGIRATZEA

Erabilitako *E. coli* andui eta plasmidoak 2.1. eta 2.2. tauletan laburbildurik agertzen dira, hurrenez hurren. Andui desberdinak hazteko erabili ziren antibiotiko kontzentrazioak 2.3. taulan aurkezten dira.

2.1. taula. Erabilitako *E. coli* anduiak.

Anduia	Ezaugarriak	Erreferentzia
BL21(DE3)	*F^+ hsds gal (DE3)*	Studier eta Moffatt (1986)
BL21C41(DE3)	*F^+ hsds gal (DE3)*	Miroux eta Walker (1996)
DH5α	*F^- supE44 DlacU169(f80lacZDM15) hsdR17 recA1 endA1 gyrA96 thi-1 relA1*	Grant et al. (1990)
JM109	*RecA1 endA1 gyrA96 thi relA1 hsdR17supE44 Δ(lac-proAB) F´(traD36 proAB $lacI^q$ lacZ ΔM15)*	Yanisch-Perron et al. (1985)
Lemo21(DE3)	*fhua2 (lon) ompT gal (λ DE3) (dcm) ΔhsdS/ pLemo(CamR)* *λ DE3 = λ sBamHlo ΔEcoRI-B int::(lacI::PlacUV5::T7 gene1) i21 Δnin5* *pLemo =* pACYC184-*PRHABAD-LYSY*	Wagner et al. (2008)
OmniMAX™2	*F' {proAB$^+$ $lacI^q$ lacZΔM15 Tn10(Tet^R) Δ(ccdAB)} mcrA Δ(mrr-hsdRMS-mcrBC) φ80(lacZ)ΔM15 Δ(lacZYA-argF) U169 endA1 recA1 supE44 thi-1 gyrA96 relA1 tonA panD*	Invitrogen
Rosseta™ (DE3) pLysS	F^- *ompT* $hsdS_B(r_B^- m_B^-)$ *gal dcm* (DE3) pLysSRARE (Cam^R)	Novagen
UB1637	*F^- lys his trp rpsL recA56*	de la Cruz eta Grinsted, (1982)

2.2. taula. Erabilitako plasmidoak.

Plasmidoa	Deskribapena	Fenotipoa	Erreferentzia
pET22b(+)	Gain-adierazpenerako bektorea	Amp^R	Novagen
pET24a(+)	Gain-adierazpenerako bektorea	Kan^R	Novagen
pIP501	Plasmido naturala	Chl^R, MLS^R, Inc18	Evans eta Macrina (1983)
pKM101	Plasmido naturala	Amp^R, TRA_N, IncN	Langer eta Walker (1981)
pKM101Δ*traJ*	pKM101::Δ*traJ*	Amp^R, TRA_N, IncN, $TraJ^-$	Lan hau
pKM101Spc^r_Δ*traJ*	pKM101::Δ*traJ* eta Spt^R erresistentzia kassetearekin	Spt^R, TRA_N, IncN, $TraJ^-$	Whitaker et al. (2016)
pQTEV-*orf10*	pQTEV:: $traJ_{pIP501}$	Amp^R, $TraJ_{pIP501}$-TEV-H_7 T5 promotorearen menpean	Abajy et al. (2007)
pSU1456	R388::Δ*trwB*	Su^R, Tmp^R, TRA_W, IncW, $TrwB^-$	Llosa et al. (1994)
pSU1547	pET22b(+)::*trwA*	Amp^R, TrwA-H_6 T7 promotorearen menpean	Moncalián eta de la Cruz, (2004)
pSU4637	pET3a´::*trwBΔN70*	Amp^R, Rep (pMB8), TrwBΔN70 T7 promotorearen menpean	Cabezón (1996)
pSU4814	pSU19::$mob_{CloDF13}$	Chl^R, Rep (p15A), MOB (CloDF13)	Núñez eta De La Cruz (2001)
pSU4833	pSU4814::Δ*mobB*	Chl^R, Rep (p15A), $MobB^-$	Núñez eta De La Cruz (2001)
pUB3	pET22b(+)::*trwB*	Amp^R, TrwB-H_6 T7 promotorearen menpean	Hormaeche et al. (2004)
pUB48	pET22b(+)::$traJ_{pIP501}$	Amp^R, TraJ-H_6 T7 promotorearen menpean	Lan hau
pUB49	pET24a(+)::*mobC*	Kan^R, $MobC_{CloDF13}$-H_6 T7 promotorearen menpean	Lan hau
pUB7	pET22b(+)::*trwBTMD*	Amp^R, TMD_{TrwB}-H_6 T7 promotorearen menpean	Segura et al. (2014)
pUB9	pWaldo-GFPe::*trwB-GFP*	Kan^R, TrwB-TEV-GFP-H_8 T7 promotorearen menpean	Segura et al. (2014)
pUBQ1	pET22b(+)::*traJTMD-TEV-trwBCD*	Amp^R, TMD_{TraJ}-TEV-CD_{TrwB}-H_6 T7 promotorearen menpean	Lan hau

pUBQ2	pET24a(+)::*traJTMD-TEV-trwBCD*	Kan^R, TMD_{TraJ}-TEV-CD_{TrwB}-H_6 T7 promotorearen menpean	Lan hau
pUBQ3	pET22b(+)::*trwBTMD-traJ*$_{P501}$	Amp^R, $TMD_{TrwB}TraJ_{pIP501}$-H_6 T7 promotorearen menpean	Lan hau
pUBQ4	pET24a(+)::*traJTMD-trwBCD*	Kan^R, $TMD_{TraJ}CD_{TrwB}$-H_6 T7 promotorearen menpean	Lan hau
pUBQ4GFP	pWaldo-GFPe::*traJTMD-trwBCD-GFP*	Kan^R, $TMD_{TraJ}CD_{TrwB}$-TEV-GFP-H_8 T7 promotorearen menpean	Lan hau
pUBQ4(K142T)	pET24a(+)::*traJTMD-trwBCD(K142T)*	Kan^R, $TMD_{TraJ}CD_{TrwB}$-H_6 K142T mutazioarekin CD_{TrwB} domeinuan T7 promotorearen menpean	Lan hau
pUBQ5	pET22b(+)::*traI*$_{pIP501}$-*traJ*$_{pIP501}$	Amp^R, $TraI_{pIP501}TraJ_{pIP501}$-$H_6$ T7 promotorearen menpean	Lan hau
R388	Plasmido naturala	Tmp^R, TRA_W, IncW	Datta eta Hedges (1972)

2.3. taula. Erabilitako antibiotikoak. 2.1. eta 2.2. tauletan bakterio andui eta plasmido bakoitzak kodetzen dituzten antibiotikoen aurkako erresistentziak adierazten dira. Honen arabera, bakterio desberdinak hazteko Luria Bertani (LB) kultibo eta LB-agar plakei antibiotiko egokiak gehitu zitzaizkien, taula honetan adierazitako kontzentrazioak erabiliz. Antibiotikoen laburdurak *American Society for Microbiology*-k ezarritakoak dira.

Antibiotikoa	Laburdura	Kontzentrazioa (µg/mL)
Anpizilina	Amp	100
Espektomizina	Spt	50
Estreptomizina	Str	50
Kanamizina	Kan	50
Karbenizilina	Car	50
Kloranfenikola	Chl	12,5-25
Nalidixikoa	Nal	30
Trimetoprima	Tmp	10

DNA plasmidikoaren laginak 4°C eta -20°C-tan biltegiratu ziren. Horretaz gain, haiekin *E. coli* DH5α zelulak transformatu egin ziren gordekin iraunkorrak izateko. Bakterio andui desberdinak gordetzeko, zelulak 2 mL LBn hazi ziren gau osoan zehar 37°C-tan, antibiotiko egokia gehituz. Lortutako kultibo asetik 800 µL hartu eta %80 (b/b) glizerol 800 µL-rekin nahastu ziren. Lortutako bakterio esekidurak -80°C-tan gorde ziren.

2.2. BIOLOGIA MOLEKULARRA

Biologia molekularrak intereseko proteina kodetzen duen genearen isolatzea, anplifikazioa, eta aldaketa egitea ahalbidetzen du. Lan honetan biologia molekularreko teknika klasikoak erabili dira (Sambrook and Russell, 2001), bai itu-proteinak kodetzen dituzten sekuentziak gain-adierazpen bektoreetan klonatzeko, baita proteina hauen mutante desberdinak (adibidez, delezio mutanteak eta mutante puntualak), zein kimerak lortzeko. Horretaz gain, murrizte-entzimak erabili dira pKM101Spc^r_Δ*traJ* bektoreak kodetzen duen antibiotikoaren aurkako erresistentzia aldatzeko.

2.2.1. DNAren ANPLIFIKAZIOA ETA KLONAKETA

Intereseko DNA klonatzeko zenbait pausu jarraitu behar dira: (i) DNA moldearen lorpena; (ii) polimerasaren kate-erreakzio (*Polymerase Chain Reaction*, PCR) bidezko DNA zatikiaren anplifikazioa, murrizte-entzimak ezagutzen dituzten itu sekuentziak gehituz; (iii) lortutako DNA eta bektorearen murrizte-entzimen bidezko liseriketa; (iv) DNA zatikiaren eta bektorearen arteko ligazioa; (v) *E. coli* andui konpetenteen transformazioa; eta (vi) bektorean txertatutako DNA zatikiaren presentziaren baieztapena sekuentziazioaren bidez.

2.2.1.1. DNA PLASMIDIKOAREN ISOLAKETA

PCR bat burutzeko, lehenengo eta behin anplifikatu nahi den DNAren moldea behar da. Tesi honetan *E. coli* DH5α anduietan biltegiratutako plasmidoak erabili dira molde gisa, pIP501 plasmidoa izan ezik, *E. faecalis*-en biltegiratzen dena. DNA plasmidikoaren isolatze azkarra burutzeko kit komertzialak erabili dira, hain zuzen ere *QIAGEN Plasmid Kits*, *NucleoBond® Xtra Midi* eta *NucleoSpin® Plasmid*. Purutasun altuko DNA kantitate handiak lortzeko Midi-prestaketak burutu ziren eta gainontzeko kasuetan Mini-prestaketak, beti etxe komertzialek eskainitako protokoloak jarraituz. DNA plasmidikoaren isolaketa erabili da bai PCRentzat DNA moldea lortzeko, baita klonaketaren azken pausuko transformanteetatik bektoreak isolatzeko ere.

pIP501 plasmidoa erauzteko, ordea, *E. faecalis* JH2-2 anduia erabili zen. Horretarako, zelula hauen kultibo ase baten 100 µL zentrifugatu ziren (12.100 *g*, 1 min). Jalkina 20 µL *E. faecalis lisi indargetzailearekin* berreseki eta 20 minutuz 95°C-tan inkubatu zen. Bukatzeko, lortutako laginari 180 µL Milli-Q ur gehitu zitzaizkion.

2.2.1.2. POLIMERASAREN KATE-ERREAKZIOA

PCR teknika alboetan bi sekuentzia jakin dituen itu DNAren anplifikazioa burutzeko erabiltzen da. Lehenengo eta behin hasleak diseinatu behar dira anplifikatu nahi den itu sekuentziaren muturrekin hibridatzeko eta bide-batez itu DNAn bektorean ligatzeko beharrezkoak diren murrizte gune egokiak sortzeko. Lan honetan erabilitako hasleak *Eurofins Genomics*-en (Eurofins Scientific, Brusela, Belgika) erosi ziren eta 2.4. taulan laburbildurik agertzen dira.

2.4. taula. PCR erreakzioetan erabilitako hasleak. Lehenengo zutabeak anplifikatutako DNA (genea edo gene zatia) adierazten du eta bigarrenak lortutako anplikoia zein konstrukto lortzeko erabili zen. F eta R *forward* eta *reverse* hasleak dira, hurrenez hurren. Haslearen sekuentzian etra lodiz nabarmenduriko nukleotidoak, azken zutabeko murrizte-entzimek ezagutzen dituzten itu sekuentziak dira, jatorrizko DNA zatiari gehitu zaizkionak.

Anplifikatutako produktua	Mutantea	Haslea (5' → 3')	Murrizte-entzima
***mobC*$_{CloDF13}$**	*mobC*$_{CloDF13}$	F1: GACA**CATATG**GCACTGGAGCGATAC	*Nde*I
		R1: GTCA**CTCGAG**CTCCGTTGTCATAAA	*Xho*I
***traI*$_{pIP501}$**	*traI*$_{pIP501}$-*traJ*$_{pIP501}$	F2: GTGCA**CATATG**GCGAAGAAGAAGCAAG	*Nde*I
		R2: GAAT**GGATCC**GTCATTTTTCCCCCTC	*Bam*HI
***traJ*$_{pIP501}$**	*trwBTMD-traJ*$_{pIP501}$	F3: CCGCCG**CTCGAG**ACTAGTTTATTAGCAGAA	*Xho*I
		R3: GGTTC**CTCGAG**AAATGGTAATTCGCTGTT	*Xho*I
	traI$_{pIP501}$-*traJ*$_{pIP501}$	F4: CGGC**GGATCC**ACTAGTTTATTAGCA	*Bam*HI
	traJ$_{pIP501}$	F5: GCCG**CATATG**ACTAGTTTATTAGCAG	*Nde*I
	traJ$_{pIP501}$ eta *traI*$_{pIP501}$-*traJ*$_{pIP501}$	R4/5: CACT**CTCGAG**AAATGGTAATTCGCT	*Xho*I
traJTMD	*traJTMD-TEV-trwBCD*	F6: GGAATTC**CATATG**GACGATAGAGAAAGAGGC	*Nde*I
		R6: TCC**CCCGGG**ACCCTGAAAATACAAATTCTCACG ATAAATCTTTTTGAATCTTTCG	*Ava*I
traJTMD-trwBCD	*traJTMD-trwBCD-GFP*	F7: CCG**CTCGAG**ATGGACGATAGAGAAAGAGG	*Xho*I
		R7: CGC**GGATCC**GATAGTCCCCTCAAC	*Bam*HI
trwBCD	*traJTMD-TEV-trwBCD*	F8: TCC**CCCGGG**TTGAATAGCGTCGGACAAGGC	*Ava*I
		R8: CCTTGG**CAATTG**GCCGATTAC	*Mfe*I

PCR erreakzioetan *PfuTurbo* DNA polimerasa erabili zen, etxe komertzialaren aholkuak jarraituz. Erreakzioak *Pfu reaction buffer*-ean burutu ziren bolumena 25 µL-ra doituz eta osagaien ondoko kontzentrazioak erabiliz: 2 ng/µL DNA molde, 0,8 mM dNTP nahasketa, 2,5 ng/µL hasle bakoitzeko, eta 0,05 U *PfuTurbo* DNA polimerasa. PCRak *C1000TM Thermal Cycler* batean egin ziren 2.5. taulan agertzen diren baldintzak erabiliz erreakzio bakoitzerako. Kasu guztietan hasierako desnaturalizazio bat burutu zen (45 seg, 95°C-tan) eta bukaerako luzapen bat (10 min, 72°C-tan). Tartean hiru pausu errepikatu ziren ziklo kopuru desberdinetan, PCR protokoloaren arabera (2.5. taula): 1. Desnaturalizazioa, 2. Hasleen parekaketa, 3. Luzapena.

2.5. taula. PCR erreakzioetan erabilitako zikloen protokoloa. Lehenengo, bigarren eta hirugarren zutabeek anplifikatutako genea, molde gisa erabilitako DNA plasmidikoa eta hasle bikotea adierazten dute, hurrenez hurren. Zenbakidun zutabeek protokoloaren pausuak adierazten dituzte: 1. Desnaturalizazioa. 2. Hasleen parekaketa. 3. Luzapena. Hiru pausu hauek azken zutabeak adierazitako alditan errepikatu ziren.

Anplifikatutako produktua	DNA moldea	Hasle bikotea	1	2	3	Ziklo kopurua
mobC	pSU4814	F1, R1	94°C, 45 seg	58°C, 45 seg	72°C, 80 seg	27
$traI_{pIP501}$	pIP501	F2, R2	95°C, 45 seg	60°C, 45 seg	72°C, 60 seg	30
$traJ_{pIP501}$	pIP501	F3, R3	95°C, 45 seg	60°C, 90 seg	72°C, 90 seg	30
$traJ_{pIP501}$	pIP501	F4, R4	95°C, 45 seg	56°C, 45 seg	72°C, 120 seg	35
$traJ_{pIP501}$	pIP501	F5, R5	95°C, 45 seg	56°C, 45 seg	72°C, 120 seg	35
traJTMD	pKM101	F6, R6	95°C, 60 seg	64°C, 60 seg	72°C, 120 seg	30
traJTMD-trwBCD	pUBQ4	F7, R7	98°C, 10 seg	66°C, 30 seg	72°C, 60 seg	25
trwBCD	pUB3	F8, R8	94°C, 20 seg	95°C, 30 seg	72°C, 60 seg	21

PCRtik lortutako anplikoiak %1 (p/b) agarosazko gel elektroforesi bidez aztertu ziren, *TAE indargetzailea* eta *Sybr™ Safe* tindatzailea erabiliz. Tamaina egokia zutela ziurtatzeko *1 kb Plus DNA ladder* pisu molekularreko patroia erabili zen. Gelen bistaratzea *Gel Doc™ EZ Imager* batean burutu zen. Banda ez-espezifikoak agertu zirenean, anplikoiak geletik purifikatu ziren, gainontzeko kasuetan PCR laginaren garbiketa zuzena burutu zen heinean. Horretarako *Gel/PCR extraction kit* edota *NucleoSpin® Gel and PCR Clean-up* kit komertzialak erabili ziren. Lortutako DNAren kontzentrazioa eta purutasuna ezagutzeko *NanoDrop™ Lite Spectophotometer* bat erabili zen, 230 eta 260 nm-tako absorbantzia neurtuz.

2.2.1.3. LISERIKETA ETA LIGAZIOA

Klonaketa burutzeko anplikoia eta bektorea murrizte-entzima egokiekin liseritu ziren, elkarren artean ligatu ahal diren mutur itsaskorrak lortuz. Aurreko atalean esan bezala, PCR hasleen bidez anplikoien muturretan murrizte-entzimak ezagutzen dituzten itu sekuentzia egokiak gehitu ziren. Erreakzioak entzimen etxe komertzialen argibideak jarraituz burutu ziren. Bektore hutsen ligazioa ekiditeko (adibidez, murrizte-entzima bakar batek soilik erabili zen kasuetan), bektoreen laginak *Shrimp Alcaline Phosphatase*-rekin tratatu ziren murrizte-entzimen tratamenduaren ostean. Ondoren, lagin guztiak 65°C-tan 20 minutuz inkubatu ziren, laginetan zeuden entzimak inaktibatzeko. Liseritutako produktuak agarosazko gel elektroforesi bidez purifikatu ziren, aurreko atalean azaldu bezala. Jarraian, anplikoia eta bektorea T4 DNA ligasa entzimaren bidez ligatu ziren. Erreakzioak 4:15 (mol:mol) bektore:anplikoi erlazioan burutu ziren etxe komertzialak eskainitako protokoloa jarraituz. Ligazioaren ostean, entzima 20 minutuz 65°C-tan inkubatuz inaktibatu zen.

2.2.1.4. TRANSFORMAZIOA

Bakterioek beste bakterioetatik edota ingurunetik DNA molekulak barneratzeko zenbait mekanismo aurkezten dituzte, hauetako bat transformazioa izanik. Mekanismo honetan oinarrituz, posible da itu plasmidoa bakterioetan barneratzea *in vitro* prozesu baten bidez. Transformazioa burutzeko, errendimendu desberdina duten bi teknika erabili egin dira. Alde batetik $CaCl_2$-an oinarritutako metodo kimikoa (Cohen et al., 1972) eta bestaldetik elektroporazioa, aurrekoa baino 50 aldiz eraginkorragoa dena (Dower et al., 1988). Transformazioa burutzeko *E. coli* zelulak konpetente (hau da, iragazkorrak) bihurtu behar dira, lehenengo kasuan kimiokonpetenteak ($CaCl_2$-aren bidez) eta bigarrenean elektrokonpetenteak (pultsu elektriko baten bidez), hurrenez hurren.

BAKTERIOEN PRESTAKETA

Bakterio **kimiokonpetenteen** prestaketarako -80°C-tan biltegiratutako zelula gordekina abiapuntu moduan erabiliz, bakterioak antibiotiko gabeko LB-agar petri plaka batean hazi ziren gau osoan zehar 37°C-tan. Plaka horretan hazitako kolonia bat aukeratu eta antibiotiko gabeko LBn (10 mL) hazi zen baldintza berdinetan. Hurrengo egunean 1:100 diluzioa burutu zen (3 mL kultibo 300 mL LBn), bakterioak 37°C-tan hazten utziz 600 nm-tan dentsitate optikoaren balioa (OD_{600}) 0,4-koa izan arte. Pausu honetatik aurrera protokolo guztia 4°C-tan burutu zen. Bakterio zelulak 50 mL-ko 6 *falcon* hodietan banandu ziren eta ondoren 5 minutuz 4°C-tan utzi ziren. Jarraian hodiak zentrifugatu (3.260 *g*, 10 min), gain-jalkina deuseztatu eta hodi bakoitzeko jalkina 5 mL 100 mM $CaCl_2$-rekin berreseki zen, ondoren bolumena 50 mL-ra doituz. Suspentsioak berriz baldintza berdinetan zentrifugatu eta berreseki ziren 5 mL 100 mM $CaCl_2$ erabiliz, baina kasu honetan hiru hoditako suspentsioak *falcon* bakarrean elkartu ziren, bakoitzean bolumena 50 mL-ra doituz (guztira 100 mL suspentsio izanez). Zelulak berriz zentrifugatu ziren aurreko baldintzetan eta prozesua errepikatu zen, bi hodietako jalkinak *falcon* bakarrean elkartuz, bolumena 50 mL-ra doituz eta berriz zentrifugatuz modu berean. Gain-jalkina deuseztatu eta bakterioak 5 mL 100 mM $CaCl_2$/glizerola %15 (b/b) disoluzioarekin berreseki ziren, berriz zentrifugatuz. Azkenik jalkina soluzio beraren 500-2.000 µL-rekin berreseki zen eta hortik 50 µL-tako alikuotak egin ziren. Bakterio esekidura hauek nitrogeno likido bidez izoztu eta -80 °C-tan gorde ziren transformazioak egiteko erabili arte.

Zelula **elektrokonpetenteak** prestatzeko protokolo bera jarraitu zen, baina $CaCl_2$-a ur destilatuarekin ordezkatuz. Izan ere, zelulak konpetenteak bihurtuko dituen pultsu elektrikoa eman ahal izateko esekiduran ezin da gatzik egon.

$CaCl_2$ BIDEZKO TRANSFORMAZIOA

Izozturiko zelula kimiokonpetenteak transformatzeko orduan lehenengo eta behin bakterioak izotzetan desizoztu eta ligazio produktuekin nahastu ziren, izotzetan 30 minutuz inkubatuz. Ostean, laginei 42°C-tan 45 segundoko talka termiko bat eman zitzaien. Zelula esekidura berriz izotzetan 2 minutuz mantendu ondoren, giro-tenperaturan izandako 300 µL LB esterilarekin nahastu eta 37°C-tan 45 minutuz inkubatu zen. Azkenik, zelulak zentrifugatu ziren (6.000 *g*, 2 min), gain-jalkinetik 200 µL deuseztatuz eta jalkina gainontzeko bolumenean

berresekiz. Lortutako laginak antibiotiko egokidun LB-agar petri plaketan erein ziren eta gau osoan zehar 37°C-tan inkubatu ziren.

Transformazio batetik lortutako kolonia bat **bigarren plasmido batekin transformatzeko**, lehenengo eta behin, kolonia horretako bakterioak (plasmido bat jada bazutenak) konpetente bihurtu ziren. Horretarako kolonia gau osoan zehar 37°C-tan hazi zen antibiotiko egokidun 10 mL LBn. Hurrengo goizean, kultiboak diluitu ziren 1:20 erlazioan (500 µL kultibo 10 mL LBn) eta 37°C-tan hazi ziren. Zelula esekiduraren OD_{700} 0,3 lortutakoan 2 mL kultibo hartu eta zentrifugatu ziren (4.200 *g*, 1 min). Lortutako jalkina aldez aurretik hoztutako 1 mL 100 mM $CaCl_2$-rekin berreseki eta izotzetan 30 minutuz mantendu zen. Lagina berriz zentrifugatu (3.300 *g*, 1 min, 4°C), gain-jalkinetik 900 µL deuseztatu eta jalkina gainontzeko 100 µL-tan berresiki zen, izotzetan beste 30 minutuz inkubatuz. Honen ostean 40 µL-ko alikuotak egin ziren, transformatzeko prest. Bigarren plasmidoa gehitzeko transformazio prozesua aurretik azaldutakoaren antzekoa da, aldaketa gutxi batzuekin. Alde batetik, DNArekin burutzen den hasierako inkubazioa 15 minutukoa zen eta talka termikoa 90 segundokoa. Horretaz gain, talka termikoaren ostean bakterio esekidurei zuzenean giro tenperaturan izandako 500 µL LB gehitu zitzaien 37°C-ko inkubazioaren aurretik.

ELEKTROPORAZIO BIDEZKO TRANSFORMAZIOA

Aldez aurretik prestatu eta -80°C-tan gordetako bakterioak izotzetan desizoztu ziren eta 50 µL zelula 4 µL ligazio produkturekin nahastu ziren. Nahasketa 0,2 cm-tako *Gene Pulser*® elektroporazio kubeta batera igaro zen, izotzetan inkubatu zena 15 minutuz. Ondoren kubetari *Gene Pulser Xcell™ Total System* elektroporadorean 4-5 milisegundotako pultsu bat eman zitzaion ondoko parametroak erabiliz: 2.500 V, 25 µF, 200 Ω. Berehala zelulak aldez aurretik hozturiko 1 mL LB esterilarekin nahastu eta *eppendorf* hodi batera igaro ziren, izotzetan hutzi zena 15 minutuz. Azkenik, zelulak 37°C-tan inkubatu ziren 50 minutuz, 650 rpm-ko irabiaketarekin. Transformazioaren produktuak antibiotiko egokia zuten LB-agar petri plaketan erein ziren, gau osoan zehar 37 °C-tan inkubatu zirenak.

2.2.1.5. ZATIKIAREN PRESENTZIAREN BAIEZTAPENA

Petri-plaketan bakterio koloniak agertuz gero, hauetako batzuk aukeratu eta antibiotiko egokidun 5 mL LBn hazi ziren, 37°C-tan inkubatuz gau osoan zehar. Zelula kultibo hauetatik DNA plasmidikoaren erauzketa burutu zen Mini-prestaketak eginez. Anplikoiaren txertaketa PCR eta liseriketa bidez (murrizte-entzimak erabiliz) aztertu zen, klonaketaren lehenengo pausuetan erabilitako protokoloak jarraituz. Erreakzio hauetatik lortutako produktuak agarosazko gel elektroforesi bidez aztertu ziren. Bi frogaketetan anplikoiaren tamainako banda aurkezten zuten Mini-prestaketekin *E. coli* DH5α zelulak transformatu ziren eta lortutako kolonietatik DNA erauzi zen, Midi-prestaketak eginez kasu honetan. PCR erreakzioan emandako mutazioen presentzia baztertzeko, lagin hauek Sanger sekuentziazioaren bidez aztertu ziren Sekuentziazio eta Genotipo Azterketen SGIker Unitatean (SGIker, UPV/EHU).

2.2.2. MUTAGENESI GUNERATUA

Mutagenesi guneratua proteinen funtzioan eta egituran parte hartzen duten aminoazidoak aztertzeko teknika baliagarria da. Tesi honetan teknika hau T4CPen Walker A motiboaren lisina kontserbatua treonina batengatik ordezkatzeko erabili da. Teknika hau burutzeko *QuikChange II Site-Directed Mutagenesis Kit* sistema komertziala erabili zen, etxe komertzialak eskainitako protokoloa jarraituz.

Mutagenesi guneratua ohiko klonaketa tekniketan oinarritzen da, baina aldaketa gutxi batzuekin prozesua errazteko. Hasleak (2.6. taula) *QuikChange Primer Design (https://www.genomics.agilent.com/primerDesignProgram.jsp)* programa informatikoaren bidez diseinatu ziren. PCR bidez pUBQ4 bektorea anplifikatu zen, mutazioa zeramaten hasleak erabiliz, mutazio hori sekuentzian txertatzeko. Erreakzioa kit-eko gomendioak eta produktuak erabiliz egin zen. Erabilitako profil termikoa ondokoa izan zen: hasierako desnaturalizazioa 95°C-tan 30 segundoz, anplifikaziozko 18 zikloz jarraiturik (desnaturalizazioa 95°C, 30 segundo; hasleen parekaketa 55°C, 60 segundo; luzapena 68°C, 8,5 min) eta bukaerako luzapena 72°C, 10 minutuz. Honen ostean PCR produktuaren 40 µL *Dpn*I murrizte-entzimarekin tratatu ziren ordu batez 37°C-tan, metilatutako DNA moldea liseritzeko. Bukatzeko bakterio kimiokonpetenteak lortutako laginarekin transformatu ziren aurreko atalean deskribaturiko protokoloa jarraituz. Alde batetik kit-ak eskainitako *E. coli* XL1-Blue anduia erabili zen eta bestaldetik *E. coli* DH5α anduia, bakterio koloniak azken kasuan soilik lortuz. Kolonietatik DNA plasmidikoaren erauzketa egin zen, aurretik azaldu bezala, sekuentziaren balioztapena burutzeko.

2.6. taula. Mutagenesi erreakzioetan erabilitako hasleak. Mutagenesi batean PCR bidez lorturiko anplikoia plasmido molde bera da, baina sekuentzia aldatuarekin. FM eta RM mutagenesi *forward* eta mutagenesi *reverse* hasleei dagokie, hurrenez hurren.

Anplifikatutako produktua	Mutantea	Haslea (5' → 3')
pUBQ4(K142T) bektorea *(*pET24a(+)::*traJTMD-trwBCD(K142T))*	*traJTMD-trwBCD(K142T)*	FM1: AAGCAACACCGATGTACCCGTACCAGTGGCA RM1: GTGCCACTGGTACGGGTACATCGGTGTTGCTT

2.2.3. ETEKIN-HANDIKO KLONAKETA

Oxford Protein Production Facility UK-n (OPPF-UK, Research Complex at Harwell, Didcot, UK) 96 putzutako plaketan oinarritutako protokolo bat diseinatu zen modu erraz batean klonaketa ugari burutzeko (Bird, 2011). Honen bidez gene jakin bat, edota batzuk, bektore bilduma batean denbora laburrean *In-fusion™ ligase-less* teknologiari esker klonatu daitezke. Tesi honetan T4CPen azterketa sakonago bat burutu ahal izateko $MobB_{CloDF13}$, $MobB\Delta TMD_{CloDF13}$, $TMD_{TrwB}TraJ_{pIP501}$ eta $TraJ_{pIP501}$ proteinak kodetzen dituzten sekuentziak 12 gain-adierazpen bektore desberdinetan txertatu egin ziren. Bektore hauetako bakoitzak (2.7. taula) etiketa desberdin bat gehitu zion klonatutako proteinari, azterketa biokimiko eta biofisikoak burutzerakoan erabilgarriak izan daitezkeenak.

2.7. taula. Bektore gisa erabilitako plasmidoak. Plasmido hauek guztiak pOPIN gain-adierazpen bektore taldekoak dira (Berrow et al., 2007). ***POI**: Intereseko proteina; N-HIS: N-muturreko His_6 etiketa; C-HIS: C-muturreko His_6 etiketa; 3C: Rhinovirus 3C proteasarako murrizketa gunea; BAP: *Biotin acceptor peptide*; STREPII: *Streptavidin biding peptide II*; TRX: *E. coli Thioredoxin reductase*; MBP: *Maltose binding protein*; SUMO: *Small ubiquitin like modifier*; TF: *Trigger factor*; GST: *Glutathione-S-transferase*; eGFP: *Enhanced green fluorescent protein*; HALO7: *Halo 7 etiketa* (Promega); FLAG: DYKDDDDK sekuentzia aminoazidikoa duen antigenoa.

	Bektorea	Etiketa*	Erresistentzia
1	pOPINE	**POI**-C-HIS	Amp
2	pOPINFB	N-HIS-3C-**POI**-BAP	Amp
3	pOPINFS	N-HIS-3C-**POI**-C-STREPII	Amp
4	pOPINTRX	N-HIS-TRX-3C-**POI**	Amp
5	pOPINM	N-HIS-MBP-3C-**POI**	Amp
6	pOPINS3C	N-HIS-SUMO-3C-**POI**	Amp
7	pOPINTF	N-HIS-TF-3C-**POI**	Amp
8	pOPINCDM	N-HIS-MBP-3C-**POI**	Str
9	pOPINRSJ	N-HIS-GST-3C-**POI**	Kan
10	pOPINE-3C-eGFP	**POI**-3C-eGFP-C-HIS	Amp
11	pOPINE-3C-HALO7	**POI**-3C-HALO-C-HIS	Amp
12	pOPINEneo-FLAG	**POI**-3C-FLAG-HIS_8	Amp

2.2.3.1. ETEKIN-HANDIKO POLIMERASAREN KATE ERREAKZIOA

Beharrezko anplikoiak lortzeko PCR entsegu desberdinak burutu ziren. Klonaketa hauek 0,6 µM hasle pare egoki, 0,2 µL DNA molde eta *Phusion Flash Master Mix* erabiliz burutu ziren, 50 µL-tako bolumenean. Hasleen diseinurako *In-Fusion*™ teknika bidez klonatzeko gehitu behar ziren sekuentziak eta aukeratutako itu bektorearen ezaugarriak (2.7. taula) kontutan hartu ziren. Erabilitako profil termikoa ondokoa izan zen: hasierako desnaturalizazioa 98°C-tan 5 segundoz, anplifikaziozko 30 zikloz jarraitua (desnaturalizazioa 98°C, 5 segundo; hasleen parekaketa 60°C, 5 segundo; luzapena 72°C, 1 min) eta bukaerako luzapena 72°C, 1 minutu. PCR entsegu hauetan erabilitako hasle pareak S2.1. taulan aurkezten dira.

5 µL PCR produktu 2 µL *DNA karga indargetzaile*rekin nahastu ziren eta %1,25 (p/b) *TBE indargetzailea*n prestatutako agarosazko gel elektroforesi bidez aztertu ziren, *SYBR*™ *Safe* tindatzailea eta *Hyperladder* I pisu molekularreko patroia erabiliz. Behin anplikoien tamaina egokia zela ziurtaturik, PCR produktuak *Dpn*I entzimarekin (5 U) tratatu ziren ordu batez 37°C-tan, metilaturiko DNA moldea liseritzeko. Honen ostean anplikoiak purifikatu ziren *AmPure*™ *XP-PCR purification system* erabiliz eta etxe komertzialaren gomendioak jarraituz.

Purifikaturiko DNA produktuak agarosazko gel elektroforesi bidez aztertu ziren, aurretik azaldutako baldintzetan.

2.2.3.2. *IN-FUSION*™ ERREAKZIOAK ETA ETEKIN-HANDIKO TRANSFORMAZIOA

In-fusion™ erreakzioen bidez, DNA anplikoi bakoitzaren txertaketa egin zen pOPIN taldeko bektore desberdinetan. Klonaketa bakoitzeko, aldez aurretik *Kpn*I-*Hind*II murrizte-entzimekin linealizaturiko 1 µL pOPIN bektore (100 ng) eta 2 µL PCR produktu (10-100 ng) nahastu ziren, 10 µL-tako bolumenean. Lorturiko lagin bakoitzari 10 µL *In-Fusion*™ entzima gehitu zitzaizkion. Erreakzioak 42°C-tan egin ziren, 30 minutuz, *Veritithermocycler* batean. Ostean 40 µL *TE indargetzaile*rekin diluitu eta izotzetan mantendu ziren.

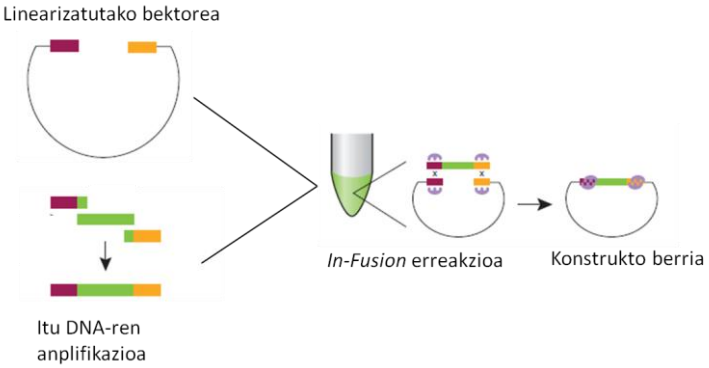

2.1. irudia. *In-fusion* erreakzioaren irudikapen eskematikoa. 15 base paretako sekuentzia osagarriak granate eta laranjaz adierazten dira. Itu genearen sekuentzia berdez adierazten da. Konstrukto berria lortzeko linearizatutako bektorea eta PCR anplikoia *In-fusion* entzimarekin nahastu ziren, 30 minutuz 42°C-tan inkubatuz.

Etekin-handiko transformazioa *E. coli Omnimax*™*2 T1-Phage resistant* bakterio kimiokonpetenteetan burutu zen. *In-Fusion*™ erreakzio bakoitzetik lortutako 3 µL aldez aurretik izotzetan desizoztutako 50 µL zelulekin nahastu ziren. Nahasketak izotzetan inkubatu ziren 30 minutuz eta ostean talka termiko bat burutu zen 42°C-tan, 40 segundoz. Bakterio esekidurak berriz izotzetan 2 minutuz inkubatu ziren eta ondoren 300 µL *Super Optimal Broth* katabolitoen errepresiodun hazkuntza medio (SOC) gehitu zitzaien. Ondoren, zelulak 37°C-tan inkubatu ziren ordu batez eta LB-agar plaketan erein ziren. Kasu honetan, LB-agarrari antibiotiko egokia, X-Gal %0,02 (p/b) [%20 (p/b) kontzentrazioko *stock*-aren 1:1000 diluzioa dimetilformamidan (DMF)] eta 1 mM isopropil-β-D-tiogalaktosido (IPTG) gehitu zitzaizkion. Zelulekin ereindako plakak 37°C-tan inkubatu ziren gau osoan zehar.

2.2.3.3. KLONAKETAREN BAIEZTAPENA ETA GLIZEROL GORDEKINEN PRESTAKETA

Gau osoko inkubazioaren ostean zelula kolonia zuri eta urdinak lortu ziren LB-agar plaketetan. Kolonia urdinak plasmido hutsekin erlazionaturik zeuden, hau da, anplikoia txertatu ez zitzaien plasmidoekin. Kolonia hauek jatorrizko bektorea linearizatu ez denean edota bektorea murrizte-entzima bakar batekin moztu eta berzirkularizatzen denean ager daitezke. Konstruktoak aztertzeko, transformazio bakoitzetik 2 kolonia zuri aukeratu ziren eta bakoitza antibiotikorekin aberastutako 1,2 mL LBn gau osoan zehar 37°C-tan hazi zen. Hurrengo egunean, kultibo guztien glizerol gordekin bana prestatu zen. Horretarako kultibo bakoitzeko 100 µL esterilizaturiko LB-glizerol %30 (b/b) 100 µL-rekin nahastu ziren. Lortutako bakterio suspentsioak -80 °C-tan biltegiratu ziren.

Konstruktoak bi entsegu desberdin erabiliz aztertu ziren. Lehenengoa frogaketa azkar bat izan zen, ideia orokor bat lortzeko. Horretarako glizerol gordekin bakoitzaren 2 µL esterilizaturiko H_2O 100 µL-tan diluitu ziren eta 100°C-tan inkubatu ziren 5 minutuz. Lagin hauek etekin-handiko PCR azterketa batean DNA molde bezala erabili ziren. Erreakzioak 25 µL-tan burutu ziren 12,5 µL 2X *Phusion Flash Master Mix*, 0,15 µL *pOPIN forward* hasle (5' GACCGAAATTAATACGACTCACTATAGGGG 3') (100 µM *stock*) eta anplikoi bakoitzerako 1,5 µL *reverse* hasle egoki (10 µM stock, S2.1. taula) erabiliz. Kasu honetan erabilitako PCR protokoloa ondokoa izan zen: hasierako desnaturalizazioa 94°C-tan, 2 minutuz; anplifikaziozko 30 zikloz jarraitua (desnaturalizazioa 94°C, 30 segundo; hasleen parekaketa 60°C, 30 segundo; luzapena 68°C, 2 min) eta bukaerako luzapena 68°C, 4 minutuz. PCR produktuak 6,5 µL *DNA karga indargetzaile*rekin nahastu ziren eta %1,5 (p/b) agarosazko gel elektroforesiz aztertu ziren aurretik azaldu bezala (2.2.3.1. atala).

Klonaketaren baieztapen zehatzago bat izateko, etekin-handiko plasmido erauzketa burutu zen. Horretarako gau osoan zehar hazitako kultiboak zentrifugazio bidez (5.000 *g*, 15 min) jaso ziren. Ondoren, gain-jalkina deuseztatu eta Mini-prestaketak egin ziren *Bio-Robot 8000* bat eta *Wizard SV96 purification system*-a erabiliz etxe komertzialaren argibideak jarraituz. Erauzitako DNA plasmidikoaren 1,5 µL molde gisa erabili ziren PCR bidezko azterketa burutzeko, aurreko paragrafoan azaldu bezala. Emaitza positiboak lortu zituzten konstruktoak sekuentziazio bidez aztertu ziren 2.8.taula adierazitako hasleak erabiliz.

2.8. taula. Sekuentziazioan erabilitako hasleak. [a]Konstrukto guztien sekuentziaziorako erabilitako haslea. [b]$MobB_{CloDF13}$ taldeko konstruktoen sekuentziaziorako erabilitako haslea. [c]$TMD_{TrwB}TraJ_{pIP501}$ eta $TraJ_{pIP501}$ konstruktoen sekuentziaziorako erabilitako haslea.

Haslea	Sekuentzia (5' → 3')
T7 forward[a]	TAATACGACTCACTATAGGG
Triexdown[a]	TCGATCTCAGTGGTATTTGTG
MobBcenter forward[b]	GATTGTGTTGGCGCG
MobBcenter reverse[b]	CAGCGACTGGTGCG
TraJcenter[c]	AAGAATTTGATCCACGCT

2.2.4. M13 BAKTERIOFAGOAREN DNAREN ERAUZKETA

VCSM13 fagoa (*Interference-Resistant Helper Phage*) M13 fagoaren mutantea da, kanamizinaren aurkako erresistentzia kodetzen duen genea daukana. Fago honen ziklo infekziosoan bi fase bereizten dira, lehenengoa zelula barneko kate bikoitzeko DNA (*double stranded DNA,* dsDNA) fasea eta bigarrena partikula infekzioso moduko ssDNA fasea.

ATP hidrolisi entseguetan *E. coli* bakterioetan hazitako fagoaren ssDNA erabili zen, erosita zein laborategian purifikatua. Azken kasu honetan *E. coli* JM109 zelulak 37°C-tan gau osoan zehar hazi ziren Nal antibiotikoarekin osaturiko 10 mL LBn. Hurrengo egunean kultiboaren 1:20 diluzioa egin zen (500 µL kultibo 10 mL LBn) eta hazten utzi zen OD_{700} 0,3 balioa lortu arte. Orduan, zelulak fagoaren 10^{10} plaka-sortzaile unitaterekin infektatu ziren, nahasketa ordu batez inkubatuz 37°C-tan. Ondoren, kultiboa kanamizinarekin osaturiko LBn diluitu zen 1:25 erlazioan (10 mL kultibo 250 mL LBn) eta 18 orduz 30°C-tan inkubatu zen irabiaketa leunarekin. Hurrengo egunean zelulak zentrifugazio bidez jaso ziren (2.000 *g*, 15 min, 4°C). Gain-jalkinari 50 mL PEG 8.000 %20 (b/b) eta NaCl 2,5 M-eko disoluzioa gehitu zitzaion, ordu batez inkubatuz 4°C-tan irabiaketa leunarekin. Jarraian, lagina zentrifugatu zen (8.000 *g,* 20 min, 4°C). Lorturiko fago jalkina 2 mL *TE indargetzaile*an berreseki zen, lorturiko suspentsioa bi alikuotetan bananduz, bat erauzketa egiteko eta bestea -20°C-tan biltegiratzeko.

ssDNAren erauzketarako 1 mL fago esekidurari 4 mL *TE indargetzaile* eta pH 8,0n orekaturiko 5 mL fenol disoluzio gehitu zitzaizkion (**2.2. irudia**). Bi minutuz irabiaketa bortitzarekin nahastu ostean, lagina zentrifugatu zen (3.000 *g*, 5 min, giro tenperatura) eta jasotako fase urtsua 5 mL fenol:kloroformorekin (1:1, b/b) nahastu zen. Nahasketa zentrifugatu zen (3.000 *g,* 5 min, giro tenperatura), fase urtsua jaso zen berriz eta 5 mL fenol:kloroformo:isopropanolekin (2,5:2,4:0,1, b/b) nahastu zen ssDNA erauzteko. Lagina berriz zentrifugatu ostean (3.000 *g,* 5 min, giro tenperatura) DNAren hauspeatzea burutu zen. Horretarako azken zentrifugaziotik lortutako fase urtsuari NaAc gehitu zitzaion bukaerako kontzentrazioa 0,3 M izan arte. Ostean, lorturiko laginaren bolumena kontutan hartuz 2,5 lagin-bolumen etanol absolutu gehitu ziren. Behin ondo nahastuta, lagina ordu batez 20°C-tan inkubatu zen. Ondoren zentrifugatu zen (17.000 *g,* 20 min, 4°C), jalkina etanol %70 (b/b)-rekin

garbituz eta berriz zentrifugatuz (17.000 *g*, 10 min, 4°C). Bukatzeko gain-jalkina deuseztatu eta jalkina ondo lehortu zen *TE indargetzailea*n berreseki aurretik. Lorturiko ssDNA kontzentrazioa *NanoDrop™ Lite Spectophotometer*-a erabiliz neurtu zen.

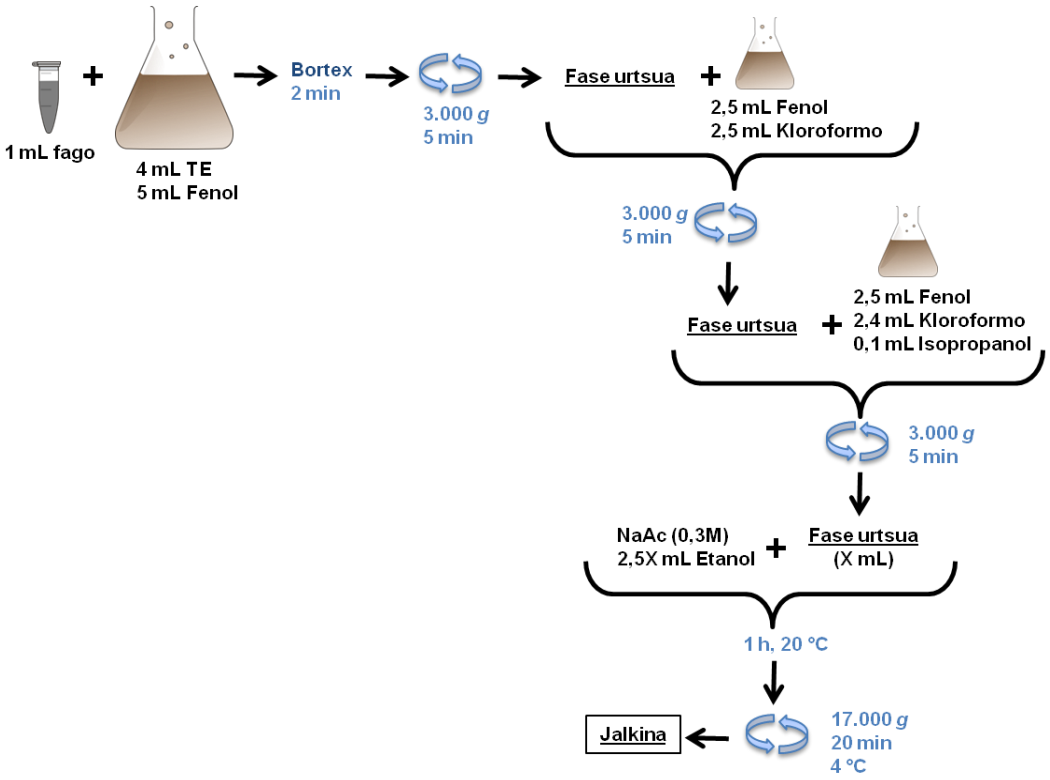

2.2. irudia. ssM13 DNAren erauzketa prozesuaren irudikapen eskematikoa. Azpimarraturiko laginak hurrengo pausuetan erabiliko diren zentrifugazio produktuei dagokie. Gezi urdinek zentrifugazio prozesu bat adierazten dute.

2.2.5. pKM101Δ*traJ*ren EKOIZPENA

Konjugazio entseguak burutzerakoan ikusi zen pKM101Spc^r_Δ*traJ* plasmidoari espektinomizinaren aurkako erresistentzia eskaintzen dion kaseteak (*spc cassette*) estreptomizinaren aurkako erresistentzia ere ematen duela. Hau bateraezina zen konjugazio saiakeretan *E. coli* UB1637 anduia hartzaile gisa erabiltzearekin, erresistentzia berdina aurkezten baitu. Hori dela eta, kasetea plasmidotik ebaki zen biologia molekularreko teknikak erabiliz. Horretarako 1 ng plasmido 8 U *EcoR*I murrizte-entzimarekin 2 orduz 37°C-tan inkubatu zen, ondoren entzima inaktibatzeko 15 minutuz 65°C-tan inkubatuz. Plasmidoa ligatu eta *E. coli* DH5α bakterio konpetenteetan transformatu zen, Amp-rekin osatutako LB-agar plaketan erein zirenak. Lortutako koloniak Amp edo Str-rekin osatutako LBn hazi ziren haien fenotipoa aztertzeko, balioztatuz Str-ren aurkako erresistentzia galdu egin zutela. Modu honetan pKM101Δ*traJ* plasmidoa lortu zen.

2.3. KONJUGAZIOA

Konjugazio prozesuan T4CP eta mutante desberdinen *in vivo* efektua aztertzeko, konjugazio entseguak burutu ziren. Entsegu hauek burutzeko bakterio emaile eta hartzaile bat nahasten dira, lan honetan *E. coli* DH5α eta *E. coli* UB1637 anduiak izan direnak, hurrenez hurren. Emaileak plasmido konjugatibo bat eta aztergai den proteina kodetzen duen gain-adierazpen plasmidoa daramatza (2.3.irudia). Horretarako, *E. coli* DH5α zelulak aldez aurretik plasmido egokiekin transformatu ziren.

Konjugazio entseguak antibiotikoen bidezko hautespenean oinarritzen dira. Zelulek daukaten plasmido bakoitzak antibiotiko jakin baten aurkako erresistentzia kodetzen du, eta horretaz gain, andui emaile eta hartzaileek erresistentzia kromosomiko desberdina aurkezten dute (2.3.irudia). Konjugazio prozesua ematen denean, zelula hartzaileak plasmido konjugatiboak kodetzen duen erresistentzia lortzen du antibiotiko horren aurkako fenotipoa lortuz, konjugazio aurretik aurkezten ez zuena. Horretan oinarrituz, antibiotiko egokidun LB-plakak erabiliz, transkonjuganteen (plasmido konjugatiboa jasotako zelula hartzaileak, alegia) kopurua ezagutu daiteke.

Entsegu honetan kontrol egokiak erabiltzea oso garrantzitsua da, gainerako mikroorganismoen kutsadurarik ez dagoela ziurtatzeko. Kontrol positibo gisa plasmido konjugatibo natiboa erabili zen, zeinaren transferentzia maiztasuna deskribaturik dagoen. Kontrol negatibo gisa T4CP ez-funtzionala kodetzen duen plasmido konjugatiboa erabili zen, proteina hau beharrezkoa baita transferentzia emateko. Bi plasmido konjugatibo hauetan oinarrituz, konjugazio bidez proteina birkonbinanteen bi ezaugarri aztertu daitezke: alde batetik, T4CP ez-funtzionala duten plasmidoen konjugazioa osatzeko aurkezten duen gaitasuna, funtzionalitate entseguen bidez; eta beste aldetik bere presentziak jatorrizko konjugazio sisteman daukan eragina, dominantzia entseguen bidez (2.3.irudia).

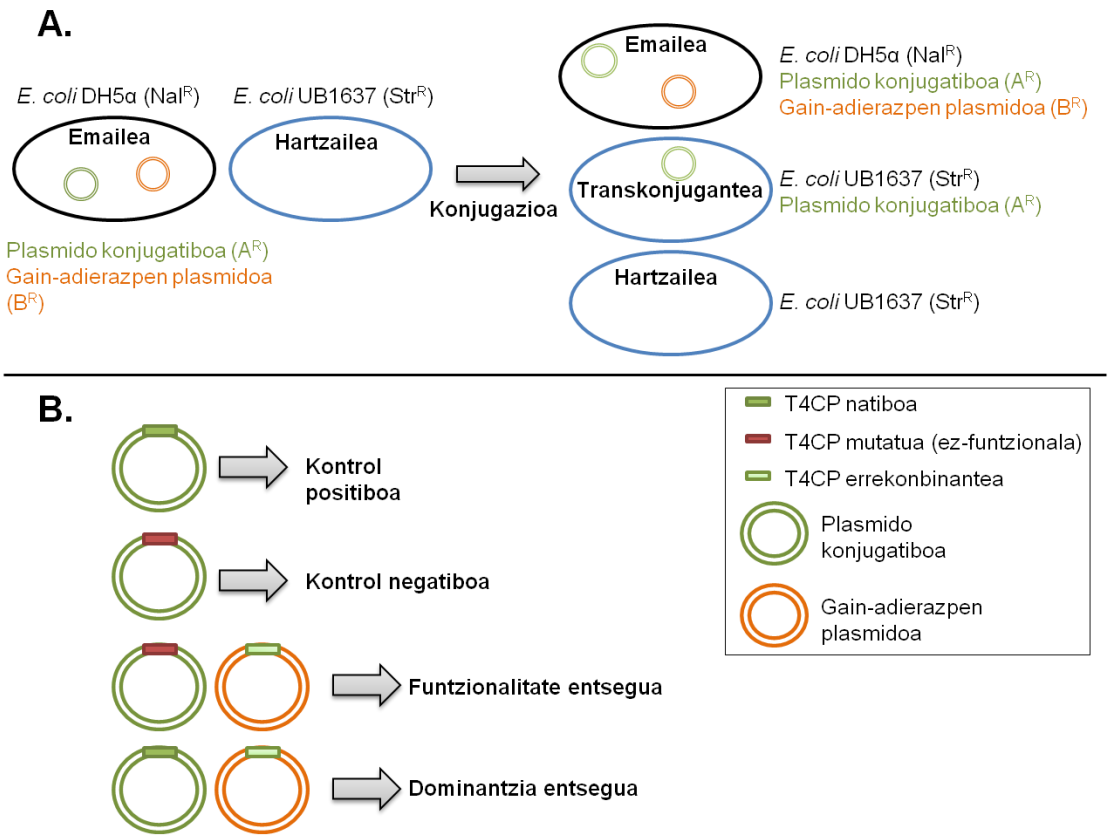

2.3. irudia. Konjugazio entseguaren irudikapen eskematikoa. Konjugazio entseguan plasmido konjugatibo bat zelula emailetik zelula hartzailera igarotzen da. Tesi honetan *E. coli* DH5α eta UB1637 anduiak erabili dira emaile eta hartzaile gisa, hurrenez hurren. **A)** Plasmido konjugatiboak konjugazio prozesurako proteinak kodetzen ditu, gain-adierazpen plasmidoak aztertu nahi den proteina akoplatzailea kodetzen duen bitartean. Konjugazio prozesuaren ostean bakterioak antibiotiko konbinazio desberdinak dituzten plaketan ereiten dira, emaile eta transkonjuganteen kopurua ezagutzeko. Honela, konjugazioaren transferentzia maiztasuna kalkula daiteke. **B)** Zelula emailean aurkitzen diren plasmidoen arabera konjugazio entseguetatik informazio desberdina lor daiteke. Plasmido konjugatibo natiboa kontrol positibo gisa erabiltzen da. Konjugazioaren kontrol negatibo gisa T4CP mutatua (ez-funtzionala) daukan plasmido konjugatiboa erabiltzen da, transferentzia burutzeko ezintasuna daukana. T4CP ez-funtzionala duen plasmido konjugatiboa T4CP birkonbinantearekin konbinatzean, azken honek konjugazioa osatzeko daukan gaitasuna aztertu daiteke. Bukatzeko, zelula emailean T4CP natiboa eta birkonbinantea agertzen direnean, bien arteko dominantzia erlazioa aztertu daiteke.

Entsegu hauek burutzeko aldez aurretik ezarritako protokoloa erabili zen (Llosa et al., 2003), aldaketa gutxi batzuekin. Andui emaile eta hartzaileak gau osoan zehar hazi ziren 37°C-tan, antibiotiko egokiekin osatutako 2 eta 10 mL LBn, hurrenez hurren. Hurrengo egunean 100 µL emaile 100 µL hartzailerekin nahastu eta zentrifugatu ostean (6.000 *g*, 2 min), jalkina 50 µL LB esterilean berreseki zen. Zelula esekidurak LB-agar plaketetan kokaturiko 0,22 µm-eko Millipore-nitrozelulosazko iragazkietan jarri ziren eta ordu batez 37°C-tan inkubatu ziren, konjugazio prozesua emateko. Ondoren iragazkiak 2 mL LB-dun 13 mL-tako saiodietara igaro ziren eta iragazkietatik bereizteko 20 minutuz irabiatu ziren. Iragazkien garbiketa prozesuaren

azken pausuan saiodi bakoitza 30 segundoz bortexeatu zen. Saiodietan lorturiko bakterio nahasketa bakoitzetik LB medioan diluzio seriatuak egin ziren (1:10, $1:10^2$, $1:10^3$, $1:10^4$ eta $1:10^5$) eta bakoitzetik 100 µL erein ziren antibiotiko egokiko LB-agar plaketan. Lagin bakoitza bi plaka motetan erein zen: alde batetik emaileak eta bestaldetik transkonjuganteak hazteko beharrezkoak ziren antibiotiko nahasketekin osaturiko plaketan. Plakak gau osoan zehar inkubatu ziren 37°C-tan eta hurrengo goizean plaka bakoitzean agerturiko kolonien zenbaketa burutu zen. Transferentzia maiztasunak transkonjugante koloniak emaile kolonia kopururekiko kalkulatu ziren. Azkenik, kolonia transkonjuganteek konjugazio plasmidoa lortu zutela baieztatzeko, plasmidoaren presentzia PCR bidez baieztatu zen.

2.4. PROTEINEN DETERMINAZIORAKO TEKNIKAK

Proteinak karakterizatzerako orduan, haien determinazioa burutu behar da, aztertzen ari den proteina itu-proteina dela ziurtatzeko eta laginean ager daitezkeen gainerako proteinen ezagupena izateko.

2.4.1. POLIAKRILAMIDAZKO GEL BIDEZKO ELEKTROFORESIA

Proteinen determinazio burutzeko tekniken artean arruntena sodio dodezil sulfatozko poliakrilamidazko gel bidezko elektroforesia (*Sodium dodecyl sulfate polyacrylamide gel electrophoresis*, SDS-PAGE) da. Horretaz gain, teknika hau karakterizazio zehatzagoak (Western-plapaketa edota masa-espektometria bidezko proteinen identifikazioa, adibidez) egiteko lehenengo pausu gisa erabili ohi da. Tesi honetan, proteinen erauzketaren jarraipena egiteko baldintza desnaturalizatzailetan %12,5 (p/b) poliakrilamidazko gelak erabili egin dira, Laemmlik ezarritako metodoa jarraituz (Laemmli, 1970). Teknika honi esker proteinak haien pisu molekularraren arabera bereizi daitezke.

SDS-PAGEak burutzeko, laginei *proteina karga indargetzailea* (6X) gehitu zitzaien bukaerako indargetzaile kontzentrazioa 1X-ra doituz. Horretaz gain, proteina solugarrien azterketa egiterakoan laginak berotu ziren (5 min, 100°C). MPak, ordea, ez ziren bero bidez desnaturalizatu, gelaren putzuetan sartzeko zailtasuna aurkezten dituzten agregatuak sortzen baitituzte irakiterakoan. Elektroforesiak *SDS-PAGE indargetzailea*n burutu ziren, orokorrean 110 V-tan 10 minutuz eta ondoren 200 V-tan 40 minutuz. Bereizitako proteinen pisuaren estimazioa egiteko pisu molekular ezaguneko proteinen eredu-patroi desberdinak erabili ziren laginaren arabera (*Prestained SDS-PAGE Standards Low range, Prestained SDS-PAGE Standards Broad range, Precision Plus Protein™ Unstained Protein Standard, Precision Plus Protein™ Dual Color Standards, eta PageRuler™ Plus Prestained Protein Ladder*). Gelen tindaketa *disoluzio tindatzailea (Stain)* erabiliz burutu zen, gutxi gora-behera gela 15 minutuz giro tenperaturan disoluzio honetan murgildurik mantenduz. Soberako tindatzailea kentzeko, *disoluzio destindatzailearekin (Destain*) behar bezain beste garbiketa egin ziren. Gelak *Bio-Rad GS-800 densitometer* edo *Bio-Rad Gel DOC™ EZ Imager* bat erabiliz bistaratu ziren.

2.4.2. POLIAKRILAMIDAZKO GEL ELEKTROFORESI URDIN-NATIBOA

Proteinen egoera oligomerikoa aztertzeko tekniken artean poliakrilamidazko gel elektroforesi urdin-natiboa (*Blue Native-PAGE,* BN-PAGE) (Schagger et al., 1994) aurkitzen da. SDS-PAGEn erabilitako baldintzek proteinen desnaturalizazioa eragiten dute, hori dela eta ezin dira proteina bakoitzak laginean aurkezten dituen egoera oligomerikoak bereizi, denak banda bakar baten moduan aurkezten baitira. BN-PAGEn, ordea, proteinen egoera natiboa mantentzen da eta horri esker proteina oligomeroak bereizteko teknika moldaerraza da. Laginei *Coomassie Brilliant Blue* koloratzaile anionikoa gehitzen zaie. Koloratzaile hau laginean dauden mintz proteinetara batzen da, bertan dauden proteina-proteina arteko elkarrekintzak mantenduz eta konplexuari karga negatiboa emanez. Horri esker mintz-proteinen agregazio joera murrizten da, elektroforesian detergenterik erabili gabe.

Elektroforesi mota hau burutzeko *NativePAGE™ Novex® Bis-Tris* gel sistema komertziala aukeratu zen, %4-16 Bis-Tris akrilamidazko gelak eta *NativePAGE™ %5 G-250* koloratzailea erabiliz. Laginak etxe komertzialaren gomendioak jarraituz prestatu ziren, nahiz eta proteina bakoitzarentzat erabilitako kontzentrazioa eta koloratzaileen presentzia optimizatu behar izan, bakoitzaren agregazio joera desberdinak zirela eta. Katodoan erabilitako indargetzaileari dagokionez, nahiz eta etxe komertzialak *urdin ilun indagertzailea* gomendatu, *urdin argi indargetzailea* erabiltzeko erabakia hartu zen, ikusi baitzen mintz-proteinek coomassie kontzentrazio altuetan agregazio joera handiagoa aurkezten zutela, gelean barneratzeko arazoak izanik. Anodoan erabilitako indargetzailea kit komertzialekoa izan zen. Pisu molekularreko markatzaile gisa *HMW Native Marker* proteina nahasketa erabili zen, 66 eta 669 kDa tarteko pisu molekularreko proteinak dituena. Elektroforesia ordu batez 150 V-tan egin zen eta beste bi orduz 250 V-tan edota aurrealdea gelaren bukaerara heldu arte. Prozesu osoa 4°C-tan burutu zen. Teknika honetan proteinen bistaratzea zuzena da, proteina konplexuek lotuta daukaten koloratzaileari esker. Hala ere, intentsitate txikiko bandak identifikatzeko aurreko atalean SDS-PAGErako deskribatutako tindaketa/destindaketa prozesua egin zen.

2.4.3. WESTERN PLAPAKETA

Lagin batean agertzen diren proteina desberdinen artean proteina zehatz baten identifikazioa burutzeko Western plapaketa (*Western blotting,* WB) edota inmuno-plapaketa teknika erabili daiteke (Yang eta Mahmood, 2012), epitopo zehatz bat (edo batzuk, antigorputz poliklonalen kasuan) ezagutzen duten antigorputzen erabileran oinarritzen dena.

WBa egin aurretik, lagineko proteinak SDS-PAGE baten bidez bereizi egiten dira, kasu honetan aldez aurretik tindaturiko proteinen patroia erabiliz. Patroi berezi hau erabilgarria izaten da proteinen mugimendua gelean zehar begi bistaz jarraitzeko. Gel elektroforesiaren ostean, proteinen transferentzia erdi-lehorra burutu zen proteinak poliakrilamidazko geletik *Protran* nitrozelulosazko mintz batera igarotzeko. Prozesu honetan beharrezkoak diren *Whatman® 3MM* filtro-paperak, nitrozelulosazko mintza eta poliakrilamidazko gela aldez aurretik *transferentzia indargetzailea*n murgildu ziren. Proteinen transferentzia 45 minutuz 15 V-tan burutu zen hurrengo ordena mantenduz (behetik gora): Trans-Blot plaka, hiru *Whatman® 3MM* filtro-paper, nitrozelulosazko mintza, poliakrilamidazko gela eta beste hiru filtro-paper.

Behin transferentzia eginda elkarrekintza ez-espezifikoak saihesteko mintzaren blokeoa burutu zen giro tenperaturan ordu batez *TBST-BSA disoluzioa* erabiliz. Jarraian, antigorputz-primarioarekin inkubazioa egin zen, ordu batez giro tenperaturan edo gau osoan zehar 4°C-tan. Antigorputz primarioek aztergai den proteinaren epitopo bat (edo batzuk, antigorputz poliklonalen kasuan) ezagutzen dute espezifikoki. Lan honetan gehien bat erabilitako antigorputz primarioa histidina etiketaren aurkako *mouse anti-His (C-term) monoclonal* antigorputza izan zen, 1:5000 (b/b)-ko diluzioa *TBST-BSA disoluzioa*n burutuz. Nitrozelulosazko mintza *TBST*-rekin garbitu zen giro tenperaturan 10 minutuz inkubatuz hiru aldiz, mintzari lotu gabeko antigorputza kentzeko. Ostean, mintza antigorputz sekundarioarekin inkubatu zen giro tenperaturan ordu batez. *Mouse anti-His (C-term) monoclonal* antigorputz primarioaren ezagupenerako *Donkey-AntiMouse IgG-HRP* antigorputz sekundarioa erabili zen, 1:1000 (b/b)-ko diluzioa *TBST-BSA disoluzioa*n burutuz. Mintza berriz garbitu zen aurreko pausuan bezala eta proteinen detekziorako *detekzio disoluzioa* prestatu zen: 7,5 mL TBST, 1 mL diaminobenzidina (6 mg/mL), 1 mL $NiNH_4SO_4{\cdot}6H_4O$ %1,4 (p/b), 0,5 mL $CoCl_2{\cdot}6H_2O$ (%1,8 p/b) eta 2 µl H_2O_2 %100 (b/b). Kasu honetan, antigorputz sekundarioari konjokatutako errefau minaren peroxidasa entzima (*Horseradish peroxidase,* HRP) diaminobenzidina substratua oxidatzeko gai da; oxidazio erreakzioa gertatzen den gune espezifiko horietan koloredun jalkinak lortuz (hau da, itu proteinen bandak koloredunak bihurtuz). Beraz, mintza *detekzio disoluzioa*n murgildu zen proteinen bandak agertu arte. Azkenik mintzen garbiketa burutu zen ur distilatuarekin bost minututako hiru garbiketa eginez.

2.4.4. MASA ESPEKTROMETRIA

Masa espektrometria proteinen azterketarako erabiltzen den teknika da, masaren inguruko informazio zehatza ematen duena. Tesi lan honetan teknika hau erauzitako $TMD_{TraJ}CD_{TrwB}$ laginen kalitatearen azterketa bikoitza burutzeko erabili egin zen: alde batetik proteina kutsatzaileen izaera ezagutzeko eta beste aldetik aztergai den proteinaren osotasuna ziurtatzeko. Masa espektrometria saiakuntzak Proteomika Unitatean burutu ziren (SGiker, UPV/EHU).

Laginetan proteina kutsatzaileen presentzia aztertzeko, aldez aurretik ezarritako protokoloa erabili zen (Arechaga et al., 2008). 30 µg proteinadun laginak SDS-PAGE bidez banandu ziren. Beirazko petri kutxatila batean gela *disoluzio tindatzailea*rekin inkubatu ondoren ur destilatuarekin destindatu zen, metanolaren trazak saihesteko. Laginean itu proteinaren ehunekoa oso altua zenez, gainerako proteinen estaldura ez gertatzeko $TMD_{TraJ}CD_{TrwB}$ri ezarritako banda bisturi batekin ebaki zen, gainerako proteinen estaldura ekiditeko. Gainontzeko gel kalea hiru zatitan banandu zen, banandurik Mili-Q uran gorde zirenak. Gel zati bakoitza tripsinarekin tratatu zen gel-barneko proteinen liseriketa burutuz (Shevchenko et al., 1996). Tripsinaren bidezko tratamendua jasandako lagin hauek banandurik kromatografia likido-tandem masa espektometria (*Liquid chromatography-tandem mass spectrometry*, LC-MS/MS) bidez aztertu ziren, espektroak *CapLC* kapilaritatezko kromatografia sistema batekin konektaturiko *Q-Tof Micro* masa espektrometro baten bidez jasoz. Teknika honen bidez lorturiko espektroak *ProteinLynx global server* erabiliz prozesatu ziren, eta *E. coli*-ren proteinak dituen NCBIprot 20161127 datu-basearekin alderatu ziren MASCOT bilaketa motorra erabiliz.

Beste aldetik, proteinaren degradazio eza eta pisu molekularra aztertzeko, zuzenean purifikazioaren ondoren lortutako lagina erabili zen. Azterketa hau burutzeko, lehenengo eta behin purifikatutako proteina laginaren indargetzaile aldaketa burutu zen, jatorrizko indargetzaileak detergentea, gatz-kontzentrazio altua eta glizerola baitzeukan. Horretarako 145 µg proteina alderantzizko fase kromatografia zutabetik (*C4 Micro Spin column*) igaro ziren, *MS indargetzailea*n berresekiz. Zoritzarrez, pausu horretan proteinaren galera gertatu zenez ezin izan zen entseguarekin aurrera jarraitu.

2.5. PROTEINEN ERAUZKETA

Biologia molekularraren bidez itu-proteinak kodetzen dituzten geneak gain-adierazpen plasmidoetan txertatuta ziren. Plasmido hauek zelula egokietan transformatuz gero, intereseko proteinen adierazpena erregulatu daiteke, ondoren zelula kultibo hauetatik gain-adierazitako proteinen erauzketa burutzeko. Behin proteina puruak izanda, haien karakterizazio biokimiko eta biofisikoa egin daiteke *in vitro*.

Tesi honetan erauzitako proteina bakoitzarentzat erabilitako protokolo zehatza hirugarren kapituluan aurkezten da.

2.5.1. PROTEINEN GAIN-ADIERAZPENAREN AZTERKETA

Proteina baten azterketa molekularra burutzeko, proteina hori zeluletatik erauzi egin behar da kantitate eta purutasun maila egokietan. Oro har, MPen adierazpen maila naturala baxuegia da haien erauzketa burutzeko (Wagner et al., 2008), hori dela eta gain-adierazpen sistemak erabili ohi dira. Proteina baten gain-adierazpenean faktore desberdinek eragiten dute, hala nola erabilitako zelula anduia, induktorearen kontzentrazioa, indukzio denbora eta tenperatura. Tesi honetan, proteina bakoitzaren gain-adierazpen protokolo onena aurkitzeko faktore desberdin hauen konbinazioak aztertu dira metodo desberdinen bidez.

Metodorik arrunt eta azkarrena SDS-PAGE eta WB bidezko analisia da. Horretarako bakterioak hazi eta proteinen gain-adierazpena aztertu nahi ziren baldintzetan burutu zen. Indukzioaren une desberdinetan laginak hartu ziren, haien OD_{600} balioa neurtuz. Laginak zentrifugatu (14.000 *g*, 10 min, 4°C) eta *SAB 3X* (*SAB 6X*: H_2O nahasketa 1:1 (b/b) erlazioan) *proteina karga indargetzailea*n berreseki ziren, OD_{600} 0,2ra doituz. Zelula suspentsio hauetatik 15 µL hartu eta SDS-PAGE eta WB bidez aztertu ziren. Modu horretan gain-adierazpen baldintza desberdinetan lorturiko proteinaren konparaketa kuantitatiboa, baina ez kualitatiboa, burutu zen.

2.5.1.1. ETEKIN-HANDIKO GAIN-ADIERAZPENAREN AZTERKETA

2.2.3. atalean lortutako konstruktoek kodetzen dituzten proteinen adierazpen azterketa burutzeko etekin-handiko gain-adierazpen entsegua burutu zen. Bertan zelula andui desberdinak eta medio desberdinak proteinen gain-adierazpenean daukaten eragina aztertu zen. Honetarako OPPF-UK-n (Bird, 2011) ezarritako protokoloa erabili zen, mintz-proteinen ezaugarriak kontutan hartzeko aldaketa gutxi batzuekin.

GAIN-ADIERAZPENERAKO *E. coli* ANDUIEN TRANSFORMAZIOA

Entsegu honetan bi *E. coli* andui desberdin erabili ziren: Lemo21(DE3) eta Rosseta™(DE3) pLysS. Erabilitako transformazio protokoloa 2.2.3.2. atalean azaldutakoaren antzekoa izan zen, aldaketa gutxi batzuekin: bakterio kimiokonpetenteen 50 µL izotzetan desizoztu ziren eta hauei gain-adierazpen plasmido egokiko 3 µL gehitu zitzaien. Nahasketak izotzetan 30 minutuz inkubatu ostean, talka termiko bat burutu zen 42°C-tan, 30 segundoz. Zelula suspentsioak izotzean jarri ziren 2 minutuz eta ondoren lagin hauei 300 µL *Power Broth* (PB) hazkuntza medio gehitu zitzaien. Laginak ordu batez 37°C-tan inkubatu ostean, 30 µL zelula suspentsio hartu eta antibiotiko egokiekin osaturiko LB-agar plaketan erein ziren. Plasmido bakoitzari zegokion antibiotikoaz gain, plakei Chl (35 µg/mL) ere gehitu zitzaien, pLemo edo pLysSRARE plasmidoen mantentzerako. Plakak gau osoan zehar 37°C-tan inkubatu ziren.

GAIN-ADIERAZPENA ETA ZELULEN UZTA

Adierazpen baldintza gehiago aztertzeko, bi *E. coli* anduiez gain, bi indukzio metodo ere erabili ziren: IPTG bidezko indukzioa eta *Overnight Express™ Instant TB Medium* (TBONEX), auto-indukzio hazkuntza medio bat dena. Bi kasuetan lehenengo eta behin plaka bakoitzetik kolonia bana aukeratu zen, antibiotikoekin osaturiko 0,7 mL PBn inokulatu zena. Kultibo hauek gau osoan zehar 37°C-tan hazi ziren. Hurrengo goizean bi diluzio desberdin burutu ziren. Alde batetik, 150 µL[Lemo21(DE3)] edo 250 µL [Rosseta™ (DE3) pLysS] kultibo antibiotikodun 3 mL LBrekin diluitu ziren. Beste aldetik, bolumen bereko diluzioak egin ziren TBONEX medioan. Diluituriko bi zelula taldeak 37°C-tan hazi ziren OD_{595} 0,5 balioa lortu zuten arte. Une horretan TBONEX kultiboak 20-24 orduz 25°C-tan hazi ziren. LB kultiboak, ordea, giro tenperaturara egokitu ziren eta kultibo bakoitzari 1 mM IPTG gehitu ostean, gau osoan zehar 20°C-tan inkubatu ziren.

Zelulen uztarako, 96-putzu sakonetako bi plaka erabili ziren, bat IPTGdun kultiboentzat eta beste bat TBONEX medioan hazitako kultiboentzat. Putzu bakoitzean 1 mL kultibo gehitu zen eta blokeak zentrifugatu ziren (6.000 *g*, 10 min). Ondoren, gain-jalkina deuseztatu, plakak zigilatu eta -80°C-tan gorde ziren 20 minutuz gutxienez.

MINIATURAZKO NI^{2+}-NTA ADIERAZPEN PROTOKOLOA

Tesi honetan aztergai diren proteina gehienak MPk izanik, erauzketa egiteko orduan *Qiagen BioRobot 8000*an erabili ohi den protokoloa MPentzat moldatu egin zen (Bird, 2011).

Bi estrategien bidez (IPTG eta TBONEX medioa, alegia) lorturiko zelula jalkinak desizoztu eta 200 µl *NPI-10-Tween indargetzaile*rekin berreseki ziren, jarraian 4°C-tan 20 minutuz irabiaketa orbitalarekin inkubatuz. Lehenengo 10 minutuen ostean, laginei lisozima eta DNasa I (*DNase I*) gehitu zitzaien, 1 mg/mL eta 400 U/mL kontzentrazioetan, hurrenez hurren; 20 minutu igaro ondoren laginei %1 (p/b) *n-Dodecyl-β-D-maltopyranoside* (DDM) eta proteasa inhibitzaileen koktela gehitu zitzaien. Laginak beste ordu batez baldintza berdinetan inkubatu ostean zentrifugatu ziren (6.000 *g*, 30 min, 4°C) jalkina deuseztatuz, non apurtu gabeko zelulak zeuden. Lorturiko gain-jalkinak behealde-laueko 96-putzutako plaka batera igaro ziren putzu bakoitzak Ni-NTA *bead* magnetikodun esekidura baten 20 µL zituelarik. Ondoren aldez aurretik ezarritako protokoloa jarraitu zen, baina indargetzaile guztiei DDMa gehituz.

96-putzutako plaka *Qiagen BioRobot 8000*ren imanaren gainean minutu batez kokatu zen eta putzu bakoitzeko gain-jalkina deuseztatu zen. Ondoren putzu bakoitzean zeuden *bead* magnetikoak 200 µL *NPI-20 Tween-DDM indargetzailea* erabiliz garbitu ziren. Horretarako, plaka berriz imanaren gainean minutu batez kokatu zen eta gain-jalkina deuseztatu zen, prozesua birritan errepikatuz. Behin garbiketak eginda, putzu bakoitzari 50 µL *NPI-250 Tween-DDM* gehitu zitzaizkion, jarraian plaka minutu batez irabiatzailearen gainean kokatuz eta ondoren beste minutu batez imanaren gainean. Bukatzeko, gain-jalkinak (eluituriko proteinak zituztenak) plaka garbi batera igaro ziren.

Metodo honen bidez erauzitako proteinak SDS-PAGE bidez aztertu ziren. Horretarako, lagin bakoitzetik 10 µL hartu eta 10 µL *proteina karga indargetzaile II*-rekin nahastu ziren. Nahasketa bakoitzetik 10 µL kargatu ziren *NuPAGE™Novex 10% Bis-Tris Midi* gel komertzialetako kale bakoitzean. Elektroforesia *MES indargetzailea*n 45 minutuz 200 V-tan burutu zen. Ondoren gelak *Instant Blue*-rekin ordu batez tindatu ziren eta destindatzeko ur-destilatuarekin behar bezain beste garbiketa burutu ziren.

2.5.1.2. eGFP BIDEZKO GAIN-ADIERAZPENAREN AZTERKETA

MPen gain-adierazpenaren optimizazioa burutzeko estrategia desberdinak garatu egin dira, haien artean zelula-andui espezifiko edota hobeturiko proteina berde fluoreszenteen (*enhanced Green Fluorescence Protein,* eGFP) fusio-proteinen erabilera. Azken estrategia honek adierazpenaren jarraipen zuzen, azkar eta kuantitatiboa burutzea ahalbidetzen du (Drew et al., 2001). Izan ere, eGFP domeinuak fluorokromo izaera soilik dauka modu egokian tolesturik aurkitzen denean, beraz fusio-proteina baten kasuan proteina osoa era egokian tolesturik aurkitu behar da fluoreszentzia izateko. Honetan oinarrituz, zelula kultiboen fluoreszentzia azter daiteke, modu egokian tolesturiko itu-proteina kantitatearekin zuzenean erlazionatzen dena.

Entsegu hau $MobB_{CloDF13}$ eta $TMD_{TrwB}TraJ_{pIP501}$ proteinekin burutu zen, aldez aurretik ezarritako protokoloa jarraituz aldaketa gutxi batzuekin (Drew et al., 2008). Lehenengo eta behin itu-proteinen eGFP fusio-proteinak lortu ziren eta konstruktoekin zelulen transformazioak egin ziren. Biak MPak izanik, *E. coli* BL21C41(DE3) eta Lemo21(DE3) anduiak erabiltzea erabaki zen, proteina mota honen gain-adierazpenerako egokiak baitira bereziki. BL21C41(DE3) zelulen kasuan indukzio osteko hazkuntza bi tenperaturetan egin zen, 25 eta

30°C-tan. Lemo21(DE3)-ren kasuan indukzioa 30°C-tan egin zen, baina T7 lisozimaren ekoizpena erregulatu zen, rhamnosa bidez induzigarria zena. Bi kasu hauetan proteinaren adierazpena LB eta PB kultibo medioetan aztertu zen.

Entsegua burutzeko zelula kolonia bana antibiotiko egokiekin osatutako 2 mL LB edo PB-en hazi zen gau osoan zehar 37°C-tan. Hurrengo egunean 1:50 diluzioak egin ziren (200 µL kultibo 10 mL antibiotikodun LB edo PBn) eta zelulak OD_{600} 0,4ko balioa lortu arte 37°C-tan hazi ziren. Orduan kultiboak 0,4 mM IPTGrekin induzitu ziren eta Lemo21(DE3) zelulen kasuan rhamnosa ere gehitu zitzaien kontzentrazio jakinetan (0, 100, 200, 250, 500, 1000 edo 2000 µM). Proteinen indukziorako tenperatura egokia ezarri zen (25 edo 30°C) eta zelulak gau osoan zehar hazi ziren. Indukzio osteko adierazpen maila 4 ordu eta 20 ordu igaro ondoren aztertu zen. Horretarako hiru lagin desberdin hartu ziren: alde batetik OD_{600} neurtzeko, beste aldetik SDS-PAGE eta WBak burutzeko eta azkenik fluoreszentziaren azterketa egiteko.

Elektroforesia burutzeko, 500 µL kultibo zentrifugatu ziren (6.000 *g*, 5 min, 4°C). Ondoren gain-jalkina deuseztatu eta zelula jalkina OD_{600} 0,2ra berreseki zen SAB 3X *proteina karga indargetzailea*n (SAB 6X: H_2O nahasketa 1:1 (b/b) erlazioan). Lagin hauetatik 15 µL gehitu ziren bi SDS-PAGE geletara, gel bat coomassie bidezko tindaketa egiteko eta bestea WBerako.

Fluoreszentziaren azterketarako 1 mL zelula kultibo zentrifugatu zen (6.000 *g*, 5 min, 4°C). Jalkina 100 µL *PBS*rekin berreseki eta izotzetan 15 minutuz inkubatu zen. Ostean 900 µL *PBS* gehitu eta lagina berriz zentrifugatu, berreseki eta baldintza berdinetan inkubatu zen. Zelula suspentsioa 96 putzutako plaka batera igaro zen eta neurketa *SinergyHT* plaka irakurle batean burutu zen, *Gen5* softwarea erabiliz. Laginak 485 nm-tan kitzikatu ziren eta fluoreszentzia igorpena 512 nm-tan jaso zen.

2.5.2. PROTEINEN PURIFIKAZIOA

Proteina baten purifikazioa bere karakterizaziorako eman behar den lehenengo pausua da, gainerako kutsatzaile proteikorik gabe lan egitea ahalbidetzen duelako. Tesi honetan aztertutako proteina desberdinen purifikazio protokoloak garatzeko, $TrwB_{R388}$ proteinarentzat ezarritakoa erabili egin zen abiapuntu gisa (Vecino et al., 2010).

Protokolo bat garatu aurretik komenigarria da ahalik eta informazio gehien izatea itu-proteina eta berarekin erlazionaturiko proteinei buruz, hau lagungarria baita purifikazio protokoloan erabiliko diren teknika kromatografiko egokienak aukeratzeko. Tesi honetan tresna bioinformatikoak erabili ziren proteinen ezaugarri orokorrak aztertzeko. Honetarako ExPASy baliabide bioinformatikoen ataria erabili egin zen (https://www.expasy.org/), batez ere UniprotKB (https://www.uniprot.org/) eta ProtParam (https://web.expasy.org/protparam/). Hauetaz gain mintz-proteinen topologiaren azterketa burutzeko TOPCONS (http://topcons.cbr.su.se/) softwarea erabili egin zen (Tsirigos et al., 2015).

2.5.2.1. HASIERAKO PAUSU AMANKOMUNAK

GAIN-ADIERAZPENA ETA ZELULEN UZTA

Purifikazioa burutzeko, lehenengo eta behin gain-adierazpenerako egokiak diren zelulak itu-proteina kodetzen duen konstruktoarekin transformatu ziren. Ondoren zelula hauen aurre-kultibo bat burutu zen, zelulak antibiotikoekin osatutako LB bolumen txiki batean haziz gau osoan zehar, 37°C-tan. Hurrengo egunean zelula hauek 1:50 erlazioan diluitu eta 37°C-tan hazten utzi ziren kultiboa hazkuntza esponentzialeko puntu egokira heldu arte, OD_{600} bidez neurtu zena. Une horretan proteinaren ekoizpena martxan jarri zen IPTG bidezko indukzioz.

Behin proteinaren indukzioa eginda zelulak tenperatura eta denbora jakinean inkubatu ziren. Ondoren zelulen uzta egin zen zentrifugazio bidez (8.000 *g*, 15 min, 4°C). Zelula jalkina *zelula indargetzailea*n berreseki zen (orokorrean 20 mL/zelula kultibo L-ko) eta lortutako zelula suspentsioak nitrogeno likidorekin izoztu eta -80°C-tan biltegiratu ziren haien erabilpenera arte.

ZELULEN LISIA

Izoztutako zelula suspentsioak 37°C-ko ur-bainuan desizoztu ziren. Ondoren zelulen lisia egin zen, metodo entzimatiko edota mekanikoen bidez. Lisi entzimatikoan lagina %0,07 (p/b) lisozimarekin inkubatu zen, 4°C edo izotzetan, 30-45 minutuz. Pausu honetan proteinen egonkortasunerako lagungarriak diren erreaktiboak gehitu ziren protokoloaren arabera, haien artean ditiotreitol agente erreduktorea (DTT), $MgCl_2$, DNasa I, proteasen inhibitzaileak [fenilmetanosulfonil fluoruroa (PMSF)] edota proteasen koktel inhibitzaileak.

Lisi entzimatikoaren ostean zelulen lisi mekanikoa egin zen, lagina tartekatu ziren bi alikuotetan bananduz eta *MSE Soniprep 150* sonikadorea erabiliz. Purifikazio protokolo gehienetan lau aldiz errepikatutako 10 ziklo egin ziren. Ziklo bakoitzean 10 segundoz sonikatzen zen, 10 segundoz atseden eginez, laginaren beroketa ekiditeko. Izan ere, sonikazioak laginaren tenperatura igotzen du, proteinen agregazioa eragin dezakeena. Hori dela eta, laginak ur-izotz bainuan mantendu ziren sonikazio prozesu osoan zehar. Bukatzeko laginaren zentrifugazioa burutu zen (8.000 *g*, 15 min, 4°C) apurturiko eta apurtu gabeko zelulen banaketa lortzeko.

Proteina solugarrien purifikazioa egiterakoan azken zentrifugazio hori ultrazentrifugazio (105.000 *g*, 45 min, 4°C) batekin ordezkatu zen. Modu horretan apurtu gabeko zelulekin batera, inklusio gorputzak eta mintz-frakzioa ere jalkitzen ziren, gain-jalkinean proteina solugarriak soilik geratuz.

2.5.2.2. MINTZ-PROTEINEN SOLUBILIZAZIOA

MPen purifikazioa konplexuagoa da, hauek mintz-plasmatikotik erauzi behar direlako. Oro har, proteina hauen erauzketarako detergenteak erabiltzen dira mintza solubilizatzeko gai direlako, proteina-detergente , lipido-detergente eta lipido-proteina-detergente konplexuak sortuz.

Lehenengo eta behin mintz-frakzioa proteina solugarrietatik banandu zen, apurturiko zelulen gain-jalkina zentrifugatuz (105.000 *g*, 45 min, 4°C). Zelulen mintz-frakzioa jalkinean geratu zen, kontu handiz berreseki zena, zentrifuga saiodiak izotzetan mantenduz. Honetarako 19,6 mM DDM, 600 mM NaCl eta 0,1 mM PMSFrekin osatutako indargetzailea (*solubilizazio indargetzailea*) erabili zen. Hazitako zelula litroko 10 mL *solubilizazio indargetzaile* erabili ziren, hau da, 4 L zeluletik lortutako mintz frakzioa 40 mL-tan berreseki zen. Mintz-suspentsioa 90 minutuz 4°C-tan irabiaketa leunarekin inkubatu ostean, berriro zentrifugatu zen (105.000 *g*, 60 min, 4°C) solubilizaturiko MPak gain-jalkinean lortuz.

2.5.2.3. TEKNIKA KROMATOGRAFIKOAK

Proteina bat lehenengo aldiz purifikatzerakoan metodoaren aukeraketa enpirikoa egin behar da, baita zenbait protokolo saiatu optimoa aurkitu arte ere. Entsegu kopurua murriztearren, aldez aurretik purifikaturiko eta antzeko propietateak dauzkaten proteinen protokoloak erabili ohi dira abiapuntu gisa. Aurreko pausuetan lorturiko erauzkin gordinetik itu-proteina isolatzeko teknika desberdinak daude, proteinaren propietate espezifikoetan oinarritzen direnak. Hauen artean erabilienak teknika kromatografikoak dira. Era berean kromatografia mota desberdinak daude, zeinetan proteinen banaketa propietate fisiko desberdinen arabera egiten den. Normalean proteina bat purifikatzeko orduan, kromatografia mota desberdinen konbinazioak erabili ohi dira. Tesi honetan ioi-truke, afinitatezko eta gel-iragazpeneko kromatografiak erabili egin dira. Orokorrean kromatografia zutabeak *ÄKTA-FPLC* sistemetara konektatu ziren eta proteinen eluzioa absorbantzia 280 nm-tan neurtuz jarraitu zen.

IOI TRUKEZKO KROMATOGRAFIA: P-11 FOSFOZELULOSA ERRETXINA

Whatman® P-11 fosfozelulosazko erretxina zelulosa sare bati atxikituriko ortofosfato ioiez osaturik dago. Ioi hauek negatiboki kargaturik aurkitzen dira pH 4tik aurrera, hori dela eta, erretxina hau ioi truke kationikoko kromatografiak burutzeko egokia da.

Erretxina etxe komertzialaren argibideak jarraituz prestatu egin zen. 70 mL erretxina lortzeko, 18 g fosfozelulosa 0,5 M NaOH 25 bolumenekin nahastu ziren, irabiaketa leunarekin 5 minutu mantenduz. Erretxina jalkitzen utzi zen, gain-jalkina deuseztatu eta jarraian Milli-Q urarekin garbiketak errepikatuz, gain-jalkinaren pHa 11 edo baxuagoa izan arte. Orduan, erretxina 0,5 M HCl disoluzio batekin nahastu zen, 5 minutuz inkubatuz. Ondoren, Milli-Q urarekin garbiketak errepikatu ziren pH 3 lortu arte. Bukatzeko, erretxina 50 mM Tris-HCl (pH 7,8) disoluzioarekin orekatu eta 4°C-tan ilunpetan biltegiratu zen. Kromatografia bakoitzean erretxina berria erabili egin zen, errendimendu egokia lortzeko.

Aktibaturiko erretxinarekin tamaina egokiko zutabe bat paketatu zen (70 mL erretxina 4 zelula litro kultibotik lorturiko erauzkin gordineko) ponpa peristaltiko baten laguntzaz. Jarraian erretxina kromatografia indargetzailearen bi bolumenekin orekatu zen. Lagina gau osoan zehar zutabetik 4°C-tan birzirkulatzen utzi zen. Ondoren oreka indargetzailearen bi bolumen igaro ziren erretxina ez-espezifikoki itsatsitako proteina kutsatzaileetatik garbitzeko. Azkenik erretxinari lotutako proteinaren eluzioa burutu zen *ÄKTA-FPLC* batean, kasu bakoitzerako protokolo egokia jarraituz.

AFINITATEZKO KROMATOGRAFIA: *HisTrap™ FF*

Immobilizaturiko metalen bidezko afinitate kromatografian (*Immobilized Metal Affinity Chromatography,* IMAC) trantsiziozko metalak, hala nola Ni^{2+}, erretxina ez-disolbagarri batean immobilizatzen dira. Nikel ioiek histidinen albo-kateetan dauden elektroi taldeekin elkarrekintzak burutzen dituzte. Elkarrekintza hauen bidez loturiko proteinen eluzioa burutzeko, imidazoldun indargetzaileak erabili ohi dira, imidazolak histidinekin lehiatzen baitu nikel ioiekin elkarrekiteko. Printzipio hauetan oinarrituz, purifikazio prozesua errazten duten histidina ugariko kateak kokatu ohi dira itu-proteinetan. Hain zuzen ere, tesi honetan erabilitako proteina guztiek, TrwBΔN70k izan ezik, karboxilo muturrean sei edota zortzi histidinetako katea aurkezten dute eta *HisTrap™ FF* zutabe bidez purifikatu egin dira.

Nahiz eta proteina bakoitzerako protokolo jakin bat jarraitu, orokorrean nikeldun erretxina kromatografia imidazol kontzentrazio baxuko indargetzailearen bi zutabe-bolumenekin orekatu zen eta lagina gau osoan zehar zutabetik igarotzen utzi zen, batura-errendimendu ona lortzeko. Ondoren *ÄKTA-FPLC* sistema bat erabiliz, ez-espezifikoki itsatsitako proteinen garbiketa egin zen, oreka indargetzailearen 10 bolumen erabiliz. Bukatzeko, imidazol kontzentrazio altuagoko indargetzaile bat erabiliz erretxinari loturiko proteinen eluzioa egin zen.

Erabilera bakoitzaren ostean zutabearen garbiketa eta birsorkuntza egin zen ponpa peristaltiko baten laguntzaz. Horretarako zutabetik 25 mL *disoluzio birsortzaile* igaro arazi ziren, ondoren 15 mL Milli-Q ur eta bukatzeko 10 mL etanol (zutabea 4°C-tan biltegiratzeko). Zutabea berrerabiltzeko zutabetik banan-banan 15 mL Milli-Q ur, 2,5 mL *nikel disoluzio*, 20 mL Milli-Q ur eta 10 mL kromatografia indargetzaile (itu-proteinaren araberakoa) igaro ziren, orden horretan.

GEL-IRAGAZPENEKO KROMATOGRAFIAK

Gel-iragazpeneko kromatografietan (*Size-exclusion chromatography,* SEC) fase geldikorra tamaina jakineko poroak dauzkan erretxina batez osatua dago, hori dela eta, biomolekulak haien tamainaren arabera banandu egiten dira. Horren arabera, proteinen tamainak proteinak zutabean zehar egiten duen ibilbidea ezartzen du; handienak ibilbide laburragoa eginez, erretxinaren poroetatik ezin baitira sartu. Aurretik azaldutako bi kromatografien kasuan, proteinek erretxinarekin elkarrekintzak sortzen dituzte, haietara lotuta geratuz. SECetan, ordea, ez da proteina eta erretxinaren artean elkarrekintzarik sortzen.

Bereizmen ahalmen desberdineko erretxinak daude, itu-proteinaren tamainaren eta deuseztatu nahi diren gainerako proteinen arabera aukeratzen direnak. Tesi honetan

Superosa-6 (5-5.000 kDa) eta *Superdex-200* (10-600 kDa) erretxinak erabili dira bolumen desberdinetako zutabeetan, laginaren eta helburuaren arabera hautatu zirenak.

SECak burutzeko, etxe komertzialaren gomendioak jarraitu ziren fluxu eta lagin bolumenari dagokienez. Lehenengoz zutabea indargetzaile egokiaren bi zutabe bolumenekin orekatu zen. Bitartean, laginak zentrifugatu ziren agregatuak deuseztatzeko (17.000 *g*, 10 min, 4°C). Ondoren, bolumen egokiko lagina (zutabearen tamainaren araberakoa) zutabera txertatu zen eta oreka indargetzaile bera erabiliz kromatografia burutu zen.

Tesi honetan *Superose 6 PC 3.2/30* eta *10/300 GL* zutabeak erabili dira aldez aurretik purifikaturiko proteina lagin batean egon daitezken egoera oligomeriko desberdinak aztertzeko. Itu-proteinen eta haien oligomero desberdinen pisu molekularra ezagutzeko, pisu molekular ezaguneko proteina nahasketa erabili ohi da patroi gisa. Kasu honetan, zutabearen kalibrazioa egiteko Sigmako kit komertzialen nahasketa bat erabili zen, pisu molekular desberdineko proteinak nahastuz: Tiroglobulina (669 kDa), Ferritina (440 kDa), Aldolasa (128 kDa), Konoalbumina (75 kDa), Erribonukleasa A (13,7 kDa) eta Aprotinina (6,5 kDa). Zutabeen bolumen hila kalkulatzeko Urdin-dextrano 2000 (1 mg/mL) erabili zen. Hau polisakarido konplexu bat da, zeinaren pisu molekularra bereizmen tartetik gora dagoen.

Kromatografia mota hauek lagineko indargetzailea aldatzeko ere erabili ohi dira, izan ere, indargetzaile aldaketa burutzeko zutabe komertzial espezifikoak daude. Lan honetan *Sephadex G-25* erretxinako *PD SpinTrap* eta *PD-10 desalting* zutabeak erabili egin dira helburu honekin, bolumen txikiko (100-180 µL) eta erdiko (1,75-2,5 mL) laginetan indargetzailea aldatzeko, hurrenez hurren. Entsegu hauek etxe komertzialak gomendatutako protokoloak jarraituz egin ziren.

2.5.2.4. PROTEINAK KONTZENTRATZEKO TEKNIKAK

Tesi honetan proteinak kontzentratzeko 15 mL-tako *Amicon® Ultra* amikoiak erabili egin dira, proteina bakoitzaren pisu molekularraren araberako iragazkiak (*Molecular weight cut-off*, MWCO) erabiliz (15, 30, 50 edo 100 kDa). Lehenengo eta behin amikoia Milli-Q urarekin zentrifugatu zen (2.850 *g*, 5 min, 4°C). Ondoren ura deuseztatu eta izotzetan hoztutako lagina gehitu zen. Lagina, lortu nahi zen kontzentrazio edo bolumen finalaren arabera, denbora aldakorrean zentrifugatu zen (2.850 *g*, 4°C). Kontzentrazio prozesu luzeetan 15 minututako zentrifugazio txandak egin ziren, bi txanden artean lagina berresekiz, iragazkian proteinaren agregazioa saihesteko. Behin bolumen egokia lortuta lagina *eppendorf* saiodietara igaro zen bertan azkeneko zentrifugazio bat burutuz (13.000 *g*, 10 min, 4°C) proteina kontzentratzeko prozesuan sortutako agregatuak kentzeko.

2.5.2.5. $TrwA_{R388}$ren PURIFIKAZIOA

$TrwA_{R388}$ proteinaren purifikazioa egiteko aldez aurretik deskribaturiko protokoloa erabili zen, aldaketa gutxi batzuekin (Moncalián et al., 1997). *E. coli* BL21(DE3) zelula konpetenteak pSU1547 plasmidoarekin transformatu ziren. Zelula koloniak anpizilinadun 10 mL LBn hazi ziren gau osoan zehar 37°C-tan. Goizean, kultiboen 1:50 diluzioa burutu zen (guztira 3 L zelula suspentsio haziz 500 mL-tako matrazetan) eta berriz 37°C-tan hazten utzi

ziren. OD_{550} 0,6-0,8 balioa lortzerakoan matrazeei 1 mM IPTG gehitu zitzaien proteinaren gain-adierazpena martxan jartzeko eta bost orduz 37°C-tan inkubatu ziren. Ondoren zelulen uzta egin zen zelula suspentsioak zentrifugatuz (8.000 *g*, 15 min). Jalkina 120 mL *TrwA1 indargetzailea*n berreseki, nitrogeno likido bidez izoztu eta -80°C-tan biltegiratu zen.

Purifikazio prozesurako zelulak ur-bainuan desizoztu ziren eta ur-izotz bainuan mantentzen ziren bitartean, *MSE Soniprep 150* sonikatzaile bat erabiliz lisatu ziren. Horretarako 14-15 mikroietako anplitudea erabili zen, 10 segundo pizturik, 10 segundo amataturik tartekatzen zituen 10 ziklo burutuz. Ondoren lagina bitan banandu zen eta protokolo bera birritan errepikatu zen alikuota bakoitzeko. Bukatzeko, azken sonikazio bat burutu zen bi laginak elkartuz. Lortutako zelula suspentsioa zentrifugatu zen (105.000 *g*, 25 min, 4°C) eta lortutako gain-jalkinari imidazola gehitu zitzaion, bukaerako kontzentrazioa 20 mM imidazol izan arte. Erauzkin gordin hori, aldez aurretik nikelarekin kargaturiko eta *TrwA2 purifikazio indargetzailea*rekin orekaturiko 5 mL-tako *HiTrap Chelating FF* zutabe batera gehitu zen. Erretxina 15 mL indargetzaile berarekin garbitu ostean, zutabea *ÄKTA-FPLC* batean konektatu zen eta bertatik proteina eluitu zen. Proteinaren eluziorako 2,5 mL-ko fluxua erabiliz 100 mL-ko 20-500 mM imidazoleko gradientea erabili zen, *TrwA2* eta *TrwA3 purifikazio indargetzaileak* erabiliz. Zutabetik 2 mL-ko frakzioak jaso ziren eta haietan $TrwA_{R388}$ren presentzia SDS-PAGE bidez aztertu zen. Itu-proteina zuten frakzioak elkartu eta *Amicon Ultra-15 YM-30* bat erabiliz kontzentratu ziren, 2,2 mL-ko bolumena lortu arte. Lagina zentrifugatu (17.000 *g*, 10 min, 4°C) eta aldez aurretik *TrwA4 purifikazio indargetzailea*rekin orekaturiko *Superdex HR 75 16/60 HiLoad* gel-iragazpeneko zutabe batean injektatu zen. Horretarako, 2 mL lagin xiringatu ziren eta indargetzaile bera erabili zen proteinaren eluziorako, 1 mL/min-ko fluxuan, 2 mL-ko frakzioak jasoz. TrwA aurkezten zuten frakzioak elkartu eta 4°C-tan gorde ziren haien erabilpenera arte.

2.5.2.6. TrwBΔN70ren PURIFIKAZIOA

Jarraitutako protokoloa Tato et al. (2005) artikuluan deskribaturikoa izan zen, baina indargetzaileetan $MgCl_2$ gehitu barik. BL21C41(DE3) anduia erabili zen, pSU4637 plasmidoarekin transformatua. Zelula hauekin anpizilinarekin osaturiko 10 mL LBdun zortzi matraze hazi ziren gau osoan zehar 37°C-tan. Hurrengo egunean 1:50 diluzioak burutu ziren, guztira 4 L zelula suspentsio lortuz 500 mL-dun zortzi matrazetan. Zelula esekidurei OD_{550} 0,6-0,8 balioa lortu zutenean 1 mM IPTG gehitu zitzaien. Proteinaren adierazpenaren indukzioa 4 orduz 37°C-tan egin zen. Zelula suspentsioak zentrifugatu (8.000 g, 15 min, 4°C) ostean, jalkina 60 mL *TrwBΔN70-1 purifikazio indargetzailea*rekin berreseki, nitrogeno likidorekin izoztu eta -80°C-tan biltegiratu zen.

Purifikazio prozesurako zelulak 37°C-ko ur-bainuan desizoztu ziren. Ondoren, laginei lisozima 0,8 mg/mL eta 2,5 mM benzamidina gehitu zitzaien zelulen lisia emateko eta proteolisia saihesteko, hurrenez hurren. Puntu honetatik aurrera, pausu guztiak 4°C-tan burutu ziren. Lagina 45 minutuz izotzetan inkubatu ostean, *TrwBΔN70-2 purifikazio indargetzailea*rekin diluitu zen 1:1 erlazioan, irabiaketa bidez nahastuz eta azkenik zentrifugatuz (138.000 *g*, 30 min, 4°C).

Aurreko zentrifugazioan lortutako gain-jalkina *TrwBΔN70-1 purifikazio indargetzailea*rekin diluitu zen, bukaerako NaCl kontzentrazioa 150 mM izan arte. Lagina 1 mL/min-ko fluxuarekin 35 mL-tako fosfozelulosa P-11 zutabe batean gehitu zen. Kasu honetan *TrwBΔN70-3 purifikazio indargetzailea* erabili zen zutabea orekatzeko eta garbitzeko. Proteinaren eluziorako, berriz, 60 mL *TrwBΔN70-4 purifikazio indargetzaile* erabili ziren. Jasotako frakzioak SDS-PAGE bidez aztertu ziren. Honela, itu-proteina zuten laginak elkartu eta *TrwBΔN70-1 purifikazio indargetzailea*rekin diluitu ziren bukaerako kontzentrazioa 150 mM NaCl izan arte. Jarraian, 5 mL-ko *Hitrap-SP* zutabea 15 mL *TrwBΔN70-3 purifikazio indargetzailea*rekin orekatu zen lagina bertan kargatzeko 1 mL/min-ko fluxuan. Ondoren, zutabea indargetzaile berarekin garbitu zen. TrwBΔN70ren eluziorako, 150 mM eta 1 M tarteko NaCl gradientea erabili zen, 120 mL-tan eta 2,5 mL/min-ko fluxuan. Kromatografiatik 2 mL-tako frakzioak jaso, SDS-PAGE bidez aztertu zirenak. Itu-proteina zeukatenak elkartu eta *Amicon Ultra-15 YM-30* bat erabiliz kontzentratu ziren, bukaerako lagin bolumena 5 mL izan arte. Jarraian, laginean egon zitezkeen agregatuak zentrifugazio bidez (100.000 *g*, 20 min, 4°C) kendu egin ziren. Ondoren, aldez aurretik 240 mL *TrwBΔN70-5 purifikazio indargetzailea*rekin orekaturiko *Hi Load 26/60 Superdex 200* gel-iragazpeneko kromatografia zutabean 2,5 mL lagin xiringatu ziren. Kromatografia indargetzaile berdina erabiliz burutu zen, 2 mL-tako frakzioak jasoz. Prozesua gainontzeko 2,5 mL-ak xiringatuz errepikatu zen.

Lortutako frakzioak SDS-PAGE bidez aztertu eta TrwBΔN70 zuten laginak elkartu ziren. Laginari glizerola gehitu zitzaion %20 (b/b)-era doituz eta nitrogeno likido bidez izoztu ziren alikuotak gin ziren. Bukatzeko, TrwBΔN70 proteinadun alikuota hauek -80°C-tan biltegiratu ziren bere erabilerara arte.

2.5.3. PROTEINEN KONTZENTRAZIOAREN DETERMINAZIOA

Edozein entsegu burutzeko proteinen kontzentrazio zehatzak ezagutu egin behar dira. Horretarako lan honetan hiru teknika desberdin erabili egin dira: 280 nm-tan absorbantzia neurtuz, Bradford saiakuntza bidez (Bradford, 1976) eta azido bizinkoninikoan (*Bicinchoninic acid*, BCA) oinarrituriko kit komertziala erabiliz.

2.5.3.1. 280 nm-tako ABSORBANTZIAREN NEURKETA

Tirosina eta triptofano aminoazido aromatikoei esker proteinek 280 nm-tan ultramore absortzio espektro berezia aurkezten dute. Horretaz gain, proteinetan egon daitezken fenilalanina aminoazido aromatikoek eta disulfuro zubiek ere eragin ahula izan dezakete uhin luzera honetako absorbantzian. Honetan oinarrituz eta Lambert-Beer ekuazioa erabiliz (2.1. ekuazioa), soluzioan dagoen proteina jakin baten kontzentrazioa determinatu daiteke. Honetarako, proteina bakoitzaren absortzio-koefiziente molar teorikoa (ε) *ProtParam* erreminta bioinformatikoaren bidez kalkulatu zen. Absorbantziaren neurketa *NanoDrop Lite Spectophotometer* bat erabiliz egin zen.

$$Absorbantzia = \varepsilon \times c \times l$$

2.1. ekuazioa. Lambert-Beer ekuazioa. ε: absortzio koefiziente molarra ($M^{-1} cm^{-1}$), c: molekula aktiboen kontzentrazioa (M), l: argiak laginean zehar burutzen duen ibilbidearen luzera (cm).

2.5.3.2. BRADFORD SAIAKUNTZA

Teknika hau *Coomassie Brilliant Blue* molekularen propietate espektroskopikoetan oinarritzen da, proteinekin elkarrekiten duenean bere absorbantzia 465 nm-tatik 595-nm-tara lekualdatzen baita. 2 mg/mL-ko behi serumaren albumina (*Bovine serum albumin,* BSA) erabiliz patroi zuzena egin zen, 0 eta 16 µg artean, bolumena 100 µL-ra doituz. Laginak 1:10 erlazioan purifikazio infargetzailearekin diluitu ziren, bolumena era berean doituz. Saiodi bakoitzera 1 mL Bradford erreaktibo (1:5 diluzioan) gehitu zen, ondo nahastuz eta 15 minutuz giro tenperaturan inkubatuz. Patroia eta laginen absorbantzia 595 nm-tan neurtu zen *Jenway 6300* espektofotometroa erabiliz.

2.5.3.3. *BCA™ PROTEIN ASSAY KIT*

BCA metodoa burutzeko Smith et al. (1985) deskribaturiko entseguaren aldaera bat erabili zen, *BCA™ Protein Assay Kit* komertziala erabiliz. Horretarako BSA erabiliz 0 eta 12 µg arteko patroi zuzena egin zen eta purifikaturiko laginak (itu-proteinak zituztenak) diluitu ziren.

Entsegua 96 putzutako plaka batean burutu zen. Zuzen patroiko lagin bakoitzetik 25 µL gehitu ziren eta aztergai ziren laginetik 2 µL (purifikaturiko laginen kasuan 1:10 erlazioan diluiturik zeudenak). Azken hauei 23 µL indargetzaile gehitu zitzaien (proteinak zuen indargetzaile bera). Ondoren putzu bakoitzari 200 µL BCA erreaktibo gehitu zitzaien eta plaka 37°C-tan 30 minutuz inkubatu zen. Bukatzeko absorbantzia 562 nm-tan neurtu zen *PowerWave™ XS* plaka irakurle batean, *Gen5* softwarea erabiliz.

2.5.4. PROTEINEN BILTEGIRATZEA

Behin proteinen erauzketa prozesua eginda, hauek -80°C-tan biltegiratu ziren erabiliak izan arte. Horretarako purifikaturiko laginei glizerola gehitu zitzaien %20 (b/b) bukaerako kontzentrazioa izan arte. Bolumen egokiko alikuotak egin ziren, nitrogeno likido bidez izoztu zirenak eta -80°C-tan gorde egin zirenak.

2.6. PROTEINEN KARAKTERIZAZIOA

2.6.1. ESPEKTROSKOPIA INFRAGORRIA

Espektroskopia infragorria (*Infrared spectroscopy*, IRS) nahiz eta bereizmen altuko teknika ez izan, proteinen bigarren mailako egiturari buruzko informazioa eskaintzen duen teknika da. Horretarako, izpi-infragorrien absorbantzia burutzen da (10.000 eta 100 cm^{-1} artean) sistema interferometriko bat erabiltzen duten tresnen bidez. Espektroaren zarata murrizteko eta haien harrera azkartzeko, Fourier bidezko izpi-infragorrien eraldaketa izeneko prozesu matematikoa erabiltzen da (Arrondo et al., 1993; Goméz-Moreno Caleras and Sanz, 2003). Teknika hau oso erabilgarria suertatu da proteinen konformazio eta dinamikaren azterketan. Bere oinarria izpi-infragorrien absorbantzia egitean lotura atomikoek pairatzen dituzten bibrazio eta errotazioen aldaketen azterketa da. Proteinen egituran dauden patroi

errepikakorrei esker, espektroak espero baino sinpleagoak dira eta bibrazio frekuentzien eta egitura motiboen artean erlazio bat ikusten da. IRS oso erabilgarria da MPen azterketa burutzerakoan, proteinaren tamaina edota ingurune lipidikoak ez dutelako eraginik (Arrondo eta Goñi, 1999). Horretaz gain, espektroskopia mota honetan itu-proteinari ez zaio inolako zundarik gehitu behar.

Biomolekulen talde funtzional eta loturek bibrazio oso zehatzak aurkezten dituzte. Proteinen kasuan lotura peptidikoak eragiten duen amida banda da ezagunena. Banda honen barruan bibrazio talde desberdinak bereiz daitezke amida I banda izanik erabiliena, konformazio aldaketen aurrean erakusten duen sentikortasunagatik eta albo kateek beregan daukaten eragin urriagatik. Izan ere, amida I banda proteinan aurkezten diren bigarren mailako egitura desberdinen seinaleen gainjartzearen ondorioa da. Bigarren mailako egitura bakoitzak uhin-luzera jakinetan burutzen du izpi infragorrien absorbantzia, hori dela eta proteinaren ikerketa burutzeko amida I bandaren deskonposaketa egin ohi da.

Ur-disoluzioetan IRS neurketak burutzea zailtasunak dakartza, urak proteinek argiaren absorbantzia burutzen duten uhin-luzeretan interferentziak sortzen baititu. Hau saihesteko metodorik arruntena ur astunaren erabilera da (D_2O), honek argia uhin-luzera txikiagoetan xurgatzeko ahalmena baitu. Hala ere, aldaketa burutzea konplexua izan daiteke, prozesuan zehar proteinen desnaturalizazioa gerta daitekelako. D_2O indargetzaileak lortzeko lehenengo entseguan, ur-disoluziozko indargetzaileak liofilizatu ziren, baina teknika hau ez zen egokitzat suertatu detergenteen presentzia zela eta; beraz, zuzenean D_2O indargetzaileak prestatzea erabaki zen.

MobBΔTMD proteina disolbagarriaren indargetzaile aldaketa dialisi bidez egin zen. Horretarako MobBΔTMDren purifikazio indargetzailea prestatu zen glizerolik gabe (neurketetan zailtasunak sortu ditzakeena) eta D_2O-a erabiliz H_2O-ren tokian (*MobBΔTMD IRS indargetzailea*). Ondoren indargetzaile hori erabiliz lagina 5 mg/mL proteina kontzentraziora diluitu zen. Hortik 170 µL hartu eta 1 mL *MobBΔTMD IRS indargetzaile*rekin dializatu ziren, *D-Tube™ Dyalizer Midi* (MWCO 3,5 kDa) bat erabiliz, 4°C-tan, bi indargetzaile aldaketa burutuz 2 orduro (guztira 3 mL indargetzaile erabiliz). Lortutako lagina 75 µL-tako amaierako bolumenera kontzentratu zen, IRS bidez aztertu zena.

$MobB_{CloDF13}$ren kasuan estrategia bera erabili zenean, proteina agregatu egin zen. Hori dela eta, dialisi ordez D_2O indargetzailearekin diluitzea eta ondoren kontzentratzea erabaki zen. 40 µL lagin (10,6 mg/mL proteina kontzentrazioan) *MobB IRS indargetzaile*rekin diluitu ziren 200 µL-ko bolumenera doituz. Ondoren lagina 120 µL-ra kontzentratu zen, 0,5 mL-tako edukiera eta 100 kDa-eko poro tamaina zuen amikoia (*Amicon® Ultra 0,5 ml, MWCO 100 kDa*) erabiliz. Prozesua H_2O-ren arrastoa desagertu arte errepikatu zen, guztira lagina bost bider diluituz eta jatorrizko bolumenera kontzentratuz. Bukatzeko lagina agregatuak kentzeko zentrifugatu zen (13.000 *g*, 10 min, 4°C) eta lortutako gain-jalkina IRS bidez aztertu zen.

$TMD_{TraJ}CD_{TrwB}$ren kasuan tarteko estrategia bat erabili zen. 25 µL lagin (12,5 mg/mL proteina kontzentrazioan) 200 µL *$TMD_{TraJ}CD_{TrwB}$ IRS indargetzailea*rekin diluitu ziren eta lortutako diluzioa indargetzaile berdinaren 1 mL aurrean dializatu zen bi orduz, prozesua birritan errepikatuz. Ondoren laginari 100 µL indargetzaile gehitu zitzaizkion eta aurreko

kasuan bezala amikoi bidez kontzentratu zen. Bukatzeko $MobB_{CloDF13}$ren prozesuan jarraitutako pausu berberak burutu ziren.

IRS bidez egitura sekundarioaren eta egonkortasun termikoaren azterketak egin ziren. Lehenengo kasuan neurketak 20°C-tan burutu ziren, eta bigarren kasuan laginak 20°C-tik 80°C-ra berotu ziren 1°C/min-ko abiaduran. Infragorri espektroak 25 µm-ko luzera optikoa erabiliz jaso ziren *Thermos Nicolet Nexus* espektofotometro batean, nitrogeno likidorekin errefrigeraturiko merkurio-kadmio-teluro detektore batekin hornituta zegoena eta tenperaturaren kontrolerako *TempComp*^{TM} peltier bat zuena. 15 µL lagin (beti 1 mg/mL-ko kontzentraziotik gorakoak) kaltzio fluorurozko leiho batean kokatu ziren eta orokorrean espektro bakoitzeko 370 ekortze burutu ziren, lagina zein indargetzailearenak, 2 cm^{-1}-eko erresoluzioarekin eta minuturo batez bestekoa eginez. Espektroak *OMNIC* (Nicolet) softwarea erabiliz jaso ziren eta datu tratamenduak *OMNIC* eta *SpectraCalc* bidez egin ziren, aldez aurretik ebatzitako metodoak jarraituz (Arrondo eta Goñi, 1999; Arrondo et al., 1993).

2.6.2. TRIPTOFANOAREN BEREZKO FLUORESZENTZIA

Proteinek berezko fluoreszentzia aurkezten dute haien aminoazido sekuentzian aurkitzen diren hiru fluoroforo naturalei esker: triptofanoa, tirosina eta fenilalanina aminoazidoak (Lakowicz, 2006). Aminoazido hauek haien artean ezaugarri desberdinak aurkezten dituzte, ala nola kitzikapen eta igorpen uhin-luzera desberdinak, baita erdi-bizitza eta errendimendu kuantiko desberdinak ere (2.4. irudia). Triptofanoa, fluoreszentzia altueneko aminoazidoa da, bere propietate espektroskopikoei esker. Honen ondorioz (baita beste aminoazidoetan ematen diren erresonantzia bidezko energia transferentziak direla eta) hiru aminoazido aromatikoak dituen proteina baten igorpen espektroa, triptofanoak duen igorpen espektroaren antzekoa izango da. Fenilalanina eta tirosinaren ekarpenak alboratuz Triptofanoaren igorpen espektroa aztertzeko lagina 295 nm-tako uhin luzerarekin kitzikatu egin behar da.

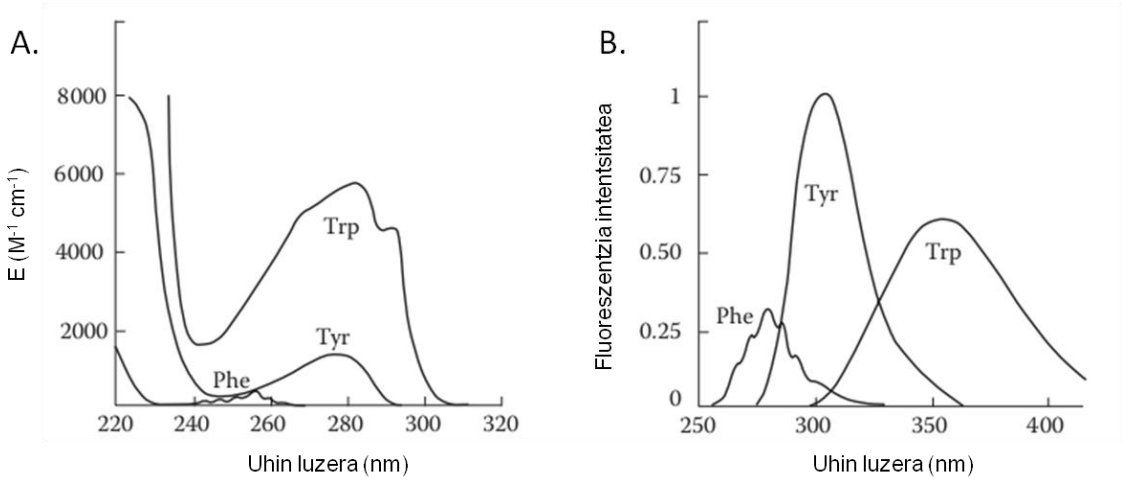

2.4. irudia. Aminoazido aromatikoen absorbantzia (A) eta fluoreszentzia igorpen (B) espektroak. Trp: Triptofanoa, Tyr: Tirosina, Phe: Fenilalanina. Absorbantzia uhin luzerarekiko absortzio-koefiziente gisa irudikatu da. Fluoreszentziaren intentsitatea unitate arbitrarioetan adierazita dago. Irudia Lakowicz (2006)-tik egokitua dago.

Proteinen berezko fluoreszentzia inguruneko polaritatearen aldaketen aurrean oso sentikorra da. Triptofanoaren kasuan, inguruneko polaritatea handitzen denean, bere igorpen uhin luzera maximoa handitu egiten da (gorrirantz desplazatuz 10-20 nm-tan), fluoreszentziaren intentsitatea handitzen den heinean. Propietate hau erabilgarria da triptofanoak zein ingurunetan aurkitzen diren ezagutzeko, baita proteinan eman ahal diren egitura aldaketak aztertzeko ere (Greene eta Pace, 1974). Tesi honetan, teknika hau indargetzaile desberdinetan proteinek aurkezten duten egonkortasuna aztertzeko erabili egin da.

Entseguak burutzeko proteina bakoitza 20 µM-eko kontzentraziora diluitu zen, proteina horri zegokion purifikazio indargetzailearekin nahastuz. Ondoren diluituriko 5 µL lagin aztergai zen indargetzailearen 95 µL-rekin nahastu ziren, nahasketa *Suprasil*^{R} kuartzozko kubeta batera igaroz (1 µM proteina, 100 µL-ko bolumenean). Neurketak 25°C-tan burutu ziren, lagina 295 nm-tan kitzikatuz, 3 nm-tako arraildurak erabiliz, *FluoroMax*^{R}*-3* espektro-fluorimetro batean. Espektroak egiteko, fluoreszentziaren igorpena 310 eta 420 nm tartean neurtu zen. Zinetikak burutzeko, espektroen bidez identifikatutako igorpen uhin-luzera maximoaren intentsitatea neurtu zen ordu batez.

2.6.3. ULTRAZENTRIFUGAZIO ANALITIKOA

Ultrazentrifugazio analitikoa (*Analytical ultracentrifugation*, AUC) zentrifugazio indarraz baliatzen da soluzioan dauden makromolekulen azterketa burutzeko, honek proteinen propietate hidrodinamiko eta termodinamikoen azterketa ahalbidetzen du, inolako erretxina edo gainazalen beharrik gabe (Lebowitz et al., 2002). Solubilizaturiko MPen laginak osagai anitzetako sistema konplexuak dira, non detergente mizelak eta proteina-detergente konplexuak (*Protein-detergent complex,* PDC) dauden, lipido kantitate desberdinekin lotuak. AUCren erabilpenen artean sedimentazio abiadura entseguak aurkitzen dira. Hauetan solutoaren sedimentazio joera aztertzen da denboraren menpean, errotazio ardaratzarekiko distantzia irizpidetzat hartuz. Horretarako, proteinen kasuan, absorbantzia neurtzen da 280 nm-tan. Solutoak zentrifugazio indarra jasotzean zentrifugazio zelularen hondorantz jotzen du, laginaren meniskoan solutoaren kontzentrazioa murriztuz. Modu horretan kontzentrazio lerro bat eratzen da denbora aurrera joan ahala hondorantz jotzen duena. Soluto muga honen mugimenduak sedimentazio koefizientea (s) ezartzen du (Correia eta Stafford, 2015).

Sedimentazio koefizientea Svedberg ekuaziotik lortzen da (2.2. ekuazioa) eta Svedberg unitateetan (S) ematen da (1 S = 10^{-13} seg). Ekuazio honek sedimentazio koefizientea soluto eta disolbatzailearen ezaugarri fisiko-kimikoen araberakoa dela frogatzen du. Disolbatzaile desberdinetan aztertutako makromolekulen artean konparaketak egin ahal izateko s balio esperimentalak egoera estandarretara (H_2O, 20°C: $s_{w,20}$) zuzendu ohi dira software informatikoen laguntzaz.

$$s = \frac{v}{\omega^2 r} = \frac{M(1-\bar{v}p^\circ)}{N_A f} = \frac{M D (1-\bar{v} p^\circ)}{R T} = \frac{M (1-\bar{v} p^\circ)}{N_A 6 \pi n^\circ R_s}$$

2.2. Ekuazioa. Svedberg ekuazioa eta bere aldaerak. v: makromolekularen abiadura; $\omega^2 r$: indar zentripetua; M: masa molarra; $\bar{v}$: bolumen espezifiko partziala; p°: disolbatzailearen dentsitatea; N_A: Avogradoren zenbakia; f: marruskadura koefizientea; D: difusio koefizientea; R: gasen konstantea; T: tenperatura; n°: disolbatzailearen biskositatea; R_s: makromolekularen erradio hidrodinamikoa.

Sistema heterogeneoetan, non makromolekula bat baino gehiago dauden (edota proteina bera egoera desberdinetan), kontzentrazio muga desberdinak agertzen dira zentrifugazioan zehar. Datu esperimental hauen azterketa burutzeko sedimentazio koefizienteen banaketa (*c(s)*) izeneko modelo analitikoa erabiltzen da. Honetarako s eta D balioen arteko erlazio zehatz bat onartzen da $v, f, p^\circ \; eta \; n^\circ$ balio zehaztuak erabiliz (Ebel, 2011).

Tesi honetan teknika hau erabili da $TrwB_{R388}$, $TMD_{TraJ}CD_{TrwB}$, $MobB_{CloDF13}$, eta MobBΔTMD purifikaturiko proteina laginek indargetzaile desberdinetan aurkezten duten egonkortasuna aztertzeko, baita disoluzioan aurkitzen diren espezie oligomeriko desberdinen identifikazioa egiteko ere.

Lehenengo eta behin proteinak aztergai ziren indargetzailera igaro ziren. Horretarako Sephadex G-25 erretxinako *PD SpinTrap* zutabeak erabili egin ziren etxe komertzialaren aholkuak jarraituz, zentrifugazioak 10°C-tan burutuz eta laginak izotzetan mantenduz. Behin indargetzaile aldaketa eginda, proteinaren kontzentrazioa neurtu zen, haien absorbantzia 280 nm-tan neurtuz, itu-kontzentraziora doitzeko.

Sedimentazio abiadura azterketak indargetzaile eta proteina kontzentrazio egokiarekin burutu ziren 129.000 edo 185.800 *g* eta 20°C-tan *UV-Vis* optika detekzio sistemadun *XL-A* ultrazentrifuga analitikoan, *An50Ti* errotorea eta 12 mm-tako sektore bikoitzeko erdiko piezak erabiliz. Lagin bakoitzetik datuak bost minuturo jaso ziren argi absorbantzia 280 nm-tan neurtuz. Sedimentazio koefizienteen banaketa kalkulatzeko sedimentazio abiadura datuak karratu-txikieneko muga modeloa jarraituz tratatu ziren, *SEDFIT* softwarean (National Institute of Health, Bethesda, MD, USA) ezarritako *c(s)* metodoa erabiliz (Schuck et al., 2002). Kalkulatutako s balioak $s_{w,\,20}$ egoera estandarretara zuzendu ziren *SEDNTERP* (Biomolecular Interaction Technologies Center, University of New Hampshire, NH, USA) softwarea erabiliz.

2.6.4. PROTEOLISI ENTSEGUAK

Proteolisi entseguak K proteinasa erabiliz egin ziren, aldez aurretik deskribaturiko protokoloa erabiliz (Vecino et al., 2011), aldaketa gutxi batzuekin. Bi indargetzaile (*Tris0 eta MP purifikazio indargetzaileak*) eta bi tenperatura (25 eta 37°C) desberdin erabili ziren. Lehenengo eta behin 2 µg proteina aukeratutako indargetzailearen 9 µL-tako bolumen finalean 10 minutuz inkubatu ziren, entsegua burutuko zen tenperaturan, DNAren presentzian (0,5 µg pUC18 plasmido edo 45-mer oligonukleotido) edo absentzian. 45-mer oligonukleotidoa (3' TCGCCACGTTTCGCCGTTTGCGGGGGTTTCTGCGAGGAACTTTGG 5') aurretik erabilia izan da $TrwB_{R388}$rekin egindako *in vitro* azterketetan (Tato et al., 2005, 2007). Ondoren K proteinasa

gehitu zen 1:500 (p/p, proteasa:proteina) erlazioan eta laginak beste 10 minutuz inkubatu ziren. Erreakzioak 5 mM PMSF gehituz gelditu ziren. Bukatzeko, lisian lorturiko produktuak SDS-PAGE elektroforesi bidez aztertu ziren.

2.6.5. MUGIKORTASUN ELEKTROFORETIKOAREN ALDAKETAREN ENTSEGUA

DNA eta proteinen arteko elkarrekintzak gel bidezko elektroforesi bidez azter daitezke, mugikortasun elektroforetikoaren aldaketaren entseguen (*Electrophoretic Shift Mobility Assay, EMSA)* bidez (Hellman eta Fried, 2007). Bi molekula hauek haien artean elkarrekiten dutenean, tamaina handiagoko konplexu bat eratzen dute, elektroforesi bidez molekula askeetatik bereizi daitekeena. Lan honetan teknika hau purifikaturiko proteinen eta DNA molekula desberdinen arteko elkarrekintzak aztertzeko erabili da, aldez aurretik deskribaturiko protokoloa jarraituz (Larrea et al., 2017)

Entseguak bi indargetzaile desberdinetan burutu ziren (*Tris0 eta MP purifikazio indargetzaileak*), 10 µL-tan, proteina kontzentrazio desberdinak (1-12 µg tartekoak) eta 0,3 (linearizaturiko plasmido bikatenarioa) edo 0,5 µg DNA (gainontzeko DNA molekulak) erabiliz. Proteina eta DNA laginak indargetzaile egokian nahastu eta 10 minutuz inkubatu ziren, 37°C-tan. Inkubazio honen ostean erreakzioak *DNA karga indargetzailea* gehituz gelditu ziren. Emandako elkarrekintzak aztertzeko, laginak %0,7 (p/b) agarosazko gel elektroforesi bidez banandu ziren, *TAE indargetzailea* erabiliz. DNA molekulak bistaratzeko *SYBR™ Safe* tindatzailea eta *Gel Doc™ EZ imager* aparatua erabili ziren.

2.6.6. ATParen HIDROLISI ENTSEGUAK

T4CPek nukleotidoak lotzen dituzten proteinetan dauden bi motibo kontserbatu aurkezten dituzte, Walker A (edota P-loop) eta Walker B motiboak alegia (Walker et al., 1982). Are gehiago, TrwBΔN70ren hiru dimentsiotako egiturak F_1-ATPasa eta helikasa hexamerikoen antza dauka (Gomis-Rüth et al., 2001; Ye et al., 2004). Proteina hauek nahiz eta mekanismo desberdinak erabili, motore molekular gisa jarduten dute, ATParen hidrolisitik lortzen den energia erabiliz zelulan lan mekanikoak burutzeko. Hala ere, orain arte T4CPen *in vitro* ATPasa aktibitatea soilik TMDrik gabeko mutanteetan deskribatu da. TrwBΔN70 mutanteak DNA-menpeko ATPasa aktibitatea erakusten du *in vitro*, ATParekiko kooperatibitate positiboa aurkeztuz (Tato et al., 2005). Horretaz gain TrwA proteina lagungarriak eta G-kuadruplex egiturak sortzen dituzten DNA molekulek aktibitate hau areagotzen dute (Matilla et al., 2010; Tato et al., 2007). Tesi honetan aktibitate honen funtzio eta erregulazioa hobeto ulertzeko T4CP aldaera desberdinen aktibitatea aztertu da entzimen entsegu akoplatua erabiliz.

Metodo espektrofotometriko hau Kreuzer eta Jongeneelek deskribatu zuten (Kreuzer and Jongeneel, 1983). Bertan ATP hidrolisia, pirubato kinasa (*pyruvate kinase,* PK) eta L-laktato deshidrogenasaren (*lactate dehydrogenase,* LDH) aktibitate konbinatuen ondorioz nikotinamida adenina dinukleotidoaren (*nicotinamide adenine dinucleotide hydrogen*, NADH) oxidazioarekin akoplatzen da (2.5. irudia), zeinaren desagerpena 340 nm-tan absorbantzia neurtuz jarrai daiteken. Era berean, sistema honen bidez ATPa birsortzen da, produktuaren (*adenosine diphosphate,* ADP) bidezko inhibizioa saihestuz.

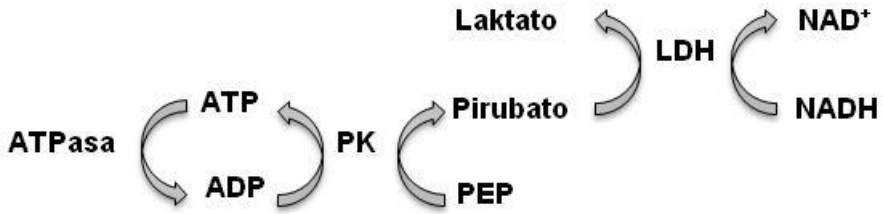

2.5. irudia. ATParen hidrolisia jarraitzeko erreakzioen irudikapen eskematikoa. ATPa PK entzimak PEPa pirubatora transformatzen duen heinean birsortzen da. Sortutako pirubatoa laktatora eraldatzen da LDH entzimak burututako erreakzioaren bitartez, zeinetan NADHa NAD^+era oxidatzen den. NADHaren oxidazioa zuzenki proportzionala da ATP hidrolisiarekiko eta 340 nm-tako absorbantzia neurtuz jarrai daiteke.

340 nm-tan absorbantziaren murrizketa *Cary 300 Bio* espektofotometroa (kubetetan) edota *SinergyHT* plaka irakurlea (96 putzutako plaketan) eta *Gen5* softwarea erabiliz neurtu zen. Proteina desberdinen ATPasa aktibitatearen karakterizazioa burutzerakoan baldintza desberdinak frogatu ziren, hala nola, indargetzaileen konposaketa (pHa, indar ionikoa, edota detergente kontzentrazioa) eta tenperatura. Kontrakoa adierazi ezean, erreakzioak 200 µL-ko bolumenean burutu ziren, sistema birsortzaileko (*Regenerator System*, RS) ondoko kontzentrazioak erabiliz: 17 µg/mL LDH, 0,25 mM NADH, 0,5 mM fosfoenol pirubato (*phosphoenol pyruvate,* PEP) eta 60 µg/mL PK. Entseguak burutzeko, lehenengo eta behin erreakzio indargetzailean 20X RSa prestatu zen, izotzetan mantendu zena. Ondoren erreakzio indargetzailea kubeta edota putzuetara gehitu zen, jarraian 10 µL 20X RS, eta bukatzeko kontzentrazio eta bolumen jakinera doitutako proteina (aurretik 13.000 *g*-n zentrifugatu zena agregatuak kentzeko). Gainerako osagaiak erabiliz gero (DNA edota $TrwA_{R388}$ proteina lagungarria) une honetan gehitu ziren baita. DNAdun entseguak 6 nM (pisu molekular) pUC18 edo ssM13rekin burutu ziren. $TrwA_{R388}$ren efektua aztertzeko 0,2 mg/mL proteina gehitu ziren. Kontu handiz pipetaren laguntzaz erreakzioak nahastu eta neurketa burutuko zen tenperaturan 15 minutuz inkubatu ziren. Denbora hau igarota, kubeta edo plaka tenperatura berdinean mantenduz, ATPa gehitu (5 mM, ATP titulazioetan ezik), nahastu eta 340 nm-tako absorbantziaren neurketa burutu zen. Kontrol negatibo gisa nahasketa berdinak burutu ziren baina proteinarik gabe.

Lambert-Beer legean (2.1. ekuazioa) oinarrituz 2.3. ekuazioan ikusten da 340 nm-tan neurtutako absorbantziaren murrizketatik lorturiko malda zuzenki proportzionala dela ATParen hidrolisiarekiko.

$$malda = \frac{\Delta absorbantzia}{\Delta denbora}$$

$$\Delta c = \frac{malda}{\varepsilon \times l}$$

$$ATPasa\ aktibitatea = \frac{malda \times 10^6}{6220 \times l}$$

2.3. ekuazioa. ATPasa aktibitatearen neurketa. ATPasa aktibitatea desagerturiko µM ATP/min moduan kalkulatzen da. ε: NADHaren absortzio koefiziente molarra, 6220 $M^{-1}\,cm^{-1}$.

Entsegu hauek burutzeko $TrwA_{R388}$ eta TrwBΔN70 proteinak purifikatu ziren, proteina lagungarri eta kontrol gisa erabiltzeko, hurrenez hurren. Horretaz gain, pUC18 eta ssM13 plasmidoen erauzketa burutu zen DNAren eragina ATPasa aktibitatean aztertzeko.

ATP bidezko titulazioetan lortutako datuetan oinarrituz $TMD_{TraJ}CD_{TrwB}$ eta MobBΔTMD proteinen ATPasa aktibitatearen zinetika aztertu zen. Lehenengo eta behin, substratuaren eragina aztertzeko titulazioan lortutako datuak Michaelis-Menten modelora egokitzen ote ziren aztertu zen (2.4. ekuazioa) (Cornish-Bowden, 1979).

$$v = \frac{V_{max}\,[S]}{K_m + [S]}$$

2.4. ekuazioa. Michaelis-Menten ekuazioa. Ekuazio honen bidez erreakzioaren abiadura eta substratuaren kontzentrazioa erlazionatu egiten dira. *v*: erreakzioaren abiadura (substratuaren desagerpen gisa), V_{max}: sistemak lortu dezakeen abiadura maximoa, K_m: Michaelis-konstantea, abiadura maximo balioaren erdia lortzen den substratu kontzentrazioari dagokiona.

Lortutako datuen Michaelis-Menten modeloaren egokitasuna ziurtatzeko Hill ekuazioa erabili zen. Ekuazio honetan, substratuaren eta proteinaren arteko batura aztertzen da, substratuaren kontzentrazioaren menpe. Hori dela eta, Hill ekuazioa substratuen kooperatibitatea aztertzeko erabili ohi da, Hill-koefizientearen (*n*) kalkuluaren bidez. Michaelis-Menten modelora egokitzen diren entzimen kasuan ez da kooperatibitaterik ematen eta koefiziente honen balioa bat da. Hill ekuazioaren aldaerak burutuz, grafikoki zuzen baten moduan irudikatu daiteken ekuazioa lortzen da (2.5. ekuazioa), Hill grafikaren irudikapenerako erabili ohi dena. Ekuazioa jarraituz, lortzen den zuzenaren malda bat dator Hill-koefizientearekin.

$$\log\left(\frac{v}{V_{max} - v}\right) = n\log[S] - \log[S]_{0,5}$$

2.5. ekuazioa. Hill ekuazioaren aldaera. Aldaera hau Hill-ekuazioaren irudikapen grafikoa burutzeko erabili ohi da. *v*: erreakzioaren abiadura (substratuaren desagerpen gisa); V_{max}: sistemak lortu dezakeen abiadura maximoa; *n:* Hill-koefizientea; $[S]_{0,5}$: abiadura maximoaren erdia lortzen duen substratu kontzentrazioa, kooperatibitate eza dagoenean K_m-ren baliokidea dena.

Horretaz gain, Lineweaver-Burk ekuazioa (2.6. ekuazioa) erabili zen abiadura maximoaren (V_{max}) balioa modu zehatzean kalkulatzeko. Izan ere, Lineweaver-Burk grafikan *y*-ardatzaren ebaki puntuak V_{max} balioaren alderantzizkoari dagokio.

$$\frac{1}{v} = \frac{K_m}{V_{max}[S]} + \frac{1}{V_{max}}$$

2.6. ekuazioa. Lineweaver-Burk ekuazioa. Ekuazio hau Michaelis-Mente ekuazioaren aldaera da, V_{max} balioaren kalkulua burutzeko. V_{max}: sistemak lortu dezakeen abiadura maximoa; K_m: Michaelis-konstantea, abiadura maximo balioaren erdia lortzen den substratu kontzentrazioari dagokiona.

2.7. PROTEINEN KRISTALIZAZIOA

Proteinen egitura aztertzeak hainbat kasuetan garrantzitsua izan daitekeen informazioa eskaintzen du, hala nola teknika konputazionalen bidez ligando potentzialak identifikatzeko orduan. Hori dela eta, proteinen hiru dimentsiotako egituraren ebazpena lortzea oso lagungarria izan daiteke proteina hauen mekanismo eta funtzio biologikoa aztertzeko. T4CPen kasuan, $TrwB_{R388}$ mutante solugarriaren, TrwBΔN70, kristalizazioa lortu eta bere egitura tridimentsionala ebatzi zen (Gomis-Rüth et al., 2001); baina oraindik ezin izan da lortu T4CP natibo baten kristalik. Redzej et al. (2017) egindako ikerketan NS-EM bidez lortutako irudiak lagungarriak izan dira $TrwB_{R388}$ sekrezio konplexuarekiko nola dagoen kokatuta aztertzeko (Redzej et al., 2017), non bi dimero moduan kokatzen zen. Hala ere, oraindik informazio asko falta da. Izan ere, ez da inolako deskribapenik egin proteina natiboen egitura osoari buruz edota TMDaren presentziak zelako eragina daukan aurretik deskribaturiko CDaren egituran. Galdera hauek IRS bidez erantzuten saiatu dira (Vecino et al., 2011), baina tesi honetan $TrwB_{R388}$ren kristalizazio entseguak burutzea erabaki zen erresoluzio altuko egiturak lortzeko. Horretaz gain, MobBΔTMD mutantearen kristalizazio prozesua martxan jarri da.

2.7.1. $TrwB_{R388}$ren KRISTALIZAZIOA

$TrwB_{R388}$ren kristalizazio entseguak *Membrane Protein Laboratory*-n (*Diamond Light Source Ltd, Harwell Science and Innovation Campus, Oxford, UK*) burutu ziren. Lehenengo eta behin proteinaren purifikazioa egin zen Vecinok deskribaturiko protokoloa erabiliz (Vecino et al., 2011) aldaketa batzuekin. Laburbilduz, *E. coli* BL21C41(DE3) zelulak pUB3 bektorearekin transformatu ziren. Lortutako koloniak anpizilinarekin osatutako LBn hazi ziren, gau osoan zehar 37°C-tan. Hurrengo egunean kultiboaren diluzioak (1:50) egin ziren, guztira 6 L lortuz. Kultiboak 37°C-tan hazi ziren OD_{650} 0,7 lortu arte. Orduan laginei 1 mM IPTG gehitu zitzaien eta 25°C-tan hazi ziren lau orduz proteinaren gain-adierazpena lortzeko. Horren ostean, zelulak zentrifugazioz uztatu ziren (8.000 *g*, 15 min). Gain-jalkina *zelula indargetzailea*ren 65 mL-tan berreseki zen eta lortutako esekidura nitrogeno likidoz izoztu eta -80°C-tan biltegiratu zen.

Proteinaren purifikaziorako, zelulak desizoztu ziren eta lagin hauei 0,02 mg/mL DNasa I, 1 mM $MgCl_2$ eta 1 mM *Pefabloc*^{TM} *SC* gehitu zitzaien, *zelula indargetzailea*rekin 200 mL-tako bolumen finalera doituz. Zelulak *MC Constant Cell Disruption* sistema erabiliz apurtu ziren, 25 KPSI-ko presioarekin, 15,6°C-tan. Ondoren lagina zentrifugatu zen (24.000 *g*, 13 min, 4°C) eta lortutako gain-jalkina berriz zentrifugatu zen (105.000 *g*, 1h, 4°C) mintz-frakzioa lortzeko. Jalkina 40 mL *zelula indargetzaile*n berreseki zen, bitan banandu zena eta nitrogeno likidoz izoztu zena -80°C-tan gordetzeko. Purifikazioa egiteko orduan lorturiko mintz-frakzio erdia ur bainu bidez desizoztu eta *TrwB C1 indargetzailea* erabiliz 23 mL-tik 65 mL-ra eraman zen indargetzailearen bukaerako kontzentrazioak doituz. Mintzak solubilizatzeko lagina 90 minutuz 4°C-tan irabiaketarekin utzi zen. Ondoren, suspentsioa zentrifugatu zen (190.000 *g*, 30 min, 4°C), solubilizaturiko proteinak gain-jalkinean lortuz.

Lagina aldez aurretik *TrwB C2 indargetzailea*rekin orekaturiko *HisTrap*^{TM} *FF* zutabe batera gehitu zen 1 mL/min-ko fluxuan. Indargetzaile berdina erabiliz zutabearen garbiketa egin zen eluituaren absorbantzia 280 nm-tan zerora heldu arte. Ondoren 22 mL *TrwB C3*

*indargetzailea*rekin $TrwB_{R388}$ren eluzioa egin zen. Lortutako proteina 100 kDa-eko porodun amikoiak erabiliz kontzentratu zen gel-iragazpenerako kromatografia burutzeko. Orduan lagina bitan banandu zen *Superdex 200 Increase 10/300 GL* gel-iragazpeneko kromatografiatik igarotzeko, kasu batean *TrwB C4 indargetzailea* erabiliz eta bestean *TrwB C5 indargetzailea*. Lortutako frakzioen osagai proteikoak SDS-PAGE bidez aztertu ziren *NuPAGE 4-12%* gelak erabiliz eta $TrwB_{R388}$ zeukatenak elkartu eta berriz kontzentratu ziren. Bukaeran 4 eta 1 mg proteina lortu ziren DDM eta LDAOdun indargetzaileetan, hurrenez hurren.

Lortutako laginak gel-iragazpeneko kromatografia bati akoplatutako angelu anitzeko laser argi dispertsioz (*Size Exclusion Chromatography-Multi Angle Laser Light Scattering*, SEC-MALLS) aztertuz ziren, tresna oso baliogarria dena PDCen ikerketarako. Honen bidez detergente soluzioan aurkitzen den MParen egitura eta masa era zehatzean aztertu daiteke, ez direlako konformazio edo formaren inguruko presuntziorik hartzen (2.7. ekuazioa); SEC, AUC eta Native-PAGE tekniketan egiten den bezala (Slotboom et al., 2008). Horretarako kontzentrazioaren eta argi dispertsio intentsitatearen neurketa zehatzak banaketa teknika batekin konbinatzen dira. SEC saiakera bati MALLS analisia gehitzerakoan lortzen diren abantailak honako hauek dira: zutabeen kalibrazioan burututako akatsak eta atxikipen denbora saihestea eta neurri hidrodinamikoekin eta masa molarrekin lotutako hipotesiak ezabatzea. Horretaz gain, SEC-MALLS neurketak laginaren homogeneotasuna eta agregatuen presentzia aztertzeko baliogarriak dira. SEC-MALLs entsegua *Superdex 200 increase 10/300 GL*-rekin hornitutako *Viscotek GPCmax* (*Solvent sampling module VE 2001 GPC*) batean egin zen. Azterketa burutzeko laginak 1 mg/mL-ra diluitu ziren eta 0,6 mL/min-ko fluxua erabiliz 30°C-tan zutabetik igaro ziren.

$$Mw = \frac{\Delta LS}{K \cdot (\frac{dn}{dc})^2 \cdot c}$$

2.7. ekuazioa. SEC-MALLS bidez masa molekularraren kalkulurako ekuazioa. Mw: itu proteinaren masa molekularra; ΔLS: argi dispertsioaren aldaketa; K: indargetzaile bakoitzerako ezartzen den konstantea; dn/dc: proteinaren errefrakzio indizearen handipen espezifikoa kontzentrazioarekiko; c: proteinaren kontzentrazioa (mg/mL). Mintz proteinen kasuan Mw, dm/dc eta c PDCari dagozkio.

Behin laginen egokitasuna azterturik, kristalizazio entseguak burutu ziren, hiru plaka komertzial desberdin erabiliz: *MemGold*^{TM}, *MemGold2*^{TM} (alfa-helizedun mintz-proteinen kristalizazioa errazten duten baldintzadunak) eta *MemMeso*^{TM}. Proteina bakoitzeko sei plaka prestatu ziren, baldintza guztiak 4 eta 20°C-tan frogatzeko (guztira 12 plaka). Laginak 15 mg/mL-ra diluitu ziren eta *sitting drop* teknika erabiliz plaketan kokatu ziren *Mosquito*^{R} *LCP* bat erabiliz.

2.7.2. MobBΔTMDren KRISTALIZAZIOA

MobBΔTMDren kristalizazio entseguak burutzeko, lehenengo eta behin purifikazio protokolo egokia garatu zen. Bertan *E. coli* BL21(DE3) bakterioak pOPINE-*mobBΔTMD* bektorearekin (S2.1. taula) transformatu ziren. Lortutako zortzi koloniekin anpizilinarekin osaturiko 10 mL LBdun zortzi matraze inokulatu ziren, gau osoan zehar 37°C-tan hazten utzi

zirenak. Hurrengo egunean kultiboen diluzioak (1:50) egin ziren, 4 L kultibo lortuz, berriz hazten utzi zirenak OD_{600} 0,5-0,6 arteko balioak izan arte. Orduan kultiboei 1 mM IPTG gehitu zitzaien eta 25°C-tan 16 orduz proteinen gain-adierazpena burutu zen. Kultiboak zentrifugatu ziren (8.000 *g*, 15 min, 4°C) eta jalkinak 50 mL *zelula indargetzaile*rekin berreseki ziren. Lortutako zelula esekidurak nitrogeno likido bidez izoztu eta -80°C-tan biltegiratu ziren.

Proteinen erauzketa egiteko zelula suspentsioa 37°C-tako ur bainuan desizoztu zen eta 1 mM DTT, %0,07 (p/b) lisozima, 0,2 mM PMSF eta proteasen koktel inhibitzailea gehitu zitzaion. Nahasketa 30 minutuz inkubatu zen 4°C-tan irabiaketa leunarekin eta ondoren zelulen lisi mekanikoa burutu zen sonikazio bidez (2.5.2.1. atala). Lisatua zentrifugatu zen (138.000 *g*, 45 min, 4°C), proteina solugarrien frakzioa lortuz gain-jalkinean.

Proteinen erauzkin gordinari 50 mM imidazol gehitu zitzaizkion. Ondoren, lagina aldez aurretik *MobBΔTMD1 indargetzailea*rekin orekaturiko 5 mL-ko *HisTrap™ FF* zutabe batean kargatu zen, gau osoan zehar 4°C-tan birzirkulatzen utziz. Hurrengo egunean zutabea *ÄKTA-FPLC* sistema batera konektatu zen eta atxikitu ez ziren proteinen garbiketa egiteko 25 mL *MobBΔTMD1: MobBΔTMD2 (70:30, b/b) indargetzaile* igaro ziren. Itu-proteinaren eluzioa burutzeko *MobBΔTMD1:MobBΔTMD2 (35:65, b/b) indargetzaile* nahasketa erabili zen, 2 mL/min-ko fluxuan eta 1 mL-ko frakzioak jasoz. Hauek SDS-PAGE bidez aztertu ziren eta MobBΔTMD aurkezten zuten frakzioak elkartu eta 1 mL-ra kontzentratu ziren 30 kDa-eko iragazkidun amikoia erabiliz. Lagina zentrifugatu zen (13.000 *g*, 10 min, 4°C) agregatuak deuseztatzeko eta aldez aurretik *zelula indargetzaile*rekin orekaturiko *Superdex 200 HR 10/30* zutabe batean xiringatu zen 500 µL-ko bi txandetan, 0,8 mL/min-ko fluxua erabiliz. 500 µL-ko frakzioak jaso eta aztertu ziren, itu-proteina zeukatenak elkartuz.

Kristalizazio entseguak burutzeko, lehenengo eta behin proteina dializatu edota kontzentratu zen, kristalizazio baldintzen beharraren arabera. Lehenengo kristalizazio entseguak burutzeko 96-putzu 2-tantako *MRC* kristalizazio plaka komertzialak erabili ziren. Behin baldintza interesgarriak identifikaturik, 48-putzutako *MRC Maxi* optimizazio plakak erabili ziren. Kasu guztietan *sitting drop* kristalizazio teknika erabili zen *Mosquito® LCP* bat erabiliz. 96-putzutako plaketan 250 nL proteina disoluzio 250 nL itu-soluziorekin nahastu ziren tanta bakoitzean eta 48-putzutako plaketetan bolumen bikoitza. Kristalen hazkuntza jarraitzeko argazkiak *Rock Imager®* softwarearen bidez jaso ziren.

2.8. BERRERAIKITAKO EREDU SISTEMAK

2.8.1. MINTZ-EREDUEN SISTEMAK

MPekin *in vitro* entseguak burutzeko baldintza optimoak haien jatorrizko egoeratik hurbilen aurkitzen direnak dira, hau da, bigeruza lipidikoaren antzeko ezaugarriak eskaintzen dituztenak. Hau lortzeko dauden abiapuntuen artean mintz-eredu moduan jarduten duten lipido sistemak daude, hala nola besikula lamela-bakar txikiak (*Small Unilamellar Vesicles*, SUV), besikula lamela-bakar handiak (*Large Unilamellar Vesicles,* LUV) eta besikula lamela-bakar erraldoiak (*Giant Unilamellar Vesicles*, GUV).

2.8.1.1. LIPIDOEN PRESTAKETA

Erabilitako lipido konposaketaren eta burututako entseguaren arabera lipidoen prestaketa protokoloa aldaera desberdinak izan zituen, baina orokorrean ondoko pausuak jarraitu ziren. Lehenengo eta behin lipidoak kloroformotan berreseki ziren, ondoko kontzentrazioetara: 50 mg/mL dioleilfosfokolina (*1,2-dioleoyl-sn-glycero-3-phosphocholine* DOPC), 25 mg/mL fosfatidiletanolamina (*Phosphatidylethanolamine*, PE), 20 mg/mL fosfatidilglizerol (*Phosphatidylglycerol,* PG), 25 mg/mL kardiolipina (*Cardiolipine*, CL) eta 0,5 mg/mL *E. coli* lipidoen nahasketa. Ondoren lipidoak proportzio egokietan nahastu ziren 10 mg lipidoko nahasketak lortuz. Hauek bortexeatu eta lipido kantitate jakineko alikuotetan banandu ziren (helburuaren arabera). Kloroformotan zeuden laginak nitrogeno gasa erabiliz lehortu ziren eta saiodi bakoitzean lortutako lipido filmak 2 orduz huts-ponpa batean utzi ziren, disolbatzaile organikoaren arrastorik ez geratzeko. Lortutako alikuotak -20°C-tan mantendu ziren haien erabilerara arte. Erabiltzeko orduan indargetzaile bolumen egokiarekin (edo kloroformoarekin GUVen prestaketa prozesuan) berreseki ziren, entseguak egiteko kontzentrazioetara doituz.

2.8.1.2. BESIKULA LAMELA-BAKAR TXIKIAK

Tesi honetan eutsitako bigeruza lipidikoak (*Supported lipid bilayers*, SLB, ikusi 2.8.3.4. atala) sortzeko abiapuntu gisa SUVak erabili egin dira gehien bat, hain zuzen ere DOPC-SUV eta bakterioen barne mintzekin egindako besikulak (*Bacterial Inner Membrane Vesicles*, BIMV, ikusi 2.8.3.2. atala).

DOPC-SUVak 2,5 mg/mL-ko kontzentraziora prestatu ziren, 50 µL DOPC (10 mg/mL *PBS*n) 150 µL entsegu indargetzailearekin nahastuz. BIMVen kasuan 1-2 µg proteina lagin 150 µL indargetzailetan diluitu ziren. Zenbait kasutan, beharraren arabera, nahasketari DiD zunda fluoreszentea (*1,1'-Dioctadecyl-3,3,3',3'-Tetramethylindodicarbocyanine perchlorate*) gehitu zitzaion. Lipidoak giro tenperaturara egokitu ostean bortexeatu ziren, besikula lamela-anitz handiz (*Multilamellar large vesicles*, MLV) osaturiko esne koloredun suspentsio uniformea lortuz. Hau giro tenperaturan 10 minutuz ultrasoinuen bainu bidez sonikatu zen, jarraian bortexeatuz eta berriz sonikatuz. Prozesua errepikatu zen lipidoen esekidura gardendu arte. Sonikazio prozesu honi esker lamela anitzeko besikulak apurtu/desegin eta SUVak lortu ziren.

2.8.1.3. BESIKULA LAMELA-BAKAR HANDIAK

Lehenengo eta behin lipido nahasketak prestatu ziren 2.8.1.1. ataleko protokoloa jarraituz, bolumen eta kontzentrazio egokiak erabiliz, bukaeran 15 mg-ko lipido filmak lortuz. LUVak lortzeko, lipido filmak *liposoma indargetzailean* berreseki ziren 30 mg/mL-ko bukaera kontzentraziora. Nahasketa ondo bortexeatu zen MLVak lortuz. Hauei izozte-desizozte 15 ziklo egin zitzaien, nitrogeno likidoa eta 45°C-ko ur bainua tartekatuz, pausu bakoitzaren ostean ondo bortexeatuz. Prozesu honen ondorioz izoztu-desizoztutako lamela-anitzeko besikulak (*Freezed-thawed* MLV, FT-MLV) lortu ziren, estrusio bidez homogeneizatu zirenak. Horretarako lipido esekidura polikarbonatozko 0,1 µm-eko porodun bi filtroetatik 35-41 aldiz igaro arazi zen *Liposofast-Basic* bat erabiliz. Modu honetan tamaina homogeneoko (120 nm inguruko diametroa) LUVak lortu ziren. Bukaerako lipido kontzentrazioa neurtzeko kolina

kuantifikatzeko *Phosphatidylcholine Assay Kit*-a erabili zen, etxe komertzialak eskainitako protokoloa jarraituz.

2.8.1.4. BESIKULA LAMELA-BAKAR ERRALDOIAK

GUVak lortzeko estrategia desberdinak erabili ziren: elektroformazioa, ganbara zein ITO estalkietan, eta gel bidezko hantura.

ELEKTROTRANSFORMAZIO GANBARAK

Elektroformazioa GUVak sortzeko metodo erabiliena da, Angelova eta Dimitrov-ek (1986) garatutakoa. Bertan soluzio urtsu batean lipidoen hantura espontaneoa kanpo eremu elektriko baten aplikazioz modulatzen da.

GUVak lortzeko lipido filmak desizoztu ziren eta zunda fluoreszente bat gehitu zitzaien, DiD edo DiO (3,3'-dioctadezilloxakarbozianina perkloratoa), lipidoekiko 0,05-0,1 (mol:mol) erlazioan. Ondoren saiodiei kloroformoa gehitu zitzaien, lipidoak 1 edo 2 mg/mL-ko kontzentrazioetara doituz, eta bortizki bortexeatu ziren. Elektroformazioa burutzeko, fase organikoan disolbaturiko lipido suspentsioaren 2,5 µL tantaz tanta banandu ziren platinozko bi harien gainazalean zehar. Behin disolbatzailea lurrundurik, prozesua errepikatu zen, berriz lurruntzen utziz. Bitartean teflonezko putzu bakoitzera 4°C-tan gordetako 350 µL sakarosa disoluzio (300 mM) gehitu ziren (*PBS*arekiko isosmotikoa zena), non lipidodun hariak murgildu ziren. Korronte elektrikoa jasotzean hidratataturiko lipidoen hantura ematen da, maiztasuna jaisterakoan harietatik askatzen direnak GUV moduan. Horretarako platinozko hariak sorgailu baten elektrodoetara konektatu ziren 10 Hz-ko maiztasuna eta 1,5 V-ko tentsioa ezarriz 105 eta 120 minutu artean. Osaturiko GUVak harietatik askatzeko, maiztasuna 2 Hz-tara jaitsi zen, baldintza hauetan 45-60 minutuz mantenduz. Entsegu desberdinetan protokolo honen aldaera desberdinak erabili ziren, tenperatura, tentsio edota maiztasuna aldatuz.

Behin GUV askeak lorturik, zortzi putzutako *Nunc™ Lab-Tek™* bistaratze ganbarak prestatu ziren. GUVak putzuen azpialdearekin ez fusionatzeko, putzu bakoitzean 400 µL BSA (10 mg/mL) gehitu ziren eta giro tenperaturan 45 minutuz utzi ziren, beirazko gainazala blokeatzeko. Honen ostean ganbaren garbiketa egin zen, hiru aldiz ur destilatua erabiliz eta beste hiru aldiz *PBS* erabiliz. Bukatzeko 250 µL *PBS* gehitu ziren ganbara bakoitzean, gainean elektroformaturiko 50 µL GUV jarriz kontu handiz.

ITO ESTALKIAK

Elektroformazioan oinarrituriko beste teknika bat ITOz (*Indium Tin Oxide,* ITO) estalitako estalkien erabilera da (García-Sáez et al., 2010). Metodologia honen bidez GUVen formazioa fluoreszentziazko mikroskopio konfokalean zuzenean bistara daiteke.

Lehenengo eta behin estalkien prestakuntza egin zen, ITO gainestaldurarekin erosi zirenak. Estalkiak hauspeakin-ontzi batean etanolean murgildu ziren eta 10 minutuz ultrasoinuen bainu sonikatzaile batean mantendu ziren, estalkien gainazalean egon zitekeen zikinkeria (aurreko saiakuntzen lipido arrastoak, adibidez) bertatik kentzeko. Ondoren etanola deuseztatu eta H_2O-rekin hiru garbiketa burutu ziren, azkenengoan sonikazio prozesua

errepikatuz. Jarraian isopropanolean murgildu ziren bost minutuz eta behin disolbatzaile hau kenduta lehortzen utzi ziren. Muntaia egin aurretik estalkien konduktibitatedun aldea (hau da, ITOz estalitako aldea) identifikatu zen, estalkiaren alde bakoitzean tentsioa neurtuz.

GUVen formazioa burutzeko zunda fluoreszentedun lipido suspentsioa estalkiaren gainean *zig-zag* moduan edo tantaz tanta jarri eta lehortzen utzi zen lipido filma sortzeko. Ondoren euskarriaren muntaia egin zen 2.6. irudia azaldu bezala.

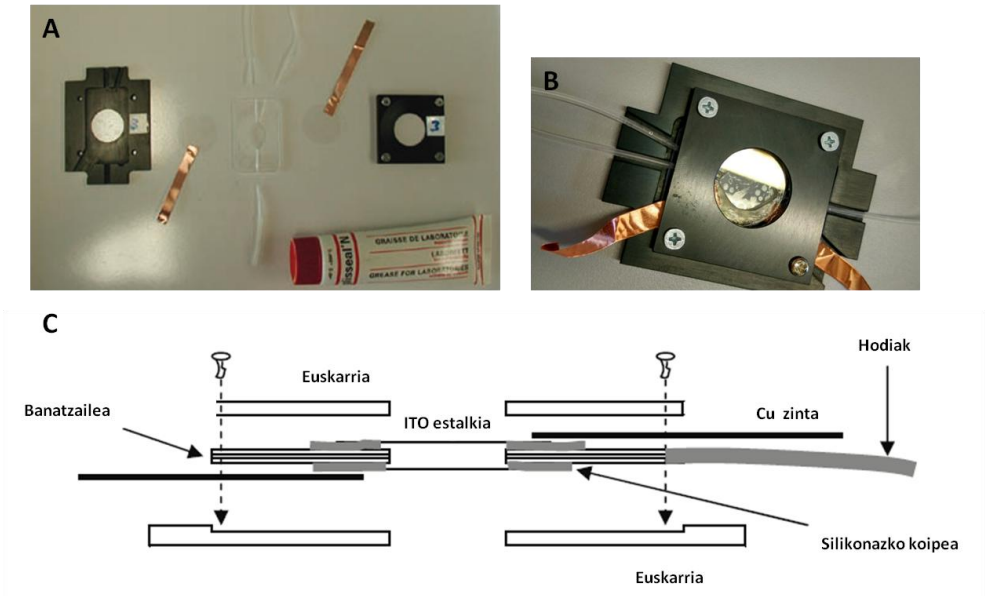

2.6. irudia. ITO estalkien ganbararen muntaia. A) Ganbararen osagai desberdinak: metalezko euskarriak, plastikozko banatzailea, hodiak, ITO estalkiak, kuprezko zintak eta silikonazko koipea. **B)** Muntaturiko ganbara. **C)** Muntaiaren irudikapen eskematikoa. Hau lortzeko plastikozko hiru hodi banatzailearen zirrikituetatik sartu behar dira. Ondoren banatzailearen bi aldeetatik silikonazko koipea jarri behar da, ganbara guztiz zigilaturik geratzeko (hau da, lipido nahasketa sakarosadun soluzioan murgilduta egoteko eta soluzio hau ganbaran mantentzeko). Banatzailearen alde bakoitzean ITO estalki bana kokatzen da. Ezinbestekoa da lipidodun estalkia ganbararen bekaldean egotea (mikroskopioaz bistaratu ahal izateko), estalkien konduktibitatedun aldeak barnera begira egotea (hau da, ITO estaldura barnera begira) eta kuprezko zintak ITO estaldurarekin kontaktuan egotea eta hutsuneekin ondo egokitzea. Behin dena kokaturik dagoela, estalkiak eta banatzailea euskarri metalikoen artean kokatzen dira, eta dena torlojuen bidez ziurtatzen da. A eta C irudiak García-Sáez et al. (2010)-tik egokituak izan dira.

Behin muntaia eginda, sakarosazko soluzioa behealdeko hoditik (hodi bakarra daukan aldea) 45°-ko inklinazioa mantenduz xiringatu zen, burbuilen formazioa saihesteko. Soluzioa beste bi hodietatik irten arte gehitu zen eta orduan hodiak pintzen bidez zigilatu ziren. Euskarria mikroskopioan kokatu zen objektiboaren gainean dH_2O kokatuz (*C-Apochromat 40×1.2 water immersion* objektiboa erabili baitzen). Ondoren kuprezko zinta bakoitza generadore elektrikoan konektatu zen, zinten arteko kontaktua saihestuz. Elektroformazio protokolo desberdinak frogatu ziren, 5. kapituluan azaltzen direnak.

Agarosa gel bidezko GUVen formazioak (2.7. irudia) zenbait abantaila aurkezten ditu elektroformazioaren aurrean, batez ere ekipamendu espezializatuari dagokionez. Horretaz gain, indargetzaile fisiologikoetan proteo-GUVak egiteko orduan, proteina dentsitate banaketa homogeneoagoak lortzen dira, nahiz eta GUV etekina baxuagoa izan. Tesi honetan aurretik deskribaturiko protokoloa jarraitu da (2.7. irudia) (Garten et al., 2015).

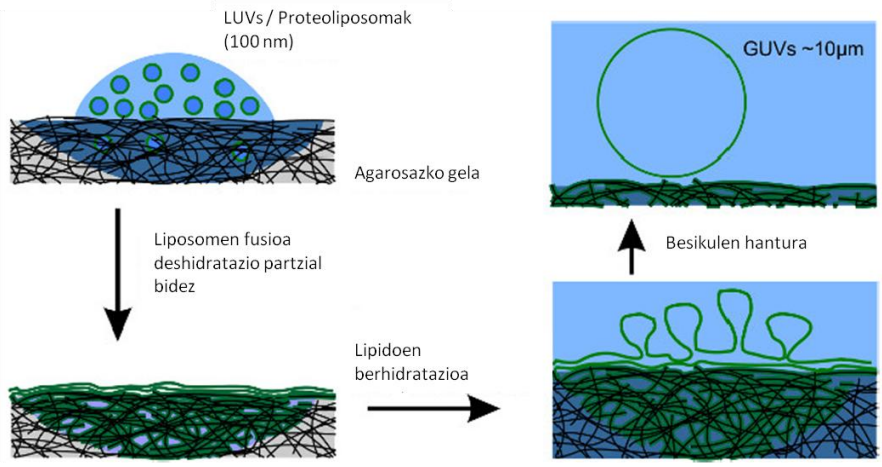

2.7. irudia. Gel bidezko hanturaz bideratutako GUVen formazioaren irudikapen eskematikoa. Liposomadun suspentsio baten tantak agarosa gelaren gainazalean zehar sakabanatzen dira. Ondoren N_2 korronte baten bidez tantak deshidratatu egiten dira liposomen fusioa emanez eta lipido film bat sortuz. *GUV hantura indargetzailea* gehitzerakoan, filma berhidratatu egiten da eta agarosazko gelaren poroetatik GUVak ateratzen dira gainazalera. Hauek 10 µm ingurura arte haz daitezke, hantura eta GUVen arteko fusio bidez. Irudia Garten et al. (2015)-tik egokitua izan da.

Lehenengo eta behin %1 (p/b) agarosa soluzioa prestatu zen eta beirazko estalkiak *Mucasol*^{TM} detergentea erabiliz garbitu ziren. Ondoren 22 x 22 mm^2-ko estalki bakoitzaren gainean epeldutako 200 µL agarosa gehitu ziren, gainazal guztian zehar ondo bananduz. Jarraian estalkia bertikalki kokatu zen, beheko ertza paper baten gainean kokatuz, gehiegizko agarosa soluzioa kentzeko. Modu horretan agarosazko geruza mehe eta leun bat lortu zen estalkian. Hauek 60°C-tan 30 minutuz mantendu ziren ondo lehortzeko, eta ondoren giro tenperaturan hozten utzi ziren.

Bitartean GUVak lortzeko abiapuntu gisa erabiliko ziren LUVak edo proteoliposomak (ikusi 2.8.3.1. atala) prestatu ziren. Lehenengo kasuan 10 µL LUV (1,33 mM lipido) 0,2 µL DiDrekin (50 µM *stock*) bortex bidez nahastu ziren. Ondoren nahasketaren 5 µL estalki osoan zehar tantaz tanta sakabanatu ziren, eta behin lehorturik gainerako 5 µL-ak ere sakabanatu ziren. Proteoliposomen kasuan 5 µg DOPC-SUV (300 mM sakarosa indargetzailetan prestatuak) 15 µL proteoliposomekin (0,023 mM lipido) nahastu ziren eta LUVekin erabilitako protokolo bera jarraituz nahasketa guztia agarosa geruzaren gainazalean zehar sakabanatu zen.

Liposomen indargetzailearen lurrunketa N_2 korronte baten bidez burutu zen, 10-15 minutuz, tanten lehorketa ikusi arte. Orduan *GUV hantura indargetzailea* gehitu zen petri kutxatilan, estalkia bertan murgildurik geratu arte (1 mL inguru). Hantura prozesua 30 minutuz

burutu zen. GUVen askapena lortzeko petri kutxatilaren alboetan kolpe leunak eman ziren zenbait aldiz. Ondoren pipetaren punta (moztuta, GUVak ez apurtzeko) estalkiaren gainetik igaro zen kontu handiz, azalera guztitik igaroz eta 50 µL jasoz, aurretik prestaturiko bistaratze ganbara batera gehitu zirenak.

2.8.2. PROTEINEN MARKAKETA ZUNDA FLUORESZENTEEN BIDEZ

Fluoreszentziazko mikroskopioen bidez proteinen azterketa burutzeko, molekula fluoreszenteak erabili behar dira. Proteina fluoreszenteak lortzeko tekniken artean haietara fluorokromo izaera duten zundak kimikoki atxikitzea dago. Mota desberdinetako zundak daude, erreakzio mota desberdinen bidez proteinetara atxikitzen direnak. Tesi honetan erabilitako Atto zunden atxikipena zunden maleimida taldeen eta proteinetan dauden zisteinen artean ematen diren erreakzioetan oinarritzen da. Hau $TrwB_{R388}$, TrwBΔN70 eta $TMD_{TraJ}CD_{TrwB}$ proteinekin burutu zen, zisteina bakarra daukatenak agerian (Vecino et al., 2010). Hiru zunda desberdin erabili ziren etxe komertzialaren aholkuak jarraituz, bi gorri (Atto 633 eta Atto 655) eta berde bat (Atto 488).

Lehenengo eta behin proteinen indargetzaile aldaketa burutu zen, zundek pH 7,0an burutzen baitute markaketa optimoa eta proteinak pH 7,8 ($TrwB_{R388}$ eta $TMD_{TraJ}CD_{TrwB}$) eta pH 6,0an (TrwBΔN70) aurkitzen zirelako. Horretarako *Vivaspin 500*® kontzentratzeko iragazkiak erabili ziren. $TrwB_{R388}$ eta $TMD_{TraJ}CD_{TrwB}$ *MP markaketa indargetzailea*rekin eta TrwBΔN70 *TrwBΔN70 markaketa indargetzailea*rekin diluitu ziren 50 µL proteina eta 150 µL indargetzaile nahastuz. Ondoren laginak kontzentratzeko iragazkian zentrifugatu ziren (15.000 *g*, 15 min, 4°C), prozesua hirutan errepikatuz (pausu bakoitzean 100 µL indargetzaile gehituz). Behin indargetzaile aldaketa eginda, proteinak *eppendorf* hodi batean zentrifugatu ziren (13.000 *g*, 10 min, 4°C) agregatuak kentzeko. Ondoren kontzentrazioa neurtu zen *Thermo Scientific Multiskan GO* espektofotometroa erabiliz. Markaketa burutzeko, proteina (10-20 µM), zunda [1:10 edo 1:20 (mol:mol) proportzioan] eta Tris (2-karboxietil) fosfina [*Tris (2-carboxyethyl) phosphine,* TCEP] erreduktorea [1:10 (mol:mol) proportzioan] ondo nahastu ziren, bolumena 200 µL-ra doituz. Erreakzioa gau osoan zehar utzi zen 4°C-tan, ilunpetan eta irabiaketa leunarekin.

Lotu gabeko zundaren garbiketa egiteko estrategia desberdinak frogatu ziren. Lehenengo eta behin $TrwB_{R388}$ eta $TMD_{TraJ}CD_{TrwB}$ laginentzat afinitate kromatografia bidezko garbiketa burutu zen, Ni-NTA agarosazko erretxina erabiliz. Horretarako 200 µL erretxina 1 mL-tako zutabe batean paketatu, Milli-Q uraz garbitu eta *MP markaketa indargetzailea*rekin orekatu zen. Ondoren lagina gehitu eta erretxinarekin ondo nahastu zen, ordu batez 4°C-tan irabiaketa leunarekin mantenduz. Zutabea berriz paketatu zen soberako indargetzailea deuseztatuz. Proteinaren eluziorako 150 mM imidazol zuen *MP markaketa indargetzailea* gehitu zen. Erretxina indargetzailearekin berreseki eta berriz inkubatu zen, ordu batez 4°C-tan irabiaketarekin. Proteinaren eluzioa egiteko, erretxina paketatu eta 150 mM imidazoldun *MP markaketa indargetzailea* igaro zen zutabetik frakzioak jasoz. Lortutako laginaren proteina eta zunda kontzentrazioak aztertu ziren, absorbantzia 280 nm-tan eta zunda bakoitzari zegokion uhin-luzeran aztertuz, hurrenez hurren.

Aurreko teknikaren bidez proteina ugari galdu zen prozesuan zehar eta gainera teknika hori ez zen itu-proteina guztientzat egokia, TrwBΔN70k ez baitu histidina etiketarik. Hori dela eta, zunden garbiketarako bigarren estrategia bat erabili zen, *Pierce™ Dye Removal Columns* kit komertziala erabiliz, etxe komertzialak eskainitako protokoloa jarraituz. 400 µL erretxina erabili ziren eta lagina zutabetik birritan igaro zen, garbiketa optimizatzeko. Hala ere, prozesu honen ostean oraindik zunda aske ugari geratzen zenez, hasieran erabilitako indargetzaile aldaketarako estrategia erabili zen. Laginak indargetzaile egokiarekin diluitu ziren eta *Vivaspin 500®*-etan zentrifugatu ziren (15.000*g*, 10 min, 4°C). Prozesua bezain beste aldiz errepikatu zen iragazian zundaren presentzia desagertu arte. Orduan laginak *eppendorf* hodi batera igaro eta zentrifugatu ziren (13.000 *g*, 10 min, 4°C) agregatuak kentzeko. Bukatzeko gain-jalkinaren proteina eta zunda kontzentrazioak aztertu ziren aurreko paragrafoan azaldu bezala.

2.8.3. BERRERAIKITAKO SISTEMAK

Behin *E. coli*-ren barne mintza antzeratzen zuten mintz-ereduak lortuta, haietan itu-proteinen berreraikitzea egin zen. Tesi honetan proteoliposoma mota desberdinak erabili dira, beti ere molekula bakarreko entseguak egiteko proteo-GUVak lortzeko helburuarekin.

2.8.3.1. PROTEO-LUVak

Proteo-GUVak lortzeko estrategietako bat abiapuntu gisa proteo-LUVak erabiltzea izan zen. Hauek aurretik deskribaturiko protokoloa erabiliz egin ziren (Vecino et al., 2011), aldaketa txikiekin.

Lehenengo eta behin, aurreko atalean azaldutako teknikak erabiliz, GUVak sortzeko konposizio lipidikoa optimizatu zen. Lortutako emaitzetan oinarrituz DOPC:PE:PG:CL (50:26,3:19,6:4,1) (mol:mol) lipido nahasketarekin LUVak osatu ziren, 2.8.1.3. atalean azaldu bezala.

LIPOSOMEN SOLUBILIZAZIOA ETA PROTEINAREN TXERTATZEA

Hurrengo pausua, LUVen solubilizazioa burutzea izan zen. Lan honetan *n-octyl-β-D-glucopyranoside* (OG) detergentea erabili egin zen honetarako. Solubilizazio kontzentrazioa ezagutzeko 200 µL-ko bolumenean 2,5 mM LUV OG kontzentrazio goranzkorrekin inkubatu ziren, 0tik 28 mM-era (*Liposoma indargetzailea*n prestatutako 500 mM-eko OG diluzioa erabiliz). Liposomen solubilizazioa uhertasunaren aldaketa aztertuz jarraitu zen, absorbantzia 520 nm-tan neurtuz (Goñi eta Alonso, 2000). Behin kontzentrazioa ezaguturik, liposomen solubilizazioa eta proteinen txertaketa egin ziren. Horretarako 6,25 mM LUV 74,78 mM OGrekin inkubatu ziren 25°C-tan, 30 minutuz, irabiaketarekin. Ondoren purifikaturiko proteinak gehitu ziren(25 µM proteina, 250:1 lipido:proteina erlazioan) bolumena 500 µL-ra doituz eta suspentsioa 25°C-tan beste 30 minutuz inkubatuz.

Detergentea kentzeko *Bio-Beads™ SM2* (BB) poliestirenozko partikulak erabili ziren. Hauek aldez aurretik garbitu egin ziren Holloway-ek (1973) deskribatu bezala: 10 g partikulen gainean 500 mL etanol gehitu ziren, giro tenperaturan irabiaketarekin 30 minutuz inkubatuz eta garbiketa hau hirutan errepikatuz. Ondoren 1 L Milli-Q ur gehitu zen, baldintza berdinetan

beste hiru inkubazio burutuz. Ura kendu eta BBak (bustita mantenduz) ilunpetan gorde ziren. Entsegu bakoitzean BB berriak erabili ziren. Detergentea kentzeko lehenengo eta behin lipido-proteina-detergente nahasketari 100 mg BB gehitu zitzaizkion, hiru orduz 4°C-tan irabiaketa leunarekin inkubatuz. Ondoren, beste 100 mg gehitu ziren, ordu batez egoera berdinetan inkubatuz. Bukatzeko, 200 mg BB gehitu ziren eta gau osoan zehar 4°C-tan irabiaketarekin inkubatu ziren. BBak kentzeko laginak zentrifugatu ziren (4.500 *g*, 2 min, 4°C) eta gain-jalkina pipeta bidez jaso zen.

ESPEZIE DESBERDINEN BANAKETA SAKAROSA GRADIENTE BIDEZ

Nahasketan zeuden espezie desberdinak banatzeko (proteoliposomak, liposomak eta agregaturiko proteina) sakarosa gradiente bidezko flotazio zentrifugazioa erabili zen (Rigaud and Lévy, 2003). Horretarako sakarosa dentsitate gradiente eten bat prestatu zen 4 mL-ko zentrifuga hodietan, *liposoma indargetzailea*n prestaturiko sakarosa soluzio desberdinak (% p/b) erabiliz. Horretarako zentrifuga hodian 500 µL-ko geruzak pixkanaka gehitu ziren, ondoko ordenean: lagina, %60, %40, %30, %20, %10, %5 eta %2,5. Laginen difusio egokirako %60ko soluzioa %0,05 Tritoi X-100rekin osatu zen. Zentrifugazioa *SW-60 Ti* errotorearekin burutu zen (100.000 *g,* 3 h, 4°C). Zentrifugazioan liposomek eta proteinadun liposomek gorantz flotatzen dute gradientean zehar, proteina askea eta agregatua beheko geruzan geratzen diren heinean. Zentrifugazioa bukatzerakoan 500 µL-ko alikuotak jaso ziren (lorturiko banden arabera).

Lagin hauek SDS-PAGE bidez aztertu ziren proteinadun frakzioak identifikatzeko. Horretaz gain, lipidoen kuantifikazioa burutu zen kolina kuantifikatzeko *Phosphatidylcholine Assay Kit* komertziala erabiliz, lipido:proteina erlazio egokia aurkezten zuten frakzioak identifikatzeko. Hauek *liposoma indargetzailea*rekin diluitu ziren 9 mL-ra arte eta *Ti-50* errotorean zentrifugatu ziren (100.000 *g*, 2 h, 4°C) sakarosa kentzeko. Lortutako jalkinak *liposoma indargetzailea*ren 50 µL-tan berreseki ziren, 4°C-tan biltegiratuz.

PROTEINAREN DETERMINAZIOA

Proteo-LUVen proteina kontzentrazioaren determinazioa SDS-PAGE bidez egin zen. Horretarako purifikaturiko $TrwB_{R388}$ proteina kontzentrazio desberdinetan (2 µg-tik 30 µg-ra) aztertu zen poliakrilamidazko gel batean eta tindaturiko banden intentsitatea *FIJI* softwarearen bidez neurtu zen kontzentrazioarekiko patroi zuzen bat egiteko. Proteo-LUVen laginak modu berean aztertu ziren eta haien proteina kontzentrazioa patroi zuzenarekin konparatuz kalkulatu zen.

Proteinen orientazioa mintzarekiko tiol erreaktibo iragazkor eta iragazgaitzak erabiliz determinatu zen (Sanowar eta Le Moual, 2005). Erreaktibo hauek proteinetan dauden zisteinei lotzeko gaitasuna daukate. Laburbilduz, proteo-LUVak (1,5 µM proteina) 22°C-tan 10 minutuz inkubatu ziren tiol erreaktibo bakoitza gehitu ostean. Liposomen solubilizazioa OGrekin 22°C-tan egin zen, 30 minutuz. Lehenengo erreaktiboekin inkubatu ostean, laginak *liposoma indargetzaile*rekin 8 mL-tara diluitu eta zentrifugatu ziren (105.000 *g*, 2 h, 4°C) soberako erreaktiboa deuseztatzeko.

Proteina totala determinatzeko proteo-LUVak 220 mM OGrekin solubilizatu ostean 0,33 mM fluoreszeina 5-iodoazetamidarekin (*5-iodoacetamide fluorescein,* 5-IAF) inkubatu

ziren (2.8. irudia, A). Tiol erreaktibo fluoreszente hau mintzarekiko iragazgaitza da, beraz zitosoleko domeinua kanporantz zuzenduta daukan proteina kantitatea zuzenean determinatzeko balio du (2.8. irudia, B). Aldiz, zitosoleko domeinua liposomen barnerantz zuen proteina kantitatea ezagutzeko, proteo-LUVak 0,33 mM azido 4-azetamido-4'-maleimidilstilben-2 2'-disulfonikoarekin (*4-Acetamido-4'-Maleimidylstilbene-2,2'-Disulfonic Acid*, AmdiS), mintzarekiko tiol erreaktibo iragazgaitza, inkubatu ziren, kanpo proteina blokeatzeko. Ondoren, proteo-LUV horiek 220 mM OGrekin solubilizatu eta 0,33 mM 5-IAFrekin inkubatu ziren, barnerantz zuzendutako proteina soilik markatzeko (2.8. irudia, C). Bukatzeko, markaketa ez-espezifikoa neurtu zen bi entsegu desberdinen bidez (2.8. irudia, D). Alde batetik proteo-LUVak 10 mM N-etilmaleimidarekin (*N-Ethylmaleimide*, NEM), mintzarekiko tiol erreaktibo iragazkor ez fluoreszentea, inkubatu ziren eta ostean 5-IAF 0,33 mM-rekin. Beste aldetik, 220 mM OGrekin inkubatu ziren, jarraian 0,33 mM AmdiSrekin eta ondoren 0,33 mM 5-IAFrekin inkubatuz. Modu honetan erabilitako erreaktiboen elkarrekintza inespezifikoen eza frogatu zen.

Erreakzio guztiak *Laemmli 6X indargetzailea* 1X bukaerako kontzentraziora gehituz gelditu eta SDS-PAGE bidez aztertu ziren. 5-IAF bidez markaturiko proteinak *ChemiDoc*^{TM} bidez ikusi ziren. Fluoreszentziaren azterketa egin ostean, gela tindatu egin zen *tindatzeko disoluzioa* erabiliz, kale guztietan proteina kantitate berdina zegoela frogatzeko.

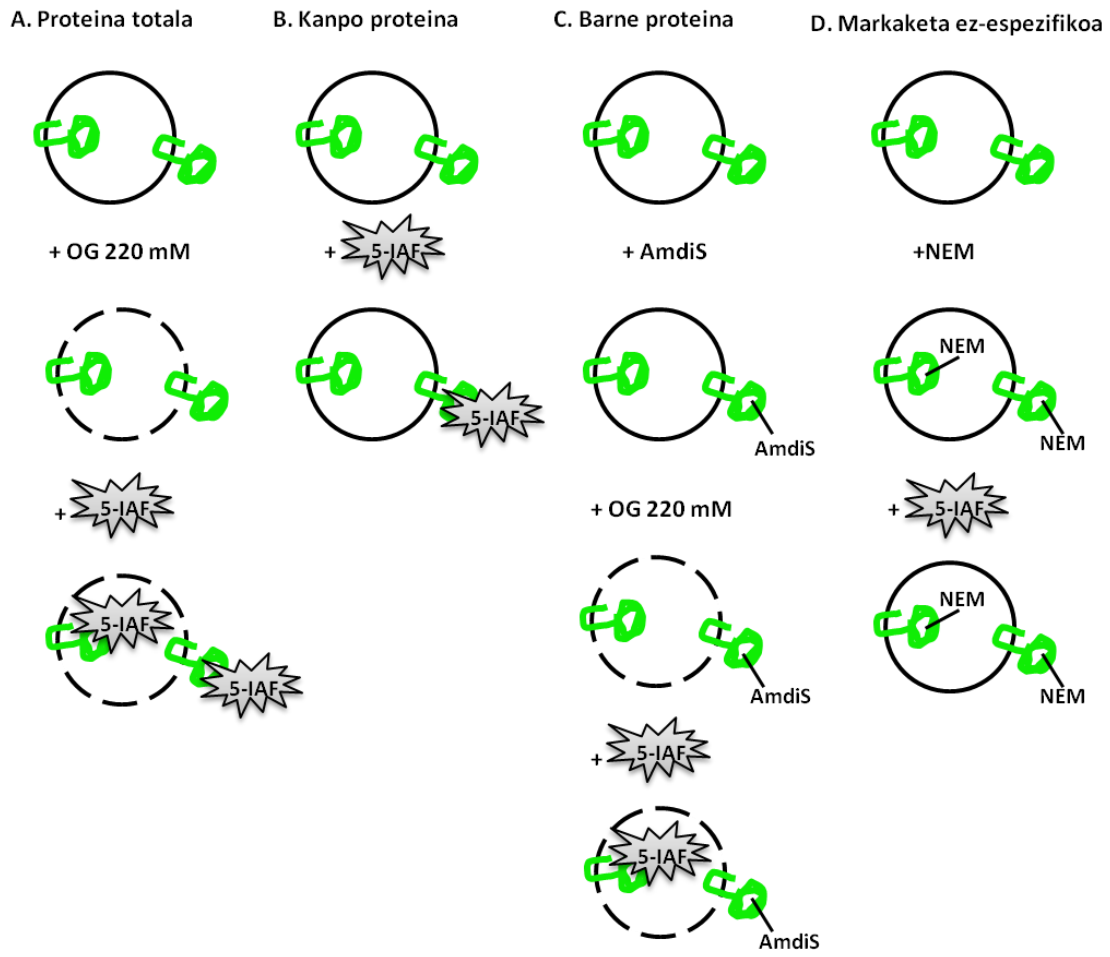

2.8. irudia. Proteo-LUVetan berreraikitako proteinen orientazioaren azterketaren irudikapen eskematikoa. Proteinak zisteinekin erreakzionatzen duten tiol erreaktiboekin markatu ziren. Horretarako proteoliposomak erreaktiboekin 10 minutuz 22°C-tan inkubatu ziren. Liposomak beltzez adierazita daude, proteina berdez eta 5-IAF erreaktibo fluoreszentea grisez. Mintz-etenak OG bidez solubilizaturiko liposomak adierazten ditu. **A)** Proteina totalaren markaketa. **B)** Domeinu disolbagarria kanporantz orientaturiko proteinaren markaketa. **C)** Domeinu disolbagarria barrurantz orientaturiko proteinaren markaketa. **D)** Fluoreszentzia ez-espezifikoa.

2.8.3.2. BAKTERIOEN BARNE MINTZEKO BESIKULAK

Lehenengo eta behin itu-proteinadun BIMVak lortu ziren, literaturan deskribaturiko protokoloa jarraituz (Jiménez et al., 2011; De Vrije et al., 1987) aldaketa gutxi batzuekin. Laburbilduz, *E. coli* BL21C41(DE3) zelulak pUB9 eta pOPINe-MobBGFP plasmidoekin transformatu egin ziren. Lortutako koloniak antibiotikodun 120 mL LBn hazi ziren, 37°C-tan gau osoan zehar. Hurrengo egunean 1:50 diluzioak egin ziren andui bakoitzeko 2 L-ko bi matraze eta 1 L-ko matraze bana prestatuz, 37°C-tan hazten utzi zirenak. OD_{600} 0,6 ($TrwB_{R388}GFP$) eta 0,4 ($MobB_{CloDF13}GFP$) balioak lortzean, bakterioak 1 mM IPTGrekin induzitu ziren, 25°C-tan inkubatzen utzi zirenak. Une horretan andui bakoitzeko 1 L-dun matrazeko zelulak jaso ziren, 6.000 *g*-n zentrifugatuz. Lortutako jalkin bakoitza 10 mL *BIMV1 indargetzaile*rekin berreseki zen eta -20°C-tan biltegiratu zen ("0 lagina" moduan izendatuz). Indukziotik ordu batera lagin

bakoitzeko 2 L-dun matrazetako batekin prozesu bera errepikatu zen, kasu honetan 20 mL indargetzaile erabiliz jalkina berresekitzeko (“1 lagina” moduan izendatuz). Andui bakoitzeko geratzen zen 2 L-ko matrazearekin protokolo bera erabili zen indukziotik bi ordu igarota (“2 lagina” moduan izendatuz).

BIMVak isolatzeko lehenengo eta behin zelula suspentsioak ur bainu bidez desizoztu ziren. Une horretatik aurrera protokolo guztia 4°C-tan burutu zen. Azpimarratu beharra dago 0 laginentzat bolumen erdiak erabili zirela. Laginei 40 µL DNasa I (10 mg/mL-ko kontzentrazioan) eta 1 M $MgCl_2$ gehitu zitzaien eta French prentsa erabiliz lisatu ziren. Apurtu gabeko zelulak deuseztatzeko laginak zentrifugatu egin ziren (8.000 *g,* 15 min) eta gain-jalkina berriz zentrifugatu zen (116.760 *g*, 45 min). Jalkinak (mintz frakzioak) 2 mL *BIMV2 indargetzaile*rekin berreseki ziren.

Bakterioen barne mintza isolatzeko sakarosa gradiente bat erabili zen. Horretarako %62 (p/b) sakarosa disoluzioa prestatu zen 4°C-tan. Disoluzio hau erabiliz eta 1 mL *BIMV sakarosa indargetzaile* gehituz, 10,5 mL-tako (Milli-Q urarekin doituz) %35, %45, %50 eta %55 (p/b) sakarosa diluzio desberdinak prestatu ziren. Ondoren *SW-60* errotorerako 4,2 mL-tako saiodietan sakarosa gradientea prestatu zen 2.9. irudian adierazten den moduan. Tratamendu hau izotzetan egin zen, soluzio bakoitza kontu handiz gehituz sakarosa geruzak elkarren artean ez nahasteko. Zentrifugazioaren (262.710 *g,* 40 min) bukaera balazta erabili gabe burutu zen, dentsitatearen bidez banandutako geruzen nahasketa ekiditeko.

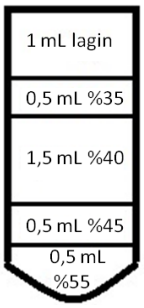

2.9. irudia. Sakarosa gradientearen irudikapen eskematikoa. Sakarosa gradiente etenaren bidezko banaketa burutzeko sakarosa disoluzio desberdinak pixkanaka gehitu ziren zentrifugazio hodietan, irudian adierazitako ordenean.

Behin gradientea eginda, barne mintzari zegokion banda gorrixka bat ikusi zen %35-%45 geruzen tartean, zeinaren gainetik kanpo mintzen banda zurixka zegoen. Barne-mintzari zegokion banda pipeta baten laguntzaz eta kontu handiz jaso zen eta *BIMV2 indargetzailea*rekin 1:5 proportzioan diluitu zen. Ondoren diluzioak zentrifugatu ziren (120.000 *g,* 90 min), sakarosa aztarnak kentzeko. Lortutako jalkinak itu proteinadun *E. coli* barne mintzak ziren, 500 µL *BIMV2 indargetzaile*tan berreseki zirenak. 25 µL-tako alikuotak egin ziren eta nitrogeno likidoa erabiliz izoztu ziren -80°C-tan biltegiratzeko. Lagin bakoitzean lortutako proteina kontzentrazio totala 280 nm-tan absorbantzia neurtuz kalkulatu zen.

2.8.3.3. PROTEO-GUVak

Fluorescence Cross-Correlation Spectroscopy (FCCS) izeneko teknikaren bidezko entseguak proteo-LUV eta BIMVekin burutzerakoan, populazio mailako azterketa bat egiten da. Ondorioz, lortzen diren emaitzak populazioaren batezbestekoari dagozkio. Aldiz, proteo-GUVak erabiltzean, GUV-bakarreko entseguen bidez mintzean bertan ematen diren aldaketak era kontrolatu batean jarrai daitezke. FCCS entseguak burutzeko helburua izanda, T4CPak GUVetan berreraikitzeko saiakera desberdinak burutu ziren proteoliposomak eta BIMVak abiapuntu gisa erabiliz (Dezi et al., 2013).

DETERGENTE GABEKO FUSIOA

GUVen formazio entsegu desberdinak burutu ziren 2.8.1.4. atalean aurkeztutako elektroformazio eta ITO estalkien protokoloak jarraituz. Azken kasuan, BIMVak DOPC-SUVekin erlazio desberdinetan nahastu ziren GUVen formazioa erraztu nahian.

DETERGENTE BIDEZKO FUSIOA

Detergenteak erabiliz proteo-GUVak lortzeko estrategia desberdinak daude. Tesi honetan Dezi et al. (2013) ezarritako protokoloen hiru aldaera desberdin erabili egin dira (2.10. irudia):

1. **GUVen prestaketa detergenteen presentzian, ondoren detergente bidez purifikaturiko mintz proteinekin fusionatzeko.** Entsegu hauek burutzeko baldintza desberdinak frogatu ziren: lipido konposizio desberdinak, elektroformazio ganbarak zein ITO estalkiak, 300 mM zein 400 mM sakarosadun indargetzaileak eta elektroformazio protokolo desberdinak [(10 Hz, 1,5 V, 2 h eta 2 Hz, 1,5 V, 1 h) edo (10 Hz, 1,1 V, 3,5 h)]. GUVen formaziorako 2 mg/mL-ko lipido esekidurak erabili ziren (5 µL) zeinei DiO %0,1 gehitu zitzaien. Detergentea lipido esekidurari edo *GUV hantura indargetzaileari* gehitu zitzaion, 0,2 mM DDM izanik hantura prozesuan zehar.

2. **BIMV eta DOPC-SUVen detergente bidezko fusioa proteo-GUVen formaziorako abiapuntu gisa.** Honetarako DOPC-SUVak eta BIMVak banandurik prestatu eta solubilizatu ziren. DOPC-SUVak *SUV fusio indargetzailea*n prestatu ziren, 2,5 mg/mL DOPC eta 0,025 µM DiD kontzentraziora, 200 µL-tan. Hauek 41,3 mM OGrekin solubilizatu egin ziren, 45 minutuz giro tenperaturan inkubatuz. BIMVak kantitate desberdinetan (2, 10, 25 eta 50 µg proteina totala) diluitu ziren *SUV fusio indargetzailea*n, 136 µL-ko bolumenera. Hauek OGrekin solubilizatu egin ziren baldintza berdinetan, 2 µg proteinako 4 µM OG erabiliz. Ondoren, solubilizaturiko 64 µL DOPC-SUV BIMV disoluzio desberdinekin elkartu ziren, 0,8 mg/mL DOPCdun 200 µL-tako laginak lortuz. Ordu batez 25°C-tan inkubatu ostean nahasketari 15 mg BB gehitu zitzaizkion. 30 minutu geroago beste 15 mg gehitu ziren eta berriz 30 minutu igarota 30 mg gehiago, gau osoan 4°C-tan inkubatuz. Protokolo honen bidez proteo-SUVak (BIMV-DOPC-SUVak) lortu ziren. Kontrol negatibo gisa, protokolo bera jarraitu zen, baina detergenterik erabili gabe. 2 eta 10 µg proteinadun proteo-SUVak abiapuntu gisa erabiliz (detergenterekin tratatuak eta kontrol negatiboak) gel bidezko hantura burutu zen proteo-GUVak (BIMV-DOPC-GUVak) lortzeko.

3. **BIMVak aldez aurretik formaturiko DOPC-GUVekin fusionatzeko entseguak.** BIMVak (0,2 mg/mL proteina) DOPC-GUVekin inkubatu ziren erlazio desberdinetan gau osoan zehar. Bi besikulen arteko fusioa emateko DDMrekin osatutako *GUV fusio indargetzailea* erabili zen. Indargetzaileko Triton X-100 detergentea BIMVen solubilizazioa burutzeko erabili zen, DDMa DOPC-GUVen solubilizazioa burutzeko erabili zen heinean [2:1 (p/p) lipido:DDM erlazioa erabiliz]. Nahasketak gau osoan zehar giro tenperaturan inkubatu ziren, irabiaketarik gabe GUVak ez apurtzeko. Hurrengo goizean laginei 15 mg BB gehitu zitzaien eta bost orduz utzi ziren baldintza berdinetan. Lortutako proteo-GUVen bistaratzea 2.8.1.4. atalean azaldu bezala burutu zen.

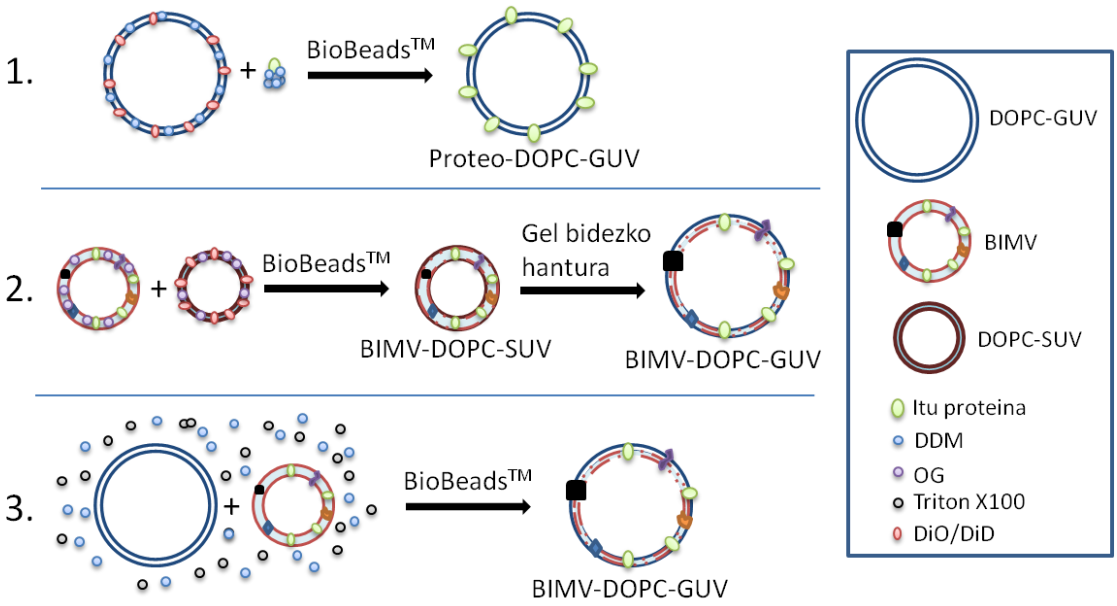

2.10. irudia. Detergente bidezko proteo-GUVen formaziorako burututako entseguen irudikapen eskematikoa. 1. Detergenteen presentzian formatutako GUVen eta purifikatutako proteinen arteko fusioa. 2. Aldez aurretik solubilizaturiko BIMV eta DOPC-SUVen fusioa, gel bidezko hanturaren bidez proteo-GUVen lortzerako. 3. Aldez aurretik formatutako GUVen eta BIMVen detergente bidezko solubilizazioa eta ondoko fusioa.

2.8.3.4. EUTSITAKO BIGERUZA LIPIDIKOAK

Orain arte deskribaturiko besikuletan bigeruza lipidikoak ingurune urtsu bat inguratuz kokatzen dira. Eutsitako bigeruza lipidikoetan, ordea, bigeruza lipidikoak euskarri solido baten gainean kokatzen dira gainazal lau bat sortuz. Zenbait tekniketan, adibidez *Atomic Force Microscopy* (AFM) edota *Total Internal Reflection Fluorescence Microscopy* (TIRFM) tekniketan, gainazal solido lau handi batekin lan egiteak prozesuak errazten ditu. TIRFM oligomeroen estekiometria aztertzeko teknika bikaina da, protokolo jakinen bidez SLBak sortzean proteinak modu estatikoan geratzen baitira beiran atxikiturik, lipidoak mugitzen diren heinean. SLBak sortzeko abiapuntu gisa BIMV-DOPC nahasketak erabili ziren. Horretarako Dodd et al. (2008) deskribaturiko protokoloen optimizazioa burutu zen, parametro desberdinen (proteina

kantitatea, BIMV:DOPC erlazioa, DiD kontzentrazioa, fusio metodoa, eta abar) konbinazioak frogatuz.

Lehenengo eta behin beirazko estalkien (#1, 0,13-0,16 mm) eta bistaratze ganbaren prestaketa egin zen (Subburaj et al., 2015). Estalkiak garbitzeko, momentuan prestaturiko azido sulfurikozko (%95-97, b/b) eta hidrogeno peroxidozko (%30, b/b) 3:1 (b/b) nahasketa batean murgildu ziren ordu batez. Honen bidez hondakin organikoak garbitu eta beirazko gainazalaren hidrofilizatea areagotu zen. Ondoren, Milli-Q urarekin ondo garbitu eta bost minutuz sonikatu ziren. Bukatzeko, N_2 korronte bidez lehortu ziren. Erabiltzerako orduan zortzi putzutako *Nunc™ Lab-Tek™* ganbarei beirazko zorua kendu zitzaien, haietara garbitutako estalkiak itsatsiz.

Nahiz eta protokoloaren aldaera desberdinak erabili (ikusi 5.5. TIRFM entseguen prestaketa), orokorrean jarraitutako pausuak ondokoak izan ziren (2.11. irudia): lehenengo eta behin *SLB indargetzailea*n DOPC-SUVak prestatu ziren 2,5 mg/mL-ko kontzentrazioan. Era berean, BIMVak (0,375 µg proteina) *SLB indargetzailea*n DiDaren kontzentrazio egokiarekin nahastu ziren bolumena 100 µL-ra doituz, ostean SUVak lortzeko sonikazio prozesua burutuz. Ondoren bistaratze ganbarak 37°C-tara berotutako termobloke baten gainean kokatu ziren. BIMV laginak 50 µL DOPC-SUVekin nahastu eta ganbaretara gehitu ziren. Jarraian, $CaCl_2$ gehitu zen 3 mM-eko bukaerako kontzentraziora, 15 minutuz inkubatuz besikulen fusioa emateko. Bukatzeko, fusionatu gabeko SUVen garbiketa egin zen, ganbarak epeldutako *SLB indargetzaile*rekin 20 aldiz garbituz. Azken garbiketan 300 µL gehitu ziren, bertan laginak 20 minutuz inkubatuz. Horren ondoren laginak mikroskopio bidez bistaratzeko prest zeuden.

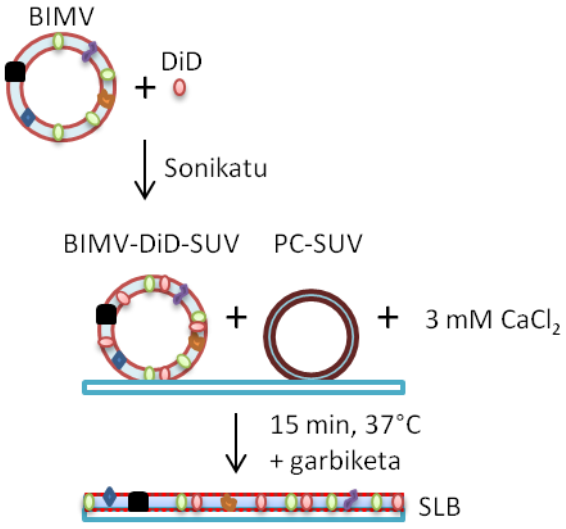

2.11. irudia. Eutsitako bigeruza lipidikoen formazioa. Purifikaturiko BIMVak DiD zundarekin nahastu eta sonikatu ziren, BIMV-DiD-SUVak lortzeko. Hauek, aldez aurretik sorturiko DOPC-SUVekin nahastu eta *Nunc™ Lab-Tek™* ganbaretara gehitu ziren. Fusioa emateko 3 mM $CaCl_2$ gehitu ziren, ostean ganbarak 15 minutuz 37°C-tan inkubatuz. Fusionatu gabeko besikulak garbitu ostean eutsitako bigeruza lipidikoak lortu ziren, TIRFM entseguak burutzeko.

Hala ere, protokolo honen bidez lorturiko emaitzak ez ziren esperotakoak izan (besikulen fusio desegokia, eGFP seinale biziegia eta abar eman zirelako). Hori dela eta aldaera

desberdinak frogatu ziren, adibidez detergente bidezko solubilizazioak erabiltzea, SLB optimoak lortzeko.

2.9. TEKNIKA MIKROSKOPIKOAK

Lan honetan, proteinen azterketan sakontzeko, fluoreszentziazko mikroskopiaren aldaera desberdinak erabili egin dira. Mikroskopia teknika hau substantzia jakin batzuek, fluorokromo deituak, uhin-luzera jakin bateko argia jasotzeko eta beste uhin-luzera handiago batean igortzeko duten gaitasunean oinarritzen da. Fluorokromoak laginaren parte izan daitezke, adibidez eGFPdun fusio-proteinak, edota laginean fixatu daitezke, aldez aurretik azaldutako zunda fluoreszenteak bezala. Fluorokromodun lagin bat uhin-luzera egokiarekin kitzikatzen bada, ikusgarri bihurtzen da bere igorpen uhin-luzera soilik igarotzen uzten duen iragazki bat erabiliz gero. Modu horretan fluorokromoa distiratsu agertzen da atzeko plano ilun baten gainean, igorritako argiaren intentsitatea eta kolorea erabilitako molekula fluoreszentearen araberakoak izanik.

Fluoreszentziazko mikroskopioa ohiko mikroskopioaren antzekoa da, baina kasu honetan iragazki bat dago zeinak fluorokromoa kitzikatuko duen uhin-luzera soilik igarotzen uzten duena. Era berean, laginak igorritako argia bigarren iragazki batetik igarotzen da, fluorokromoak igorritako uhin luzerako argia soilik igarotzen uzten duena. Mikroskopio konfokalak zenbait abantaila aurkezten ditu epifluoreszentziako mikroskopioen aurrean. Alde batetik laginaren gune jakin batean soilik fokatzen den argi-iturri bat (laser bat, alegia) erabiltzen du. Bestaldetik bi arrailduren (*pinhole)* erabilera: (i) kitzikatze arraildura (*Illumination pinhole*), argi iturriaren ostean kokaturikoa, zeinak plano fokalaren goi eta bekaldetik datorren argia deuseztatzen duen; eta (ii) detekzio arraildura (*Confocal pinhole)*, foto-detektagailura iristen den fluoreszentzia mugatzen duena. Honek plano fokalean aurkitzen ez diren puntuek igorritako erradiazioaren deuseztapena ahalbidetzen du. Ezaugarri hauei esker irudien bereizmen optikoa hobea da, irudi hauek erresoluzio altuagoa aurkeztuz eta plano bakarrean fokaturik egonik.

2.9.1. PROTEINEN KOKAPEN AZPIZELULARRA

2.9.1.1. eGFP FUSIO-PROTEINEN KOKAPENA

Aurretik azaldu bezala, biologia molekularraren bidez T4CP-eGFP fusio proteina desberdinak lortu ziren. Behin proteina hauen *in vivo* funtzionalitatea konjugazio entseguen bidez frogaturik, haien kokapen azpi-zelularra aztertu zen. eGFP proteinek soilik ondo tolesturik daudenean daukatenez fluoroforo izaera, haien bistaratzeak proteina funtzionalen azterketa ziurtatzen du, desnaturalizaturik edota inklusio gorputzetan daudenak baztertuz (Drew et al., 2006). eGFP-fusio proteinen kokapen azpi-zelularra prozesu konjugatiboan parte hartzen duten gainerako proteinen absentzian zein presentzian (plasmido konjugatibodun anduietan, alegia) aztertu zen, proteina hauek T4CPen kokapenean izan dezaketen eragina ezagutzeko. Entsegu hauetan Segura et al. (2014)-n aurkeztutako protokoloa erabili zen, aldaketa batzuekin.

Lehenengo eta behin, gain-adierazpena burutzeko zelulak plasmido egokiekin transformatu ziren (pUB9 $TrwB_{R388}$GFPrako, pUBQ4GFP $TMD_{TraJ}CD_{TrwB}$GFPrako, pOPINE-3C-eGFP-*$tmd_{TrwB}traj$* TMD_{TrwB}TraJ-GFPrako, pOPINE-3C-eGFP-*traj* $TraJ_{pIP501}$GFPrako, pOPINE-3C-eGFP-mobB $MobB_{CloDF13}$GFPrako, eta pOPINE-3C-eGFP-*mobB*Δ*TMD* MobBΔTMDGFPrako). Zehazki *E. coli* BL21(DE3) eta BL21C41(DE3) bakterioak erabili ziren proteina disolbagarriak eta MPak adierazteko, hurrenez hurren. Zelulak antibiotiko egokiekin osatutako 10 mL LBn gau osoan zehar 37°C-tan hazi ziren. Hurrengo goizean, kultiboak 1:50 proportzioan diluitu (500 µL kultibo 25 mL LBn) eta OD_{600} 0,4 balioa lortu arte 37°C-tan hazi ziren. Orduan, 1 mM IPTGrekin induzitu eta 1 mL-tako lagin bat hartu zen (0 denbora) bere OD_{600}a neurtuz. Zelulak 25°C-tan hazten utzi ziren eta 4 eta 20 ordu ostean 1 mL-ko laginak jaso ziren berriz. Lagin bakoitza jaso bezain laster zentrifugatu zen (8.000 *g*, 2 min) eta *PBS*rekin 3 garbiketa burutu ziren. Ostean, berriz zentrifugatu eta gain-jalkina deuseztatu zen. Zelulak ezartzeko jalkina 500 µL paraformaldehido %4 (p/b) soluzioan berreseki eta giro tenperaturan 10 minutuz inkubatu zen. Laginak zentrifugatu ziren (8.000 *g*, 5 min) eta behin paraformaldehidoa deuseztaturik *PBS*rekin beste hiru garbiketa burutu ziren. Protokoloaren une honetan, gelditu eta laginak 4°C-tan gorde daitezke.

Zelulak estalkien gainean atxikitzeko, estalki esterilak 24-putzutako plaka batean kokatu eta 200 µL polilisinarekin gaineztatu ziren. Ordu batez giro tenperaturan inkubatu ostean, pipeta baten laguntzaz polilisina kendu eta plaka lehortzen utzi zen 37°C-tan, 30 minutuz. Bitartean zelula laginak 1 mL-ko bolumenera eta OD_{600} 0,32 baliora doitu ziren *PBS*a erabiliz. Honi esker estalki guztietan antzeko zelula dentsitatea lortu zen. Lehortutako estalkien gainean 500 µL zelula suspentsio gehitu eta zentrifugatu ziren (800 *g*, 10 min, giro tenperatura). Ondoren, plaka 30 minutuz giro tenperaturan inkubatu zen, ilunpetan. Atxiki ez ziren zelulen garbiketa burutzeko, gain-jalkina pipeta baten laguntzaz kendu eta *PBS*arekin hiru garbiketa egin ziren.

Estalkien muntaia burutzeko, portak etanolarekin garbitu eta lehortzen utzi ziren. Ostean, estalkiak H_2O-rekin garbitu eta aldez aurretik portan jarritako 2 µL *ProLong Gold antifade reagent* gainean kokatu ziren. Behin laginak prestatuta, hozkailuan gorde egin ziren. Laginen behaketa *Leica TCS SP5* mikroskopio konfokalean egin zen, 60X olio objektiboa, 488 nm-tako kitzikapena eta 525 nm-tako igorpena erabiliz. Lortutako irudien tratamendua *Huygens Essential* eta *ImageJ* programa informatikoen bidez egin zen. eGFP fusio-proteinen 6 kokapen desberdin identifikatu ziren (2.12. irudia). Hala ere, zenbait kasutan eGFPri zegokion fluoreszentzi berdeko irudietan ez zen argi geratzen proteinen kokapena. Hori dela eta, irudiak *ImageJ* softwarearen bidez tratatu ziren, aldez aurretik ezarritako *ICE* izeneko filtroa erabiliz (2.12. irudia, beheko ilara).

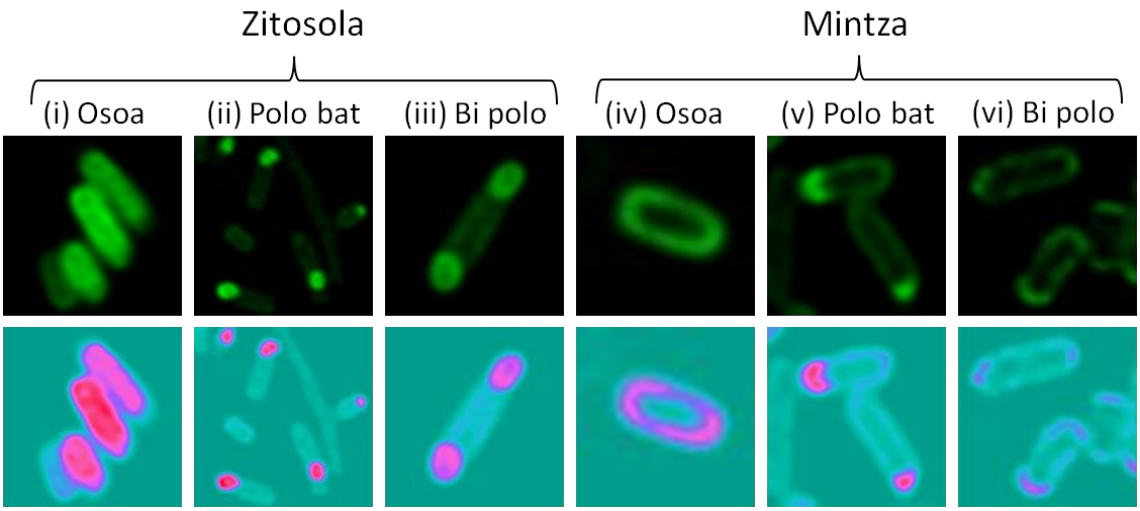

2.12. irudia. T4CP-eGFP fusio-proteinen kokapen desberdinen sailkapena. Fluoreszentziaren intentsitate maximoa aurkezten zuen kokapen azpi-zelularraren arabera sei proteina-kokapen desberdin deskribatu ziren: (i) zitosol osoan zehar; (ii) zitosoleko polo bakarrean; (iii) zitosoleko bi poloetan; (iv) mintz osoan zehar; (v) mintzeko polo bakarrean; (vi) mintzeko bi poloetan. Goiko lerroan fluoreszentzia berdea adierazita dago eta beheko lerroan zenbaketa egiteko erabili zen *ICE* filtroa. Irudiak ondoko laginetatik jasoak dira: (i) eGFP indukziotik 4 ordura; (ii) MobBΔTMD-GFP indukziotik 4 ordura; (iii) $TraJ_{pIP501}$GFP indukziotik 4 ordura; (iv) $TrwB_{R388}$GFP indukziotik 4 ordura; (v) $TrwB_{R388}$GFP pSU1456 plasmidoaren presentzian indukziotik 20 ordura; (vi) $MobB_{CloDF13}$GFP pSU1456 eta pSU4833 plasmidoen presentzian indukziotik 4 ordura.

2.9.1.2. IMMUNOFLUORESZENTZIA BIDEZKO KOKAPENA

Immunofluoreszentzia hainbat arlotan erabiltzen den teknika da. Bertan, fluoreszenteki markatutako antigorputzak erabiltzen dira, aztergai den molekula edota antigeno jakina ezagutzen duen beste antigorputz bat espezifikoki detektatzen dutenak. Tesi honetan immunofluoreszentzia teknika erabili zen eGFP fusio-proteinekin lortutako emaitzen balioztapena egiteko. Bi metodologien protokoloak nahiko antzekoak dira, baina kasu honetan fluorokromoa bigarren mailako antigorputz bat zen. Ondoren azaldutako protokoloko pausu guztien artean laginak hiru aldiz garbitu ziren *PBSa*rekin.

Zelula laginen lortze prozesua aurreko protokoloan bezala burutu zen, paraformaldehido tratamenduaren osteko garbiketetara arte. Behin garbiketa horiek eginda, zelulak iragazkor bihurtu ziren antigorputzak zelula barnera sartu ahal izateko. Horretarako zelulak berriz zentrifugatu eta jalkina 1,5 mL *iragazkortasun indargetzailea*n berreseki zen, 10 minutuz 4°C-tan inkubatuz. Jarraian, aldez aurretik 24 putzutako plaka batean kokaturiko eta polilisinarekin trataturiko estalkien gainean 20 µL zelula esekidura gehitu ziren. Giro tenperaturan 10 minutuz inkubatu ostean, 200 µL *PBS*rekin estalkien hiru garbiketa egin ziren, azken garbiketan *PBS*a bertan mantenduz lagina ez lehortzeko. Jarraian plaka zentrifugatu zen (3.000 *g*, 5 min), putzu bakoitzeko *PBS*a deuseztatu, eta estalkiak -20°C-tan gordetako metanolarekin inkubatu ziren 4 minutuz. Metanola kendu eta garbiketen ostean, plaka izotz gainean mantenduz, estalki bakoitza -20°C-tan gordetako azetonan murgildu zen 20 segundoz.

Ondoren, blokeoa burutu zen *blokeatze disoluzio*aren 200 µL erabiliz eta ordu batez 37°C-tan inkubatuz. Jarraian laginak gau osoan zehar 200 µL *mouse anti-His (C-term) monoclonal* lehen mailako antigorputzarekin (1:200 diluzioa *blokeatze disoluzioan*) inkubatu ziren 4°C-tan. Hurrengo egunean estalkiak *PBSa*rekin garbitu eta ilunpetan, giro tenperaturan, 3 orduz 10 µg/mL *Alexa Fluor 488 goat anti-mouse* bigarren mailako antigorputzarekin (*blokeatze disoluzioan* diluitua) inkubatu ziren. Bukatzeko, lotu gabeko antigorputzaren garbiketak burutu ziren, estalkiak *PBSa*rekin garbituz.

Estalkien muntaia aurreko atalean bezala burutu zen, baina kasu honetan irudien eskuratzea "Biomedikuntzan Mikroskopia Analitiko eta Bereizmen Handikoa" zerbitzuaren bidez egin zen (SGIker, UPV/EHU), *Olympus Fluoview*^{TM} *500* mikroskopio konfokala erabiliz.

2.9.2. *FLUORESCENCE CROSS-CORRELATION SPECTROSCOPY (FCCS)*

FCCS bidez bi molekulen arteko elkarrekintzak aztertzen dira. Horretarako itu-molekulak zunda fluoreszente desberdinekin etiketaturik egon behar dira. Ondoren mikroskopio konfokal bat erabiliz, lagineko bi fluorokromoen intentsitate gorabeherak aztertzen dira. Aldakuntza hauek bi fluorokromoen fluoreszentzia-espektroak parekaturik daudela adierazten du, hau da, bi molekulak bolumen fokalean zehar elkarrekin mugitzen direla. Lan honetan FCCS teknika proteo-SUVetan itu-proteinen okupazioa aztertzeko erabili da, deskribaturik baitago %20ko proteina okupazioa duten besikulek TIRFM bidezko estekiometria azterketak burutzeko SLB egokiak sortzen dituztela (Subburaj et al., 2015). Nahiz eta entseguen baldintzak guztiz berdinak ez izan irizpide hau abiapuntu gisa erabili zen.

Tesi honetan BIMVetan isolaturiko eGFP-fusio proteinak (fluoreszentzia berdea) erabili ziren, lipidoak DiD zundarekin (fluoreszentzia gorria) markatu zirelarik. BIMV-PC-SUVak 2.8.3.4. atalean azaldu bezala lortu ziren eta fluoreszentziazko mikroskopio konfokalaz aztertzeko bistaratze ganbaretan kokatu ziren.

FCCS entseguak *LSM710* mikroskopio konfokal bat erabiliz burutu ziren. Mikroskopioa *ConfoCor3*, *C-Apochromat 40* x N.A. 1,2 ur inmertsiozko objektiboarekin eta 488 eta 633 nm-tan kitzikatzeko laserrekin ekipaturik zegoen. Fluoroforo desberdinek igorritako fotoiak ispilu dikroikoen bidez banandu eta iragazki egokien ostean kokaturiko *Avalanche* foto diodoen (APD) bidez detektatu ziren (eGFPrentzat 505-540 nm-tako iragazkia eta zunda gorrientzat >655 nm-takoa). APDak detektore oso sentikorrak dira, FCCS entseguak burutzeko oso egokiak izanda. Erlazio-gurutzatuko kurbak lortzeko behar bezain beste datu jasotzeko, lagin bakoitza bere difusio denbora baino 10.000 aldiz gehiago neurtu zen. Difusio denbora, difusio koefizienteak, proteina kontzentrazioa eta erlazio-gurutzatuak "*3D Brownian difusion*" funtzioan oinarrituta kalkulatu ziren. Neurketa guztietan 3 errepikapen tekniko burutu ziren (30 segundokoak) eta neurketak kaltetu zezaketen partikula fluoreszente handien aztarnak kendu ziren.

2.9.3. *FLUORESCENCE RECOVERY AFTER PHOTOBLEACHING*

Fluorescence Recovery After Photobleaching (FRAP) izeneko teknika molekulen zinetikak edota difusio mugimenduak aztertzeko erabiltzen da. Bere oinarria laserraren

menpean egoteagatik ematen den fluorokromoen amatatzearen ondoren fluoreszentziaren aldaeraren azterketa da. Tesi honetan SLBen fluidotasuna, eta beraz lipidoen alboko difusioa, aztertzeko erabili egin da.

Entsegu hauek egiteko SLBak prestatu eta mikroskopio konfokal bidez aztertu ziren. Horretarako laginaren gune batean DiDaren hasierako fluoreszentzia bistaratu zen. Jarraian gune horren puntu konkretu bat (oro har azalera totalaren %30-50 tartean dagoena) uhin-luzera egokiko laserrarekin (DiDaren kasuan, 633 laserra) irradiatu zen. Puntu horretako fluorokromoek (hau da, DiD molekulek) argi intentsitate handia jasotzearen ondorioz (laserraren intentsitatea %0,5etik %100ra igotzeagatik) fluoreszentzia bizitza azkar agortu zuten, laginean gune ilun bat agertuz. SLBan lipidoen difusioa ziurtatu zen fluoreszentziaren berreskurapena lortu baitzen (berreskurapen prozesuan zehar %0,5eko laser intentsitatea erabiliz eta irudiak hartuz gune ilunak fluoreszentzia balio maximo batera heldu arte). Fenomeno hau gune ilunaren ingurunean dauden partikula fluoreszenteen difusioan oinarritzen da. Gune ilunetik kanpo dauden molekula fluoreszenteei frakzio mugikorra deritzo, gune argi eta ilunaren artean trukatu ezin diren molekulei frakzio ez-mugikorra deitzen zaien bitartean. Beraz, gune argitik ilunera molekula fluoreszenteen difusioa ematean, molekula fluoreszente hauek gune ilunean zeuden molekulak (aldez aurretik amataturikoak, alegia) ordezka ditzakete, gune iluna berriz fluoreszente bihurtuz. Normalean, FRAP irudikapen batean hasierako fluoreszentzia intentsitatea minimo batera jaisten da foto-amataketaren ostean eta gero berriz fluoreszentzia berreskuratzen da gune ilunean balio konstante batera heldu arte, fluoreszentziaren berreskurapen maila frakzio mugikorraren eta ez-mugikorraren araberakoa izanik.

2.9.4. *TOTAL INTERNAL REFLECTION FLUORESCENCE MICROSCOPY*

TIRFM molekula bakarreko teknika da. Tesi honetan teknika hau bakterioen barne-mintzean aurkitzen diren T4CP oligomero populazio desberdinen azterketa egiteko erabili da; hain zuzen ere $TrwB_{R388}$GFP eta $MobB_{CloDF13}$GFP proteinena. Horretarako fluoreszentziaren analisia edota foto-amataketa entseguak burutu ziren. Izan ere TIRFM bidezko foto-amataketa erabiliz espezie bakoitzean dauden fluoroforo kantitatea azter daiteke (Subburaj et al., 2015).

Lan honetan BIMVak erabiliz azterketa hau burutzeko protokoloa garatu eta optimizatu da. Lehenengo eta behin FCCS eta FRAP bidez abiapuntuko baldintza egokiak ezarri ziren. Behin protokoloak optimizaturik, konposizio egokiko SLBak prestatu eta mikroskopio entseguak burutu ziren *Zeiss Axiovert 200* mikroskopioa erabiliz (100X olio objektiboa, TIRF angelua: 5,7). TIRFM entseguan erabilitako parametroak 2.9. taulan laburbiltzen dira.

2.9. taula. TIRFM entseguetan erabilitako parametroak.

Laserra	488 (%10)
Tenperatura	-79°
Esposizio denbora	35 ms
Irakurketa	10 MHz; 14 bit
Em irabazi anitza	300
Irabazia	1
Tartea	0
Denbora osoaren atzerapena	35
Marko kopurua	500

CHAPTER 3:

COUPLING PROTEIN PRODUCTION FOR THE STUDY OF THE ROLE OF THEIR TRANSMEMBRANE DOMAIN

3. COUPLING PROTEIN PRODUCTION FOR THE STUDY OF THE ROLE OF THEIR TRANSMEMBRANE DOMAIN

All plasmids used in this work are listed in table 2.2. All reagents and buffers are listed on tables A.1 and A.2 of the appendix, respectively. All the proteins used in this work contain a poly-histidine tag (H_x-tag) on their C-term except for TrwBΔN70. All the eGFP fusion-proteins are namedy as GFP to simplify the nomenclature.

3.1. INTRODUCTION

T4CPs are essential elements in cT4SSs and are also key elements in many pT4SSs. The members of this family display a high sequence, length, and domain architecture heterogeneity. In fact, the only conserved features through all T4CPs are the Walker A and B motifs in the NBD. For this reason, they are classified according to the different domain architectures in the following manner (figure 1.5) (Llosa and Alkorta, 2017): (i) the VirD4-type subfamily, which is composed of integral MPs; (ii) TraG-J pairs, which are MPs but additionally present a physical and functional association with another MP; (iii) T4CPs without TMD, which could or could not have a linked MP, like the pair $TraJ_{pIP501}$ and $TraI_{pIP501}$; (iv) FtsK-like T4CPs and (v) Archaeal T4CPs. The structural paradigm of the T4CPs, $TrwB_{R388}$ (the T4CP of conjugative plasmid R388) falls inside the VirD4-type group, which is the most studied subfamily. $TrwB_{R388}$ is composed of a TMD formed of two transmembrane α-helices connected through a periplasmic loop at the N-term and a globular CD that contains an NBD with the Walker A and Walker B motifs and a small membrane-distal AAD (Gomis-Rüth et al., 2001). However, the huge heterogeneity of the T4CP family questions if the characteristics described for the conjugative $Gram^-$ paradigmatic T4CPs from the VirD4-type subfamily are universally applicable.

As mentioned above, the most studied T4CPs are MPs, which need the precise use of detergents during their purification to maintain their stability once they are out of their natural environment, the membrane. But paradoxically, this treatment endangers the integrity of the protein while complicating and slowing the process of obtaining protein samples in proper conditions for further functional and structural studies. Due to this fact, the only full-length T4CP that has been successfully purified to date is $TrwB_{R388}$ (Hormaeche et al., 2002; Redzej et al., 2017), while trials for purifying other membrane T4CPs have not rendered the sufficient amounts of high quality solubilised protein for performing *in vitro* assays (Chen et al., 2008). For this reason most of the *in vitro* studies of T4CPs have been achieved using deletion mutant proteins that lack the TMD (Larrea et al., 2017; Schroder and Lanka, 2003; Tato et al., 2007). However, after studying the properties of $TrwB_{R388}$ in comparison to its deletion mutant, TrwBΔN70, it was observed that they presented significant differences regarding biological activity (such as *in vivo* function, *in vitro* nucleotide-binding and *in vitro* ATPase activity), oligomerization pattern, subcellular location and stability (Hormaeche et al., 2002, 2004, 2006; Moncalián et al., 1999; Segura et al., 2013, 2014; Vecino et al., 2010, 2011). For this reason it has been concluded that the TMD of $TrwB_{R388}$ accomplishes a role beyond the anchorage of the protein to the membrane, determining the location, stability and activity of this T4CP.

On the way to identifying specific inhibitors of T4CPs it is indispensable to begin with unravelling the universal characteristics related to all T4CPs and gaining deeper knowledge on the role of the TMD. For this reason we decided to **study a set of T4CPs** of different origins and characteristics. Specifically T4CPs from four different cT4SS have been studied in this work: on the first place **$TrwB_{R388}$** from the $Gram^-$ plasmid R388 of *E. coli*, which is the structural paradigm of the T4CPs (Llosa and Alkorta, 2017) and has been studied in our group for over 20 years. Secondly **$MobB_{CloDF13}$**, which is the T4CP of the mobilizable plasmid CloDF13 from *Enterobacter cloacae.* It is an interesting system to study since it is part of the rare MOB_{C1} family plasmids, which are mobilizable plasmids that encode their T4CP (Smillie et al., 2010). Additionally, $MobB_{CloDF13}$ has been described as an atypical T4CP, due to its dual role in DNA transfer, since it acts as an accessory protein in CloDF13 relaxation process and also as a T4CP (Núñez and De La Cruz, 2001). Thirdly, **$TraJ_{pIP501}$**, which is the T4CP of the conjugative plasmid pIP501, originally isolated from a $Gram^+$ clinical *Streptococcus agaliactae* strain (Evans and Macrina, 1983). $TraJ_{pIP501}$ belongs to the group of T4CPs that lack a TMD but are linked to a MP (Alvarez-Martinez and Christie, 2009). It is located in the cytosol and it has been postulated that it could perform its coupling activity together with a small MP named $TraI_{pIP501}$ (see T4CPs without TMD), forming a potential two-protein fusion T4CP (Grohmann et al., 2016). Hence, it must present different characteristics to those described for the VirD4-like T4CPs. Finally, a forth T4CP was chosen, **$TraJ_{pKM101}$** of the conjugative plasmid pKM101 from *E. coli*. $TraJ_{pKM101}$ is the phylogenetically closest T4CP to $TrwB_{R388}$, with a sequence homology of 37% (Alvarez-Martinez and Christie, 2009; Paterson et al., 1999), and it has been described that both T4CPs can interact with the T4SS of R388 and pKM101 (Llosa et al., 2003).

To perform a wide study, together with the four native proteins, different mutant proteins have been characterised in this thesis. On one hand a **deletion protein lacking the TMD of $MobB_{CloDF13}$, MobBΔTMD,** has been constructed. On the other hand, **chimera proteins** that contain combinations of TMD and CD of the chosen heterologous T4CPs, **$TMD_{TraJ}CD_{TrwB}$ and $TMD_{TrwB}TraJ_{pIP501}$**, have been constructed to analyse the role of the different domains. This strategy has already been used for the study of components of cT4SSs, showing interesting results (Bourg et al., 2009). Specifically, through the chimera protein approach the function of the AAD of $VirD4_{At}$ from the T-plasmid of *Agrobacterium tumefaciens* (Whitaker et al., 2016) and of the N-terminal HUH domain of $TrwC_{R388}$ (Agúndez et al., 2018) have been analysed.

3.2. CONSTRUCTION OF RECOMBINANT AND MUTANT PROTEINS

The first step in this study was to clone the genes encoding for these proteins and their respective mutants into different expression vectors. This was performed using traditional molecular biology methods and a high-throughput (HTP) assay developed in the Oxford Protein Production Facility-UK (OPPF-UK). The sequences of all the plasmid constructions performed in this work were checked by Sanger sequencing in the General Genomics Sequencing and Genotyping Unit (SGIKER, UPV/EHU).

3.2.1. SEQUENCE ANALYSIS

In order to construct different mutants of the chosen T4CPs (*i.e.* $TrwB_{R388}$, $MobB_{CloDF13}$, $TraJ_{pIP501}$, and $TraJ_{pKM101}$) their sequences were analysed through bioinformatics tools. First, the different characteristics of the proteins, such as MW and isoelectric point, were analysed using *ProtParam* (https://web.expasy.org/protparam/). Second, the topology of the MPs was studied using *Topcons* (http://topcons.cbr.su.se/). The obtained results for the wild type T4CPs studied in this work are shown in figure 3.1. As expected, $TraJ_{pIP501}$ does not contain any transmembrane region. On the contrary, $TraI_{pIP501}$, which is not a T4CP but might interact with $TraJ_{pIP501}$ (Grohmann et al., 2016), has two predicted transmembrane helices.

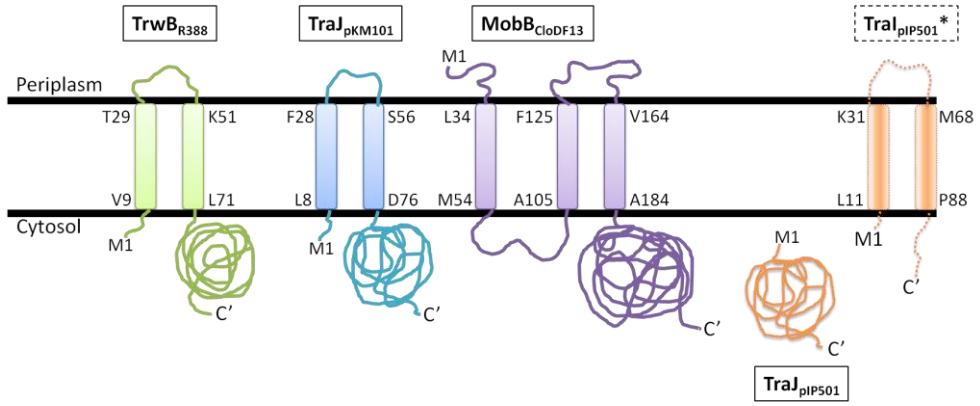

Figure 3.1. Predicted membrane topology of $TrwB_{R388}$, $TraJ_{pKM101}$, $MobB_{CloDF13}$, $TraJ_{pIP501}$ and $TraI_{pIP501}$. Membrane topology of the different T4CPs was predicted using *Topcons* software. The black lines represent the inner bacterial membrane. M1: N-term; C': C-term. The first and last residues of each transmembrane helix are shown next to the corresponding helix and represented with the single letter amino acid code and their position in the sequence. Proteins from R388, pKM101, CloDF13, and pIP501 plasmids are shown in green, blue, purple and orange, respectively. * $TraI_{pIP501}$ is shown with dashed lines for it is not a T4CP.

Once the location of the different transmembrane helixes in the protein sequence was known, this information was used to design the mutant proteins as follows (for complete sequences see Protein sequence and information):

- **$TMD_{TraJ}CD_{TrwB}$**: amino acids M_1 to D_{76} from $TraJ_{pKM101}$ followed by amino acids L71 to I507 from $TrwB_{R388}$.
- **$TMD_{TrwB}TraJ_{pKM101}$**: amino acids M_1 to G_{75} from $TrwB_{R388}$, followed by the linker sequence -QGELE- and the amino acids T_2 to F_{551} from $TraJ_{pIP501}$.
- **$MobB\Delta TMD_{CloDF13}$:** amino acids D_{185} to Y_{653} from $MobB_{CloDF13}$.
- **$TraI_{pIP501}TraJ_{pIP501}$**: amino acids M_1 to D_{143} from $TraI_{pIP501}$ followed by the amino acids –GS- and amino acids T_2 to F_{551} from $TraJ_{pIP501}$.

3.2.2. TRADITIONAL CLONING

As explained in the previous chapter, target genes can be cloned into expression vectors by applying PCR, restriction and ligation techniques. This has been used to directly clone wild-type genes, but also to create genes encoding for chimera T4CPs.

3.2.2.1. PROTEINS RELATED TO R388 SYSTEM

As one of the aims of this thesis is to gain deeper knowledge in the role of the TMD of T4CPs, two different chimera variations of $TrwB_{R388}$ have been constructed, switching its TMD or CD with domains from another T4CP. Specifically, T4CPs $TraJ_{pKM101}$ and $TraJ_{pIP501}$ were used to change the TMD and CD of $TrwB_{R388}$, respectively.

$TMD_{TraJ}CD_{TrwB}$

The first chimera protein is composed of the TMD of the T4CP $TraJ_{pKM101}$ (TMD_{TraJ}) and the CD of $TrwB_{R388}$ (CD_{TrwB}). The target sequence for TEV protease was added in between both domains (through the PCR primers, table 2.4), so that they could be separated after purification and individually studied.

The strategy used for the construction of this protein is described in section 2.2.1. Briefly, the sequence encoding for the TMD of $TraJ_{pKM101}$ was amplified using plasmid pKM101 as a template and the encoding sequence of CD_{TrwB} was amplified using plasmid pUB3 as template. Obtained amplicons were inserted into pET22b(+) expression vector, which adds a H_6-tag at the C-term and encodes for Amp resistance (Amp^R). After restrictions, ligation into pET22b(+) vector and transformation into *E. coli* DH5α cells, a set of putative clones was obtained. Plasmid DNA was extracted from the colonies and the presence of the insert was checked by PCR (figure 3.2, A) and digestion with restriction enzymes (figure 3.2, B). A band of 1548 Kb and bands of 5493 and 1548 Kb in PCR and restriction analysis, respectively, indicated positive results in the cloning of $TMD_{TraJ}CD_{TrwB}$ chimera. The resultant plasmid was named **pUBQ1 (**figure 3.2, C), which contained the sequence for protein **TMD_{TraJ}-TEV-CD_{TrwB} with a H_6-tag at the C-term and encoded for Amp^R** (figure 3.2, D).

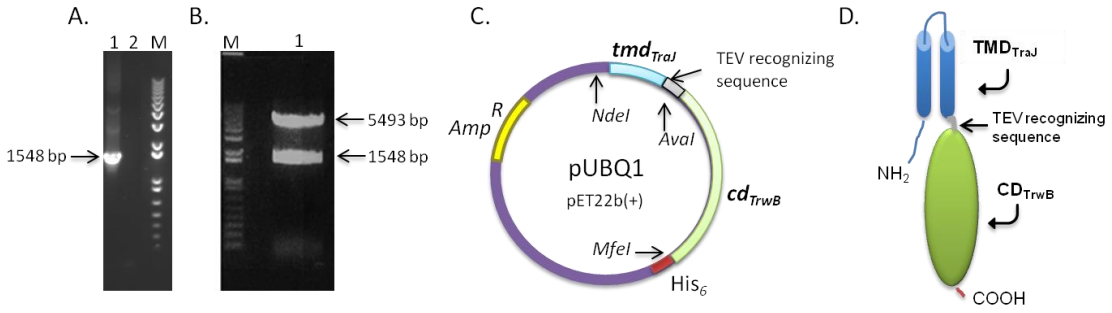

Figure 3.2. Cloning of *tmd_{TraJ}-TEV-cd_{TrwB}*. Products obtained in all the reactions were analysed by 1% (v/v) agarose gel electrophoresis in *TAE buffer* and dyed with *Sybr™ Safe*. M: *1 kb plus DNA ladder*. **A)** *E. coli* DH5α cells were transformed with the product of the ligation and plasmid DNA was extracted from the obtained colonies. This DNA was used as a template for PCR amplification of *$tmd_{TraJ}cd_{TrwB}$*. 1: amplified product; 2: negative control. Band in lane 1

shows the expected size of 1548 base pairs (bp), pointed by the arrow. **B)** Plasmids that gave positive results in the previous test were digested with *Nde*I and *Xho*I restriction enzymes. Two bands were obtained, pointed by the arrows. The upper band corresponds to the backbone of the pET22b(+) vector (5493 bp) and the lower band to the insert (1548 bp). **C)** Schematic representation of pUBQ1 vector. Used restriction sites are pointed by arrows. The H_6-tag is represented in red, while the genes encoding for Amp^R are in yellow. Sequence for TEV protease is represented in grey. DNA fragment encoding for tmd_{TraJ} and cd_{TrwB} are shown in blue and green, respectively. **D)** Schematic representation of the chimera protein encoded in pUBQ1 vector, TMD_{TraJ}-TEV-CD_{TrwB}. Colour code as in C.

To perform conjugation assays, it was necessary to co-transform cells with pKM101 and pUBQ1 plasmids, both coding for Amp^R. Therefore it was decided to subclone the new protein into the pET24a(+) vector, which encoded for Kan antibiotic resistance (Kan^R). Once pUBQ1 vector was obtained, it was digested with *NdeI* and *MfeI* enzymes and the fragment corresponding to tmd_{TraJ}-*TEV*-cd_{TrwB} was ligated into pET24a(+) expression vector, which had been previously digested with the same restriction enzymes. The colonies were analysed using the same protocol as in pUBQ1. Finally, pUBQ2 plasmid was obtained, which also had the sequence encoding for TMD_{TraJ}-TEV-CD_{TrwB} with an H_6-tag at the C-term, but encoded Kan^R.

Subsequently, during purification of TMD_{TraJ}-TEV-CD_{TrwB} protein (see section S3.5.1.3.) a spontaneous hydrolysis through the TEV recognition sequence was observed. Although different purification protocols were attempted, the hydrolysis was unavoidable. Therefore, for the sake of celerity, it was decided to purchase a new construct, plasmid pUBQ4, in which the genes encoding for both domains would be right after each other, without TEV recognizing sequence or sequence for restriction enzymes in between them. The construction of this plasmid was made by TOP Gene Technologies, Inc. (Saint-Lauren, QC-Canada). They synthesized $tmd_{TraJ}cd_{TrwB}$ sequence *de novo* and inserted it into pET24a(+) plasmid using *Nde*I and *XhoI* restriction sites. From that moment on, **pUBQ4** plasmid was the one used in this thesis for the study of **$TMD_{TraJ}CD_{TrwB}$ chimera protein**.

$TMD_{TraJ}CD_{TrwB}$GFP

To perform subcellular location studies, it was necessary to obtain the eGFP fusion variant of $TMD_{TraJ}CD_{TrwB}$. The construction was performed as explained in section 2.2. Briefly, the $tmd_{TraJ}cd_{TrwB}$ sequence was amplified using pUBQ4 plasmid as a template for the PCR reaction. Amplified DNA fragment and plasmid pUB9 were independently digested with *Xho*I and *Bam*HI restriction enzymes. From pUB9 digestion, two fragments were obtained: $TrwB_{R388}$GFP and pWaldo-GFPe vector backbone. They were separated by 1% (w/v) agarose gel electrophoresis in *TAE buffer* and the fragment corresponding to the vector backbone was purified. Digested $tmd_{TraJ}cd_{TrwB}$ was ligated with the vector backbone and the obtained sample was used to transform *E. coli* DH5α cells. Plasmid DNA was extracted from the obtained colonies and analysed for the presence of the insert through digestion and PCR amplification (figure 3.3). In this manner, **pUBQ4GFP** plasmid was obtained. This plasmid coded for **Kan^R and $TMD_{TraJ}CD_{TrwB}$ protein followed by a recognition site for the TEV protease, an eGFP domain and a H_8-tag** ($TMD_{TraJ}CD_{TrwB}$-TEV-eGFP-H_8, named in short as $TMD_{TraJ}CD_{TrwB}$GFP).

.

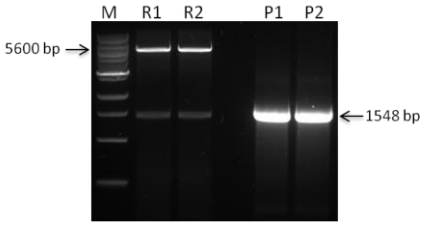

Figure 3.3. Clone testing for $TMD_{TraJ}CD_{TrwB}GFP$ construction. Plasmid DNA was extracted from two of the colonies obtained from the transformation with the ligation products. Obtained samples were on one hand digested with *Xho*I and *Bam*HI (R1 and R2), and on the other hand, they were used as templates for PCR amplification of $tmd_{TraJ}cd_{TrwB}$ (P1 and P2). The upper arrow points to the vector backbone obtained after digestion (5600 bp), while the lower band points to $tmd_{TraJ}cd_{TrwB}$ DNA fragment (1548 bp).

$TMD_{TrwB}TraJ_{pIP501}$

The second chimera protein is composed of the TMD of $TrwB_{R388}$ (TMD_{TrwB}) and the coupling protein $TraJ_{pIP501}$. In order to construct this protein the $traJ_{pIP501}$ sequence was inserted into pUB7 vector [pET22b(+) expression vector that encodes for TMD_{TrwB}]. To ensure the cloning, plasmid DNA from different candidate clones was analysed by agarose gel electrophoresis (figure 3.4, A). Plasmids that presented the expected size were used as DNA templates for PCR amplification of $traJ_{pIP501}$ to confirm the presence of the insert (figure 3.4, B). Plasmids that presented the expected size amplicon in the PCR amplification (1656 bp) were further analysed. Since the cloning strategy was based on a single restriction site (*Xho*I), it was also necessary to check the orientation of the insert. To do so, restriction with *Pvu*I-HF enzyme was performed by taking advantage of having two *Pvu*I-HF restriction sites; one inside the insert and another one in the vector backbone. When the amplicon had been properly oriented, bands of 1297 and 5922 bp had to be observed (figure 3.4, C). The obtained plasmid was named **pUBQ3** (figure 3.4, D), which contained the sequence for protein **$TMD_{TrwB}TraJ_{pIP501}$ with a C-term H_6-tag and encoded for Amp^R** (figure 3.4, E).

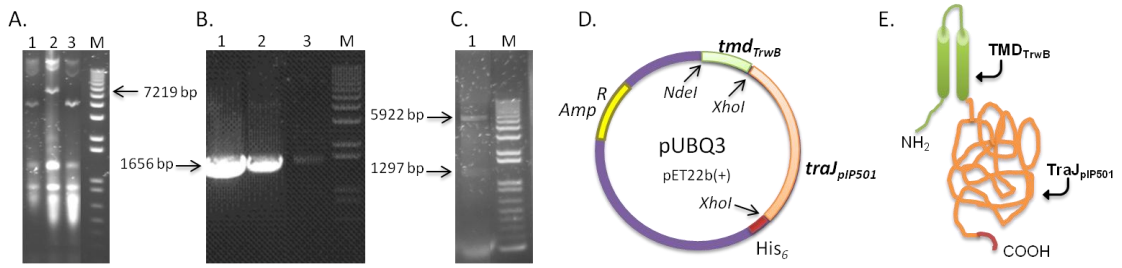

Figure 3.4. Cloning of $tmd_{TrwB}traJ_{pIP501}$. Products obtained in all the reactions were analysed by 1% (v/v) agarose gel electrophoresis in *TAE buffer* and dyed with *Sybr™ Safe*. M: *1 kb plus DNA ladder*. **A)** *E. coli* DH5α cells were transformed with the product of the ligation and plasmid DNA was extracted from the obtained colonies. Lanes 1 and 3 are negative clones that contain recircularized empty vectors, while lane 2 shows a plasmid with the proper size (7219 bp, pointed by the arrow). **B)** Extracted DNA was used as a template for PCR amplification of *traJ.*

1: amplified product; 2: positive control; 3: negative control. Bands in lanes 1 and 2 show the expected size of 1656 bp (pointed by the arrow). **C)** Insert orientation check by restriction enzymes. The proper bands of 1297 and 5922 bp were observed (pointed by the arrows). **D)** Schematic representation of pUBQ3 vector: used restriction sites are pointed by arrows. The H_6-tag is represented in red, while the genes encoding for Amp^R are in yellow. DNA fragments encoding for tmd_{TrwB} and $traJ_{pIP501}$ are shown in green and orange, respectively. **E)** Schematic representation of the protein encoded in pUBQ3 vector, $TMD_{TrwB}TraJ_{pIP501}$. Colour code as in D.

3.2.2.2. PROTEINS RELATED TO CloDF13 SYSTEM

$MobB_{CloDF13}$ and MobBΔTMD were cloned using a high throughput protocol in OPPF-UK (see below, section 3.2.4.)

$MobC_{CloDF13}$

Mobilizable plasmids contain an *oriT* and a relaxase encoding region, in addition to a T4CP in the case of the MOB_{C1} family plasmids (Smillie et al., 2010). CloDF13 plasmid falls into this category encoding in its MOB region for its *oriT,* the protein $MobC_{CloDF13}$, and the T4CP $MobB_{CloDF13}$. This organization suggested the role of $MobC_{CloDF13}$ as the relaxase of the system, which was proved by *in vivo and in vitro* assays (Núñez and De La Cruz, 2001). Conversely, $MobC_{CloDF13}$ does not show any sequence similarity with previously reported relaxases. Additionally, it has been described that it is not able to relax CloDF13 plasmid *in vivo* in the absence of $MobB_{CloDF13}$, showing a unique substrate processing reaction performed by both proteins. These special characteristics together with its interactions with the T4CP turn $MobC_{CloDF13}$ into an interesting protein to study.

In order to perform the cloning, *mobC* gene was amplified by PCR and the product was digested with *NdeI* and *Xho*I restriction enzymes. The digested DNA fragment was ligated into a previously digested pET24a(+) vector. *E. coli* cells were transformed with the ligation product and plasmid DNA was extracted from the obtained colonies to check the presence of the insert and its sequence. In this manner plasmid **pUB49, encoding Kan^R and $MobC_{CloDF13}$ with a C-term H_6-tag,** was obtained.

3.2.2.3. PROTEINS RELATED TO pIP501 SYSTEM

$TraJ_{PIP501}$

Although $traJ_{pIP501}$ had been previously cloned in different vectors [such as pQTEV-*orf10,* Abajy et al. (2007)], it was decided to clone it in pET22b(+) in order to attempt new purification methods. After amplification of $traJ_{pIP501}$ by PCR, the same protocol as for $MobC_{CloDF13}$ was followed, but using pET22b(+) vector instead of pET24a(+). In this manner plasmid **pUB48 ,encoding for Amp^R and $TraJ_{pIP501}$ with a C-term H_6-tag,** was obtained.

As previously said, it has been postulated that the soluble T4CP $TraJ_{pIP501}$ might perform its coupling activity upon interaction with the small MP $TraI_{pIP501}$. This association could form a complex similar to the paradigmatic VirD4-type T4CPs. For this reason, it was decided to create a fusion-protein between $TraJ_{pIP501}$ and $TraI_{pIP501}$ to study its characteristics. The cloning was performed in two steps. First, $TraI_{pIP501}$ was amplified, digested with *Nde*I and B*amH*I and inserted into pET22b(+) vector, as explained in section 2.2.1. and the pET22b(+)*traI* construction was obtained. Simultaneously, $traJ_{pIP501}$ gene was amplified and digested with *BamH*I *and Xho*I. pET22b(+)*traI* was digested likewise and the obtained vector backbone (including $traI_{pIP501}$ gene) was ligated with the digested $traJ_{pIP501}$ DNA fragment. The obtained sample was used to transform *E. coli* DH5α cells. DNA from the grown colonies was extracted and checked by PCR (figure 3.5, A), digestion, and Sanger sequencing. In this manner plasmid **pUBQ5** was obtained (figure 3.5, B), which contained the sequence for the fusion-protein **$TraI_{pIP501}TraJ_{pIP501}$ with a C-terminus H_6-tag and encoded for Amp^R** (figure 3.5, C).

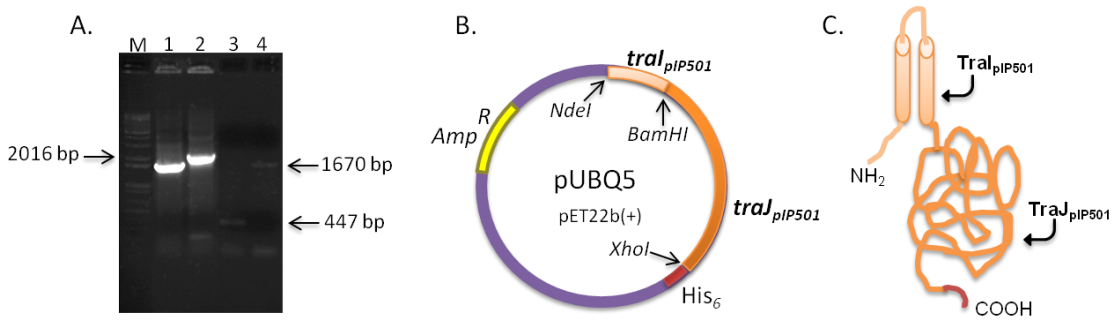

Figure 3.5. Cloning of $traI_{pIP501}traJ_{pIP501}$. Products obtained in all the reactions were analysed by 1% (v/v) agarose gel electrophoresis in *TAE buffer* and dyed with *Sybr™ Safe*. M: *1 kb plus DNA ladder*. **A)** *E. coli* DH5α cells were transformed with the product of the ligation and plasmid DNA was extracted from the obtained colonies. This DNA was used as a template for PCR amplification of $traJ_{pIP501}$ *and traItraJ.* 1: amplification of *traJ* (1670 bp); 2: amplification of *traItraJ* (2016 bp); 3: positive control for $traI_{pIP501}$ (447 bp); 4: positive control for $traJ_{pIP501}$. **B)** Schematic representation of pUBQ5 vector. Used restriction sites are pointed by arrows. The H_6-tag is represented in red, while the genes encoding for Amp^R are in yellow. DNA fragments encoding for *traI* and *traJ* are shown in light and dark orange, respectively. **C)** Schematic representation of the protein encoded in pUBQ5 vector, $TraI_{pIP501}TraJ_{pIP501}$. Colour code as in B.

3.2.3. SITE-DIRECTED MUTAGENESIS: $TMD_{TraJ}CD_{TrwB}$(K142T)

Site-directed mutagenesis is a straight forward technique to change a specific DNA sequence within a plasmid, whether it is a nucleotide exchange, insertion or deletion (Bachman, 2013). Studies have been made with the homologous mutant of $TrwB_{R388}$, TrwBK136T, and it has been described that this mutation abolishes the transfer ability of $TrwB_{R388}$ (Moncalián et al., 1999). Additionally, mutant TrwBΔN70(K136T) did not show ATPase activity in comparison to TrwBΔN70 (Tato et al., 2005). Analogously, in this work, we used side-directed mutagenesis to study the role of the conserved lysine in the Walker A motive present in $TMD_{TraJ}CD_{TrwB}$ chimera (K142T). This mutation was constructed as explained in

section 2.2.2. To do so, *QuikChange II Site-Directed Mutagenesis Kit* was used following the instructions given by the manufacturer. In this manner **pUBQ4(K142T)** plasmid was obtained, encoding for **$TMD_{TraJ}CD_{TrwB}$ with the K142T mutation and an H_6-tag at the C-term**.

3.2.4. HIGH-THROUGHPUT CLONING

Note: Due to the high amount of plasmid constructions performed in this section the results are summarised in supplementary data table S3.1. To simplify data analysis, each construction is named with a code (capital letter followed by a number) whose translation is shown on the aforementioned table.

It has been described that problems to express and solubilise proteins might be solved when expressing them as fusion-proteins. This strategy has been performed with $TraJ_{pIP501}$ and $TMD_{TrwB}TraJ_{pIP501,}$ to optimize their expression and purification, and with the proteins related to CloDF13 system, $MobB_{CloDF13}$ and its soluble mutant MobBΔTMD. On that account, an HTP cloning and expression protocol designed by OPPF-UK (Berrow et al., 2007) was used (section 2.2.3.). Through this method, **the genes encoding for these proteins were cloned into a set of pOPIN vectors.** Each of these vectors added a different fusion-tag in the N- or C-term of the target protein, which could be helpful when performing experiments with different requirements. The main advantage of this HTP method is its savings in time and money since all the reactions are performed simultaneously. Additionally, some of the pOPIN vectors have the same single-chain sequences when linearised, hence some PCR products aimed for different vectors are the same. This is advantageous in case a negative result is obtained in one of the PCRs since it might be substituted for another one in the *In-fusion*™ reaction.

The base of this HTP cloning method was the use of the *In-Fusion*™ enzyme and the pOPIN set of vectors (OPPF, UK). This is a ligase independent single-step technology, where the enzyme catalyses the union of DNA duplexes through the exposition of complementary single-chain sequences (figure 2.1). To do so, complementary sequences to the ones present in the target vectors (15 bp approximately) were added by the PCR primers to the target sequences (table S2.1). As explained before, even if a single PCR product could be used to obtain different constructs, due to the HTP design of the assay, all the PCR reactions were always performed, even though some of them gave the same product. It must be pointed out that according to the HTP nature of the method, after obtaining all the amplicons, the rest of the reactions were performed straightforward, from the *In-fusion*™ reaction until the final PCR checks, even if some negative results were obtained in the intermediate steps. Once a whole trial had been performed, the obtained results were analysed and a second small trial was carried out for the constructs that had given negative results on the first round.

First of all, to obtain the target genes, 47 HTP PCR amplifications were performed; using three different DNA templates (table S2.1). The set of PCR products was analysed by agarose gel electrophoresis (figure 3.6, A). Some of the amplifications related to $tmd_{TrwB}traJ_{pIP501}$ and all the amplifications related to $traJ_{pIP501}$ gave negative results; therefore a second trial for all the constructs related to these genes was performed (figure 3.6, B). The obtained PCR products from both trials were digested with *Dpn*I enzyme, purified, and analysed likewise (figure 3.6, C). All the amplicons except for G6 (for nomenclature see table

S3.1) were obtained; however, since the product of this amplification was the same as the one of E6 and F6 reactions, F6 amplicon was used as the substrate for the G6 *In-Fusion*™ reaction.

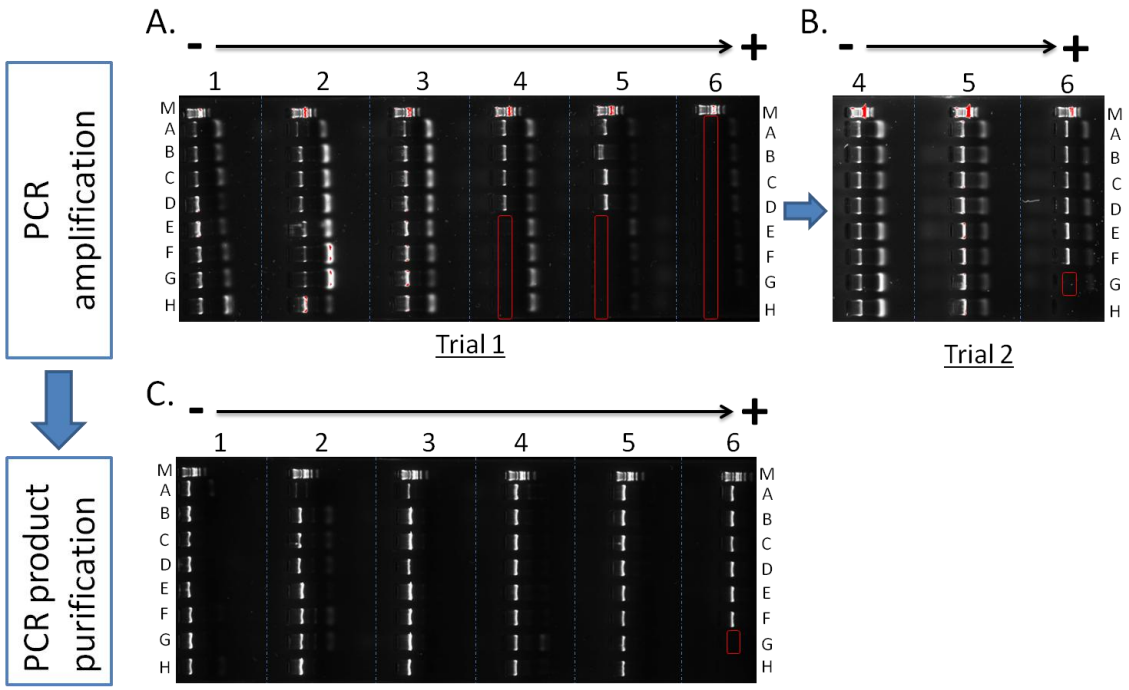

Figure 3.6. Analysis of the HTP-PCR products. Obtained products were analysed by 1.25% (w/v) agarose gel electrophoresis in *TBE buffer*. M: *Hypperladerl*™ *DNA MW marker*. Numbers in columns and letters in lines represent the coordinates that encode for each construct (table S3.1). Red boxes mark the negative results. Black arrows show the direction of DNA movement. **A)** First PCR trial. **B)** Second PCR Trial. **C)** Purification of PCR products.

Purified samples were joined by *In-Fusion*™ technology into the corresponding vectors and the resulting plasmids were used to transform *E. coli* OmniMAX™2 competent cells. The following day white and blue colonies related to successful *In-Fusion*™ reactions and recircularized vectors, respectively, were obtained. Two putative positive clones of each construct were checked by PCR using two approaches: (i) boiled samples of the cell cultures grown for the DNA extraction and (ii) Mini-prep purified DNA samples (figure 3.7, A and B, respectively).

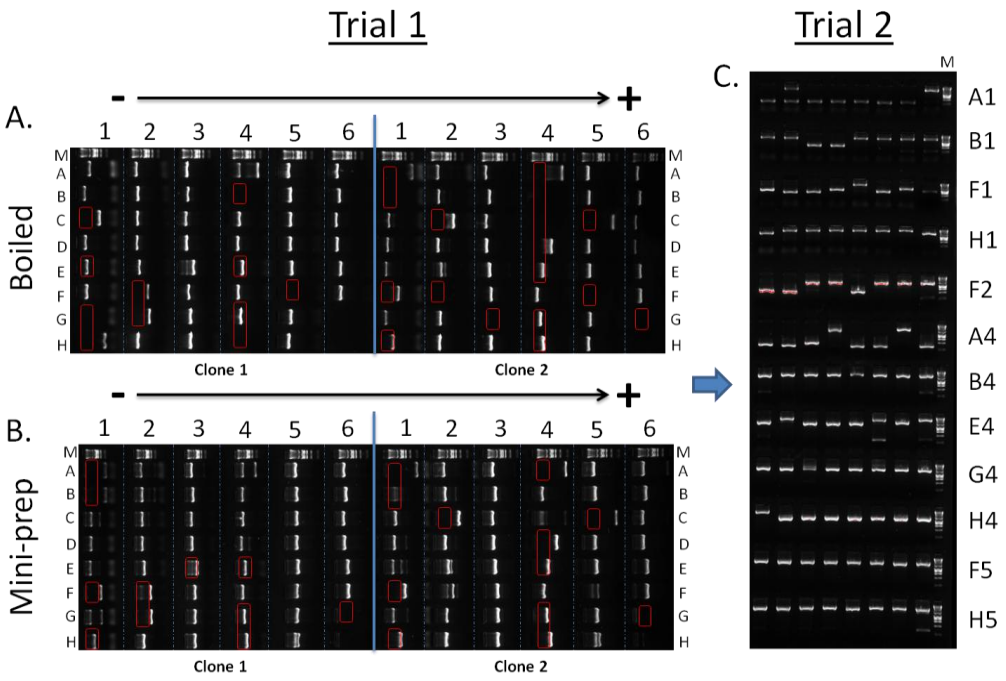

Figure 3.7. Results of the PCR tests. Two putative positive clones of each experiment were tested by PCR reactions using two different approaches: **A)** Crude cell extracts as DNA templates. **B)** Mini-prep purified samples as DNA templates. Obtained products were analysed by 1.25% (w/v) agarose gel electrophoresis in *TBE buffer*. M: *Hypperladerl™ DNA MW marker*. Numbers in columns and letters in lines represent the coordinates that code for each construct. Red boxes mark the negative results. Black arrows show the direction of DNA movement. **C)** A second trial was performed for the clones that gave negative results using new mini-prep purified DNA samples.

By doing two different approaches it was easier to decide about some ambiguous results and double-check the negative ones. In some constructs no positive results were obtained in any of the PCRs. On the one hand, all the constructs related to pOPINFB vector gave negative or unclear results. This could have been because the pOPINFB vector used for the *In-Fusion*™ reactions might have not been properly linearised. For this reason, the four *In-Fusion*™ reactions performed with pOPINFB (B1, F2, B4, F5) were repeated using another batch of the linearised vector. Eight white colonies obtained from these new transformations were tested together with another eight colonies of each construct that had given negative or unclear results on the first trial (A1, F1, H1, A4, E4, G4, H4, and H5). In this case, PCRs were performed by using Mini-prep purified DNA samples as templates. The products of these new reactions were analysed by agarose gel electrophoresis as described previously (figure 3.7). A graphical summary of the results can be seen in supplementary data (table S3.1).

After performing all the tests, **46 out of the 47 constructs were obtained** (table S3.2). In this manner, a broad catalogue of T4CP variants was obtained ready to be used in further studies when required. At this point it is necessary to stress that **if these constructs would have been done by conventional non-HTP methods, the amount of time and money spent would have been considerably higher**; as an example, instead of 25 days, it would have taken between 6 to 12 months.

3.3. *IN VIVO* ACTIVITY OF THE DIFFERENT PROTEINS: MATING ASSAYS

T4CPs are essential elements in the conjugative process (Cabezón, 1996). Therefore, conjugation or mating assays allow determining whether a T4CP variant is active or not *in vivo* (Segura et al., 2013). In this thesis mating assays were used to test the effect of the H_6- and eGFP-H_6-tags in the *in vivo* activity of the proteins and also to evaluate the effect of switching heterologous domains between T4CPs. Specifically, these experiments were used to study two different properties of the constructed proteins: (i) their capacity to complement the conjugative process in the absence of another T4CP (functionality studies) and (ii) how their presence affects the native conjugative system, being the native T4CP present (dominance studies) (see section 2.3.).

Assays related to $MobB_{CloDF13}$ and its variants were a little different since this T4CP is original from a mobilizable plasmid and therefore it needs the presence of a co-resident cT4SS for its transfer. For this reason, these experiments were performed in the presence of the MOB region of CloDF13 (pSU4814 and pSU4833 plasmids with or without functional $MobB_{CloDF13}$, respectively) and pSU1456 plasmid (encoding for R388 conjugative system except for $TrwB_{R388}$). Results obtained in mating assays are summarised in table 3.1 and figures 3.8 and 3.9.

$TraJ_{pIP501}$ and its different variants ($TraJ_{pIP501}$GFP, $TMD_{TrwB}TraJ_{pIP501}$ and $TraJ_{pIP501}TraI_{pIP501}$) should have been studied in the presence of pIP501 and pIP501 lacking $TraJ_{pIP501}$, $TraI_{pIP501}$ or both proteins. To do so, the construction of in-frame knockout mutants of pIP501 was addressed following the protocol described by Fercher and co-workers (Fercher et al., 2016). Our collaborators in Dr. Grohmann's group managed to obtain the pIP501Δ*traI,* pIP501Δ*traJ,* and pIP501Δ*traItraJ* knockout plasmids. Conjugation experiments with these plasmids in the absence of any T4CP showed that both proteins, **$TraJ_{pIP501}$ and $TraI_{pIP501}$, are essential for the conjugative process** (personal communication with Dr. Grohmann).

Since pIP501 is a conjugative plasmid with a $Gram^+$ origin, mating assays had to be performed on a $Gram^+$ bacteria, for which *Enterococcus faecalis* strains was used (Arends et al., 2013). Unfortunately, the pIP501 related proteins (*i.e.* $TraJ_{pIP501}$, $TMD_{TrwB}TraJ_{pIP501}$, $TraI_{pIP501}TraJ_{pIP501}$, and their eGFP variants) had been cloned into pET or pOPIN expression vectors, which are not compatible with *E. faecalis.* Therefore, these proteins had to be subcloned in pEU327 expression vector, suitable for *E. faeca*lis. At the present moment, this work is being done in Dr. Grohmann's laboratory and up to date two complementation plasmids have been obtained: pEU327-*traJ* (that contains $TraJ_{pIP501}$) and pEU327-*trai-traj* (which contains **$TraI_{pIP501}$** and **$TraJ_{pIP501}$ proteins** separately, not as a fusion-protein). According to Dr. Grohmann's personal communication, both plasmids were able to **complement the conjugative process of the knockout plasmids to the same frequencies as native pIP501**. From this point on, chimera proteins $TMD_{TrwB}TraJ_{pIP501}$ and $TraJ_{pIP501}TraI_{pIP501}$ will be cloned into pEU327 vector to obtain data about their functionality through mating assays. Those results will be needed for performing further biochemical and biophysical studies.

Table 3.1. Transfer frequencies of plasmids. Transfer frequencies of plasmids pSU1456, pKM101Δt*raJ,* and pSU4833 complemented with different T4CP recombinant proteins were studied. Additionally, the effect of $TMD_{TraJ}CD_{TrwB}$ in the conjugative process of R388 and pKM101 was analysed (dominance assays). *E.coli* DH5α and UB1637 strains were used as donor and recipient cells, respectively. Transfer frequencies were normalised to the number of transconjugants per donor and are the mean value of at least five independent experiments. Lines shaded in white are related to control assays. (+) Positive control; (-) negative control; NA: does not apply to this case; Ø: no T4CP; WT: wild type T4CP. [a]Data from Segura *et al.,* 2013. [b]Data from Whitaker *et al.,* 2016.

	Conjugative Plasmid (T4CP)	Complementation plasmid (T4CP)	Mobilizable plasmid (T4CP)	Transfer frequency
Conjugation	R388 (+) ($TrwB_{R388}$, WT)	NA	NA	**0.21** [a]
	pKM101 (+) ($TraJ_{pKM101}$, WT)	NA	NA	**0.22** [b]
	pSU1456 (-) (Ø)	NA	NA	**$<10^{-8}$**
	pKM101Δt*raJ* (-) (Ø)	NA	NA	**$<10^{-8}$**
	pSU1456 (Ø)	pUBQ3 ($TMD_{TrwB}TraJ_{pIP501}$)	NA	**$<10^{-8}$**
	pSU1456 (Ø)	pUBQ4 ($TMD_{TraJ}CD_{TrwB}$)	NA	**1.82×10^{-4}**
	pSU1456 (Ø)	pUBQ4(K142T) [$TMD_{TraJ}CD_{TrwB}$(K142T)]	NA	**$<10^{-8}$**
	pSU1456 (Ø)	pUBQ4GFP ($TMD_{TraJ}CD_{TrwB}$GFP)	NA	**3.33×10^{-6}**
	pKM101Δt*raJ* (Ø)	pUBQ4 ($TMD_{TraJ}CD_{TrwB}$)	NA	**$<10^{-8}$**
Mobilization	pSU1456 (Ø)	NA	pSU4814 (+) ($MobB_{CloDF13}$, WT)	**2.42×10^{-2}**
	pSU1456 (Ø)	NA	pSU4833 (-)	**$<10^{-8}$**
	pSU1456 (Ø)	pOPINE-*mobB* ($MobB_{CloDF13}$)	pSU4833	**1.75×10^{-2}**
	pSU1456 (Ø)	pOPINE-3C-eGFP-*mobB* ($MobB_{CloDF13}$GFP)	pSU4833	**1.53×10^{-3}**
	pSU1456 (Ø)	pOPINE-*mobBΔTMD* (MobBΔTMD)	pSU4833	**$<10^{-8}$**
	pSU1456 (Ø)	pOPINE-3C-eGFP-*mobBΔTMD* (MobBΔTMDGFP)	pSU4833	**$<10^{-8}$**
Dominance	R388 ($TrwB_{R388}$, WT)	pUBQ4 ($TMD_{TraJ}CD_{TrwB}$)	NA	**1.13×10^{-2}**
	pKM101 ($TraJ_{pKM101}$, WT)	pUBQ4 ($TMD_{TraJ}CD_{TrwB}$)	NA	**1.10×10^{-2}**

Transfer capability of $TMD_{TraJ}CD_{TrwB}$ was studied by complementation of two different conjugative systems, R388 and pKM101, being functional on the first case, but non-functional on the second (figure 3.8). These results can be explained as the **necessary specific interactions between the CD of the T4CP and its cognate relaxase** for transfer to happen (Cabezón et al., 1997; Hamilton et al., 2000; Llosa et al., 2003). In agreement with this, it seems that when complementing pSU1456, TMD_{TraJ} was able to interact with the heterologous T4SS from R388, while CD_{TrwB} interacted with its cognate relaxase $TrwC_{R388}$, therefore conjugation happened. On the contrary, when complementing pKM101Δ*traJ* even if TMD_{TraJ} interacted with its cognate $T4SS_{pKM101}$, CD_{TrwB} did not recognize $TraI_{pKM101}$ relaxase, impeding conjugation. Analogously, when the transfer capacity of $TMD_{TrwB}TraJ_{pIP501}$ was studied using the T4SS of R388 plasmid it was unable to conjugate. Once again the CD of the chimera ($TraJ_{pIP501}$) could not interact with the heterologous $TrwC_{R388}$ relaxase. Nevertheless, an additional cause for this negative result could be the fact that domains of proteins from $Gram^-$ and $Gram^+$ related conjugative systems have been used to construct the chimera $TMD_{TrwB}TraJ_{pIP501}$. Unfortunately, the transfer capacity of $TMD_{TrwB}TraJ_{pIP501}$ using the T4SS of pIP501 could not be studied due to the lack of $TraI_{pIP501}$ and $TraJ_{pIP501}$ knockout plasmids.

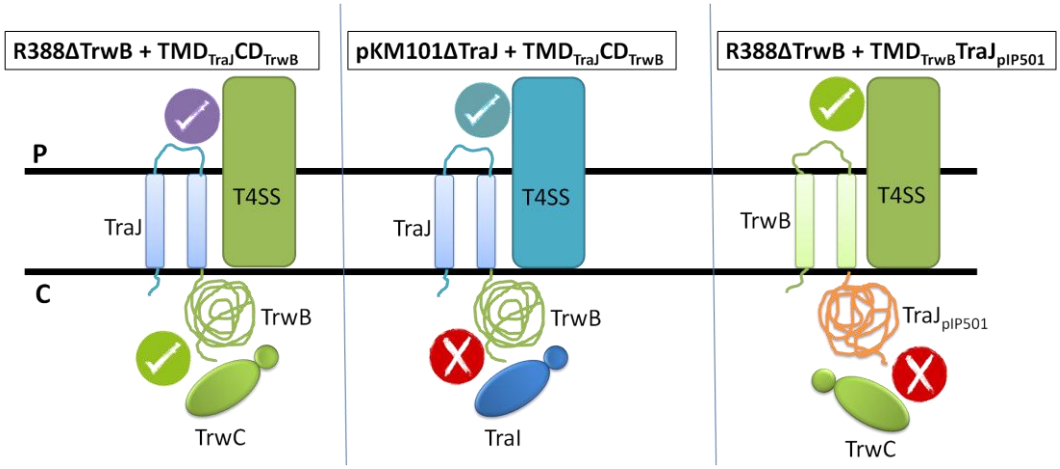

Figure 3.8. Schematic representation of the interactions present in the conjugation assays with the chimera proteins. The relaxase, T4CP, and T4SS present in each assay are shown. R388, pKM101 and pIP501 related proteins are shown in green, blue and orange, respectively. Purple tick represents interactions between proteins of heterologous systems, while green and blue ticks represent interactions between proteins of R388 and pKM101 systems, respectively. Red crosses represent non-effective interactions between heterologous systems. P: periplasm; C: cytoplasm.

Additionally, when the transfer capacity of $TMD_{TraJ}CD_{TrwB}$ was studied using the T4SS of R388 plasmid, this protein showed a transfer capacity three orders of magnitude smaller than the wild type protein. This decrease may be due to two causes: (i) to conformational changes in the CD of $TrwB_{R388}$ as a consequence of the chimera formation, rendering a less active protein; or (ii) the heterologous interaction between TMD_{TraJ} and the T4SS of R388. In fact, the transfer frequency of pKM101 using $TraJ_{pKM101}$ and $T4SS_{R388}$ was established as 1.8×10^{-2} transconjugants per donor, one order of magnitude lower than using the cognate T4SS of pKM101 (Llosa et al., 2003). Another result that we have observed for this chimera protein, is that the point mutation in the Walker A domain, **$TMD_{TraJ}CD_{TrwB}$(K142T), resulted in a non-**

functional phenotype underlining on the one hand the crucial role of that residue as it has been previously reported (Gunton et al., 2005; Kumar and Das, 2002; Moncalián et al., 1999) and on the other hand suggesting that $TMD_{TraJ}CD_{TrwB}$ is functionally similar to $TrwB_{R388}$ despite the results obtained in the complementation studies.

Next, in **dominance assays,** we studied what happened when two different T4CPs were present. First, it was observed that $TMD_{TraJ}CD_{TrwB}$ reduced the transfer frequency of R388 and pKM101 in an order of magnitude (figure 3.9). A possible explanation for the case of R388 is that **competition for the substrate** between both T4CPs ($TMD_{TraJ}CD_{TrwB}$ and $TrwB_{R388}$) could occur, obtaining an overall conjugative rate value between the one corresponding to $TMD_{TraJ}CD_{TrwB}$ and $TrwB_{R388}$. However, this explanation is not appropriate for the negative dominance observed when pKM101 system was used ($TMD_{TraJ}CD_{TrwB}$ and $TraJ_{pKM101}$) since conjugation assays previously showed that the chimera protein was not able to recognize the relaxosome of pKM101 system (figure 3.8). Therefore, an alternative explanation could be that **competition for the T4SS** could also occur, since it has been reported that TMD_{TraJ} can interact with both, R388 and pKM101 secretion channels (Larrea et al., 2017; Llosa et al., 2003). According to this hypothesis, when transferring pKM101 the chimera protein would have interacted with the secretion channels, sequestering them from interacting with $TraJ_{pKM101}$ and reducing the conjugative rate (figure 3.9, D). A third possible explanation would be that **non-functional heteroligomers** were made between the native and the chimera proteins, competing for the conjugative machinery and therefore lowering the transfer frequency (figure 3.9, C and F). Any of these alternatives would have caused a decrease in the plasmid transfer rate, as observed in the dominance mating assays.

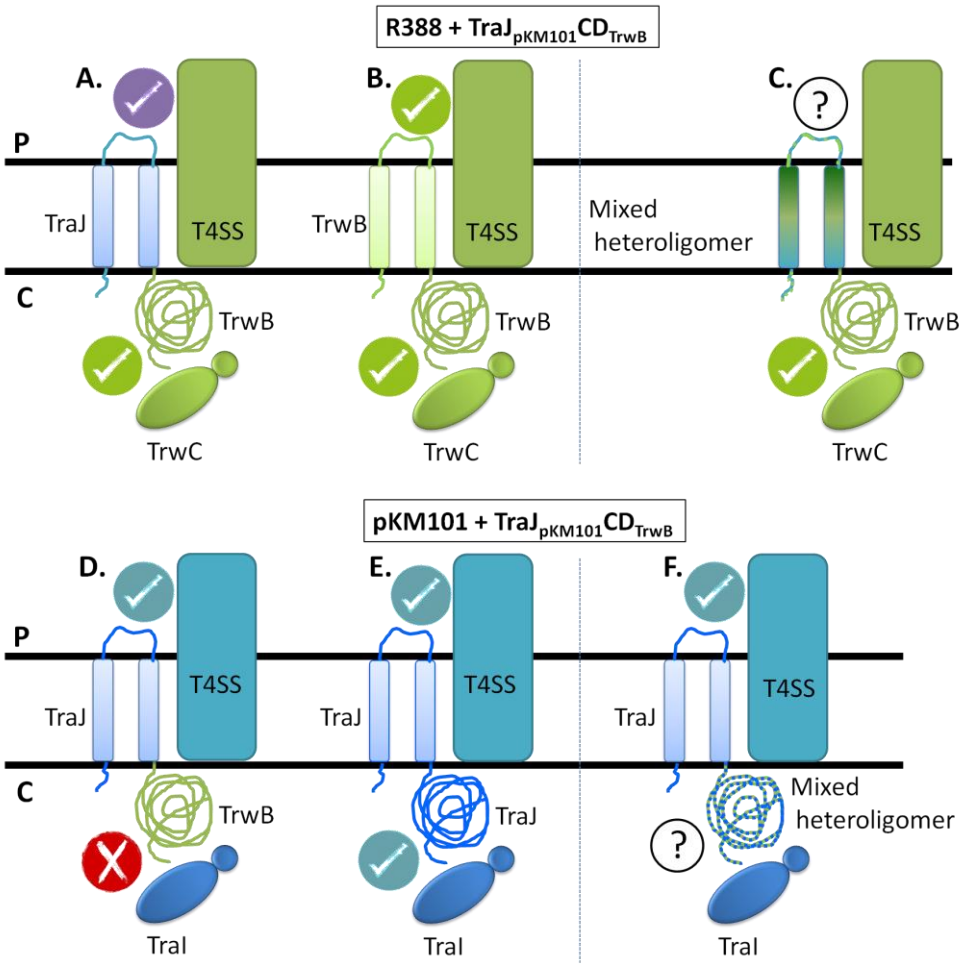

Figure 3.9. Schematic representation of the dominance assays performed with $TMD_{TraJ}CD_{TrwB}$. The relaxase, T4CPs, and T4SS present in each assay are shown. R388 and pKM101 related proteins are shown in green and blue, respectively. Purple tick represents interactions between proteins of heterologous systems, while green and blue ticks represent interactions between R388 and pKM101 systems, respectively. Red crosses represent non-effective interactions between heterologous systems. Interrogation: hypothetical heteroligomer formation. P: periplasm; C: citoplasm

Regarding **CloDF13 system**, it was observed that **$MobB_{CloDF13}$ was functional** when the T4SS of R388 was used, showing that the H_6-tag does not affect the activity of this T4CP, in agreement with what has been previously published for $TrwB_{R388}$ (Hormaeche et al., 2006). Similarly, the deletion of the TMD, **MobBΔTMD mutant, rendered a non-functional phenotype** as it occurs with other T4CP mutants that lack the TMD such as TrwBΔN70 and PcfCΔN103 (Chen et al., 2008). It has been described that the TMD is necessary for oligomerization (Hormaeche et al., 2002; Mihajlovic et al., 2009; Schroder and Lanka, 2003) and subcellular location (Kumar and Das, 2002; Segura et al., 2014), suggesting that these characteristics are needed for the *in vivo* functioning of T4CPs. However, a TcpA mutant lacking the TMD, but not the N-term cytosolic amino acids, $TcpA_{\Delta 46\text{-}104}$, was able to perform conjugation, although at a frequency lower than the wild type plasmid. Non-published experiments with TrwBΔN8, which lacks the N-term cytosolic eight amino acids, showed a decrease in the transfer rate of more than three orders of magnitude (Vecino, 2009). Taken

together these results, it seems that not only the TMD (α helixes and periplasmic loop) but also the N-term cytosolic amino acids have an important role in the activity of T4CPs. In this context, it has already been described the importance of this small region in specific interactions with the relaxosome (Llosa et al., 2003; Schroder and Lanka, 2003). In the case of $MobB_{CloDF13}$ its N-term is located in the periplasm (figure 3.1), which could be an important feature for recognizing an interacting with the secretion channel coded by the co-resident conjugative plasmid.

Finally, the *in vivo* activity of the different **eGFP fusion-proteins** was tested. It was observed that **$TMD_{TraJ}CD_{TrwB}$GFP and $MobB_{CloDF13}$GFP** were able to complement the transfer of pSU1456 and pSU4833 plasmids, respectively. However the presence of the eGFP-domain had a mild effect in the proteins (a reduction of 1 or 2-logs, (De Paz et al., 2010); specifically $TMD_{TraJ}CD_{TrwB}$GFP complemented conjugation in a frequency two orders of magnitude lower than $TMD_{TraJ}CD_{TrwB}$, and $MobB_{CloDF13}$GFP one order of magnitude lower than $MobB_{CloDF13}$. Conversely, results previously published by our group with $TrwB_{R388}$GFP (Segura et al., 2014) reported that the eGFP domain did not affect the conjugative rate. It can be postulated from these results that in this case **the bulky eGFP domains did somehow obstruct but not inhibit the functioning of the T4CPs since they remained functional at lower rates**. Regarding MobBΔTMDGFP, as expected, it was not able to complement conjugation.

3.4. EXPRESSION SCREENING

The first step to obtaining high-quality protein samples for further biochemical and biophysical studies is to develop an appropriate purification method in terms of quality and quantity. This requires developing a suitable expression procedure, which is of particular concern when dealing with MPs (Sjöstrand et al., 2017). Most of the proteins studied in this work are MPs which are usually poorly expressed not only in their natural systems but also when cloned and expressed following conventional methods. Therefore, in order to obtain enough high-quality protein samples to perform *in vitro* studies, it is necessary to overexpress them (Wagner et al., 2006). To achieve this, different expression conditions (*e.g.* bacterial strain, induction temperature, induction time) were tested for each protein.

All the genes encoding for the proteins studied in this work were under the T7*lac* promoter, therefore they were expressed in strains that contained the λDE3 lysogen and thus contain T7 RNA polymerase (T7RNAP) under control of the *lac*UV5 promoter. In these strains the addition of IPTG induces the expression of T7RNAP, which performs the transcription of the genes under the T7*lac* promoter. Unfortunately, expression of MPs in lysogenic strains like *E. coli* BL21(DE3) is usually toxic, mainly because of the overload of transcription and translocation machineries, since transcription by T7RNAP is 10 times higher than by *E. coli* RNAP, which implies a high expression of mRNA of the target protein. This causes the overload of the translation machinery, causing ribosome destruction and growth arrest (Dong et al., 1995). In addition, naked mRNA is degraded, in some cases faster than the transcripted one, obtaining a lower yield of protein (Arechaga et al., 2003). Simultaneously, the translocation machinery gets saturated, rendering misfolded MPs (Wagner et al., 2008). In this context, it

has been described that induction by IPTG can lower the level of properly folded and inserted MPs obtained in BL21(DE3) when comparing with the leakage expression in non-induced cells (Angius et al., 2016). These issues can be overcome by the use of lysogenic strains that offer different expression strategies, such as the two commonly used variants of BL21(DE3) strain: *E. coli* Lemo21(DE3) and *E. coli* BL21C41(DE3).

On the one hand, BL21C41(DE3) strain has mutations in *lac*UV5 and *lac*I promoters, resulting in lower production of T7 RNA polymerase (Kwon et al., 2015). Hence, the risks associated with the expression of MPs are reduced. On the other hand, Lemo21(DE3) contains the pLemo plasmid, which codes for the natural inhibitor of the T7RNAP, T7 lysozyme (Moffatt and Studier, 1987) under a tritable promoter. This allows tuning the amount of T7RNAP by regulating the expression of T7 lysozyme through induction with rhamnose (figure 3.10) (Schlegel et al., 2012). This can be helpful when expressing MPs since it is possible to get a lower recombinant mRNA expression level in order to avoid overload issues and somehow mimic the effect of the mutations on BL21C41(DE3) strain. However, it must be taken into account that in the absence of rhamnose, Lemo21(DE3) functions as BL21(DE3) strain.

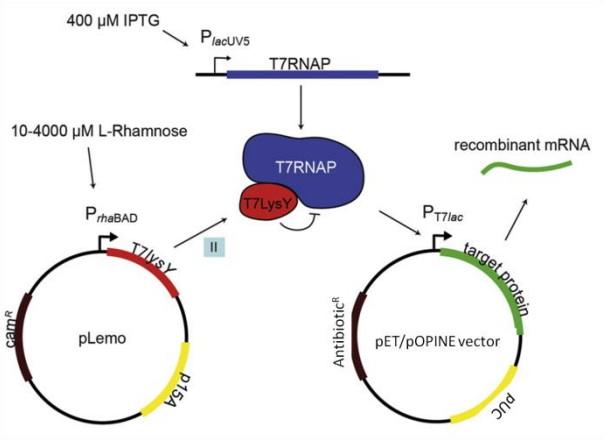

Figure 3.10. Schematic representation of the mechanism of *E. coli* Lemo21(DE3) strain. On the one hand, the expression of the chromosomally located gene encoding for T7RNAP is governed by the IPTG-inducible *lac*UV5 promoter. On the other hand, pLemo plasmid codes for the gene of the inhibitor of the T7RNAP, T7 lysozyme. Transcription of T7*lys*Y is governed by the rhamnose promoter (P*rha*BAD), which is easier to titrate than the *lac*UV5 promoter. In this study, the gene encoding for the target protein was cloned on a pET or pOPINE vector and its expression was governed by the T7*lac* promoter. On that account, expression of the target protein could be optimized by combining induction with IPTG and regulation with rhamnose. Figure modified from Schlegel et al., (2012).

Additionally, a third strain was also used, *E. coli* Rosseta™ (DE3) pLysS. This strain is suitable to express eukaryotic proteins, as it is suitable for codons rarely used in *E. coli*. Even if it is not specific for MPs, it was used because it is part of the HTP expression screening developed by OPPF-UK (see section 2.5.1. and 3.4.2.).

3.4.1. WESTERN-BLOTTING BASED EXPRESSION SCREENING

WB assays based on the recognition of the C-term His-tag present in the different proteins were used to study a set of expression conditions with some of the target proteins, [*i.e.* $MobB_{CloDF13}$, $TraJ_{pIP501}$ (coded in pQTEV-*orf10* plasmid), $TMD_{TrwB}TraJ_{pIP501}$, and $TraI_{pIP501}TraJ_{pIP501}$]. In these assays different expression conditions were analysed for each target protein, such as the bacterial strain, OD_{600} at which induction was performed, IPTG concentration, and expression temperature. To do so, cells were grown and induced in the chosen conditions and samples were taken at different times. Cell suspensions were treated as explained in section 2.5.1. and analysed by SDS-PAGE and WB using *mouse anti-His (C-term) monoclonal* antibody.

This analysis only provided a **quantitative approach**, because no information on the folding state of the proteins was obtained, therefore it was only used as a preliminary expression screening. More exhaustive (quantitative and qualitative) analysis were performed with $MobB_{CloDF13}$GFP and $TMD_{TrwB}TraJ_{pIP501}$GFP fusion-proteins (see section 3.4.3.), whereas new constructs for $TraJ_{pIP501}$ were made in order to improve the results visualised on the preliminary WB assays.

An example of these studies performed with the chimera protein **$TraI_{pIP501}TraJ_{pIP501}$** is shown in supplementary data (figure S3.1). In this expression screening combinations of three strains [BL21C41(DE3), Lemo21(DE3) and Rosseta™ (DE3) pLysS], two induction OD_{600} values (0.4 and 0.6), three IPTG concentrations (0.4, 0.6 and 1 mM), two expression temperatures (25 and 30°C) and two different expression times (4 h and 20 h) were made (figure 3.11). In this manner, a total amount of **96 different expression conditions** was tested.

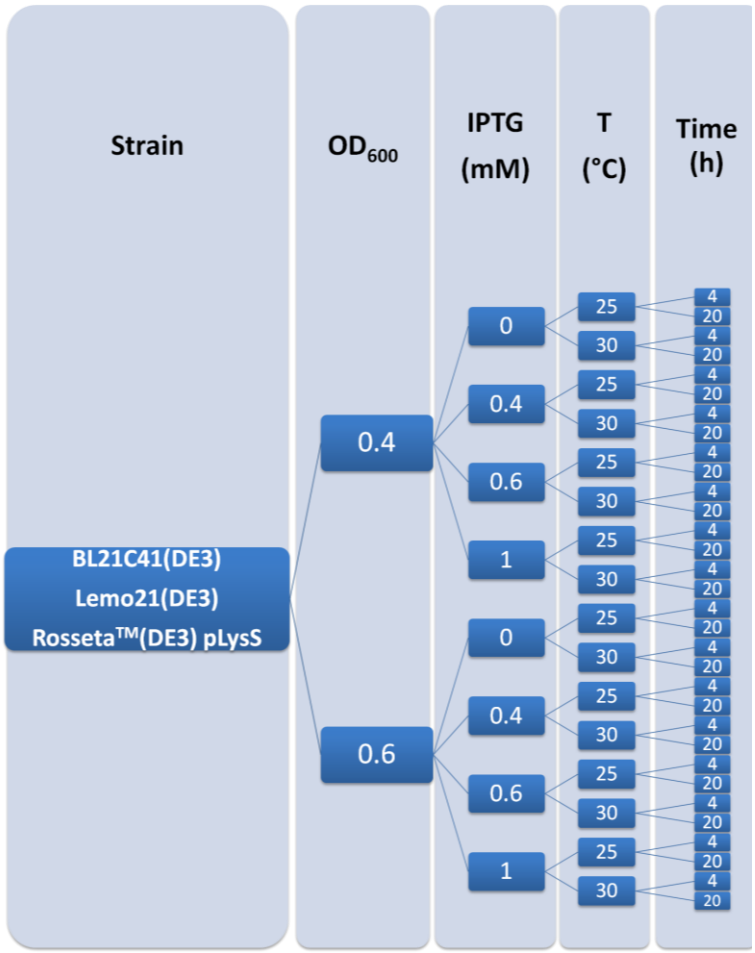

Figure 3.11. Strains and parameters tested in the expression screening of $TraI_{pIP501}TraJ_{pIP501}$ chimera protein. Expression of the target protein was performed combining the five different parameters shown in columns, testing a total of 96 expression conditions.

After the analysis of the results, BL21C41(DE3) was chosen as the best bacterial strain to perform the expression of this protein. Hydrolysis was seen in many Lemo21(DE3) conditions, while Rosseta™ (DE3) pLysS strain showed a lower expression level, in addition to some hydrolysis in some of the tested conditions (figure S3.1). When **BL21C41(DE3)** strain was used, the best expression was obtained when induction was done at **OD_{600} 0.6** and the expression at **30°C.** No difference was observed among the three concentrations of IPTG used; therefore the lowest one, **0.4 mM**, was chosen.

3.4.2. HIGH-THROUGHPUT EXPRESSION SCREENING

Note: Due to the high amount of proteins analysed in this section the results are summarised in supplementary data (table S3.2). To this end, each construction is named with a code (capital letter followed by a number) whose translation is on table S3.2.

To analyse the expression of the constructs obtained in the HTP cloning, a small-scale HTP expression screening was performed. The protocol used was the one described by OPPF-UK (Bird, 2011). This protocol was **based on the presence of a C-term His_6-tag** in all the constructs, which allowed purifying all of them simultaneously by an automated method. Even

though only half of the proteins were supposed to be MPs, the whole set was purified using an alternative protocol adapted to MPs. Four different expression conditions were analysed for each protein consisting of two *E. coli* strains [Lemo21(DE3) and Rosseta^{TM}(DE3) pLysS)] combined with two different induction strategies [IPTG and Overnight Express^{TM} Instant Terrific Broth (TBONEX)] as described in section 2.5.1. TBONEX media promotes growth to high density and induces protein expression from *lac* promoters without the addition of IPTG, obtaining a high-level protein production.

Upon the first round of construct verification, cells were transformed with the proper plasmid for each construct (table S3.1, column 7), including those samples that gave negative results on the construct verification. The reason for this was to maintain the 96-code during the whole assay (*i.e.*, cloning, overexpression, and purification). To study all the target proteins, a second small-scale expression screening was performed with the second set of constructs. In both cases, a single colony of each construct was picked and grown overnight at 37°C. After growth and induction, 4 sets of cell cultures were obtained: (i) Lemo21(DE3) in LB, (ii) Lemo21(DE3) in TBONEX, (iii) Rosseta^{TM}(DE3) pLysS in LB and (iv) Rosseta^{TM}(DE3) pLysS in TBONEX. These samples were used to perform a Ni^{2+}-NTA small-scale protein purification, adjusting its standard protocol to MP purification by adding DDM to the different buffers (as in the purification of $TrwB_{R388}$; Hormaeche et al., 2002). Finally, the obtained proteins were analysed by SDS-PAGE (figure S3.2).

In total, **188 different samples were analysed, 47 proteins expressed in four different conditions**. In this method, the analysis relies on the amount of final purified proteins that were visually estimated and qualified as: (-) not identified, (+) low, (++) medium and (+++) high. Since the intermediate steps such as the expression and proper folding could not be analysed, it was not possible to know whether negative results were due to unsuccessful expression, folding level, and/or purification steps. When the results were unclear a question mark (?) was added next to the qualification. Taking together both trials, **out of 46 constructs obtained in the HTP cloning 33 fusion-proteins were visualised** (table 3.2). Specifically, 27 proteins presented low expression-solubilisation levels in all the conditions tested, only one protein (G3) reached a medium level at most, and the remaining seven proteins reached a high level at least in one of the tested conditions. All the fusion-proteins that achieved a high expression-solubilisation level were MobBΔTMD constructions.

Table 3.2. Overexpression of proteins produced by HTP cloning. Four different expression conditions were tested to express the 47 fusion-proteins of this study. The numbers in the first row represent the cloning vector (as in table 2.6). The numbers inside the table represent the conditions where the fusion-protein was identified. 1: Lemo21(DE3) induced with IPTG. 2: Lemo21(DE3) induced with TBONEX. 3: Rosseta™(DE3) pLysS induced with IPTG. 4: Rosseta™(DE3) pLysS induced with TBONEX. ✓: the fusion-protein was identified in all the conditions tested n.i.: the fusion-protein was not identified in any of the conditions tested. n.c.: fusion-protein not constructed. *: unclear identification. [a]out of 12; [b]out of 44; [c]out of 188.

	1	2	3	4	5	6	7	8	9	10	11	12	Total (out of 48)
$MobB_{CloDF13}$	✓	n.i.	X	n.i.	n.i.	n.i.	✓	n.i.	✓	✓	✓	n.i.	20+4*
MobBΔTMD	✓	✓	✓	✓	✓	✓	✓	✓	✓	✓	✓	✓	48
$TMD_{TrwB}TraJ_{pIP501}$	✓	1?	3,4	n.i.	1?	n.i.	n.i.	3	✓	1	1,2,4	2	16+2*
$TraJ_{pIP501}$	3	1?	2,3,4	✓	✓	1,2	1,2,3	2,3,4	n.c.	✓	✓	✓	32+1*[b]
Total (out of 16)	13	4+2*	13	8	8+1*	6	11	8	12[a]	9+4*	15	9	116 + 7*[c]

3.4.2.1. COMPARISON BETWEEN SOLUBLE AND MEMBRANE PROTEINS

As expected, the best results (tables 3.2 and S3.2) were obtained for the soluble proteins **MobBΔTMD and $TraJ_{pIP501}$**, especially with the first one since all of its fusion-proteins were observed. Regarding $TraJ_{pIP501}$, all the fusion-proteins were visualised in at least one of the tested conditions, although the identification of $TraJ_{pIP501}$-BAP was not clear. However, comparing to MobBΔTMD fusion-proteins, $TraJ_{pIP501}$ related ones showed a lower expression/solubilisation level.

Although the expression conditions used (*i.e.* long incubation periods at low temperature) have been reported in the bibliography to avoid the formation of inclusion bodies and to obtain functional MPs (Drew et al., 2008), the **expression levels obtained for MPs were not as high as for soluble proteins.** For **$MobB_{CloDF13}$ and $TMD_{TrwB}TraJ_{pIP501}$, six and nine fusion-proteins were identified, respectively** (table 3.2), all of them with low expression-solubilisation levels. Some of these proteins showed protein-bands higher than expected when compared to the MW markers in SDS-PAGEs (table S3.2 and figure S3.2). These results can be explained because MPs tend to migrate differently than soluble proteins on SDS-PAGE gels (Rath et al., 2009). Additionally, in some samples (14 out of 138), instead of the fusion-protein, only the fusion-tag was visualised. This could be due to an incorrect cloning or to proteolysis during the purification process.

3.4.2.2. FUSION-TAGS

When thinking about the different fusion-tags used in this screening, it must be taken into account that the most common tag used for protein purification in the bibliography is the His_6-tag, which was the common tag used for this HTP purification. Bird (2011) recommended that when obtaining a good expression with **His_6-tag**, there is not much advantage in making fusion-proteins. Therefore, and since most of these constructs were identified in all the conditions, the His_6-tag constructs were chosen for performing further studies. Nevertheless, $TraJ_{pIP501}$ cloned in pOPINE showed a mutation on its sequence and, hence, it had to be cloned again (section 3.2.2.3.).

Taking into account the total number of fusion-proteins identified, the best results were obtained with the **GST-tag**, since all the constructs were identified in all the conditions tested. However, the expression-solubilisation level obtained was low in all of them, even with MobBΔTMD. These results are in agreement with the ones described by Bird (2011), where the GST fusion-proteins generally gave lower levels of expression. However, based on the results of this work, the best tag cannot be chosen taking into account the obtained level of expression-solubilisation, since a low level was obtained in most of the cases. Medium or high levels were only obtained with MobBΔTMD, thus the expression level seems to be more related to the protein nature and not to the used tag.

Regarding **eGFP fusion-proteins**, although a low expression-solubilisation level was visualised when analysing all the constructs by SDS-PAGE, a specific in-cell eGFP fluorescence-based analysis showed a good expression level when performing the induction by IPTG. These results suggested that these fusion-proteins do express, but that the solubilisation process is not the optimal one.

3.4.2.3. STRAINS AND INDUCTION METHODS

During the expression, solubilisation, and purification of a protein, many variables affect protein production apart from the nature of the protein or the fusion-tag. To optimise this process as much as possible, four different expression strategies were tested. Taking into account the total identified proteins and the different expression levels, differences between the four conditions were not statistically significant (figure 3.12). However, when analysing the presence of each protein, differences were seen between each condition; in fact, a few proteins were only identified in one of the tested conditions (table S3.2). These results point to the **need of testing different strains and induction methods when trying to overexpress proteins**, especially challenging proteins such as MPs.

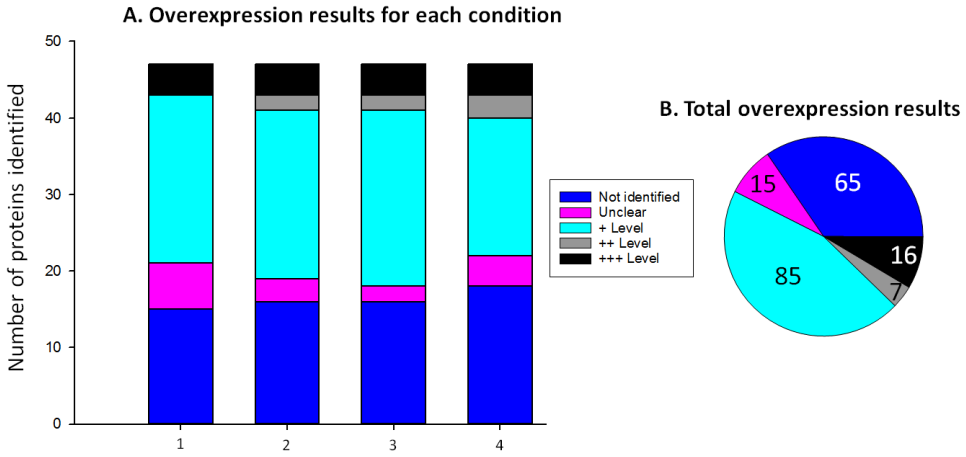

Figure 3.12. Expression screening results. Purified protein samples were analysed by SDS-PAGE. The expression and solubilisation level of the purified proteins was estimated visually and qualified as: (-) not identified, (?) unclear, (+) low, (++) medium and (+++) high. **A)** Expression results for each tested condition. Numbers in the *x*-axis are: 1: Lemo21(DE3) induced with IPTG. 2: Lemo21(DE3) induced with TBONEX. 3: Rosseta™ (DE3) pLysS induced with IPTG. 4: Rosseta™ (DE3) pLysS induced with TBONEX. **B)** Total number of proteins in each expression level.

To sum up, although the HTP small-scale expression screening allowed testing **the expression of 46 fusion-proteins in a short time, many ambiguous results were obtained**. To clarify these results the related constructs should be checked using a specific expression screening instead of the HTP method. Additionally, regarding MPs (*i.e.* $MobB_{CloDF13}$ and $TMD_{TrwB}TraJ_{pIP501}$), their expression could also be analysed using different *E. coli* strains, such as the Walker strain BL21C41(DE3) or Lemo21(DE3) strain, but adjusting in the later the expression level by rhamnose. Similarly, the same procedure should be undertaken with the rest of fusion-proteins that showed low expression-solubilisation levels.

3.4.3. eGFP BASED EXPRESSION SCREENING OF MEMBRANE PROTEINS

As indicated in the previous section, finding the optimal conditions for the expression of MPs can be a challenging task. To ease this process, different strategies have been developed, amongst them the use of specific strains, such as the Walker strains, which improve the expression of MPs; or the use of fusion-proteins, such as the eGFP (Heim and Tsien, 1996), whose intense fluorescence allows monitoring the protein expression at the cell level in a fast and quantitative way (Drew et al., 2001). One of the most interesting properties of these fusion-proteins is that the eGFP domain only presents fluorescence when properly folded and therefore as part of a fusion-protein it is a good reporter of proper folding.

The two MPs, **$MobB_{CloDF13}$ and $TMD_{TrwB}TraJ_{pIP501}$, did not show a proper expression level in any of the conditions tested in the HTP assay**. For this reason, specific expression screenings were performed for both proteins as proposed in the previous section; on the one hand, tuning the expression in Lemo21(DE3) strain through rhamnose (Drew et al., 2008) and

on the other hand using the Walker BL21C41(DE3) strain. To do so, eGFP fusion-proteins were used to monitor the expression level at the different conditions.

Briefly, as explained in section 2.5.1.2., the first **screening was performed in *E. coli* Lemo21(DE3)** at 30°C. Cells were transformed with pOPINE-3C-eGFP-*mobB* or pOPINE-3C-eGFP-$tmd_{TrwB}traJ_{pIP501}$ and grown in LB or PB media. The later one is indicated for improved expression of recombinant proteins in *E. coli,* obtaining cell yields up to four times higher than with LB Broth according to manufacturers. The expression of the target proteins was induced using 0.4 mM IPTG and seven different rhamnose concentrations (0, 100, 200, 250, 500, 1000, or 2000 µM). For each tested condition fluorescence emission at 512 nm and OD_{600} were measured 4 and 20 hours after induction. Fluorescence was analysed using a *SinergyHT microplate reader*, exciting the samples at 485 nm and measuring emission at 512 nm (F_{512}). OD_{600} was measured using a *Jenway 6300 spectrophotometer*. The ratio between the obtained values showed a quantitative and qualitative approach of the properly folded eGFP fusion-proteins (fluorescence) per OD unit (F_{512}/OD_{600}), being high values optimal (more properly folded protein per cell). Non-induced cells were used as a negative control, while cells expressing eGFP were used as a positive control.

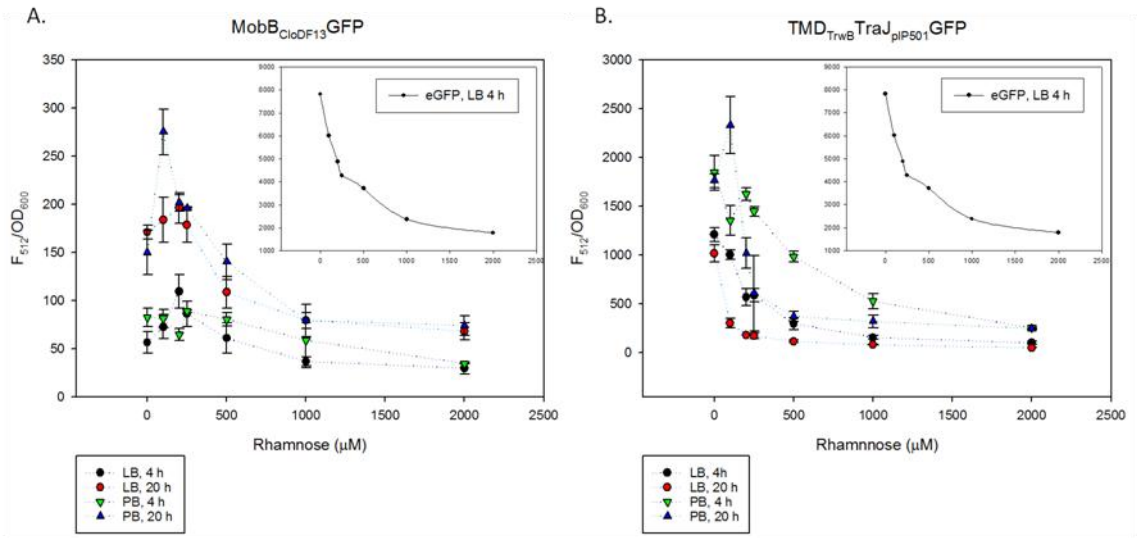

Figure 3.13. Expression of MobB$_{CloDF13}$GFP and TMD$_{TrwB}$TraJ$_{pIP501}$GFP fusion-proteins in *E. coli* Lemo21(DE3) strain. The expression of the target proteins in the different conditions was monitored after 4 and 20 h by measuring F_{512} and OD_{600}. Obtained data were normalised by dividing the fluorescence value with the OD_{600} value of the sample. eGFP protein was used as the positive control, but due to the high values obtained, only the results of expression in LB after 4 h of induction are shown. **A)** Overexpression of MobB$_{CloDF13}$GFP. **B)** Overexpression of TMD$_{TrwB}$TraJ$_{pIP501}$GFP.

Very **different results were observed for each protein** (figure 3.13). In both cases, the highest amount of protein per cell was obtained after 20 h of expression in PB but while MobB$_{CloDF13}$ expression reached a maximum F_{512}/OD_{600} rate of 275.27, TMD$_{TrwB}$TraJ$_{pIP501}$ showed an F_{512}/OD_{600} rate almost ten times higher (2331.87). Regarding the effect of the medium and the rhamnose concentration, MobB$_{CloDF13}$ best expression results in LB were obtained with 200 µM after 4 h and in PB with 100-250 µM after 20 h. On the contrary, for TMD$_{TrwB}$TraJ$_{pIP501}$ the

use of rhamnose did not show a positive effect in the expression of properly inserted and folded protein, since higher rhamnose concentrations related to a lower F_{512}/OD_{600} ratio, as seen for the positive control protein eGFP. These results, together with the low expression values obtained, suggest that $MobB_{CloDF13}$ could be more toxic for the cells, although obtained OD values were not significantly different between both proteins (figure S3.3). When comparing both growth mediums, higher F_{512}/OD_{600} values were obtained with PB, although observed differences between them were not statistically significant. Unfortunately, PB results were not as reproducible as the ones obtained with LB.

To obtain more information, the same measurements were taken in ***E. coli* BL21C41(DE3) strain**, after induction with 0.4 mM IPTG and expression at 25 and 30°C (figure 3.14). For **$MobB_{CloDF13}$GFP best results were obtained at 25°C after 20 h of induction**, without significant differences between both mediums. The convenience of using 25°C instead of 30°C was expected since lower induction temperatures are usually recommended for laborious MPs. Probably this temperature caused a lower rate of expression, avoiding the saturation of the folding and translocation machinery in the membrane and resulting in a higher amount of properly folded protein after 20 h of expression. Regarding expression time, after 20 h of induction F_{512}/OD_{600} values obtained by tuning $MobB_{CloDF13}$GFP expression in Lemo21(DE3) and by expressing it in BL21C41(DE3) were significantly different. According to Schlegel et al. (2012), regulating the expression in Lemo21(DE3) through the addition of rhamnose somehow mimics MP expression levels that are achieved in BL21C41(DE3). However, this did not happen when expressing $MobB_{CloDF13}$GFP, since results obtained in BL21C41(DE3) after 20 h of induction doubled those obtained in Lemo21(DE3) in the same conditions. Nevertheless, quite **different results** were obtained with **$TMD_{TrwB}TraJ_{pIP501}$**. On the one hand, it **showed higher F_{512}/OD_{600} values than $MobB_{CloDF13}$GFP in all the conditions tested**, obtaining at 25°C lower protein amount than at **30°C**, except for expression in LB after 20 h. It seems that slowing down the expression was not proper for this protein, since the best results in Lemo21(DE3) were also obtained in the absence of rhamnose (figure 3.13, B). On the other hand, results obtained between both mediums were significantly different, obtaining a higher amount of protein per cell with **PB**. Additionally, in this case, expression in Lemo21(DE3) gave better or similar results to those obtained in BL21C41(DE3).

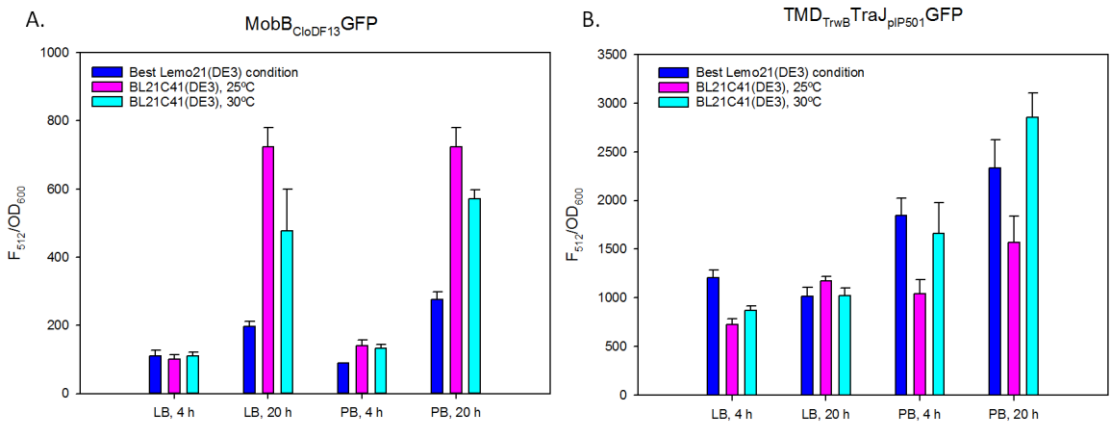

Figure 3.14. Expression screening of $MobB_{CloDF13}$GFP and $TMD_{TrwB}TraJ_{pIP501}$GFP fusion-proteins. The expression of the target proteins in the different conditions was monitored after

4 and 20 h by measuring F_{512} and OD_{600}. Obtained data was normalized by dividing the fluorescence value with the OD_{600} value of the sample. Graphics show the comparison between the best result obtained in Lemo21(DE3) and the different conditions tested in BL21C41(DE3). **A)** Overexpression of $MobB_{CloDF13}GFP$. **B)** Overexpression of $TMD_{TrwB}TraJ_{pIP501}GFP$.

From these results the best conditions for expressing $MobB_{CloDF13}GFP$ and $TMD_{TrwB}TraJ_{pIP501}GFP$ proteins were postulated. Before doing so, it was taken into account that the prize of PB is three times higher than the prize of LB, therefore it would have only been used in cases were expression in LB was very low. Thereby, **it was chosen to express both proteins in BL21C41(DE3) cells grown in LB medium, for 20 h at 25°C**.

3.5. PURIFICATION

To address biochemical and biophysical characterization high-quality pure protein samples are needed. To achieve this task when dealing with MPs, in addition to the issues related to the expression, it must be taken into account that most purification techniques have been developed for soluble proteins, while MPs present different needs. First, MPs must be taken out of their native lipid environment and become soluble in an aqueous condition, which is usually accomplished by the use of detergents. Then MPs are usually purified using mainly the same techniques as soluble proteins but in the presence of detergent, which conditions some of the general approaches used for the purification of soluble proteins. As a consequence, general protocols cannot be developed and finding the proper method to purify an MP is an empirical time-consuming process. This is one of the reasons why despite the relevance of MPs (around 30% of the proteins and more than 50% of drug targets are MPs) they only represent around 3.4% of the 3D atomic structures that have been solved to date (The Protein Data Bank).

In this thesis, **specific purification protocols have been developed for the different T4CPs** and their mutants, based on the main steps shown in figure 3.15 and section 2.5.2. Briefly, cells were grown in the conditions chosen from the overexpression study of each target protein. Then, cells were harvested by low-speed centrifugation, resuspended in the proper buffer and frozen by liquid N_2 to avoid water crystals. Next, cells overexpressing the target-protein were thawed and from that point onwards all the steps of the purification were carried at 4°C to reduce protein denaturation. Cells were disrupted by enzymatic lysis using lysozyme. However, since this method offers a low yield, it was followed by mechanical lysis through ultrasonication. After this step, unbroken cells were discarded by low-speed centrifugation and membrane fraction was obtained by ultracentrifugation of the supernatant.

Once the membrane fraction was obtained, solubilisation of the MPs was performed. This is one of the most critical steps of MP purification where aggregation and loss of function of the protein can occur. To avoid that, the detergent must be carefully chosen and the physical conditions such as temperature and stirring must be as mild as possible. Due to their amphipathic nature detergents disintegrate the membrane while incorporating lipids and proteins in micelles. In this work, the non-ionic detergent DDM was used. It is considered a mild non-denaturing detergent and has been previously used for the purification of $TrwB_{R388}$

(Hormaeche et al., 2006). After a successful solubilisation, stable PDCs or protein-lipid-detergent complexes were obtained.

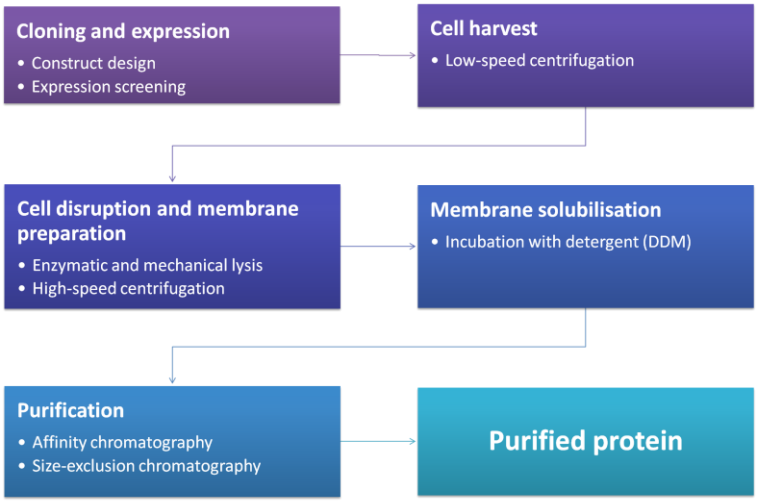

Figure 3.15. Workflow overview for membrane protein solubilisation and purification.

To keep the protein in a stable form, the purification process was always conducted right after solubilisation. Non-solubilised proteins and inclusion bodies were removed by ultracentrifugation and the obtained extract was passed through a set of chromatography columns. In these steps, detergent concentration was lowered, but kept above the critical micelle concentration (CMC) since the presence of free detergent is necessary to maintain the native state of MPs. Chromatographies based on two separation principles were used: (i) affinity and (ii) size-exclusion. In the first case, *HisTrap*^{TM} *FF* columns were used. These columns have immobilized Ni^{2+} ions, which interact with the His_6-tags of the target proteins. In the second case, *Superdex 200* columns were mainly used. This was usually the last step of the purification protocol, where aggregates were removed and proteins were transferred to a suitable buffer. Between the different steps, ultrafiltration-based protein concentration was performed. To avoid the concentration of detergent micelles, a proper MWCO (usually 100 kDa for full-length T4CPs) was used.

3.5.1. PURIFICATION OF $TrwB_{R388}$ RELATED PROTEINS

In our group, different purification protocols have been developed for $TrwB_{R388}$. First, it was purified without a His_6-tag (Hormaeche et al., 2002) but to optimize the obtained yield, an improved purification protocol that involved the use of a His_6-tag was published (Hormaeche et al., 2006). Through these protocols it was possible to separate $TrwB_{R388}$ monomers and hexamers, however, this was not always necessary and a third purification protocol was developed for the reconstitution of $TrwB_{R388}$ into liposomes (Vecino et al., 2010). In this thesis, after trying all the alternatives for purifying the different versions of $TrwB_{R388}$ (*i.e.*, $TrwB_{R388}$, $TMD_{TraJ}CD_{TrwB}$, $TMD_{TraJ}CD_{TrwB}K136T$, and $TMD_{TrwB}TraJ_{pIP501}$), a combination of the previous protocols was developed to perform comparative studies between them. Most of the

modifications were made based on our empirical data and recommendations from the Purifying Challenging Proteins: Principles and Methods Handbook (GE Healthcare, 2007).

In the **common protocol** (figure 3.16) *E. coli* BL21C41(DE3) cells were transformed with the corresponding plasmids (pUB7, pUBQ4, pUBQ4K136T, and pUBQ3 for $TrwB_{R388}$, $TMD_{TraJ}CD_{TrwB}$, $TMD_{TraJ}CD_{TrwB}$K136T, and $TMD_{TrwB}TraJ_{pIP501}$, respectively). Obtained colonies were used to inoculate eight flasks containing 10 mL LB supplemented with the corresponding antibiotics, which were grown overnight at 37°C with continuous shaking. Next, cells were diluted 1:50 (v/v) with fresh LB supplemented with antibiotics to prepare 4 L of culture (8 flasks of 500 mL) and were grown at 37°C with continuous shaking until an OD_{600} of 0.4-0.5 was reached. Next, overexpression was induced by the addition of 1 mM IPTG and cells were grown with continuous shaking at 25°C overnight. Cells were harvested by centrifugation at 8,000 *g* for 15 min at 4°C. The pellet was suspended in 80 mL of *Cell buffer*, frozen with liquid N_2 and stored at -80°C.

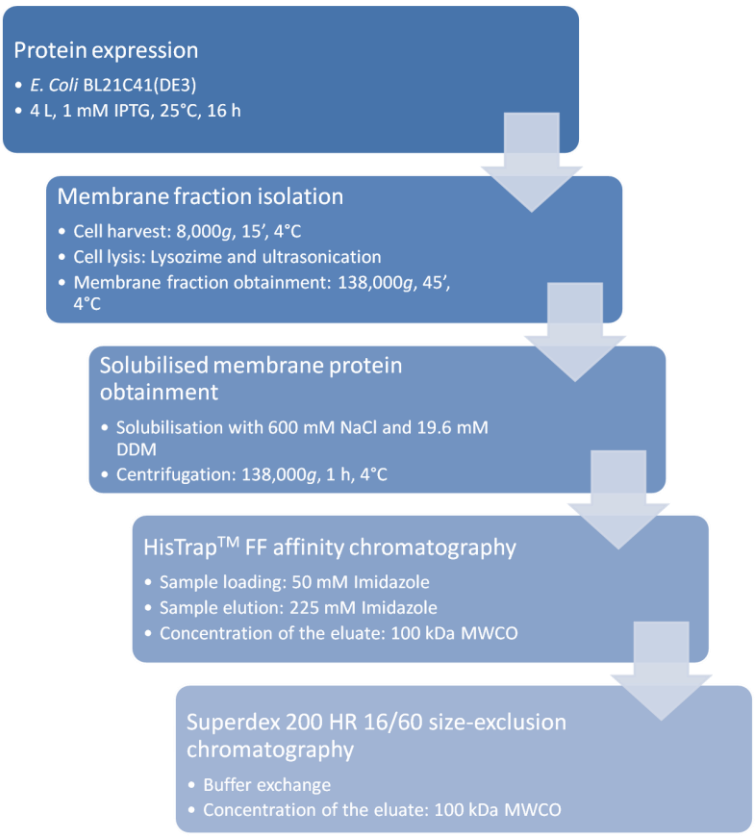

Figure 3.16. Schematic representation of the common protocol for the purification of $TrwB_{R388}$ and its mutant proteins.

For purification, cells were thawed at 37°C and 0.02 mg/mL DNase I, 1 mM DTT, 0.07% (w/v) lysozyme, 1 mM $MgCl_2$, 1 mM PMSF and 2 tablets of protease inhibitor cocktail were added. From this point onwards, the whole process was performed at 4°C to avoid aggregation of the proteins. After 45 min of incubation with agitation, cells were disrupted by sonication. Afterwards, the sample was centrifuged at 8,000 *g* for 15 min to remove the non-lysed cells. The supernatant, containing the broken cells, was centrifuged at 138,000 *g* for 45 min to

sediment the membrane fraction. The supernatant with the soluble proteins was discarded and the pellet was carefully resuspended in 30 mL of *Cell buffer*. Then DDM and NaCl were added to a final concentration of 19.6 mM and 600 mM, respectively, and the volume was adjusted to 40 mL. The mixture was incubated for 90 min with continuous stirring and then centrifuged at 138,000 *g* for 1 hour.

The supernatant containing the target protein was mixed 1:1 (v/v) with *MP1 buffer* to decrease the concentration of DDM and NaCl to 8.3 mM and 300 mM, respectively. Then, the sample was supplemented with 50 mM imidazole and loaded onto a 5 mL *HisTrap™ FF* column which had been previously equilibrated with *MP2 buffer*. To increase the binding of the protein, the sample was left recirculating overnight through the column. Next, it was connected to an *ÄKTA-FPLC system* and it was washed with 50 mL of *MP2 buffer* at a flow rate of 2 mL/min until the absorbance at 280 nm reached the baseline. Bound proteins were eluted with *MP3 buffer*, at a flow rate of 1.5 mL/min and fractions of 1 mL were collected. Obtained samples were analysed by SDS-PAGE and the ones containing the target protein were pulled-down and concentrated to 100 µM using a centrifugal filter with a MWCO of 100 kDa.

The resulting sample was loaded onto a *Superdex 200 HR 16/60* column and the gel filtration was performed in *MP purification buffer* at a flow rate of 0.5 mL/min. The peak fractions corresponding to the target protein were pulled-down and concentrated as explained before. Glycerol was added to a final concentration of 20% (v/v) and protein concentration was determined by measuring absorption at 280 nm. Finally, aliquots were stored at -80 °C.

As previously said, the common purification protocol differs in some aspects with the previously published protocols for the purification of $TrwB_{R388}$. These changes were made at different points of the purification process. Briefly, expression conditions were changed by using **4 L of cell culture, inducing at OD_{600} 0.4-0.5 and expressing for 20 h at 25°C**. The next change performed was the **addition of $MgCl_2$ and DNase I** to the lysis suspension. It was chosen to **avoid the use of the P-11 ion-exchange** chromatography used in the previous protocols since it seemed unnecessary (it was time-consuming and did not improve the obtained sample) if no separation of the different oligomers was being made. The next change was the use of **centrifugal filters with a MWCO of 100 kDa to avoid the concentration of the DDM micelles**. Taking into account that MW of $TrwB_{R388}$ (57.33 kDa) is below this cut-off, the size of $TrwB_{R388}$-DDM complex was analysed by SEC-MALLS to ensure that $TrwB_{R388}$ would be retained (figure S3.4). In this manner, it was seen that the MW of the PDC is 112.98 kDa, which is big enough to use 100 kDa filters. After protein concentration, a **SEC was performed** to change the buffer, which also served for increasing the purity of the sample.

3.5.1.1. PURIFICATION OF $TrwB_{R388}$

An example of the results obtained from the purification of $TrwB_{R388}$ through the common purification protocol is shown below. $TrwB_{R388}$ has a theoretical MW of 57.33 kDa and it appears a little higher than the 5th lane of the *PageRuler™ Plus Prestained Protein Ladder* (55 kDa). Therefore, the whole purification process was followed by the visualisation of this band.

The SDS-PAGE analysis of the expression, solubilisation, and affinity chromatography offered much information (figure 3.17). It was seen how, even in the absence of IPTG (lane a),

due to the leakage of the T7 expression system, $TrwB_{R388}$ was the most expressed protein in the cell. Additionally, it was observed that $TrwB_{R388}$ appeared in the membrane fraction as expected (lane d). The solubilisation protocol was highly efficient since the total amount of the target protein obtained in the solubilised fraction was similar to its total amount on the membrane (lanes d and e). By using 50 mM imidazole when loading the sample into the affinity column, most of the contaminant proteins were discarded, even if some target protein was lost in the process too (lane f). Since fractions 6 to 10 showed a high percentage of contaminant proteins [figure 3.17, fractions between red lines (A) and shaded in red (B)] they were discarded when pulling-down the fractions for the next step (2 to 5 and 11 to 57) (figure 3.17, B, shaded in blue).

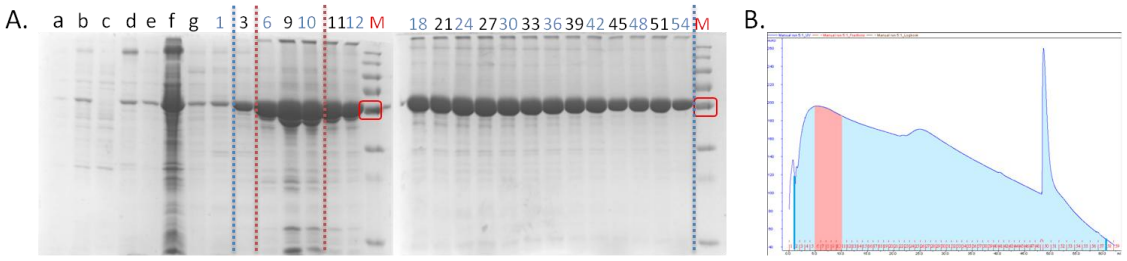

Figure 3.17. SDS-PAGE analysis and chromatogram of the *HisTrap™ FF* affinity chromatography. A) SDS-PAGE analysis of the obtained samples. Five µL of each sample were loaded (samples a to e were diluted 1:100). a: non induced cells; b: broken cells; c: soluble proteins; d: membrane fraction; e: solubilised membranes after dilution with *MP1 buffer*; f: flow-through *His-trap™ FF* column; g: washed unbound proteins; 1 to 54: fractions eluted from the *His-trap™ FF* column. M: *PageRuler™ Plus Prestained Protein Ladder*. The red square marks the band of 55 kDa. Fractions between the blue lines were pulled-down, except for the ones between the red lines that were discarded. **B)** The chromatogram obtained from the affinity column. Protein elution was followed by measuring light absorbance at 280 nm. Fractions shaded in blue were pulled-down while the ones in red were discarded.

The obtained sample was concentrated and loaded onto a *Superdex 200 HR 16/60* column to perform a SEC in two injections of 5 mL each. The chromatography was performed in *MP purification buffer*, at a flow rate of 0.5 mL/min and taking 0.5 mL fractions. Figure 3.18 shows the results obtained on the first injection, being the results of the second one equals. During the SEC three main peaks were obtained with the following elution volumes (V_e): 47, 54 and 59 mL. In this regard, it must be pointed out that the target protein was present in all the fractions collected through the three peaks. Several explanations can be given for this result. On the one hand, different $TrwB_{R388}$ oligomeric species might have been distributed through these peaks. On the other hand, these peaks could have been related to contaminant proteins that eluted at different points of the chromatography together with the target protein. What is more, a mixture of both scenarios could have happened. Consequently, fractions containing $TrwB_{R388}$ were pulled-down separately for the three peaks. Sample one was composed of the fractions related to the first peak of each injection (figure 3.18, light blue, fractions 10 to 18). These fractions seemed to have part of aggregated or high MW complexes, which were unable to enter the polyacrylamide gel. Sample two was composed of the fractions from the second peak (figure 3.18, medium blue, fractions 19 to 25), which seemed to have a bigger percentage

of contaminant proteins. Finally, sample three was composed of the fractions that formed the third peak (figure 3.18, dark blue, fractions 26 to 36). The three obtained samples were concentrated separately and analysed through different techniques.

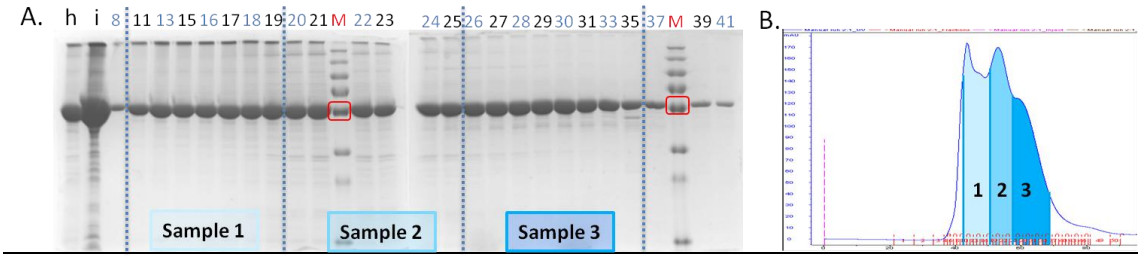

Figure 3.18. SDS-PAGE analysis and chromatogram of the SEC. A) SDS-PAGE analysis of fractions obtained in the first chromatography round (five µL of each sample). h: eluate from *HisTrap™ FF* affinity chromatography column; i: concentrated eluate; 8 to 41: eluted fractions. M: *PageRuler™ Plus Prestained Protein Ladder*. The red square marks the band of 55 kDa. Fractions between lines represent the fractions that were pulled-down to obtain each final sample (figure 3.19). **B)** Chromatogram obtained from the first injection onto the *Superdex 200 HR 16/60* column. Protein elution was followed by measuring absorption at 280 nm. Different shades represent the fractions that were pulled-down together for obtaining each final sample.

Sample one was concentrated to 53.44 µM (3.06 mg/mL and 2 mL), obtaining 6.12 mg protein. The big-sized complex was still visible in the SDS-PAGE, but not on the western blot (figure 3.19). The reason for this could be that it corresponded to a contaminant protein, but probably it was a $TrwB_{R388}$ aggregate were the His_6-tags were hidden. Regarding the BN-PAGE, five different bands were observed (figure 3.19, C, lane 1, pointed by arrows 1 to 5), confirming the oligomer mixture on the sample. Sample two was concentrated at 68.70 µM (3.103 mg/mL and 1 mL), obtaining 4.13 mg protein. Although the protocol used was the same as for sample 1, a smearing was observed on the BN-PAGE. Nevertheless, the lowest three bands could be observed (figure 3.19, C, lane 2, pointed by arrows 1 to 3), being number one the most intense, then number three, and number 2 very faint. Sample three was concentrated at 66.12 µM (3.89 mg/mL and 1.8 mL), obtaining 6.82 mg protein. The protein in this sample showed some hydrolysis as it can be seen on the western blot (figure 3.19, B, lane 3). Regarding the BN-PAGE, no conclusions could be taken since no bands were visualised. In total 17.07 mg protein were obtained from 4 L of culture (yield: 4.27 mg/L).

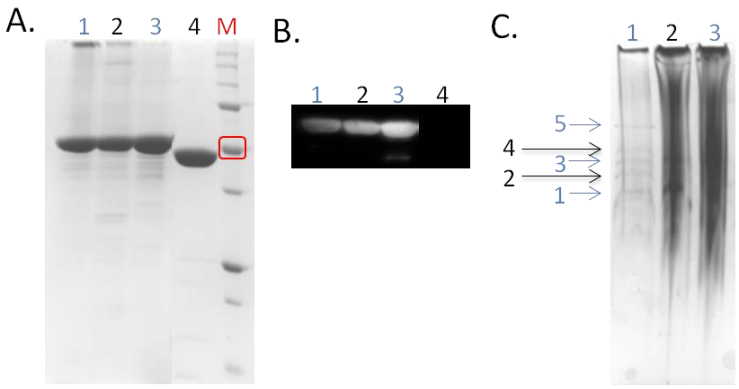

Figure 3.19. Final samples obtained in the purification of $TrwB_{R388}$. A) Analysis via SDS-PAGE of the final samples. Two µg of protein were loaded. 1: sample 1; 2: sample 2; 3: sample 3; 4: TrwBΔN70 for WB control. M. *Precision Plus Protein™ Unstained Protein Standard*. The red square marks the band of 50 kDa. **B)** WB analysis of the purified samples. *Mouse anti-His (C-term) monoclonal* and *Donkey-AntiMouse IgG-HRP* antibodies were used as primary and secondary antibodies, respectively. Lanes as in A. TrwBΔN70 was used as negative control. **C)** BN-PAGE of the purified samples. Lanes as in A. Each arrow points to a different band.

3.5.1.2. PURIFICATION OF $TMD_{TraJ}CD_{TrwB}$ AND $TMD_{TraJ}CD_{TrwB}$(K142T)

It has been already mentioned in this chapter (section 3.2.2.1.) that $TMD_{TraJ}CD_{TrwB}$ chimera protein was firstly coded in plasmids pUBQ1 and pUBQ2 as TMD_{TraJ}-TEV-CD_{TrwB}. However, when trying to purify it, spontaneous hydrolysis occurred through the TEV domain (figure S3.5). Consequently, a new construction of the protein without the TEV domain was designed (plasmid pUBQ4) to be used in all the studies regarding this chimera protein.

Several purification protocols based on previous studies of our group (Hormaeche et al., 2006; Vecino et al., 2010) were followed to address oligomerization, stability and reconstitution studies of the chimera protein. Nevertheless, in this section, the results obtained for the purification of $TMD_{TraJ}CD_{TrwB}$ and $TMD_{TraJ}CD_{TrwB}$(K142T) through the common purification protocol for $TrwB_{R388}$ related proteins are shown. $TMD_{TraJ}CD_{TrwB}$ has a theoretical MW of 58.28 kDa, which runs a little higher than the 6th lane of *Precision Plus Protein™ Unstained Protein Standard* (50 kDa). Therefore, the whole purification process was followed by the visualisation of this band.

Expression and solubilisation levels (figure 3.20, A, lanes b to e) were similar to those obtained with $TrwB_{R388}$ (figure 3.17, A) As with $TrwB_{R388}$, the first purification step was an affinity chromatography. The obtained chromatogram showed two peaks, being the first one bigger than the second (figure 3.20, B). The fractions associated with the first peak had a higher amount of contaminant proteins and were discarded. Therefore, fractions of the second peak (25 to 51) were pulled-down together, concentrated to 5 mL and centrifuged to remove aggregates.

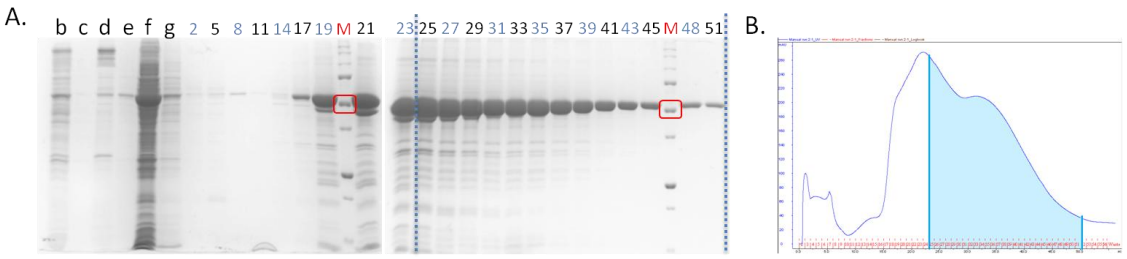

Figure 3.20. SDS-PAGE analysis and chromatogram of the *HisTrap™ FF* affinity chromatography. A) SDS-PAGE analysis of obtained samples. Five µL of each sample were loaded (samples b to e were diluted 1:100). b: broken cells; c: soluble proteins; d: membrane fraction; e: solubilised membranes after dilution with *MP1 buffer*; f: flow-through *His-trap™ FF* column; g: washed unbound proteins; 2 to 51: fractions eluted from the *His-trap™ FF* column. M: *Precision Plus Protein™ Unstained Protein Standard*. The red square marks the band of 50 kDa. Fractions between the lines were pulled-down. **B)** The chromatogram obtained from the affinity chromatography. Protein elution was followed by measuring absorption at 280 nm. Fractions shaded in blue were pulled-down together for the next steps.

The obtained sample was loaded onto *a Superdex 200 HR 16/60* column and the chromatography was performed as explained for $TrwB_{R388}$. Two peaks were obtained on the SEC chromatogram, with V_es of 58 and 71 mL, respectively (figure 3.21, B). This result was quite different from that obtained for $TrwB_{R388}$, were three peaks with V_es of 47, 54 and 59 mL were obtained. These results suggest that the chimera protein was present in two smaller species than $TrwB_{R388}$, as the first V_e corresponded to the latest obtained for the native protein. When analysing the obtained fractions via SDS-PAGE, it was seen that the target protein was distributed through both peaks; similar to $TrwB_{R388}$. Fractions from 45 to 56 showed a contaminant protein with a MW of approximately 30 kDa (figure 3.21, A). Since the elution of this contaminant is related to the second peak it was chosen to pull-down the two peaks separately: (i) fractions 29 to 41 were pulled-down as sample 1 (S1) and (ii) fractions 43 to 66 were pulled-down as sample 2 (S2). S1 was concentrated to 93.47 µM (6.78 mg/ml and 0.7 mL) (figure 3.23, lane 1), while S2 was concentrated to 61.16 µM (4.43 mg/ml and 2.2 mL) (figure 3.23, lane 2). In total 14.49 mg protein were obtained from 4 L of culture (yield: 3.72 mg/L).

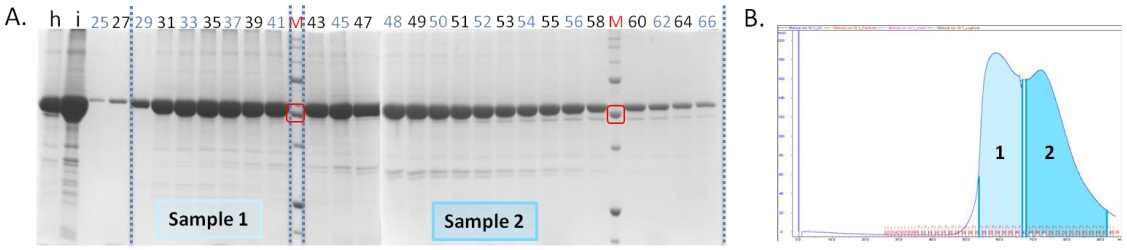

Figure 3.21. SDS-PAGE analysis and chromatogram of the SEC. A) SDS-PAGE analysis of fractions obtained on the SEC (five µL of each sample). h: pull-down of the eluate from the affinity chromatography; i: concentrated eluate; 25 to 66: fractions containing $TMD_{TraJ}CD_{TrwB}$ protein eluted from SEC. M: *Precision Plus Protein™ Unstained Protein Standard*. The red square marks the band of 50 kDa. Fractions between lines were pulled-down to obtain each final sample (figure 3.23). **B)** Chromatogram obtained from the *Superdex 200 HR 16/60*

column. Protein elution was followed by measuring absorption at 280 nm. Different shades represent the fractions that were pulled-down together for obtaining each final sample.

To validate the possible ATP hydrolase activity that $TMD_{TraJ}CD_{TrwB}$ could show, it was chosen to construct and purify the mutant protein $TMD_{TraJ}CD_{TrwB}$(K142T). This is a homologue of the transfer deficient mutant TrwBK136T (Hormaeche et al., 2006) in which the conserved lysine in the Walker A motif was changed for a threonine. A similar mutant was constructed for the soluble protein TrwBΔN70, TrwBΔN70(K136T) (Moncalián et al., 1999), which lacked ATPase activity. $TMD_{TraJ}CD_{TrwB}$(K142T) was expressed and purified following the common protocol for $TrwB_{R388}$ and its mutants (figure 3.16).

As with $TMD_{TraJ}CD_{TrwB}$, obtained expression level was similar to that of $TrwB_{R388}$ and it had a high solubilisation yield (figure 3.22, A, comparison between lanes d and e). Conversely, the elution profile obtained from the affinity chromatography was not similar to the ones obtained with the previously purified proteins. Additionally, it showed a lower proportion of the chimera mutant and a higher presence of contaminant proteins. Fractions 22 to 77 were pulled-down together, discarding the ones related to the first peak that had many contaminants. The obtained sample was concentrated to 5 mL, centrifuged and loaded on to a *Superdex 200 HR 16/60* column (figure 3.22, D). 1 mL fractions were collected and analysed through SDS-PAGE. The chromatogram showed a main peak with a V_e of 90 mL and an elbow on the left, with an approximate V_e of 81 mL. This result points to a MW smaller than the ones present in $TrwB_{R388}$ and $TMD_{TraJ}CD_{TrwB}$ samples. Regarding the results observed on the SDS-PAGE, as in the previous column, a high amount of contaminant proteins was obtained together with the target protein. These proteins, which eluted mainly between fractions 88 to 95, might have been the causative of the second peak and not a different oligomeric state of the chimera protein. Owing to the discordances with $TMD_{TraJ}CD_{TrwB}$ purification, it was not easy to establish a common pattern to perform the pull-down of the fractions containing $TMD_{TraJ}CD_{TrwB}$(K142T). Finally, it was chosen to put together fractions from 77 to 101, which were concentrated to 1.75 mL and 139.74 µM (10.14 mg/ml), obtaining a total of 17.7 mg (4.43 mg per cell culture L).

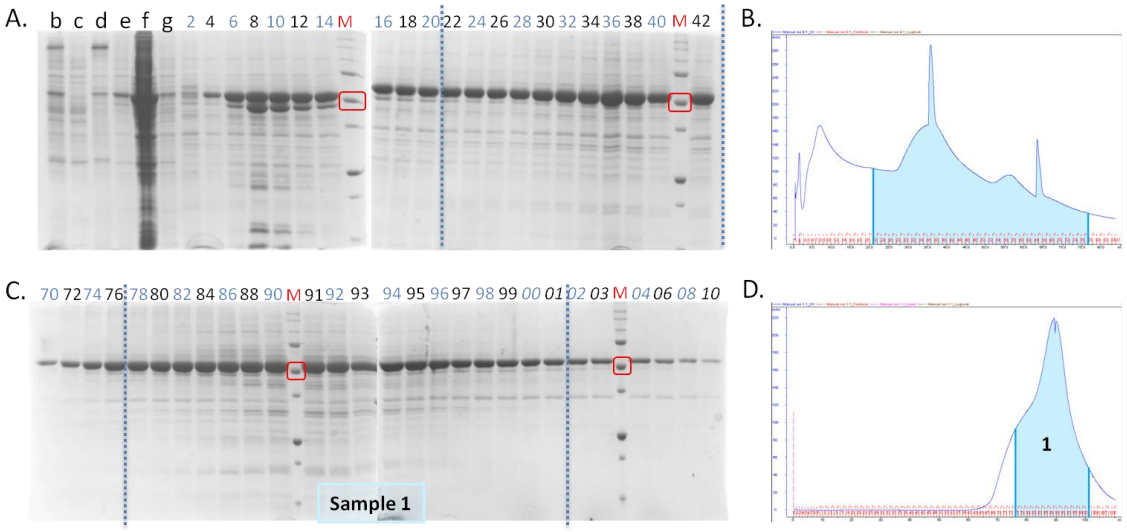

Figure 3.22. Purification of $TMD_{TraJ}CD_{TrwB}$(K142T). A) SDS-PAGE analysis of obtained samples. Five µL of each sample were loaded (samples b to e were diluted 1:100). b: broken cells; c: soluble proteins; d: membrane fraction; e: solubilised membranes after dilution with *MP1 buffer*; f: flow-through *His-trap™ FF* column; g: washed unbound proteins; 2 to 42: fractions eluted from the *His-trap™ FF* column. M: *Precision Plus Protein™ Unstained Protein Standard*. The red square marks the band of 50 kDa. Fractions between the lines were pulled-down. **B)** The chromatogram obtained from the affinity column. Protein elution was followed by measuring light absorbance at 280 nm. Fractions shaded in blue were pulled-down. **C)** SDS-PAGE analysis of fractions obtained on the SEC (five µL of each sample). 70 to *10*: obtained fractions. M: *Precision Plus Protein™ Unstained Protein Standard*. Numbers in italics represent the fraction number above one hundred. The red square marks the band of 50 kDa. Fractions between lines were pulled-down to obtain the final sample (figure 3.23). **D)** Chromatogram obtained after the *Superdex 200 HR 16/60 column*. Protein elution was followed by measuring light absorbance at 280 nm. Fractions shaded in blue were pulled-down together to obtain the final sample.

Finally, the samples obtained at the purification of both $TMD_{TraJ}CD_{TrwB}$ and $TMD_{TraJ}CD_{TrwB}$(K142T) proteins were analysed (figure 3.23). S1 of $TMD_{TraJ}CD_{TrwB}$ showed the highest purity, while S2 presented the contaminant protein of 30 kDa observed with $TrwB_{R388}$. Regarding $TMD_{TraJ}CD_{TrwB}$(K142T), even after following the same protocol as with $TMD_{TraJ}CD_{TrwB}$, a sample with less purity was obtained. WB results showed no hydrolysis for any of the proteins, while BN-PAGE results were surprisingly uneven, although the same protocol was performed for the three samples. While no clear band could be seen for S1, S2 showed three bands with some smearing (figure 3.23, C, lane 2). These species were also present in $TMD_{TraJ}CD_{TrwB}$(K142T), in addition to another one with high MW. The observed oligomeric states showed the same size as the ones seen for Sample 1 of $TrwB_{R388}$, except for number 4 (figure 3.19, lane 1 and figure 3.23, C, lane 3). These results point to the fact that although obtained profiles on the SEC chromatograms differed from each other this was not due to the presence of different oligomeric species (the oligomeric differences between $TrwB_{R388}$ related proteins are further discussed in section 4.4.).

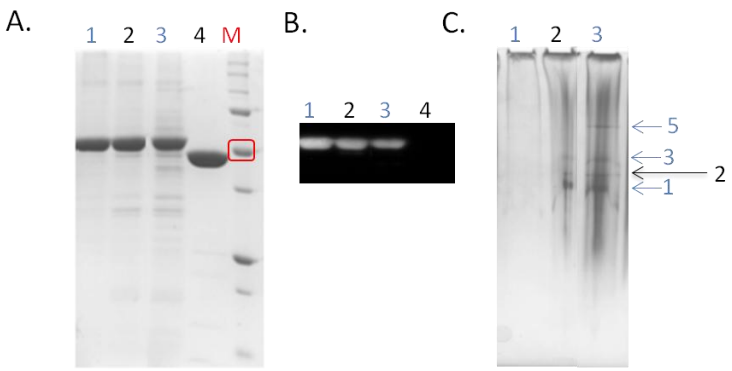

Figure 3.23. Final samples obtained in the purifications of $TMD_{TraJ}CD_{TrwB}$ and $TMD_{TraJ}CD_{TrwB}$(K142T) A) Analysis via SDS-PAGE of the final samples. Two µg of each sample were loaded. 1: sample 1 of $TMD_{TraJ}CD_{TrwB}$; 2: sample 2 of $TMD_{TraJ}CD_{TrwB}$; 3: final sample of $TMD_{TraJ}CD_{TrwB}$(K142T); 4: TrwBΔN70 for WB control. M: *Precision Plus Protein™ Unstained Protein Standard*. The red square marks the band of 50 kDa. **B)** WB of the purified samples. *Mouse anti-His (C-term) monoclonal* and *Donkey-AntiMouse IgG-HR*P antibodies were used as primary and secondary antibodies, respectively. Lanes as in A. TrwBΔN70 was used as the negative control. **C)** BN-PAGE of the purified samples. Lanes as in A. Each arrow points to a different band.

3.5.1.3. PURIFICATION OF $TMD_{TrwB}TraJ_{pIP501}$

Results of the expression screening of $TMD_{TrwB}TraJ_{pIP501}$GFP (section 3.4.3.) suggested optimal expression conditions in PB medium, BL21C41(DE3) strain and 30°C. However, the use of this medium was discarded for economical reasons. When looking at the results obtained with LB, expression obtained in BL21C41(DE3) strain at 25°C after 20 h, gave one of the best results. As the aim of studying this protein was to compare it with $TrwB_{R388}$ and the other mutants, the employed purification protocol was the previously described common one.

An example of the results obtained during $TMD_{TrwB}TraJ_{pIP501}$ purification is shown below. This protein has a theoretical MW of 72.7 kDa, which runs together with the 7th lane of the *Precision Plus Protein™ Unstained Protein Standard* (75 kDa). Therefore, the whole purification process was followed by the visualisation of this band. The expression and membrane location of this chimera protein were analysed via SDS-PAGE (figure 3.24). Expression level turned out to be lower than that of $TrwB_{R388}$, but it was located in the membrane as expected. A single peak was obtained on the affinity column chromatogram, although many contaminant proteins eluted together with the target protein, especially on the first fractions. Nevertheless, as a SEC would be performed afterwards, fractions from 4 to 20 were pulled-down together and concentrated to 5 mL. The obtained sample was centrifuged to get rid of the contaminants and loaded onto a *Superdex 200 HR 16/60* column.

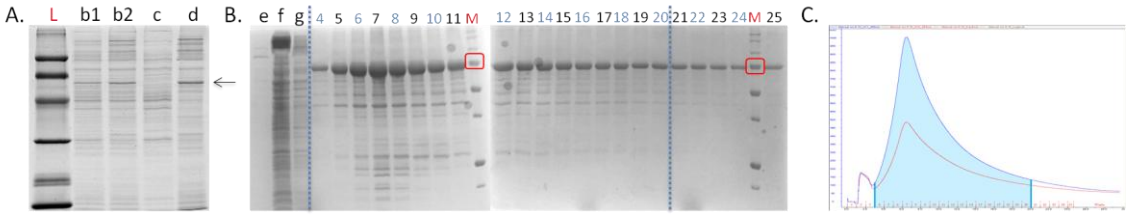

Figure 3.24. SDS-PAGE analysis and chromatogram of the *HisTrap™ FF* affinity chromatography. A) SDS-PAGE analysis of the samples obtained during cell lysis and membrane fraction isolation. Two µg of protein per well were loaded. b1 and b2: broken and unbroken cells, respectively; c: soluble proteins; d: membrane fraction; L: *Prestained SDS-PAGE Standard Low Range*. The black arrow points to the target protein. **B)** SDS-PAGE analysis of samples obtained from the affinity chromatography. e: solubilised membranes after dilution with *MP1 buffer*; f: flow-through *His-trap™ FF* column; g: washed unbound proteins; 4 to 25: fractions eluted from the *His-trap™ FF* column. M: *Precision Plus Protein™ Unstained Protein Standard*. Red square marks the band of 75 kDa. Fractions between lines were pulled-down. **C)** The chromatogram obtained from the *HisTrap™ FF* column. Protein elution was followed by measuring light absorbance at 280 nm. Fractions shaded in blue were pulled-down for the next steps.

The SEC run was performed as for the rest of $TrwB_{R388}$ related proteins. However, it must be pointed out that some kind of trouble happened during the chromatography since the protein had a V_e higher than expected. In contrast to sample 1 of $TrwB_{R388}$, which had a V_e of 47 mL, the chimera protein appeared after 120 mL, which corresponds to the size of the column. In this case, two main peaks were obtained on the SEC (figure 3.25, B). As with $TrwB_{R388}$, the first one might be associated with high MW complexes or aggregates, as can be observed in the SDS-PAGE (figure 3.25, A, lanes 95 to 98). Due to the oligomeric mixture seen in all the samples from the previous purifications, it was chosen not to pull-down the fractions according to the obtained peaks. Instead, the first ones were discarded and also the last ones that had a contaminant protein of low MW (**Figure 3.25**, lanes *17* to *21*). After concentration, 1.05 mL were obtained at 38 µM (2.76 mg/mL), resulting in 2.90 mg protein in total (0.725 mg per cell culture L). Taking into account the low yield and the purity degree obtained, it can be postulated from these results that the described common protocol might not be the best for purifying $TMD_{TrwB}TraJ_{pIP501}$ chimera protein. This may happen due to the different properties it has in comparison to the other ones presented in this chapter. Therefore, to deeply study $TMD_{TrwB}TraJ_{pIP501}$, a different purification protocol should be optimized.

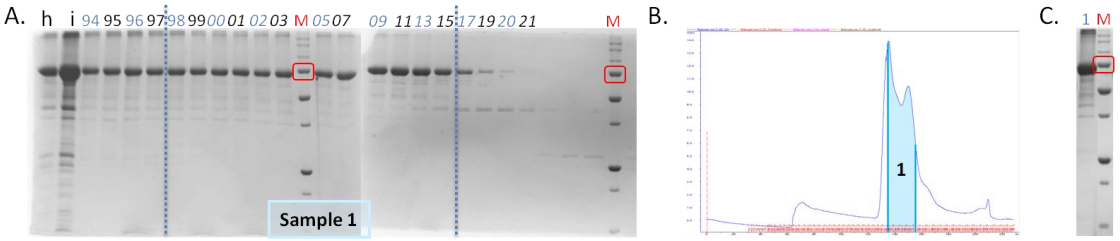

Figure 3.25. SEC and final sample of $TMD_{TrwB}TraJ_{pIP501}$ purification. A) SDS-PAGE analysis of fractions obtained on the SEC (five µL of each sample). h: pull-down of the eluate from the affinity chromatography; i: concentrated eluate; 94 to *21*: fractions eluted in the chromatography. Numbers in italics represent the fraction number above one hundred. M: *Precision Plus Protein™ Unstained Protein Standard*. The red square marks the band of 75 kDa. Fractions between lines were pulled-down to obtain the final sample. **B)** Chromatogram obtained after the *Superdex 200 HR 16/60* column. Protein elution was followed by measuring absorption at 280 nm. Fractions shaded in blue were pulled-down to obtain the final sample. **C)** Analysis via SDS-PAGE of the final sample. Five µL were loaded. M: *Precision Plus Protein™ Unstained Protein Standard*. The red square marks the band of 75 kDa.

Figure 3.26 shows a summary of the proteins purified through the common protocol (except for TrwBΔN70, which was loaded as a control). It can be seen how $TrwB_{R388}$ and $TMD_{TraJ}CD_{TrwB}$ samples present a high purity degree, while the one obtained for $TMD_{TrwB}TraJ_{pIP501}$ should be optimized. Besides, the yield obtained for this protein was low when comparing it to the other proteins. In fact, it is said that protein purification with a yield below 1 mg/L is not worth performing due to the low results/cost relation (Angius et al., 2016).

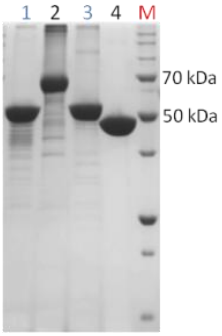

Figure 3.26. Purified proteins through the common protocol for $TrwB_{R388}$ and its mutants. A set of proteins related to $TrwB_{R388}$ was purified following the same protocol. Obtained final samples were analysed together via SDS-PAGE. Two µg of protein were loaded per well. 1: $TrwB_{R388}$, Sample 1; 2: $TMD_{TrwB}TraJ_{pIP501}$; 3: $TMD_{TraJ}CD_{TrwB,}$ sample 1; 4: TrwBΔN70 purified as explained in section 2.5.2.6.. M: *Precision Plus Protein™ Unstained Protein Standard*.

3.5.2. PURIFICATION OF PROTEINS FROM THE ClODF13 SYSTEM

Plasmid CloDF13 is a mobilizable plasmid that originated in *Enterobacter cloacae.* Its mobilizable region is composed of the *oriT* sequence and the sequences encoding for $MobB_{CloDF13}$ and $MobC_{CloDF13}$ (Núñez and De La Cruz, 2001). Regardless of the interesting characteristics they presented via *in vivo* assays, these proteins have not been purified and *in vitro* characterized so far. Since the main aim of this work is to study T4CPs and their properties, we have focused on $MobB_{CloDF13}$, while only preliminary assays have been performed with $MobC_{CloDF13}$ (figure S3.6).

3.5.2.1. PURIFICATION OF $MobB_{CloDF13}$

Purification protocol for $MobB_{CloDF13}$ was developed by using the one described for $TrwB_{R388}$ (Vecino et al., 2011) as a starting point and advises from MP purification handbooks. Later on, it was seen that it could be properly purified using the common protocol for the purification of $TrwB_{R388}$ and its related mutants. $MobB_{CloDF13}$ has a theoretical MW of 73.95 kDa, and runs between the bands corresponding to 50 and 75 kDa of the *Precision Plus Protein™ Unstained Protein Standard* in SDS-PAGE analysis. Therefore, the whole purification process was followed by the visualisation of this band.

Expression conditions were chosen taking into account the results obtained on the expression screening of $MobB_{CloDF13}$GFP (section 3.4.3.). Briefly, E. *coli* BL21C41(DE3) cells were transformed with pOPINE-*mobB* plasmid (table S3.1). Cells were grown at 37°C with shaking in 4 L of LB supplemented with Amp until OD_{600} of 0.4-0.5 was reached. Expression was induced by addition of 1 mM IPTG and cells were grown at 25°C for 20 h. Cells were harvested by centrifugation at 8,000 *g* and the obtained pellet was suspended in 80 mL of *Cell buffer*, which was frozen using liquid N_2 and stored at -80°C. From this point on the performed protocol was as the one described for $TrwB_{R388}$ and its related proteins (section 3.5.1.).

Although the first samples from the purification were too diluted, the presence of $MobB_{CloDF13}$ could be observed in the ones related to broken cells and membrane fraction, suggesting a high expression level (figure 3.27, A, lanes b and d). Fractions 4 to 42 obtained in the *HisTrap™*FF affinity column were pulled-down, discarding fractions 7, 8 and 9 that had an extra protein band right under the one related to $MobB_{CloDF13}$. The obtained sample was concentrated using a *Centricon YM-100* to a final volume of 10 mL. The resulting sample was loaded in two steps onto a *Superdex 200 HR 16/60* column and the SEC was performed in *MP purification buffer* at a flow rate of 0.5 mL/min and taking 1.0 mL fractions (figure 3.28).

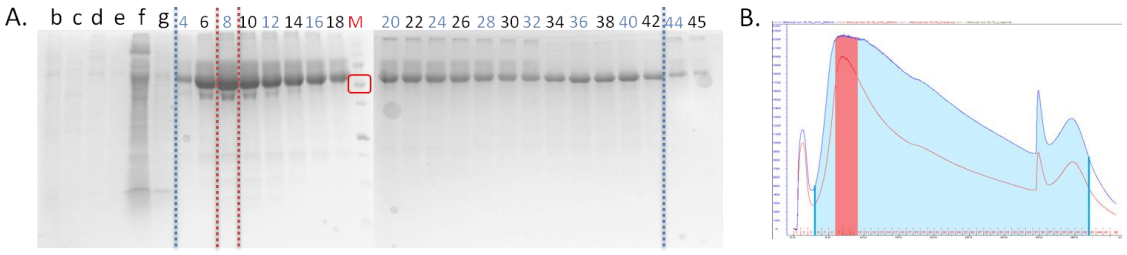

Figure 3.27. SDS-PAGE analysis and chromatogram of the *HisTrap™ FF* affinity chromatography. A) SDS-PAGE analysis of obtained samples. Five µL of each sample were loaded (samples b to e were diluted 1:100). b: broken cells; c: soluble proteins; d: membrane fraction; e: solubilised membranes after dilution with *MP1 buffer*; f: flow-through *His-trap™ FF* column; g: washed unbound proteins; 4 to 45: fractions eluted from the *His-trap™ FF* column. M: *Precision Plus Protein™ Unstained Protein Standard*. The red square marks the band of 50 kDa. Fractions between the blue lines were pulled-down, while fractions between the red ones were discarded. **B)** The chromatogram obtained from the affinity chromatography. Protein elution was followed by measuring absorption at 280 nm. Fractions shaded in blue were pulled-down for the next steps.

Elution curves obtained from both runs were similar, presenting a main peak with a V_e of 61 mL. Additionally, an elbow to the left of the peak was observed, but the fractions related to it were discarded when pulling-down the fractions that contained $MobB_{CloDF13}$ (57 to 70 of both runs). The sample was concentrated and glycerol was added to a final concentration of 20% (v/v). As a result 0.98 mL sample was obtained at 208.6 µM (15.37 mg/mL) (figure 3.28, C), resulting in 15.06 mg protein (3.86 mg per cell culture L).

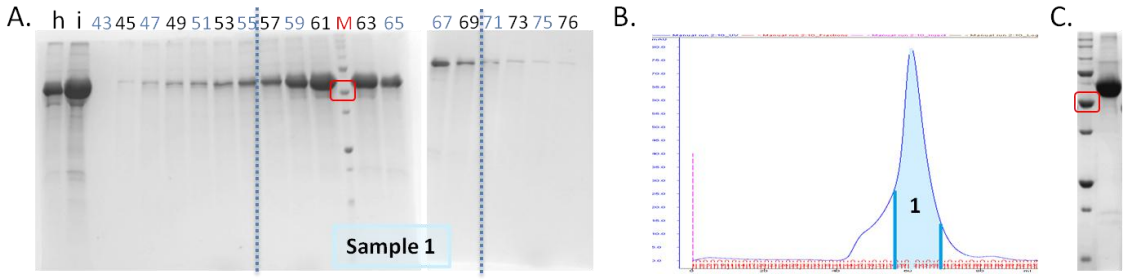

Figure 3.28. SDS-PAGE analysis and chromatogram of the SEC. A) SDS-PAGE analysis of fractions obtained from the SEC (five µL of each sample). h: pull-down of the eluate from the affinity chromatography; i: concentrated eluate; 43 to 76: fractions eluted in the chromatography. M: *Precision Plus Protein™ Unstained Protein Standard*. The red square marks the band of 50 kDa. Fractions between the blue lines were pulled-down to obtain the final sample. **B)** Chromatogram obtained after the *Superdex 200 HR 16/60* column. Fractions shaded in blue were pulled-down to obtain the final sample. **C)** Analysis via SDS-PAGE of the final sample. Five µL were loaded. M: *Precision Plus Protein™ Unstained Protein Standard*. Red square marks the band of 50 kDa.

3.5.2.2. PURIFICATION OF MobBΔTMD

To analyse the role of the TMD in $MobB_{CloDF13}$, a mutant that lacks this domain was constructed, named MobBΔTMD. This is a strategy that has been long used when studying T4CPs (*e.g.,* $TrwB_{R388}$ and TrwBΔN70, $TraG_{RP4}$ and TraGΔ2, $PcfC_{pCF10}$ and PcfCΔN103). MobBΔTMD has a theoretical MW of 53.13 kDa and runs together with the 5th band of the *PageRuler™ Plus Prestained Protein Ladder* (55 kDa) on SDS-PAGE. Therefore, the whole purification process was followed by the visualisation of this band.

In order to purify the TMD-less mutant, a protocol similar to the one used for $MobB_{CloDF13}$ was developed, adapting it to a soluble protein. *E. coli* Lemo21(DE3) cells were transformed with pOPINE-*mobBΔTMD* plasmid (table S3.1) and obtained colonies were grown at 37°C with shaking in 4 L of LB supplemented with Amp until an OD_{600} of 0.5-0.6 was reached. Expression was induced with 1 mM IPTG and performed for 20 h at 25°C. Cells were harvested by centrifugation at 8,000 *g*, for 15 min, at 4°C and the obtained pellet was suspended with 80 mL of *Cell buffer*. The mixture was frozen in liquid N_2 and stored at -80°C.

The cell suspension was unfrozen and the same lysis protocol as the one used for $MobB_{CloDF13}$ was followed, keeping the sample at 4°C for the whole process. After ultrasonication, the obtained sample was ultracentrifuged at 138,000 *g* for 45 min, to pellet the membrane fraction and the inclusion bodies. The supernatant with the soluble proteins was supplemented with 50 mM imidazole and loaded onto a 5 mL *HisTrap™ FF* column, which had been previously equilibrated with *MobBΔTMD1 buffer*. Affinity chromatography was performed as with $MobB_{CloDF13}$, but using *MobBΔTMD1 buffer* for washing and *MobBΔTMD2 buffer* for elution.

MobBΔTMD showed a higher expression level than the purified MPs. Additionally, since the sample processing before the first chromatography was shorter than with MPs, the protein loss was decreased. These factors turned in a high protein recovery after the *His-trap™ FF* column (figure 3.29). Although some contaminant proteins were present, their abundance next to the target protein was low. Fractions 5 to 13 were pulled-down and concentrated using a *Centricon YM-30* to a final volume of 600 µL. The resulting sample was centrifuged in order to get rid of the aggregates and loaded onto a *Superdex 200 HR 10/30* column. SEC was performed in *Cell buffer* at a flow rate of 0.3 mL/min and collecting 0.5 mL fractions.

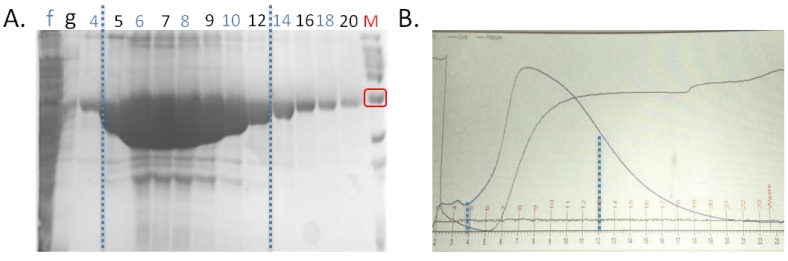

Figure 3.29. SDS-PAGE analysis and chromatogram of the *HisTrap™ FF* affinity chromatography. A) SDS-PAGE analysis of obtained samples. Three µL of samples f and g and 5 µL of each fraction were loaded. f: flow-through *His-trap™ FF* column; g: washed unbound proteins; 4 to 20: fractions eluted from the *His-trap™ FF* column. M. *PageRuler™ Plus*

Prestained Protein Ladder. The red square marks the band of 55 kDa. Fractions between the lines were pulled-down. **B)** The chromatogram obtained from the affinity chromatography. Protein elution was followed by measuring absorption at 280 nm. Fractions between the dashed lines were pulled-down.

Due to the high amount of protein, the saturation of the UV-lamp happened while performing the chromatography (figure 3.30, B). As in the previous chromatography, fractions had contaminant proteins, but they were highly enriched in the target protein. For this reason, fractions 11 to 21 were pulled-down and without further concentration of the sample, they were centrifuged to discard the aggregates. Glycerol was added to a final concentration of 20% (v/v) and aliquots were made. A final volume of 5 mL was obtained at 115.44 µM (6.82 mg/mL) (figure 3.31, A), with a yield of 34.1 mg protein (8.52 mg per cell culture L).

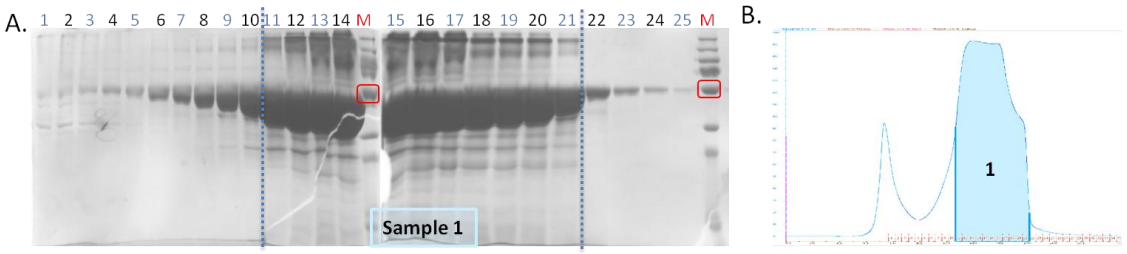

Figure 3.30. SDS-PAGE analysis and chromatogram of the SEC. A) SDS-PAGE analysis of fractions obtained on the SEC (five µL of each sample). 1 to 25: fractions eluted in the chromatography. M: *PageRuler™ Plus Prestained Protein Ladder*. The red square marks the band of 55 kDa. Blue lines represent the fractions that were pulled-down to obtain the final sample. **B)** Chromatogram obtained after the *Superdex 200 HR 16/60* column. Protein elution was followed by measuring absorption at 280 nm. Fractions shaded in blue were pulled-down together to obtain the final sample.

Since the SEC chromatography did not give a nice resolution, the obtained sample was further analysed by loading 30 µL at 20 µM in a *Superose 6 PC 3.2/30* column. This is a 2.4 mL column for performing SEC with a resolution between 5 and 5.000 kDa and small volume samples. The run was performed in *Cell buffer* supplemented with 10% (v/v) glycerol, at room temperature and a flow rate of 0.03 mL/min. The obtained chromatogram showed a single peak, in contrast to the SEC performed during the purification process (figure 3.31, B).

Although obtained purity degree was enough to perform most of the studies, there are other techniques, like crystallization that require the highest purity degree possible. For this assays, an alternative protocol was used, which is described in section 2.7.2. The difference between both protocols is an extra washing step with 100 mM imidazole at the affinity chromatography and elution of the protein with 164 mM instead of 225 mM imidazole. In this manner, a lower purification yield was obtained (3.87 mg per cell culture L), but the sample showed higher purity (figure 3.31, C).

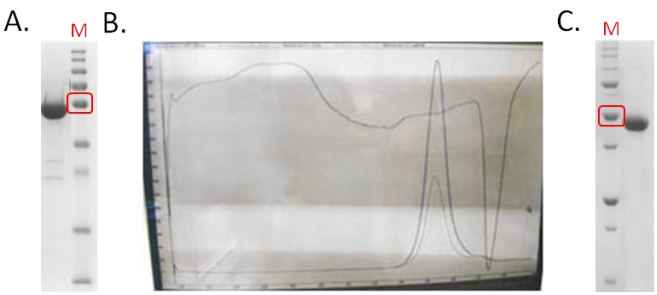

Figure 3.31. Final samples obtained in the purifications of MobBΔTMD. A) Analysis via SDS-PAGE of the final sample. Two µg of protein were loaded. M: *PageRuler™ Plus Prestained Protein Ladder*. The red square marks the band of 55 kDa. **B)** The chromatogram obtained after the *Superose 6 PC 3.2/30* column. An analytical SEC was performed with 30 µL (20 µM) of the final sample. The run was performed in *Cell buffer* supplemented with 10% (v/v) glycerol, at room temperature and a flow rate of 0.03 mL/min. Protein elution was followed by measuring absorption at 280 nm. **C)** Two µg of MobBΔTMD sample purified using the protocol for crystallization described in section 2.7.2. were analysed via SDS-PAGE. M: *Precision Plus Protein™ Unstained Protein Standard*. The red square marks the band of 50 kDa.

3.6. SUBCELLULAR LOCATION

As explained in section 1.3.3., the subcellular location of different T4CPs has been studied in-depth rendering ambiguous results (Gunton et al., 2005; Kumar and Das, 2002; Segura et al., 2014). Intending to gain a deeper knowledge of this matter, we have studied the location of native T4CPs and related mutant proteins of three different conjugative systems. On the one hand, the T4CP variants related to the R388 conjugative system: $TrwB_{R388}$ and the chimera proteins $TMD_{TraJ}CD_{TrwB}$ and $TMD_{TrwB}TraJ_{pIP501}$; on the other hand the T4CP from the pIP501 conjugative system: $TraJ_{pIP501}$; and finally the T4CP variants related to the mobilizable plasmid CloDF13: $MobB_{CloDF13}$ and MobBΔTMD.

To study the location of these proteins, two different approaches based on confocal fluorescence microscopy were used: (i) immunofluorescence and (ii) eGFP-labelling, as explained in section 2.9.1. Preliminary studies were performed using both techniques; however, since eGFP-labelling offered clearer and more reproducible results, it was the chosen technique to perform the whole study. Additionally, since the eGFP moiety only emits fluorescence when properly folded (Drew et al., 2005), the eGFP based approach allowed only visualizing properly folded proteins. Nevertheless, a sample of images acquired through immunofluorescence microscopy is shown in supplementary data (figure S3.7).

Since eGFP-tag can affect the activity of the target protein, the *in vivo* activity of the eGFP fusion-proteins was studied by mating assays proving their functionality (section 3.3.). It was decided to use *E. coli* BL21C41(DE3) (for MPs) and BL21(DE3) strains (for soluble proteins). The comparative use of *E. coli* BL21C43 strain for studying the subcellular location was dismissed since it had been previously described that similar location results were obtained with both Walker strains (Segura et al., 2014). Afterwards, expression conditions were selected

based on the results obtained in the expression screenings shown in section 3.4.3. To have a common expression protocol, it was decided to perform the induction with 1 mM IPTG and express the target proteins in LB for 4 and 20 h at 25°C. The study was complemented by analysing the effect of the presence of other conjugative proteins in the location of the full-length T4CPs, to take into account possible interactions that could affect the location pattern.

$MobB_{CloDF13}$, as the T4CP of a mobilizable plasmid, performs conjugation through interaction with its cognate relaxase ($MobC_{CloDF13}$) and a secretion channel coded in a co-resident conjugative plasmid. Therefore, its location was also studied in the presence of both, a conjugative helper plasmid (pSU1456, R388 lacking functional $TrwB_{R388}$) and the mobility region of CloDF13 (pSU4833, $MOB_{CloDF13}$ lacking $MobB_{CloDF13}$) (table 2.2).

Fluorescence images of the different samples were acquired in a *Leica TCS SP5* confocal fluorescence microscope, with a 60X oil immersion objective. Sample excitation was performed with 488 nm wavelength, while fluorescence emission was measured between 505 and 525 nm. Obtained images were treated and analysed using *Huygens* and *ImageJ* softwares. Observed fluorescence indicated the location of the eGFP fusion-proteins. All the images can be seen in supplementary data (figure S3.8).

Table 3.3. Subcellular locations of different T4CP-eGFP fusion-proteins at different expression times and in the absence or presence of a T4SS. The eGFP variants of the different T4CPs (first column) were expressed in *E. coli* BL21C41(DE3) strain by induction with 1 mM IPTG for 4 (white rows) and 20 (blue rows) hours. The images of fluorescence were acquired in a *Leica TCS SP5* confocal fluorescence microscope, with a 60X oil immersion objective. Sample excitation was performed with 488 nm wavelength, while fluorescence emission was measured between 505 and 525 nm. Numbers are percentages calculated up to the total amount of cells counted for each sample (between 50 and 200). The main location for each condition is marked in bold. M: location through the perimeter of the cell membrane; 1P: location at a single-pole; 2P: location at both poles. -: without relevance for this study. N.d.: not determined. *Proteins expressed in *E. coli* BL21(DE3) and polar location in the cytosol.

	Expression time (h)	Without T4SS (%)			$T4SS_{R388}$ (%)			$T4SS_{R388}$ and $MOB_{CloDF13}$ (%)		
		M	1P	2P	M	1P	2P	M	1P	2P
$TrwB_{R388}$	4	**77**	9	14	**84**	8	8	-		
	20	15	**75**	10	6	**90**	4			
$TMD_{TraJ}CD_{TrwB}$	4	**83**	11	6	**76**	18	6	-		
	20	40	**51**	8	14	**67**	18			
$TMD_{TrwB}TraJ_{pIP501}$	4	33	**44**	23	10	**51**	38	-		
	20	4	**56**	40	4	**57**	39			
$TraJ_{pIP501}$*	4	0	**56**	44	-			-		
	20	0	44	**56**						
$MobB_{CloDF13}$	4	18	8	**74**	19	14	**68**	5	13	**82**
	20	18	21	**61**	15	15	**70**	4	22	**74**
MobBΔTMD*	4	0	**95**	5	N.d.			N.d.		
	20	0	**95**	5						

Regarding the **location of each protein at different expression times,** different patterns were observed (figure 3.32). In regard to $TrwB_{R388}$ and $TMD_{TraJ}CD_{TrwB}$, after 4 h of expression, the main location was through the whole cell membrane, which switched to a single-pole after 20 h, being this change smaller in the case of the chimera protein. The location of $TMD_{TrwB}TraJ_{pIP501}$ showed more similarities with $TraJ_{pIP501}$ than with $TrwB_{R388}$. It had a predominant single-pole location at both times, similar to $TraJ_{pIP501}$, which switched with time from one pole to two poles, with a small percentage difference. In the case of $MobB_{CloDF13}$, it was predominantly located at both poles in all the studied conditions, showing a little increase in one pole location after 20 h. Regarding its soluble mutant MobBΔTMD, 95% of the cells had the T4CP-eGFP fusion-protein located on a single pole at both tested times. These patterns and the main location observed for all the proteins were the same, both, in the absence or presence of a conjugative system (table 3.3). However, although $MobB_{CloDF13}$ kept two poles as its main location, in the presence of pSU1456 it did not partially switch to a single-pole after 20 h, as in the absence of it.

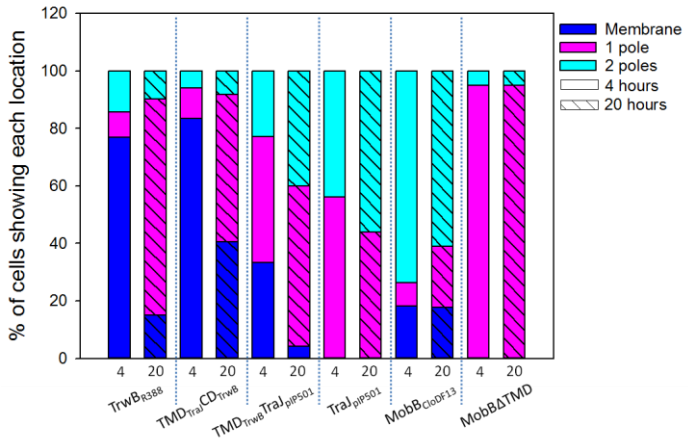

Figure 3.32. Location of the different eGFP fusion-proteins 4 and 20 hours after induction. The graph shows the percentage of cells showing membrane periphery (dark blue), 1 pole (pink) or 2 pole (light blue) locations, 4 or 20 hours (stripped) after induction in the absence of type IV secretion machinery. In the case of TraJ$_{pIP501}$ and MobBΔTMD the polar locations were in the cytosol instead of the membrane. Percentages are taken from table 3.3.

With relation to **the influence of the presence of a T4SS** (lacking a functional T4CP that could interact with the studied protein), the general observed pattern was that it enhanced the percentage of cells with the T4CP at the predominant location after 20 h (figure 3.33). The percentage of cells showing TrwB$_{R388}$ and TMD$_{TraJ}$CD$_{TrwB}$ at a single pole increased, as did the presence of TMD$_{TrwB}$TraJ$_{pIP501}$, although in a very smaller percentage. The reason for this could be that TraJ$_{pIP501}$, as a soluble T4CP lacking a TMD, does not perform the same kind of interactions with the T4SS. This issue should be further studied by analyzing its location and the location of TraJ$_{pIP501}$ in the presence of pIP501 plasmid. MobB$_{CloDF13}$ showed the same pattern, increasing its percentage at both poles. Furthermore, the additional presence of its cognate MOB$_{CloDF13}$ region enhanced the effect produced by T4SS$_{R388}$. Taking all into account, it seems that the different interactions that occur between T4CPs and the different T4SS components are an additional recruitment mechanism for their subcellular location.

The goal of this study was to unravel the different aspects that take part in the location of T4CPs. For that, we studied T4CPs of different origins and characteristics, together with mutant and chimera T4CPs. Regarding the full-length proteins, TrwB$_{R388}$ located at the membrane after 4 h of expression and at a single pole after 20 h. These results are not in agreement with the ones presented in Segura et al. (2014), where the polar location of TrwB$_{R388}$ was observed after 4 h. However, the starting OD$_{600}$ values of both experiments were different (0.4 *vs.* 0.7, respectively), probably rendering to a different growth phase between both populations after 4 h of induction. On the contrary, MobB$_{CloDF13}$ was located at both poles only 4 h after induction. However, it must be pointed out, that after 4 h a fluorescent perimeter around the cell could also be visualized, while the intensity observed at the poles increased after 20 h. Intriguingly, TraJ$_{pIP501}$, which is a soluble T4CP, also located at the cytosol poles in the absence of any other conjugative protein. Up to date, no location studies had been made with soluble full-length T4CPs, but it was postulated that they were recruited to their final location by a small associated MP, like TraI$_{pIP501}$ (Grohmann et al., 2016).

In this regard, surprising results were obtained with MobBΔTMD, which located at a single cell pole in the absence of other conjugative proteins, unlike the rest of TMD-less mutant T4CPs. These results suggest that soluble T4CPs and the ones related to mobilizable plasmids localize at the cellular poles through different mechanisms than the ones present in VirD4-type T4CPs. The result obtained with the chimera protein $TMD_{TrwB}TraJ_{pIP501}$ reinforced this affirmation, since it showed a polar location only 4 h after the induction, unlike $TrwB_{R388}$ and $TMD_{TraJ}CD_{TrwB}$. It has been speculated that the polar location of T4CPs could be related to interactions with the cardiolipin enriched membrane poles (Mileykovskaya and Dowhan, 2009; Segura et al., 2014), but at the same time mediated by complex and dynamic changes in transduction, cytoskeleton proteins, etc (Shapiro et al., 2002). As many of these interactions seem to happen through the TMD, soluble T4CPs could have evolved to develop different mechanisms to interact with the membrane and ensure their polar location. A similar scenario could have happened with mobilizable plasmid related T4CPS. As their interactions with T4SSs are not specific, all their interaction mechanisms might have changed to adapt to this scenario, including the ones related to the polar location on the membrane.

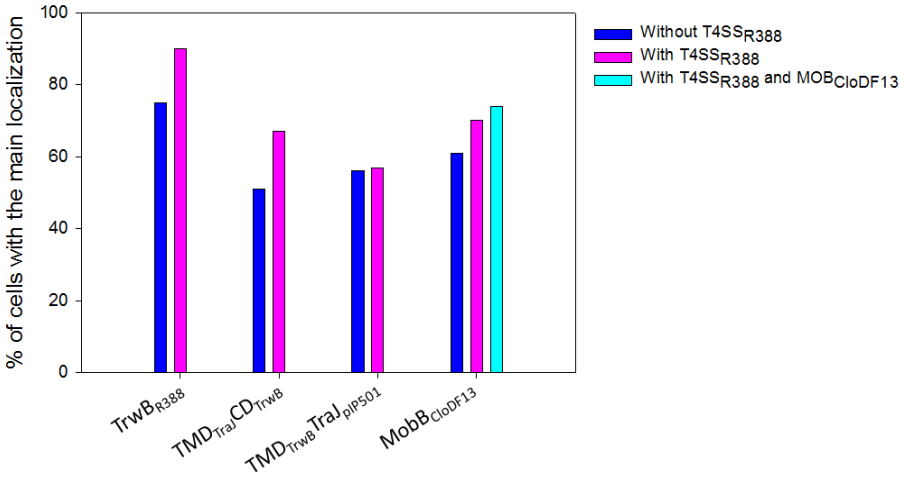

Figure 3.33. Influence of the presence of a conjugative system in the location of the different T4CPs. $TrwB_{R388,}$ $TMD_{TraJ}CD_{TrwB}$, and $TMD_{TrwB}TraJ_{pIP501}$ had a predominant location at one pole of the membrane, while $MobB_{CloDF13}$ was mainly present at both poles. Percentages are taken from table 3.3.

Regarding the interaction with the T4SS, even if previous studies (Gunton et al., 2005; Kumar and Das, 2002; Segura et al., 2014) have shown that the location of the T4CP is independent to the presence of the rest of the conjugative proteins; our results suggest that they do have some kind of effect on it (figure 3.33). Specifically, the presence of a conjugative system (a MOB region and a secretion channel) seems to enhance the polar location of the studied full-length proteins, except for $TMD_{TrwB}CD_{TraJ}$. A possible explanation for this is that due to its chimera nature, it presented a behavior in between the one shown by $TrwB_{R388}$ and $TraJ_{pIP501}$, hiding the effect of the conjugative plasmid. Another suggestion is that the observed enhancement was associated with the specific interactions between the soluble domain of the T4CP and its cognate relaxosome. It has been suggested that the relaxosome components spatially position the substrate at the periphery to stimulate substrate docking with the T4CP, which could enhance the polar location of the T4CPs (Chen et al., 2008). According to this

hypothesis, $TMD_{TraJ}CD_{TrwB}$ would have interacted with $TrwC_{R388}$ and $TrwA_{R388}$ (coded in plasmid pSU1456) through its soluble domain, but not $TMD_{TrwB}CD_{TraJ}$. Similar observations have been seen in regard to $MobB_{CloDF13}$, although its location at both poles was enhanced in the presence of $T4SS_{R388}$, it was further enhanced when $MOB_{CloDF13}$ was also present.

Taking all together, it seems that **different factors condition the subcellular location of T4CPs**, such as their nature (VirD4-type or soluble), their origin (conjugative or mobilizable plasmid) and the presence of a conjugative system. For this reason, further studies should be performed to gain knowledge about this matter.

3.7. DISCUSSION/SUMMARY

T4SSs are macromolecular transport systems related to bacterial conjugation (cT4SS) and virulence processes (pT4SS). The study of these systems has been enhanced in the last years, due to their implication in the spread of genes related to antibiotic resistance and in pathogenic processes of bacteria (Christie et al., 2014).

T4CPs are ubiquitous in all cT4SS, present in many plasmids that code for pT4SS and in some mobilizable plasmids too, which makes them an interesting study subject. The different roles of this protein family are open to debate. Their main function in cT4SS is to connect the substrate with the secretion channel at the cell membrane (Llosa et al., 1994). In addition, they seem to take part in the energetic part of the conjugative process together with VirB4 and VirB11 proteins since mutations in the Walker A domain inhibit both the ATPase activity of the soluble domains and the plasmid transfer (Tato et al., 2005). They also take part in the signal transmission of the conjugative process (Cascales and Christie, 2004b) and might act as a channel for DNA translocation according to the "*Shoot and Pump*" model (Llosa et al., 2002). Despite their importance, T4CPs have not been fully characterized, mainly because of the troubles associated to their condition as integral MPs. For this reason, most of the *in vitro* studies regarding T4CPs have been performed with soluble mutants that lack the TMD. However, comparative studies between the full-length proteins and these mutants have shown the importance of the TMD in many aspects such as biological activity, oligomerization, subcellular location and stability (Kumar and Das, 2002; Mihajlovic et al., 2009; Segura et al., 2014; Vecino et al., 2011).

This work has a double aim of studying T4CPs beyond their paradigmatic subfamily (The $Gram^-$ conjugative VirD4-type proteins, such as $TrwB_{R388}$) and further analysing the role of the TMD. To do so, a set of native and mutant T4CPs have been constructed using traditional molecular cloning techniques and a HTP method. It must be reminded that all the proteins constructed in this thesis have an H_6-tag at their C-term. Through the traditional approach, two native proteins have been obtained: the relaxase $MobC_{CloDF13}$ from the mobilizable plasmid CloDF13 and the soluble T4CP $TraJ_{pIP501,}$ from the $Gram^+$ plasmid pIP501. Additionally, three chimera proteins have been constructed: $TMD_{TraJ}CD_{TrwB}$, composed of the TMD of $TraJ_{pKM101}$ and the CD of $TrwB_{R388}$; $TMD_{TrwB}TraJ_{pIP501}$, composed of TMD of $TrwB_{R388}$ and the full-length $TraJ_{pIP501}$; and $TraI_{pIP501}TraJ_{pIP501}$, composed of the small transmembrane protein $TraI_{pIP501}$ and $TraJ_{pIP501}$, which are suggested to interact *in vivo* creating a VirD4-like structure. The use of

chimera proteins to investigate the role of each domain and their mechanisms is an approach that has been highlighted by top experts in the area of bacterial conjugation and used in recent papers (Li and Christie, 2018; Whitaker et al., 2016). Traditional molecular cloning techniques were also used to obtain the walker A mutant and the eGFP variant of $TMD_{TraJ}CD_{TrwB}$, $TMD_{TraJ}CD_{TrwB}$(K142T) and $TMD_{TraJ}CD_{TrwB}$GFP, respectively.

In order to obtain more options to work with, it was decided to perform a HTP cloning and expression protocol designed by OPPF-UK (Berrow et al., 2007; Bird, 2011). Twelve different pOPIN vectors were chosen each of which added a fusion-tag that could be advantageous for the purification or characterization process of the target protein. Four proteins were chosen to be constructed with the different tags: $TraJ_{pIP501}$ and $TMD_{TrwB}TraJ_{pIP501}$, which had given troubles when trying to purify them, and $MobB_{CloDF13}$ from CloDF13 plasmid, together with its soluble mutant MobBΔTMD. The main advantage of using this HTP method was that it allowed obtaining several constructs of different proteins at the same time while saving time and money. In this manner, 46 out of the targeted 47 constructs were obtained.

The first step in the characterisation of the obtained constructs was to test their *in vivo* activity, in other words, their ability to perform the conjugative process. It has been long known that *trw genes* can be taken out of their plasmid context to mediate conjugation (Bolland et al., 1990). Through mating assays it was validated that the new constructs expressed in *trans* were able to complement conjugation of a T4SS lacking a functional T4CP. The main conclusions obtained in this assays agreed with those previously described in the literature: (i) the presence of a H_6-tag at the C-terminus of T4CPs does not impair their functioning (Hormaeche et al., 2006; Segura et al., 2013); (ii) T4CP chimera proteins can be functional *in* vivo, as seen with the transfer of pSU1456 by $TMD_{TraJ}CD_{TrwB}$ (Whitaker et al., 2016); (iii) the specific interactions between the soluble domain of the T4CP and the relaxosome are necessary for the conjugative process to happen (Cabezón et al., 1997), (iv) point mutations at the Walker A domain inhibit the T4CP function (Gunton et al., 2005; Kumar and Das, 2002; Moncalián et al., 1999) and (v) TMD-less mutants lose their ability to perform conjugation (Cascales et al., 2013; Chen et al., 2008). Additionally, it was seen that the chimera protein $TMD_{TraJ}CD_{TrwB}$ presented negative dominance against the native proteins $TrwB_{R388}$ and $TraJ_{pKM101}$. This could happen due to competition for the secretion channel and/or the presence of non-functional heteroligomers composed of both T4CPs present in the system. Finally, on the contrary to what is described in the literature (Segura et al., 2014), the presence of an eGFP domain at the C-terminus of the T4CP has a mild effect on protein functionality, decreasing the plasmid transfer rate. A possible explanation for this is that the presence of the bulky eGFP domain could somehow difficult the proper functioning of the T4CPs without totally inhibiting it. Since no mating assays could be performed with the pIP501 system, the study of $TraJ_{pIP501}$ and the chimera protein $TraI_{pIP501}TraJ_{pIP501}$ have been belated.

The next step was to obtain high-quality protein samples, pure and homogeneous, to do *in vitro* assays with. One of the most important factors for a successful purification is the starting material. In order to identify the optimal expression conditions for each protein, a variety of small-scale expression screenings was performed. The H_6-tag based assays (either by the HTP expression screening or by WB) although useful, were not the best alternative, since they only offered quantitative but not qualitative results. For this reason, it was chosen to

perform studies based on eGFP fusion-proteins, in which fluorescence is observed only if the proteins are properly folded (Drew et al., 2008). Taking together the results obtained in the expression screenings it was chosen to use *E.coli* BL21C41(DE3) strains, perform the induction at an OD_{600} of 0.4 with 1 mM IPTG and expressing the proteins for 20 h at 25°C. Additionally, after analyzing the cost/yield relation of LB and PB growth, it was chosen to use the first one. Although this screening was performed with eGFP fusion-proteins, the identified optimal conditions were extrapolated to the H_6-tagged proteins.

Additionally, the performance of a HTP expression screening in which two induction methods, two bacterial strains, and 12 different fusion-tags were compared provided much information. This screening was based on a small-scale purification assay through affinity chromatography and the visualization of the results by SDS-PAGE as performed by Bird (2011). Therefore, the total quantity of each protein was observed, without distinguishing between properly folded or aggregated proteins. In this manner, the expression and solubilisation level of 188 different samples was scored by visual inspection of the bands in the gels and qualified as null (-), low (+), medium (++) or high (+++). 36 out of the 47 initial fusion-proteins were identified in at least one of the tested conditions, obtaining the best results with the soluble proteins. The use of two different strains and two induction methods turned out to be useful since some of the constructs were only visualised in one of the tested conditions. However, no significant differences were seen between the four different expression strategies in the amount of identified proteins or expression levels. This result could have been expected, since the advantages of using Lemo21(DE3) and Rosseta^{TM}(DE3) pLysS strains were not exploited (the regulation through rhamnose and the expression of eukaryotic proteins, respectively).

Regarding the different tags, even if the best results were obtained with the GST-tag, Halo-tag also gave quite good results. STREPII-tag, which has been widely used for protein purification, also gave good results, since all the constructs were visualised in at least one of the tested conditions and a few of them with medium and high solubilisation levels. On the contrary BAP, MBP (cloned in pOPINM) and SUMO-tags only gave results with the soluble proteins. Furthermore, even though the fusion-proteins were not visualised, both MBP and SUMO-tags were observed. This could be related to the proteolysis described by Bird (2011) that affected the larger fusion-proteins. However, in this study, the proteolysis would not have been related to the weight of the fusion-protein but to their nature, as it was only seen with MPs. It could be that those proteins were not properly folded and that they were hydrolysed while in the cell or during the purification process. Other tags (*i.e.,* TRX, FLAG-His_8 and MBP cloned in pOPINCDM) gave similar results, but in these cases the MP constructs were identified at least in one condition with a low expression-solubilisation level. TF-tag showed quite better results than those ones, though all its fusion-proteins had a low expression-solubilisation level and proteolysis related to $TMD_{TrwB}TraJ_{pIP501}$ was also visualised.

Once the expression conditions were fixed, purification protocols were developed for the different proteins. As mentioned above, purifying MPs is one of the most difficult projects in the biochemistry field (Stroud et al., 2018). The traditional method in which proteins are extracted from their native lipid environment through the use of detergents usually results in protein samples with low activity and stability. For this reason, up to date, the only full-length T4CP that has been purified is $TrwB_{R388}$, although trials to purify different T4CPs have been

performed. For example, purification of $PcfC_{pCF10}$ did not render sufficient amounts of soluble protein (Chen et al., 2008) and $DotL_{L.\ pneumophila}$ constructs containing the ATPase domain were very unstable (Kwak et al., 2017).

The starting point for purifying $TrwB_{R388}$ and its related proteins [$TMD_{TraJ}CD_{TrwB}$, $TMD_{TraJ}CD_{TrwB}$(K142T) and $TMD_{TrwB}TraJ_{pIP501}$] were the published protocols for $TrwB_{R388}$ (Hormaeche et al., 2006; Vecino et al., 2010). Each of these protocols had a different aim; while the first one was focused on obtaining pure monomers and hexamers separately, the second one tried to get a bigger amount of pure protein. In this thesis, both protocols were used similarly and after observing the obtained results it was chosen to create a new protocol using the chosen expression conditions and mixing both purification protocols. Additionally, SEC-MALL analysis with $TrwB_{R388}$ purified sample showed the real size of the PDCs, which was taken into account when choosing the MWCO for the concentration of the samples. The new protocol was used for purifying the four $TrwB_{R388}$ related proteins in the same manner so that comparative studies could be carried with them. Although the chromatograms obtained on the SECs highly differed between the different proteins, BN-PAGE analysis showed that the same oligomeric species were mainly present in all the samples. Purification of $TrwB_{R388}$ and $TMD_{TraJ}CD_{TrwB}$ presented a high yield and purity degree of the target protein. On the contrary, this protocol did not give proper results for the purification of $TMD_{TrwB}TraJ_{pIP501}$, which should be further optimized.

Regarding the purification of the proteins related to CloDF13 system, protocols were developed for $MobB_{CloDF13}$ and the TMD-less mutant MobBΔTMD. For the full-length protein the common protocol for $TrwB_{R388}$ related proteins was used, rendering good yield and purity results. For MobBΔTMD two different protocols have been developed. On the first one more protein amount was obtained, but a few contaminants were present; on the contrary, on the second one, the obtained protein amount was decreased in favour of higher purity.

Finally, the subcellular location of the different T4CPs has been studied. It has been described that the polar location of proteins in bacteria is a characteristic that underlines their sophisticated internal organization. It is important in many processes like chemotaxis and cellular division (Howard, 2004) and according to our results in conjugation too. Through the purification protocols, it has been proven that $TrwB_{R388}$, $TMD_{TraJ}CD_{TrwB}$, $TMD_{TrwB}TraJ_{pIP501}$ and $MobB_{CloDF13}$ are located in the bacterial membrane. Furthermore, $TrwB_{R388}$GFP, $TMD_{TraJ}CD_{TrwB}$GFP, and $MobB_{CloDF13}$GFP have been purified together with the bacterial inner membrane (see section 5.3.2.). $TraJ_{pIP501}$ and MobBΔTMD, on the contrary, are located on the cytosol, as expected from the lack of a TMD in their predicted structure. Taking this into account, subcellular location assays were performed with the different proteins to know their exact situation through the membrane or cytosol. Studies in the literature do not show a consensus pattern either in the location of the T4CPS nor in the role of each domain in this property (Bauer et al., 2011; Kumar and Das, 2002; Segura et al., 2014).

Our results have shown that no universal location patterns can be attributed to T4CPs. On the one hand, $TrwB_{R388}$ related proteins located mainly at a single pole of the cell on the stationary phase, although this behaviour was less prominent in the chimera proteins. Strikingly, in the case of $TMD_{TrwB}TraJ_{pIP501}$ its location seemed to be influenced by the cytosolic

domain since it was located at a single-pole only after 4 h, unlike $TrwB_{R388}$ but similar to $TraJ_{pIP501.}$ On the other hand, $MobB_{CloDF13}$ located at both poles after just 4 hours of expression. Unexpectedly, the soluble proteins located at the poles of the cells too. Up to know T4CPs that lacked the periplasmic loop or the TMD located at the membrane periphery or the cytosol, respectively, in the absence of other conjugative proteins (Kumar and Das, 2002; Segura et al., 2014). Besides, the TMD of $TrwB_{R388}$ located at the membrane poles without the need for the cytosolic domain (Segura et al., 2014). These results suggested a leading role for the TMD in the subcellular location of the T4CPs. However, $TraJ_{pIP501}$ located at one or both poles of the cell, while MobBΔTMD did it at a single-pole, suggesting different mechanisms guiding their subcellular location. Apart from this, even if previous studies have shown that the rest of the conjugative system is not necessary for the polar location of the T4CPs; our results suggest that the presence of other transfer proteins enhances the percentage of cells showing the T4CP at the pole(s). Taking all together three conclusions can be undertaken: (i) T4CPs localize either at a single pole or both poles, depending on the system; (ii) the presence of a TMD is not essential for the polar location of TMD-less and mobilizable plasmid associated T4CPs (iii) the presence of a cT4SS enhances the polar location of T4CPs.

CHAPTER 4:

IN VITRO MOLECULAR CHARACTERIZATION OF TYPE IV COUPLING PROTEINS

4. *IN VITRO* MOLECULAR CHARACTERIZATION OF TYPE IV COUPLING PROTEINS

All plasmids used in this work are listed on table 2.2. All reagents and buffers are listed on tables A.1 and A.2 of the appendix, respectively. All the proteins used in this work contain a poly-histidine tag (H_x-tag) on their C-term except for TrwBΔN70.

4.1. INTRODUCTION

T4CPs are essential proteins in the conjugative process, a key mechanism in the spread of antibiotic resistance among bacteria. Additionally, they are also present in many systems related to pathogenic processes. This makes T4CPs interesting candidates as drug targets for both controlling HGT via conjugation and the transfer of effectors during pathogenic situations. To do so, a thorough knowledge of their function and way of action is needed. However, despite their fundamental role, mainly due to their nature as MPs, there are many questions to be answered.

Characterizing full-length MPs is a challenging issue, mainly due to the difficulties derived from their expression and purification processes. Therefore, most of the studies with T4CPs have been performed with soluble mutants that lack the TMD. However, many studies performed with $TrwB_{R388}$ have shown that the results obtained with those mutants do not allow to infer how the native protein works (Hormaeche et al., 2002, 2004, 2006; Moncalián et al., 1999; Segura et al., 2013, 2014; Vecino et al., 2010, 2011). For this reason, this thesis aims to provide full-length T4CPs to accomplish different biochemical and biophysical studies that will contribute to unravel the role of their TMD.

To achieve these objectives two approaches have been carried out. On the one hand, the chimera protein $TMD_{TraJ}CD_{TrwB}$ has been constructed and purified. A comparison between this protein and published results from $TrwB_{R388}$ and TrwBΔN70 would help to elucidate the role of the TMD. On the other hand, $MobB_{CloDF13}$ and its soluble mutant protein, MobBΔTMD, have also been constructed and purified. As previously said, $MobB_{CloDF13}$ is one of the few T4CPs belonging to mobilizable plasmids and therefore it necessarily has to interact with a distant T4SS. This, compared to the usual fact in conjugative plasmids in which the T4CP interacts with its specific T4SS, makes $MobB_{CloDF13}$ an excellent system for studying the interactions required in bacterial conjugation.

Along this chapter different characteristics of different T4CPs have been investigated. Specifically, the *in vitro* stability, DNA-binding, oligomerization patterns, structure, and ATPase activity of $TMD_{TraJ}CD_{TrwB}$ (in some cases together with $TrwB_{R388}$), $MobB_{CloDF13}$, and MobBΔTMD, have been studied. The comparative study of each wild type T4CP ($TrwB_{R388}$ and $MobB_{CloDF13}$) and their soluble and chimera proteins ($TMD_{TraJ}CD_{TrwB}$, TrwBΔN70 and MobBΔTMD) will shed light on the role of T4CPs.

4.2. STABILITY

Since MPs are especially prone to denaturalization, before further *in vitro* studies were accomplished, the stability of the target protein at different conditions had to be evaluated. The stability of a protein can be defined as the resistance of the native conformation against denaturation due to external factors (González Flecha, 2017). On the one hand, a folded and functional protein can lose its tertiary structure rendering a disordered polypeptide. This process is called denaturation and may be reversible since no chemical changes have been produced in the polypeptide chain. The resistance of the protein against these processes is defined as thermodynamic or conformational stability. On the other hand, proteins can suffer adverse reactions that could cause an irreversible function loss due to adverse conditions, with the consequent protein aggregation and precipitation. The resistance of the protein against this processes is called long-term or kinetic stability (Ó'Fágáin, 2017). Precisely, the aim of this section is to assess the kinetic stability of T4CPs.

As soon as MPs are solubilised out of the membrane by detergents, they become unstable and are in constant competition between folding and aggregation (Metola, 2017). Protein stability can be disturbed by many parameters, such as temperature, ionic strength, and the presence of ligands (Booth et al., 2001). For this reason, before performing any *in vitro* assays, it is important to make a careful screening of the propensity of the protein to lose its native state during the time that a given reaction lasts (Hardy et al., 2018). To do so, techniques based on different physical or chemical principles have been commonly used, for instance enzymatic activity (Cattoni et al., 2008), solvent denaturation (Hormaeche et al., 2004; Schellman, 2002), proteolysis assays (Endo et al., 1985; Vecino et al., 2011), circular dichroism (Kelly and Price, 2000; Miles and Wallace, 2016), intrinsic fluorescence from Trp residues (Hellmann and Schneider, 2019; Moon and Fleming, 2011), and IRS (Arrondo and Goñi, 1999; Vecino et al., 2012).

In this thesis we have studied the stability of $TrwB_{R388,}$ $MobB_{CloDF13}$, and their respective mutants and chimeras at different temperatures, ionic strength, and pH conditions using some of the above-mentioned techniques. In this manner, the optimal conditions to perform *in vitro* assays to characterize the different T4CPs have been established.

4.2.1. $TrwB_{R388}$ RELATED PROTEINS

$TrwB_{R388}$ has been extensively studied but as there are still open questions about its molecular mechanism, in this thesis two chimera proteins have been constructed switching its domains with those of other T4CPs (section 3.2.): (i) $TMD_{TraJ}CD_{TrwB}$, using the TMD of its phylogenetically closest homologue, $TraJ_{pKM101}$; and (ii) $TMD_{TrwB}TraJ_{pIP501}$, using the soluble $Gram^+$ related T4CP $TraJ_{pIP501.}$ However, for technical reasons no conjugative studies could be performed to prove the *in vivo* activity of $TMD_{TrwB}TraJ_{pIP501}$, and, therefore, our studies have been focused on $TMD_{TraJ}CD_{TrwB}$.

4.2.1.1. THERMAL STABILITY

Thermal stability of $TMD_{TraJ}CD_{TrwB}$ solubilised with DDM was studied through IRS (section 2.6.1.), as previously done with $TrwB_{R388}$, TrwBΔN50, and TrwBΔN70 (Vecino et al., 2012). Briefly, sample buffer was exchanged to D_2O [*$TMD_{TraJ}CD_{TrwB}$ IRS (D_2O) buffer*] and IR spectra were recorded in a *Thermos Nicolet Nexus 5700* spectrometer equipped with a liquid nitrogen-refrigerated mercury–cadmium–telluride detector using a Peltier-based temperature controller and a 25 µm optical path. The information regarding the denaturalization was obtained through analysis of the 1700-1600 cm^{-1} region of the IR spectrum, which corresponds mainly to the C=O stretching vibrations of the peptide bonds and is called the amide I band. The use of the amide I band for studying denaturalization of the protein is a useful tool since its characteristics change when the protein loses its native conformation. Specifically, two bands appear at 1615-1620 cm^{-1} and 1680 cm^{-1} when the protein aggregates. The appearance of these bands allows monitoring the denaturalization process of the protein and the calculation of the mid-point denaturation temperature (T_m) (figure 4.1).

The results obtained with the different proteins were compared. In order to perform a proper comparison, in this case, the final DDM and NaCl concentrations used in the purification of $TMD_{TraJ}CD_{TrwB}$ were changed to the ones described in the purification protocols of $TrwB_{R388}$ and TrwBΔN50 (*i.e.,* 0.2 mM DDM and 200 mM NaCl instead of 0.6 mM DDM and 300 mM NaCl). Experiments were performed as explained in section 2.6.1. In short, the thermal stability was monitored by analysing the amide I band spectral shape width at half-height (WHH) as a function of temperature. To do so, the temperature was increased at 1°C/min starting at 20°C and finishing at 80°C. IR spectra collection and data analysis were performed as explained in Vecino et al. (2012).

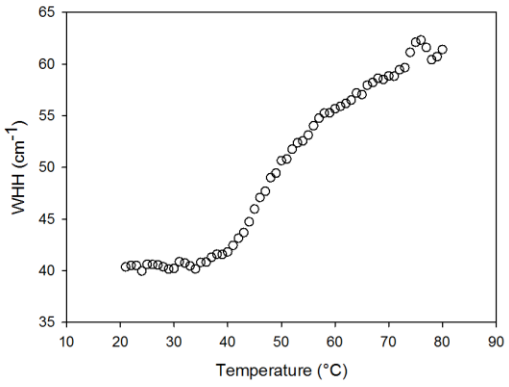

Figure 4.1. Thermal denaturation of $TMD_{TraJ}CD_{TrwB}$ followed by IRS. The widths at half-height (WHH) of the amide I bands are plotted as a function of temperature (°C). Thermal denaturation is marked by an abrupt increase in band-width. Experiments were performed as explained in section 2.6.1.

The thermal denaturation of $TMD_{TraJ}CD_{TrwB}$ starts at 35°C at the tested conditions, achieving its T_m at 51.1°C. These results resemble those obtained with $TrwB_{R388}$ and the mutant lacking the first transmembrane helix, TrwBΔN50 (table 4.1). According to these results, since the denaturalization of the target protein starts at 35°C, *in vitro* experiments should be carried

out below this temperature because above 35°C the concentration of active protein would decrease. Therefore subsequent characterization assays were performed at 25°C, as some previous studies performed with $TrwB_{R388}$ (Hormaeche et al., 2006; Vecino et al., 2010).

Table 4.1. Mid-point denaturation temperatures of R388 related T4CPs. [a]Data from Vecino et al. (2011); [b]Data from Vecino et al. (2012) [c]unpublished data from Vecino.

	$TrwB_{R388}$ [a]	$TMD_{TraJ}CD_{TrwB}$	TrwBΔN50[b]	TrwBΔN70[c]
T_m (°C)	48	51	48	63

4.2.1.2. INFLUENCE OF THE IONIC STRENGTH, pH AND DETERGENT CONCENTRATION

It has been already mentioned that MPs solubilised in detergent are in constant competition between folding and aggregation. Many factors affect this equilibrium, including the physicochemical properties of the detergent and the buffer, such as the electrical charge of the surfactant and its concentration, or the pH and the ionic strength of the solution. If the conditions are not optimal and the hydrophobic surfaces are not properly shield, protein insolubility happens, which can sometimes be seen as protein aggregates. Therefore, the effects of these parameters were studied using different techniques.

PRELIMINARY AGGREGATION ASSAYS

A preliminary assay of the tendency to aggregate of $TMD_{TraJ}CD_{TrwB}$ in different conditions was performed. It was based on the assumption that protein aggregates are orders of magnitude heavier than the properly folded protein particles. This increase in the MW is directly related to the increase in the sedimentation coefficient, which makes the aggregates possible to be separated by centrifugation. To do so, two different pHs (6.2 *vs.* 7.8) combined with two different detergent concentrations (0.3 mM *vs.* 0.5 mM DDM) and two different ionic strengths (75 mM *vs*. 200 mM NaCl) were studied. The chimera protein was incubated at 25°C in each buffer for 15 and 30 minutes and afterwards the solution was centrifuged to remove protein aggregates (17.000 *g*, 10 min, 4°C). Then, the remaining protein concentration on the supernatant was measured and it was compared with the initial concentration (figure 4.2).

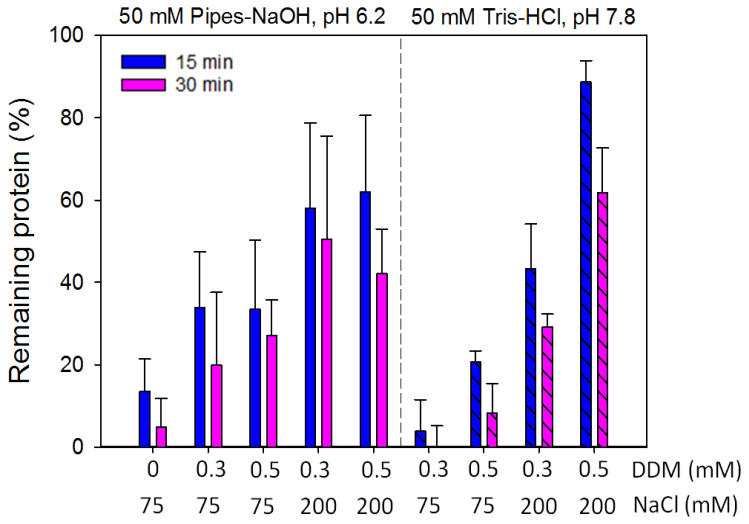

Figure 4.2. $TMD_{TraJ}CD_{TrwB}$ solubility assay. The chimera protein was incubated at 25°C for 15 (blue) and 30 (pink) minutes in *50 mm Pipes-NaOH (pH 6.2)* or *50 mM Tris-HCl (pH 7.8)* (striped bars) buffers supplemented with the corresponding DDM and NaCl concentrations. The bars represent the percentage of the remaining protein in the supernatant after discarding the aggregated fraction and are the mean value of three independent experiments. All buffers contained 5% (v/v) glycerol and 6 mM $MgCl_2$.

It was observed that the percentage of aggregation was lower at 200 mM NaCl and that the increase of DDM concentration helped in protein stability. At both pH values, the same tendency was observed regarding ionic strength and detergent concentration; although results obtained at pH 7.8 were more reproducible than at pH 6.8. Taking all this into account **the highest protein stability was achieved at pH 7.8, 0.5 mM DDM** and **200 mM NaCl**. However, even at this condition, after 15 minutes of incubation 11% of the protein was lost because of the formation of protein aggregates. Even more, after 30 minutes the protein loss increased to a 38%.

ANALYTICAL ULTRACENTRIFUGATION

To gain deeper knowledge on protein stability, the presence of high MW aggregates in $TrwB_{R388}$ and $TMD_{TraJ}CD_{TrwB}$ samples was studied by AUC as explained in section 2.6.3. Briefly, protein buffer was exchanged by the buffer to be analysed using *Sephadex G-25 PD SpinTrap* columns. Once the protein concentration was adjusted to 5.23 µM $TrwB_{R388}$ and 5.15 µM $TMD_{TraJ}CD_{TrwB}$, runs were performed at 129,000 *g* and 20°C in an *XL-A analytical ultracentrifuge* using an *AN50Ti rotor* and 12-mm double-sector centerpieces. Data from each sample was registered every 5 minutes by measuring absorption at 280 nm. Sedimentation coefficient distributions [*c(s)*] were calculated by least-squares boundary modelling of sedimentation velocity data using the *c(s)* method as implemented in the *SEDFIT* program. Additionally, obtained sedimentation coefficients (s) were corrected to the standard conditions (in water and at 20°C) using the *SEDNTERP* software to obtain the standard s-values ($s_{w,20}$); and from here onwards all the results will be expressed as standard s-values. Additionally, those populations whose s-value was above 20 S were defined as aggregated species. The

abundance of each population (%) is calculated as the area below the corresponding peak in comparison to the total area below the curve of the *c(s)* profile.

First of all, the **effect of the ionic strength** was tested. To do so, detergent concentration was maintained at 0.2 mM DDM as in the last step of the previously used $TrwB_{R388}$ purification protocol (Vecino et al., 2010), while different NaCl concentrations were added. The rest of the buffer components were: *50 mM Tris-HCl (pH 7.8), 0.1 mM EDTA and 5% (v/v) glycerol*.

At these conditions, $TrwB_{R388}$ and $TMD_{TraJ}CD_{TrwB}$ proteins showed aggregates with high s-values (figure S4.1). However, in all cases, a main peak with a smaller s-value was observed, which probably contained a mixture of different oligomeric species. When analysing the abundance of the main peak in each experiment, it was seen that it was directly proportional to the salt concentration (figure 4.3). These results showed that **raising the ionic strength of the solution reduced the presence of protein aggregates.** It must be noticed that in the case of $TrwB_{R388}$, the abundance of species with a high MW (oligomers higher than hexamers or protein aggregates) was smaller, showing a higher stability than the chimera protein at the tested conditions. At 150 mM NaCl, a main peak (80.6% abundance) of a $s_{w,20}$ of 3.7 S was observed in $TrwB_{R388}$ sample. This is intriguing, because it is a low value to be related to the monomeric form of the protein, since the lowest $s_{w,20}$ attributed to $TrwB_{R388}$ monomer in the rest of the conditions tested in this work has been 4.3 S. This discrepancy could be associated with protein degradation.

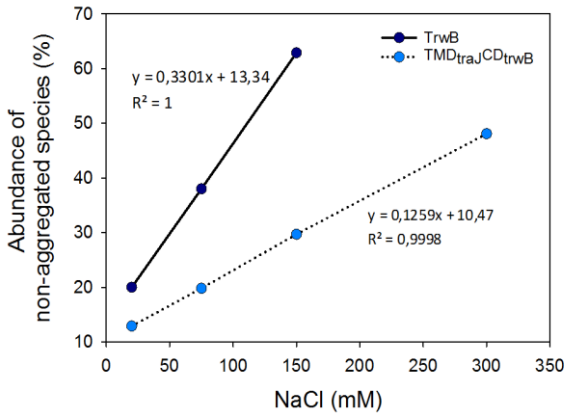

Figure 4.3. Stability of $TrwB_{R388}$ and $TMD_{TraJ}CD_{TrwB}$ at different ionic strengths. The sedimentation profile of both proteins was studied in buffer *50 mM Tris-HCl (pH 7.8), 0.2 mM DDM, 0.1 mM EDTA* and *5% glycerol (v/v)*, at increasing NaCl concentrations. Assays were carried out as explained in section 2.6.3. and the *c(s)* were analysed using *SEDFIT* software. It was defined as non-aggregated species those whose sedimentation coefficient was beneath 20 S.

Next, the effect of the **detergent concentration** was studied. The DDM concentration used in the previous assays was 0.2 mM, which is close to the critical micellar concentration (CMC) (0.12 mM in the presence of 200 mM NaCl). Experiments to assess if higher detergent concentrations (0.3 and 0.5 mM DDM) could improve protein stability were carried out. At low salt concentration (50 mM NaCl) both proteins showed aggregated profiles (see Analytical

ultracentrifugation assays) independently of DDM concentration, suggesting that a **high ionic strength is a requisite to reduce aggregation of these proteins independently to the detergent concentration used**. At high salt concentration (300 mM NaCl) *c(s)* profiles with better-defined peaks and smaller s-values were obtained, especially at 0.5 mM DDM, even if some species with high MW were still present.

These results demonstrated that the detergent concentration used in previous $TrwB_{R388}$ purification protocols [(0.2 mM DDM (Vecino et al., 2010)] was too low to maintain the protein in a homogeneous stable form. Nevertheless, as mentioned in chapter 3, probably due to the centrifugal filters used in those studies the real DDM concentration was above 0.2 mM although the exact detergent concentration was not known (section 3.5.1.).

INTRINSIC TRYPTOPHAN FLUORESCENCE

The kinetic stability studies were performed through fluorescence assays. As explained in section 2.6.2., proteins present **intrinsic fluorescence** due to the aromatic amino acids in their sequence. The main contribution to the intrinsic fluorescence spectra is due to the Trp residues, which in terms of wavelength and intensity are very sensitive to changes in the environment. Specifically, when the polarity of the environment increases, the emission maximum increases too, causing a red-shift of the emission. In this manner, in a highly hydrophobic environment, the emission maximum is around 310 nm, while it can be as high as 350 nm in a polar aqueous environment. As during protein unfolding Trp residues become exposed to a less hydrophobic environment and their emission spectrum changes, this property has made Trp intrinsic fluorescence a widely used technique to study protein conformational changes (Ghisaidoobe and Chung, 2014; Hellmann and Schneider, 2019; Lakowicz, 2006; Moon and Fleming, 2011). Due to the red-shift caused by the change to a polar environment, the measured fluorescence intensity at the initial emission maximum (I_0) tends to decrease through time (I). In this manner, by calculating the ratio between I and I_0 (I/I_0) the unfolding of the protein at different conditions can be analysed and compared.

In this work, the changes in the intrinsic fluorescence of $TrwB_{R388}$ and $TMD_{TraJ}CD_{TrwB}$ were measured through 60 minutes to study the effect of the ionic strength, detergent concentration, and pH. Assays were performed as explained in section 2.6.2. using a *FluoroMax^{R}-3 spectro-fluorimeter*. First of all, emission spectra between 310 and 420 nm were measured in every buffer for each protein. In this manner, it was observed that the initial emission maximum was at 344 nm; therefore, this was the wavelength used to monitor the changes in fluorescence against time.

It was seen that the fluorescence I/I_0 ratio measured with $TrwB_{R388}$ and $TMD_{TraJ}CD_{TrwB}$ decreased in all the tested conditions probably due to a red-shift of the emission. Hence, both proteins show a tendency to denaturalize through time in all the conditions tested (figure 4.4). However, statistically significant differences (Mann-Whitney U Test) were observed in the denaturalization kinetics between buffers with low ionic strengths (0, 75, and 150 mM NaCl) and buffers with a higher ionic strength (300 mM NaCl), except in the absence of detergent. Regarding the effect of detergent concentration in stability, at 300 mM NaCl a significant difference was observed between the results obtained with 0.2 mM DDM and the rest of the

tested detergent concentrations. These results come in agreement with those obtained in the previous sections. Consequently, it was decided to perform all the following assays (unless otherwise specified) at buffers containing **0.6 mM DDM and 300 mM NaCl.**

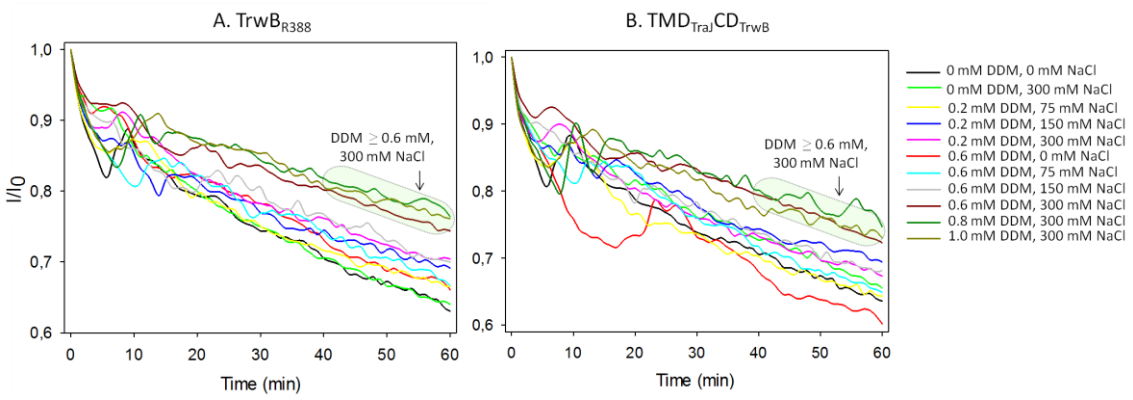

Figure 4.4. Effect of ionic strength and detergent concentration on TrwB$_{R388}$ (A) and TMD$_{TraJ}$CD$_{TrwB}$ (B) stability. Experiments were performed at 1 µM protein in 100 µL buffer and at 25°C. Buffer composition was *50 mM Tris-HCl (pH 7.8), 0.1 mM EDTA and 10% (v/v) glycerol*, containing different DDM and NaCl concentrations (as specified in the figure). Sample excitation was performed at 295 nm and fluorescence emission was collected at 344 nm. Assays were carried out in a *FluoroMax^R-3* using 3 nm slits. Graphs show the fluorescence intensity ratio *vs.* time. I: emission fluorescence intensity at each moment; I_0: initial emission fluorescence intensity. Represented curves are the mean value of at least three independent measurements.

Finally, the effect of pH on the stability of both proteins was studied (figure 4.5). TrwB$_{R388}$ and TMD$_{TraJ}$CD$_{TrwB}$ have theoretical isoelectric points of 9.2 and 9.0, respectively, and therefore are positively charged at all the tested pHs (5.6, 6.2, and 7.8). However, it was observed that both proteins were significantly more unstable at pH 7.8 than at 6.2 and 5.6. These results could be related to the increase of positive charges at acidic pHs. This increase could cause an increase in the repulsive electrostatic force, diminishing the tendency of proteins to aggregate (Guo et al., 2005; Kyne et al., 2017).

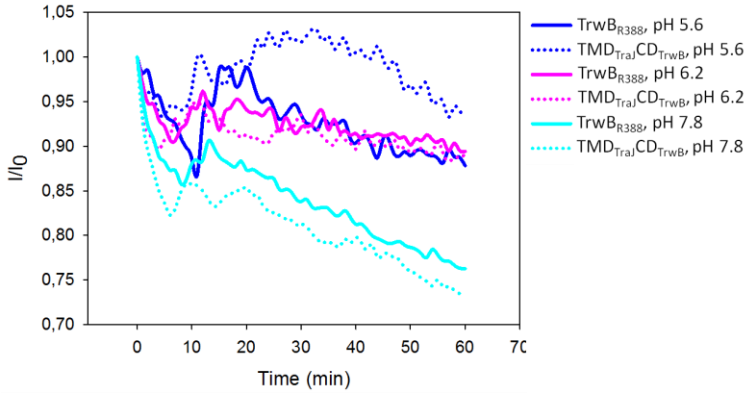

Figure 4.5. Effect of pH on TrwB$_{R388}$ and TMD$_{TraJ}$CD$_{TrwB}$ stability. Experiments were performed at 1 µM protein in 100 µL buffer and at 25°C. The following buffers were used: 50 mM

CH_3COONa (pH 5.6), 50 mM Hepes (pH 6.2) and 50 mM Tris-HCl (pH 7.8). All buffers were supplemented with *0.6 mM DDM, 0.1 mM EDTA, 10% (v/v) glycerol, 6 mM $MgCl_2$ and 300 mM NaCl*. Sample excitation was performed at 295 nm and fluorescence emission was collected at 344 nm. Assays were carried out in a *FluoroMax^R-3* using 3 nm slits. Graphs show the fluorescence intensity ratio *vs.* time. I: emission fluorescence intensity at each moment; I_0: initial emission fluorescence intensity. Represented curves are the mean value of at least three independent measurements.

4.2.1.3. INFLUENCE OF DNA PRESENCE AGAINST PROTEOLYTIC DIGESTION

The binding of ligands is a factor that can alter the conformation of a protein and therefore change the accessibility of proteinases, rendering different digestion patterns. On that account, since it has been described that T4CPs interact with DNA in a sequence-independent manner (section 1.3.4.), the possible effect of DNA molecules on the conformation of T4CPs was studied. To do so, protease K digestion of $TrwB_{R388}$, $TMD_{TraJ}CD_{TrwB}$, and TrwBΔN70 proteins was accomplished in the absence or presence of DNA.

Assays were performed as explained in Vecino et al. (2011) (section 2.6.4.), where this technique was employed to analyse the stability of $TrwB_{R388}$ in detergent solution *vs.* reconstituted into proteoliposomes. Nevertheless, in this study preliminary trials to establish the reaction conditions were performed. First of all, the digestion time (5, 10, and 20 minutes) and temperature (25 and 37°C) were tested. Since the observed differences between the three digestion times were not significant, in the following assays the digestion time was 20 minutes. Regarding temperature, higher digestion levels were achieved at 37°C. However, as the digestion pattern was the same at both temperatures, only results at 25°C are shown. To study the possible effect of DNA-binding, two different DNA molecules were chosen (i) pUC18 dsDNA and (ii) a 45 base pair oligonucleotide (45-mer: 3' TCGCCACGTTTCGCCGTTTGC**GGGGG**TTTCTGCGAGGAACTTTGG 5') which had previously been used in ATP hydrolysis studies with TrwBΔN70 (Tato et al., 2005, 2007). Furthermore, two different buffers were employed: Buffer A (figure 4.6, A), which lacked detergent and NaCl; and Buffer B (figure 4.6, B), which was supplemented with the detergent and NaCl concentrations in which maximum stability had been achieved in the previous experiments (*i.e.*, 0.6 mM DDM and 300 mM NaCl).

The stability of each sample was evaluated according to the hydrolysis degree by comparing visually the intensity of the negative control band against the digested ones. In this regard, the soluble mutant showed the highest stability, followed by the chimera protein and finally the wild type protein (figure 4.6).

Concerning both buffers (figure 4.6, A *vs.* B), in general a **higher hydrolysis rate was observed in the buffer with low ionic strength and no detergent**, both in the absence or presence of DNA. The only exception was TrwBΔN70, which in the absence of DNA showed a higher digestion rate in the buffer with 0.6 mM DDM and 300 mM NaCl. These results come in agreement with the values presented in the previous sections were $TrwB_{R388}$ and $TMD_{TraJ}CD_{TrwB}$ showed more stability in the presence of detergent and high ionic strength.

Regarding the effect of DNA presence against proteolysis, differences were observed in the low strength buffer (figure 4.6, A) but were not significant in the buffer containing 0.6 mM DDM and 300 mM NaCl (figure 4.6, B). Broadly, the presence of DNA molecules during digestion with proteinase K seemed to enhance the hydrolysis in all the tested conditions, especially regarding the soluble mutant TrwBΔN70.

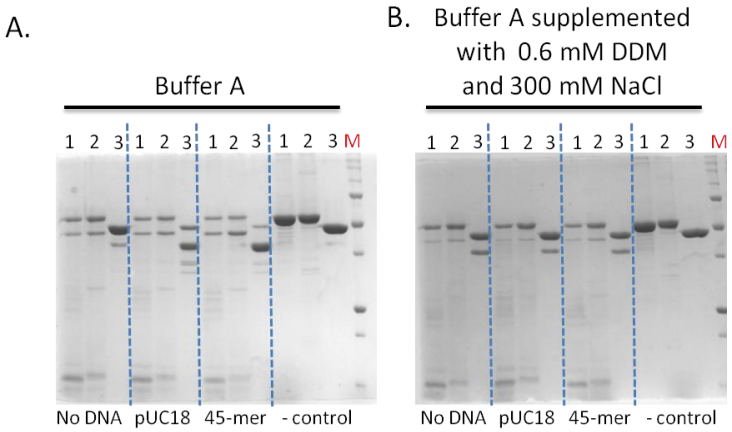

Figure 4.6. Proteinase K digestion of $TrwB_{R388}$, $TMD_{TraJ}CD_{TrwB}$, and TrwBΔN70 at 25°C. Proteinase K digestions at a 1:500 enzyme:protein ratio (w/w) were carried out with 2 µg of the target protein in a final volume of 10 µL, in the absence or presence of 0.5 µg DNA. Reactions were performed in *Buffer A* [*50 mM Tris-HCl (pH 7.8), 0.1 mM EDTA and 10 % (v/v) glycerol*] or *Buffer B* [*50 mM Tris-HCl (pH 7.8), 0.6 mM DDM, 0.1 mM EDTA, 10 % (v/v) glycerol* and *300 mM NaCl*]. After digestion, samples were analysed via SDS-PAGE. Each number is related to a protein sample: 1. $TrwB_{R388}$; 2. $TMD_{TraJ}CD_{TrwB}$; 3. TrwBΔN70. Controls are non-digested proteins. M. *PageRuler™ Plus Prestained Protein Ladder*.

These observations suggest that **the presence of DNA alters the conformational state of the proteins making them more accessible to the protease**. However, this effect seems to be reduced in a solution containing high ionic strength and detergent.

4.2.2. $MobB_{CloDF13}$ RELATED PROTEINS

With the aim of obtaining a more general sight of the properties shared by different T4CPs, stability assays were also performed with $MobB_{CloDF13}$ and its mutant lacking the TMD, MobBΔTMD.

4.2.2.1. THERMAL STABILITY

Thermal stability of $MobB_{CloDF13}$ and MobBΔTMD was studied through IRS. The specific protocol followed for these proteins is explained in section 2.6.1. As depicted in figure 4.7, the denaturation of the native protein starts at 47°C, achieving its T_m at 56°C, while the denaturation of MobBΔTMD starts at 55°C, achieving its T_m at 62°C.

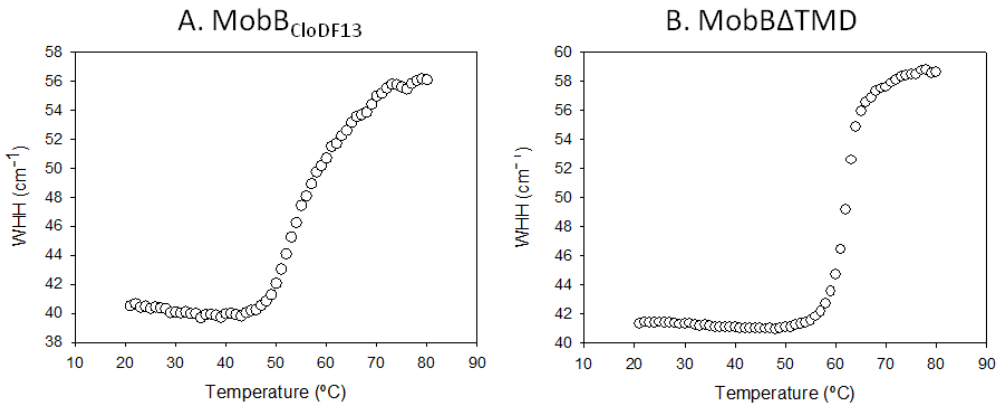

Figure 4.7 Thermal denaturation of MobB$_{CloDF13}$ and MobBΔTMD followed by IRS. The widths at half-height (WHH) of the amide I bands are plotted as a function of temperature (°C). Thermal denaturation is marked by an abrupt increase in band-width. Experiments were performed as explained in section 2.6.1.

Results between TrwB$_{R388}$ and MobB$_{CloDF13}$-related proteins were compared (**Table 4.2**). MobBΔTMD and TrwBΔN70 showed similar denaturation temperatures (T_m 62°C and 63°C, respectively). Regarding full-length proteins, it was observed that MobB$_{CloDF13}$ was more stable than TrwB$_{R388}$ against thermal denaturation (T_m 56°C and 48°C, respectively). However, as both native proteins were characterized in different buffers the obtained results should be taken with care. Therefore, to properly compare TrwB$_{R388}$ and MobB$_{CloDF13}$ further thermal stability assays should be performed in parallel for both proteins.

	MobB$_{CloDF13}$	MobBΔTMD	TrwB$_{R388}$[a]	TrwBΔN70[b]
T_m (°C)	56	62	48	63

Table 4.2. Mid-point denaturation temperatures of the wild type and TMD-less mutants related to CloDF13 and R388 systems. [a]Data from Vecino et al. (2011); [b] Unpublished data from Vecino.

4.2.2.2. INFLUENCE OF THE IONIC STRENGTH, pH AND DETERGENT CONCENTRATION

The purification protocol of MobB$_{CloDF13}$ was designed based on all the stability knowledge gained from the study of TrwB$_{R388}$ and TMD$_{TraJ}$CD$_{TrwB}$. While the later proteins had been previously purified following different protocols and with different buffers, MobB$_{CloDF13}$ was purified from the beginning in a buffer containing 0.6 mM DDM and 300 mM NaCl (section 3.5.2.1.). For this reason, fewer stability studies were done regarding this protein. As for the soluble mutant, its stability was studied in parallel with that of the native MobB$_{CloDF13}$.

First, the homogeneity of the sample and the presence of aggregated species in the purification conditions of each protein were analysed by AUC (figure 4.8). Unlike $TrwB_{R388}$ related proteins, the *c(s)* profiles obtained from the study of **$MobB_{CloDF13}$ and MobBΔTMD** did not show aggregated species. Each protein presented a main peak that was attributed to their monomeric form (see section 4.4.2.). In the case of $MobB_{CloDF13}$ this species covered 84.7% of the profile with an $s_{w,20}$ of 5.8 S. Additionally, a minority species (13.2%) with a smaller sedimentation coefficient was observed ($s_{w,20}$ of 4.7 S), which could be associated to hydrolysed protein. Although the same phenomenon was seen in some other $MobB_{CloDF13}$ AUC assays (see Analytical ultracentrifugation assays), it was not clear what the cause for such hydrolysis was. Regarding MobBΔTMD, the predominant species (97.9% of the profile) had an $s_{w,20}$ of 3.2 S.

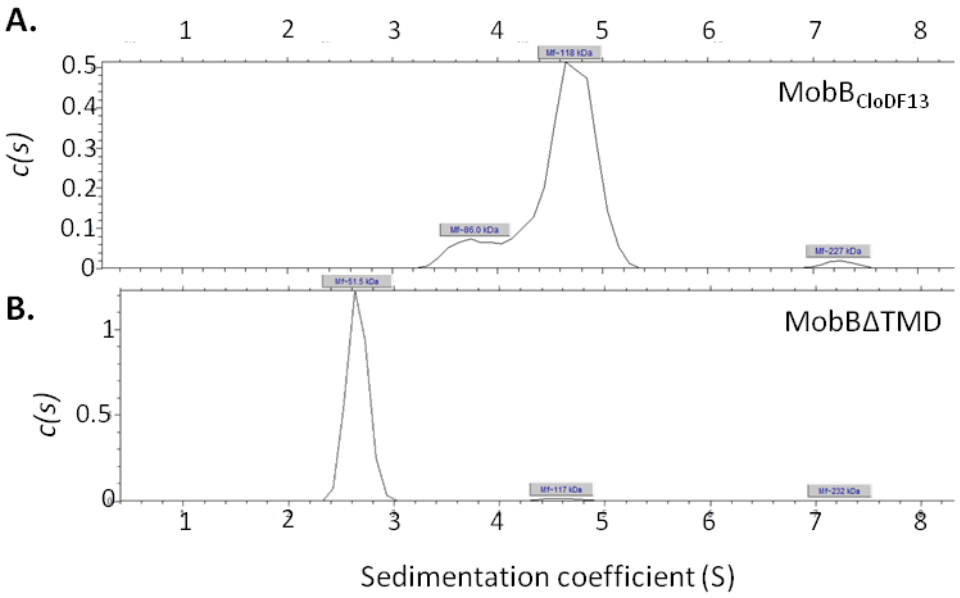

Figure 4.8. Sedimentation coefficient distribution of $MobB_{CloDF13}$ (A) and MobBΔTMD (B). A) 3.38 µM $MobB_{CloDF13}$ were analysed in 50 *mM Tris-HCl (pH 7.8), 0.6 mM DDM, 0.1 mM EDTA, 5% (v/v) glycerol and 300 mM NaCl* buffer. **B)** 8.47 µM MobBΔTMD were analysed in *50 mM Tris-HCl (pH 7.8), 0.1 mM EDTA, 5% (v/v) glycerol and 200 mM NaCl* buffer. Both runs were performed at 129,000 *g* and 20°C in an *XL-A analytical ultracentrifuge* using an *AN50Ti rotor* and 12-mm double-sector centerpieces. Data from each sample was registered every five minutes by measuring absorption at 280 nm. The *c(s)* were calculated as explained in section 2.6.3.

In agreement with the previously presented results, it is well known that high ionic strength is widely applied to stabilize MPs in solution. This phenomenon is known as salting-in, which happens because salt ions ease the accommodation of hydrophobic surfaces in aqueous solutions (Vogel et al., 2001). By contrast, soluble proteins can be stable at lower ionic strengths or even precipitate at higher ones (salting out). The soluble mutant TrwBΔN70 has been usually studied at NaCl concentrations lower than 200 mM (Tato et al., 2005, 2007; Vecino, 2009) and even if MobBΔTMD did not aggregate at that concentration it was decided

to study its solubility at 20, 75 and 150 mM NaCl too. No significant changes were seen in the sedimentation profile at any of the conditions tested (see Analytical ultracentrifugation assays), showing that **MobBΔTMD is soluble in the 20-200 mM NaCl range**.

Table 4.3. Sedimentation coefficients and percentages of the different MobBΔTMD species obtained at different NaCl concentrations. AUC assays were performed with 8.45 µM MobBΔTMD in *50 mM Tris-HCl (pH 7.8), 0.1 mM EDTA, and 5% (v/v) glycerol buffer* supplemented with different NaCl concentrations. AUC runs and data analysis was performed as previously described.

	$s_{w,20}$ and % of each species
20 mM NaCl	3.2 S (94.7%), 5.2 S (5.3%)
75 mM NaCl	3.4 S (97.9%), 5.9 S (2.1%)
150 mM NaCl	3.2 S (97.8%), 5.5 S (2.2%)
200 mM NaCl	3.2 S (97.9%), 5.5 S (2.1%)

INTRINSIC TRYPTOPHAN FLUORESCENCE

As performed with $TrwB_{R388}$ related proteins the kinetic stability of $MobB_{CloDF13}$ and MobBΔTMD was studied by monitoring the changes in the intrinsic Trp fluorescence. An emission spectrum analysis between 310 and 420 nm was performed, seeing that the emission maximum of these proteins was at 340 nm; therefore, this was the chosen wavelength at which stability assays were performed. Specifically, two different buffers [*50 mM Tris-HCl (pH 7.8)* and *50 mM CH_3COONa (pH 5.6)*, both supplemented with *0.1 mM EDTA and 10% (w/v) glycerol*] were tested with different DDM and NaCl concentrations (figure 4.9).

Even if $MobB_{CloDF13}$ was not fully stable in any of the tested conditions, its kinetic stability was higher at an acidic pH (pH 5.6), as observed with $TrwB_{R388}$ and $TMD_{traJ}CD_{TrwB}$. At this pH, only an 18% protein loss was obtained at the highest DDM and NaCl concentrations tested (0.8 mM DDM and 300 mM NaCl). As expected, in the absence of detergent in Tris-HCl buffer the denaturation tendency increased significantly.

Regarding the stability of MobBΔTMD, controversial results had been previously described for the TMD-less mutant TrwBΔN70. On the one hand, DDM showed a protective effect against denaturation (Hormaeche et al., 2004), but on the other hand, it seemed to decrease its stability and ATPase activity (Vecino, 2009). In this study it has been seen that the kinetic stability of MobBΔTMD diminished more than 20% in buffers lacking detergent, with no significant protein denaturation at 0.6 or 0.8 mM DDM. Additionally, no significant differences were seen between both tested pHs.

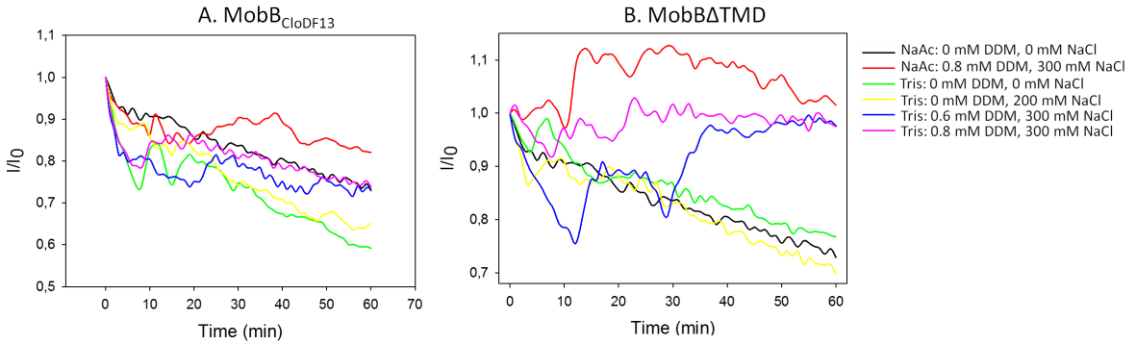

Figure 4.9. The effect of ionic strength, detergent concentration and pH on MobB$_{CloDF13}$ (A) and MobBΔTMD (B) stability. Experiments were performed at 1 µM protein in 100 µL buffer and at 25°C. *50 mM Tris-HCl (pH 7.8)* and *50 mM CH_3COONa (pH 5.6)* buffers were employed, both supplemented with *0.1 mM EDTA and 10% (w/v) glycerol*, in addition to the correspondent DDM and NaCl concentrations. Sample excitation was performed at 295 nm and fluorescence emission was collected at 340 nm. Assays were carried out in a *FluoroMax^R-3* using 3 nm slits. Graphs show the fluorescence intensity ratio *vs.* time. I: emission fluorescence intensity at each moment; I_0: initial emission fluorescence intensity. Represented curves are the mean value of at least three independent measurements.

Taking all into account, **the best stability results for all the tested proteins of R388 and CloDF13 systems were obtained at pHs below 7.8 and high detergent and salt concentrations**. It must be underlined that in the *MP purification buffer* (pH 7.8, 0.6 mM DDM and 300 mM NaCl) TrwB$_{R388}$, TMD$_{TraJ}$CD$_{TrwB}$, and MobB$_{CloDF13}$ showed similar stability results (table 4.3).

Table 4.3. Protein denaturation percentages at different pHs and buffers supplemented with 0.6 mM DDM and 300 mM NaCl. Protein denaturation percentage is represented as the fluorescence emission intensity decrease after 60 minutes of incubation in each buffer. Data taken from figures 4.4, 4.5, and 4.9. pH 5.6: *50 mM CH_3COONa*; pH 6.2: 50 mM Hepes; pH 7.8: *50 mM Tris-HCl*. All buffers were supplemented with *0.6 mM DDM, 0.1 mM EDTA, 10% (w/v) glycerol and 300 mM NaCl*. n.d.: not determined. *0.8 mM DDM.

	pH 5.6	pH 6.2	pH 7.8
TrwB$_{R388}$	13	11	24
TMD$_{TraJ}$CD$_{TrwB}$	7	11	28
MobB$_{CloDF13}$	18*	n.d.	27
MobBΔTMD	0*	n.d.	3

4.2.2.3. INFLUENCE OF DNA PRESENCE AGAINST PROTEOLYTIC DIGESTIONS

Finally, the effect of DNA-binding against proteolytic digestion with proteinase K was examined. In this case, reactions performed at 37°C showed more defined digestion profiles than at 25°C and therefore both sets of experiments are shown (figure 4.10). Since in the assays performed with $TrwB_{R388}$ related proteins no significant differences were seen between pUC18 and 45-mer DNA molecules section 4.2.1.3.), in this case only pUC18 was used. As observed with $TrwB_{R388}$ related proteins, the TMD-less mutant, MobBΔTMD, was more stable against digestion than the native protein. Additionally, higher hydrolysis rates were observed in the buffer lacking detergent as well, which comes in agreement with the stabilizing effect of DDM described in the previous section. Lastly, the presence of DNA did not seem to have any effect against proteolytic digestion, except for $MobB_{CloDF13}$ in the buffer without detergent, in which digestion was increased. These results resemble to those observed with $TrwB_{R388}$ related proteins.

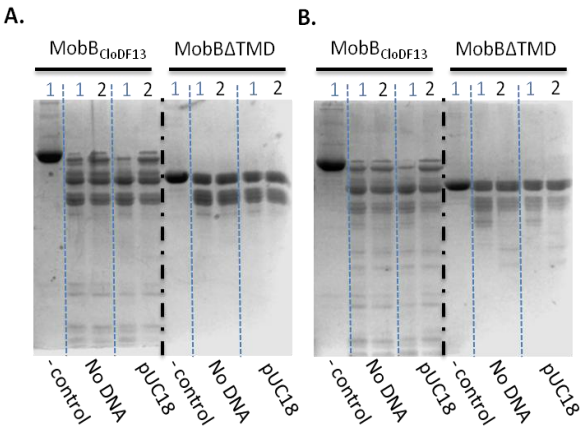

Figure 4.10. Proteinase K digestión of $MobB_{CloDF13}$ and MobBΔTMD at 25°C (A) and 37°C (B). Proteinase K digestions at a 1:500 enzyme:protein ratio (w/w) were carried out with 2 µg of the target protein in a final volume of 10 µL, in the absence or presence of 0.5 µg DNA. Reactions were performed in *Buffer A* [*50 mM Tris-HCl (pH 7.8), 0.1 mM EDTA and 10 % (v/v) glycerol*] or *Buffer B* [*50 mM Tris-HCl (pH 7.8), 0.6 mM DDM, 0.1 mM EDTA, 10 % (v/v) glycerol* and *300 mM NaCl*]. After digestion, samples were analysed via SDS-PAGE. M. *PageRuler™ Plus Prestained Protein Ladder*.

Taking into account all the results obtained with both $TrwB_{R388}$ related and $MobB_{CloDF13}$ related proteins, **it seems that in buffers lacking detergent and with a low ionic strength DNA-binding makes the proteins more susceptible to hydrolysis by proteinase K, probably due to a conformational change**. To better understand this effect, it should be further studied, for example by characterizing the interaction between these T4CPs and the tested DNA molecules.

4.3. DNA-BINDING

During the conjugative process T4CPs take part in a dynamic set of interactions with both the substrate and the T4SS, as explained in chapter one. Many previous studies have described the interaction between T4CPs and DNA molecules (Cascales and Christie, 2004b; Chen et al., 2008; Moncalián et al., 1999). Through *in vivo* assays, it has been described that these interactions are highly regulated inside the mating process, while *in vitro* assays have shown that the binding is unspecific to the DNA sequence but specific to G4-DNA structures (Matilla et al., 2010).

In general, DNA-protein interactions can be characterized using a variety of techniques, both *in vitro* and *in vivo* (Dey et al., 2012). In particular, the study of T4CP-DNA interactions has been mostly based on techniques that monitor the appearance of complexes with a higher MW such as EMSA (Larrea et al., 2017; Moncalián et al., 1999; Schroder and Lanka, 2003), SEC, and AUC (Matilla et al., 2010).

4.3.1. ELECTROPHORETIC MOBILITY SHIFT ASSAY

When a protein interacts with a DNA molecule they form a complex of high MW. The principle of EMSA is that when analysing the DNA-protein mixture through electrophoresis this complex presents a shift in mobility in comparison to the free molecules. In this thesis, agarose gel based EMSAs were performed (Seo et al., 2019).

Interactions between different T4CPs (*i.e.,* $TrwB_{R388,}$ $TMD_{TraJ}CD_{TrwB}$, TrwBΔN70, $MobB_{CloDF13}$, and MobBΔTMD) and different DNA molecules (*i.e.,* ssM13 plasmid, dspUC18 plasmid both in linear and circular/supercoiled state, and the mer-45 oligo) were characterized at different protein:DNA ratios. Assays were performed as explained in section 2.6.5. (Larrea et al., 2017). Additionally, with the aim of further studying the results obtained in the proteinase K digestion assays, *Bufer A* and *Buffer B* were used to perform the EMSAs. By doing so the effect of the ionic strength and detergent in DNA-binding could be unravelled. Since no significant differences between the different DNA molecules were observed only the results obtained with the circular form are shown (figure 4.11, A), except in the case of $TMD_{TraJ}CD_{TrwB}$ for which the four tested DNA molecules are shown (**Figure 4.11**B).

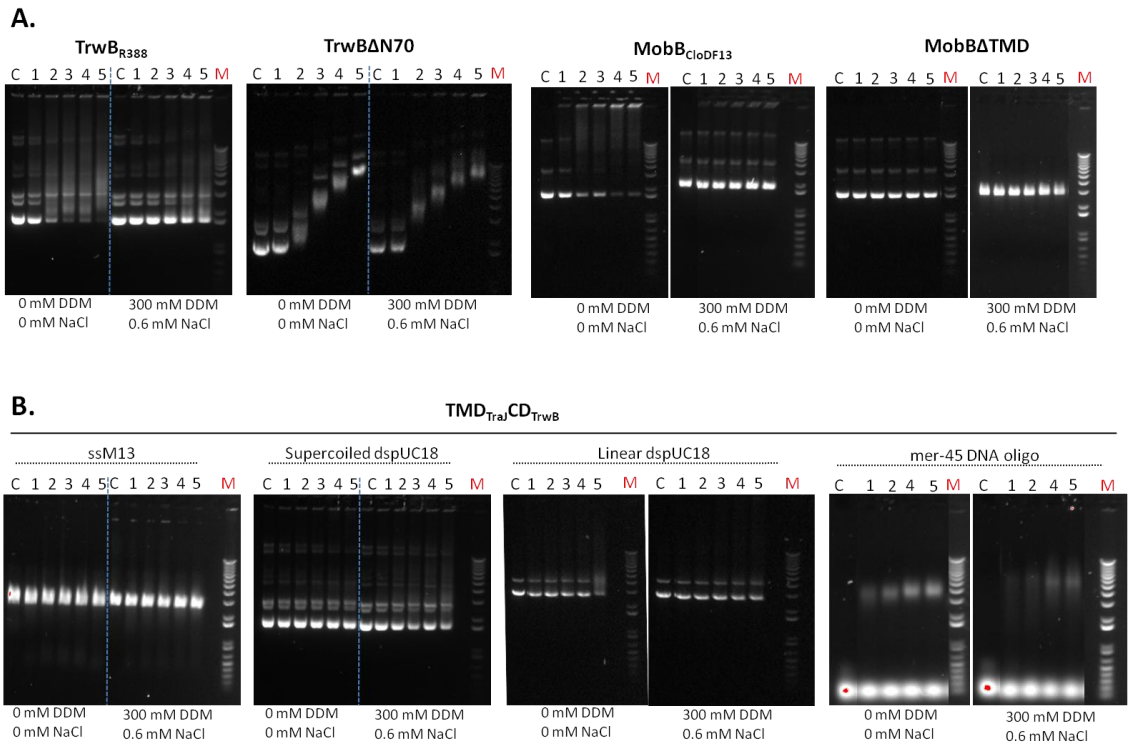

Figure 4.11. Interaction between different T4CP variants and DNA. A) Binding of TrwB$_{R388}$, TrwBΔN70, MobB$_{CloDF13}$, and MobBΔTMD to circular/supercoiled dspUC18 plasmid. **B)** Binding of TMD$_{TraJ}$CD$_{TrwB}$ to different DNA molecules. Binding assays were performed by mixing 0.5 µg DNA and increasing protein concentrations and incubating them for 10 minutes in a final volume of 10 µL and 25°C. Employed buffers were *Buffer A* [*50 mM Tris-HCl (pH 7.8), 0.1 mM EDTA and 10 % (v/v) glycerol*] or *Buffer B* [*50 mM Tris-HCl (pH 7.8), 0.6 mM DDM, 0.1 mM EDTA, 10 % (v/v) glycerol and 300 mM NaCl*]. Reactions were stopped by addition of *DNA loading buffer* and *SYBR™ Safe* was added for the visualization of DNA molecules. Samples were analysed by 0.7% (w/v) agarose gel electrophoresis. The numbers above the lanes represent the protein micrograms present in each reaction. C: negative control, 0.5 µg DNA; M: *1 kb Plus DNA Ladder*.

Protein-DNA-binding was observed as a shift in the electrophoretic mobility of the DNA molecule in all the tested proteins, although it was almost imperceptible in the soluble mutant MobBΔTMD. Even if only qualitative results were obtained from these assays, it is noteworthy that the **binding was higher at low ionic strength and in the absence of detergent** in all the tested samples, except for the binding between the chimera protein and the supercoiled dspUC18 plasmid. However, as this lack of interaction was not seen in the other tested DNA molecules (figure 4.11, B), it was assumed that a technical error in the electrophoresis assay of interaction between TMD$_{TraJ}$CD$_{TrwB}$ and dspUC18 plasmid could have occurred. The fact that DNA-binding is higher in the absence of NaCl and detergents could explain why the effect of DNA presence in the proteinase K hydrolysis assays was only seen in those buffer conditions; suggesting that in *buffer A* DNA would be able to bind and change the conformation of the T4CP making it more accessible to the protease K. On the contrary, in *buffer* B, the presence of detergent and high ionic strength would impede DNA-binding, no conformational change would happen and therefore the lysis rate would be smaller. As previously said, T4CP-DNA

interactions are sequence unspecific. In general, unspecific protein:DNA interactions are based on ionic interactions between positively charged residues of the protein and the DNA backbone and therefore are extremely sensitive to changes in ionic strength (Smeekens and Romano, 1986). In relation to this, it has been reported that lysine residues are involved in substrate translocation of $TrwB_{R388}$ (Larrea et al., 2017). Taking into account the results presented in this section, it could be that at 300 mM NaCl interactions between these lysine residues and DNA molecules are hindered. Additionally, the presence of a non-ionic detergent in addition to the high ionic strength could enhance the binding-impediment (Thermo Scientific Pierce, 2010). The appearance of smeared bands in the gels could be due to different factors such as excessive gel heating or excessive conductivity. However, since it is only observed in the samples were binding happens it is probably due to DNA becoming gradually unbound during the electrophoretic movement (Sidorova et al., 2010).

In these assays, **TrwBΔN70 showed the highest binding propensity.** As seen in Larrea et al. (2017) with pUC8 DNA, **interactions happened at multiple protein:DNA ratios** depending on protein concentration, as it can be inferred from the different sized molecular complexes seen in our results (figure 4.11, A). On the contrary, the soluble mutant **MobBΔTMD did not show any significant DNA-binding** in the tested conditions, which also comes in agreement with the results observed in the proteolytic digestion assay, where no DNA effect was seen in the lysis patterns (section 4.2.2.3.). This is an intriguing result taking into account that the native protein $MobB_{CloDF13}$ did show DNA-binding capacity. The observed differences between the native $MobB_{CloDF13}$ and the TMD-less mutant MobBΔTMD suggest that the presence of the TMD in mobilizable plasmid related T4CPs is necessary for the protein to perform its DNA-binding activity *in vitro*, opposite to what has been described for the conjugative plasmid related $TrwB_{R388}$ and its mutant TrwBΔN70.

Regarding MPs, an additional assay testing higher protein concentrations in the absence of DDM and NaCl was tested (figure 4.12). It was observed that $MobB_{CloDF13}$ and $TrwB_{R388}$ presented similar binding properties, having the total amount of DNA bound with 10 µg protein. Regarding $TMD_{TraJ}CD_{TrwB}$, it presented lower binding rates than the native T4CPs. As the binding happens in the CD, the difference observed between $TrwB_{R388}$ and $TMD_{TraJ}CD_{TrwB}$, which share the same CD, suggests an **effect of the heterologous TMD in the overall structure and mechanism of the chimera protein**. This difference in the DNA-binding affinities might be one of the possible explanations of the differences observed in the *in vivo* mating assays, where $TMD_{TraJ}CD_{TrwB}$ performed conjugation in a smaller frequency than $TrwB_{R388}$ (see section 3.3.). In that section, it was hypothesised that the chimera protein could present conformational changes in the CD that impeded its optimal functioning, which could also be the cause of the lower DNA-binding affinities described in this section.

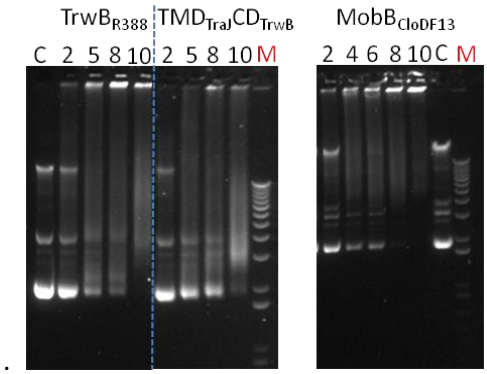

Figure 4.12. Interaction between TrwB$_{R388}$, TMD$_{TraJ}$CD$_{TrwB}$ and MobB$_{CloDF13}$ and circular pUC18 plasmid. Binding assays were performed as explained in figure 4.11 in *buffer A* [*50 mM Tris-HCl (pH 7.8), 0.1 mM EDTA and 10 % (v/v) glycerol*]. The numbers above the lanes represent the protein micrograms present in each reaction. C: negative control, 0.5 µg pUC18; M: *1 kb Plus DNA Ladder*.

Nevertheless, since the results obtained through this method are hardly quantifiable, further experiments should be carried out to obtain T4CP:DNA-binding parameters with different DNA molecules. There are several techniques available to perform such studies, amongst them up to date single-molecule techniques such as nanopore technology, which offers excellent capabilities to unravel the mechanism and kinetics of protein:DNA interactions (Celaya et al., 2017). In this account, preliminary studies through AUC have been made to study the interaction between pUC18 and TMD$_{traJ}$CD$_{TrwB}$. In the EMSA assay at a 20 protein:DNA (w/w) ratio it was seen that most of the DNA was bound in high MW complexes (figure 4.12, TMD$_{traJ}$CD$_{TrwB}$, lane 10). A similar ratio (19.5) was analysed through AUC showing the appearance of two complexes of theoretical molecular weights of 581 and 835 kDa, as estimated by *SEDNTERP* software (figure S4.2). This data suggests that **upon DNA-binding oligomerization of the protein could happen**. These results come in agreement with the ones published about the oligomerization of TrwBΔN70 upon interaction with DNA molecules (Matilla et al., 2010).

4.4. OLIGOMERIZATION

The role of oligomerization of T4CPs and its functional implications in bacterial conjugation have long been debated (section 1.3.2.3.). In this thesis, to deepen the knowledge around this matter, different methods have been applied such as SEC, BN-PAGE and AUC. The first two techniques are based on the use of a matrix to separate the different populations, while AUC is based on the use of a centrifugal field. It must be said that both approaches have advantages and disadvantages, which is the reason to combine them. Focusing on the disadvantages of each method, when using a matrix for characterization, bound detergent and lipids affect the migratory behaviour of MPs, usually leading to overestimation of the MW and compromising the reliability of the technique (Hill et al., 2014; Slotboom et al., 2008). Conversely, AUC methodology is not reliable when analysing multi-component mixtures, even if this methodology provides quite accurate MW determination for monodisperse samples

(Chaton and Herr, 2015). Therefore, the obtained results with each approach must be taken with care and conclusions must be drawn considering all the mentioned aspects.

4.4.1. $TrwB_{R388}$ RELATED PROTEINS

Published studies from our group have widely analysed the oligomeric state of $TrwB_{R388}$. These works have underlined the importance of the purification protocol and the concentration method in the oligomeric nature of the obtained sample. On the one hand, the procedure described by Hormaeche et al. (2004) rendered monomers and hexamers separately by using a combination of different chromatography columns. On the other hand, the protocol employed by Vecino et al. (2010) offered a higher protein yield but as a polydisperse sample composed of a mixture of different oligomeric species. In this thesis, $TMD_{TraJ}CD_{TrwB}$ chimera protein has been isolated using both approaches and the heterogeneity of those samples has been studied.

4.4.1.1. PROTOCOL FOR THE OBTAINMENT OF MONOMERS AND HEXAMERS

To separately obtain monomers and hexamers, $TMD_{TraJ}CD_{TrwB}$ was purified as described in Hormaeche et al. (2004). Through that protocol, Hormaeche and co-workers obtained separated $TrwB_{R388}$ monomers and hexamers by separated elution with 500 mM and 1 M NaCl containing buffers in the cationic exchange chromatography. Additionally, they described that the protein concentration process had an effect in the oligomeric state of $TrwB_{R388}$.

After purification through this approach (the exact protocol to obtain each sample is shown in section S4.4.1.2.), five different $TMD_{TraJ}CD_{TrwB}$ (theoretical MW: 58.28 kDa) samples were obtained: FI.0, FI.1, FII.0, FII.1, and FII.2 (figure 4.13). The main two samples FI and FII, which rendered the subsequent ones, were obtained after the elution of the *Phosphocellulose P-11* column with buffers containing 500 mM or 1 M NaCl, respectively.

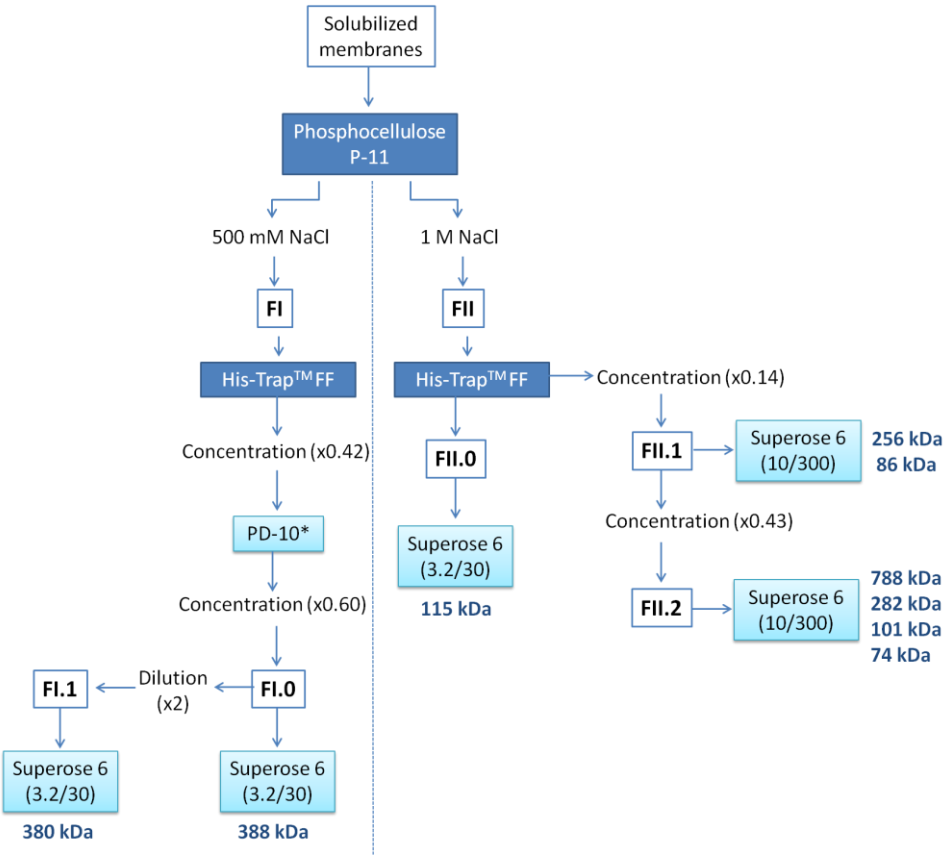

Figure 4.13. Schematic representation of $TMD_{TraJ}CD_{TrwB}$ purification protocol. White boxes represent obtained samples. Dark blue boxes represent non-size-exclusion chromatographies and light blue boxes represent size-exclusion chromatographies. The MWs of the different species observed in each SEC are shown next to the corresponding light blue box. Dilution and concentration factors are shown between parentheses. **PD-10* was used as a buffer exchange chromatography and therefore did not give information about the oligomeric state of the sample.

SIZE-EXCLUSION CHROMATOGRAPHIES

Analyses of the oligomeric composition were performed via SEC using *Superose 6 PC 3.2/30* or *Superose 6 GL 10/300* columns, depending on the sample characteristics. This type of matrix offers a resolution capacity between 5 and 5,000 kDa for globular proteins. Even if SEC is not the most suitable approach to establish the MW of a MP purified in detergent, it can give an insight into its polydispersity and oligomeric state. Prior to characterizing $TMD_{TraJ}CD_{TrwB}$ samples, both columns were calibrated using a protein standard mix as explained in section 2.5.2.3. Since in these chromatographies molecules are separated according to their size, the obtained V_es from the standard protein elutions were used to obtain the formula that correlates the V_es obtained in each sample with their MWs.

First of all FI.0, FI.1 and FII.0 samples were analysed using the analytical *Superose 6 PC 3.2/30* column. To do so 30 µL of each sample: FI.0 (12 µM protein), FI.1 (6 µM protein) and FII.0 (14 µM protein) were injected and the chromatography was performed with *TrwB oligomers 7 buffer* at 40 µL/min and room temperature (figure 4.14). In this column the void-

volume, established by the V_e of Blue-dextran 2000, was 1.0 mL; therefore peaks with a lower V_e were considered aggregates. Likewise, V_e values higher than 2.0 mL (related to a MW of 22.85 kDa) were considered hydrolysed products.

The chromatogram of the **FI.0** sample (figure 4.14, A) showed two fused-peaks related to the void volume of the column and three peaks assigned to small-sized molecules. The main peak of the chromatogram corresponded to 1.623 mL V_e (**380 kDa**, according to the calibration pattern). **FI.1** sample (figure 4.14, B) presented a similar elution profile, although with only one peak at the void-volume and two peaks associated with small-sized molecules. In this case, the main peak was related to 1.620 mL V_e (**388 kDa** according to the calibration pattern), probably being the same species as the one observed in FI.0 sample. However, since in both cases the main peaks did not present a symmetric form, they could contain different populations.

The chromatogram obtained from **FII.0** sample (fraction 5 of the affinity chromatography performed with FII sample, figures S4.4 and figure 4.14) showed a smaller peak related to the void-volume, while the main peak appeared at a V_e of 1.783 mL (**115.3 kDa**). Taking into account that the $TrwB_{R388}$-DDM PDC has a MW of 112.98 kDa (see section S3.5.1.2.), this fraction of 115.3 kDa most probably corresponds to the monomeric form of the chimera. However, the width of the peak suggests that it might have more species. This result is intriguing since according to the literature (Hormaeche et al., 2004) FII sample should be related to hexamer elution. Different hypotheses can be drawn to explain this discordance: (i) that the higher abundance of monomers in FII.0 caused an elution peak on the SEC that masked the rest of the populations present in the sample or (ii) that monomers eluted from this column at different imidazole concentrations than higher-order oligomers.

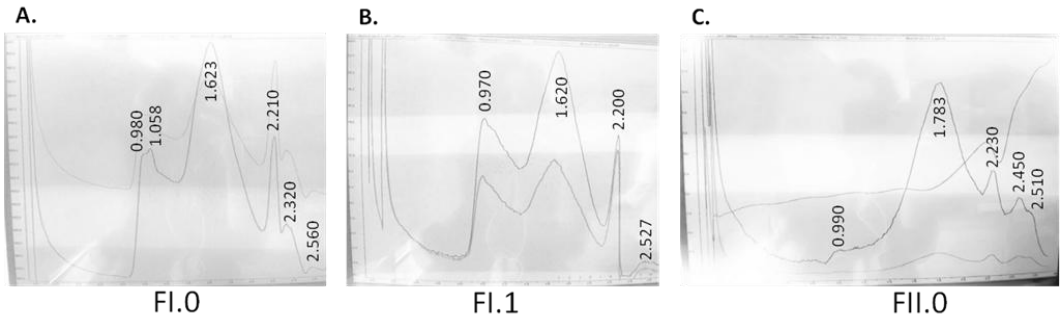

Figure 4.14. Chromatograms of FI.0, FI.1 and FII.0 samples obtained from the *Superose 6 (3.2/30)* column. Sample preparation and chromatography were performed as described in section 2.5.2.3. Protein elution was followed by measuring absorption at 280 nm. Numbers next to each peak represent the V_e (mL).

Next FII.1 and FII.2 samples were run through a *Superose 6 (10/300)* column to analyse the effect of the concentration on the distribution of oligomeric species (figure 4.15). The column had been previously equilibrated with two volumes of *TrwB oligomers 7 buffer*, which was also used during the chromatography. The run was performed at 0.5 mL/min and 0.5 mL fractions were collected.

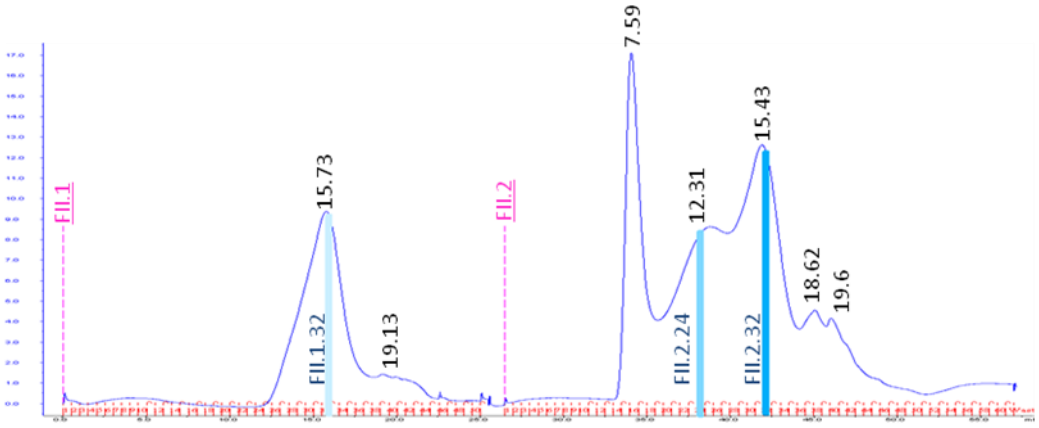

Figure 4.15. Chromatogram of the elution of FII.1 and FII.2 samples from the *Superose 6 (10/300)* column. Sample preparation and chromatography runs were performed as described in section 2.5.2.3. Protein elution was followed by measuring absorption at 280 nm. Pink dashed lines indicate the injection point of each sample. Numbers on top of each peak represent the V_e (mL). Vertical blue lines indicate the fractions that were further analysed via BN-PAGE (Blue-native page).

In the *Superose 6 (10/300) chromatography* **FII.1** sample showed two peaks with V_es of 15.73 and 19.13 mL (**256.3** and **86.17 kDa,** respectively), which differed from the main one observed in FII.0 sample (**115.3 kDa**). The concentration of FII.1 sample caused a different elution profile in FII.2 sample. FII.2 related SEC chromatogram showed five different elution peaks: the first one, at the void-volume of the column, was possibly associated with aggregated protein; the second one with a V_e of 12.31 mL (**766.4 kDa**), was most likely high-order oligomers; the third peak with a V_e of 15.43 mL (**282.2 kDa)** could be related to the first peak observed in FII.1 sample; the forth peak with a V_e of 18.62 mL (**101.5 kDa**) and the last one with a V_e of 19.6 mL (**73.9 kDa**). Taking into account that FII.1 and FII.2 sample only differed in the concentration step, a third hypothesis for the single presence of monomers in sample FII.0 could be drawn: it could be that no monomer-hexamer separation had been performed in the P-11 *column* and that the whole FII.0 sample was composed of monomers, which oligomerized during the concentration step. Additionally, this theory could explain why a species bigger than the monomer was observed in FI.0 and FI.1 samples, which in the purification of $TrwB_{R388}$ were related to monomers (Hormaeche et al., 2004).

A summary of the observed populations for each case is presented in table 4.4. It must be noted that due to the width of the observed elution peaks, different oligomeric species might be present in each peak. Considering the similarities between $TMD_{TraJ}CD_{TrwB}$ and $TrwB_{R388,}$ the smallest species (73.9 and 86.2 kDa) might have been a hydrolysed form of the chimera while the second ones (101.5 and 115.3 kDa) might be related to the monomeric form in complex with DDM. Regarding the other species, this technique does not allow establishing to which oligomeric form they were related since different oligomers might require different protein:detergent relations in the formation of the PDC.

Table 4.4. Summary of the species observed in the SECs of $TMD_{TraJ}CD_{TrwB}$ samples. Samples from different steps of the purification process were analysed by *Superose 6 (3.2/30)* or *Superose 6 (10/300)* columns. The MW of each population, related to the V_e of each peak, was calculated using calibration curves as explained in section 2.5.2.3. Peaks related to the void-volume of the column are attributed to protein aggregates. Dilution and concentration factors are shown between parentheses.

	Concentration steps (volume changes)	Identified species (kDa)
FI.0	2 steps (x0.42, x0.6)	Aggregated, 388
FI.1	1:1 dilution of FI.0 (x0.42, x0.6, x2)	Aggregated, 380
FII.0	0 steps	115.3
FII.1	1 step (x0.14)	256.3, 86.2
FII.2	2 steps (x0.14, x0.43)	Aggregated, 766.4, 282.2, 101.5, 73.9

BLUE-NATIVE PAGE

To deepen the oligomerization studies, fractions obtained in the FI and FII chromatography were analysed via Blue-Native PAGE. Assays were performed as explained in section 2.4.2. Specifically, 20 µg of each sample were loaded and the electrophoresis was performed at 4°C for 120 min, half the time at 150 V and then at 250 V. Although the samples did slightly aggregate during the run, some bands could be distinguished (figure 4.16).

A total of six bands could be perceived in sample **FI.0**, reinforcing the idea that through this protocol monomers and hexamers of the chimera protein were not isolated by elution with different NaCl concentrations (500 mM and 1M) and that the peaks obtained by SECs contained **a mixture of different oligomeric species**. Even if due to the quality of the gel these results must be taken with care, it seems that the smallest band, with a MW between 67 and 140 kDa, could be related to the monomeric species. Next, there were two bands in between 140 and 232 kDa, another one between 323 and 440 kDa, the fifth band below 669 kDa, and the last one above 669 kDa. The later was slightly present in all the samples and it could be related to a high-order oligomer or an aggregated state of the protein. Regarding FII related samples, although smearing of the samples happened, **FII.1.32** and **FII.2.32** showed similar profiles with a strong band around 100 kDa, possibly related to the **monomer**ic form, and some faint bands. As the estimated MWs for these fractions through the SEC calibration were 256 and 282 kDa, respectively, it seems that they were overestimated and are truly related to the monomer. This result suggests that the species observed in FII.2 chromatogram related to higher V_es might have been hydrolysed products. Although **FII.2.24** sample did not show a clear band pattern, a slight band could be observed between 140 and 232 kDa, equivalent to the third band observed in FI.0. Although the MW of this population was estimated at 766 kDa in the SEC, it was probably much lower, being related to **dimer or trimers**.

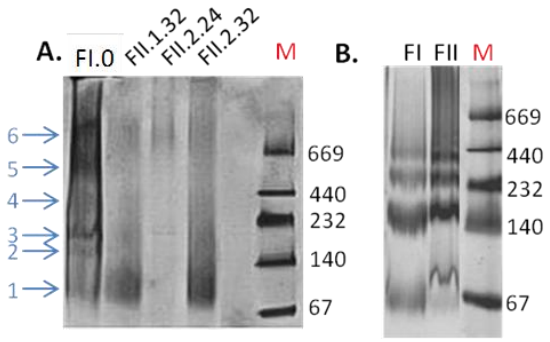

Figure 4.16. Blue-Native PAGE of different samples obtained from the monomer/hexamer purification process of $TMD_{TraJ}CD_{TrwB}$ (A) and TrwBΔN50 (B). BN-PAGE gel was performed as explained in section 2.4.2. **A)** Analysis of the FI.0, FII.1.32, FII.2.24 and FII.2.32 samples. The later three are related to the fractions obtained in the *Superose 6 (10/300)* chromatography of FII.1 and FII.2 (figure 4.15, vertical blue lines). M: *HMW Native Marker*. Arrows point at the bands that appear in the different lanes. **B)** BN-PAGE of TrwBΔN50 samples purified following the same protocol with slight modifications. The gel shows the analysis of the obtained FI and FII samples. B image taken from Vecino (2009).

In summary, it can be said that FII.0, FII.1 and FII.2 samples contained a mixture of species. Therefore, it seems that regarding $TMD_{TraJ}CD_{TrwB}$ **the two-step elution process from the cation-exchange chromatography did not render in the isolation of monomers and hexamers**. This behaviour was already seen with the mutant lacking the first transmembrane helix, TrwBΔN50 (figure 4.16), and is opposite to what was described for $TrwB_{R388}$ (Vecino, 2009). It must be underlined that protein concentration seems to affect the formation of oligomeric species in the sample, in agreement with previous results obtained for the native protein. Specifically, it was described that the equilibrium between the different species of $TrwB_{R388}$ is displaced towards the hexamer when increasing the concentration (Vecino, 2009). This can be observed when comparing the results obtained with FII.1 and FII.2 samples, which only differed in the concentration steps but showed very different oligomeric patterns. However, hypothesising that no oligomer separation had been made during the elution from the P-11 column and taking into account that FI.0 was studied at a lower concentration than FII.0 sample (12 µM *vs.* 14 µM), observed oligomerization could be related to the concentration process *per se* and not to the protein concentration on the sample. In this case, the influence of the concentration steps in the protein could create oligomeric species that might not come in hand with their biological significance. On that account, it must be underlined that dilution does not seem to affect the oligomeric state since the diluted FI.I sample (6 µM) showed the same species as FI.0 sample (12 µM).

4.4.1.2. COMMON PURIFICATION PROTOCOL

$TrwB_{R388}$ (theoretical MW: 57.33 kDa) and $TMD_{TraJ}CD_{TrwB}$ (theoretical MW: 58.28 kDa) samples isolated through the common purification protocol (section 3.5.1.) were analysed in parallel to compare their oligomeric behaviour. In addition to the SEC and BN-PAGE studies, in this case, samples were also analysed through AUC.

In the SEC results, both proteins showed a different distribution, even if they had two species with similar V_es (figure 4.17). Shown V_es are the mean value of three independent experiments and the MWs were calculated using a calibration curve as explained in gel-iragazpeneko kromatografiak. In both cases, the first peaks (V_es of 0.977 and 0.974 mL for $TrwB_{R388}$ and $TMD_{TraJ}CD_{TrwB}$, respectively) were associated with the void-volume of the column and were probably related to aggregates. The second peaks (V_es 1.269 and 1.269 mL for $TrwB_{R388}$ and $TMD_{TraJ}CD_{TrwB}$, respectively) were still related to MWs higher than 1,000 kDa and therefore were most likely artefacts created during the purification process. The third peak presented in $TrwB_{R388}$ chromatogram fits with a MW of **251.2 kDa**, while the one in $TMD_{TraJ}CD_{TrwB}$ did with **367.8 kDa**. However, the width of these peaks suggested that they might contain other species. For this reason, and taking into account the previous MW overestimations performed through SEC calibration, a BN-PAGE analysis was performed. The obtained results reinforced the idea that both samples presented a mixture of oligomeric species. Probably this effect is due to the influence of the detergent in the chromatography and that each oligomer has a different protein:detergent ratio that causes similar V_es for different populations. The main difference seen in the BN-PAGE between both proteins is the abundance of each population. In the case of $TrwB_{R388}$ it seems that the main species is the monomer (figure 4.17, C, fifth arrow), while for the chimera protein it is a band with a MW above 242 kDa (figure 4.17, D, second arrow), in agreement with the main species observed in the SEC chromatogram (figure 4.17).

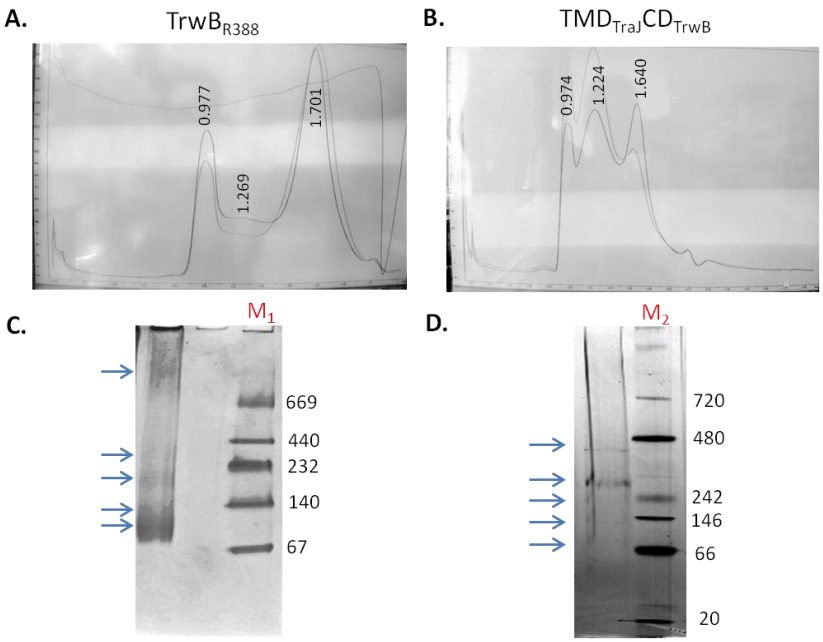

Figure 4.17. SEC and Blue-Native PAGE of $TrwB_{R388}$ (A, C) and $TMD_{TraJ}CD_{TrwB}$ (B, D) samples obtained through the common purification protocol. SEC runs were performed in a *Superose 6 (3.2/30)* column as described in section 2.5.2.3. Protein elution was followed by measuring absorption at 280 nm. Numbers next to each peak represent the V_e (mL). BN-PAGE assays were performed as described in section 2.4.2. M_1: *HMW Native Marker*; M_2: *NativeMark™ Unstained Protein Standard.*

Due to the ambiguity of these results, AUC analyses were performed to investigate the effect of protein and detergent concentrations on the oligomeric state. AUC runs were performed with four different protein concentrations (5.23, 6.97, 10.46, and 20.92 µM of $TrwB_{R388}$ and 5.15, 5.58, 10.3, and 20.6 µM of $TMD_{TraJ}CD_{TrwB}$) at two different detergent concentrations (0.5 and 1.5 mM DDM) (see Analytical ultracentrifugation assays). **All the tested conditions showed two main states and some higher-order oligomers or aggregates** (table 4.5). Regarding **$TrwB_{R388}$** the first species, which probably corresponded to the monomeric form of the protein, had an average $s_{w,20}$-value of 4.56 S (estimated MW of 86.46 kDa), while the second population had an average $s_{w,20}$-value of 8.07 S (estimated MW of 155.57 kDa). Similar results were obtained when analysing **$TMD_{TraJ}CD_{TrwB}$**. The first species presented an average $s_{w,20}$-value of 4.90 S (estimated MW of 72.77 kDa), while the second population had an average $s_{w,20}$-value of 7.64 S (estimated MW of 142.78 kDa). Even if the obtained $s_{w,20}$-values of the different runs showed slight variations these variations are common and non-significant in polydisperse samples.

Table 4.5. Summary of the main two species observed in the AUC analyses of $TrwB_{R388}$ and $TMD_{TraJ}CD_{TrwB}$ samples. *SEDNTERP* and *SEDFIT* software data analyses were performed to obtain the $s_{w,20}$ and MW values of each population, respectively. Results in the table are the mean value of six AUC runs performed at different protein:detergent ratios.

	$s_{w,20}$	MW
$TrwB_{R388}$	4.56 S (±0.23), 8.07 S (±0.53)	68.46 kDa (±3.11), 155.57 kDa (±5.96)
$TMD_{TraJ}CD_{TrwB}$	4.90 S (±0.47), 7.64 S (±1.00)	72.77 kDa (±14.45), 142.78 kDa (±21.60)

Regarding the relative abundance of these species (estimated as explained in Analytical Ultracentrifugation) significant differences were obtained between both proteins. As seen in the SEC and BN-PAGE studies, AUC results showed that the monomer proportion in $TrwB_{R388}$ was higher than in $TMD_{TraJ}CD_{TrwB}$, while the dimeric population was higher in the later in all the tested conditions (figure 4.18, A and B). Additionally, the sum of the monomer and dimers percentages in $TrwB_{R388}$ was considerably higher than in $TMD_{TraJ}CD_{TrwB}$. For both proteins, the increase in protein concentration turned out into a decrease in the abundance of the main two species and an increase in higher-order populations (figure 4.18, C).

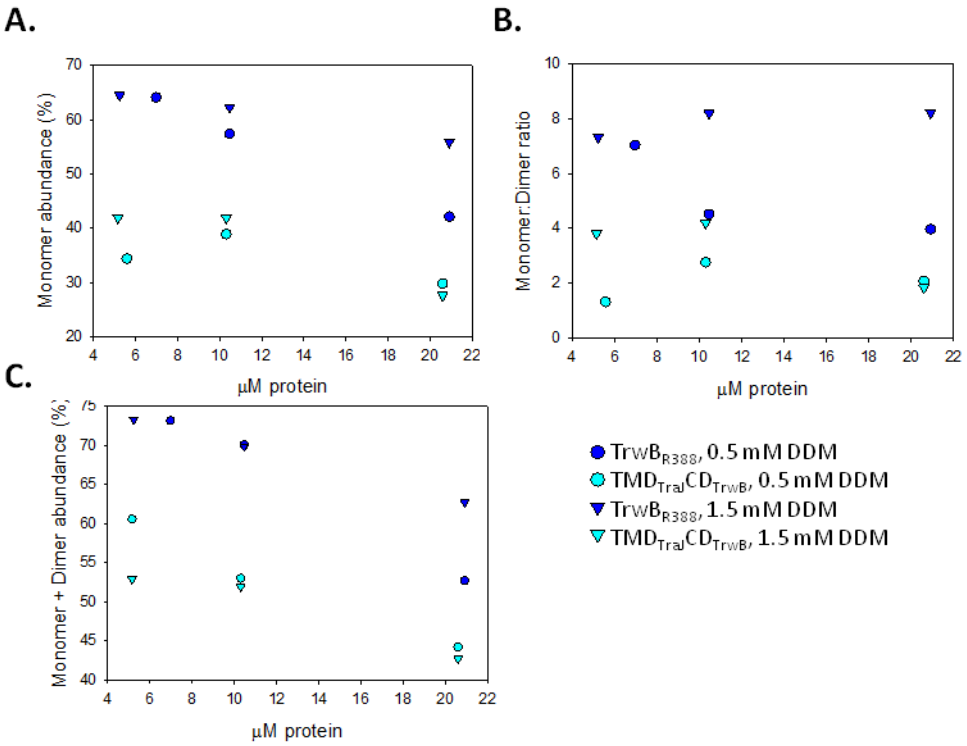

Figure 4.18. The abundance of the monomer (A), the monomer:dimer ratio (B), and the sum of the two main populations (C) observed in TrwB$_{R388}$ and TMD$_{TraJ}$CD$_{TrwB}$ samples at different protein and DDM concentrations. AUC runs and data analysis were performed as explained in section 2.6.3. Sedimentation coefficient distribution graphs are shown in Analytical ultracentrifugation assays). The abundance is the amount of each population as a percentage of total populations.

All the data collected through both purification protocols and the different techniques showed ambiguous results. Therefore, the different estimations of sample composition and population masses were not accurate enough to support stoichiometry determination. However, qualitatively it can be seen that TrwB$_{R388}$ and TMD$_{TraJ}$CD$_{TrwB}$ **behave differently regarding oligomerization**. On one hand, no monomer and hexamer separation could be performed with TMD$_{TraJ}$CD$_{TrwB}$ using the protocol established for TrwB$_{R388}$, similar to what was described for the mutant TrwBΔN50 (Vecino, 2009). On the other hand, when both proteins were purified using the same protocol, they presented different chromatography profiles and bands in the BN-PAGE, being the main differences the **higher abundance of the monomer in TrwB$_{R388}$ sample.** AUC experiments allowed a more specific characterization of the sample polydispersity and reinforced the previously observed results. Two main conclusions can be drawn from this data. First: **the TMD does have an influence in the oligomerization of the protein since T4CPs with the same soluble domain but a different TMD show a different oligomeric behaviour**. This observation comes into agreement with previous results showed in this work, where it has been proven that TrwB$_{R388}$ and TMD$_{TraJ}$CD$_{TrwB}$ show different *in vivo* conjugation rates and *in vitro* DNA-binding affinities. Second: **the purification protocol, specifically each concentration step, could promote the appearance of higher-order oligomers**. Owing to this, it is difficult and risky to draw conclusions regarding oligomerization using purified MP samples and these techniques. For this reason, it was chosen to characterize

the different populations through single-molecule studies of T4CPs in their native membrane environment to (see 5. Molekula-bakarreko Entsegu baldintzen optimizazioa).

4.4.2. $MobB_{CloDF13}$ RELATED PROTEINS

A similar study was performed with $MobB_{CloDF13}$ and its soluble mutant MobBΔTMD, both purified as explained in section 3.5.2. These proteins were analysed by SEC, BN-PAGE, and AUC.

Regarding $MobB_{CloDF13}$ (theoretical MW: 73.95 kDa), the chromatogram obtained from the elution of the analytical *Superose 6 PC 3.2/30* column showed a different profile to the ones obtained with $TrwB_{R388}$ and $TMD_{TraJ}CD_{TrwB}$. It presented a single peak with a V_e of 1.602 mL, related to a MW of 553.5 kDa, according to the column calibration performed with protein standards in *MP purification buffer* (figure 4.19, A). However, as suggested by its width, the peak could contain different species, as later confirmed by the BN-PAGE analysis, where three main bands were observed (figure 4.19, C). The first one had a MW of approximately 100 kDa and was most likely related to the monomer. The second one, which was the main population, had a MW around 200 kDa. Finally, a third faint band could be observed just above the second, with a MW above 232 kDa. These results suggested the presence of monomers and most likely dimers and trimers.

As obtained with $MobB_{CloDF13}$, the SEC chromatogram of the soluble mutant MobBΔTMD (theoretical MW: 53.13 kDa) showed a symmetrical peak (figure 4.19, B). Its V_e (1.840 mL) corresponded to a MW of 72.06 kDa, slightly above the theoretical MW of the monomer. The BN-PAGE results agreed with the SEC, where a main population of approximately 70 kDa was observed, plus two other bands of approximately 130 and 200 kDa, most likely related to dimers and trimers (figure 4.19, D).

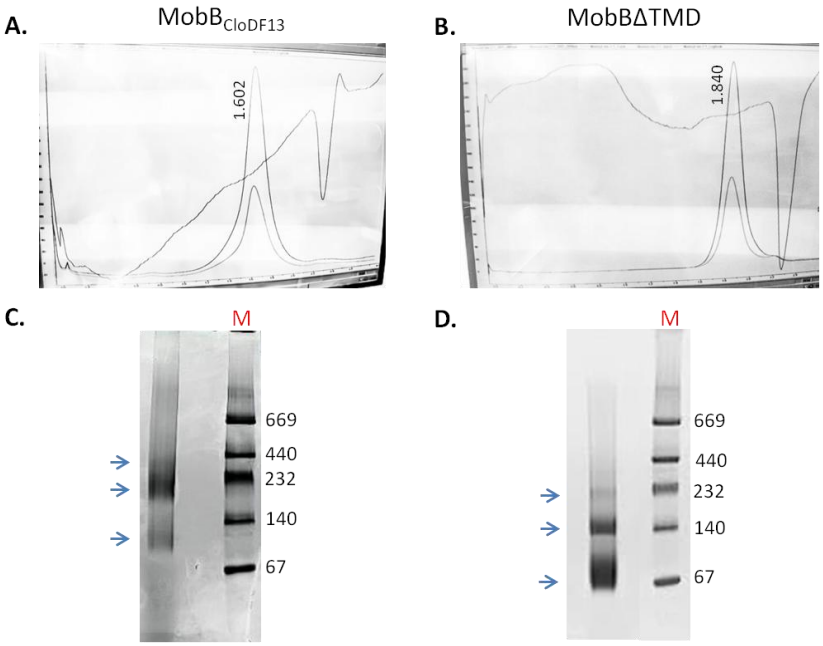

Figure 4.19. Size-exclusion chromatographies and Blue-Native PAGEs of $MobB_{CloDF13}$ (A, C) and MobBΔTMD (B, D) samples. SECs were performed in a *Superose 6 (3.2/30)* column as

described in section 2.5.2.3. Protein elution was followed by measuring absorption at 280 nm. Numbers next to each peak represent the V_e (mL). Blue-Native PAGE assays were performed as described in 2.4.2. poliakrilamidazko gel elektroforesi urdin-natiboa. M: *HMW Native Marker*.

AUC studies with $MobB_{CloDF13}$ were performed at three different protein (3.38, 8.12, and 13.54 µM) and two different DDM (0.6 and 1.5 mM) concentrations. All the tested conditions showed a main population with a $s_{w,20}$-value of 5.9 S and an estimated MW of 119.2 kDa (table 4.6 and Analytical ultracentrifugation assays).

Even though it presented higher values than expected for its theoretical MW, in comparison with the results observed for $TrwB_{R388}$ that showed an $s_{w,20}$ of 4.56 S, this population was attributed to the monomer. Some of the runs showed additional populations, out of which two hypothetical species were estimated: On the one hand, in 67% of the runs a species which had an average $s_{w,20}$ and MW of 9.4 S and 232 kDa, respectively, and which could be related to dimers was observed. On the other hand, a species present in the two runs performed with the highest protein concentration (13.54 µM) was observed. This species had an average $s_{w,20}$ and MW of 13.1 S and 346 kDa, respectively. Assuming the estimated MW of 119.2 kDa per monomer, this species could be related to trimers. Nevertheless, as the MW estimation through AUC of polydisperse samples is limited, these results should be taken with care. This suggests that $MobB_{CloDF13}$ tends to oligomerize when increasing protein concentration although further studies in this matter should be performed to corroborate the hypothesis. As pointed in Analytical ultracentrifugation, a species with a low $s_{w,20}$-value which was attributed to hydrolysed protein was also observed in two of the runs. When comparing these results with the ones obtained in the BN-PAGE and taking into account the limits of both techniques, it seems that **$MobB_{CloDF13}$ presents three different oligomeric states at the tested conditions, probably related to monomer, dimer and trimer. However, these findings also suggest that higher-order oligomers could be observed at higher protein concentrations.**

With regard to MobBΔTMD, AUC runs were performed at different protein concentrations (8.47, 16.94, 33.89 µM), NaCl concentrations (20, 75, 150, 200 mM), CH_3COONa concentrations in substitution for NaCl (20, 75, 150 mM), and pH values (5.6, 6.0, 7.0) (see Analytical ultracentrifugation assays). In spite of the different conditions, similar results were obtained in all the trials (table 4.6). They all showed a main species (average of 97.2%) with an average $s_{w,20}$-value of 3.1 S and an estimated average MW of 50.4 kDa which was attributed to the monomeric species. Additionally, a small percentage of a second population was observed in all the runs (average of 2.2%). This population presented an average $s_{w,20}$-value of 5.25 S, and an estimated average MW of 112.8 kDa and was, therefore, assigned to the dimeric species. In addition to the main species, AUC results showed one or two additional populations in small percentages. An average MW of 181.1 kDa was estimated for the first one, which was observed in 77% of the runs; while an average MW of 244.7 kDa was estimated for the second one, present in 38% of the runs. These species could be related to trimers and tetramers, respectively. These results come in agreement with the ones obtained in the SEC and in the BN-PAGE. Hence, from such observations, it was concluded that **MobBΔTMD is mainly purified as monomers, with a small dimer percentage and fewer trimers and tetramers. It must be underlined that this pattern was independent of any of the parameters tested in the AUC runs.** Once again, the results obtained with MobBΔTMD

differed from those described for TrwBΔN70; as the soluble mutant of $TrwB_{R388}$ has only been purified as a monomer, forming oligomeric complexes merely in the presence of G4-DNA structures (Matilla et al., 2010).

Table 4.6. Summary of the main species observed in the AUC analyses of $MobB_{CloDF13}$ and MobBΔTMD samples. *SEDNTERP* and *SEDFIT* software data analyses were performed to obtain the $s_{w,20}$ and MW values of each population, respectively. Results for $MobB_{CloDF13}$ are the mean value of six AUC runs performed at different protein:detergent ratios, while results for MobBΔTMD are the mean value of 13 AUC runs performed at different conditions (see Analytical ultracentrifugation assays).

	$S_{w,20}$ (S)	MW (kDa)
$MobB_{CloDF13}$	5.9 (±0.19), 9.39 (±0.65), 13.14 (±0.50)	119.2 (±18.0), 232.4(±6.4), 346.3(±16.3)
MobBΔTMD	3.1 (±0.18), 5.2 (±0.41)	50.4 (±2.3), 112.9 (±5.7)

4.5. STRUCTURE

The solved high-resolution structure is one of the most powerful tools to study and understand the biological role of a protein. Both, the secondary structure elements and the tridimensional (3D) model structure can give reliable information about different aspects of the protein such as the stability, protein interactions, and molecular mechanism. Up to date, there are only two crystal structures related to T4CPs: On one hand, the crystal structure of TrwBΔN70, the mutant protein lacking the TMD of the conjugative T4CP $TrwB_{R388}$ (section 1.3.2.2.) (Gomis-Rüth et al., 2001) and on the other hand, the C-term extension of $DotL_{Legionella}$ as part of the Dot/Icm holocomplex from the pathogenic T4SS of *L. pneumophila* (Kwak et al., 2017). Therefore, there is not a high-resolution structure model of a full-length T4CP yet and as a result relevant information is missing.

Even if these questions were partially answered through IRS assays performed with $TrwB_{R388}$ (Hormaeche et al., 2004; Vecino et al., 2011, 2012), there is still the need for further studies and new crystal structures. In this thesis, IRS assays of $TMD_{TraJ}CD_{TrwB}$, $MobB_{CloDF13}$, and MobBΔTMD have been performed to add information about T4CP secondary structure to the already existing one about $TrwB_{R388}$. Additionally, crystallization trials with $TrwB_{R388}$ and MobBΔTMD have been performed and preliminary single-molecule electron microscopy assays have been carried with $TrwB_{R388}$ in collaboration with Dr. Ronnie Berntsson from Umeå University, Sweden.

4.5.1. SECONDARY STRUCTURE STUDIES VIA INFRARED SPECTROSCOPY

To analyse the secondary structure components of $TMD_{TraJ}CD_{TrwB}$, $MobB_{CloDF13}$, and MobBΔTMD the protocol explained in section 2.6.1. was performed. The information regarding

the secondary structure was obtained through the analysis of the amide I band. Band decomposition and data treatment were performed as described in Vecino et al. (2012).

The secondary structure of $TMD_{TraJ}CD_{TrwB}$ was studied so that it could be compared with those of the native $TrwB_{R388}$ and its mutants TrwBΔN50 and TrwBΔN70 (Vecino et al., 2012). The decomposed and curve-fitted spectrum of the amide I region is shown in supplementary data (figure S4.6). The corresponding parameters such as band position, percentage area, and structure assignation, are displayed in table 4.7 together with those presented in Vecino et al. (2012). It must be taken into account that band assignation is not always a straightforward process since its position can be altered by the environment. The spectrum of the chimera protein exhibited four bands related to protein structure. As in the native protein the component at 1654 cm^{-1} was assigned to α-helix, while the bands at 1626 and 1676 cm^{-1} were associated with the high and low-frequency vibrations of β-sheet, even if the later also had a β-turns component. A sizeable proportion of the structure gave off a signal centred at 1640 cm^{-1}, as seen in the deletion mutants but not in $TrwB_{R388}$, which was assigned to flexible, non-periodic elements.

Table 4.7. Secondary structure components of $TrwB_{R388}$, $TMD_{TraJ}CD_{TrwB}$, TrwBΔN50 TrwBΔN70. The different components were obtained through band decomposition of the amide I band of IR spectra recorded in D_2O medium. The spectra are shown in figure S4.6. Only areas above 5% are shown. Area percentages are compared to the ones of the chimera protein: green represents a difference in area higher than 5%, while red represents lower than 5%. β-T: β-turns; β-S: β-sheet; α-H: α-helix. [a]Data taken from (Vecino et al., 2012).

	$TrwB_{R388}$[a]		$TMD_{TraJ}CD_{TrwB}$		TrwBΔN50[a]		TrwBΔN70[a]	
Assignment	Position (cm^{-1})	Area (%)	Position (cm^{-1})	Area (%)	Position (cm^{-1})	Area (%)	Position (cm^{-1})	Area (%)
β-T + β-S	1676	5	1671	14	1676	2	1675	8
β-T	1661	27	/	/	1665	11	1665	11
α-H	1647	41	1654	35	1654	27	1653	26
Unordered + β-S	/	/	1640	30	1641	37	1640	39
β-S	1631	27	1626	17	1628	17	1627	12

With the aim of further studying if the deletion of the TMD has the same effect in all T4CPs, the same study was carried out with $MobB_{CloDF13}$ and its deletion mutant MobBΔTMD. The decomposed and curve-fitted spectra of the amide I regions are shown in supplementary data (figure S4.6). In this case, both proteins exhibited four main bands that were assigned as shown in table 4.8. As in the previous proteins, the component at 1653/1652 cm^{-1} was assigned to α-helix and the bands at 1666/1665 cm^{-1} were associated with β-turns, as seen in the proteins studied in Vecino et al. (2012), but not in $TMD_{TraJ}CD_{TrwB}$. Likewise, the signal centred at 1677/1682 cm^{-1} was assigned to low-frequency vibrations of β-sheet and β-turns. Similar to the results obtained with the chimera protein, both $MobB_{CloDF13}$ and MobBΔTMD had a band at 1639 cm^{-1}, related to 30% of the structure, assigned to unordered structures.

Table 4.8. Secondary structure components of $MobB_{CloDF13}$ and MobBΔTMD. The different components were obtained through band decomposition of the amide I band of IR spectra recorded in D_2O medium. The spectra are shown in supplementary data. Only areas above 5% are shown. Area percentages of MobBΔTMD are compared to the ones of $MobB_{CloDF13}$: green represents a difference in area higher than 5%, while red represents lower than 5%. β-T: β-turns; β-S: β-sheet; α-H: α-helix.

	$MobB_{CloDF13}$		MobBΔTMD	
Assignment	Position (cm^{-1})	Area (%)	Position (cm^{-1})	Area (%)
β-T + β-S	1677	7	1682	3
β-T	1666	13	1665	22
α-H	1653	35	1652	29
Unordered + β-S	1639	29	1639	30

For the past decades, IRS has proven to give reliable information about the secondary structure of proteins (Arrondo and Goñi, 1999; López-Lorente and Mizaikoff, 2016). Specifically, regarding T4CPs, it has been widely used to study $TrwB_{R388}$ and it was observed that removing the TMD had important structural and functional consequences. It was described that the predominant secondary structures in $TrwB_{R388}$ were α-helixes, while TrwBΔN70 had a higher proportion of β and unordered structures. This suggested that the presence of the small TMD enabled the whole protein to fold in a more ordered and compact manner (Hormaeche et al., 2004). Additionally, it was seen that the single deletion of the first α-helix in the mutant TrwBΔN50 was enough to cause similar changes in the secondary structure of the CD as the deletion of the whole TMD (Vecino et al., 2012). On this account, the aim of the IRS studies performed in this work was to further analyse how the change or loss of the TMD modifies the overall protein conformation.

Regarding $TMD_{TraJ}CD_{TrwB}$, one of the most predominant changes in comparison with $TrwB_{R388}$ was that a band at 1640 cm^{-1} represented an important percentage of the secondary structure (30%). This band, which was also present in TrwBΔN50 and TrwBΔN70 mutant proteins but not in$TrwB_{R388,}$ has been mainly assigned to flexible structures (non-periodic elements) related to a less compact overall structure (Agopian et al., 2016). For instance, it represented a 20% of the sarcoplasmic reticulum Ca^{2+}-ATPase (Echabe et al., 1998). It was hypothesised that such high proportion of flexible loops would only be possible in a structure where the cytoplasmic domain consisted of periodic secondary structures connected by long loops. As the crystal structure of TrwBΔN70 shows this kind of loops (Gomis-Rüth et al., 2002a), the presence of the 1640 cm^{-1} band in $TMD_{TraJ}CD_{TrwB}$, TrwBΔN50, and TrwBΔN70 mutant proteins could be explained (table 4.7) as the loss of the compact structure of $TrwB_{R388}$ due to the deletion of its cognate TMD (Hormaeche et al., 2004).

Previous studies about TrwBΔN70 and TrwBΔN50 showed that the band at 1640 cm^{-1} also had a β-sheet component (Vecino et al., 2012). To elucidate if this also happened in $TMD_{TraJ}CD_{TrwB}$, IRS experiments at different temperatures were performed (20, 40, 60 and 80°C). In this matter, it was published that at higher temperatures the band at 1640 cm^{-1} split showing a β-sheet related band, which would not happen if the band was purely composed of unordered structures (Andraka et al., 2017). Through this assay it was seen that the 1640 cm^{-1}

band in the chimera protein was composed of both unordered and β-sheet elements. Along these lines, it has to be noticed that the band at 1626 cm^{-1}, also assigned to β-sheet elements, was 10% lower in the chimera than in the native T4CP. Additionally, the band around 1671 cm^{-1}, which also had a β-sheet component, was 9% higher in the chimera in comparison to $TrwB_{R388}$. Bearing all in mind, it could be that the total percentage of β-sheet in $TMD_{TraJ}CD_{TrwB}$ is just slightly smaller to that of $TrwB_{R388.}$ However, as the bands related to this secondary structure appeared mixed with other structural elements, it is risky to adjudge them an exact percentage.

Concerning β-turns, the band assigned to them in the $TrwB_{R388}$ related proteins, 1661-1665 cm^{-1}, was not observed in the chimera protein. However, it can be postulated that the increase seen in $TMD_{TraJ}CD_{TrwB}$ of the band at 1671cm^{-1}, assigned to both β-turns and β-sheet structures, was partially related to the β-turns component seen in the mutants at 1665 cm^{-1}. This would imply that the β-turns component of the chimera protein is lower than the one of the native protein and similar to the TMD deletion mutants.

Finally, concerning the helical structures, $TMD_{TraJ}CD_{TrwB}$ presented a decrease in α-helix in comparison with $TrwB_{R388}$, but an increase in comparison to the mutants. Therefore it seems that **$TMD_{TraJ}CD_{TrwB}$ has qualitative and quantitative features in between the native protein and the deletion mutants**. **These results suggest that the presence of a heterologous full-length TMD does provide a more compact and ordered structure to the T4CP in comparison to the TMD deletion mutants, even if it does not reach the level of the native protein.** This result comes in agreement with previously presented results in this work, which have demonstrated that although the chimera resembles the native protein, their functional and structural features are not the same. Some of those results have suggested that the presence of the heterologous TMD might influence processes happening in the CD (*e.g.,* substrate interaction). The observed structural changes reported here might be the explanation for those changes in functionality.

To test if the results described for $TrwB_{R388}$ could be extrapolated to other T4CPs, the secondary structure of $MobB_{CloDF13}$ and its soluble mutant, MobBΔTMD, were studied. When full-length native proteins ($TrwB_{R388}$ and $MobB_{CloDF13}$) were compared it was observed that the 1631 cm^{-1} band assigned to β-sheet structures in $TrwB_{R388}$ (27%) was missing in $MobB_{CloDF13}$. Also an increase in the same proportion of the band at 1639 cm^{-1} was observed in $MobB_{CloDF13}$. As seen with the $TMD_{TraJ}CD_{TrwB,}$ protein, this band was assigned to unordered and β-sheet structures. Therefore, as hypothesized for $TMD_{TraJ}CD_{TrwB,}$ it could be possible that the increase of the 1639 cm^{-1} band is partially covering the β-sheet structures assigned in $TrwB_{R388}$ to the 1631 cm^{-1} band.

Surprisingly, MobBΔTMD presented an IR spectra quite similar to the one obtained for $MobB_{CloDF13}$. It had smaller and higher helical structure and β-turns percentages, respectively, but both showed similar unordered and β-sheet percentages. This result leads to think that in this T4CP the presence of the TMD does not have the same effect in the structure of the CD as it does in $TrwB_{R388}$ related proteins. As $MobB_{CloDF13}$ has to interact with heterologous T4SSs, it could be that the TMDs of this mobilizable plasmid related T4CPs have differently evolved to perform those unspecific interactions without altering the CD where the specific interactions

with its cognate system happen. Similar effects have been already described in this work, as the TMD of $MobB_{CloDF13}$ is not a limiting element for the polar localization of the protein (section 3.6.) or its oligomerization (section 4.4.). Therefore, **care should be taken when extrapolating the results obtained with the paradigmatic protein $TrwB_{R388}$ to the rest of the T4CP family members**.

4.5.2. $TrwB_{R388}$ TERTIARY STRUCTURE PRELIMINARY ASSAYS

As mentioned before, elucidating the structure of a protein is a key step in understanding its biological function and dynamics. To do so, many biophysical techniques have been developed during the years, such as nuclear magnetic resonance, X-ray crystallography, electronic microscopy, circular dichroism, etc. However, as previously explained, when it comes to working with MPs, there are a lot of added difficulties. These proteins have mostly a complex biogenesis and sample preparation, making it complicated to obtain the high protein concentrations and purity needed for structural studies. Additionally, due to the employed purification techniques, these samples tend to be unstable and to have low functionality. For these reasons, even if 20-30% of all proteins encoded by the genome are MPs, nowadays they only cover a very small percentage of high-resolution 3D-structures (Pedro et al., 2019). However, after the publication of the first results about the structure of $TrwB_{R388}$ by X-ray crystallography and EM (Gomis-Rüth et al., 2001; Hormaeche et al., 2002), thanks to the advances in this area, in the last years the knowledge regarding the tertiary structures of T4SS has increased. Specifically, studies performed with cryo-electron tomography (Hu et al., 2019; Oikonomou and Jensen, 2019) and NS-EM (Redzej et al., 2017) have shed light on the structure of T4SS and have given a new insight into the role of T4CPs inside these systems.

In spite to all the advances, there is still no high-resolution structure of an isolated full-length T4CP. In this matter, attempts to crystallize purified $TrwB_{R388}$ were unfruitful (Vecino, 2009). In this thesis, new crystallization trials were performed in collaboration with the Membrane Protein Laboratory (MPL) at Diamond Light Source (Oxford-UK) under the guidance of Dr. Moraes. To do so a three-step protocol was performed (section 2.7.1.). In the first place, a new $TrwB_{R388}$ purification protocol was established, afterwards, the quality of the samples was analysed using SEC-MALS (section S3.5.1.2.), and finally crystallization trials at 4 and 20°C were performed using *MemGold™*, *MemGold2™*, and *MemMeso™* commercial plates. Unfortunately, no crystal structures were observed in any of the conditions tested.

In addition to X-ray crystallography, cryo-electron microscopy (Cryo-EM) was also chosen as an alternative strategy for the obtainment of high-resolution structures of $TrwB_{R388}$. Preliminary assays have been made in collaboration with Dr. Berntsson (Umeå University, Sweden). First of all, purified $TrwB_{R388}$ (section 3.5.1.1.) was analysed by NS-EM (figure 4.20). As the obtained images looked proper, the same protein samples were used for vitrifying grids for Cryo-EM. Afterwards, Dr. Berntsson performed a preliminary Cryo-EM assay in the *Thermo Scientific™ Titan/Krios* transmission electron microscope and collected the data. Even though the particle density in each grid square was low, an initial processing of the data was performed with 9000 particles. These were suitably classified into 2D classes and it was observed that they adopted a predominant orientation on the grid. In the light of these results,

the next steps in this matter would be to try different grids to get more particle density inside the grid squares. In this manner, more data would be collected to have enough particles to work with in trying to solve the structure.

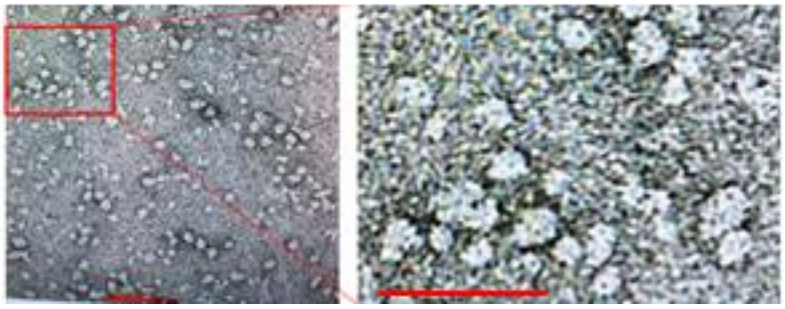

Figure 4.20. $TrwB_{R388}$ electron microscopy images by NS-EM. Original and zoomed area (marked with a red box). Scale bar: 50 nm. Images taken by Dr. Berntsson.

4.5.3. MobBΔTMD CRYSTALLIZATION PRELIMINARY ASSAYS

The difficulties that arise from working with MPs have been many times simplified by studying their soluble mutants. Even if it has been widely proven that the TMD of T4CPs is not merely an anchor to the membrane and that it has an important role in the *in vivo* function and *in vitro* properties of the protein, we decided to perform crystallization studies with MobBΔTMD. In this manner the obtained structure would be compared to the ones solved for TrwBΔN70 and the possible structural differences amongst conjugative and mobilizable plasmid related T4CPs would be defined.

Preliminary studies in commercial *96-well 2-drop MRC* crystallization plates were performed, so that afterwards the crystallization conditions could be optimized using *48-well MRC Maxi* crystallization plates. After the first crystallization attempts (plates 1703-1708; table S4.1) a crystal was observed in only one condition (plate 1705, drop G3). The crystal was 220x200 µm and appeared after 120 days (figure 4.21, A). It was harvested in a 20% ethylenglycol cryoprotective solution and kept in liquid N_2. To get better crystals, an optimization plate was set up (optimization plate 1721, table 4.9) and a crystal was formed in drop B6 (figure 4.21, B).

Table 4.9. Optimization of conditions from drop G3 in plate 1705. The starting conditions for the optimization plate 1721 were: *100 mM MES pH 6.5, 10 mM ZnSO4, 25% PEG 550 MME*. The concentration of ZnSO4 (0-20 mM) was changed through rows and the concentration of PEG 550 MME (20-30%) was changed through columns. *100 mM MES pH 6.5* was used as buffer in the top four rows (A-D), while *100 mM HEPES pH 7.5* was used in the bottom four rows (E-H).

[PEG]		20%	25%	30%	20%	25%	30%
[Zn]		**1**	**2**	**3**	**4**	**5**	**6**
0 mM	**A**	MES	MES	MES	MES	MES	MES
5 mM	**B**	MES	MES	MES	MES	MES	MES
10 mM	**C**	MES	MES	MES	MES	MES	MES
20 mM	**D**	MES	MES	MES	MES	MES	MES
0 mM	**E**	HEPES	HEPES	HEPES	HEPES	HEPES	HEPES
5 mM	**F**	HEPES	HEPES	HEPES	HEPES	HEPES	HEPES
10 mM	**G**	HEPES	HEPES	HEPES	HEPES	HEPES	HEPES
20 mM	**H**	HEPES	HEPES	HEPES	HEPES	HEPES	HEPES

The crystal was 50x20 µm and appeared after 90 days. It was harvested in a 20% ethylenglycol cryoprotective solution and kept in liquid N_2. The crystals from 1705G3 and 1721B6 were sent to the ALBA synchrotron in Barcelona to get some diffraction data but unfortunately they did not diffract. Nevertheless, the obtained diffractograms confirmed that the crystals were protein crystals and not salt crystals.

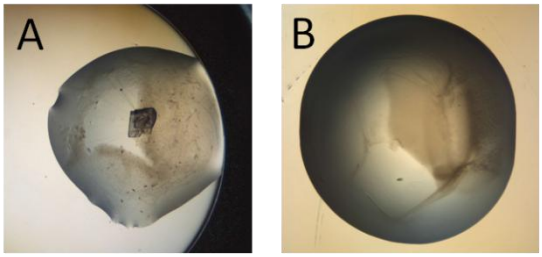

Figure 4.21. MobBΔTMD crystals. A) Crystal from condition 1705G3. **B)** Crystal from condition 1721B6.

To test the influence of the presence of glycerol in the protein buffer, several commercial screens (plates 1722-1724 and 1763-1768) were attempted in a glycerol free buffer (*cell buffer*). The previously formed crystal in 1705G3 did not show up in plate 1764G3. Similarly, in plates where the conditions were those of the previously formed crystals (1769 and 1770) no crystals were observed in the absence of glycerol. On the other hand, new crystals of protein grew in *cell buffer* in conditions that had been unsuccessful with *MobBΔTMD* crystallization buffer (table 4.10 and figure 4.22), leading to the conclusion that the presence of glycerol may favour the formation of protein crystals in some conditions but it

can hamper it in some other. Other possible explanation may be that these crystals were growing from a more concentrated protein solution than the one tested with buffer A. Crystals of protein in buffer B were also formed in plates 1766 and 1767 in conditions not tested with buffer A (table 4.10 and figure 4.22).

Table 4.10. Growing conditions of MobBΔTMD crystals in the absence of glycerol.

	Plate number	Drop number	Concentration (mM)	Conditions
A	1765	G6_1	0.560	*200 mM Na malonate pH 7.0, 20% PEG 3350*
B	1765	H11_1	0.56	*100 mM Bis-Tris pH 5.5, 200 mM MgCl2, 25% PEG 3350*
C	1766	A2_2	0.28	*10 mM Tris pH 8.0, 1.20 M Na citrate*
D	1766	A8_2	0.28	*20 mM MES pH 6.5, 20 mM NaCl, 20 mM CaCl2, 10 mM MgSO4, 7.7% PEG 1500*
E	1766	C11_1	0.56	*10 mM HEPES pH 7.0; 20 mM NiSO4, 33% Jeffamine-M600*
F	1767	B3_1	0.56	*20 mM MES pH 6.0; 20 mM MgCl2, 3.5% PEG 3350*

Unfortunately, it was not possible to harvest these crystals because most of them dissolved when the cryoprotective solution was applied, probably because they had grown in supersaturated conditions. Some other crystals were so strongly attached to the bottom of the well that it was impossible to harvest them.

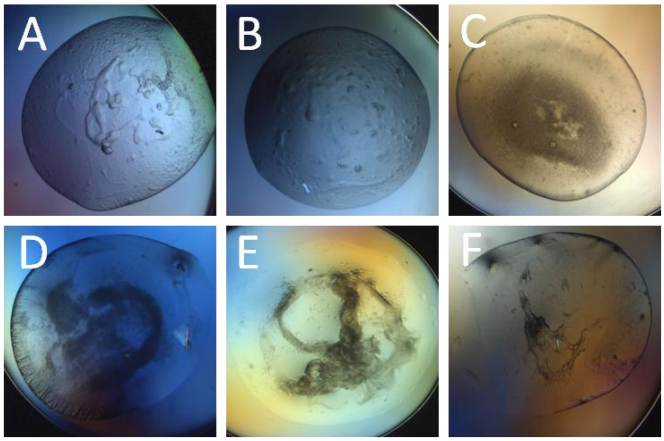

Figure 4.22. Images of MobBΔTMD crystals in the absence of glycerol. A to F letters are related with the conditions shown in table 4.10.

To sum up, it can be stated that it **is possible to grow protein crystals from MobBΔTMD** even though no diffracting crystal has been obtained so far. Several conditions in which crystals could be obtained were found, so there is room for the optimization of

conditions. As the influence of protein concentration and protein buffer formulation is still unclear, there are many different factors to be explored in the future.

4.6. ATP HYDROLASE ACTIVITY

The biogenesis and substrate transport in T4SS requires a considerable amount of energy, which is fulfilled by the presence of three ATPases in the system: VirB4-like, VirB11-like, and VirD4-like (T4CPs) proteins. These proteins are amongst the RecA/AAA+ family, which are ring shape hexameric ATPases associated with diverse cellular activities. T4CPs, as the other components of the family, present a NBD with Walker A and Walker B conserved motifs in their CD (Moncalián et al., 1999). T4CPs with point mutations in the Walker A motif have shown that this is essential for the ATPase activity of the protein (Hormaeche et al., 2004; Lang and Zechner, 2012; Schroder and Lanka, 2003). However, nowadays no *in vitro* ATPase activity has been described for any full-length T4CP, even if it has been observed in TMD deletion mutants (Llosa and Alkorta, 2017; Schröder and Lanka, 2005; Tato et al., 2005).

The most studied protein of the family regarding the ATPase activity is $TrwB_{R388}$, specifically through the characterization of its TMD deletion mutant TrwBΔN70. This mutant protein presents an *in vitro* ATPase activity with positive cooperativity stimulated by DNA and by $TrwA_{R388}$ accessory protein. The first works showed that the ATPase activity is enhanced by oligonucleotides with a minimum length of 45 nucleotides and dsDNA (Tato et al., 2005, 2007). Moreover, it has been described that TrwBΔN70 is at least 25 times more efficient in its ATPase activity in the presence of an oligonucleotide which contains guanine-rich sequences forming G4-DNA structures (Matilla et al., 2010). Additionally, the accessory protein $TrwA_{R388}$ stimulated 10-fold the ATPase activity in the presence of dsDNA, while it did not alter the values obtained with oligonucleotides (Tato et al., 2007).

In previous works in our group, the activity of the full-length protein has been long studied with unsuccessful results, suggesting that it could be regulated by the TMD or by the interaction of this domain with another component of the T4SS or the membrane (Vecino, 2009). These results put forward that there are still many unknown details regarding the function and modulation of the ATP hydrolase activity of T4CPs. In this thesis, we have continued with the search of that activity by optimizing the ATP hydrolysis assay conditions (section 2.6.6.) and by studying different T4CP variants.

4.6.1. ATPase ACTIVITY OF $TMD_{TraJ}CD_{TrwB}$

In the preliminary assays for the characterization of the ATPase activity of the chimera protein the effect of ATP concentration, pH, ionic strength (NaCl and KCl concentrations), and the presence of DNA (ssM13 and dsPUC18 DNA, 6 nM) were studied. Coupled enzyme assays were carried out as described for TrwBΔN70 (Tato et al., 2007) with 1.56 µM protein at 37°C in *50 mM Tris-HCl (pH 8), 6 mM $MgCl_2$ and 75 mM NaCl* buffer. Obtained data did not fit into a Michaelis-Menten equation, showing negative cooperativity with a maximum activity at 5 mM ATP, 40°C, pH 8.0 and 20 mM NaCl, with no effect of the presence of DNA (data not shown). However, the lack of detergent and the low salt concentration in the buffer caused the protein

to aggregate. In agreement with the results obtained in the stability assays (section 4.2.1.2.), it was observed that around 80% of the protein aggregated during the reaction time, impeding the calculation of the specific activity.

Coupled enzyme assays have been mainly used for studying the ATPase activity of soluble T4CP mutants (Cabezón and Arechaga, 2020), however, when using full-length MPs, measuring the absorbance has always been a problem due to the aggregation and therefore turbidity of the samples (Vecino, 2009). For this reason, the next step was to study the effect of the detergent in the assay. To do so, three different DDM concentrations were tested (0, 0.2, and 0.4 mM) using ADP instead of ATP and no protein. It was seen that the detergent does not cause any effect in the coupled enzyme assay *per se,* even if it has been described that it reduces TrwBΔN70's activity in 50% (Vecino, 2009). Therefore to prioritize protein stability DDM was used while setting up the optimal activity parameters.

To characterize the elution profile, the ATPase activity of the different fractions obtained during the SEC was determined. Additionally, this experiment was employed to optimize the ionic strength used during the coupled enzyme assay by simultaneously testing all the samples at 100 and 200 mM NaCl (figure 4.23). The results showed that the observed activity was mainly related to the proteins eluted in the second peak and that even if the protein stability was improved with 200 mM NaCl, the ATPase activity decreased an average of 40.1%. This result underlines a persistent problem when working with MPs, since the buffers in which the protein is more stable are not the most suited ones for its activity. However, as there was still aggregation of protein during the reaction, it was decided to further increase the ionic strength and reduce the reaction temperature to 25°C in the following experiments, even if those conditions would decrease the obtained velocity.

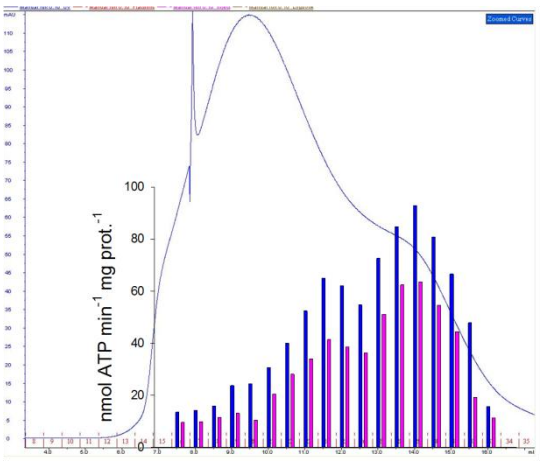

Figure 4.23. Correlation of ATPase activity and protein elution profiles in SEC of $TMD_{TraJ}CD_{TrwB}$. Coupled enzyme assays were performed at 37°C with 1.56 µM protein in a buffer containing *50 mM Tris-HCL (pH 7.8), 0.5 mM DDM, 0.1 mM EDTA, 5% (v/v) glycerol, 6 mM $MgCl_2$ and the RS (17 µg/mL LDH, 0,25 mM NADH, 0,5 mM PEP and 60 µg/mL PK) supplemented with 100 or 200 mM NaCl* (blue and pink columns, respectively). Reactions were performed using 5 mM ATP as explained in section 2.6.6. and absorbance was measured using a *SinergyHT* plate reader and the Gen5 software.

As $TrwB_{R388}$ had not shown any ATPase activity in the tested conditions, the next step was to ensure that the aforementioned activity belonged to $TMD_{TraJ}CD_{TrwB}$ and not a contaminant protein or the hydrolysis of the soluble domain. To address this problem the point-mutation variant $TMD_{TraJ}CD_{TrwB}$K142T was constructed, as it has been described that this change in the Walker A domain impedes conjugation and inhibits the *in vitro* ATPase activity of T4CPs (Hormaeche et al., 2006; Moncalián et al., 1999; Tato et al., 2005). As a preliminary test the inability to perform conjugation of $TMD_{TraJ}CD_{TrwB}$K142T was confirmed via mating assays (section 3.3.). Afterwards, its *in vitro* activity was analysed through coupled enzyme assay together with the full-length native protein; the two samples of $TMD_{TraJ}CD_{TrwB}$ and the soluble mutant TrwBΔN70 (figure 4.24). This set of experiments was also performed in the presence of 6 nM pUC18 DNA and/or 14.9 µM $TrwA_{R388}$, however as no changes on the activity were observed the data related to the presence of DNA and $TrwA_{R388}$ is not shown.

At the tested conditions no activity was obtained for $TrwB_{R388}$, in agreement with the in-depth study made by Vecino in which no ATPase activity was seen for this protein in a wide variety of conditions (Vecino, 2009). As for TrwBΔN70, it must be taken into account that the reaction conditions (buffer and temperature) were far from its optimal conditions, which could explain the observed lack of activity (Tato et al., 2005). Regarding the chimera protein, only the second sample presented activity, consistent with the results observed in the previous assay in which the activity was adjudged to the second peak of the SEC. Surprisingly the sample related to $TMD_{TraJ}CD_{TrwB}$K142T showed the highest activity at the tested conditions.

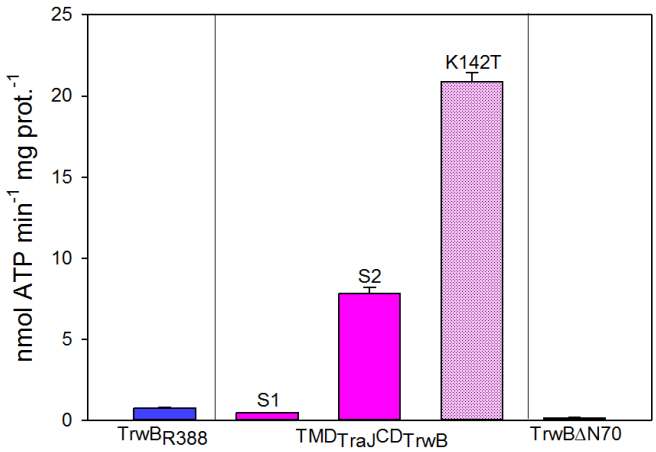

Figure 4.24. ATPase activity of $TrwB_{R388}$ related proteins. Coupled enzyme assays were performed at 25°C with 3 µM protein in a buffer containing *50 mM Tris-HCL (pH 7.8), 0.4 mM DDM, 0.1 mM EDTA, 10% (v/v) glycerol, 6 mM $MgCl_2$, 300 mM NaCl* and the RS (*17 µg/mL LDH, 0,25 mM NADH, 0,5 mM PEP and 60 µg/mL PK*). Reactions were performed using 5 mM ATP as explained in section 2.6.6. and absorbance was measured using a *SinergyHT* plate reader. Results are the mean value of three independent experiments.

Given the fact that this mutation impedes the *in vivo* activity through inhibition of nucleotide-binding and therefore ATP hydrolysis, the observed ATPase activity should be ascribed to a contaminant protein or some artefacts in the coupled enzyme assay. These data suggest that the ATPase activity shown by $TMD_{TraJ}CD_{TrwB}$ could be related to one of the proteins that appear in the second sample of $TMD_{TraJ}CD_{TrwB}$ and $TMD_{TraJ}CD_{TrwB}$K142T in the SDS-PAGE,

but not in the first sample of the chimera (figure 3.23, A). To confirm this hypothesis protein samples were validated through LC-MS/MS (section 2.4.4.) but no conclusive results were obtained. Taking into account that S1 presents a higher purity degree and that it has not shown any ATPase activity at the tested conditions, it can be postulated that as $TrwB_{R388}$, **$TMD_{TraJ}CD_{TrwB}$ does not present ATPase activity *in vitro*** at the tested conditions.

4.6.2. ATPase ACTIVITY OF MobBΔTMD

To compare MobBΔTMD with TrwBΔN70 the kinetic parameters of their ATPase activity were studied by coupled enzyme assays. As with the chimera protein, the effect of pH, ionic strength, and ATP concentration were tested. Experiments were performed at 37°C with 3 µM protein and 3 mM ATP as explained in section 2.6.6., in *sodium acetate buffer (pH 5.6)* containing *6 mM $MgCl_2$, 75 mM NaCl* and the components of the RS (*17 µg/mL LDH, 0.25 mM NADH, 0.5 mM PEP and 60 µg/mL PK*), unless otherwise indicated. In all the assays a negative control in the absence of protein was performed to ensure that no spontaneous hydrolysis of ATP was happening due to the reaction conditions.

First of all the activity at different pH values was studied in the range between pH 5.0 and 7.0. To do so, sodium acetate buffer (pH 5.0, 5.25 and 5.6), HEPES sodium buffer (pH 6.0 and 6.5), and Tris-HCl (pH 7.0) buffers were used (figure 4.25, A). It was observed that at the tested conditions the protein showed its highest activity at pH 5.6, being this activity almost zero at higher pHs. This result comes along with what was described for TrwBΔN70, which showed **optimal activity between pH 5.25 and 6.25** (Tato et al., 2005). Next, the effect of the NaCl was analysed at three different NaCl concentrations (75, 150, and 200 mM) and three different temperatures (25, 30, and 37°C) (figure 4.25, B). As expected the highest activity was obtained at the highest temperature and lowest ionic strength (*i.e.*, 37°C and **75 mM NaCl**), as it has been seen that activity tends to decrease when increasing NaCl concentration above 100 mM (see previous section and Tato et al., 2005). To perform a further temperature screening, the activity was evaluated in a range from 20°C to 50°C (figure 4.25, C). It was seen that the maximum activity was obtained at **45°C**, which is the temperature in which the protein starts to lose its native conformation and aggregates (figure 4.7). However, in order to perform a more accurate comparison with TrwBΔN70 assays were performed at 37°C.

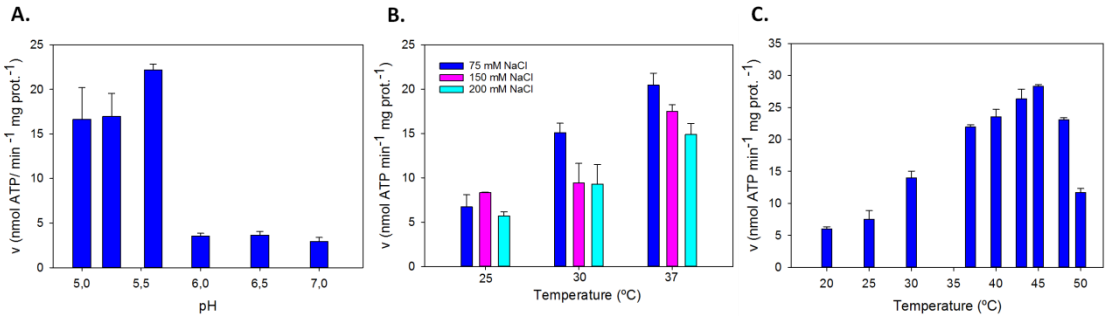

Figure 4.25. ATPase activity of MobBΔTMD at different pH values (A), NaCl concentrations (B), and temperatures (C). Coupled enzyme assays were performed at 37°C with 3 µM protein in *sodium acetate buffer (pH 5.5) containing 6 mM $MgCl_2$, 75 mM NaCl and the RS (17 µg/mL LDH, 0,25 mM NADH, 0,5 mM PEP and 60 µg/mL PK*) unless otherwise indicated. Reactions

were performed in the presence of 3 mM ATP as explained in section 2.6.6. and absorbance was measured using a *Cary 300 Bio Spectophotometer.* Results are the mean value of three independent experiments.

Next, the effect of ATP concentration in the ATPase activity of MobBΔTMD was studied through ATP titration (figure 4.26, A). Obtained data were further analyzed using the Hill equation in which, assuming that the reaction rate is proportional to the fractional saturation of the enzyme, the Hill coefficient can be calculated (n_h) (figure 4.26, B). This parameter can be interpreted as the minimum number of protomers within the oligomeric structure involved in ATP cooperative binding. For MobBΔTMD it was seen that the ATPase activity increased with increasing ATP concentration until **saturation was reached at 2.5 mM**. Obtained data fitted into a simple hyperbolic curve, which is related to the **Michaelis-Menten kinetics** model (equation 2.4). The analysis of the Hill plot (equation 2.5) supported this observation since an n_h of 0.95 was obtained, meaning that no cooperative binding of the substrate occurs, as in the Michaelis-Menten model. This is opposite to the results obtained for TrwBΔN70, which showed positive cooperativity involving at least three protomers (Tato et al., 2005). A possible explanation for the cooperativity shown by TrwBΔN70 could be that it was described in the presence of DNA, which stimulates the ATPase activity of TrwBΔN70 and therefore changes the kinetic parameters of the reaction. In order to check this hypothesis in MobBΔTMD, ATPase coupled enzyme assays were performed in the presence of dspUC18 and ssM13 DNA molecules as explained in 2.6.6. ATParen hidrolisi entseguak. However, unlike with TrwBΔN70, used here as a positive control, no changes in the activity rates of MobBΔTMD were observed. Nevertheless, these results are consistent with the ones observed in the previous sections, in which **the presence of DNA had no effect** in protein stability (section 4.2.2.3.) nor did it bind to it at the tested conditions (section 4.3.1.).

Based on the ATP titration data, the Lineweaver-Burk equation (equation 2.6) was used to calculate the maximum hydrolysis rate (V_{max}). In this plot, the *y*-intercept is equivalent to the inverse of V_{max} (figure 4.26, C). In this manner, **V_{max} value at the tested conditions was of 22.7 nmol ATP min^{-1} mg^{-1}**, not far from the one showed by TrwBΔN70 in the absence of DNA or $TrwA_{R388}$ [30 nmol ATP min^{-1} mg^{-1}, (Tato et al., 2005)].

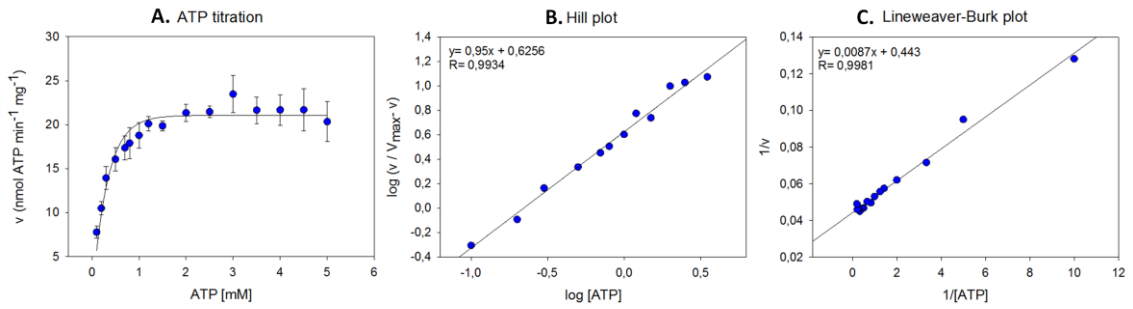

Figure 4.26. Effect of ATP concentration in MobBΔTMD ATP hydrolysis. Coupled enzyme assays were performed at 37°C with 3 µM protein in sodium *acetate buffer (pH 5.5) containing 6 mM $MgCl_2$, 75 mM NaCl and the RS (17 µg/mL LDH, 0,25 mM NADH, 0,5 mM PEP and 60 µg/mL PK*). Reactions were performed as explained in section 2.6.6. using different ATP concentrations. Absorbance was measured using a *Cary 300 Bio Spectrophotometer.* Results are the mean value of three independent experiments. **A)** The curve obtained in the ATP

titration showed a Michaelis–Menten behavior. **B)** The slope of the lines in the Hill plot in the range of 0.1 mM ATP (log[ATP]: -1) to 3.5 mM ATP (log[ATP]: 0.54) was estimated as the apparent Hill coefficient (n_h) with a value of 0.95. **C)** Lineweaver-Burk plot was used to calculate the maximum hydrolysis rate (V_{max}). The *y*-intercept of this graph is equivalent to the inverse of V_{max} (22.7 nmol ATP min^{-1} mg^{-1}).

In summary, results obtained with MobBΔTMD presented similarities and discrepancies with those described for TrwBΔN70. On the one hand, both proteins are active at acidic pH and show a similar ATPase rate in the absence of accessory proteins and DNA molecules. On the other hand, MobBΔTMD does not present positive cooperativity or enhanced activity in the presence of DNA molecules. In order to clarify these discrepancies, the main requirement should be to demonstrate that the observed ATP hydrolysis is indeed performed by MobBΔTMD. To do so, the cloning of m*obBΔTMDK270T* is being performed which codes for the homologue of the inactive Walker A mutant TrwBΔN70K136T, MobBΔTMDK270T. Once the legitimate ATPase activity is confirmed it should be further characterized at different conditions, such as in the presence of $MobC_{CloDF13}$ (section S3.5.2.) and/or G-quadruplex DNA structures.

4.7. DISCUSSION/SUMMARY

This chapter has been focused on the characterization of T4CPs through biochemical and biophysical techniques. Due to their essential role in the conjugative process, a few of these proteins have been deeply studied during the last decades. T4CPs are a broad family of proteins essential for conjugation. In fact, in a genetic study performed with 1,000 plasmids, 255 T4CPs were found by expert annotation (Smillie et al., 2010). Nevertheless, only a few T4CPs have been studied, mainly associated with T4ASS, in particular of the $Gram^-$ VirD4-type subfamily, such as $VirD4_{A.\ tumefaciens}$ (Atmakuri et al., 2004; Cascales et al., 2013; Li and Christie, 2018; Whitaker et al., 2015), $TraD_F$ (Haft et al., 2007; Lu and Frost, 2005; Lu et al., 2008) and $TrwB_{R388}$ (Hormaeche et al., 2006; Segura et al., 2014; Vecino et al., 2011). T4CPs from other subfamilies have also been characterized, although not in such depth. Among these ones there is the prototype of the TraG-J subfamily, $TraG_{R27}$ (Gunton et al., 2005, 2007), and the $Gram^+$ related $PcfC_{pCF10}$ (Chen et al., 2008) and $TcpA_{pCW3}$ (Steen et al., 2009). Additionally, in the last years, due to their importance in pathogenic processes, the study of T4CPs related to T4BSS has increased. In this case, the most studied ones have been $DotL_{L.\ pneumophila}$ (Kwak et al., 2017; Sutherland et al., 2012) and $Cagβ_{H.\ pylori}$ (Chang et al., 2018; Hu et al., 2019). In all those works, different aspects of T4CPs have been analysed, being the most common ones their phylogeny, the interactions with the relaxosome and the T4SS, the structure and the role of the different domains, the ATPase and nucleotide-binding activities, and the subcellular location. It must be underlined that, due to the difficulties of working with MPs, most of the *in vitro* studies carried out in these works were performed with soluble variants of the T4CPs.

To gain knowledge about T4CPs this work has been focused on two main aspects: (i) the role of the TMD of the paradigmatic VirD4-type T4CPs by the analysis of chimera proteins that interchange the TMD of different T4CPs; and (ii) the study of the T4CP of the mobilizable

plasmid CloDF13, $MobB_{CloDF13}$, since T4CPs of mobilizable plasmids are scarce and have not been characterized up to now. To do so, in the previous chapter a set of genes coding for T4CPs was cloned and their *in vivo* activities were tested. Once their functionality was proven, their expression conditions were optimized and purification protocols were developed. Additionally, in the previous chapter, the *in vivo* localization of the different T4CPs at different times and conditions was analysed. From the results obtained in the mating and purification assays, it was chosen to perform further biochemical and biophysical studies with the chimera protein $TMD_{TraJ}CD_{TrwB}$ and the $MobB_{CloDF13}$-MobBΔTMD pair. In particular, in this chapter their *in vitro* stability, DNA-binding capacity, oligomerization, structure, and ATP hydrolysis have been characterized. All the results obtained in the assays performed with $TMD_{TraJ}CD_{TrwB}$ and the $MobB_{CloDF13}$-MobBΔTMD have been compared with both $TrwB_{R388}$ and its TMD-less mutant TrwBΔN70 to better understand the role of the TMD and the differences between diverse members of the family.

During the characterization of the different T4CP variants, , their **stability was studied** first of all since keeping the proteins stable is essential to perform further *in vitro* assays. The initial conditions and the different assays that were performed were based on those previously published with $TrwB_{R388}$ (Hormaeche, 2003; Hormaeche et al., 2004; Vecino et al., 2011). In particular, the effects of temperature, ionic strength, pH, and DNA-binding upon stability were studied. Regarding $TMD_{TraJ}CD_{TrwB}$, it was seen that in the purification buffer its denaturation started at 35°C with a T_m of 51.1°C and therefore it was chosen to perform the *in vitro* characterizations at 25°C to avoid possible aggregation of the sample during reactions. This result suggested that the chimera protein could be slightly more stable against temperature than the native protein, which had a T_m of 48°C; however, it must be taken into account that $TrwB_{R388}$ was studied in less favourable conditions (lower DDM and NaCl concentrations) (Vecino et al., 2011). Additionally, the difference between the T_m of $TrwB_{R388}$ and TrwBΔN70 was more than twice the T_m difference between $MobB_{CloDF13}$ and MobBΔTMD, suggesting a different effect of the presence of the TMD in each system.

Afterwards, through AUC and Trp intrinsic fluorescence assays it was observed that the best conditions for maintaining $TrwB_{R388}$ and $TMD_{TraJ}CD_{TrwB}$ stability were pH 6.2, 0.6 mM DDM, and 300 mM NaCl, in which only 11% of protein loss was observed after 60 minutes. Additionally, it was seen that ionic strength below 300 mM NaCl was a limiting factor for the stability independently to the detergent concentration used. The Trp intrinsic fluorescence analysis performed with $MobB_{CloDF13}$ showed less protein loss at pH 5.6 and with detergent and salt concentrations above 0.6 mM DDM and 300 mM NaCl, respectively; in agreement with the stability patterns described for $TrwB_{R388}$ and $TMD_{TraJ}CD_{TrwB}$. On the contrary, AUC assays showed that $MobB_{CloDF13}$ did not form aggregates (species with an s-value higher than 20 S) as the R388 related proteins. Concerning the soluble mutant MobBΔTMD, it showed higher stability than all the tested MPs. Its thermal denaturation started at 55°C, achieving its T_m at 63°C, in a similar way to that observed with TrwBΔN70. Regarding the influence of detergent, it was seen that it had a protective effect, fully reducing protein denaturation in the tested conditions. The digestion assays performed with proteinase K reinforced the aforementioned results. In these experiments two different buffers were tested: Buffer A [*50 mM Tris-HCl (pH 7.8), 0.1 mM EDTA, and 10 % (v/v) glycerol*] and Buffer B (Buffer A supplemented with *0.6 mM DDM and 300 mM NaCl*). As expected, TrwBΔN70 and MobBΔTMD soluble mutants were more

stable than $TrwB_{R388}$ and $MobB_{CloDF13,}$ respectively. Additionally, the previously reported protective effect of DDM in MobBΔTMD was also observed. Regarding the full-length proteins, in agreement with the previous results, a reduction in the hydrolysis rate performed by protease K was observed in the presence of 0.6 mM DDM and 300 mM NaCl. Finally, these assays showed that the presence of DNA could affect the stability of T4CPs. Most likely, DNA-binding would cause a conformational change in the T4CP, a process observed in many DNA-binding proteins (Mizuguchi and Ahmad, 2014), and make the T4CPs more accessible for protease digestion, especially in the absence of detergent and low ionic strength.

To further study the **interaction between T4CPs and DNA** EMSAs were performed, as it had been previously done with TrwBΔN70 (Moncalián et al., 1999). These assays were performed in the same buffers as the proteinase K digestion. On the one hand, it was observed that in all the tested conditions DNA-binding rates were higher in the buffer lacking NaCl and detergent. A possible explanation for this could be that the presence of detergent surrounding the proteins together with the effect of high ionic strength impeded the binding of DNA to the protein. This hypothesis would explain why the effect of DNA in the hydrolysis performed by proteinase K was different in both tested buffers. On the other hand, significant differences were found between full-length proteins and their soluble mutants, reinforcing the role of the TMD in processes that happen in the CD, such as DNA-binding. Although binding capacity was higher in TrwBΔN70, $TrwB_{R388}$ and $TMD_{TraJ}CD_{TrwB}$ did also interact with DNA. Additionally, preliminary assays performed with the chimera protein suggested that DNA-binding could promote oligomerization of the protein, as seen with TrwBΔN70 (Matilla et al., 2010). Surprisingly, $TrwB_{R388}$-TrwBΔN70 and $MobB_{CloDF13}$-MobBΔTMD pairs showed opposite patterns concerning the role of the TMD in DNA-binding. Specifically, TrwBΔN70 showed a higher binding capacity than $TrwB_{R388}$, while the binding capacity of MobBΔTMD was lower than the one observed for $MobB_{CloDF13}$. In this regard, we have hypothesized that the TMDs of T4CPs of conjugative and mobilizable plasmids present different roles, as the later has to be more versatile to interact with different T4SSs that are not encoded by the mobilizable plasmid.

As the results obtained in the DNA-binding studies performed with $TMD_{TraJ}CD_{TrwB}$ suggested oligomerization processes, the next step was to analyse the **oligomeric behaviour** of the different proteins. Even though there still are many unknowns regarding the role of T4CPs during conjugation, the last studies have underlined their dynamic participation, in which changes in the oligomeric state would be required (Waksman, 2019). As studying the oligomerization stoichiometry and equilibrium is a difficult task, partly due to the difficulties associated with the calculation of the MW of MPs, three complementary approaches were used: SEC, BN-PAGE, and AUC. Even if each of them has its drawbacks, it was expected that their combination would shed light on the question of stoichiometry and oligomerization equilibrium of T4CPs. Unluckily, mainly regarding R388 related proteins, ambiguous results were obtained depending on the employed methodology. This observation emphasizes the importance of using different techniques when characterizing a protein. Even though $TrwB_{R388}$ and $TMD_{TraJ}CD_{TrwB}$ showed a mixture of oligomers, whose percentages varied according to the purification protocol and the experimental conditions of each assay, it seems that the most abundant species were the monomer and the dimer. The main difference when comparing both proteins was the higher monomer abundance in the native protein. Regarding CloDF13-related proteins, three main species were identified in varying percentages in $MobB_{CloDF13}$

samples, which were probably related to monomer, dimer, and trimer. The soluble mutant MobBΔTMD presented a similar behaviour, although in this case, the monomeric population was predominant (about 98.0%).

From such observations, different conclusions were drawn. On the one hand, regarding sample handling during purification, our findings suggested that the oligomer population of $TMD_{TraJ}CD_{TrwB}$ was affected by the concentration steps which promoted the oligomerization of the sample. Therefore, these steps should be avoided when performing oligomerization studies or when the oligomeric state of the protein is essential. On the other hand, it seems that our results with the different T4CP variants could reflect some of the different populations present *in vivo*. However, no hexamers were observed in our studies, which until now have been considered the active form of the protein. This absence could be related to different aspects: Firstly, to the purification protocol used to obtain the protein sample, as it has been widely proven that different oligomers can be obtained through different protocols (Hormaeche et al., 2002). Secondly, to the lack of the regulatory mechanisms present *in vivo* during the conjugative process, such as interactions with the relaxosome or other proteins from the T4SS that could influence the oligomeric state of T4CPs. Finally, to the conditions in which the experiments were carried out, such as protein concentration and ionic strength that could avoid the oligomerization equilibrium towards hexameric species. Additionally, the data obtained with $TMD_{TraJ}CD_{TrwB}$ underscored once again the importance of the TMD, as it did not behave like the native protein, showing similar patterns to those observed in TrwBΔN50, a mutant lacking the first transmembrane helix. The differences shown in the oligomerization pattern between the native and the chimera protein could be one of the explanations of the differences observed in the mating assays frequency, where $TMD_{TraJ}CD_{TrwB}$ performed conjugation at lower rates than $TrwB_{R388}$.

On another note, the results observed with the proteins of the CloDF13 system highlighted the importance of performing broad studies before extrapolating the data obtained from a single protein to its whole family. Specifically, our results with $MobB_{CloDF13}$ and MobBΔTMD have suggested that T4CPs related to conjugative and mobilizable plasmids could not share the same features. In this specific case, while the TMD is essential for the oligomerization of $TrwB_{R388}$, the absence of the TMD in MobBΔTMD protein did not seem to make any difference in comparison to $MobB_{CloDF13}$. With the aim of further studying this matter, the focus of the next chapter will be to reconstitute T4CPs in model membranes so that the different populations can be characterized through single-molecule techniques.

The next step in the characterization process was to study the **structure** of $TMD_{TraJ}CD_{TrwB}$ and the $MobB_{CloDF13}$-MobBΔTMD pair. First of all, their secondary structure components were analysed using IRS so that obtained results could be compared with the current literature (Hormaeche et al., 2004; Vecino et al., 2011, 2012). When analysing the obtained data it must be taken into account that due to the rearrangement of the bands and the presence of bands with mixed components it is difficult to establish the exact ratios between secondary structure elements. Nevertheless, it seems that the chimera protein showed structural features in between those described for $TrwB_{R388}$ and its TMD deletion mutants, with more periodical elements than the mutants, but still a less compact structure than the native protein. As the differences observed in the oligomerization pattern, these

structural differences could also be the cause of its lower functionality *in vivo*. This result underlined once again the importance of the TMD in the overall structure of a T4CP. Surprisingly, when using the same approach with $MobB_{CloDF13}$ and its soluble mutant both proteins presented similar spectra. These results come in agreement with those previously discussed regarding oligomerization, advocating that the effect of the TMD of $MobB_{CloDF13}$ upon its CD is not similar to that long-described for $TrwB_{R388}$.

Additionally, preliminary assays for establishing the 3D of $TrwB_{R388}$ and MobBΔTMD have been carried out. First of all, crystallization trials with the native protein were made under the supervision of Dr. Moraes in the MPL. Unluckily no crystals were obtained in any of the tested conditions, underlining the difficulties associated with MP crystallization (Birch et al., 2018). As an alternative approach, in collaboration with Dr. Berntsson from Umeå University, initial Cryo-EM assays are being performed, a revolutionary technique regarding structural studies with MPs (Cheng, 2018). The first trials have reported promising results, showing the protein in a predominant orientation on the grid. Next step would be to try different grids in order to increase the particle density inside each grid square. Regarding MobBΔTMD, as done with $TrwB_{R388}$, crystallization trials have been performed. However, in this case, through optimization of the growing conditions, several protein crystals were observed, even if they were not optimal for data harvest. In order to identify the best conditions in which to obtain diffracting crystals, the influence of protein concentration and glycerol have been studied up to now.

Finally, the **ATP hydrolysis activity** of $TMD_{TraJ}CD_{TrwB}$ and MobBΔTMD was studied with the aim of comparing the obtained results with the ones already published about TrwBΔN70 (Tato et al., 2005, 2007). The characterization of the chimera protein is particularly important because no ATPase activity of any wild type T4CP has been described to date. In addition, several comparative studies between $TrwB_{R388}$ and its soluble mutant point to a possible regulatory role of TMD in such activity. This chimera protein gives the opportunity to see if a heterologous TMD could deregulate the ATPase activity of a full-length T4CP

as it has been proven that the heterologous TMD affects the properties of the T4CP (*i.e., in vivo* activity, *in vitro* stability, oligomerization, DNA-binding, and structure). Although the first assays pointed to a possible ATPase activity, it was found to be a contaminant protein related to the S2 sample of $TMD_{TraJ}CD_{TrwB}$. Therefore, it seems that the presence of the heterologous TMD is enough to inhibit the activity presented by TrwBΔN70. This result could be related to the fact that the chimera protein is able to take part in conjugation and hence its activity must be regulated as the one of the native protein. It could be possible to speculate that regarding ATPase activity the T4CP could be in a latent non-active state in the cell and that once the conjugative process initiates, a series of signals could be transmitted along the T4SS, leading to a conformational change in the T4CP that would switch this protein to an active state. As postulated for the oligomeric behaviour, this signal could be transmitted through interactions with other proteins from the secretion system. It has been described that $TrwB_{R388}$ interacts with $TrwE_{R388}$ (the VirB10-like protein of R388 system) through their TMDs (Segura et al., 2013). Therefore, it could be hypothesized that as TrwBΔN70 lacks the TMD, its soluble domain would be permanently folded in the active state, unlike the full-length proteins.

At long last, a similar characterization was performed with MobBΔTMD. It showed an ATPase activity following a non-cooperative Michaelis-Menten kinetics, optimal at low ionic strength (75 mM NaCl), 45°C and pH 5.6. At the tested conditions this activity was not enhanced by the presence of DNA molecules, although more assays should be realized prior to drawing any conclusion, in addition to testing the Walker A MobBΔTMDK270T mutant.

5. KAPITULUA:

MOLEKULA-BAKARREKO ENTSEGU BALDINTZEN OPTIMIZAZIOA

5. MOLEKULA-BAKARREKO ENTSEGU BALDINTZEN OPTIMIZAZIOA

Kapitulu honen garapena García-Sáez laborategian burutu zen *Interfaculty Institute for Biochemistry* (IFIB)-n (Universität Tübingen, Tübingen, Alemania).

eGFP fusio-proteina guztiak GFP gisa izendatu dira nomenklatura errazteagatik.

5.1. SARRERA

Organismo desberdinen genomen azterketek genomaren %20-30a inguru MPez eraturik dagoela erakutsi dute (Wallin eta von Heijne, 1998). Proteina hauek hainbat funtzio burutzen dituzte zeluletan, batez ere garraio eta seinaleztapenarekin erlazionatuak. Arrazoi honengatik, hainbat gaixotasunekin erlazionaturik daude eta horren ondorioz farmakoen itu-molekulen %60a baino gehiago MPak dira (Hopkins et al., 2006). Egitate horrek proteina mota hau aztertzearen garrantzia azpimarratzen du. Hala ere, zelula-mintzaren konplexutasuna dela eta, MPen ekintza mekanismoei buruzko informazioa haien jatorrizko ingurunean lortzea ez da prozesu erraza. Horrenbestez, orokorrean, MPak aztertzeko estrategia erabiliena purifikazio bidez haien isolamendua egitea izan da. Erronka handia suposatzen duen zeregin hau oso konplexua denez, ez dago informazio askorik purifikaturiko MPen egitura edo portaera tridimentsionalaren inguruan (Seddon et al., 2004).

MPak isolatzeko mintzetik atera behar dira; hau normalean detergenteak erabiliz burutzen da eta urrats mugatzailea izan ohi da, 3. kapituluan azaldu bezala. Kontuan hartu behar da detergente guztiek ez dutela efektu bera proteinarengan, hau da, proteinaren disolbagarritasunerako detergente optimoak bere jarduera galaraz dezakeela, funtzioa mantentzen duen detergenteak egonkortasunerako desegokia izan daitekeen bitartean. Gainera, zelula mintza ingurune oso erregulatua dela kontutan hartuz, MPek mintzaren ezaugarriak behar dituzte haien funtzioa behar bezala betetzeko, hala nola, lipidoen eta beste proteinen presentzia. Hori dela eta, PDCak ez dira MPak aztertzeko sistema egokiena. MP batekin *in vitro* azterketak burutzeko egoera aproposena bere egoera natibora, hau da, proteina *in vivo* inguratzen duen bigeruza lipidikora, ahalik eta gehien gerturatzen den ingurumena lortzea izango litzateke. Hori dela eta, gaur egungo ikerketa askok MPak mintz-ereduetan berreraikitzea dute helburu.

Gaur egunera arte gehien aztertu diren T4CPak MP integralak dira, TMDrik gabeko mutanteak erabiliz aztertu direnak. Hori dela eta, oraindik erantzun gabeko galdera ugari daude T4CPen funtzionamenduaren alderdi dinamikoekin zuzenean lotuak.Besteak beste, oligomerizazioa eta ATPasa aktibitatea emateko beharrezko elkarrekintzak zeintzuk diren, zein den egoera oligomeriko funtzionala, edota zein den T4CParen kanalaren erabilera DNAren transferentzian zehar. Galdera hauek eraginkortasunez argitu daitezke gaur egun eskuragarri dauden teknika espektroskopikoak erabiliz. Teknika hauek bilakaera bizkorra jasan dute azken urteetan, bereizmen handiko mikroskopiaren garapena ekarriz. Haien erabilerak bio-zientzien arloan iraultza bat suertatu da, planteamendu kuantikoen bidezko prozesu biologikoen ikerketak ahalbidetuz. Gainera, teknika hauen erabilpenerako MPak mintz-ereduetan berreraiki behar dira eta hori, lehen esan bezala, haien ikerketarako ingurune aproposena da.

Teknika hauen artean GUV-bakarreko teknika esperimental bat garatu da, zeinaren bidez banakako GUV-en lotura eta iragazkortze zinetikak, besikulen tindatzaile betetze maila, eta egoera iragazkorren egonkortasunaren azterketa burutu daitekeen (Bleicken et al., 2016). Planteamendu metodologiko hau etorkizuneko proiektuetan erabil daiteke T4CP kanalen eraketan eta egonkortasunean sakontzeko, DNA garraiatzaile gisa duen eginkizunaren azterketarekin batera. Horretaz gain, bereizmen handiko mikroskopia tekniken artean, TIRFM teknika aurkitzen da, egokia dena MP integralen eta mintzekin elkarrekiten duten proteinen azterketak burutzeko. Teknika hau molekula-bakarreko irudien azterketa bidezko MPen estekiometria eta albo-difusioaren ikerketak egiteko erabili da era arrakastatsuan (Subburaj et al., 2016). TIRFM bidezko T4CP desberdinen azterketak informazio berria emango luke proteina hauen oligomerizazio mekanismo, estekiometria, eta dinamikari buruz. Halaber, mutante jakinak erabiliz, TMDak prozesu honetan duen eginkizun espezifikoa azter genezake. Hori guztia kontuan hartuta, kapitulu honen helburu nagusia **molekula-bakarreko saiakerak burutu ahal izateko protokoloak optimizatzea eta mintz-ereduetan berreraikitako T4CP lagin egokiak lortzea izan da**.

5.1.1. MINTZ-EREDUAK

Berreraikitze prozesuan zehar itu MPa bere jatorrizko ingurunearen antza duen bigeruza lipidikoan txertatzen da (Geertsma et al., 2008; Rigaud eta Lévy, 2003). Estrategia honen arazo nagusia arau oso gutxi egotea da, are gehiago, ez dago MP ororentzat erabilgarria den protokolo egokirik. Hori dela eta, berreraikitze prozesuak ahalegin enpiriko handia eskatzen du. Gaur egun, mintz-eredu ugari daude, normalean bi taldetan sailkatzen direnak: (i) berreraikitze-sistema simetrikoak edota (ii) konpartimentuetan oinarritutako berreraikitze-sistemak (Skrzypek et al., 2018); eta ikerketaren helburuak zein sistema aukeratzen den ezartzen du. Adibidez, ikerketa-sistema simetrikoetan non MPak bi aldeetatik eskuragarri dauden, hala nola nanodiskoetan (Denisov eta Sligar, 2017; Yokogawa et al., 2019), espektroskopia, batura eta elkarrekintzen azterketak burutu daitezke; ordea, ezin da garraio edota transferentzia entsegurik burutu, horretarako bi konpartimentutako sistemak behar baitira, hala nola, besikula lipidikoak. Aitzitik, proteinak sistema konpartimentalizatuetan berreraikitzerakoan bi noranzko desberdinetan koka daitezke. Normalean proteina bakoitzak zein joera izango duen ezin denez aurreikusi, faktore honek besikula lipidikoen erabilera muga dezake. Gaur egun gehien erabiltzen diren mintz-ereduak monogeruza lipidikoak, SLBak, eta besikula lipidikoak dira, liposoma moduan ere ezagunak. Tesi lan honetan SLBak eta liposomak erabili dira, baina lehenengoak bigarrenetatik eratorri zirenez, aurrerago azalduko dira.

Liposomak fosfolipido bigeruza batek nukleo urtsu bat inguratzen duenean sortzen diren besikulak dira (5.1. irudia). Lehenengo aldiz 1965. urtean deskribatu ziren (Bangham et al., 1965) eta geroztik haien erabilera asko hedatu da; izan ere, gaur egun liposomak farmakoen garraiorako eta bioezagumendurako tresna erabilienak dira (Lamichhane et al., 2018; Mazur et al., 2018). Besikula lipidikoak lamela-bakar edota lamela-anitzekoak izan daitezke. **MLV**ak era kontzentrikoan antolatutako bigeruza lipidikoen multzoak dira, haien artean ingurune urtsuz banandurik daudenak. Berez sortzen dira fosfolipido jakinak disoluzio urtsu batean aurkitzen direnean, zazpi eta hamar arteko geruzak izan ohi dituzte, eta 100 eta 5000 nm arteko diametroa. Ezaugarri hauen ondorioz ez dute inolako mintz-biologikoren antzik eta beraz normalean ez dira entsegu biofisikoak burutzeko erabiltzen.

Besikula lamela-bakarrak hiru talde desberdinetan sailkatzen dira haien tamainaren arabera (5.1. irudia): (i) **SUV**ak 200 nm baino txikiagoko lipido besikulak dira (normalean 20 eta 50 nm artekoak). Beren neurri txikiagatik kurbadura erradio txikia eta kanpoko monogeruzan lipido kopuru handiagoa dute (Szoka eta Papahadjopoulos, 1980). (ii) **LUV**ak, ordea, 200 eta 1000 nm arteko tamaina daukate (normalean 200 edo 400 nm-tako iragazkiekin sortzen dira), kapsulatze ahalmen altuarekin. Horretaz gain, lipidoen banaketa ia simetrikoa erakusten dute bi geruzetan (%54a kanpokoan eta %46a barrukoan). (iii) Hirurogeiko hamarkadan aldez aurretik aipatutako **GUV**ak sortzeko metodologia desberdinak garatu ziren. Liposoma hauek 1000 nm baino handiagoak dira, ia tokiko kurbadurarik gabeak. Haien tamaina handiak mikroskopio konfokal bidezko behaketa zuzena (Geertsma et al., 2008) eta molekula-bakarreko tekniken erabilera ahalbidetzen du (Bagatolli eta Needham, 2014).

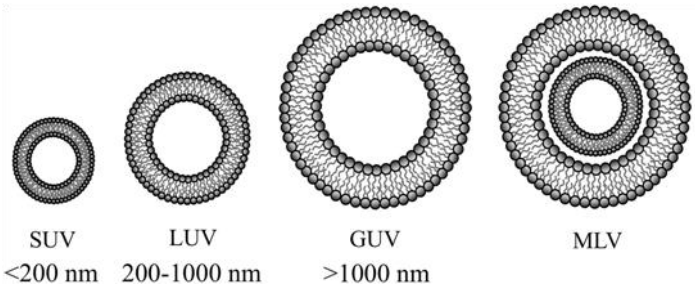

5.1. irudia. Lan honetan aurkeztutako liposoma desberdinen irudikapen eskematikoa. Lau taldetan banandu dira haien tamaina eta lamela kopuruaren arabera. Irudia Milcovich et al. (2017)-tik egokitua izan da.

Aurretik esan bezala, lipido besikulez gain beste mintz-eredu motak daude, hala nola, **SLB**ak, TIRFM entseguetan erabiltzen direnak. SLBak lortzeko liposomak (normalean SUVak) substratu solido batera fusionatzen dira, euskarri gainazaletik 10-20 Å-eko ur geruza baten bidez bananduriko bigeruza bat lortuz (5.2. irudia) (Castellana eta Cremer, 2007). Bigeruza honek mintzaren jariakortasuna mantentzen du. Mintz-eredu honek zenbait abantaila eskaintzen ditu eredu esferikoekin konparatuz, hala nola, mintz konposizio orokorraren eta lipido asimetriaren kontrola eta gainazalen erabilera espezifikoan oinarritutako hainbat tekniken erabilera (Crane eta Tamm, 2007).

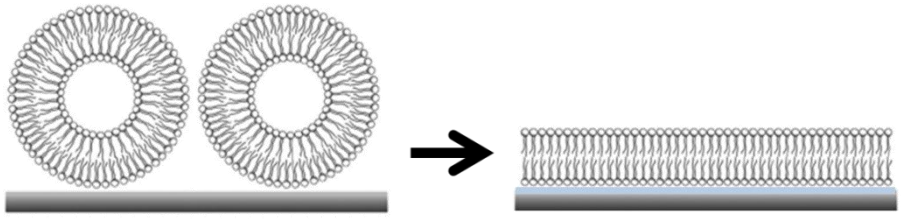

5.2. irudia. Eutsitako bigeruza lipidikoen eraketaren irudikapen eskematikoa. Gainazal solidoak liposomak xurgatzen ditu bertara fusionaturik geratuz. Modu horretan gainazal solidotik ur geruza batez bananduriko bigeruza lipidikoa lortzen da. Irudia Åkesson et al. (2012)-tik egokitua izan da.

5.1.2. PROTEINEN BERRERAIKITZERAKO METODOAK

Liposomak itu proteinen berreraikitzerako abiapuntu gisa erabili ziren. MPen berreraikitzea bere sorreratik eboluzionatu den arren (Geertsma et al., 2008; Rigaud eta Lévy, 2003; Rigaud et al., 1995), oraindik egoera bakoitzerako optimizatu egin behar da denbora asko daramaten prozesu enpirikoen bidez. TIRFM eta GUV-bakarreko entseguak burutzeko, T4CPak SLB eta GUVetan berreraiki behar dira, hurrenez hurren. MP baten berreraikitzea burutzerakoan, alderdi ugari hartu behar dira kontutan, adibidez erabiliko diren lipidoak, purifikazioan erabilitako detergentearen ezaugarriak, edota detergente hori ezabatzeko erabiliko den prozesua.

Irizpide desberdinetan oinarritutako hainbat metodo ebatzi dira LUVetan MPen berreraikitzea burutzeko. Erabilienak disolbatzaile organikoen bidezko berreraikitzea (Deamer eta Bangham, 1976), metodo mekanikoak (Racker, 1979), aldez aurretik sortutako liposometara zuzenean gehitzea (Scotto eta Zakim, 1986) eta detergente bidezko txertatzea (Rigaud et al., 1995) dira. Azken hau argitaratutako lanetan erabili da LUVetan $TrwB_{R388}$ T4CParen berreraikitzerako (Vecino et al., 2010, 2011). Hala ere, kontutan hartu beharra dago LUVetan egindako berreraikitzeak desabantaila handia dakartela karakterizazio entseguak burutzeko orduan. Izan ere, tamaina eta proteina edukiari dagokionez lortzen den proteoliposomen populazioaren izaera heterogeneoaren ondorioz, entseguetan jasotako neurriak baldintza desberdinetan aurkitzen diren proteinen batez bestekoaren islapena dira. Arazo hau saihesteko eta informazio zehatzena lortzeko aukerarik onena besikula-bakarreko entseguak dira, zehazki, aldez aurretik izendatutako GUV-bakarreko entseguak (Bagatolli eta Needham, 2014). Zoritxarrez, oraindik ez da inolako protokolorik garatu GUVetan T4CPen berreraikitzea burutzeko.

GUVen sorreran erabiltzen diren metodologia bortitzen ondorioz, oso zaila da haietan MPak berreraikitzea; hori dela eta GUVen sorrera protokoloak proteina laginekin leunagoak izateko moldatu behar dira. Honetarako hainbat metodo garatu badira ere (5.3. irudia) (Jørgensen et al., 2017), oraindik kasu bakoitzerako modu enpirikoan optimizatu behar den prozesu luzea da.

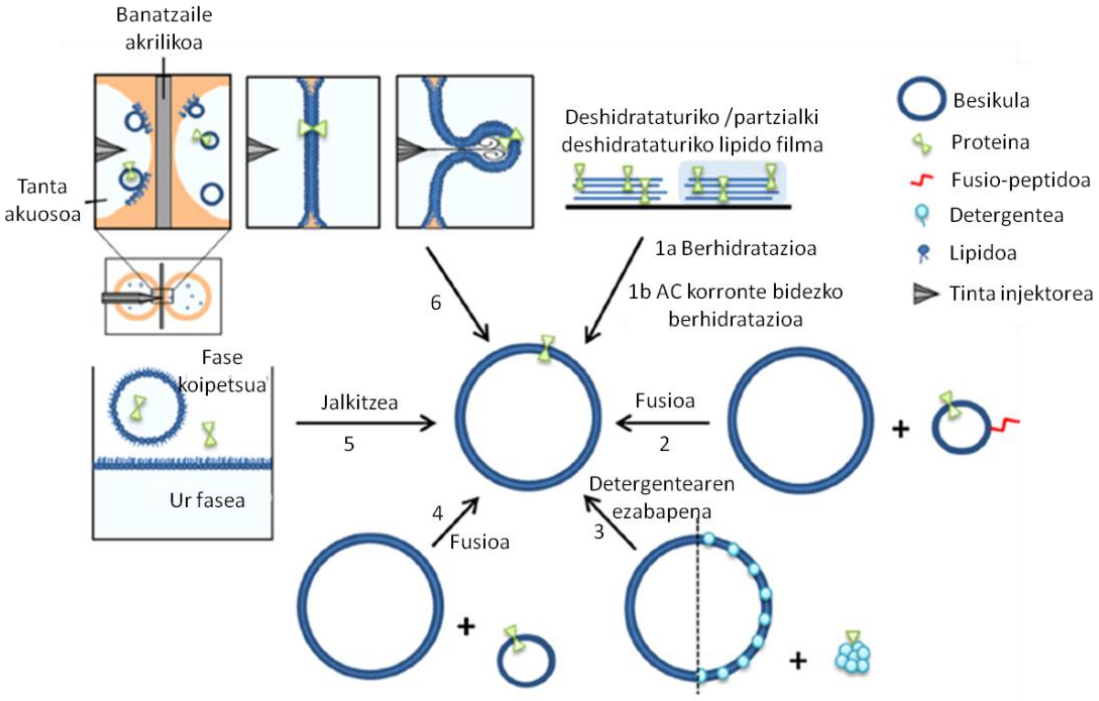

5.3. irudia. GUVetan proteinen berreraikitzea burutzeko metodo desberdinen irudikapen eskematikoa. 1: Deshidratazio-berhidratazio metodoak. Berhidratazioa bi metodo erabiliz egin daiteke: (1a) hantura espontaneo bidez edo (1b) AC korronte elektrikoa bat erabiliz. 2: Aldez aurretik sortutako GUVen fusioa peptido fusogenikoak dauzkaten proteoliposomekin. 3: Detergente bidez solubilizaturiko proteinen berreraikitzea aldez aurretik sortutako GUVetan (solubilizatu zein ez-solubilizatuak) fusioa emateko detergentearen ezabapena beharrezkoa da. 4: Aldez aurretik sortutako GUV-en eta proteoliposomen fusio espontaneoa. 5: Tanta transferentziaren metodoa: monogeruza lipidiko batez estalitako tantak beste monogeruza baten gainean jalkitzen dira. Proteinak tantaren barne zein kanpo ingurunean aurki daitezke, lortu nahi den noranzkoaren arabera. 6: Txertaketa mikrofluidikoak: soluzio koipetsu batez betetako ganbera batean banatzaile akriliko baten bidez banandurik dauden bi tanta urtsuren ertzetan monogeruza proteolipidikoak sortzen dira. Banatzailea kentzen denean monogeruzak elkartu egiten dira bigeruza proteolipidiko lau bat lortuz, zeina GUVak sortzeko erabiltzen den. Irudia Jørgensen et al. (2017)-tik egokitua izan da.

Deshidratazio-berhidratazio metodoak proteoliposomen edo purifikaturiko mintz biologikoen deshidratazioan oinarritzen dira, ondoren proteo-GUVak osatzen dituen berhidratazio bat burutuz (Poolman et al., 2005). Planteamendu honen oztopo nagusia deshidratazio urratsa da, zeinetan proteinak desnaturalizatu, agregatu edota inaktibatu ahal diren. Deshidratazio-berhidratazioa burutzeko bi estrategia desberdin daude, alde batetik (i) hantura espontaneoa (5.3. irudia, 1a**5.3. irudia**) (Reeves eta Dowben, 1969) eta beste aldetik elektroformazioa (5.3. irudia, 1b) (Angelova et al., 1992). Besikulen hantura espontaneoa burutzeko teknikarik erabiliena agarosa gel bidezko hantura espontaneoa da (Saliba et al., 2014). Dena den, ikusi da agarosaren presentzian eratutako GUVek ez dutela agarosaren ausentzian eratutakoen ezaugarri berberak. Arazo hau saihesteko, polibinil alkohol (PVA) gelak erabiltzen dituen aldaera erabiltzen hasi da (Weinberger et al., 2013). Gel bidezko hantura metodo sinplea da, non konposizio fisiologikoa duten lipido eta indargetzaileak erabil

daitezkeen. Teknika honetan tamaina desberdinetako GUVak lortzen dira eta indargetzaileetan monosakaridoen presentzia gomendatzen da proteinen desnaturalizazioa ekiditeko (Tsumoto et al., 2009). Elektroformazioari dagokionez, metodo azkarra da eta GUV homogeneoak lortzen dira eraketa prozesuan laguntzen duen AC-eremu elektriko bat aplikatuz. Metodo hau sortu zenetik optimizatu bada ere (Girard et al., 2004; Shaklee et al., 2010), oraindik eragozpen batzuk aurkezten ditu, hala nola, ekipo espezifikoen beharra edo lipido poliasegabeen oxidazio arriskua.

Deshidratazioarekin zerikusia duten arazoak ekiditeko, metodo desberdinak garatu dira zeintzuetan GUVen eraketa proteinaren berreraikitzea baino lehen burutzen den. Estrategia horiek baldintza desberdinetan GUVak eratzea ahalbidetzen dute, aztergai diren MPak kaltetu gabe. **Peptidoek eragindako fusioan** (5.3. irudia, 2), aldez aurretik sortutako proteoliposomei peptido fusogenikoak kobalenteki atxikitzen zaizkie. Ondoren, peptidodun proteoliposomak aldez aurretik eratutako GUVekin inkubatzen dira proteo-GUVak lortzeko. Metodo honen bidez, besikulen populazio homogeneoa lortzen da baina lan eskerga egin behar da eta mintzean fusio-peptidoak egotearen ondorioz berreraikitako proteina kantitatea mugaturik aurkitzen da.

Honetaz gain, proteo-GUVen lorpenerako **detergente bidezko** proteoliposomen eraketa protokoloetan oinarritutako bi aldaera garatu dira (5.3. irudia, 3) (Dezi et al. (2013). Lehenengoan, GUVak detergentearen presentzian sortzen dira, ondoren PDCekin elkartzen diren GUV ezegonkorrak lortuz. Bigarrenean, PDCak aldez aurretik eratutako GUVekin nahasten dira eta gero detergentearen kontzentrazioa igotzen da saturaziora heldu arte, non proteinak ezegonkortutako GUVetara txertatzen diren. Bi metodoak detergentearen ezabapenarekin bukatzen dira BBak erabiliz. Protokolo hauek proteoliposomak edota mintz natiboak erabiliz ere burutu daitezke, nahiz eta etekin baxuagoa lortu. Detergente bidezko berraraikitzeak metodo sinplea badirudi ere, egoera eta proteina bakoitzarentzat optimizatu behar da.

GUV eta proteoliposomen arteko **fusio espontaneoa**, nahiz eta metodo sinplea izan, geldoa eta proteina txertaketa etekin baxukoa da(5.3. irudia, 4) (Varnier et al., 2010). Hala ere, kontrako kargadun besikulak erabiltzen dituen aldaera bat deskribatu da (Biner et al., 2016). Aldaera horretan karga positibodun lipidoak dauzkaten proteoliposomak karga negatibodun GUVekin elkartzen dira. Teknika interesgarria da proteinen noranzkoa mantentzen delako. Hala ere, gerta liteke zenbait proteinek kargadun lipidoekin bateraezinak izatea.

GUVetan proteinen berreraikitzea burutzeko azken bi teknikak **tanta transferentziaren metodoa** (5.3. irudia, 5) (Walde et al., 2010) eta **txertaketa mikrofluidikoa** (5.3. irudia, 6) (Richmond et al., 2011) dira. Biak hiru pausutako metodoak dira, zeintzuetan baldintza fisiologikoak erabil daitezken eta banaketa asimetrikozko bigeruza lipidikoa lortzen den proteinen noranzko kontrolatuarekin. Optimizazioa behar duten protokolo erronkatsuak dira eta txertaketa mikrofluidikoaren kasuan ekipamendu oso espezifikoa ere ezinbestekoa da.

Kapitulu honetan, aurrerago molekula-bakarreko saiakerak burutzeko asmoz, metodo hauetako batzuk optimizatu dira **GUVetan T4CPen berreraikitzea** egiteko, hain zuzen ere agarosa gel bidezko hantura espontaneoa, elektroformazioa eta detergente bidezko berreraikitzea.

5.2. LIPIDO KONPOSAKETAREN OPTIMIZAZIOA

Mintz-ereduen konposaketa lipidikoa oso anitza izan daiteke, ehuneko desberdinetan nahastu daitezkeen lipidoen sorta handia dagoelako. Liposoma baten lipido konposaketa zehatzak liposomaren ezaugarriak ezartzen ditu, hala nola egonkortasuna, karga, eta mintzaren iragazkortasuna eta jariakortasuna. Frogatu egin da lipidoak MPen funtzioan eragin garrantzitsua daukatela (Gupta et al., 2017; Phillips et al., 2009); horretaz gain, zenbait proteinek lipido jakinen presentzia behar dute *in vivo* haien funtzioa burutzeko, adibidez mitokondrioetako pirubato garraiatzailea, zeinak CL behar duen funtzionatzeko; edota P-glikoproteina, zeinaren ATPasa aktibitatea kolesterolaren presentzian areagotzen den (Opekarová eta Tanner, 2003). Beraz, berreraikitze prozesua burutzeko aukeratzen den lipido konposaketa oso garrantzitsua da (Daghastanli et al., 2004). Proteinen berreraikitzerako fosfolipido erabilienak jatorri naturaletik lortutako fosfatidilkolina (PC) molekulak dira (Rigaud eta Lévy, 2003). Hauek oso arruntak dira haien koste baxuagatik, karga neutroa aurkezteagatik eta kimikoki inerteak izateagatik. Dena den, nahasketan kargadun lipidoak gehitzea gomendatu ohi da, karga negatiboek liposomen fusioa eragozten dutelako haien agregazioa oztopatuz.

Tesi honetako ikergaia T4CPak dira, bakterioen barne-mintzean (*bacterial inner membrane*, BIM) aurkitzen direnak. Lan honetan *E. coli* anduietan gain-adierazi direnez, haien inguruneko lipido konposizioa *E.coli* BIMena da: %74 PE, %5-19 PG eta %3-20 CL (Gennis, 1989). Gure taldean $TrwB_{R388}$rekin egindako aurreko lan batean aztertu zen ea bere funtzioa berreraikitze prozesuaren edota erabilitako lipido konposizioaren ondorioz kaltetzen zen (Vecino et al., 2011). Honetarako hiru lipido konposizio desberdin aztertu ziren: (i) PE:PG:CL (76,3:19,6:4,1), BIMa imitatzen duena; (ii) PE:PG:CL:Besteak (57,5:15,1:9,8:17,6), *E.coli* lipidoen aterakin komertziala; eta (iii) PC liposomak. Nahiz eta *E.coli* BIMean PCrik ez egon, berreraikitzerako fosfolipido erabiliena denez bere ikerketa ere egin zen. $TrwB_{R388}$ren berreraikitzea hiru konposaketa desberdin hauetan burutu zen, etekin desberdinak lortuz, eta lehenengo konposaketa arrakastatsuena izanik. Entsegu hauen bidez ikusi zen berreraikitzeak $TrwB_{R388}$ren nukleotidoekiko lotura afinitatea eta ATParekiko espezifikotasuna areagotzen zuela.

Hala ere, lipido konposaketaren optimizazioa burutu behar izan zen GUVetan berreraikitzea egin ahal izateko, lipido konposaketa guztiek ez baitute liposoma mota guztiak sortzeko balio. Honetarako Elektrotransformazio ganbarakazaldutako elektroformazio metodoa erabili zen. PE (*E. coli* jatorrikoa), PG (*E. coli* jatorrikoa), CL (behi bihotzekoa) eta DOPC (oilo arrautzekoa) lipidoak erabili ziren, DiO tindatzailearekin nahastu zirenak haien bistaratzerako. BIMa imitatzen duen lipido konposaketa erabiliz (PE:PG:CL, 76,3:19,6:4,1) egitura tubularrak lortu ziren, GUV txiki batzuekin (5.1. taula). GUV-bakarreko entseguak burutzeko beharrezko GUV handiak lortzeko liposomen konposaketa optimizatu zen, PE edukia DOPCrekin ordezkatuz ehuneko desberdinetan (PG eta CL ehunekoak 19,6 eta 4,1ean mantendu ziren, hurrenez hurren). Horretaz gain, *E. coli* lipidoen aterakin komertziala ere erabili zen DOPCarekin ehuneko desberdinetan nahastuz. Lortutako emaitzak 5.1. taulan laburbildurik agertzen dira eta irudi guztiak datu gehigarrietan aurkitzen dira (S5.1. irudia).

5.1. taula. Lipido konposaketa desberdinekin lortutako GUV laginen laburpena. *E. coli*-ren BIMa imitatzen zuten bi lipido nahasketa desberdin erabili ziren: (i) *E. coli* lipidoen aterakin komertziala eta (ii) PE:PG:CL (76,3:19,6:4,1) nahasketa. Lehenengo kasuan lipido aterakina DOPCrekin ordezkatu zen ehuneko desberdinetan. Bigarren kasuan, PEa DOPCarekin ordezkatu zen ehuneko desberdinetan, PG eta CL ehunekoak mantendu ziren bitartean. Lipidoak DiOrekin tindatu eta GUVak elektroformazioz eratu ziren, 2.8.1.4. atalean azaldu bezala. Laginen bistaratzea *ZEISS LSM 710 ConfoCor 3* fluoreszentziazko mikroskopio konfokalean burutu zen. z.g.: zehaztu gabea; ø: diametroa.

	***E. coli* lipido aterakina**	**PE:PG:CL:DOPC**
%0 DOPC	Besikula txikien kantitate urria (gehienez 20 µm ø)	Egitura tubularrak besikula gutxi batzuekin
%5 DOPC	z.g.	GUV txikiak (~20 µm) egitura tubularrekin
%10 DOPC	Besikula txikien kantitate urria (gehienez 20 µm ø)	GUV gutxi batzuk (gehienez 30 µm ø)
%20 DOPC	Besikula txikien kantitate urria (gehienez 30 µm ø)	GUV handiagoen ehuneko altuagoa (gehienez 30 µm ø)
%30 DOPC	z.g.	GUV handiagoen ehuneko altuagoa (gehienez 50 µm ø)
%40 DOPC	GUVen kantitate handia (gehienez 70 µm ø)	Lipido ia guztia GUVak eratzen aurkitzen da (gehienez 60 µm ø)
%50 DOPC	GUVen kantitate handia MLV askorekin (gehienez 50 µm ø)	GUV handiagoen ehuneko altuagoa (gehienez 70 µm ø)

Mintz baten kurbadura bere osagaien berezko kurbadurarekin oso lotuta dago (Marsh, 1996). Haien geometria molekularrean oinarriturik lipidoen berezko kurbatura negatibo, neutro edo positibo gisa sailkatzen da. Berezko kurbatura negatiboa daukaten lipidoak, PE bezala, bigeruza lipidikoaren kurbatura areagotzen dute, kurbatura neutrodunak, DOPC bezala, bigeruza lauak edota kurbatura baxuko besikulak sortzeko joera duten heinean (Kurczy et al., 2014). Honetan oinarrituz, PE ehuneko altuko lipido konposaketek egitura tubularrak edota besikula txikiak eratzeko joera dute, *E. coli* lipido aterakinarekin eta BIMa antzematen duen konposaketarekin GUVak lortzeko saiakeran ikusi bezala. Konposaketa horietan DOPCaren gehitzeak eragin bikoitza izan zuen: alde batetik lortutako GUVen kopurua handitu zen DOPC ehunekoa handituz joan ahala eta beste aldetik GUV horien tamaina baita handitu zen.

Lehen aipatu bezala, kapitulu honen helburuetako bat GUV-bakarreko saiakerak burutu ahal izateko proteo-GUVak lortzea zen. Atal honetan erakutsitako emaitzek frogatzen dute LUVetan $TrwB_{R388}$ren berreraikitzea egiteko erabili zen lipido konposaketa ez zela egokia GUVen eraketarako. Hala ere, GUVen eraketarako lipido konposaketa optimizatzerakoan batez-besteko 70 µm-ko tamaina zuten **GUV kopuru egokia lortu zen DOPC:PE:PG:CL (50:26.3:19.6:4.1) lipido nahasketa erabiliz** (5.4. irudia). Beraz, lipido konposaketa hau erabili zen GUVetan T4CPen berreraikitzea burutzeko entseguetan.

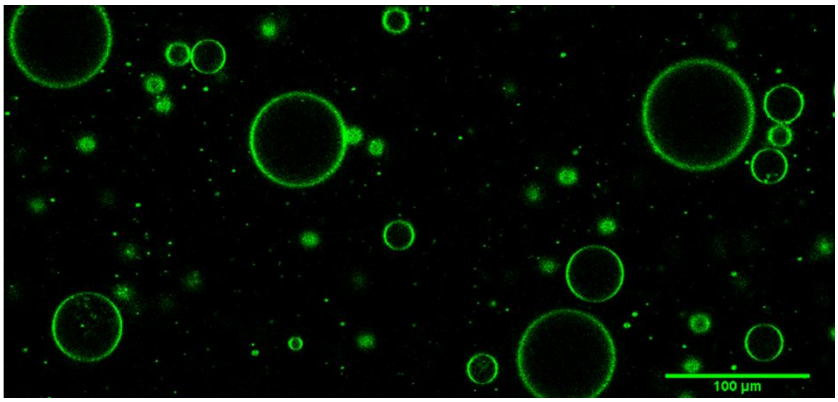

5.4. irudia. DOPC:PE:PG:CL (50:26.3:19.6:4.1) lipido nahasketarekin lortutako GUVak. DiOren presentzian sortutako GUVak *ZEISS LSM 710 ConfoCor 3* fluoreszentziazko mikroskopio konfokalean bistaratu ziren. Laginen kitzikapena 488 nm-tan burutu zen, fluoreszentziaren igorpena 505-540 nm tartean neurtu zen bitartean.

5.3. PROTEINA FLUORESZENTEEN EKOIZPENA

Proteina bat fluoreszentziako mikroskopio konfokalaren bidez aztertzeko fluoreszentzia igorpen iturri bat izan behar du, hau da, fluoroforo bat. Proteina fluoreszenteak estrategia desberdinen bidez lor daitezke, adibidez, aldaketa genetikoen bidez domeinu fluoreszentedun fusio-proteinak sortuz (Enterina et al., 2015), molekula fluoreszenteekin konjokaturiko antigorputzen bidezko immunomarkaketa erabiliz (Giepmans et al., 2006), edota zunda fluoreszenteak erabiliz markaketa kimiko zuzena burutuz (Toseland, 2013).

5.3.1. MARKAKETA KIMIKO ZUZENA

T4CP fluoreszenteen lorpenerako aldez aurretik purifikaturiko T4CPak Atto zunda fluoreszenteekin kimikoki konjokatzea erabaki zen (Bleicken et al., 2013). Zehazki Atto maleimidak erabili ziren, proteinen tiol taldeekin erreakzionatzen dutenak 7,0-7,5 pH tarte optimoan. Zunda berde bat (Atto 488) eta bi zunda gorri (Atto 633 eta Atto 655) erabili ziren. Markaketa $TrwB_{R388}$ren CDa zuten proteinei egin zitzaien ($TrwB_{R388}$, TrwBΔN70, eta $TMD_{TraJ}CD_{TrwB}$), zisteina eskuragarri bat daukatenak (Vecino et al., 2010). $TraJ_{pIP501}$ eta $MobB_{CloDF13}$rekin erlazionaturiko proteinek hiru eta zazpi zisteina zeuzkaten sekuentzian, hurrenez hurren. Zisteina hauen eskuragarritasuna ezezaguna zenez zunda kopuru desberdinen lotura gerta liteke, estekiometria azterketetarako baliogarria ez dena.

Proteinen markaketa 2.8.2. atalean azaldu bezala burutu zen. Laburbilduz, lehenengo eta behin indargetzaileen aldaketa burutu zen, laginen pHa maleimida erreakzioen pH optimora doitzeko. Horretarako laginak indargetzaile egokiarekin diluitu ondoren *Vivaspin 500*® zentrifuga kontzentratzaileak erabiliz kontzentratu ziren. Behin proteinaren kontzentrazioa neurturik, lagin bakoitza zunda kontzentrazio egokiarekin inkubatu zen gau osoan zehar. Hurrengo egunean lotu gabeko zunda garbitu zen. Horretarako, hasiera batean *His-Trap* zutabeetan oinarritutako estrategia erabili zen baina proteinaren galera handia ematen zenez eta TrwBΔN70rentzat baliogarria ez zenez bere erabilera alboratu zen.

Zutabeen pausua ordezkatzeko kit komertzial bat erabili zen lotu gabeko zundak kentzeko, etxe komertzialaren aholkuak jarraituz. Dena den, kitaren erabileraren ostean oraindik zunda aske ugari geratzen zenez laginean, indargetzaile egokiarekin diluitu eta ondoren kontzentratuz deuseztatu zen. Hasiera batean 3 kDa MWCOko iragazkiak erabili ziren baina proteinaren agregazio bortitza eman zenez azkenean 30 (TrwBΔN70rentzat) eta 100 kDa ($TrwB_{R388}$ eta $TMD_{TraJ}CD_{TrwB}$) MWCOeko iragazkiak erabili ziren. Markaketaren eraginkortasuna 280 nm-tako absorbantzia eta zunda bakoitzaren fluoreszentzia igorpena neurtuz kalkulatu zen. Neurketa hauetan oinarrituz laginean proteina eta zundaren kontzentrazioak kalkulatu ziren Lambert-Beer ekuazioa erabiliz (2.1. ekuazioa). Zunda guztia proteinei lotuta aurkitzen zela gain hartuz, proteina eta zunda kontzentrazioen arteko erlazioak markaketa eraginkortasuna adierazten zuen.

Zunda gorrien presentzian, Atto 633 eta 655, MPak agregatzeko joera aurkezten zutela ikusi zen, proteina galera handia eta markaketa etekin baxua lortuz (5.2 taula). Zunda berdearekin ordea, **ATTO 488, emaitza egokiak lortu ziren, batez ere $TrwB_{R388}$ri dagokionez** (5.2 taula). Emaitza hauek kontutan hartuta, T4CP fluoreszenteak lortzeko aukera gisa eGFP fusio-proteinak erabiltzea erabaki zen, markaketa pausu baten beharra deuseztatuz. Honen inguruan, aipatu beharra dago $TrwB_{R388}$GFPren *in vivo* funtzionalitatea dagoeneko frogatu dela eta berarekin egindako ikerketak argitaratuak izan direla (Segura et al., 2014). Beraz, itu-proteinek fluoroforo berdea izatearen ondorioz mintz-ereduen fosfolipidoak fluoreszentzia gorria daukan DiDrekin markatzea erabaki zen.

5.2. taula. Atto zunden markaketaren eraginkortasuna. $TrwB_{R388}$, TrwBΔN70 eta $TMD_{TraJ}CD_{TrwB}$ maleimidaren erreakzioen bidez Atto zundekin markatu ziren 2.8.2. atalean azaldu bezala. Taulako balioek soberako zunda garbitu ostean erreakzio bakoitzean markaturiko proteina ehunekoa adierazten dute.

	λ_{Abs}	$TrwB_{R388}$	TrwBΔN70	$TMD_{TraJ}CD_{TrwB}$
Atto 488	501 nm	%83,6	%65	%53.6
Atto 633	630 nm	%37	n.d.	%29
Atto 655	663 nm	Agregatuak	n.d.	%33

5.3.2. BAKTERIO BARNE-MINTZEKO BESIKULEN EKOIZPENA

Aurreko atalean esan bezala, MPen markaketaren emaitzak ikusita, GFP fusio-proteinak erabiltzea erabaki zen, dagoeneko haien *in vivo* funtzionaltasuna frogatuta baitzegoen (3.3. atala) (Segura et al., 2014) eta proteina molekula bakoitzeko fluoroforo bakarra eskaintzen baitzuten. Horretarako, eGFP fusio-proteinak gain-adierazita zeuzkaten BIMak purifikatu ziren, T4CP fluoreszentedun BIMVak lortuz. Sistema honen erabilerak abantaila zein desabantailak aurkezten ditu. Alde batetik lagin kopuru handia lortzen da eta T4CPak haien jatorrizko ingurunean aurkitzen dira, BIMeko lipido eta proteina espezifikoekin, itu-proteinen egonkortasun edota oligomerizatzeko joeran eragin dezaketenak. Bestalde, BIMVetako proteina:lipido erlazioa (~60:40) ez zen egokia GUVen sorrerarako abiapuntu gisa erabiltzeko. Horretaz gain, T4CPak bi noranzkoetan kokaturik aurkitzen ziren, GUV-bakarreko entseguak burutzeko oztopoa zelarik.

BIMVak lortzeko erabilitako protokoloa 2.8.3.2. atalean deskribatu da (Jiménez et al., 2011). Laburbilduz, *E. coli* BL21C41(DE3) bakterioetan $TrwB_{R388}$GFP eta $MobB_{CloDF13}$GFP fusio-proteinen indukzioa burutu zen eta justu honen ostean (0 laginak, 1 L), indukziotik ordu batera (1 laginak, 2 L) eta indukziotik bi ordutara (2 laginak, 2 L) bakterio esekidurak jaso ziren. Ondoren, zelulak apurtu, mintza isolatu eta sakarosa gradiente bat erabiliz kanpo eta barne mintzak banandu ziren. Barne-mintzen frakzioak jaso, garbitu eta indargetzaile egokian berreseki ziren, **T4CP-GFP proteinekin aberastutako BIMVak lortuz**. Bukaeran 250 eta 500 µL-tako laginak lortu ziren induzitu gabeko eta induzitutako laginetatik, hurrenez hurren. Proteina kontzentrazio totala (T4CP-eGFP fusio-proteinak gehi BIMean aurkitzen ziren gainerako proteina guztiak) 280 nm-tako absorbantzia neurtuz kalkulatu zen (5.3. taula). Kontrol negatibo gisa, protokolo bera jarraitu zen *E. coli* BL21C41(DE3) zelulak erabiliz, inolako proteina heterologoren gain-adierazpenik burutu gabe.

5.3. taula. BIMV laginen proteina kontzentrazio totala. $TrwB_{R388}$GFP eta $MobB_{CloDF13}$GFP *E. coli* BL21C41(DE3) bakterioetan gain-adierazi ziren haietan aberastutako BIMVak lortzeko, 2.8.3.2. atalean azaldu bezala. Taulan agertzen diren balioek BIMV lagin bakoitzeko proteina kontzentrazio totala adierazten dute (T4CP-eGFP fusio-proteinak eta BIMeko proteina guztiak). [a]250 µL-ko lagina [b]500 µL-ko lagina.

	0 h[a]	1 h[b]	2 h[b]
$TrwB_{R388}$GFP	T0: 2,0 mg/mL	T1: 1,0 mg/mL	T2: 3,0 mg/mL
$MobB_{CloDF13}$GFP	M0: 2,4 mg/mL	M1: 1,6 mg/mL	M2: 1,6 mg/mL

5.4. GUVetan T4CPen BERRERAIKITZEA

Behin GUVak eratzeko lipido konposaketa egokia identifikaturik eta T4CPen aldaera fluoreszenteak lorturik, GUVetan itu proteinen berreraikitzea burutzeko estrategia desberdinak frogatu ziren.

5.4.1. BERRERAIKITZE ZUZENA: GUVen ERAKETA DETERGENTEAREN PRESENTZIAN

GUVetan T4CPen berreraikitzea egiteko lehenengo saiakera Dezi et al. (2013)-ek deskribaturiko detergente bidezko metodoan oinarritu zen (5.3. irudia). Argitaratutakoaren arabera, metodologia honen bidez detergente kontzentrazio ez-solugarridun sakarosa disoluzioetan GUVen eraketa egiten da elektroformazioz. Behin GUVak lorturik, purifikatu eta solubilizaturiko MPekin nahastu egiten dira, noranzko bakarreko proteinen txertaketa zuzena emanez. Ondoren, BBak erabiliz detergentearen ezabaketa egiten da eta proteo-GUVak entsegu indargetzaile espezifikoan diluitzen dira.

Beraz, lehenengo pausua detergentearen presentzian fluoreszenteki markaturiko GUVen eraketa burutzea izan zen. Horretarako DDMa (bukaeran 0,2 mM-eko kontzentrazioan) lipido nahastarekin elkartu zen eta 400 mM sakarosa disoluziodun elektroformazio ganbaretan GUVak sortu ziren 10 Hz eta 1,1 V erabiliz 3,5 ordutan zehar. Protokolo hau jarraituz ez zenez GUVik lortu, protokoloaren aldaera desberdinak saiatu ziren, bi sakarosa disoluzio (300 edo 400 mM sakarosa), bi elektroformazio protokolo (10 Hz, 1,1 V, 3,5 h edo 10 Hz, 1,5 V, 2 h eta 2

Hz, 1,5 V, 1 h) eta bi lipido konposaketa [(*E. coli* extract:DOPC (50:50) edo DOPC:PE:PG:CL (50:26,3:19,6:4,1)] konbinatuz. Hala ere, ez zen GUVik lortu frogatutako zortzi aldaeretan. Gerta liteke honen arrazoia detergentea lipido nahasketara eta ez sakarosa disoluziora gehitzea izatea; izan ere, elektroformazioan zehar 0,2 mM DDM izateko lipido nahasteak 14 mM DDM zeukan. Honen ondorioz, detergentea elektroformazio ganbarako sakarosa disoluzioari zuzenean gehitzea erabaki zen. Dena den, aldaketa hau egiteak ez zuen inolako eraginik izan GUVen eraketa prozesuan. Saiakera guztietan kontrol positibo gisa GUVen eraketa burutu zen detergentearen absentzian, 5.2. atalean erakutsitako emaitza berdinak lortuz. Saiakera hauekin bukatzeko, elektroformazio protokoloa ITOz estalitako estalkiak erabiliz burutu zen (ITO estalkiak) (Angelova et al., 1992; García-Sáez et al., 2010), mikroskopio konfokalaren bidez prozesuaren bistaratze zuzena egin ahal izateko. Protokolo aldaera guzti hauek frogatu arren (5.4. taula), **ez zen GUVik lortu detergentearen presentzian**.

5.4. taula. GUVen eraketarako elektroformazio bidez 0,2 mM DDMren presentzian frogatutako protokolo aldaeren laburpena. Detergentearen ondorioz ezegonkortutako GUVen eraketarako bi lipido konposaketa, bi sakarosa kontzentrazio, DDMa gehitzeko bi metodo, bi elektroformazio protokolo eta bi elektroformazio metodo frogatu ziren.

	Alternatives	
Lipido konposaketa	*E. coli* aterakina:DOPC (50:50)	DOPC:PE:PG:CL (50:26.3:19.6:4.1)
Sakarosa kontzentrazioa (mM)	300	400
DDMaren gehipena	Sakarosa disoluzioa	Lipido nahasketa
Elektroformazio protokoloa	10 Hz, 1,1 V, 3,5 h	10 Hz, 1,5 V, 2 h eta 2 Hz, 1,5 V, 1 h
Elektroformazio metodoa	Elektroformazio ganberak	ITOz estalitako estalkiak

5.4.2. PROTEO-GUVen ERAKETA PROTEOLIPOSOMAK ERABILIZ

LUVetan T4CPen berreraikitzea Vecino et al. (2010)-k deskribatu bezala burutu zen. Hori dela eta, lehenengo saiakerak egiteko aukeratutako proteina $TrwB_{R388}$ izan zen. Dena den, aurretik azaldu bezala, erabilitako lipido konposaketa aldatu zen, GUVak eratzeko konposaketa optimoa erabiliz, DOPC:PE:PG:CL (50:26,3:19,6:4,1), alegia.

5.4.2.1. PROTEOLIPOSOMEN ERAKETA

Laburbilduz, LUVak 2.8.1.3. atalean azaldu bezala eratu ziren, aukeratutako lipido konposaketa erabiliz. Konposaketa hau literaturan deskribaturikoa ez zenez, lortutako LUVen solubilizazio kurbaren azterketa burutu behar izan zen (5.5. irudia). Kurba honek PE:PG:CL (76,3:19,6:4,1) konposaketarekin lortutako kurbaren antza zeukan, hiru pausutako solubilizazio prozesua aurkeztuz (Helenius eta Simons, 1975). Lehenengo pausuan, detergentea mintzean txertatzen da asetasunera heldu arte. Puntu hau lortzen den detergente:lipido erlazioari R_{sat} deritzo. Bigarren pausuan, liposomak solubilizatu egiten dira egoera lamelarretik (besikulak) mizeletara (solubilizaturiko lipidoak) igaroz, uhertasunaren beherakada bat eragiten delarik. Azken pausuan, fosfolipidoak guztiz solubilizatzen dira, disoluzio garden bat lortuz. Puntu hau gertatzen den detergente:lipido erlazioari R_{sol} deritzo. DOPCrik gabeko konposaketarekin konparatuz, %50eko DOPCdun konposaketak R_{sat} eta R_{sol} balio altuagoak aurkeztu zituen: 10,6

7,6ren aurka eta 13,9 10,4ren aurka, hurrenez hurren. Beraz, LUVetan $TrwB_{R388}$ren berreraikitze protokoloa balio hauetara egokitu zen.

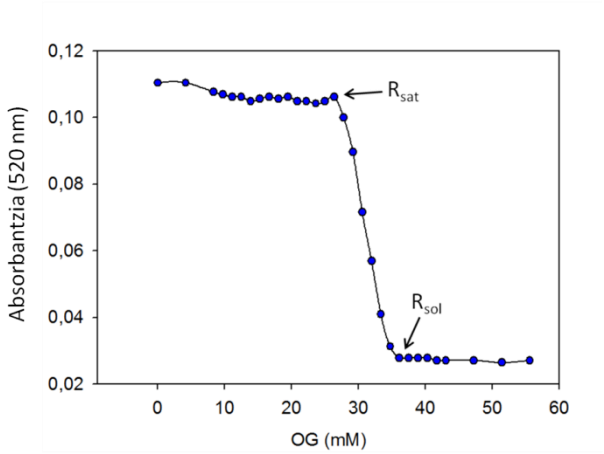

5.5. irudia. OG detergente bidezko DOPC:PE:PG:CL (50:26,3:19,6:4,1) liposomen solubilizazioa. Liposomen solubilizazio prozesua 520 nm-tan absorbantzia neurtuz jarraitu zen 2.8.3.1.atalean azaldu bezala. R_{sat} (10,6) eta R_{sol} (13,9) balioak besikulak detergentez saturaturik eta lipidoak guztiz solubilizaturik aurkitzen diren detergente:lipido erlazio balioak dira, hurrenez hurren.

Proteoliposomen eraketarako 6,25 mM liposoma 74,78 mM OGrekin solibilizatu ziren, 30 minutuz 25°C-tan inkubatuz. Ondoren, purifikaturiko 25 µM $TrwB_{R388}$ nahasketara gehitu ziren, bolumena 500 µL-ra doituz eta nahasketa berriz inkubatuz baldintza berdinetan. Kontrol negatibo gisa, prozesu berdina burutu zen proteinarik gehitu gabe. Hurrengo pausuetan Vecino et al. (2010) deskribaturiko protokoloa jarraitu zen: detergentea BBak erabiliz kendu zen eta lagineko populazio desberdinak (*i.e.,* liposoma hutsak, proteoliposomak eta agregaturiko proteina) sakarosazko gradiente zentrifugazio bidez banandu ziren. Lortutako frakzio bakoitzean lipido eta proteinaren presentzia aztertu ziren eta lipidoa soilik (liposoma hutsak) eta lipido eta proteina (proteoliposomak) zeuzkaten frakzioak jaso eta garbitu ziren bukaerako laginak lortzeko. Lortutako proteoliposomek 73,3:1 lipido:proteina erlazio molarra aurkezten zuten, 3,74 µM proteina kontzentrazioa zutelarik. Beraz, **konposaketa berriarekin DOPCrik gabeko konposaketarekin baino proteina txertatze etekin altuagoa lortu zen** (73,3:1 *vs.* 99:1, hurrenez hurren). Honetarako azalpen bat DOPCaren berezko kurbadura neutroak proteinen txertaketa erraztu izana da.

Bukatzeko, proteoliposometan $TrwB_{R388}$ren noranzkoa aztertu zen, proteinaren determinazioaazaldu bezala. Entsegu honen oinarria CDan kokaturiko zisteina bakarra eta tiol-erreaktiboen erabilera da. DOPCrik gabeko proteoliposometan gertatu bezala (Vecino et al., 2010), DOPC:PE:PG:CL (50:26,3:19,6:4,1) konposaketan **$TrwB_{R388}$ CDa besikularen kanpoko alderantz kokatuz berreraiki zen** (5.6. irudia).

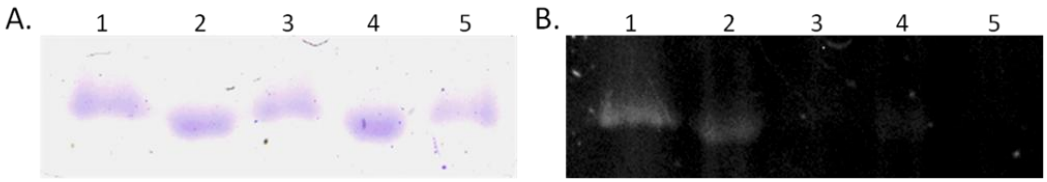

5.6. irudia. $TrwB_{R388}$ren noranzkoa DOPC:PE:PG:CL (50:26,3:19,6:4,1) proteoliposometan. Proteoliposoma laginak [$TrwB_{R388}$ DOPC:PE:PG:CL (50:26,3:19,6:4,1) liposometan berreraikita] tiol-erreaktibo iragazkor eta iragazgaitzekin inkubatu ziren 220 mM OGren presentzian edo absentzian, proteinaren determinazioaazaldu bezala. Laginen garbiketa burutu ostean, haien azterketa egin zen SDS-PAGE bidez. **A)** *Coomasie* urdin tindatzaile bidezko proteinen bistaratzea. **B)** 5-IAF zundarekin markaturiko $TrwB_{R388}$ren fluoreszentziaren bistaratzea *ChemiDoc*^{TM} bidez. 1: proteina totala; 2: kanporantz zuzendutako proteina; 3: barrurantz zuzendutako proteina; 4: kanpoko fluoreszentzia ez-espezifikoa; 5: guztizko fluoreszentzia ez-espezifikoa.

5.4.2.2. GUVen ERAKETA PROTEOLIPOSOMETATIK

Proteoliposomak deshidratazio/berhidratazio metodoak erabiliz GUVak lortzeko abiapuntu gisa erabili ziren (5.3. irudia). Zehazki, elektroformazio ganbara zein ITOz estalitako estalkietan elektroformazio saiakerak eta agarosa gel bidezko hantura espontaneozko saiakerak burutu ziren 2.8.1.4. atalean azaldu bezala (Weinberger et al., 2013).

Lehenengo eta behin, DOPCa (1 mg/mL lipido) DiDrekin (1 µM) nahastu zen, sonikazio bidez DiDrekin markaturiko DOPC-SUVak lortzeko. Lortutako besikulen 5 µL, 15 µL $TrwB_{R388}$dun proteoliposomekin nahastu ziren. Horretaz gain, berreraikitze prozesuan lortutako liposoma hutsak kontrol gisa erabili ziren. Kasu horretan 10 µL liposoma (1,33 mM lipido) bortex bidez nahastu ziren DiDrekin. Elektroformazioa burutzeko lagin bakoitzeko 5 µL erabili ziren, agarosa gel bidezko hantura espontaneorako 10 µL erabili ziren bitartean. Bi kasuetan *GUV hantura indargetzailea* (400 mM sakarosaduna) erabili zen.

Detergenteen presentzian GUVen eraketarekin gertatu bezala, ez zen GUVik lortu elektroformazioa erabiliz. Are gehiago, ITOz estalitako estalkiak erabiliz GUVen eraketa mikroskopioz bistaratzerakoan besikula txikiak zituen lehorturiko lipido geruza bat soilik ikusi zen (5.7. irudia). **Agarosa gel bidezko hantura espontaneoari dagokionez, GUVen eraketa ikusi zen liposoma hutsen kasuan zein proteoliposomen kasuan.** Liposometatik lortutako besikulek 15 µm-tako batez-besteko tamaina zeukaten, proteoliposometatik eratorritakoak 10 µm baino txikiagoak ziren bitartean. Teknika berdina erabiliz KvAP proteinadun antzeko tamainako proteo-GUVak lortu zirenez, gerta daiteke lorturiko GUV tamaina teknikarekin erlazionaturik egotea eta ez laginaren konposaketarekin (Garten et al., 2015).

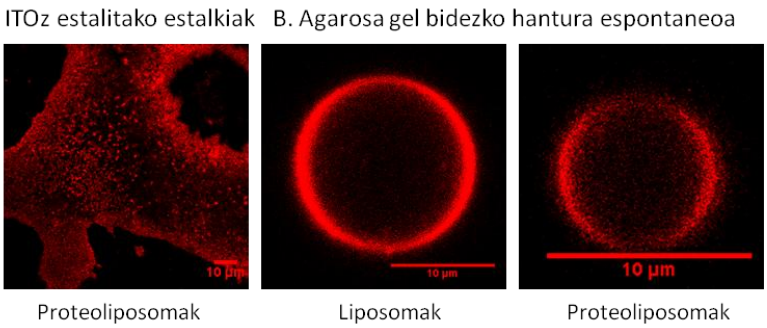

5.7. irudia. GUVen eraketa $TrwB_{R388}$ proteoliposomak abiapuntu gisa erabiliz. Aurreko atalean lortutako liposoma hutsak eta proteoliposomak GUVen eraketarako abiapuntu gisa erabili ziren. Honetarako bi teknika desberdin erabili ziren (**A**) elektroformazioa eta (**B**) agarosa gel bidezko hantura espontaneoa. Elektroformazioa burutzeko elektroformazio ganbarak eta ITOz estalitako estalkiak erabili ziren, azken hau eraketa prozesuaren bistaratze zuzena burutzeko *ZEISS LSM 710 ConfoCor 3* fluoreszentziazko mikroskopio konfokala erabiliz. Lagin guztien kitzikapena 633 nm-tan egin zen, fluoreszentzia igorpena 655 nm gainetik neurtu zen bitartean.

Aurrerago T4CPen eta G4-DNA egituren arteko elkarrekintza ikertzeko asmoz, hartu beharreko hurrengo pausua itu-proteinek proteo-GUVetan hartzen duten noranzkoa aztertzea izango litzateke; proteoliposometan bezala kanpoko noranzkoa mantentzen dutela ziurtatzeko, DNA-rekin lotura emateko ezinbestekoa dena. Ondoren, prozesu osoa proteina fluoreszenteak (Atto 488 zundarekin markatutako proteinak, zein T4CP-eGFP fusio-proteinak) erabiliz errepikatu beharko liratezke FCCS entseguak egin ahal izateko. Dena den, kontutan hartu behar da metodologia honen bidez sortutako GUVak agarosarik gabeko metodoen bidez lortutako GUVekin konparatuz ezaugarri mekaniko desberdinak erakusten dituztela. Bestalde, agarosaren presentziaren ondorioz GUV hauek izan ditzaketen portaera desberdinek funtzioaren inguruko ikerketak burutzea oztopa dezakete (Lira et al., 2014). Hori dela eta, nahiz eta agarosa gel bidezko hantura espontaneoz abiapuntu gisa erabiltzeko lagin onak lortu, T4CPak GUVetan berreraikitzeko teknika alternatiboak ere aztertu ziren.

5.4.3. BARNE-MINTZEKO BESIKULA UNILAMELAR ERRALDOIEN ERAKETA

Aurretik azaldu bezala, $TrwB_{R388}$GFP eta $MobB_{CloDF13}$ proteinez aberastutako BIMVak lortu ziren (5.3.2. atala) haietatik barne-mintzeko besikula unilamelar erraldoiak (*giant unilamellar inner membrane vesicles*, GUIMVs) lortzeko. Proteo-GUVen eraketarako BIMVak erabiltzearen abantailetako bat, proteinen purifikazio beharrik ezaz gain, proteinen funtziorako garrantzitsuak izan daitezkeen jatorrizko mintzaren osagai desberdinak GUVetan ere aurkitzen direla da (*e.g.*, mintzeko lipido eta proteinak). Dena den, BIMVak duten lipido:proteina erlazioa (~40:60) ez da GUVen eraketarako egokia. Hori dela eta, proteina kantitatea murrizteko BIMVak DOPC-SUVekin nahastea erabaki zen, proteoliposomekin egin bezala (ikusi aurreko atala). Kasu honetan hiru teknika desberdin erabili ziren: elektroformazioa, agarosa gel bidezko hantura espontaneoa eta aldez aurretik eratutako DOPC-GUVekin fusioa. Hurrengo ataletan erakusten diren lipido:proteina erlazio guztiak DOPC pisu molekular:lagineko proteina kantitate totalaren pisu molekularrari (w/w) egiten diote erreferentzia.

5.4.3.1. ELEKTROFORMAZIOA

Lehenengo eta behin, elektroformazio saiakera bat burutu zen BIMVen T2 laginarekin (5.3. taula) ITOz estalitako estalkiak eta GUVen elektroformaziorako protokolo estandarra erabiliz (2.8.1.4. atala). Honetarako DiDaren presentzian DOPC-SUVak eratu ziren sonikazioz eta ondoren BIMV T2 laginarekin nahastu ziren 80:1 erlazioan. Saiakera honetan ez zen GUVik lortu; izan ere, bazirudien DOPC-SUVak ez zirela BIMVekin guztiz nahastu deshidratazio prozesuan zehar (5.8. irudia). Emaitza hauek hobetzeko entsegu desberdinak egin ziren parametro desberdinen aldaerak erabiliz, hala nola lipido:proteina erlazioa, hantura indargetzailea, elektroformazio protokoloa, eta abar. Entsegu hauek lau saiakera desberdinetan laburbildu dira:

1. GUVen eraketa T2 eta M2 BIMV laginak erabiliz (5.3. taula) lau baldintza desberdinetan frogatu zen: DiDa BIMVetara edo DOPC-SUVetara gehituz; eta BIMVak sonikatu edo sonikatu gabe erabiliz (5.8. irudia). Aldaera guzietan, lehenengo eta behin DOPC-SUVak sonikazioz sortu eta ondoren BIMV laginekin elkartu ziren 80:1 erlazioan. Ondoren, nahasketa elektroformazio ganbaretara gehitu eta hantura burutu zen *GUV hantura indargetzailea* erabiliz (elektroformazio protokoloa: 10 Hz, 1,5 V, 105 minutuz eta 2 Hz, 1,5 V, 45 minutuz, giro tenperaturan).

2. Lehenengo saiakeraren baldintza berdinak erabili ziren (T2 eta M2 BIMV laginak, 80:1 erlazioa, eta elektroformazio protokolo berdina), baina nahasketa bi modu desberdinetan burutu zen: alde batetik BIMVak DiDaren presentzian sonikatu eta ondoren aldez aurretik sortutako DOPC-SUVekin elkartuz eta beste aldetik osagai guztiak (DOPC, BIMVak eta DiDa) elkarrekin sonikatuz

3. Saiakera honetan DOPC-SUVak 37°C-tan sonikatu ziren aldez aurretik berotutako 300 mM sakarosa disoluzioan. Bitartean BIMVak (T2 eta M2 laginak) sakarosa disoluzio berdinean diluitu (1:10 erlazioan) eta DiDaren presentzian sonikatu ziren. Ondoren, DOPC-SUVak eta BIMVak 90:1 erlazioan nahastu ziren. Elektroformazioa 37 °C-tan eta *GUV hantura indargetzailean* burutu zen (elektroformazio protokoloa: 10 Hz, 1,5 V, 105 minutuz eta 2 Hz, 1,5 V, 45 minutuz), baina 300 mM sakarosa erabiliz 400 mM ordez.

4. Azken saiakera gatz kontzentrazio fisiologikodun indargetzaile batekin burutu zen (Jiménez et al., 2011; Pott et al., 2008): *50 mM Tris-HCl (pH 7,4), 150 mM KCl eta 100 mM sakarosa*. T0, T2, M0 eta M2 laginak (10 µg proteina) DiDrekin sonikatu ziren, DOPCrik gehitu gabe. Elektroformazioa 37 °C-tan egin zen 5.5. taulan deskribatutako protokoloa erabiliz.

5.5. taula. Gatz kontzentrazio fisiologikoan GUIMVen eraketarako erabilitako elektroformazio parametroak. GUIMVen eraketarako laugarren saiakera gatz kontzentrazio altuko indargetzaile baten erabileran oinarritzen zen. Erabilitako elektroformazio protokoloak lau pausu zituen (lerro bakoitza), zeinetan potentziala eta maiztasuna aldatu ziren.

	Potentziala	Maiztasuna	Denbora	Aldaketak
1	150 mV → 3900 mV	500 Hz	30 min	750 mV igoz bost minuturo
2	3900 mV	500 Hz	90 min	/
3	3900 mV	500 Hz → 50 Hz	45 min	50 Hz jaitsiz bost minuturo
4	3900 mV	10 Hz	20 min	/

Laburbilduz, nahiz eta baldintza desberdinetan hainbat saiakera burutu, ez zen emaitza egokirik lortu. Lehenengo saiakera multzoan DiDa BIMVetara gehitu zen, baina gero DOPC-SUVetara gehitzea erabaki zen, bi lipido jatorriak kolore desberdinez markatuak egoteko eta haien fusioa bistaratu ahal izateko. Modu honetan, deshidratazio prozesuan zehar besikula desberdinak fusionatzen ez zirela ikusi zen (5.8. irudia). Hori dela eta, hurrengo saiakeretan osagai guztiak (DOPC, BIMVak eta DiDa) elkarrekin sonikatu ziren. Hala ere, ez zen desberdintasunik ikusi bi aldaeren artean. Hurrengo saiakeretan DOPC ehunekoa handitu zen, GUVen eraketa errazteko. Horretaz gain, sakarosa gutxiago erabili zen hantura indargetzailean eta elektroformazioa 37°C-tan egin zen. Baldintza horietan ez zenez GUVik lortu, azken saiakera bat burutu zen Jiménez et al. (2011) deskribatutako protokoloa erabiliz, DOPC-SUVrik erabili gabe. Zoritxarrez, **ez zen GUVik bistaratu** protokolo honen bidez, ziur asko teknikarekin erlazionaturiko aldaera guztien ondorioz, hala nola erabilitako proteina eta lipido konposaketa, elektroformazio ganbera mota, ITOz estalitako harien luzera, eta abar.

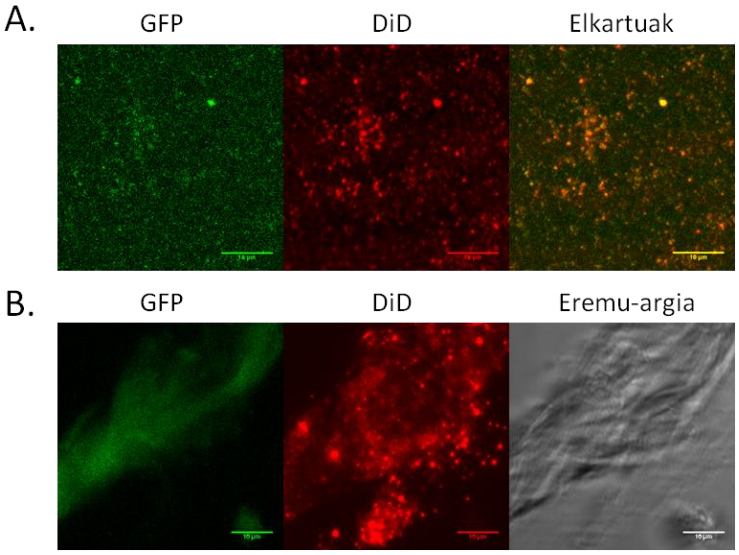

5.8. irudia. BIMVak abiapuntu gisa erabiliz GUVak lortzeko saiakerak. DOPC-DiD-SUVak T2 BIMV laginarekin nahastu ziren 80:1 erlazioan. Nahasketa GUVen eletroformaziorako lipido iturri gisa erabili zen, ondoko protokoloa erabiliz: giro tenperaturan 10 Hz, 1,5 V, 105 minutuz eta 2 Hz, 1,5 V, 45 minutuz. Laginen bistaratzea *ZEISS LSM 710 ConfoCor 3* fluoreszentziazko mikroskopio konfokalean burutu zen, kitzikapena 488 eta 633 nm-tan burutuz, GFP eta DiD fluoroforoentzat, hurrenez hurren. Fluoreszentzia igorpena 505 eta 540 nm tartean jaso zen

GFParentzat, eta 655 nm-tan DiDarentzat. **A)** Elektroformazioa ITOz estalitako estalkietan; **B)** Elektroformazioa elektroformazio ganberetan (1. saiakera). Eskala: 10 µm.

5.4.3.2. AGAROSA GEL BIDEZKO HANTURA ESPONTANEOA

BIMVak abiapuntu gisa GUVak lortzeko erabilitako bigarren teknika agarosa gel bidezko hantura espontaneoa izan zen. Nahiz eta teknika honen bidez lortutako GUVek entsegu funtzionalak burutzeko desegokiak izan, proteoliposomekin emaitza itxaropentsuak lortu zirenez, BIMVekin ere frogatu zen.

Elektroformazioan egin bezala, lehenengo eta behin sonikazioz DiD-rekin (25 nM) markaturiko DOPC-SUVak (2,5 mg/mL) eratu ziren, erabilitako indargetzailea *50 mM Hepes (pH 7,0), 500 mM KCl eta 6 mM* $MgCl_2$ izanez. Bitartean, 2 edo 10 µg BIMV (T2 lagina) 136 µL-ra diluitu eta indargetzaile berdinean sonikatu ziren. Ondoren, lagin bakoitza detergentearekin inkubatu zen 45 minutuz 25°C-tan irabiaketarekin (DOPC-SUVak 46,08 mM OGrekin eta BIMVak 4 edo 20 µM TritonX100rekin, 2 eta 10 µg-rentzat, hurrenez hurren). DOPC-SUV 64 µL BIMV laginetara gehitu ziren eta lortutako nahasketak giro tenperaturan inkubatu ziren ordu batez. Ondoren, detergentearen ezabapenerako laginak BBekin inkubatu ziren urrats desberdinetan: lehenengoz giro tenperaturan ordu erdiz 15 mg BBrekin, ondoren 30 mg BB gehiagorekin baldintza berdinetan eta bukatzeko 60 mg BB gehiagorekin (guztira 105 mg BB) gau osoan zehar 4 °C-tan. Hurrengo egunean, BBak zentrifugazio bidez kendu ziren eta lortutako laginen 10 µL agarosa gel bidezko hantura espontaneoa burutzeko abiapuntu gisa erabili ziren, 2.8.1.4. atalean azaldu bezala. Prozesu osoa detergenterik gabe ere burutu zen, detergente presentziaren kontrol gisa.

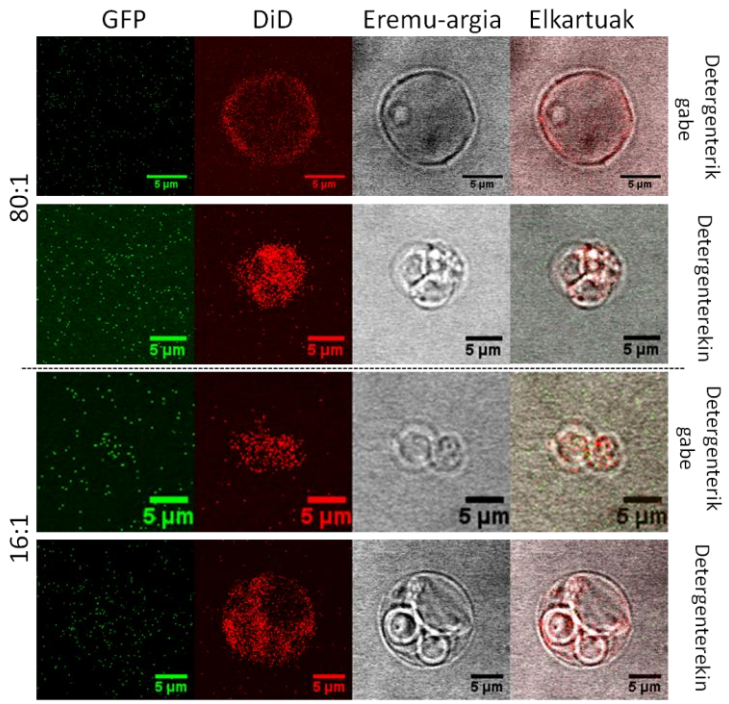

5.9. irudia. Agarosazko gel bidezko GUVen hantura espontaneoa solubilizaturiko DOPC-SUV eta BIMVak abiapuntu gisa erabiliz. Solubilizaturiko DOPC-DiD-SUVak eta $TrwB_{R388}$GFPn aberasturiko BIMVak lipido:proteina erlazio desberdinetan elkartu ziren eta lortutako

nahasketak agarosazko gel bidezko GUVen hantura espontaneorako abiapuntu gisa erabili ziren. Besikulen nahasketa detergenteen presentzian (1. eta 3. lerroak), zein absentzian (2. eta 4. lerroak) egin zen. Lortutako GUVen bistaratzea *ZEISS LSM 710 ConfoCor 3* fluoreszentziazko mikroskopio konfokal batean burutu zen, kitzikapena 488 eta 633 nm-tan burutuz, eGFP eta DiD fluoroforoentzat, hurrenez hurren. Fluoreszentzia igorpena 505 eta 540 nm tartean jaso zen eGFParentzat, eta 655 nm-tan DiDarentzat. eGFP fluoreszentzia, DiD fluoreszentzia, eremu-argiaren irudia eta aurreko hiruren elkartutako irudia 1., 2., 3., eta 4. zutabetan erakusten dira, hurrenez hurren. Eskala: 5 µm.

Ez zen emaitza egokirik lortu saiatutako baldintza desberdinetan (5.9. irudia). Izan ere, dirudienez ez zen DOPC-SUV eta BIMVen arteko fusiorik gertatu, mikroskopioz bistaraturiko besikulek fluoreszentzia gorria soilik igortzen baitzuten, DOPC lagineko DiDarekin erlazionaturik zegoena. Detergentearen absentzian, itxura unilamelarra zeukaten besikulak lortu ziren; detergentearen presentzian, ordea, bistaratutako besikula guztiak lamela-anitzekoak ziren. Nahiz eta teknika hau molda-erraza eta sinplea izan (Horger et al., 2009), berreraikitzea burutzeko deshidrataziorik gabeko beste teknikak erabiltzea erabaki zen, prozesuan zehar proteinei egindako kaltea murrizteko eta entsegu funtzionalak burutzeko GUV baliogarriak izateko.

5.4.3.3. BIMVen FUSIOA ALDEZ-AURRETIK ERATUTAKO GUVekin

Tesi honetan GUIMVak lortzeko erabilitako azken planteamendua besikulen arteko fusio espontaneoa (Varnier et al., 2010) eta detergente bidezko GUV eta besikula natiboen arteko fusioa (Dezi et al., 2013) elkartuz burutu zen. Lehenengo teknikaren etekin baxua eta detergentearen presentzian GUVak sortzeko arrakastarik gabeko saiakerak kontutan hartuz bi metodologiak nahastea erabaki zen. Horretarako GUVak detergentearen absentzian sortu eta ondoren BIMVekin elkartu ziren TritonX100ren presentzian. Modu honetan solubilizazio urrats bat gehitu zen, BBen bidezko detergentearen ezabapenaz jarraitua.

Lehenengo eta behin elektroformazioz DOPC-GUVak sortu ziren *GUV hantura indargetzailea* erabiliz. Ondoren T1 BIMV lagina (1 mg/mL bukaerako proteina kontzentrazioan) aldez aurretik sortutako DOPC-GUVekin elkartu zen lipido:proteina erlazio desberdinetan (60:1, 80:1, 100:1, eta 120:1) *GUV fusio indargetzailean*. Laginak gau osoan zehar inkubatu ziren agitaziorik gabe giro tenperaturan eta hurrengo egunean detergentearen ezabapena egin zen BBak erabiliz. Horretarako 5 mg BB gehitu ziren laginera eta lau orduz bira bertikalekin inkubatu ziren giro tenperaturan. Ondoren, BBak zentrifugazio bidez jalki eta GUVak jaso ziren fluoreszentziazko mikroskopio konfokalaz bistaratzeko (S5.2 irudia). Aztertutako lagin guztietan GUV txikiak identifikatu ziren. Dena den, GUV hauek ez ziren bi lipido iturrien nahasketak, baizik eta solubilizatu gabeko DOPC-GUVak. Are gehiago, BIMVak GUVak inguratuz kokatzen ziren, eGFParen fluoreszentziak adierazi bezala. Honen arrazoitzat TritonX100 detergenteak BIMVak baina ez DOPC-GUVak disolbatzen zituela jo zen.

Ondorioz, DOPC-GUVen solubilizazioa lortzeko bigarren saiakera bat burutu zen DDMaren presentzian. Hau egin ahal izateko, DDM bidezko DOPC-GUVen solubilizazioa aztertu zen, 25 µg/mL lipido 0,25 mM DDMrekin solubilizatzen zirela ikusiz. Erlazio hau fusio entseguetan mantendu zen. Horretaz gain, BIMV kantitatea 1 mg/mL-tik 0,2 mg/mL-ra jaitsi

zen, lehenengo saiakeran lortutako eGFP seinale bizia murrizteko. Ikusi zen DDMaren erabilerak bi besikulen fusioan laguntzen zuela (5.10. irudia) eta erabilitako lipido:proteina erlazioa garrantzitsua zela GUIMVak lortzeko. Zehazki, 400:1 erlazioan GUVak guztiz iragazkorrak bihurtzen zirela ikusi zen, 600:1 erlazioan guztiz iragazgaitzak ziren bitartean, DDMren absentzian gertatu bezala (S5.2. irudia). Ordea, 500:1 erlazioan nahasturiko laginekin emaitza itxaropentsuak lortu ziren. Nahiz eta lortutako besikulak egitura esferiko perfekturik ez izan, BIMVak DOPC-GUVekin fusionatu ziren, GUIMV txikiak lortuz. Beraz, **baldintza hauek eta garatutako fusio protokoloak abiapuntu gisa erabili beharko lirateke T4CP-eGFP proteinekin aberastutako GUIMVak erabiliz GUV-bakarreko saiakerak burutzeko**.

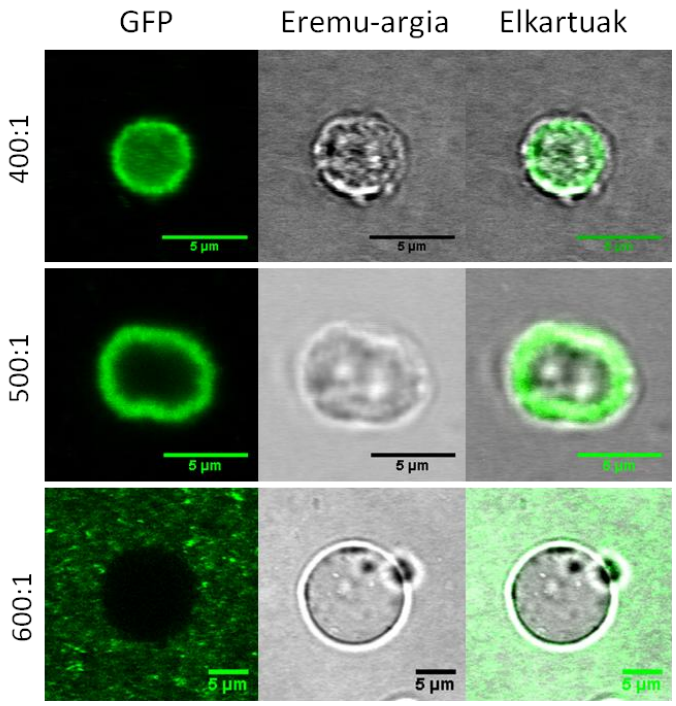

5.10. irudia. Detergente bidezko BIMVen fusioa aldez aurretik eratutako DOPC-GUVekin. DOPC-GUVak elektroformazioz eratu eta BIMVekin nahastu ziren *GUV fusio indargetzailean* lipido:proteina erlazio desberdinetan. *GUV fusio indargetzailea* TritonX100 eta DDMarekin aberastu zen BIMVen eta DOPC-GUVen solubilizaziorako, hurrenez hurren. Nahasketa gaur osoan zehar inkubatu ostean, detergentearen ezabapena burutu zen 5 mg BB erabiliz. BBak deuseztatu, GUVak jaso eta haien bistaratzea *ZEISS LSM 710 ConfoCor* 3 fluoreszentziazko mikroskopio konfokalean egin zen. eGFParen kitzikapena 488 nm-tan egin zen eta fluoreszentziaren igorpena 505-540 nm tartean jaso zen. eGFP fluoreszentzia, eremu-argiaren irudia eta aurreko bien irudi elkartua 1., 2., eta 3. zutabetan erakusten dira, hurrenez hurren. Eskala: 5 µm.

5.5. TIRFM ENTSEGUEN PRESTAKETA

Aurreko atalean T4CPekin GUV-bakarreko entseguak burutzeko protokoloen abiapuntua ezarri da, aurrerago T4CP eta DNA molekulen arteko elkarrekintzak ikertzeko asmoz. Saiakera hauekin batera T4CPekin TIRFM entseguak burutu ahal izateko protokoloen abiapuntuaren ebazpena ere egin zen, aurrerago T4CPen oligomerizazio mekanismoa, estekiometria eta dinamika aztertu ahal izateko. TIRFM entseguak egiteko protokoloak kasu bakoitzerako modu enpirikoan optimizatu egin behar dira, parametro desberdinen azterketa eginez, hala nola laginetako proteina kontzentrazioa edota irudi-jasotzearen iraupena.

Tesi lan honetan, lehenengo eta behin, SLBen jariakortasuna aztertu zen, ondoren mintzaren estaldura egokia lortzeko lipido:proteina erlazioa egokia ezarri zen, eta bukatzeko sistema osoaren optimizazioa egin zen TIRFM entseguetara egokitzeko. Abiapuntu gisa T4CP-GFP fusio-proteinekin aberastutako BIMVak erabili ziren, itu-proteinen ikerketa haien jatorrizko ingurune fisiologikoan burutzea ahalbidetzen dutelako. Hala ere, besikula hauek DOPC besikulekin fusionatu behar izan ziren, proteina kantitate totala murriztu eta SLBen eraketa errazteko (Dodd et al., 2008b). SLBak lortzeko protokolo orokorra 2.8.3.4. atalean aurkezten da. Optimizazio prozesuan zehar baldintza desberdin ugari frogatu zirenez, hurrengo ataletan egoera bakoitzeko irudi esanguratsu bat soilik erakusten da. Atal honetan adierazitako erlazio guztiak bukaerako lagineko DOPC:proteina (p:p) erlazioa adierazten dute.

5.5.1. BESIKULEN FUSIOA ETA MINTZAREN JARIAKORTASUNA

Protokolo ebazpen honen lehenengo helburuak DOPC eta BIMVen arteko fusioa eta jariakortasun egokidun mintza lortzea ziren.

Lehenengo saiakeran, 50 µg DOPC-SUV M1 (1,5 µg) eta T1 (3 µg) BIMV laginekin nahastu ziren, 83:1 eta 41:1 erlazioetan, hurrenez hurren. Kasu honetan DiDa DOPC-ra gehitu zen SUVak lortzeko sonikazioa egin aurretik, 67 nM-ko kontzentrazioan (%0,001), TIRFM entseguetan ohikoa dena (Subburaj et al., 2015). SLBak eratu eta 2.9.4. atalean azaldu bezala *ZEISS Axiovert 200* mikroskopioan bistaratu ziren. Ikusi zen 83:1 erlazioko lagina proteina kantitate egokia aurkezten zuela, 41:1 erlazioko laginean proteina kontzentrazioa oso altua zen bitartean. Bi kasuetan, DiD kontzentrazioa altuegia zen eta ez zen bere amatatzerik hauteman lau minutuko kitzikapenaren ostean (5.11. irudia). Bi besikulen arteko fusioari dagokionez, azpimarratu beharra dago eGFP fluoreszentzian mugimendu asko ikusi zela. Kontutan hartuz SLB mota honetan nahiz eta lipidoen difusioa eman proteinak beirazko gainazalera atxikitzeko joera aurkezten dutela, ikusitako mugimenduek atxiki gabeko besikulen presentzia iradokitzen dute. Horretaz gain, ez zen partikula mugikorren amatatzerik ikusi, beraz, baliteke partikula horiek proteina kantitate altuko fusionatu gabeko BIMVak izatea.

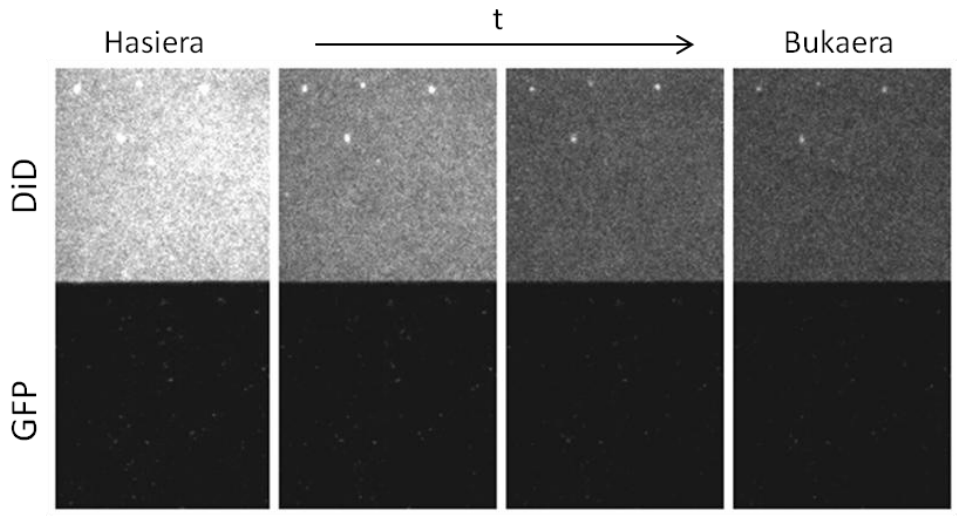

5.11. irudia. SLBen eraketaren lehenengo saiakera BIMV-DOPC-DiD nahasketa erabiliz. $MobB_{CloDF13}$GFPdun BIMVak aldez aurretik sortutako DOPC-DiD-SUVekin 83:1 erlazioan nahastu ziren. SLBak eratu eta *ZEISS Axiovert 200* mikroskopioan bistaratu ziren 2.9.4. atalean azaldu bezala. Proteina kantitatea: 1,5 µg. DiD kontzentrazioa: 67 nM. t: denbora.

Besikulen fusioa eta mintzaren jariakortasuna aztertzeko hurrengo saiakera M1 eta T1 BIMV laginekin egin zen berriz, aurreko atalean emaitza egokiak emandako 80:1 erlazioa erabiliz. DiD kontzentrazioa, ordea, hamar aldiz murriztu zen, 6,7 nM-era. Entsegu honetarako bi estrategia desberdin erabili ziren: lehenengoan SLBaren osagai guztiak (BIMVak, DOPCa eta DiDa) elkarrekin sonikatu ziren; bigarrenean, ordea, BIMVak DiDarekin sonikatu eta ondoren aldez aurretik eratutako DOPC-SUVekin nahastu ziren. SLBak C-Apochromat 40 X N.A. 1,2-ko ur-objetibo batekin hornitutako *ZEISS LSM 710 ConfoCor 3* fluoreszentziazko mikroskospio konfokalean bistaratu ziren. eGFP eta DiD fluoroforoen kitzikapena 488 eta 633 nm-tako laserrak erabiliz egin zen, hurrenez hurren; fluoreszentziaren igorpena 505-540 nm tartean eta 655 nm-tik gora jaso zen bitartean eGFP eta DiD fluoroforoentzat, hurrenez hurren.

Alde batetik, bigeruza lipidiko bat ikusi zen aztertutako lagin guztietan, BIMVak DiDarekin fusionatu zirela adieraziz. Beste aldetik, orokorrean eGFP eta DiDaren fluoreszentziak bat zetozen, nahiz eta zenbait guneek fluoroforoen banaketa ez-homogeneoa erakutsi, haietan eGFP edo DiDaren igorpena nagusituz (5.12. irudia). Erabilitako bi aldaerek antzeko emaitzak erakutsi arren, lehenengo estrategiaren bidez (BIMVak DiDarekin nahastuz eta ondoren DOPC-SUVekin) lortutako SLBek fluoreszentzia irregularreko gune gutxiago erakusten zituzten.

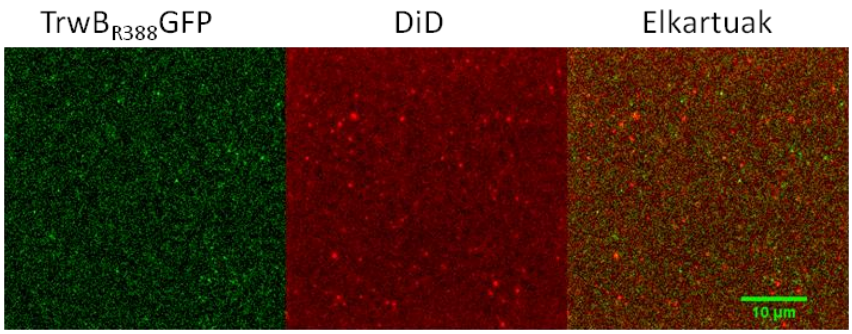

5.12. irudia. SLB eraketa eta besikulen fusioaren irudi esanguratsuak. TrwB$_{R388}$GFPrekin aberastutako BIMVak DiD eta DOPCrekin 80:1 erlazioan nahastu eta sonikatu ziren. Ondoren SLBak eratu eta *ZEISS Axiovert 200* mikroskopioan bistaratu ziren 2.9.4. atalean azaldu bezala. Proteina kantitatea: 1,5 µg. DiD kontzentrazioa: 6,7 nM. Eskala: 10 µm.

Ondoren, lortutako SLBen jariakortasuna FRAP saiakeren bidez aztertu egin zen, 2.9.3. atalean adierazi bezala. Laburbilduz, laginaren gune jakin batean DiDaren fluoreszentzia behatu zen eta ondoren gune hori intentsitate altuko argiarekin erradiatu zen, 633 nm-tako laserraren indarra %0,5tik %100era igoz. Honek DiDaren fluoreszentziaren bizitza agortzea eragin zuen, behatutako lagin azaleran gune beltz bat sortaraziz. Lipidoen alboko difusioaren ondorioz, erradiatutako gunearen kanpoan zeuden lipidoak, zeintzuen atxikitutako DiD molekulak fluoreszenteak ziren, gune beltzerantz lekualdatuz joan ziren, jatorrizko fluoreszentzia intentsitatea berreskuratu arte (5.13. irudia). Portaera hau aztertutako lagin guztietan ikusi zen. Dena den, hautemandako DiD fluoreszentzia oraindik altuegia zen TIRFM saiakerak burutzeko eta ondorioz DiDaren kontzentrazioa beste 10 aldiz jaitsi zen hurrengo entseguetan.

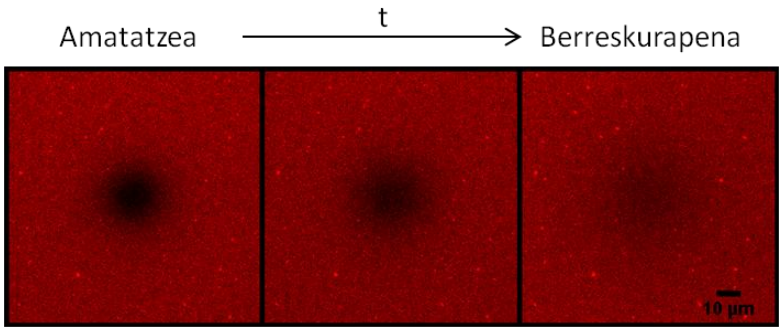

5.13. irudia. FRAP bidezko mintz-jariakortasunaren azterketaren irudi esanguratsuak. BIMVak DiDaren presentzian sonikatu eta aldez aurretik eraturiko DOPC-SUVekin elkartu ziren. Ondoren SLBak eratu eta *ZEISS LSM 710 ConfoCor 3* fluoreszentziazko mikroskopio konfokalaz bistaratu ziren. Lagineko gune bat 633 nm-tako laserrarekin erradiatua izan zen intentsitate altuan (%100 laser indarra), DiD fluoroforoen amatatzea eraginez. Lipidoen alboko difusioaren ondorioz, denbora igaro ahala belztutako gunea bertatik kanpo zeuden lipidoekin estali zen, fluoreszentziaren berreskurapena lortuz. Proteina kantitatea: 1,5 µg. DiD kontzentrazioa: 6,7 nM. Eskala: 10 µm. t: denbora.

5.5.2. MINTZEKO PROTEINA ESTALDURA

Behin SLBen jariakortasuna ziurtaturik, mintzeko proteina estaldura optimizatu zen. Aurretik argitaratutako ikerketetan ikusi egin da itu proteinen %20 inguruko estaldura aurkezten duten LUVek TIRFM saiakerak burutzeko proteina estaldura egokia duten SLBak eratzen dituztela (Subburaj et al., 2015). Lehenengo eta behin DiD kontzentrazio berria erabiliz (0,67 nM) SLBak eratu ziren, fluoreszentziaren intentsitatea, besikulen arteko fusioa eta mintzaren jariakortasuna egokiak zirela ziurtatzeko. Baldintza hauek betetzen zituzten laginen mintzeko proteina estaldura FCCS bidez aztertu zen 2.9.2. atalean azaldu bezala (Simeonov et al., 2013). Laburbilduz, SLBen eraketa protokoloa burutu zen, azken urratsa salbu ($CaCl_2$ren gehiketa), BIM-DOPC-DID besikulak lortuz. Ondoren, FCCS entseguak C-Apochromat 40 X N.A. 1,2-ko ur-objetibo batekin hornitutako *ZEISS LSM 710 ConfoCor 3* fluoreszentziazko mikroskospio konfokala erabiliz burutu ziren. eGFP eta DiD fluoroforoen kitzikapena 488 eta 633 nm-tako laserrak erabiliz egin zen, hurrenez hurren; fluoreszentziaren igorpena 505-540 nm tartean eta 655 nm-tik gora jaso zen bitartean, eGFP eta DiDrentzat, hurrenez hurren.

Lehenengo saiakeran, BIMVak (M1 lagina: 1,5 µg) DiDrekin sonikatu eta ondoren aldez aurretik sortutako DOPC-SUVekin (30 µg) nahastu ziren 20:1 erlazioan eta 0,67 nM DiD bukaerako kontzentrazioa lortuz. Kontrol gisa, BIMV-DiDak eta DOPC-DiD-SUVak erabili ziren. BIMVez soilik eraturiko SLBak ez zuen jariakortasunik, bere proteina kantitate altuaren ondorioz. DOPCz eraturiko SLBa, ordea, jariakortasuna aurkezten zuen baina ez zuen fluoreszentziarik igortzen 488 nm-tako laser argiarekin erradiatzean. Lipido nahasketadun SLBei dagokienez, jariakortasuna eta DiD kontzentrazio egokia zeukaten eta bi fluoroforoen amataketa ematen zen denboran zehar (5.14. irudia). Zoritxarrez, nahasketa honek FCCS bidez aztertzerakoan %85eko proteina estaldura erakutsi zuen, BIMVen kantitatea lau aldiz murriztu behar zela iradokiz.

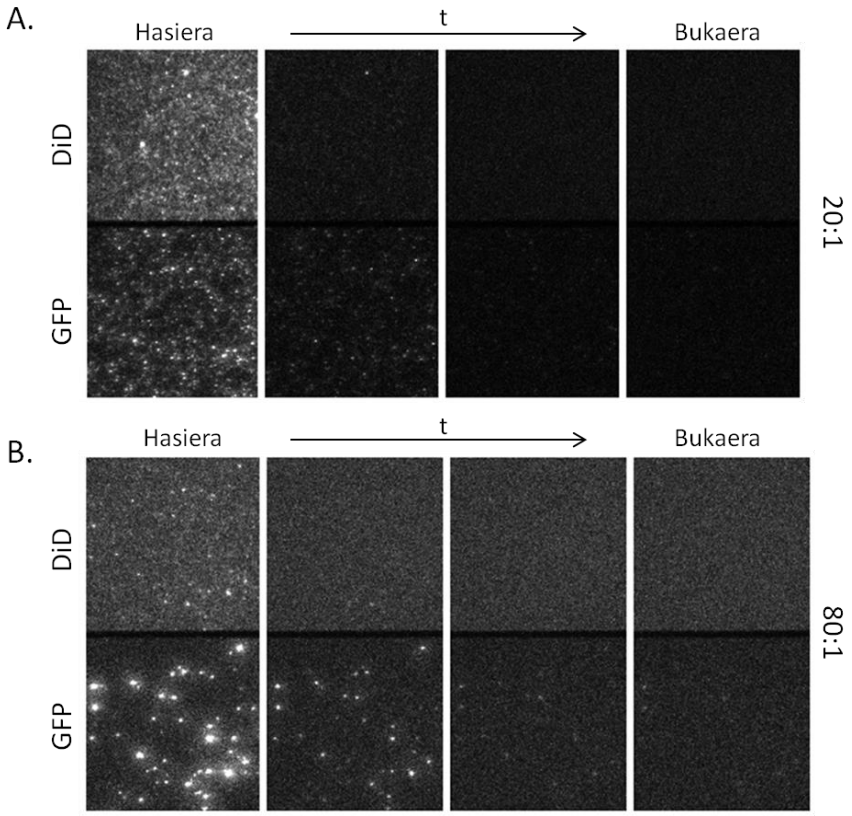

5.14. irudia. TIRFM bidezko SLB azterketen irudi esanguratsuak. BIMVak DiDrekin batera sonikatu eta ondoren aldez aurretik eratutako DOPC-SUVekin nahastu ziren. SLBak eratu eta *ZEISS Axiovert 200* mikroskopioan bistaratu ziren 2.9.4. atalean azaldu bezala. **A)** $MobB_{CloDF13}$GFPdun SLBak. Proteina kantitatea: 1,5 µg. DiD kontzentrazioa: 0,67 nM. **B)** $TrwB_{R388}$GFPdun SLBak. Proteina kantitatea: 0,375 µg. DiD kontzentrazioa: 0,67 nM.

Hurrengo saiakeran 30 µg DOPC eta 0,375 µg BIMV erabili ziren (M1 eta T1 laginak), 80:1 erlazioan nahastuz (5.5.1. atalean erabilitako erlazioaren antzekoa baina osagaien kantitate baxuagoarekin). Lagin hauek TIRFM bidez aztertzerakoan besikulak elkarren artean ez zirela ondo fusionatu zirudien, ez eta proteinak beirazko gainazalari itsatsi ere (5.14. irudia). Hala ere, FCCS entsegua burutu zen, GFP fusio-proteinen %20 inguruko mintz estaldura lortuz (5.15. irudia).

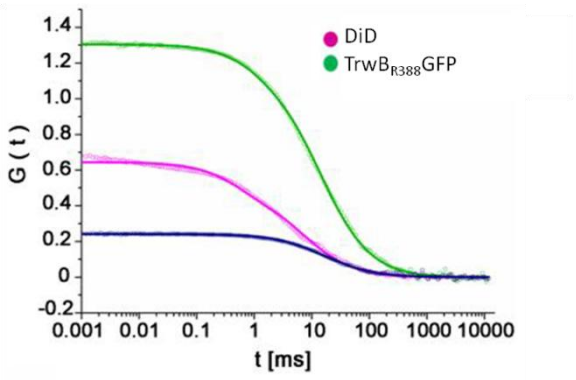

5.15. irudia. FCCS bidezko proteinen mintz estalduraren azterketa. TrwB$_{R388}$GFPdun BIMVak DiDrekin sonikatu ziren eta ondoren aldez aurretik eratutako DOPC-SUVekin nahastu ziren. Lortutako lagina FCCS bidez aztertu zen *ZEISS LSM 710 ConfoCor 3* fluoreszentziazko mikroskopio konfokala erabiliz 2.9.2. atalean azaldu bezala. Kurba urdina erlazio-gurutzatuari dagokio, mintzaren %20ko estaldura erakutsiz. Proteina kantitatea: 0,375 µg. DiD kontzentrazioa: 0,67 nM.

5.5.3. SLBen OPTIMIZAZIOA

Mintzaren jariakortasun eta estaldura egokia lortu arren, 5.14. irudia eta 5.15. irudia erakutsi bezala, bigeruzaren homogeneotasuna ez zen egokia TIRFM entseguak burutzeko. Izan ere, hainbat gunetan, proteina konplexuak egitura oso distiratsuetan elkarturik aurkitzen ziren, molekula-bakarreko analisiak egiteko baliagarria ez zena. Deskribatu denez, beirazko gainazalaren garbiketa eta prestaketa urrats kritikoa da SLB egokien ekoizpenerako (Kudalkar et al., 2016). Honetan oinarrituz, beirazko gainazalaren prestaketarako bi estrategia desberdin frogatu ziren: (i) beirazko estalkien silanizazioa eta (ii) beiraren garbiketa piraña disoluzioa erabiliz. Silanizazioan zehar perfluorodezil triklorosilanozko (FDTS) geruza hidrofobiko bat beirazko estalkiaren gainazalari atxikitzen zaio. Metodologia honek beirazko gainazala elkarrekintza hidrofobikoen bidez atxikitzen diren molekulekin estaltzen laguntzen du, adibidez antigorputzekin, nahi ez diren gainerako elkarrekintzak deuseztatuz. Piraña disoluzioari dagokionez, azido sulfuriko eta hidrogeno peroxidozko nahasketa da. Oxidatzaile indartsua da, metalen eta kutsatzaile organikoen garbiketa burutzen duena, gainazal gehienak hidroxilatzen dituen heinean. Bi modu horietan, besikulen atxikipena eta fluoreszentziaren neurketak oztopatu dezaketen molekulak desagerrarazten dira (Chandradoss et al., 2014).

Lehenengo eta behin SLBak silanizaturiko estalkietan eratu ziren. Horretarako aldez aurretik eraturiko DOPC-SUVak eta BIMV-DiD laginak (M1 eta T1, 0,375 µg) lipido:proteina erlazio desberdinetan elkartu ziren (*i.e.*, 80:1, 160:1, 500:1, 1000:1, 2000:1 eta 5000:1). Horretaz gain, besikulen atxikipena hobetzeko, SLBen eraketarako 6 mM $CaCl_2$ erabili ziren, aurretik erabilitako 3 mM $CaCl_2$-ren aldean. Lortutako SLBak 2.9.4. atalean azaldu bezala bistaratu ziren eta aurretik aipaturiko egitura distiratsu berdinak hauteman ziren frogaturiko baldintza guztietan (S5.3. irudia).

Silanizaturiko estalkien erabilera alboratu ostean, piraña bidez garbitutako beirazko estalkiak erabili ziren. Bestalde, bigeruza homogeneoak lortzeko asmoz, 5.4.3.3. atalean ebatzitako detergente bidezko BIMV eta DOPC-GUVen arteko fusio protokoloa SLBen

eraketarako egokitu zen. Honetarako BIMVak eta DOPC-SUVak elkar banandurik haien solubilizaziorako detergente egokiekin inkubatu ziren. Laburbilduz, DOPCa (2,5 mg/mL) 46,08 mM OGrekin aberastutako *SLB indargetzailetan* 45 minutuz sonikatu zen bitartean, T1 BIMV lagina (0,5 mg/mL) 150 µM TritonX100rekin aberasturiko *GUV fusio indargetzailetan* sonikatu zen 30 minutuz. Ondoren, bi laginak lipido:proteina erlazio desberdinetan nahastu ziren (*i.e.*, 100:1, 250:1 eta 500:1) detergenterik gabeko *GUV fusio indargetzailean* eta bi orduz inkubatu ziren giro tenperaturan. Bi lagin talde prestatu ziren: (i) lehenengoan detergentearen ezabapena 30 minuturo 15 mg BB gehituz egin zen, guztira 90 minutuz inkubatuz; (ii) bigarrenean, BBen hirugarren gehitzea burutzerakoan (inkubazioaren hasieratik ordu batera) 30 mg BB gehitu eta lagina giro tenperaturan gau osoan zehar irabiaketa bertikalarekin utzi zen. Detergentearen ezabapena egin ostean SLBen eraketa burutu zen 6 mM $CaCl_2$ erabiliz piraña disoluzioarekin garbitutako beirazko estalkietan. Aipatu beharra dago 250:1 erlazioan egindako nahasketarekin prozesu osoa egin zela detergenterik gabe, metodologiaren kontrol gisa erabiltzeko. SLBen bistarapena 2.9.4. atalean azaldu bezala burutu zen.

Lehenengo laginen multzoan, zeinen detergentearen ezabapena 90 minutuz egin zen, fusionatu gabeko besikula ugari ikusi ziren amatatzen ez ziren gune distiratsu gisa (S5.4. irudia). Baliteke detergentea guztiz ez ezabatu izana, laginean $CaCl_2$ren presentzian fusionatu ez ziren BIM-detergente besikulak geratuz. Bigarren lagin multzoan, zeinen detergentearen ezabapena gau osoan zehar egin zen, TIRFM saiakerak burutzeko SLB egokiak lortu ziren, jariakortasun ona eta estekiometria saiakerak egin ahal izateko GFParen amatatze aproposarekin (5.16. irudia). Nahiz eta lagin guztiek itxura egokia izan, 100:1 erlaziodun lagineko proteina dentsitatea pixka bat altua zen, ondorioz **250:1 eta 500:1 laginak aukeratu ziren haiekin molekula-bakarreko TIRFM entseguak burutzeko**.

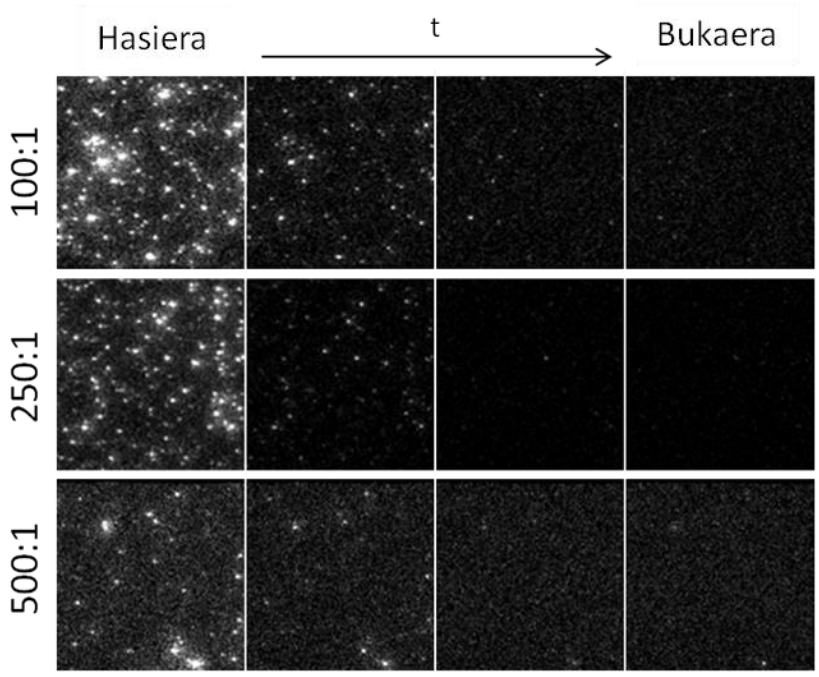

5.16. irudia. SLB eraketa detergente bidezko besikulen fusioa erabiliz. Laginen bistaratzea *ZEISS Axiovert 200* mikroskopioaren bidez egin zen 2.9.4. atalean azaldu bezala. Irudiak eGFP fusio-proteinen amatatze prozesua adierazten dute. Proteina kantitatea: 0,250 µg. DiD kontzentrazioa: 0,67 nM. t: denbora.

5.6. EZTABAIDA/LABURPENA

Kapitulu honen helburu nagusia molekula-bakarreko tekniken bidez T4CPen karakterizazioa egiteko konfigurazio esperimentala optimizatzea zen. Helburu nagusi hau bi helburu zehatzetan banatu zen: (i) **GUVetan T4CPen berreraikitzea** burutzea, molekula-bakarreko tekniken bidez DNArekiko elkarrekintzak eta T4CP kanalen azterketa burutzeko, eta (ii) T4CPen oligomerizazio mekanismoa, estekiometria eta dinamikaren azterketa TIRFM bidez egin ahal izateko **SLB egokien lorpena**.

GUV-bakarreko metodologia eta TIRFM teknikak fluoreszentziazko mikroskopian oinarritzen dira; ondorioz, protokoloen ebazpenerako egin beharreko lehenengo pausua **T4CP fluoreszenteak** lortzea zen. Horretarako, $TrwB_{R388}$rekin erlazionaturiko proteinen ($TrwB_{R388}$, TrwBΔN70, eta $TMD_{TraJ}CD_{TrwB}$) markaketa zuzena egin zen Atto maleimidak erabiliz. Nahiz eta $TrwB_{R388}$ eta Atto 488 zundaren artean emaitza onak lortu, teknika honen erabilera alboratu zen, ikerketako proteina guztientzat ez baitzen baliagarria. Alde batetik, TrwBΔN70 eta $TMD_{TraJ}CD_{TrwB}$rekin ez zen markaketa etekin egokirik lortu; eta beste aldetik, ez zen $TraJ_{pIP501}$ eta $MobB_{CloDF13}$rekin erabiltzeko aproposa, haien zisteinen eskuragarritasuna ezezaguna baita. Hori dela eta, genetikoki domeinu fluoreszente baten fusioz markaturiko T4CPak erabili ziren; 3. atalean lorturiko T4CP-eGFP fusio-proteinak, alegia. Hala ere, T4CP fusio-proteinak purifikatu ordez, haiekin aberasturiko BIM osoaren purifikazioa burutzea erabaki zen, aukera multzo berria eskainiz T4CPen ingurune natibodun GUV eta SLBen eraketarako. Ondorioz, $TrwB_{R388}$GFP eta $MobB_{CloDF13}$GFPn aberasturiko BIMVen lorpena egin zen. Ikusi da GFP domeinuaren presentziak ez duela T4CPen *in vivo* funtzioa inhibitzen, nahiz eta transferentzia maiztasuna pixka bat jaitsi (3.3. atala). Hala ere, dagoeneko eragozpen berdina duten (funtzionalitate murriztua) GFP fusio-proteinak TIRFM bidezko estekiometria saiakerak egiteko erabili dira (Leake et al., 2006).

Kapitulu honen sarreran aurkeztu bezala, mintz-eredu desberdinetan MPen berreraikitzea egiteko teknika ugari daude. SUV eta LUVetan berreraikitzea burutzeko protokolo ebatziak dauden heinean, ez dago **GUVetan berreraikitzea** burutzeko metodo orokorrik. Honetarako estrategia desberdinak deskribatu dira, haietako bakoitzak bere abantaila eta desabantailekin. Hala ere, protokolo horiek erreplikatzeko zailak dira, haietan parte hartzen duten aldagai kontrolaezinen ondorioz (Witkowska et al., 2018). Nahiz eta moldaerrazak izan, T4CPen berreraikitzea burutzeko zenbait metodo zuzenean alboratu ziren, adibidez López-Montero et al. (2013)-k deskribatutakoa. Lan horretan histidina etiketadun itu-proteinaren aldaera disolbagarria (TMD-rik gabea) erabili zuten, liposometako NTA-lipidoekin elkarrekiten zuena. Estrategia hau ez zen T4CPen ikerketarako erabili, luze frogatu baita T4CPen TMDa aingura hutsa baino gehiago dela eta ezin dela deuseztatu proteinaren berezko ezaugarriak aldatu gabe (Hormaeche et al., 2002, 2004, 2006; Moncalián et al., 1999; Segura et al., 2013, 2014; Vecino et al., 2010, 2011). Aukera desberdin guztiak kontutan hartuz, lan honetan hiru metodologia erabili dira GUVetan T4CPen berreraikitzea egiteko, haietako bakoitza oinarri desberdina izanik: (i) detergente bidezko berreraikitze zuzena (Dezi et al., 2013), (ii) GUVen eraketa proteoliposometatik (Girard et al., 2004), eta (iii) GUVen eraketa BIMVetatik (Jiménez et al., 2011).

Lehenengo bi metodoak aldez aurretik purifikaturiko eta ondoren nahasturiko lipidoez osaturiko bigeruza lipidiko artifizialen erabileran oinarritzen ziren. Aurretik argitaraturiko lanetan, $TrwB_{R388}$ BIMa antzematen zuen lipido nahasketa batez osaturiko LUVetan berreraiki zen [PE:PG:CL (76,3:19,6:4,1)] (Vecino et al., 2011). Hala ere, nahasketa hau ez zen egokia GUVen eraketarako, PE lipidoen berezko kurbadura negatiboaren ondorioz kurbadura handiko besikula txikiak edota egitura tubularrak soilik lortzen zirelako. Arazo hau nahasketaren PEa DOPCarekin ordezkatuz konpondu zen, zeinak berezko kurbadura neutroa daukan, bigeruza lauak sortzeko egokia dena. DOPC ehuneko desberdinak aztertuz, DOPC:PE:PG:CL (50:26,3:19,6:4,1) nahasketa erabiliz GUV tamaina eta kantitate egokia aurkezten zuen lagina lortu zen. Ondorioz, hau izan zen GUVen eraketarako aukeratutako lipido konposaketa.

Detergente bidezko berreraikitze zuzenean (Dezi et al., 2013) GUVak detergentearen kontzentrazio ez-solugarrietan eratu ziren sakarosa disoluzioan. Lan honetan, metodologia hau erreplikatzeko saiakerak burutu dira arrakastarik gabe. Protokoloaren aldaera gehiago frogatzeko asmoz, parametroen konbinazio desberdinak egin ziren, hala nola lipido konposaketa, sakarosa kontzentrazio, elektroformazio protokolo eta elektroformazio metodo desberdinak konbinatuz. Hala ere, ez zen GUVen eraketarik hauteman aztertutako baldintzetan eta ondorioz metodologia honen erabilera deuseztatu zen.

Bigarren aukera gisa, **proteoliposomak** GUVen eraketarako abiapuntutzat erabiltzea erabaki zen, deskribatu egin baita MPen presentziak elektroformazioarentzat mesedegarria izan daitekeela (Méléard et al., 2009). Lehenengo eta behin, LUVak lan honetan ezarritako lipido konposaketa erabiliz sortu ziren, haietatik GUVak eratu ahal izateko. Ondoren, besikula hauen solubilizazio patroia aztertu zen, proteoliposomen eraketa protokoloa konposaketa honentzat era egokian moldatzeko. Behin informazio hori izanda, LUVetan detergente bidez solubilizaturiko $TrwB_{R388}$ren berreraikitzea egin zen, Vecino et al. (2010)-k deskribaturiko protokolo moldatua erabiliz. Behin proteoliposomak lortuta, ikusi zen lipido konposaketaren aldaketak berreraikitzearen etekina areagotzen zuela mintzean proteinaren noranzkoan eraginik izan gabe. Ondoren, proteoliposomen deshidratazio/berhidratazioa burutuz GUVen eraketa frogatu zen. Aurreko metodologian bezala ez zen GUVik lortu elektroformazioz, baina agarosa gel bidezko hantura espontaneoak emaitza itxaropentsuak eskaini zituen, tamaina txikiko proteo-GUVen eraketarekin. Aitzitik, teknika honen bidez lorturiko GUVek zenbait desabantaila aurkezten dituzte. Alde batetik, proteinek haien funtzioa gal dezakete jasandako deshidratazio/berhidratazio prozesuen ondorioz; beste aldetik, lortutako GUVek ez dituzte agarosaren absentzian eratutako GUVen ezaugarri berdinak, neurketetan eragina izan ditzaketenak. Horretaz gain, kontutan hartu behar da estrategia hau erabiltzeko orduan proteinen markaketa fluoreszentea optimizatu beharko litzatekeela.

Arrazoi hauengatik, proteo-GUVen eraketarako hirugarren aukera bat erabili zen, zeinetan **BIMV**ak erabili ziren abiapuntuko material gisa. Modu honetan, T4CPen ikerketak jatorrizko ingurunetik ahalik eta gertuen dagoen egoera batean burutuko ziren. Are gehiago, ikerketa konparatibo batean deskribatu egin zen emaitza desberdinak lor daitezkelalipido nahasketa artifizialetan edo mintz natiboetan eraikitako proteinen azterketak burutzerakoan (Thoma et al., 2018), MPen funtzionamenduan ingurunearen garrantzia aldarrikatuz. Dena den, BIMVak ez dira GUVen eraketa egiteko egokiak, haien proteina kontzentrazio altuaren ondorioz; beraz, GUVak lortzeko entsegu guztietan BIMVak DOPCrekin diluitu ziren. Lehenengo

eta behin, aurretik saiaturiko deshidratazio/berhidratazio teknikak erabili ziren. Elektroformazio bidez ez zen emaitza egokirik lortu, nahiz eta protokolo orokorraren saiakera desberdinak burutu eta baldintza fisiologikoetan eraketa egiteko Jiménez et al. (2011)-ek deskribaturiko protokolo zehatza erabili (komunikazio pertsonala). Ondorioztatu zen hau gertatzearen arrazoia GUVen eraketa prozesuan parte hartzen duten faktore guztiak (*e.g.,* elektroformazio ganbaren eta ITOz estalitako harien ezaugarriak) kontrolatzeko ezintasuna zela. Agarosa gel bidezko hantura espontaneoari dagokionez, arazo nagusia DOPC-SUVen eta BIMVen arteko fusiorik ez zela gertatu izan zen, ezta detergentearen presentzian ere. Hala ere, aurretik esan bezala, metodo honen bidez lortutako GUVak ez dira ikerketa funtzionalak burutzeko optimoak.

Azkenik, proteoliposomen eraketan oinarritutako estrategia bat ebatzi zen. Protokolo honetan DOPC-GUVak detergentearen absentzian eratu ziren (proteoliposomen eraketarako LUVak sortu bezala, eta detergente bidezko berreraikitzean egindakoaren kontra) eta behin formaturik detergente bidez solubilizatu ziren. Modu honetan itu proteinaren deshidratazio/berhidratazioa saihestu zen. Bitartean BIMVak ere solubilizatu ziren eta ondoren bi laginen nahasketa burutu zen. Bukatzeko, proteoliposomen eraketa protokoloan bezala, detergentearen ezabapena egin zen BBen bitartez. Protokoloaren eta DOPC-GUV:BIMV erlazioaren optimizaziorako zenbait saiakeren ostean, ikusi zen 500:1 erlazioko nahasketetatik tamaina txikiko GUIMVak lortzen zirela. Beraz, **baldintza hauek abiapuntu gisa erabil daitezke GUV-bakarreko entseguen bidez T4CP kanalen azterketa burutu ahal izateko**.

GUVetan T4CPen berreraikitzearen protokoloa ebaztearekin batera, **T4CP fluoreszenteetan aberastutako SLBen ekoizpen protokoloa** ebatzi zen. Nahiz eta SLBak tradizionalki purifikaturiko lipidoz egindako nahasketekin eratu, azken denboraldian zelula mintz natiboetatik eratorriko SLBak (nSLBak) erabiltzen hasi dira. Joera hau jarraituz, tesi honetan BIMVak SLBak sortzeko abiapuntu gisa erabili dira, eskaintzen dituzten abantaila guztien ondorioz (*e.g.,* jatorrizko ingurunea, itu-proteinaren kantitate altua eta proteina guztientzako purifikazio protokolo amankomuna). Hala ere, lipido:proteina erlazio altuek SLBen eraketa oztopatzen dutenez, BIMVak purifikaturiko lipidoekin nahastu behar izan ziren. Izan ere, deskribatu da purifikaturiko lipido:BIMV erlazioari dagokionez muga bat dagoela SLB jarrai egokiak lortzeko (Pace et al., 2018). Are gehiago, argitaraturiko ikerketa batek erakutsi du nahasketako BIMV eta PC erlazioak lortutako SLBaren ezaugarriak ezartzen dituela (Dodd et al., 2008b). Zehazki, ikerketa horretan egindako FRAP entseguek erakutsi zuten BIMV lagina nahasketaren %40a baino gutxiago izan behar zela jariakortasun oneko SLB homogeneoak lortzeko. Horretaz gain, BIMVak atxikirik dituen PC bigeruza baten eta nahasketa homogeneodun SLB baten artean bereizi ahal izateko FRAP ikerketen garrantzia aldarrikatu zuten. Lagin egokia izanda, SLBa mintz natiboaren aldaera lau bat izan beharko litzateke, zeinetan osagai desberdinak diluituagoak dauden.

Arrazoi hauengatik, optimizazio honen lehenengo urratsak DOPC eta BIMVen arteko fusio egokia eta lortutako mintzaren jariakortasuna ziurtatzea izan ziren. SLBak eratu baino lehen lipido iturri bakoitza (*i.e.,* DOPC eta BIMVak) sonikatu zen eta ondoren SLBak lortzeko erlazio jakinetan (lipido:proteina, p/p) nahastu ziren. Teknika hau erabiltzea erabaki zen prozesuan zehar proteinen aktibitatea galtzen ez dela deskribatu delako (Pace et al., 2015). Lehenengo saiakeretan, DiD eta proteina kontzentrazio altuegiak erabili ziren, fluoreszentzia

seinale aproposa lortzeko egokitu zirenak. Ondoren, FRAP entseguen bidez, 80:1 erlazioan eraturiko SLBak homogeneotasun eta jariakortasun egokia zutela frogatu zen. Hurrengo urratsean, mintzeko proteinen estaldura aztertu zen, estekiometria azterketak burutu ahal izateko. Hau lipido:proteina erlazio berdinarekin lortu zen (80:1), baina proteinaren kantitate baxuagoa erabiliz. Dena den, SLB hauetan oraindik gune distiratsu ugari bistaratzen ziren, ziur asko fusionatu gabeko BIMVekin erlazionatuak.

Besikulen fusioa urrats kritikoa da SLBen eraketan, modu enpirikoan egokitu behar dena kasu gehienetan (Tong eta McIntosh, 2004). Gainera frogatu da lipido:proteina erlazioak fusionatu gabeko besikulen ehunekoan eta nSLBen eraketa zinetikan eragina daukala. Zehazki, fusionatu gabeko besikulen kantitatea eta bigeruzaren eraketarako beharrezko denbora handitzen dira mintz natiboa laginaren %17a baino gehiago denean (Pace et al., 2018). Honengatik, nahiz eta jariakortasun eta mintz estaldura egokiko laginak lortu, protokoloa fusionatu gabeko besikulen kantitatea murrizteko egokitu behar izan zen. Aldaera desberdinak frogatu eta besikulen fusioa areagotzeko $CaCl_2$ kontzentrazioa igo ostean, SLBen eraketarako proteo-GUVak lortzeko ebatzitako detergente bidezko protokoloaren antzeko aldaera bat erabili zen. Horrela, estekiometriaren azterketak burutzeko homogeneotasun, jariakortasun, eta fluoreszentzia egokia erakusten zuten SLBak lortu ziren 0,25 µg proteina eta 250:1 eta 500:1 lipido:proteina (p/p) erlazioak erabiliz.

BIMVak mintzaren une jakin baten isla soilik direnez, behin T4CP-eGFPen gain-adierazpen egoeran egindako estekiometria saiakerak burututa, bigarren azterketa bat egin ahalko litzateke konjugazio prozesuan zehar T4CPen oligomerizazio dinamikak aztertzeko. Are gehiago, kokapen azpizelularreko entseguetan egindakoaren antzera, zuzenean TIRFM saiakerak egin ahalko liratezke T4CP fluoreszentedun bakterioekin (Leake et al., 2006; Yamamoto et al., 2016).

SUMMARY OF THE RESULTS AND CONCLUSIONS

SUMMARY OF THE RESULTS

COUPLING PROTEIN PRODUCTION FOR THE STUDY OF THEIR TRANSMEMBRANE DOMAIN

- **Variants of coupling proteins** of different origins have been constructed through traditional molecular biology techniques: On the one hand, two chimeric proteins related to $TrwB_{R388}$, $TMD_{TrwB}TraJ_{pIP501}$ and $TMD_{TraJ}CD_{TrwB}$, in addition to two variants of the later, $TMD_{TraJ}CD_{TrwB}$GFP and $TMD_{TraJ}CD_{TrwB}$K142T. On the other hand, the soluble coupling protein of the conjugative pIP501 plasmid $TraJ_{pIP501}$ and its related $TraI_{pIP501}TraJ_{pIP501}$ chimera protein. Finally, the relaxase and the coupling protein of CloDF13 mobilizable plasmid, $MobC_{CloDF13}$ and $MobB_{CloDF13}$, respectively, together with the transmembrane deletion mutant of the later, MobBΔTMD. Besides, through a high-throughput cloning protocol, a set of fusion-protein variants of $TMD_{TrwB}TraJ_{pIP501}$, $TraJ_{pIP501}$, $MobB_{CloDF13}$, and MobBΔTMD has been obtained, to employ them in different assays as needed.
- Through mating assays, different characteristics of the ***in vivo*** **function** of coupling proteins have been studied. As previously published, it has been observed that the specific interaction with the relaxase is essential for substrate transfer (Cabezón et al., 1997; Hamilton et al., 2000; Llosa et al., 2003) and that poly-histidine tags do not interfere with the protein function (Hormaeche et al., 2006); the loss of the transmembrane domain and mutations in the Walker A domain, however, completely inhibit the process (Chen et al., 2008; Moncalián et al., 1999). On the contrary, unlike what has been previously published (Segura et al., 2014), it has been observed that the presence of a GFP domain hinders substrate transfer, even if it does not inhibit it.
- It has been shown that an in-depth study of different factors (*e.g.*, bacterial strain, induction method and inducer concentration, growth medium and temperature, and overexpression time) is essential when performing the **overexpression study** of a membrane protein because the expression of some proteins is given only under certain conditions.
- The **purification** protocol of $TrwB_{R388}$ has been optimized, successfully using it for the purifications of $TMD_{TraJ}CD_{TrwB}$ and $TMD_{TraJ}CD_{TrwB}$K142T proteins too. In addition, purification protocols for $MobB_{CloDF13}$ and MobBΔTMD proteins have been established.
- It has been shown that coupling proteins are **located at the poles** of bacteria, in a unipolar or bipolar way depending on the system. It has also been described that the presence of the rest of the secretion system enhances this location. Although the transmembrane domain has been proven to be essential for the polar location of VirD4-type conjugative coupling proteins, it was observed that this is not necessary for the transmembrane-less $TraJ_{pIP501}$ and MobBΔTMD proteins.

IN VITRO MOLECULAR CHARACTERIZATION OF COUPLING PROTEINS

- $TrwB_{R388}$, $TMD_{TraJ}CD_{TrwB}$, and $MobB_{CloDF13}$ have shown to require acidic pH (up to pH 5.6), high detergent concentration, and high ionic strength (at least 0.5 mM DDM and 300 mM NaCl) to maintain their **stability**. In addition, it has been shown that these

detergent concentration and ionic strength protect the protein against proteolysis by the K protease. Related to this, it has been described that the presence of DNA in the absence of DDM and NaCl increases the proteolysis performed by the K protease. With regard to MobBΔTMD, it has been observed that the presence of acidic pH (pH 5.6) and detergent contribute to its stability. The ionic strength, however, has no effect on its stability in the range of 20–200 mM NaCl. In the case of MobBΔTMD, although detergents and high ionic strength are also protective against proteolysis by K protease, the presence of DNA does not appear to have any effect.

- It has been observed that all the tested coupling protein variants **bind DNA**, being these interactions higher in the presence of DDM and NaCl; with the exception of MobBΔTMD, to which DNA is not bound or it is bound with low affinity under all the tested conditions.
- The secondary structure compositions of $TMD_{TraJ}CD_{TrwB}$, $MobB_{CloDF13}$, and MobBΔTMD proteins were analyzed by infrared spectroscopy for comparison with $TrwB_{R388}$ and TrwBΔN70 (see the comparison between different proteins below). In terms of three-dimensional structures, attempts have been made with cryo-electron microscopy using $TrwB_{R388}$ and MobBΔTMD crystals have been obtained, although both approaches need to be optimized.
- Conditions for performing ATP hydrolysis coupled enzyme assays with membrane proteins have been optimized, emphasizing that a lower reaction temperature (25°C instead of 37°C), high ionic strength (300 mM NaCl) and detergent are needed to ensure protein stability during the reaction time, even if these conditions reduce the hydrolysis rate. Through this technique the ATPase activities of $TMD_{TraJ}CD_{TrwB}$ and MobBΔTMD have been studied (see the comparison between different proteins below).

EXPERIMENTAL SET-UP FOR SINGLE-MOLECULE ASSAYS

- Giant unilamellar vesicles with a **lipid composition** mimicking the bacterial inner membrane were achieved using DOPC: PE: PG: CL (50: 26.3: 19.6: 4.1) lipid mixture.
- $TrwB_{R388}$ containing **proteoliposomes** and **bacterial inner membrane vesicles** containing$TrwB_{R388}$GFP or $MobB_{CloDF13}$GFP fusion proteins have been obtained.
- Regarding the **reconstitution of coupling proteins in giant unilamellar vesicles**, the best results were obtained by mixing DOPC giant unilamellar vesicles with bacterial inner membrane vesicles containing overexpressed coupling proteins in the presence of detergent.
- A protocol for obtaining coupling proteins reconstituted in supported lipid bilayers has been developed.

COMPARISON BETWEEN DIFFERENT PROTEINS

- **Comparison between $TMD_{TraJ}CD_{TrwB}$ and $TrwB_{R388}$:** the chimera protein is able to complement R388's conjugative process in the absence of the native coupling protein, but at a lower transfer frequency (0.21 and $1.82x10^{-4}$ for $TrwB_{R388}$ and $TMD_{TraJ}CD_{TrwB}$, respectively). Moreover, it shows negative dominance in the presence of $TrwB_{R388}$ and

$TraJ_{pKM101}$ coupling proteins. It appears to have higher thermal stability than $TrwB_{R388}$, but it is more unstable against low ionic strength conditions. The chimera protein shows lower DNA-binding capacity than $TrwB_{R388}$, although it seems to oligomerize upon DNA-binding, as seen with TrwBΔN70 (Matilla et al., 2010). However, it shows different oligomerization patterns compared to $TrwB_{R388}$, showing a greater resemblance to those shown by TrwBΔN50 (Vecino, 2009). Regarding the structure of $TMD_{TraJ}CD_{TrwB}$, it presents a distribution of the secondary structure elements in between the ones presented by the native protein and the transmembrane deletion mutants, being less compact than $TrwB_{R388}$ but more than TrwBΔN70 (Vecino et al., 2012). Besides, as with $TrwB_{R388}$ (Vecino, 2009), no ATPase activity of $TMD_{TraJ}CD_{TrwB}$ was detected under any of the tested conditions.

- **Comparison between MobBΔTMD and TrwBΔN70**: As TrwBΔN70, MobBΔTMD is not able to complement conjugation in the absence of the native protein (Segura et al., 2013). On the contrary, unlike TrwBΔN70, it is located in a single cell pole in the absence of the remaining conjugative proteins (Segura et al., 2014). Regarding subcellular localization, the only difference between $MobB_{CloDF13}$ and MobBΔTMD is that the native protein is located in two poles, while the mutant protein is located in a single pole. Although $MobB_{CloDF13}$ showed a clear DNA-binding capacity, it did not happen concerning MobBΔTMD, which could explain the lack of DNA effect on the K protease assay. Conversely, TrwBΔN70 showed higher DNA-binding capacity than $TrwB_{R388}$. In terms of oligomerization, although MobBΔTMD predominated as a monomer in all the studied conditions, it was also observed as a dimer and trimer; the same species identified in $MobB_{CloDF13}$ sample. In comparison, TrwBΔN70 seems to only oligomerize when interacting with G-quadruplex DNA structures (Matilla et al., 2010). MobBΔTMD performs optimal ATP hydrolysis at 45°C, acidic pH (pH 5.6), and low ionic strength; showing similar activity to that described for TrwBΔN70 in the absence of any helper molecule (22.7 and 30 nmol ATP min^{-1} mg^{-1} for MobBΔTMD and TrwBΔN70, respectively). However, MobBΔTMD presents a Michaelis-Menten type kinetics, while TrwBΔN70 presents positive cooperativity (Tato et al., 2007), bearing always in mind that the latter was described in the presence of DNA.

CONCLUSIONS

1. Coupling proteins show unipolar or bipolar location in the cell, being the presence of a transmembrane domain or the rest of the secretion system elements unnecessary for the localization of the mobilizable plasmid-related $MobB_{CloDF13}$ and the soluble T4CP $TraJ_{pIP501}$. Nevertheless, the presence of a T4SS enhances the unipolar or bipolar location in all the tested T4CP variants.
2. $TMD_{TraJ}CD_{TrwB}$, a chimera coupling protein composed of transmembrane and cytosolic domains of different origins, is able to complement the conjugation of R388, although with a lower transfer frequency. Moreover, it is capable of interacting with its both cognate systems (*i.e.*, R388 and pKM101), showing negative dominance in the presence of the native T4CPs, $TrwB_{R388}$ or $TraJ_{pKM101}$.
3. Comparing $TMD_{TraJ}CD_{TrwB}$ with $TrwB_{R388}$, it has been seen that the chimera protein presents smaller stability against low ionic strength conditions, different oligomerization patterns, and smaller DNA-binding capacity, most likely due to the secondary structural differences observed in the cytosolic domain. These results suggest that the presence of a heterologous TMD affects the cytosolic domain and the processes related to it, such as substrate-binding and, therefore, *in vivo* activity.
4. The presence of the transmembrane domain of $MobB_{CloDF13}$, on the contrary to what has been described for $TrwB_{R388}$, does not have any effect neither in the oligomerization pattern nor in the secondary structure of the cytosolic domain, even if it seems to affect DNA-binding properties.
5. The characteristics described for the conjugative plasmid related VirD4-type T4CPs and their TMDs should not be ascribed to the whole T4CP family. Specifically, it has been proven that coupling proteins that lack a transmembrane domain and mobilizable plasmid-related VirD4-type coupling proteins present different mechanisms of action.

DATU GEHIGARRIAK

S2.2.3. ETEKIN-HANDIKO KLONAKETA

S2.1. taula. HTP klonaketan erabilitako hasleak. Lau gene desberdinen klonaketa burutzeko pOPIN taldeko 12 bektore aukeratu ziren. Honetarako OPPF-UK-k ebatzitako metodoa erabili zen (2.2.3. atala). Entseguak 96-putzutako plaketetan burutu ziren, klonaketa desberdin bakoitza identifikatzeko plakako koordenatuak erabiliz (1. zutabea). Entsegu bakoitzean klonaturiko genea, erabilitako DNA moldea, bektorea eta hasleak 2., 3., 4., eta 5. zutabeetan adierazten dira, hurrenez hurren. Lortutako konstruktoak izendatzeko bektorearen izena eta bertan klonatutako genea erabili ziren (*e.g.* pOPINE-*mobB*). F eta R *forward* eta *reverse* hasleak dira, hurrenez hurren.

1	2	3	4	5
Koordenatua	Genea	DNA moldea	Bektorea	Haslea (5' → 3')
A01	*mobB*$_{CloDF13}$	CloDF13 plasmidoa	pOPINE	FA01: AGGAGATATACCATGTTTAATACGGATTCGCTTGCCTGGCAGTGG
				RA01: GTGATGGTGATGTTTGTACAGCCCCGCAAAATCATCATCACCCG
B01			pOPINFB	FB01: AAGTTCTGTTTCAGGGCCCGTTTAATACGGATTCGCTTGCCTGGCAGTG
				RB01: AGATGTCGTTCAGGCCGTACAGCCCCGCAAAATCATCATCACCCG
C01			pOPINFS	FC01: AAGTTCTGTTTCAGGGCCCGTTTAATACGGATTCGCTTGCCTGGCAGTGG
				RC01: GGTGGCTCCAGCTAGCGTACAGCCCCGCAAAATCATCATCACCCG
D01			pOPINTRX	FD01: AAGTTCTGTTTCAGGGCCCGTTTAATACGGATTCGCTTGCCTGGCAGTGG
				RD01: ATGGTCTAGAAAGCTTTAGTACAGCCCCGCAAAATCATCATCACCCG
E01			pOPINM	FE01: AAGTTCTGTTTCAGGGCCCGTTTAATACGGATTCGCTTGCCTGGCAGTGG
				RE01: ATGGTCTAGAAAGCTTTAGTACAGCCCCGCAAAATCATCATCACCCG
F01			pOPINS3C	FF01: AAGTTCTGTTTCAGGGCCCGTTTAATACGGATTCGCTTGCCTGGCAGTGG
				RF01: ATGGTCTAGAAAGCTTTAGTACAGCCCCGCAAAATCATCATCACCCG
G01			pOPINTF	FG01: AAGTTCTGTTTCAGGGCCCGTTTAATACGGATTCGCTTGCCTGGCAGTGG
				RG01: ATGGTCTAGAAAGCTTTAGTACAGCCCCGCAAAATCATCATCACCCG
H01			pOPINCDM	FH01: AAGTTCTGTTTCAGGGCCCGTTTAATACGGATTCGCTTGCCTGGCAGTGG

				RH01: ATGGTCTAGAAAGCTTTAGTACAGCCCCGCAAAATCATCATCACCCG
A02			pOPINRSJ	FA02: AAGTTCTGTTTCAGGGCCCGTTTAATACGGATTCGCTTGCCTGGCAGTGG
				RA02: ATGGTCTAGAAAGCTTTAGTACAGCCCCGCAAAATCATCATCACCCG
B02			pOPINE-3C-eGFP	FB02: AGGAGATATACCATGTTTAATACGGATTCGCTTGCCTGGCAGTGG
				RB02: CAGAACTTCCAGTTTGTACAGCCCCGCAAAATCATCATCACCCG
C02			pOPIN-3C-HALO7	FC02: AGGAGATATACCATGTTTAATACGGATTCGCTTGCCTGGCAGTGG
				RC02: CAGAACTTCCAGTTTGTACAGCCCCGCAAAATCATCATCACCCG
D02			pOPINEneo-FLAG	FD02: AGGAGATATACCATGTTTAATACGGATTCGCTTGCCTGGCAGTGG
				RD02: CAGAACTTCCAGTTTGTACAGCCCCGCAAAATCATCATCACCCG
E02	*mobBΔTMD*	CloDF13 plasmidoa	pOPINE	FE02: AGGAGATATACCATGGACGAGGCGGTGAACGCGAAAC
				RE02: GTGATGGTGATGTTTGTACAGCCCCGCAAAATCATCATCAC
F02			pOPINFB	FF02: AAGTTCTGTTTCAGGGCCCGGACGAGGCGGTGAACGCGAAAC
				RF02: AGATGTCGTTCAGGCCGTACAGCCCCGCAAAATCATCATCAC
G02			pOPINFS	FG02: AAGTTCTGTTTCAGGGCCCGGACGAGGCGGTGAACGCGAAAC
				RG02: GGTGGCTCCAGCTAGCGTACAGCCCCGCAAAATCATCATCAC
H02			pOPINTRX	FH02: AAGTTCTGTTTCAGGGCCCGGACGAGGCGGTGAACGCGAAAC
				RH02: ATGGTCTAGAAAGCTTTAGTACAGCCCCGCAAAATCATCATCAC
A03			pOPINM	FA01: AAGTTCTGTTTCAGGGCCCGGACGAGGCGGTGAACGCGAAAC
				RA01: ATGGTCTAGAAAGCTTTAGTACAGCCCCGCAAAATCATCATCAC
B03			pOPINS3C	FB03: AAGTTCTGTTTCAGGGCCCGGACGAGGCGGTGAACGCGAAAC
				RB03: ATGGTCTAGAAAGCTTTAGTACAGCCCCGCAAAATCATCATCAC
C03			pOPINTF	FC03: AAGTTCTGTTTCAGGGCCCGGACGAGGCGGTGAACGCGAAAC
				RC03: ATGGTCTAGAAAGCTTTAGTACAGCCCCGCAAAATCATCATCAC
D03			pOPINCDM	FD03: AAGTTCTGTTTCAGGGCCCGGACGAGGCGGTGAACGCGAAAC
				RD03: ATGGTCTAGAAAGCTTTAGTACAGCCCCGCAAAATCATCATCAC
E03			pOPINRSJ	FE03: AAGTTCTGTTTCAGGGCCCGGACGAGGCGGTGAACGCGAAAC
				RE03: ATGGTCTAGAAAGCTTTAGTACAGCCCCGCAAAATCATCATCAC
F03			pOPINE-3C-eGFP	FF03: AGGAGATATACCATGGACGAGGCGGTGAACGCGAAAC
				RF03: CAGAACTTCCAGTTTGTACAGCCCCGCAAAATCATCATCAC
G03			pOPIN-3C-HALO7	FG03: AGGAGATATACCATGGACGAGGCGGTGAACGCGAAAC

				RG03: CAGAACTTCCAGTTTGTACAGCCCCGCAAAATCATCATCAC
H03			pOPINEneo-FLAG	FH03: AGGAGATATACCATGGACGAGGCGGTGAACGCGAAAC
				RH03: CAGAACTTCCAGTTTGTACAGCCCCGCAAAATCATCATCAC
A04	*trwBTMD-traJ*$_{P501}$	pUBQ3 plasmidoa	pOPINE	FA04: AGGAGATATACCATGTTTAATACGGATTCGCTTGCCTGGCAGTGG
				RA04: GTGATGGTGATGTTTGTACAGCCCCGCAAAATCATCATCACCCG
B04			pOPINFB	FB04: AAGTTCTGTTTCAGGGCCCGCATCCAGACGATCAAAGAAAGGTCAGCGCC
				RB04: AGATGTCGTTCAGGCCCTCGAGAAATGGTAATTTGCTGTTGTCATTGTTGGC
C04			pOPINFS	FC04: AAGTTCTGTTTCAGGGCCCGCATCCAGACGATCAAAGAAAGGTCAGCGCC
				RC04: AGATGTCGTTCAGGCCCTCGAGAAATGGTAATTTGCTGTTGTCATTGTTGGC
D04			pOPINTRX	FD04: AAGTTCTGTTTCAGGGCCCGCATCCAGACGATCAAAGAAAGGTCAGCGCC
				RD04: ATGGTCTAGAAAGCTTTACTCGAGAAATGGTAATTTGCTGTTGTCATTGTTGGC
E04			pOPINM	FE04: AAGTTCTGTTTCAGGGCCCGCATCCAGACGATCAAAGAAAGGTCAGCGCC
				RE04: ATGGTCTAGAAAGCTTTACTCGAGAAATGGTAATTTGCTGTTGTCATTGTTGGC
F04			pOPINS3C	FF04: AAGTTCTGTTTCAGGGCCCGCATCCAGACGATCAAAGAAAGGTCAGCGCC
				RF04: ATGGTCTAGAAAGCTTTACTCGAGAAATGGTAATTTGCTGTTGTCATTGTTGGC
G04			pOPINTF	FG04: AAGTTCTGTTTCAGGGCCCGCATCCAGACGATCAAAGAAAGGTCAGCGCC
				RG04: ATGGTCTAGAAAGCTTTACTCGAGAAATGGTAATTTGCTGTTGTCATTGTTGGC
H04			pOPINCDM	FH04: AAGTTCTGTTTCAGGGCCCGCATCCAGACGATCAAAGAAAGGTCAGCGCC
				RH04: ATGGTCTAGAAAGCTTTACTCGAGAAATGGTAATTTGCTGTTGTCATTGTTGGC
A05			pOPINRSJ	FA05: AAGTTCTGTTTCAGGGCCCGCATCCAGACGATCAAAGAAAGGTCAGCGCC
				RA05: ATGGTCTAGAAAGCTTTACTCGAGAAATGGTAATTTGCTGTTGTCATTGTTGGC
B05			pOPINE-3C-eGFP	FB05: AGGAGATATACCATGCATCCAGACGATCAAAGAAAGGTCAGCGCC
				RB05: CAGAACTTCCAGTTTCTCGAGAAATGGTAATTTGCTGTTGTCATTGTTGGC
C05			pOPIN-3C-HALO7	FC05: AGGAGATATACCATGCATCCAGACGATCAAAGAAAGGTCAGCGCC
				RC05: CAGAACTTCCAGTTTCTCGAGAAATGGTAATTTGCTGTTGTCATTGTTGGC
D05			pOPINEneo-FLAG	FD05: AGGAGATATACCATGCATCCAGACGATCAAAGAAAGGTCAGCGCC
				RD05: CAGAACTTCCAGTTTCTCGAGAAATGGTAATTTGCTGTTGTCATTGTTGGC
E05	*traJ*$_{pIP501}$	pIP501 plasmidoa	pOPINEneo	FE05: AGGAGATATACCATGACTAGTTTATTAGCAGAATCAGACGGTTTAATATTGGG
				RE05: GTGATGGTGATGTTTAAATGGTAATTCGCTGTTGTCATTGTTGGC
F05			pOPINFB	FF05: AAGTTCTGTTTCAGGGCCCGACTAGTTTATTAGCAGAATCAGACGGTTTAATATTGGG

				RF05: AGATGTCGTTCAGGCCAAATGGTAATTCGCTGTTGTCATTGTTGGC
G05			pOPINFS	FG05: AAGTTCTGTTTCAGGGCCCGACTAGTTTATTAGCAGAATCAGACGGTTTAATATTGGG
				RG05: GGTGGCTCCAGCTAGCAAATGGTAATTCGCTGTTGTCATTGTTGGC
H05			pOPINTRX	FH05: AAGTTCTGTTTCAGGGCCCGACTAGTTTATTAGCAGAATCAGACGGTTTAATATTGGG
				RH05: ATGGTCTAGAAAGCTTTAAAATGGTAATTCGCTGTTGTCATTGTTGGC
A06			pOPINM	FA06: AAGTTCTGTTTCAGGGCCCGACTAGTTTATTAGCAGAATCAGACGGTTTAATATTGGG
				RA06: ATGGTCTAGAAAGCTTTAAAATGGTAATTCGCTGTTGTCATTGTTGGC
B06			pOPINS3C	FB06: AAGTTCTGTTTCAGGGCCCGACTAGTTTATTAGCAGAATCAGACGGTTTAATATTGGG
				RB06: ATGGTCTAGAAAGCTTTAAAATGGTAATTCGCTGTTGTCATTGTTGGC
C06			pOPINTF	FC06: AAGTTCTGTTTCAGGGCCCGACTAGTTTATTAGCAGAATCAGACGGTTTAATATTGGG
				RC06: ATGGTCTAGAAAGCTTTAAAATGGTAATTCGCTGTTGTCATTGTTGGC
D06			pOPINCDM	FD06: AAGTTCTGTTTCAGGGCCCGACTAGTTTATTAGCAGAATCAGACGGTTTAATATTGGG
				RD06: ATGGTCTAGAAAGCTTTAAAATGGTAATTCGCTGTTGTCATTGTTGGC
E06			pOPINE-3C-eGFP	FE06: AGGAGATATACCATGACTAGTTTATTAGCAGAATCAGACGGTTTAATATTGGG
				RE06: CAGAACTTCCAGTTTAAATGGTAATTCGCTGTTGTCATTGTTGGC
F06			pOPIN-3C-HALO7	FF06: AGGAGATATACCATGACTAGTTTATTAGCAGAATCAGACGGTTTAATATTGGG
				RF06: CAGAACTTCCAGTTTAAATGGTAATTCGCTGTTGTCATTGTTGGC
G06			pOPINEneo-FLAG	FG06: AGGAGATATACCATGACTAGTTTATTAGCAGAATCAGACGGTTTAATATTGGG
				RG06: CAGAACTTCCAGTTTAAATGGTAATTCGCTGTTGTCATTGTTGGC

S3.2.4. ETEKIN-HANDIKO KLONAKETA

S3.1. taula. HTP klonaketan lortutako emaitzen laburpena. Lehenengo zutabeak konstrukto bakoitzari ezarritako kodigoa adierazten du, erreakzioa burutu zen 96-putzutako plakaren posizioarekin bat datorrena. Klonatutako genea, kodetzen duen proteina eta erabilitako bektorea 2., 3., eta 4. zutabeetan adierazten dira, hurrenez hurren. PCRtan lortutako anplikoiak %1eko (p/b) agarosazko gel elektroforesi bidez aztertu ziren eta lortutako emaitzak 5. zutabean adierazten dira. Berde, laranja eta gorria klonaketa arrakastatsua, zalantzagarria eta arrakastarik gabea adierazten dute, hurrenez hurren. Lehenengo PCR txandan ez zirenez produktu egokirik lortu A4-tik G6-ra, erreakzio hauek errepikatu ziren. Behin HTP klonaketa burututa, zatikiaren presentziaren baieztapena burutu zen PCR bidez, konstrukto bakoitzeko bi klonetan (3.7. irudia). DNA moldea bi planteamendu desberdin erabiliz lortu zen (2.2.3.3. atala): zelulen egosketa (6. zutabea) eta mini-prestaketak (7. zutabea). Hurrengo entseguetan erabiltzeko aukeratutako klon positiboak X bidez adierazten dira. Emaitza positiborik lortu ez ziren konstruktoentzat bigarren txanda bat burutu zen. Kasu honetan, konstrukto bakoitzeko zortzi klon aztertu ziren (3.7. irudia). Txanda honetatik aukeratutako klon positiboak zenbaki bidez adierazten dira 8. zutabean . Ez ziren emaitza positiborik lortu G4 konstruktoarentzat (pOPINTF-$tmd_{TrwB}traJ$). ZG: Zehaztu gabea.

1	2	3	4	5		6		7		8
Koordenada	Genea	Proteina	Bektorea	PCR txanda		Frogaketa (Egosketa)		Frogaketa (Mini-prep)		2. txanda (x8 klon)
				1	2	1	2	1	2	
A1	*mobB*	$MobB_{CloDF13}$	pOPINE		ZG					1
B1			pOPINFB		ZG					1
C1			pOPINFS		ZG			X		
D1			pOPINTRX		ZG			X		
E1			pOPINM		ZG			X		
F1			pOPINS3C		ZG					2
G1			pOPINTF		ZG				X	
H1			pOPINCDM		ZG					2
A2			pOPINRSJ		ZG			X		
B2			pOPINE-3C-eGFP		ZG			X		
C2			pOPINE-3C-HALO7		ZG			X		
D2			pOPINEneo-FLAG		ZG			X		
E2		MobBΔTMD	pOPINE		ZG			X		
F2			pOPINFB		ZG				X	1
G2			pOPINFS		ZG				X	
H2			pOPINTRX		ZG				X	
A3			pOPINM		ZG				X	
B3			pOPINS3C		ZG				X	
C3			pOPINTF		ZG				X	
D3			pOPINCDM		ZG				X	
E3			pOPINRSJ		ZG				X	
F3			pOPINE-3C-eGFP		ZG				X	
G3			pOPINE-3C-HALO7		ZG				X	
H3			pOPINEneo-FLAG		ZG				X	
A4	tmd_{trwB}-$traJ_{pIP501}$	$TMD_{TrwB}TraJ_{pIP501}$	pOPINE							2
B4			pOPINFB							1

C4			pOPINFS						X		
D4			pOPINTRX						X		
E4			pOPINM								1
F4			pOPINS3C						X		
G4			pOPINTF								X
H4			pOPINCDM								8
A5			pOPINRSJ						X		
B5			pOPINE-3C-eGFP						X		
C5			pOPINE-3C-HALO7						X		
D5			pOPINEneo-FLAG						X		
E5	***traJ*$_{pIP501}$**	TraJ$_{pIP501}$	pOPINEneo						X		
F5			pOPINFB								1
G5			pOPINFS						X		
H5			pOPINTRX						X		
A6			pOPINM						X		
B6			pOPINS3C						X		
C6			pOPINTF						X		
D6			pOPINCDM						X		
E6			pOPINE-3C-eGFP						X		
F6			pOPINE-3C-HALO7						X		
G6			pOPINEneo-FLAG			Haslea ez zuen funtzionatu					F6 haslea erabiliz: 1

S3.4.1. HISTIDINA KATEAN OINARRITUTAKO PROTEINEN GAIN-ADIERAZPENAREN AZTERKETA: $TraI_{PIP501}TraJ_{PIP501}$

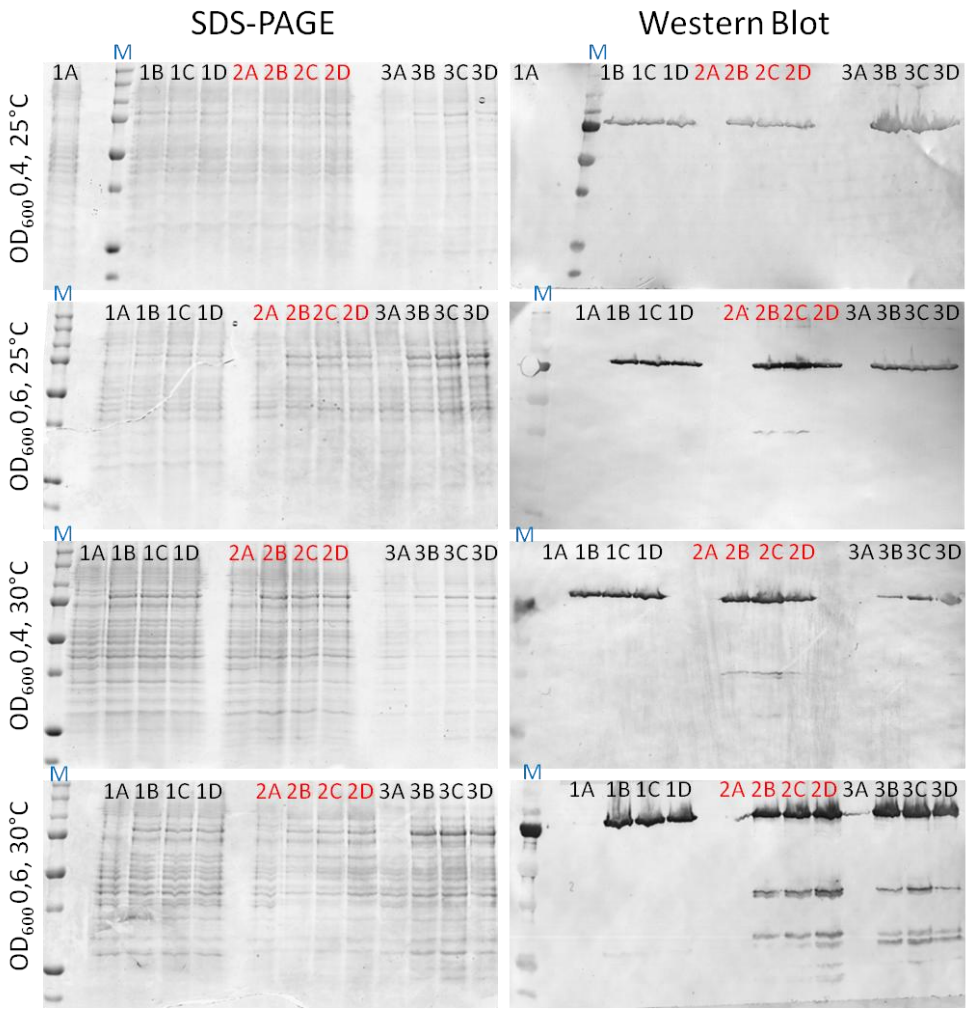

S3.1. irudia. Histidina katean oinarritutako $TraI_{pIP501}TraJ_{pIP501}$ proteinaren gain-adierazpen azterketa. *E.coli* BL21C41(DE3), Lemo21(DE3) eta Rosseta™ (DE3) pLysS anduiak pUBQ5 plasmidoarekin transformatu ziren. Zelula hauek egoera desberdinetan hazi eta induzitu ziren (3.11. irudia). Laginak lau eta hogei ordu ondoren hartu ziren gain-adierazpena aztertzeko. Zelula esekidurak 2.5.1. atalean azaldu bezala tratatu ziren. Laburbilduz, zentrifugatu ziren (14.000 *g*, 10 minutu, 4°C) eta lortutako jalkinak *SAB 3X indargetzailean* eseki ziren, zelula dentsitatea OD_{600} 0,2ra doituz. Bi SDS-PAGE burutu ziren, putzu bakoitzean 15 µL lagin jarriz. Haietako bat *Coomassie Blue* erabiliz tindatu zen, proteina guztien bistaratzea burutzeko. Bestea WB burutzeko erabili zen. *Mouse anti-His (C-term) monoclonal* eta *Donkey-AntiMouse IgG-HRP* antigorputzak erabili ziren antigorputz primario eta sekundarioa gisa, hurrenez hurren. Irudiko laburdurak: A: BL21C41(DE3), B: Lemo21(DE3), C: Rosseta™(DE3) pLysS, 1: IPTGrik gabe (kontrol negatiboa); 2: 0,4 mM IPTG; 3: 0,6 mM IPTG; 4: 1 mM IPTG. M: *Precision Plus Protein Dual Color Standard*.

S3.4.2. ETEKIN-HANDIKO GAIN-ADIERAZPEN AZTERKETA

S3.2. taula. HTP gain-adierazpen azterketan lortutako emaitzen laburpena. Lehenengo zutabeak konstrukto bakoitzari ezarritako kodigoa adierazten du, erreakzioa burutu zen 96-putzutako plakaren posizioarekin bat datorrena. Klonatutako genea, kodetzen duen proteina eta erabilitako bektorea 2., 3., eta 4. zutabeetan adierazten dira, hurrenez hurren. Itu proteinen adierazpena 2.5.1.1. atalean adierazi bezala burutu zen. Lortutako laginak SDS-PAGE bidez aztertu ziren (S3.2. irudia). Adierazpen eta solubilizazio mailak gelean agertutako banden bistaratzea burutuz baloratu eta adierazpenaren arabera hiru taldeetan banandu ziren: eza (ikurrik gabe), urria (+), erdi-mailakoa (++), altua (+++). Kualifikazio hauek Bird (2011)-k erabilitako "0,1,2,3" sistemarekin bat datoz. Zenbait konstruktoetan (horiz adieraziak) soilik bektore bidez gehitutako etiketa ikusi zen gelean. Emaitza negatibo edo zalantzagarriak emandako klonekin bigarren adierazpen azterketa bat burutu zen (gorriz adieraziak lehenengo zutabean). Bigarren txandan emaitza desberdinak lortuz gero hauek gorriz adierazita daude azken lau zutabeetan. ?: emaitza zalantzagarriak. handia: itu proteinaren banda espero baino tamaina handiagoa erakusten du SDS-PAGE gelean.

1	2	3	4	5	6			
Koordenatua	**Genea**	**Proteina**	**Bektorea**	**Pisu molekular teorikoa (Da)**	**Lemo21(DE3)**		**Rosseta™(DE3)**	
					IPTG	**TBONEX**	**IPTG**	**TBONEX**
A1	***mobB***	$MobB_{CloDF13}$	pOPINE	71720	+handia?	+handia?	+handia?	+handia?
B1			pOPINFB	71720				
C1			pOPINFS	71720	+	+	+	+
D1			pOPINTRX	84720				
E1			pOPINM	116720				
F1			pOPINS3C	71720		SUMO		SUMO
G1			pOPINTF	134720	+	+	+	+
H1			pOPINCDM	116720				
A2			pOPINRSJ	98720	+	+	+	+
B2			pOPINE-3C-eGFP	71720	+?	+?	+?	+?
C2			pOPINE-3C-HALO7	107720	+	+	+	+
D2			pOPINEneo-FLAG	71720				
E2		MobBΔTMD	pOPINE	51590	+	+++	++	+++

F2			pOPINFB	51590	+++	+++	+	+
G2			pOPINFS	51590	+++	+++	++	+++
H2			pOPINTRX	64590	+	+	+++	++
A3			pOPINM	96590	+++	+++	+++	+++
B3			pOPINS3C	64590	+++	++	+++	++
C3			pOPINTF	114590	+	+	+	+
D3			pOPINCDM	96590	+	+	+	+
E3			pOPINRSJ	78590	+	+	+	+
F3			pOPINE-3C-eGFP	78590	+	+	+	+
G3			pOPINE-3C-HALO7	87590	+	+	+	+
H3			pOPINEneo-FLAG	51590	++handia?	++handia?	+++	+++
A4	***tmd_{trwB}-$traJ_{pIP501}$***	$TMD_{TrwB}TraJ_{pIP501}$	pOPINE	69410	+	+	+	+
B4			pOPINFB	69410	+?			
C4			pOPINFS	69410			+	+handia?
D4			pOPINTRX	82410			TRX	TRX
E4			pOPINM	114410	+?	MBP	MBP	MBP
F4			pOPINS3C	82410		SUMO		
G4			pOPINTF	132410	TF	TF	TF	TF
H4			pOPINCDM	69410	MBP		+	MBP
A5			pOPINRSJ	96410	+	+	+	+
B5			pOPINE-3C-eGFP	96410	+			
C5			pOPINE-3C-HALO7	105410	+	+		+
D5			pOPINEneo-FLAG	69410		+		
E5	***$traJ_{pIP501}$***	$TraJ_{pIP501}$	pOPINEneo	60500			+	
F5			pOPINFB	60500	+?			
G5			pOPINFS	60500		+	+	+
H5			pOPINTRX	73500	+	+	+	+
A6			pOPINM	105500	+	+	+	+
B6			pOPINS3C	73500	+	+		
C6			pOPINTF	116500	+	+	+	
D6			pOPINCDM	105500		+	+	+
E6			pOPINE-3C-eGFP	87500	+	+	+	+

F6			pOPINE-3C-HALO7	87500	+	+	+	+
G6			pOPINEneo-FLAG	60500	+	+	+	+?

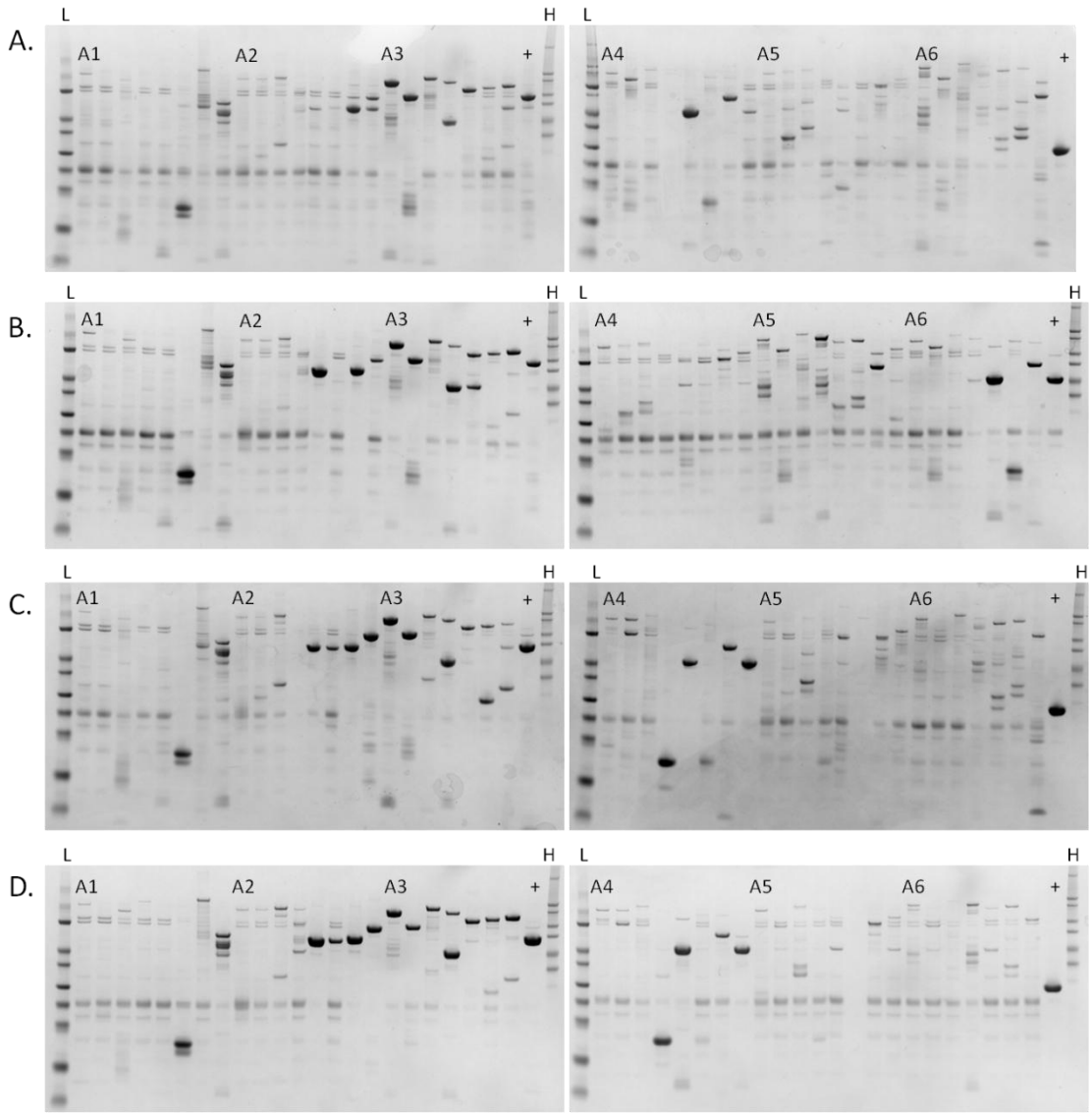

S3.2. irudia. HTP gain-adierazpenaren bidez lortutako proteinen SDS-PAGE azterketa. Proteina laginak %10 SDS-PAGE geletan kargatu ziren A1-H6 ordena jarraituz (S3.2. taula). **A)** IPTG bidez induzitutako *E.coli* Lemo21(DE3) bakterioetatik lortutako proteinak. **B)** TBONEX bidez induzitutako *E.coli* Lemo21(DE3) bakterioetatik lortutako proteinak. **C)** IPTG bidez induzitutako *E.coli* Rosseta™(DE3) pLysS bakterioetatik lortutako proteinak. **D)** TBONEX bidez induzitutako *E.coli* Rosseta™(DE3) pLysS bakterioetatik lortutako proteinak. L: *Sigma low range molecular weight marker*. H: *Sigma high range molecular weight marker*. +: Kontrol positiboa (H6): eGFP.

S3.4.3. eGFP FLUORESZENTZIAN OINARRITUTAKO GAIN-ADIERAZPEN AZTERKETA

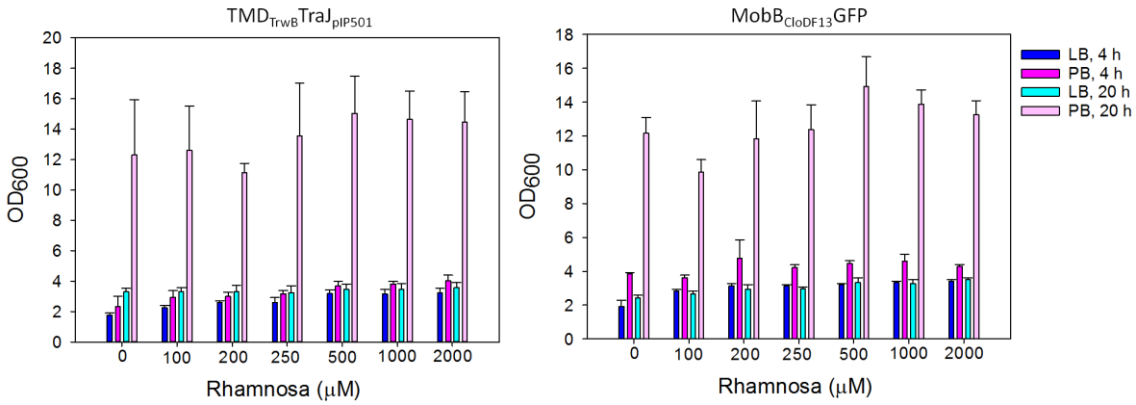

S3.3. irudia: MobB$_{CloDF13}$GFP eta TMD$_{TrwB}$TraJ$_{pIP501}$GFP proteinen gain-adierazpenaren eragina *E. coli* Lemo21(DE3) bakterioen hazkuntzan. Proteinen adierazpena LB edo PB hazkuntza medioak erabiliz burutu zen rhamnosa kontzentrazio desberdinetan. Adierazpena 0,4 mM IPTG erabiliz induzitu zen eta laginak 4 eta 20 h igarota jaso ziren. Bakterioen hazkuntza OD_{600} balioak neurtuz aztertu zen, horretarako *Jenway 6300* espektrofotometroa erabiliz.

S3.5.1.2. TrwB$_{R388}$ PROTEINAREN PURIFIKAZIOA

Soluzioan dagoen MP baten MW edota egoera oligomerikoa ezartzea ez da erreza, normalean atxikitutako detergente edota lipidoen ehunekoa ezezaguna delako. Arazo honi aurre egiteko tesi honetan TrwB$_{R388}$ purifikatu eta SEC-MALLS bidez ikertua izan zen, 2.7.1. atalean azaldu bezala. Lortutako emaitzak S3.4. irudia aurkezten dira. Kromatogramako gailur bakoitzean aurkitzen den proteina ehunekoa irizpidetzat hartuz lehenengo gailurra proteina-detergente konplexuari dagokio, bigarrena detergente mizelei dagokion bitartean (proteina %46,71 eta %6,91, hurrenez hurren). Proteina-detergente konplexuaren pisu molekularra 112,98 kDa da, DDM mizelen pisu molekularra 76,57 kDa izanik, literaturan deskribatuarekin bat datorrena (Strop eta Brunger, 2005). Datu hauetatik ondorioztatu zen TrwB$_{R388}$ren purifikazio prozesuan 50 kDa-eko iragazkia erabiltzea ez dela egokia, nahiz eta protokolo guztietan horrela egin izana (Hormaeche et al., 2002), DDMa ere kontzentratu egiten delako. Honetan oinarrituz, kontzentrazio prozesuan 100 kDa-eko iragazkia erabiltzerakoan proteinaren galerarik ez zela gertatzen frogatu zen. Behin hau frogatuta, tesi honetan TrwB$_{R388}$ edo antzeko pisu molekulardun T4CPak purifikatzerakoan 100 kDa-eko iragazkiak erabili ziren.

A.

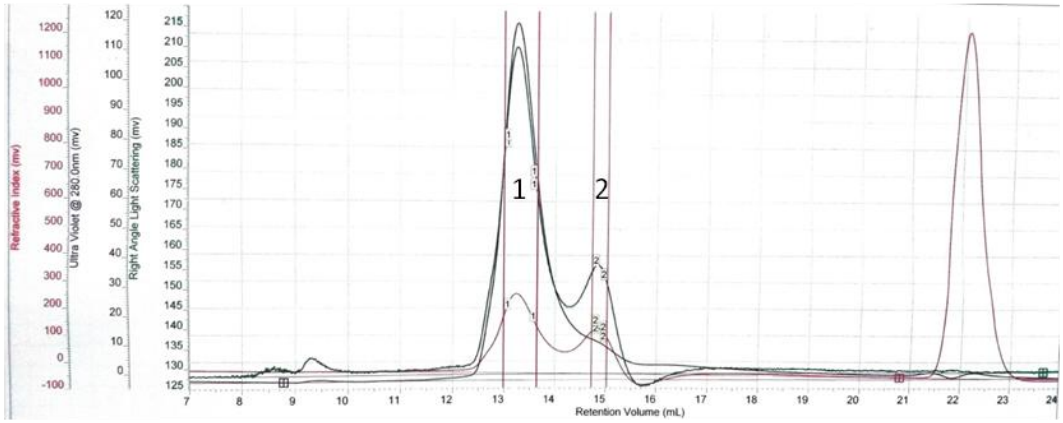

B.

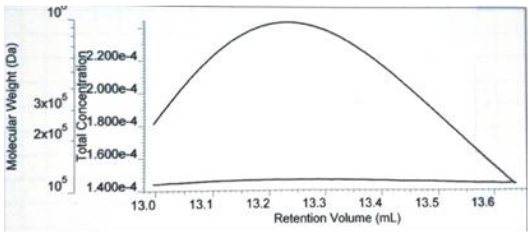

C.

Gailurra	1	2
Mw	112,982	76,567
Mw/Mn	1,000	1,000
Wt Fr (A)	0,4671	0,0691
RI Area	166,83	49,23
UV @ 280 Area	67,36	3,93
RALS Area	45,08	8,02
V_e	13,232	14,826

S3.4. irudia. $TrwB_{R388}$ren SEC-MALLS analisia. A) SEC-MALLS entseguan lortutako kromatograma. Errefrakzio indizearen (RI, gorriz), 280 nm-tan izpi-ultramoreen absorbantziaren (UV @ 280, morez), eta angelu zuzeneko argi dispertsioaren (RALS, berdez) neurketak aldi berean jaso ziren entsegu osoan zehar. Bi gailur nagusi identifikatu ziren, haietako bakoitza bi lerro gorriren bidez mugatuak. **B)** Pisu molekularraren (Da) eta kontzentrazioaren (M) banaketa SEC-ren eluzio bolumenean zehar. **C)** Lortutako emaitzen laburpena. 1. eta 2. zutabeak kromatografiaren 1. eta 2. gailurrei dagozkie, hurrenez hurren. Mw: makromolekularen pisu molekularra (proteina-detergente konplexua edo detergente mizela). Mw/Mn: kalkulaturiko pisu molekular eta batezbesteko pisu molekularraren arteko erlazioa; datuen kalitatea ebaluatzeko baliogarria dena. Wt Fr(A): A frakzioa den Mw-ren ehunekoa, proteinari dagokiona, alegia. RI Area, UV @ 280 Area eta RALS Areak gailur bakoitzarentzat mugaturiko tartean kurba bakoitzaren azpian dagoen eremua adierazten dute. V_e: gailur bakoitzari dagokion eluzio bolumena.

S3.5.1.3. TMD_{TraJ}-TEV-CD_{TrwB} PROTEINAREN PURIFIKAZIOA

TMD_{TraJ}-TEV-CD_{TrwB} kimera proteina purifikatzeko, 58,28 kDa-eko MW teorikoa daukana, $TrwB_{R388}$rentzat ebatzitako purifikazio protokoloa jarraitu zen, aldaketa batzuekin (Hormaeche et al., 2006).

Laburbilduz, lehenengo eta behin *E. coli* BL21C41(DE3) bakterioak pUBQ1 plasmidoarekin transformatu ziren. Hurrengo pausuak (gain-adierazpena, zelulen apurketa eta mintz frakzioaren lorpena eta solubilizazioa) $TrwB_{R388}$rentzat deskribatu bezala burutu ziren, prozesu osoa 4°C-tan eginez . Ondoren, solubilizaturiko lagina *50 mM Tris-HCl (pH 7,8), 1 mM DDM, 0,1 mM EDTA eta 200 mM NaCl* indargetzailearekin orekaturiko *Whatman® P-11*

fosfozelulosa ioi-truke kromatografiatik igaro zen, Ioi trukezko kromatografia: P-11 fosfozelulosa erretxina azaldu bezala. Atxikitu gabeko proteinak indargetzaile berdinarekin garbitu eta gainerako proteinak *50 mM Tris-HCl (pH 7,8), 1 mM DDM, 0.1 mM EDTA eta 1 M NaCl* indargetzailearekin eluitu ziren, 1,5 mL/min-ko fluxuan. Lortutako frakzioak SDS-PAGE bidez azter ziren, purifikazioaren lehenengo pausuetan jasotako laginekin batera. Kimera proteinadun frakzioak elkartu eta aldez aurretik *50 mM Tris-HCl (pH 7,8), 0,2 mM DDM, 0,1 mM EDTA, 20 mM imidazole eta 200 mM NaCl* indargetzailearekin orekatutako 5 mL-tako *HiTrap Chelating* afinitatezko kromatografiatik birzirkulatzen utzi ziren 1 mL/min-ko fluxuan gau osoan zehar.

Hurrengo egunean zutabea oreka indargetzailearen 50 mL-rekin garbitu zen, atxikitu gabeko proteinak deuseztatzeko. Lotutako proteinak 20tik 168 mM-era egindako imidazol gradientea erabiliz eluitu ziren, 2,5 mL/min-ko fluxuarekin, 9,5 minutuz zehar eta 2 mL-ko frakzioak jasoz (S3.5. irudia, A). Lortutako laginak SDS-PAGE bidez aztertu ziren (S3.5. irudia, B). Kromatogramak gailur bakarra aurkezten zuen, TMD_{TraJ}-TEV-CD_{TrwB} proteinaren eluzioarekin bat zetorrena. Hala ere, proteinari zegokion bandaren azpian, antzeko intentsitatedun banda bat ikusten zen kasu guztietan. Horrek iradokitzera ematen zuen kimera proteinaren zati handi bat hidrolizatzen ari zela.

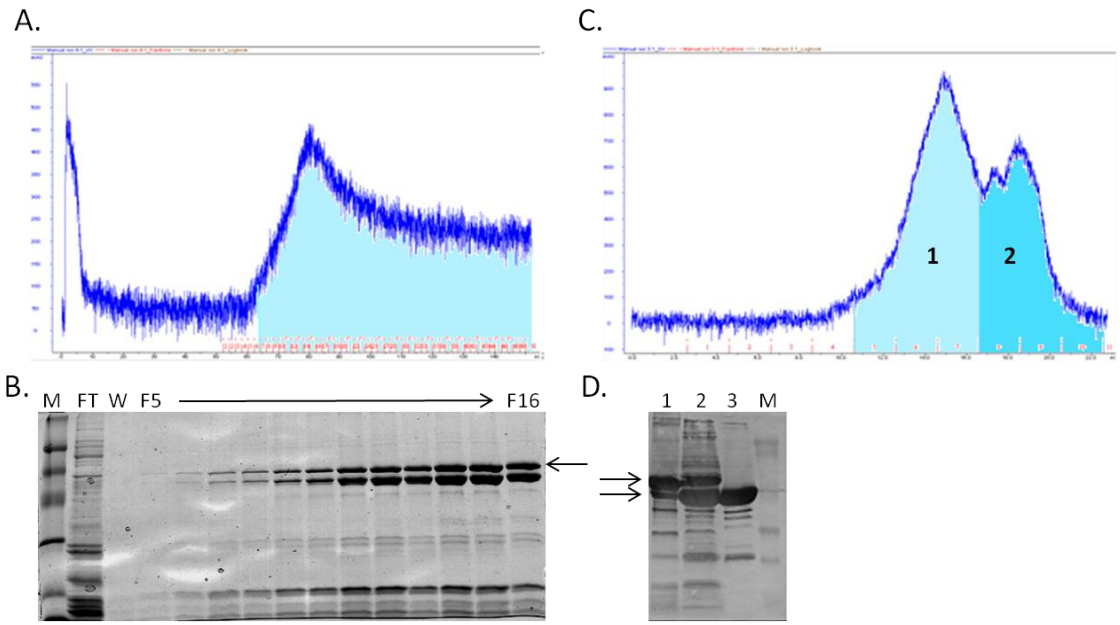

S3.5. irudia. TMD_{TraJ}-TEV-CD_{TrwB}-ren purifikazioko lehenengo saiakera. A) *HiTrap Chelating* afinitatezko kromatografiatik lortutako kromatograma. Eluzioa 280 nm-tan izpi ultramoreen absorbantzia neurtuz jarraitu zen. 2 mL-tako 50 frakzio jaso ziren. Kromatograman urdinez adierazitako frakzioak hurrengo pausuetarako elkartu ziren. **B)** *HiTrap Chelating* afinitatezko kromatografiatik lortutako frakzioen SDS-PAGE azterketa. FT: lotu gabeko proteinak (*flow through*); W: garbitutako proteinak (*wash*); F5 → F16: eluitutako frakzioak, 5.etik 16.era. **C)** *Superose 6 10/300* SEC zutabetik lortutako kromatograma. Proteinen eluzioa 280 nm-tan izpi ultramoreen absorbantzia neurtuz jarraitu zen. Urdin kolore desberdinek azken laginak lortzeko elkartu ziren bi proteina multzoak adierazten dituzte. **D)** Purifikazio protokoloaren ostean lortutako laginen SDS-PAGE analisia. 1: 1. lagina, 1. gailurreko frakzioetatik osatua; 2: 2.

lagina, 2. gailurreko frakzioetatik osatua. 3: purifikatutako TrwBΔN70, kontrol gisa. M: *Low range prestained marker*.

Itu proteina zeukaten frakzioak elkartu ziren (7.etik 50.era) eta gelean ikusitako hidrolisia saihesteko laginari PMSFa gehitu zitzaion 0,2 mM-eko kontzentraziora. Jarraian lagina 800 µL-ra kontzentratu zen eta agregatuak kentzeko zentrifugatu zen (17.000 *g*, 10 min, 4°C). Gain-jalkineko 500 µL *Superose 6 10/300* SEC zutabean gehitu ziren. Kromatografia 50 *mM Tris-HCl (pH 7,8), 0,2 mM DDM, 0,1 mM EDTA eta 200 mM NaCl* indargetzailea erabiliz burutu zen, 0,38 mL/minutuko fluxuan, 2 mL-tako frakzioak jasoz (S3.5. irudia, C). Lortutako frakzioak SDS-PAGE bidez aztertu ziren eta ikusi zen kromatogramako 1. gailurra TMD_{TraJ}-TEV-CD_{TrwB} proteinarekin erlazionaturik zegoela, 2. eta 3.a hidrolizaturiko espeziearekin erlazionaturik egonda. Frakzio desberdinak irizpide honen arabera elkartu ziren: F1, F6 eta F7 1. lagina osatuz eta 8., 9. eta 10. frakzioak 2. lagina osatuz. Lagin bakoitza kontzentratu eta SDS-PAGE bidez aztertu zen (S3.5. irudia, D). Nahiz eta TMD_{TraJ}-TEV-CD_{TrwB} bi laginetan aurkitu, hidrolizaturiko espeziea baita aurkitzen zen, proteina nagusia izanik 2. laginean. Hidrolisia TEV sekuentziatik gertatzen ari zela frogatzeko, TrwBΔN70 proteina (CD_{TrwB}ren baliokidea) erreferentzia moduan erabili zen SDS-PAGE gelean. Modu horretan hidrolizaturiko espeziearen tamaina TrwBΔN70rekin bat zetorrela ikusi zen (S3.5. irudia, D, 2. eta 3. lerroak) eta honen ondorioz gainerako entseguetan proteina hau erabiltzea deuseztatu zen.

S3.5.2. $MobC_{CloDF13}$ PROTEINAREN ADIERAZPEN ETA PURIFIKAZIOA

T4CPak ikertzearekin batera, tesi honetan $MobC_{CloDF13}$ proteina purifikatzeko lehenengo saiakerak burutu dira. Proteina hau CloDF13 plasmidoaren erlaxazioa burutzeko ezinbestekoa denez, badirudi CloDF13ren errelaxasa espezifikoa dela, nahiz eta sekuentzien azterketan gainerako errelaxasen ezaugarri komunak ez aurkeztu (Núñez eta De La Cruz, 2001). Proteina hau purifikatzearen helburua $MobB_{CloDF13}$rekin batera ikertzea zen, *in vitro* nola elkarrekiten duten aztertzeko, dagoeneko deskribatu baita elkarrekin *in vivo oriT*aren mozketa burutzen dutela (Núñez eta De La Cruz, 2001).

Lehenengo eta behin gain-adierazpen baldintzak ezarri ziren. Horretarako *E. coli* BL21C41(DE3) bakterioak pUB49 plasmidoarekin transformatu ziren eta lortutako koloniak 10 mL kanamizinarekin aberastutako 10 mL LB medioan hazi ziren gau osoan zehar 37°C-tan. Hurrengo egunean kultiboak medio berean diluitu ziren (1:20, b/b) eta 37°C-tan hazi ziren OD_{600} 0,6 balioa izan arte. Proteinaren adierazpena 1 mM IPTG gehituz induzitu zen. Kultiboak 4 orduz 37°C-tan hazten utzi, ondoren jaso eta lisatu ziren proteina adierazpenaren SDS-PAGE azterketa burutzeko (S3.6. irudia, A). $MobC_{CloDF13}$ 28,8 kDa-eko MW teorikoa dauka, gelean ikusitako banda nagusiarekin bat datorrena.

Behin proteinaren presentzia eta adierazpena frogaturik, protokoloa hiru bakterio litrora eskalatu zen baldintza berdinak erabiliz. Ostean kultiboak zentrifugazio bidez jaso (8.000 *g*, 15 min, 4°C), 50 mL *zelula indargetzaile*tan esekitu eta nitrogeno likidoan izoztu ziren. Purifikazioa burutzeko lehenengo eta behin lagina ur bainu bidez desizoztu zen 37°C-tan eta ondoren 0,02 mg/mL DNasa I, %0,07 (p/b) lisozima, 1 mM $MgCl_2$ eta 1 mM PMSF gehitu zitzaizkion bakterioen apurketa entzimatikoa burutzeko. Puntu honetatik aurrera protokolo guztia 4°C-tan burutu zen. Ordu batez lisozimarekin inkubatu ostean apurketa mekanikoa egin

zen sonikazio bidez zelulen lisia azaldu bezala. $MobC_{CloDF13}$ proteina solugarria izanik, lagina ultrazentrifugatu (105.000 *g*, 1h, 4°C) eta gain-jalkina jaso zen mintz-frakzioa deuseztatuz. Lortutako laginari 10 mM imidazol gehitu zitzaizkion eta aldez aurretik 10 mM imidazolrekin aberastutako *zelula indargetzaile*rekin orekatutako *His-trap*^{TM} *FF* zutabetik birzirkulatzen utzi zen gau osoan zehar. Hurrengo egunean, indargetzaile berdina erabiliz, lotu gabeko proteinen garbiketa burutu zen. Ondoren itu proteinaren eluzioa burutu zen imidazol kontzentrazioa hiru pausutan areagotuz: 50 mM, 170 mM (S3.6. irudia, B, lauki urdina) eta 225 mM (S3.6. irudia, B, lauki gorria). Ikusi zen proteina ez zela 50 mM imidazolrekin askatzen, hurrengo saiakeretan lagina zutabera kontzentrazio horretan gehitu ahalko zela ondorioztatuz. Hala ere, eluzioaren ostean lortutako proteina kantitatea oso urria izan zenez purifikazioa puntu horretan gelditu zen.

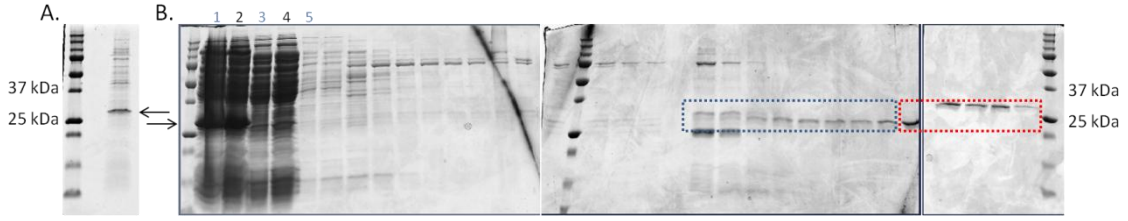

S3.6. irudia. $MobB_{CloDF13}$ proteinaren adierazpen eta purifikazio saiakera. A) $MobC_{CloDF13}$ adierazten zuten bakterio lisatuen azterketa SDS-PAGE bidez. 2 µL lagin erabili ziren. Geziak itu proteina adierazten du. **B)** *His-Trap*^{TM} *FF* afinitate kromatografia zutabetik jasotako frakzioen azterketa SDS-PAGE bidez. 3 µL (1. tik 4. laginera) edo 5 µL lagin gehitu ziren lerro bakoitzeko. 1: jasotako zelula esekidura, 2: sonikatutako bakterioak, 3: apurtutako bakterioak, 4: *His-trap*^{TM} *FF* zutabetik igarotako lagina *(flow through),* 5: estuki ez atxikitutako proteinen garbiketa. Gezia itu proteina adierazten du. Lauki urdin eta gorriak 170 eta 225 mM imidazolrekin eluitutako itu proteina adierazten dute, hurrenez hurren. *Precision Plus Protein*^{TM} *Dual Color* MW markatzaile gisa erabili zen.

Itu proteinaren urritasuna aztertzeko, purifikazio prozesuan zehar lortutako lagin ezberdinak SDS-PAGE bidez aztertu ziren (S3.6. irudia, B). Modu horretan ikusi zen $MobC_{CloDF13}$ gehiena mintz-frakzio eta proteina ez-solugarriekin batera galdu zela (S3.6. irudia, B, 2. eta 3. lerroen arteko konparaketa). Bi arrazoi egon daitezke hau gertatzeko. Alde batetik, posiblea da itu proteinaren adierazpena altua izatea, baina proteina hori modu ez-solugarrian egotea (inklusio gorputzetan); beste aldetik, gerta liteke naiz eta proteina solugarria izan, mintzeko elementuekin elkarrekiten egotea eta ondorioz haiekin batera jalkitzea ultrazentrifugazio prozesuan. Ondorioz, proteina honen purifikazio protokoloarekin aurrera jarraitu baino lehen, bere adierazpena eta zelula kokapena sakonki aztertu beharko lirateke.

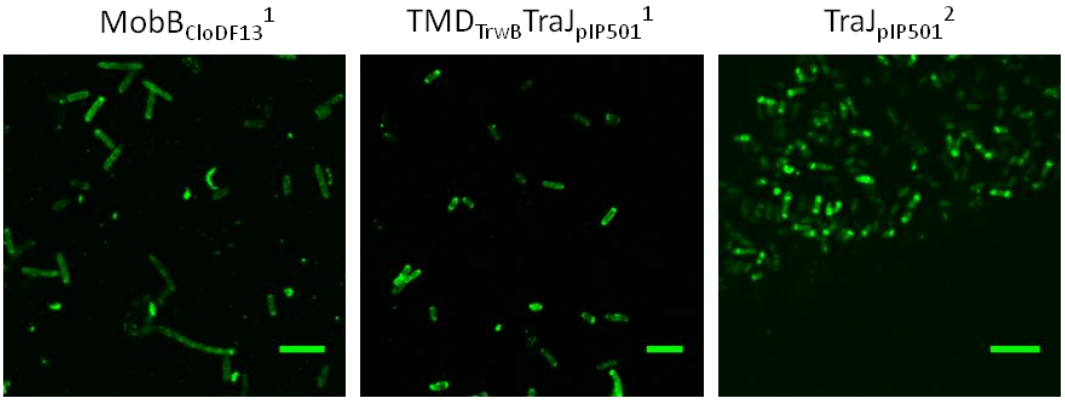

S3.7. irudia. MobB$_{CloDF13}$, TMD$_{TrwB}$TraJ$_{pIP501}$ eta TraJ$_{pIP501}$ proteinen kokapen azpizelularra immunofluoreszentzia mikroskopia bidez aztertua. Kokapen azpizelularra aztertzeko itu-proteinak *E. coli* [1]BL21C41(DE3) eta [2]BL21(DE3) bakterioetan adierazi ziren. Horretarako plasmido egokiarekin transformatutako bakterio kultiboak OD_{600} 0,4 balioan 1 mM IPTGrekin induzitu ziren, 20 orduz 25°C-tan hazten utziz. Bakterio laginak 2.9.1.2. atalean azaldu bezala prestatu ziren immunofluoreszentzia mikroskopia burutzeko. M*ouse anti-His (C-term) monoclonal* eta *Alexa Fluor goat anti-mouse* antigorputzak erabili ziren lehen maila eta bigarren mailako antigorputz gisa, hurrenez hurren. Irudiak *Olympus Fluoview^{TM} 500* mikroskopio konfokala erabiliz jaso ziren "Biomedikuntzan Mikroskopia Analitiko eta Bereizmen Handikoa (SGIker, UPV/EHU)" zerbitzuaren laguntzaz. Eskala: 5 µm.

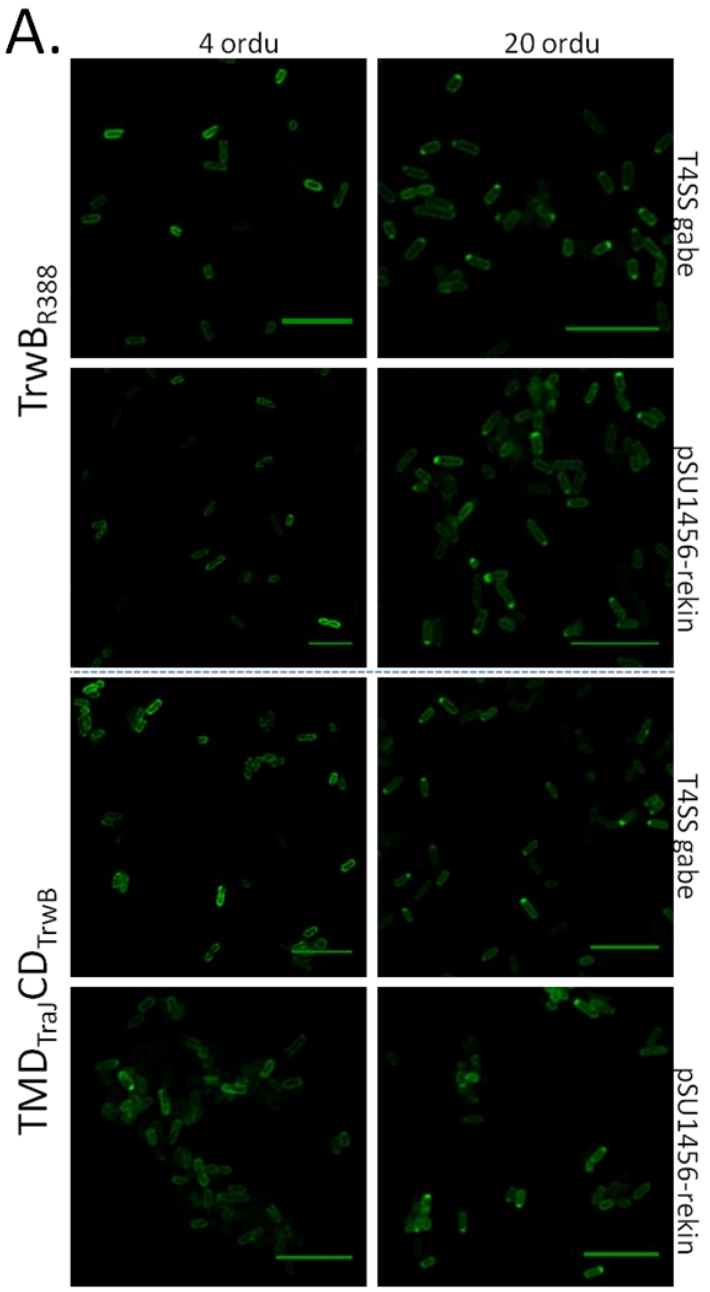
A.
4 ordu
20 ordu
TrwB$_{R388}$
T4SS gabe
pSU1456-rekin
TMD$_{TraJ}$CD$_{TrwB}$
T4SS gabe
pSU1456-rekin

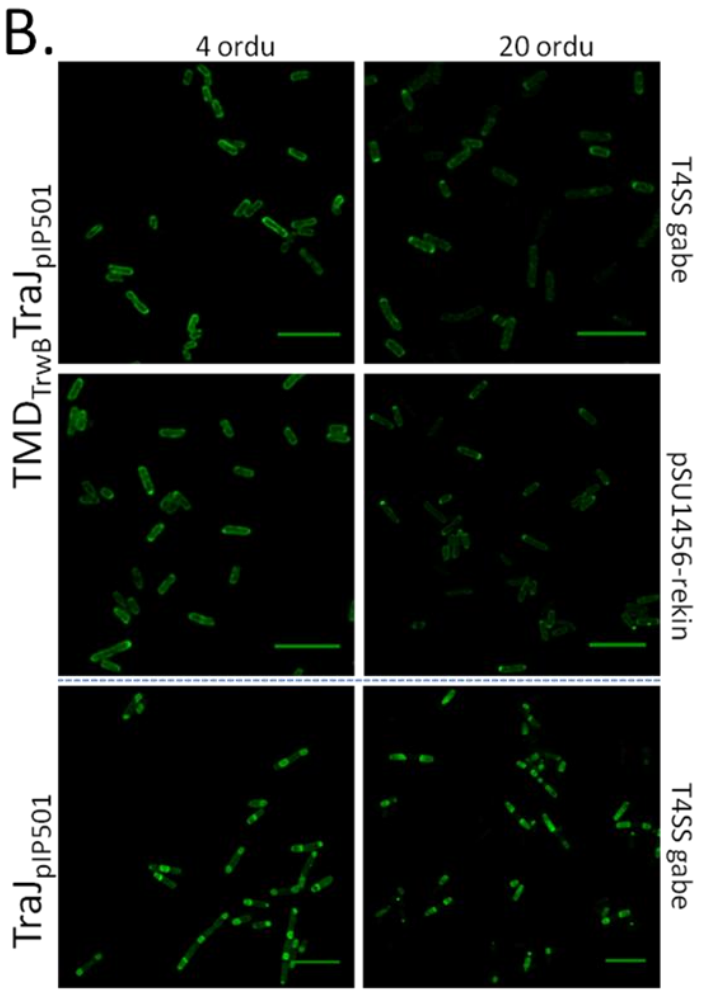
B.
4 ordu
20 ordu
TMD$_{TrwB}$TraJ$_{pIP501}$
T4SS gabe
pSU1456-rekin
TraJ$_{pIP501}$
T4SS gabe

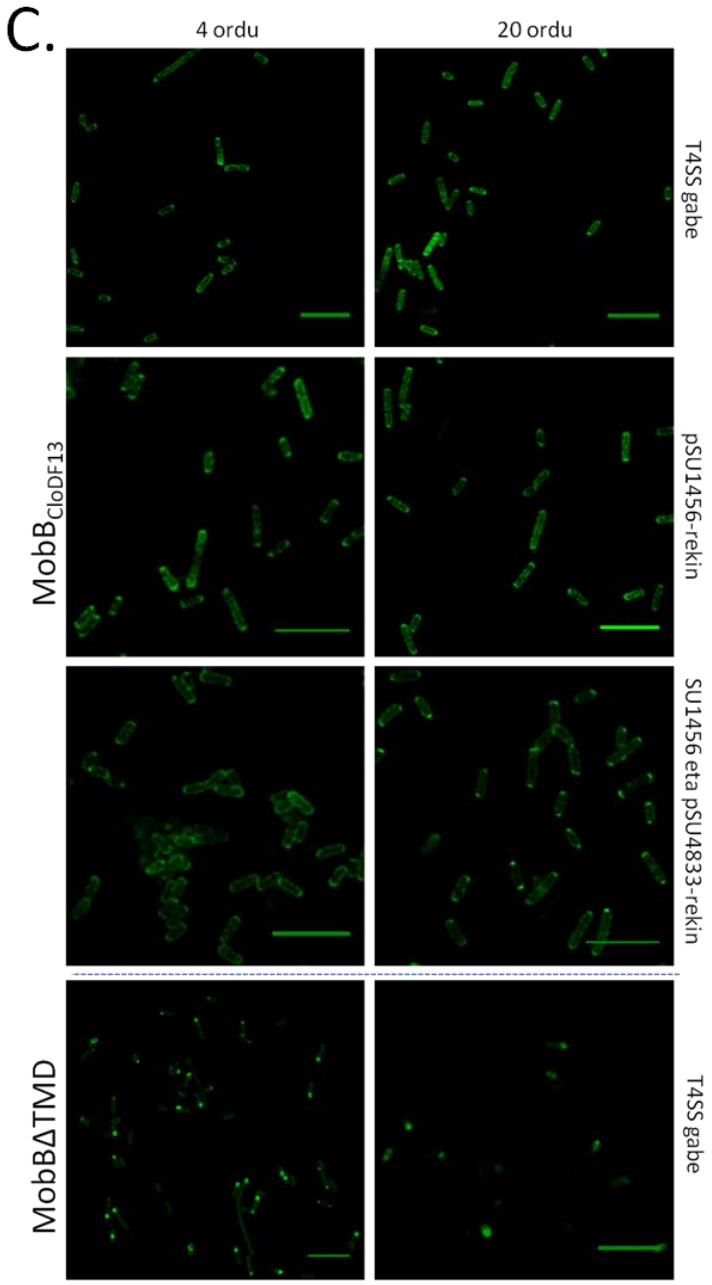

S3.8. irudia. T4CP-eGFP fusio-proteina desberdinen kokapen azpizelularra. TrwB$_{R388}$ eta TMD$_{TraJ}$CD$_{TrwB}$ (A), TMD$_{TrwB}$TraJ$_{pIP501}$ eta TraJ$_{pIP501}$ (B), eta MobB$_{CloDF13}$ eta MobBΔTMD (C) proteinen eGFP fusio-proteinak *E. coli* BL21C41(DE3)* bakterioetan adierazi ziren 1 mM IPTG erabiliz eta ondoren 4 (ezkerreko panela) eta 20 orduz (eskumako panela) 25°C-tan hazten utziz. Proteina hauen kokapen azpizelularra pSU1456 plasmidoaren presentzian, R388ren proteina konjugatibo guztiak kodetzen dituena TrwB$_{R388}$ izan ezik, edo absentzian aztertu zen. Horretaz gain MobB$_{CloDF13}$ pSU1456 eta pSU4833ren presentzian aztertu zen ere. Azken honek CloDF13ren mobilizazio proteina guztiak kodetzen ditu, MobB$_{CloDF13}$ izan ezik. Laginen behaketa *Leica TCS SP5* mikroskopio konfokalean egin zen, 60X olio objektiboa, 488 nm-tako kitzikapena eta 525 nm-tako igorpena erabiliz. Irudiak *Huygens* eta *ImageJ* softwareak erabiliz analizatu ziren. Eskala: 5 µm. * TraJ$_{pIP501}$ eta MobBΔTMD *E. coli* BL21(DE3) bakterio anduian adierazi ziren.

S4.2.1.2. INDAR IONIKO, PH ETA DETERGENTE KONTZENTRAZIOAREN ERAGINA EGONKORTASUNEAN

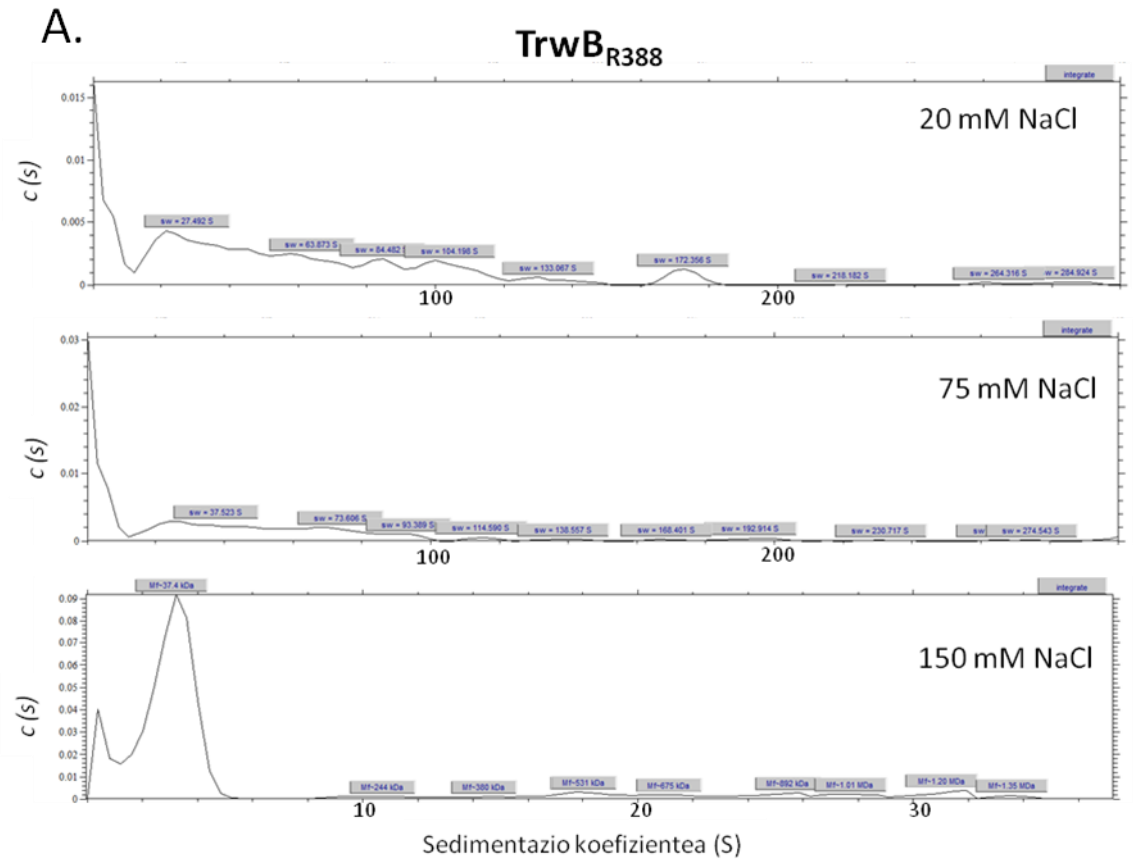

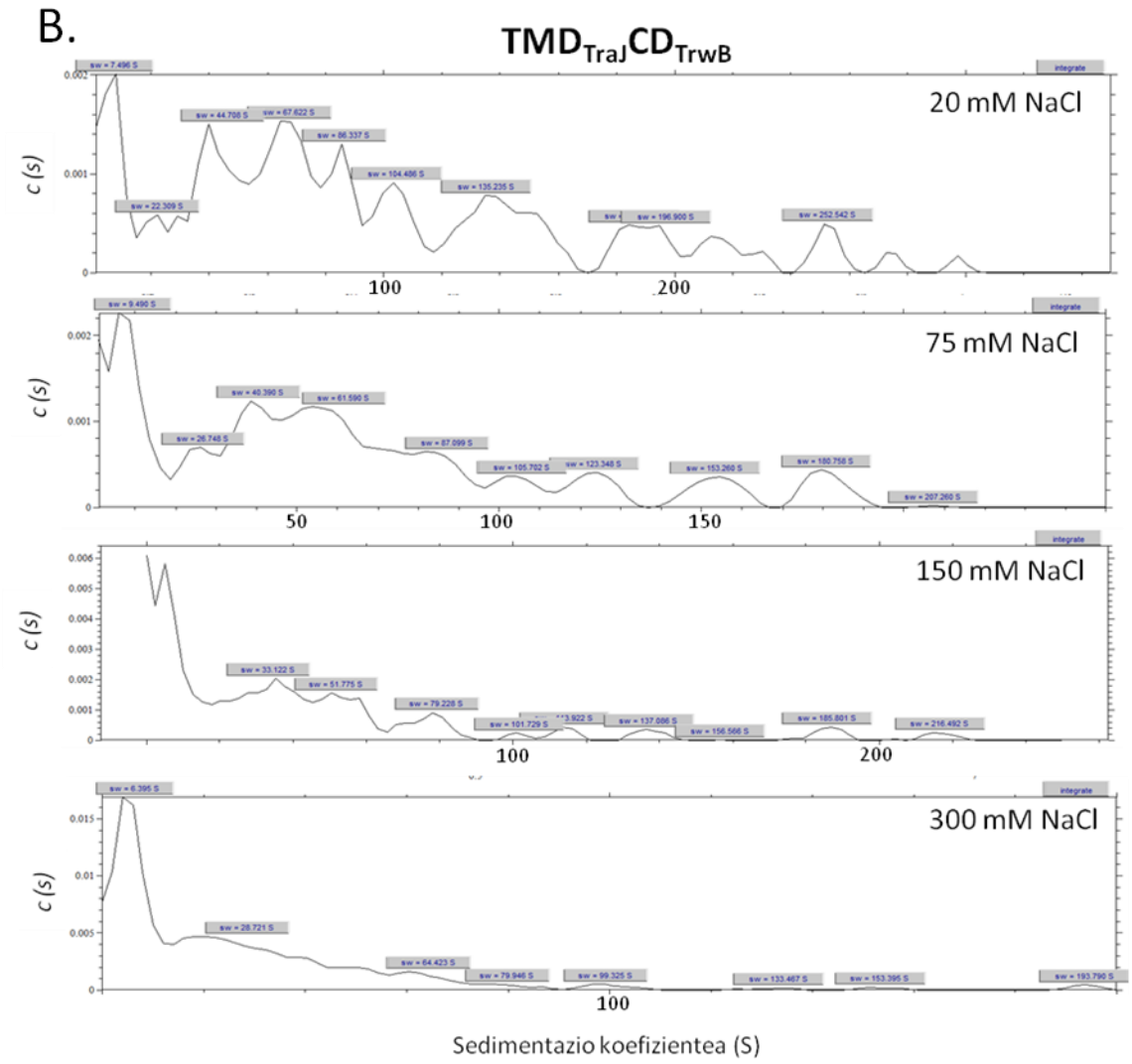

S4.1. irudia. $TrwB_{R388}$ (A) eta $TMD_{TraJ}CD_{TrwB}$ (B) proteinen sedimentazio koefizienteak indar ioniko desberdinetan. 5,23 µM $TrwB_{R388}$ eta 5,15 µM $TMD_{TraJ}CD_{TrwB}$ *50 mM Tris-HCl (pH 7,8), 0,2 mM DDM, 0,1 mM EDTA eta 5% (b/b) glizerol* indargetzailean aztertu ziren indar ioniko desberdinetan (NaCl kontzentrazioa aldatuz). Entseguak 129.000 *g* eta 20°C-tan burutu ziren *XL-A analytical* ultrazentrifuga batean *AN50Ti* errotorea eta 12 mm-tako sektore-biko erdiko piezak erabiliz. Lagin bakoitzetik datuak bost minuturo jaso ziren 280 nm-tan absorbantzia neurtuz. *c(s)*ak sedimentazio abiadurako datuen karratu txikieneko mugen modelizazio bidez kalkulatu ziren, *SEDFIT* programan ezarritako moduan.

S4.3. DNArekin ELKARREKINTZA

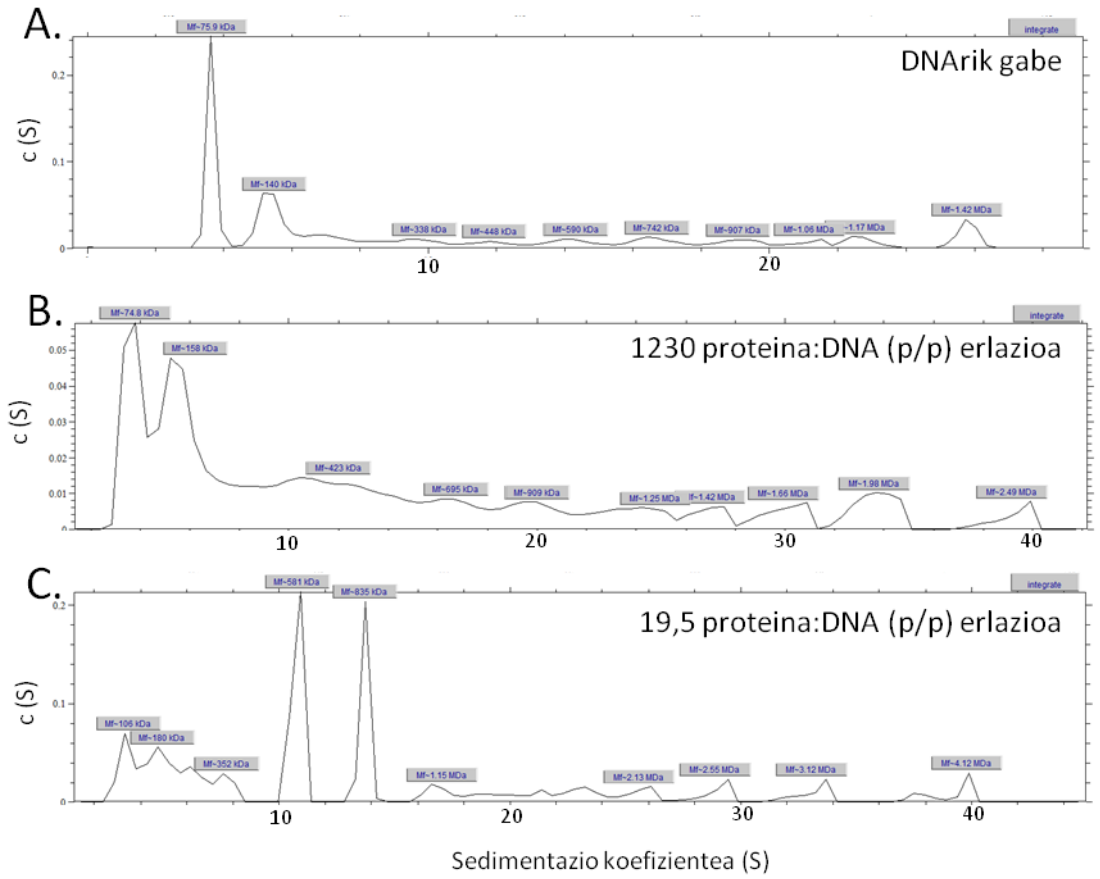

S4.2. irudia. $TMD_{TraJ}CD_{TrwB}$ren sedimentazio koefizienteak proteina:DNA (p/p) erlazio desberdinetan. 5,15 µM $TMD_{TraJ}CD_{TrwB}$ pUC18 plasmidoaren presentzian aztertu ziren *50 mM Tris-HCl (pH 7,8), 0,3 mM DDM, 0,1 mM EDTA, %5 (b/b) glizerol eta 300 mM NaCl* indargetzailea erabiliz, 6 mM $MgCl_2$rekin aberastua B eta C-n. Entseguak eta datuen analisia S4.1. irudian adierazi bezala burutu ziren.

S4.4.1.2. MONOMERO ETA HEXAMEROEN LORPENERAKO PROTOKOLOA

$TMD_{TraJ}CD_{TrwB}$ Hormaeche et al. (2004) ebatzitako prozedura jarraituz purifikatu egin zen aldaketa gutxi batzuekin.

E. coli BL21C41 (DE3) bakterio konpetenteak pUBQ4 plasmidoarekin transformatu egin ziren. Lortutako koloniak kanamizinadun 10 mL LB zortzi matraze inokulatzeko erabili ziren. Kultiboak gau osoan zehar hazi ziren eta hurrengo egunean 1:20 proportzioan diluitu ziren (500 mL-ko LB-Kan zortzi matrazetan). Bakterio suspentsioak 37°C-tan hazi ziren OD_{550} 0,6-0,8 izan arte. Orduan, gain-adierazpena induzitu zen 1 mM IPTG erabiliz eta kultiboak 25°C-tan lau orduz utziz. Lortutako kultiboak zentrifugatu ziren (8.000 *g*, 15 min, 4°C) eta jalkina 70 mL *zelula indargetzaile*n berreseki zen. Lortutako esekidura nitrogeno likidoa erabiliz izoztu eta -80°C-tan biltegiratu zen.

Purifikazio protokoloa burutzeko zelulak 37°C-tan desizoztu ziren ur bainu bat erabiliz. Pausu honetatik aurrera protokolo guztia 4°C-tan burutu zen proteinaren agregazioa saihesteko. Bakterio suspentsioa 1 mM DTT, 0,2 mM PMSF eta %0,07 (p/b) lisozimarekin inkubatu zen 30 minutuz, noizean behin astinduz. Ondoren, lagina sonikatu zen *MSE Soniprep 150* batean, 15 mikronetako anplitudea erabiliz. 10 sonikazio ziklo burutu ziren, 10 segundoz sonikatuz eta 10 segundoz geldituz. Hau burutzeko lagina bitan banandu zen eta bakoitzak bi sonikazio txanda jasan zituen. Ondoren, laginak elkartu eta berriz sonikatu ziren. Prozesu honetan zehar lagina izotz-ur bainuan mantendu zen berotzearen ondoriozko agregazioa saihesteko. Apurtu gabeko zelulak deuseztatzeko, lagina zentrifugatu (8.000 *g,* 15 min, 4°C) eta gain-jalkina jaso zen, ondoren mintz-frakzioa jasotzeko ultrazentrifugatu zena (105,000 *g,* 1 h, 4°C). Mintzak %1 (p/b) DDM eta 600 mM NaCl-dun 40 mL *zelula indargetzaile*rekin eseki ziren eta 90 minutuz 4°C-tan agitaziorekin inkubatu ziren. Jarraian, lagina ultrazentrifugatu zen (105.000 *g,* 1 h, 4°C) solubilizaturiko mintz proteinak lortuz gain-jalkinean. Lagin hau kromatografia zutabe desberdinetatik igaro zen $TMD_{TraJ}CD_{TrwB}$ren monomero eta hexameroak banandurik lortzeko.

Lehenengo eta behin, lagina *TrwB oligomers 1* indargetzailearekin diluitu zen 200 mM NaCl kontzentrazioa izan arte eta 70 mL-tako *Whatman® P-11* zutabean kargatu zen, elkartruke ionikoko kromatografia bat burutzeko. Zutabe hau aldez aurretik *TrwB oligomers 2* indargetzailearen 140 mL-rekin orekatu zen. Lagina, behin zutabetik igaro ondoren, gau osoan zehar birzirkulatzen utzi zen 1 mL/min-ko fluxuan. Ondoren erretxina 120 mL *TrwB oligomers 2* indargetzailea erabiliz garbitu zen. Proteina eluzioa bi pausutan egin zen, lehenengoa 100 mL *TrwB oligomers 3* indargetzailea erabiliz monomeroen lorpenerako (I. frakzioa, **FI**) eta ondoren *TrwB oligomers 4* indargetzailearekin hexameroen lorpenerako (II. frakzioa, **FII**).

Jasotako frakzioak SDS-PAGE bidez aztertu ziren, purifikazioaren lehenengo pausutan hartutako alikuotekin batera (S4.3. irudia, A). $TMD_{TraJ}CD_{TrwB}$ gehiena, 58,3 kDa-eko MW teorikoduna, P-11 erretxinara lotu zen 200 mM NaCl kontzentrazioan. FII frakzioak FI frakzioa baino itu proteina gehiago aurkezten zuen, baina baita proteina kutsatzaile gehiago ere. Pausu honetatik aurrera bi frakzioak banandurik, baina modu paraleloan, purifikatzen jarraitu ziren.

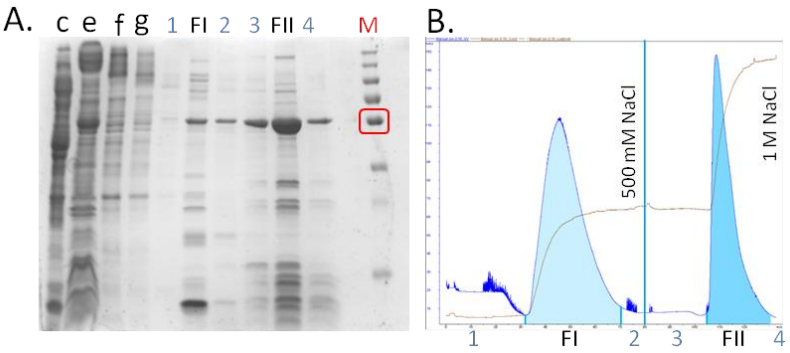

S4.3. irudia. *P-11* zutabetik lortutako laginen SDS-PAGE analisia eta kromatograma. A) Lortutako laginen SDS-PAGE azterketa. Lagin bakoitzetik 5 µL erabili ziren (c, e eta f-n soilik 3 µL). c: proteina disolbagarriak; e: solubilizaturiko MPak; f: lotu gabeko proteinak (*flow-through*); g: estuki ez atxikitatutako proteinen garbiketa; 1: 0-35 minututako eluzioa; FI: 37-70 minututako eluzioa; 2: 70-80 minututako eluzioa; 3: 80-105 minututako eluzioa; FII: 105-130

minututako eluzioa; 4: 130-140 minututako eluzioa. M: *PageRuler™ Plus Prestained Protein Ladder* MW markatzailea. Lauki gorriak 55 kDa-eko banda adierazten du. **B)** Elkartruke ionikoko kromatografian lortutako kromatograma. Proteinen eluzioa 280 nm-tako absorbantzia neurtuz jarraitu zen. Lerro urdina indargetzaile aldaketa adierazten du. Urdinez margotutako areak FI eta FII laginak lortzeko elkartutako frakzioak adierazten dituzte.

Frakzio bakoitzari 50 mM imidazol gehitu zitzaion eta paraleloki 5 mL-tako *HisTrap™ FF* afinitatezko kromatografia zutabeetara gehitu ziren, aldez aurretik nikelekin asetu eta *TrwB oligomers 5* indargetzailearen 10 mL-rekin orekatu zirenak. FI lagina hiru aldiz igaro zen zutabetik1 mL/min-ko fluxuan, FII gau osoan zehar birzirkulatzen utzi zen heinean. Ondoren, bi kasuetan, erretxina 50 mL *TrwB oligomers 5* indargetzailearekin orekatu zen eta proteinak *TrwB oligomers 6* indargetzailearekin eluitu ziren, 2 mL/min-ko fluxuan eta 1,5 mL-tako frakzioak jasoz (S4.4. irudia).

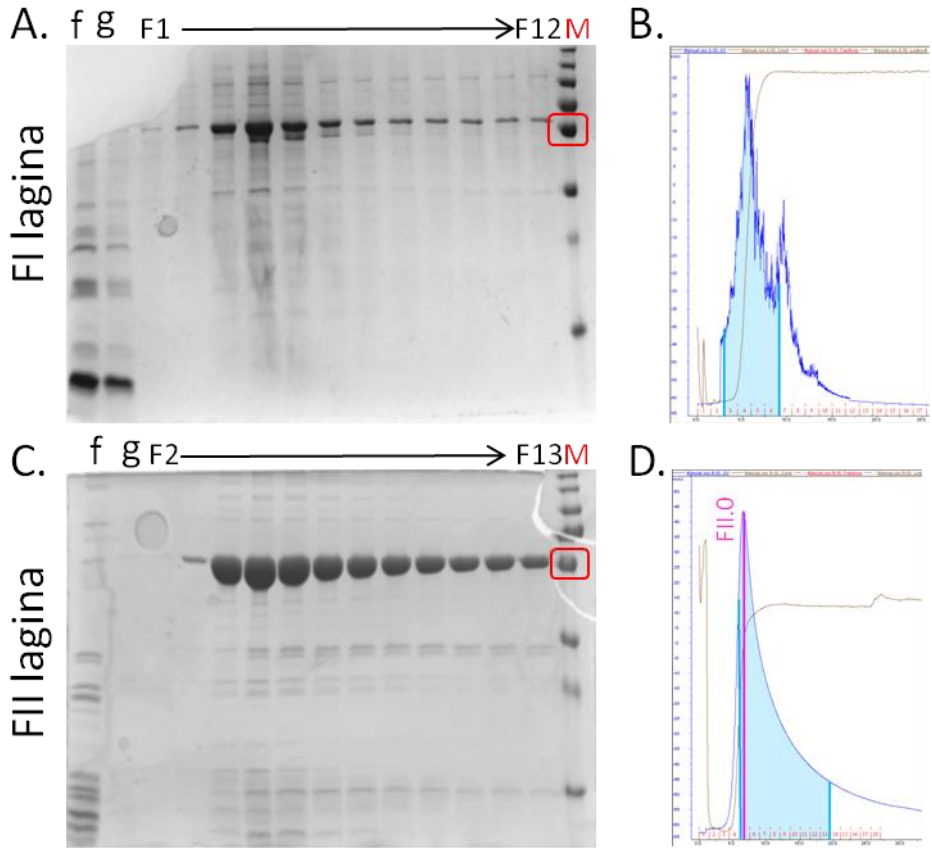

S4.4. irudia. *His-Trap™ FF* afinitatezko kromatografia zutabetik lortutako FI (A eta B) eta FII (C eta D) laginen SDS-PAGE analisia eta kromatograma. A eta C) Lortutako laginen SDS-PAGE analisia. Lagin bakoitzetik 5 µL erabili ziren. f: lotu gabeko proteinak (*flow-through*); g: estuki ez atxikitatutako proteinen garbiketa; FI.1-etik FI.12-rako frakzioak (A); FII.2-tik FII.13-rako frakzioak (C); M: *PageRuler™ Plus Prestained Protein Ladder* pisu molekularreko markatzailea. Lauki gorriak 55 kDa-eko banda adierazten du. **B eta D)** Afinitatezko kromatografian lortutako kromatograma. Proteinen eluzioa 280 nm-tako absorbantzia neurtuz jarraitu zen. Urdinez margotutako azalerak hurrengo pausuetarako elkartutako frakzioak adierazten dituzte. Marra larrosa *Superose 6 (3.2/30)* bidez aztertu zen FII.0 lagina adierazten du.

FI laginari dagokionez (S4.4. irudia, A eta B), 3., 4., 5., eta 6. frakzioak elkartu eta *Amicon Ultra-15 YM-100* bat erabiliz 2,5 mL-ra kontzentratu ziren. Ondoren lagina *PD-10* zutabe batera gehitu zen, aldez aurretik *TrwB oligomers 7* indargetzailearekin orekatu zena. Hau etxe komertzialak ezarritako grabitate bidezko protokoloa erabiliz eluitu zen, 0,5 mL (1, 4 eta 5) eta 1 mL-tako laginak (2 eta 3) jasoz. Frakzio bakoitzeko 5 µL SDS-PAGE bidez aztertu ziren, itu proteinaren presentzia egiaztatzeko (S4.5. irudia). 2., 3. eta 4. frakzioak elkartu eta aurretik egin bezala 1,5 mL-ra kontzentratu ziren, 12 µM-eko **FI.0** lagina lortuz. Bukatzeko glizerola gehitu zen %20 (b/b) kontzentrazioa izateko laginean eta 50 µL-tako alikuotetan banandurik nitrogeno bidez izoztu zen, -80°C-tan gordez haien erabilerara arte.

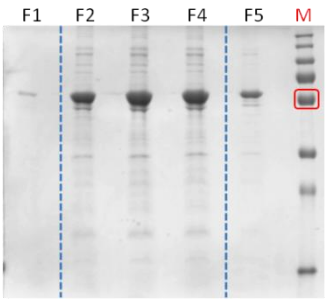

S4.5. irudia. PD-10 zutabearen eluziotik lortutako FI laginaren frakzioen analisia SDS-PAGE bidez. Lagin bakoitzetik 5 µL erabili ziren. Kale bakoitza 1etik 5era eluitutako frakzioei dagokie. M: : *PageRuler™ Plus Prestained Protein Ladder* pisu molekularreko markatzailea. Lauki gorriak 55 kDa-eko banda adierazten du. Marren arteko frakzioak bukaerako FI lagina lortzeko elkartu ziren.

FII laginari dagokionez (**S4.4. irudia**, C eta D), afinitatezko kromatografiatik lortutako 5. frakzioak purutasun eta kontzentzentrazio egokia (14.3 µM) aurkezten zuen. Hori dela eta, zuzenean frakzio honen 150 µL *Superose 6 (3.2/30)* SEC zutabea erabiliz aztertu ziren (**FII.0** lagina, **S4.4. irudia**, marra larrosa). Gainerako frakzioa 6tik 13rako frakzioekin elkartu eta 2 mL-ra kontzentratu egin zen, **FII.1** lagina lortuz.

S4.6.1. BIGARREN MAILAKO EGITURAREN AZTERKETA ESPEKTROSKOPIA INFRAGORRIAZ

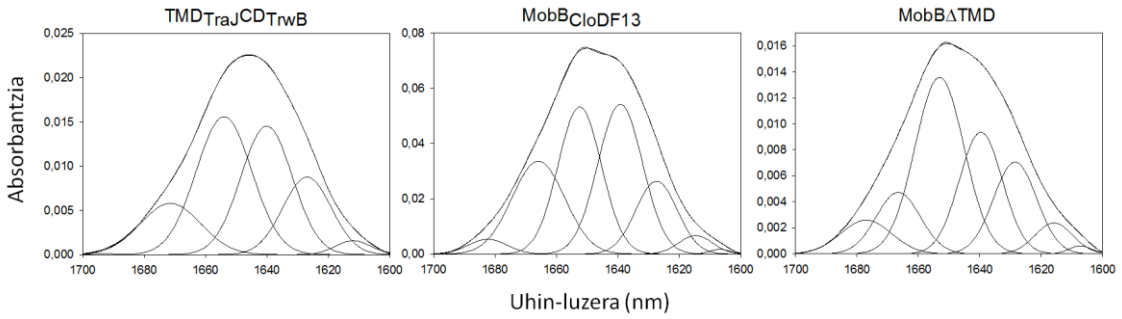

S4.6. irudia. $TMD_{TraJ}CD_{TrwB}$, $MobB_{CloODF13}$ eta MobBΔTMD proteinen infragorri espektroen Amida I eskualdeak. Entseguak 2.6.1. atalean azaldu bezala burutu ziren. Lortutako espektroak bigarren mailako estruktura osagai desberdinak erakusteko egokitu ziren, 4.7. eta 4.8. tauletan adierazi bezala.

S4.6.3. MobBΔTMD KRISTALIZAZIOAREN HASIERAKO SAIAKERAK

S4.1. taula. MobBΔTMDren kristalizaziorako frogatutako baldintzen laburpena. [a]*:* A: *MobBΔTMD kristalizazio* indargetzailea; B: *Zelula indargetzailea*. [b]: 1705 plakako G3 tantaren baldintzen optimizazioa burutu zen 48-putzutako plaka bat erabiliz (4.9. taula). [c]: 48-putzutako optimizazio plaka honen putzu guztiak 1705 plakako G3 tantaren baldintza berdinak zeuzkaten (*100 MES pH 6,5, 10 mM ZnSO4, 25% PEG 550 MME*). [d]: 48-putzutako optimizazio plaka honen putzu guztiak 1721 plakako B6 tantaren baldintza berdinak zeuzkaten (100 MES pH 6,5, 5 mM ZnSO4, 30% PEG 550 MME).

Indargetzailea[a]	Kontzentrazioa (mM)	Plaka komertziala	Plaka zenbakia
A	0,28	*JBSCreen Classic HTS I*	1703
A	0,28	*JBSCreen Classic HTS II*	1704
A	0,28	*Structure Screen 1 & 2 HT-96*	1705
A	0,28	*The Protein Complex Suite*	1706
A	0,28	*JBScreen JCSG++ HTS*	1707
A	0,28	*PACT premier HT-96*	1708
A	0,22	1705G3[b]-ren optimizazioa	1721
B	0,28	*JBSCreen Classic HTS I*	1722
B	0,28	*JBSCreen Classic HTS II*	1723
B	0,28	*PACT premier HT-96*	1724
B	0,56 (1. tanta) eta 0,56 (2. tanta)	*The Protein Complex Suite*	1763
B	0,56 (1. tanta) eta 0,56 (2. tanta)	*Structure Screen 1 & 2 HT-96*	1764
B	0,56 (1. tanta) eta 0,56 (2. tanta)	*JBScreen JCSG++ HTS*	1765
B	0,56 (1. tanta) eta 0,56 (2. tanta)	*MemGold HT-96*	1766
B	0,56 (1. tanta) eta 0,56 (2. tanta)	*MemGold2*	1767
B	0,56 (1. tanta) eta 0,56 (2. tanta)	*JBScreen Pentaerythritol HTS*	1768
B	0,56 (A1-H3) eta 0,28 (A4-H6)	1705G3[c]-ren baldintzak	1769
B	0,56 (A1-H3) eta 0,28 (A4-H6)	1721B6[d]-ren baldintzak	1770

S5.2. LIPIDO KONPOSAKETA

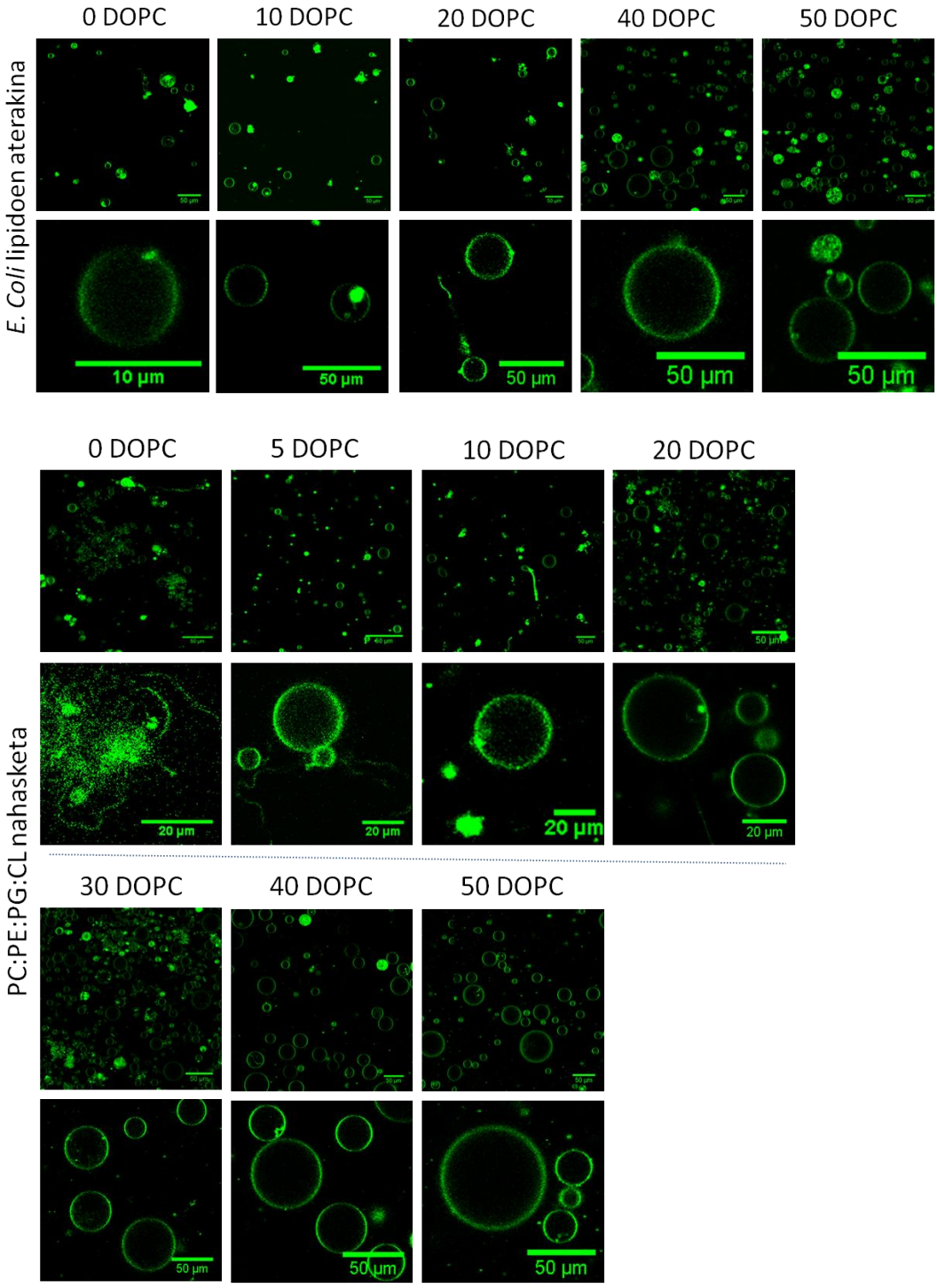

S5.1. irudia. Lipido konposaketa desberdinekin lortutako GUV laginak. Bi lipido nahasketa desberdin erabili ziren bakterioen barne mintzaren konposizio antzekoa zuten GUVen lorpenerako: (i) *E. coli* lipidoen aterakin komertziala eta (ii) PE:PG:CL (76.3:19.6:4.1). Lehenengo kasuan lipido nahasketa DOPCrekin ordezkatu zen ehuneko desberdinetan. Bigarren kasuan PEa ordezkatu zen DOPCarekin, PG eta CL ehunekoak mantendu ziren

bitartean. Lipidoak DIOrekin tindatu ziren eta GUVak elektroformazio bidez sorrarazi ziren. Laginen behaketa *ZEISS LSM 710 ConfoCor 3* mikroskopioan egin zen, 488 nm-tako kitzikapena burutuz eta 505-540 nm tarteko igorpena jasoz. Baldintza bakoitzaren goiko eta beheko irudiek lagin bakoitzeko irudi orokorra eta gertuko irudia erakusten dute, hurrenez hurren. Eskala: 50 µm.

S.5.4.3.3. BIMVen FUSIOA ALDEZ AURRETIK SORTUTAKO GUVekin

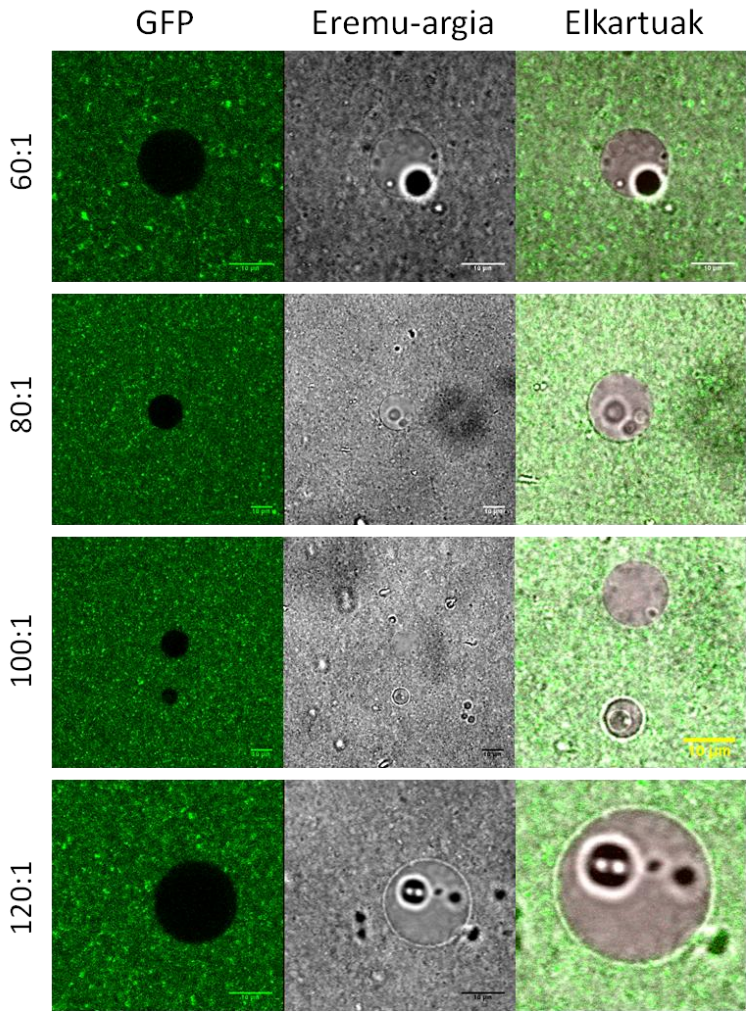

S5.2. irudia. BIMVren fusioa aldez aurretik sortutako DOPC-GUVekin. DOPC-GUVak elektroformazioz sortu eta BIMVekin (1 mg/mL bukaerako kontzentrazioa) nahastu ziren TritonX100dun *GUV fusio* indargetzailean lipido:proteina (p/p) erlazio desberdinetan. Nahasketa gau osoan zehar inkubatu ostean detergentea 5 mg BBak erabiliz kendu zen eta laginak *ZEISS LSM 710 ConfoCor 3* mikroskopioan bistaratu ziren, 488 nm-tako kitzikapena burutuz eta 505-540 nm tarteko fluoreszentzia igorpena jasoz. GFP fluoreszentzia, eremu-argiko irudia eta anplifikatu eta bateratutako irudiak 1., 2. eta 3. zutabetan erakusten dira, urrenez urren. Eskala: 10 µm.

5.5.3. SLBen OPTIMIZAZIOA

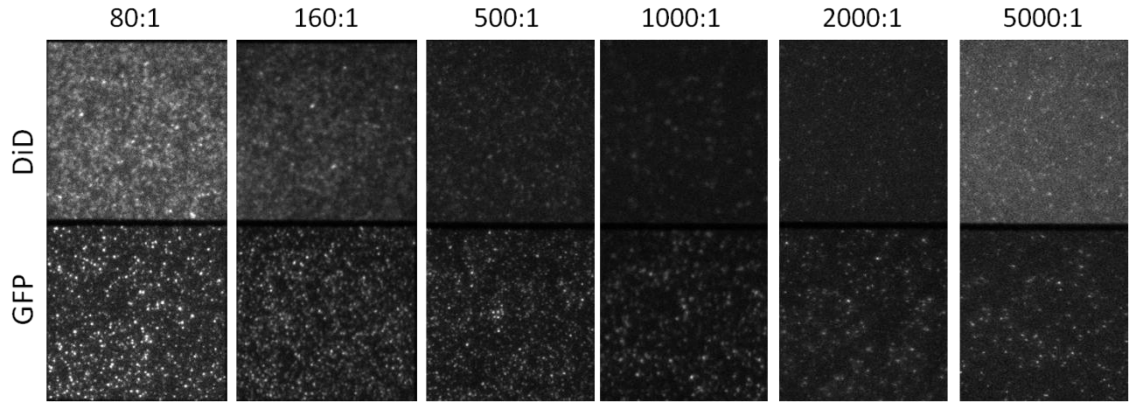

S5.3. irudia. SLBen formakuntza silanizatutako kristalezko estalkietan. $MobB_{CloDF13}$GFP-dun BIMVak DiDrekin sonikatu eta aldez aurretik formatutako DOPC-SUVekin elkartu ziren lipido: proteina erlazio desberdinetan (p/p). SLBak 6 mM $CaCl_2$ erabiliz sortu ziren silanizatutako kristalezko estalkietan eta ostean *Zeiss Axiovert 200* mikroskopioan bistaratu ziren 2.9.4. atalean azaldu bezala. Irudiak hasierako denbora adierazten dute, fluoroforoen amatatzea hasi baino lehen. Proteina eta DiD kontzentrazioak 0,375 µg eta 0,67 nM ziren, hurrenez hurren.

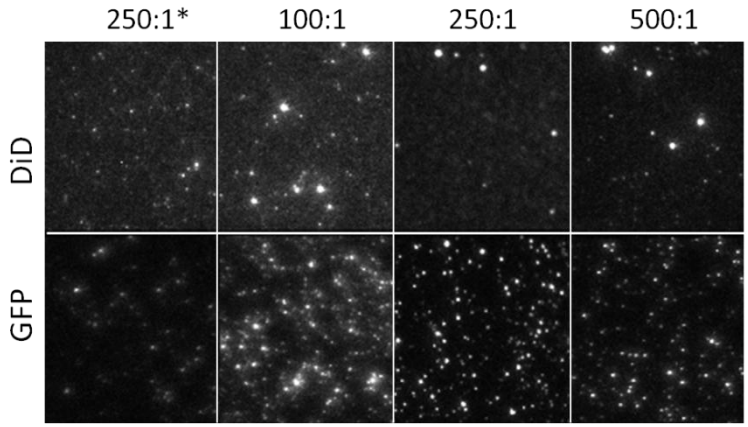

S5.4. irudia. SLBen formakuntza detergente bidezko besikulen fusioaren ostean. $TrwB_{R388}$GFPdun BIMVak DiDrekin sonikatu ziren TritonX100 detergentearen presentzian, DOPC OG detergentearen presentzian sonikatzen zen bitartean. Lortutako bi laginak lipido:proteina (p/p) erlazio desberdinetan nahastu eta elkarrekin inkubatu ziren 90 minutuz BB bidez detergentea kendu baino lehen. SLBak 6 mM $CaCl_2$ erabiliz sortu ziren piraña soluzio bidez garbitutako kristalezko estalkietan. Laginak *Zeiss Axiovert 200* mikroskopioan bistaratu ziren 2.9.4. atalean azaldu bezala. Irudiak hasierako denbora adierazten dute, fluoroforoen amatatzea hasi baino lehen. Proteina eta DiD kontzentrazioak 0,250 µg eta 0,67 nM ziren, hurrenez hurren. *Detergenterik gabeko kontrola.

ULTRAZENTRIFUGAZIO ANALITIKOKO ENTSEGUAK

Entsegu baldintzak: 20°C, 40 krpm.

a. Datu esperimentalak (%: profil osoan identifikaturiko espeziekiko ehunekoa) / b. Balio estandarrak ($S_{w,20}$).

Datuen bolumena murrizteko, proteina bakoitzeko lorturiko profil agregatuen artean soilik bi aurkezten dira.

$TrwB_{R388}$

Indargetzailea: 50 mM Tris-HCl (pH 7,8), 0,1 mM EDTA, %5 (v/v) glizerola.

Proteina (µM), DDM (mM) eta NaCl (mM) kontzentrazioak entseguaren arabera aldatu ziren.

1) 5,23 µM, 0,2 mM DDM, 20 mM NaCl

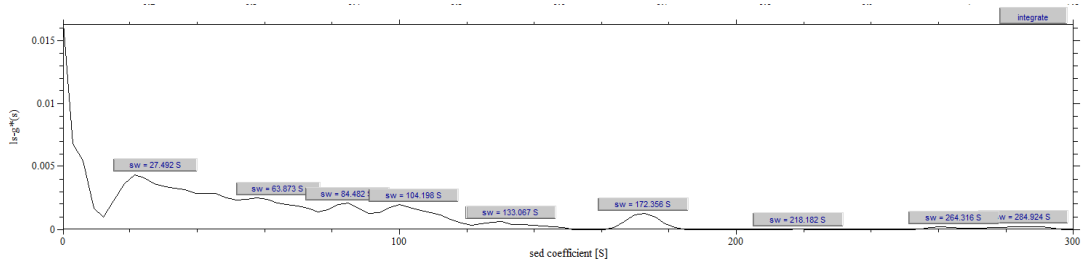

Agregatuak

2) 5,23 µM, 0,2 mM DDM, 75 mM NaCl

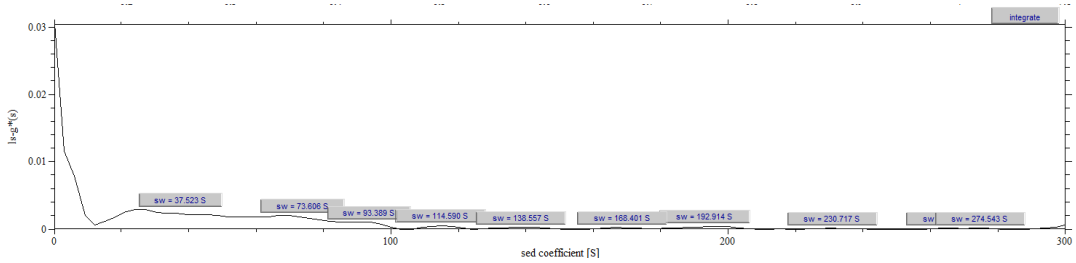

Agregatuak

3) 5,23 µM, 0,2 mM DDM, 150 mM NaCl (lagin osoko %78,0)

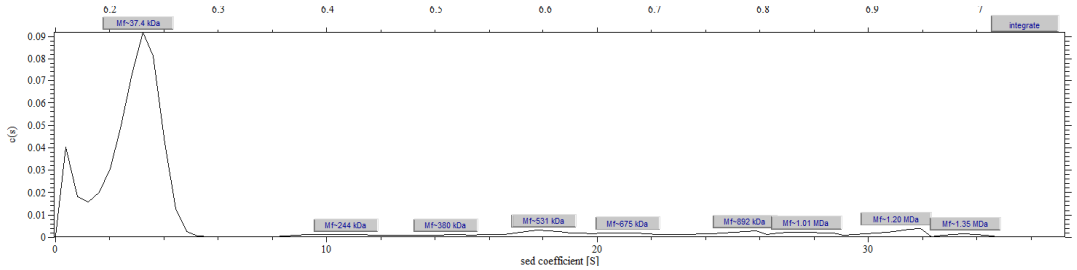

a. 3,1 S (%80,6) + Polidispertsitatea (%19,4)
b. 3,7 S + Polidispertsitatea

4) 6,97 µM, 0,3 mM DDM, 50 mM NaCl

Agregatuak

5) 6,97 µM, 0,5 mM DDM, 50 mM NaCl

Agregatuak

6) 6,97 µM, 0,3 mM DDM, 300 mM NaCl (lagin osoko %81,8)

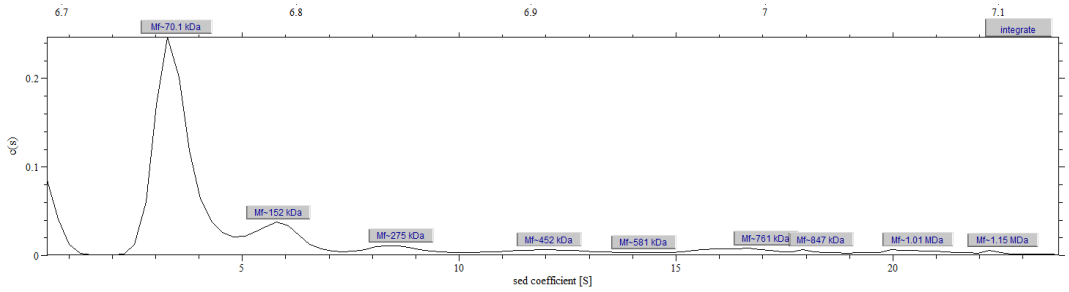

a. 3,5 S (%64,0), 5,8 S (%14,4), 8,7 S (%5,3), 12,1 S (%5,1) + Polidispertsitatea
b. 4,3 S, 7,3 S, 10,8 S, 15,0 S + Polidispertsitatea

7) 6,97 µM, 0,5 mM DDM, 300 mM NaCl (lagin osoko %97,3)

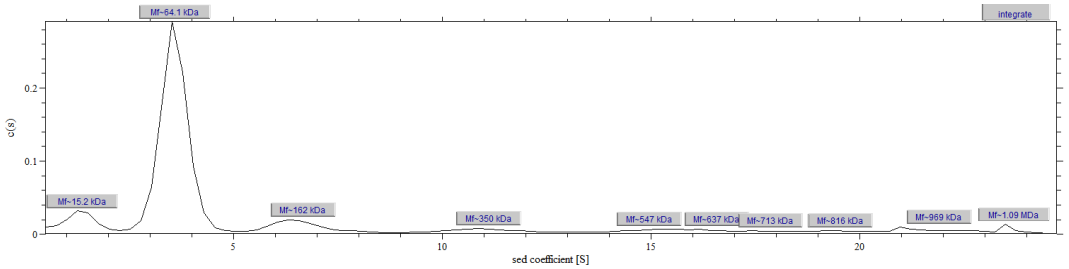

a. 1,4 S (%9,8), 3,6 S (%64,1), 6,6 S (%9,1), 11,1 S (%4,7), 15,0 S (%3,9), 19,3 S (%1,9), 21,9 S (%4,5), 23,7 S (%1,6) + Polidispertsitatea
b. 1,7 S, 4,5 S, 8,3 S, 13,8 S, 18,6 S, 24,1 S, 27,2, 29,4 + Polidispertsitatea

8) 10,46 µM, 0,5 mM DDM, 300 mM NaCl (lagin osoko %28,1)

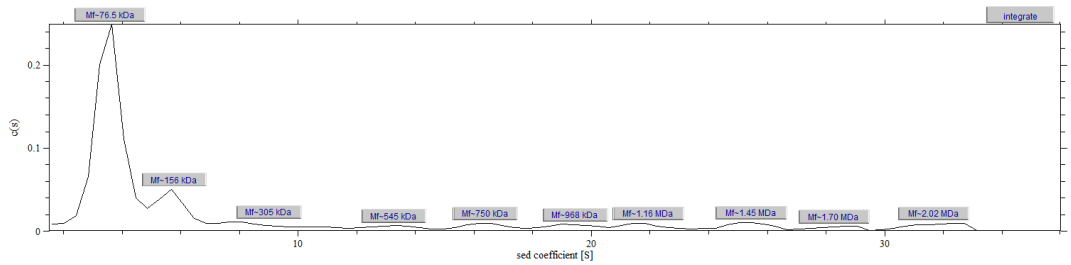

a. 3,6 S (%57,4), 5,8 S (%12,7), 9,0 S (%6,6) + Polidispertsitatea
b. 4,5 S, 7,2 S, 11,2 S + Polidispertsitatea

9) 20,92 µM, 0,5 mM DDM, 300 mM NaCl (lagin osoko %93,6)

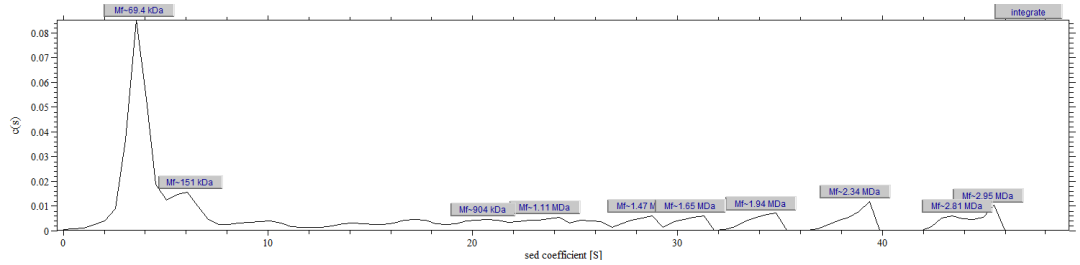

a. 3,7 S (%42,1), 6,2 S (%10,6) + Polidispertsitatea
b. 4,6 S, 7,7 S + Polidispertsitatea

10) 5,23 µM, 1,5 mM DDM, 300 mM NaCl (lagin osoko %88,8)

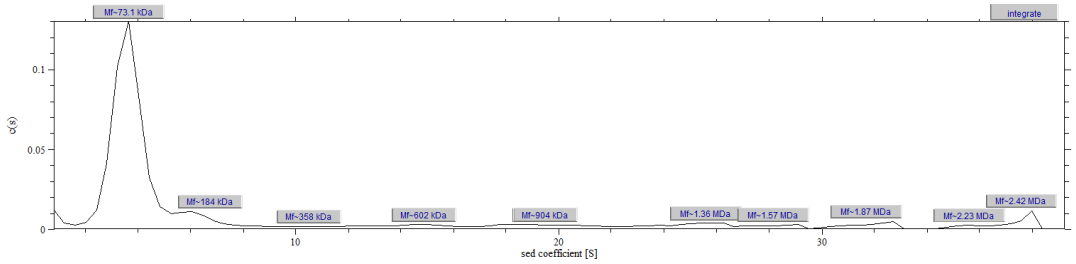

a. 3,6 S (%64,5), 6,7 S (%8,8), 9,6 → 29,5 S (%17,8), 31,7 S (%3,3), 35,6 S (%2,0), 37,6 S (%3,6) + Polidispertsitatea
b. 4,5 S, 8,4 S + Polidispertsitatea

11) 10,46 µM, 1,5 mM DDM, 300 mM NaCl (lagin osoko %95,0)

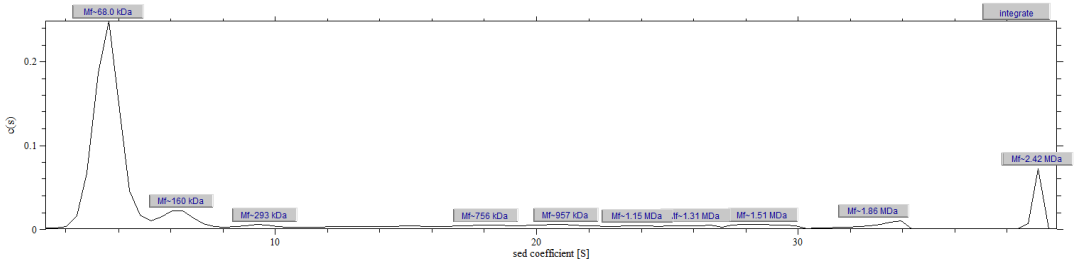

a. 3,6 S (%62,3), 6,4 S (%7,6), 9,6 S (%2,5), 10,8 S → 30,3 S (%17,2), 32,9 S (%3,5), 39,1 S (%6,9) + Polidispertsitatea
b. 4,5 S, 8,0 S, 11,9 S + Polidispertsitatea

12) 20,92 µM, 1,5 mM DDM, 300 mM NaCl (lagin osoko %84,3)

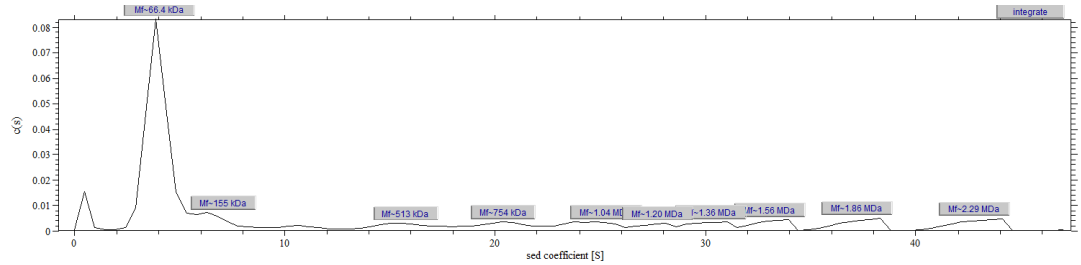

a. 4,0 S (%55,9), 7,1 S (%6,8), 9,0 S → 12,7 S (%2,3), 12,8 S → 45,1 S (%34,6) + Polidispertsitatea
b. 5,0 S, 8,8 S + Polidispertsitatea

$TMD_{TraJ}CD_{TrwB}$

Indargetzailea: 50 mM Tris-HCl (pH 7,8), 0,1 mM EDTA, %5 (b/b) glizerola.

Proteina (µM), DDM (mM) eta NaCl (mM) kontzentrazioak entseguaren arabera aldatu ziren.

1) 5,15 µM, 0,2 mM DDM, 20 mM NaCl

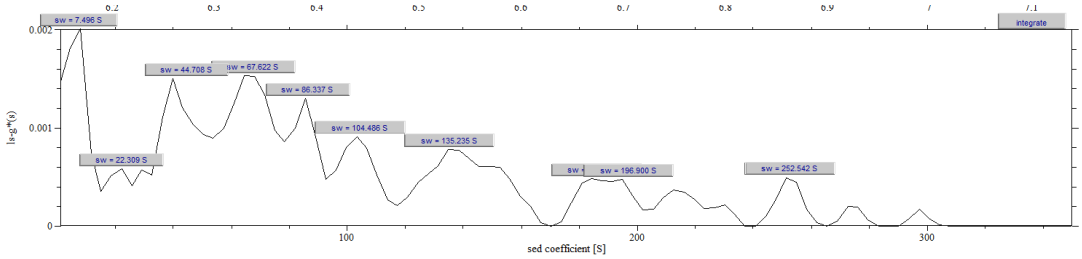

Agregatuak

2) 5,15 µM, 0,2 mM DDM, 75 mM NaCl

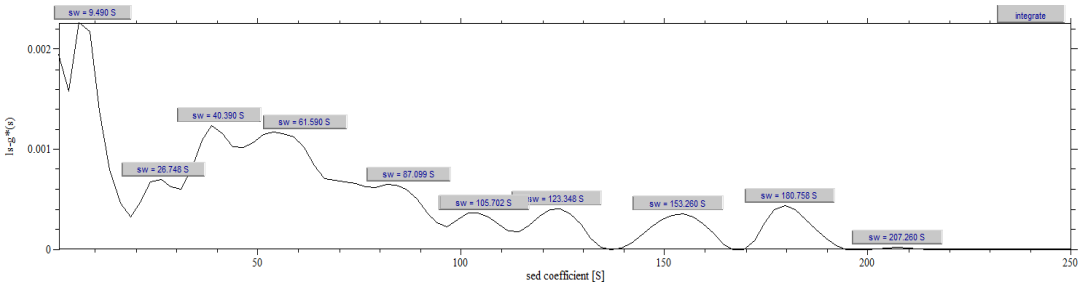

Agregatuak

3) 5,15 µM, 0,2 mM DDM, 150 mM NaCl

Agregatuak

4) 5,15 µM, 0,2 mM DDM, 300 mM NaCl

Agregatuak

5) 5,58 µM, 0,3 mM DDM, 50 mM NaCl

Agregatuak

6) 5,58 µM, 0,5 mM DDM, 50 mM NaCl

Agregatuak

7) 5,58 µM, 0,3 mM DDM, 300 mM NaCl (lagin osoko %93,7)

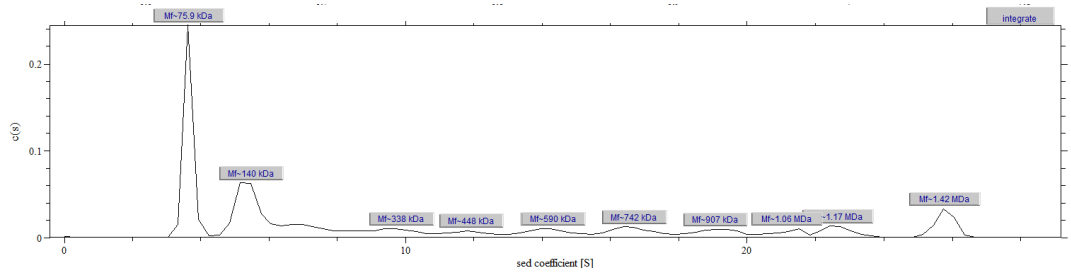

a. 3,6 S (%27,1), 5,5 S (%20,3), 6,3 → 9 S (%9,2), 9,9 S (%4,6), 11,9 S (%4,9), 14,3 S (%6,0), 16,7 S (%6,7), 19,1 S (%5,2), 21,2 S (%3,9), 22,7 S (%4,7), 25,8 S (%7,4) + Polidispertsitatea
b. 4,54 S, 6,8 S + Polidispertsitatea

8) 5,58 µM, 0,5 mM DDM, 300 mM NaCl (lagin osoko %89,4)

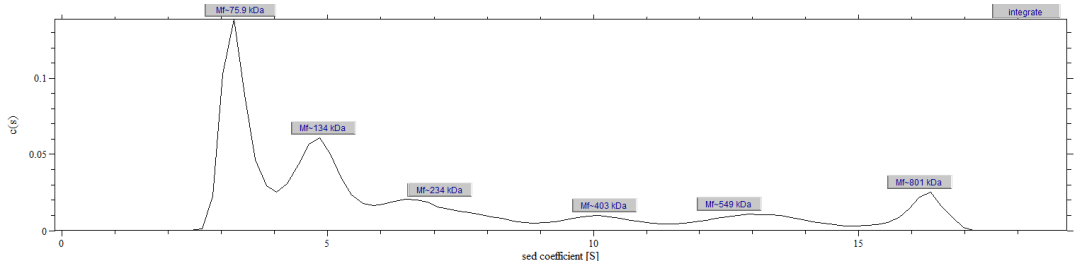

a. 3,4 S (%34,4), 4,9 S (%26,2), 7,1 S (%15,1), 10,2 S (%7,0), 11,4 S → 14,9 S (%9,2), 16,2 S (%8,1)
b. 4,17 S, 6,1 S, 8,8 S, 12,7 S + Polidispertsitatea

9) 10,30 µM, 0,5 mM DDM, 300 mM NaCl (lagin osoko %92,6)

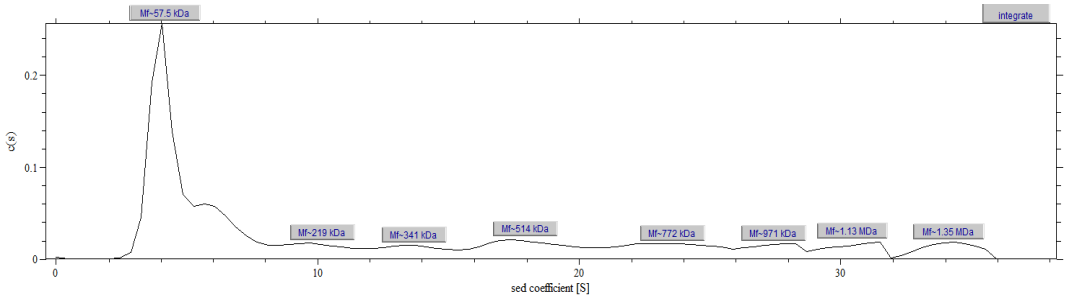

a. 4,2 S (%38,9), 5,2 S → 8,3 S (%14,1), 10,2 S (%6,3), 11,6 S → 36,1 S (%40,8) +Polidispertsitatea
b. 5,2 S + Polidispertsitatea

10) 20,60 µM, 0,5 mM DDM, 300 mM NaCl (lagin osoko %94,1)

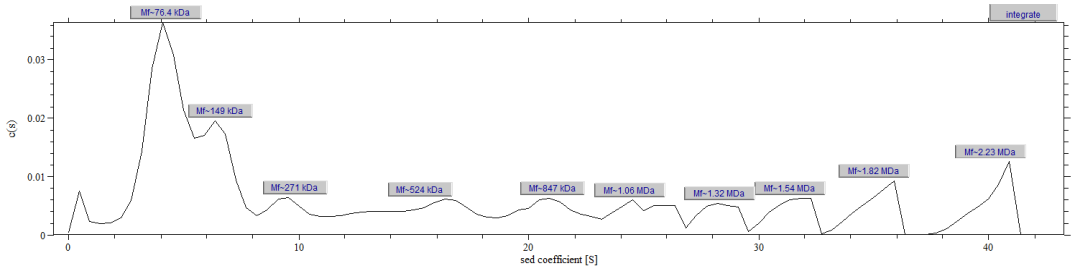

a. 4,2 S (%29,8), 6,6 S (%14,4), 9,8 S (%6,2), 11,1 S → 41,9 S (%49,5)
b. 5,3 S, 8,2 S, 12,2 S + Polidispertsitatea

11) 5,15 µM, 1,5 mM DDM, 300 mM NaCl (lagin osoko %99,8)

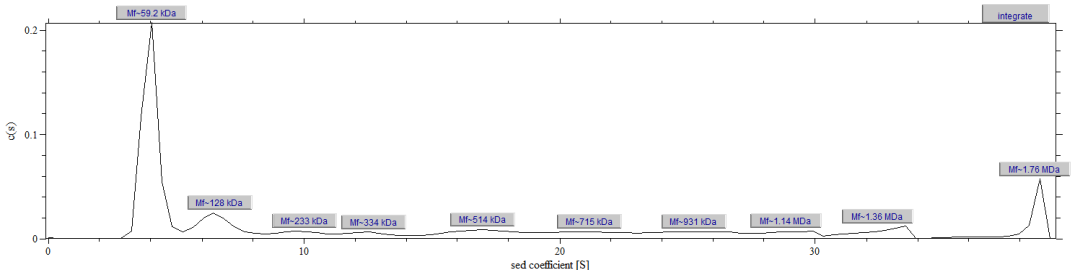

a. 4,0 S (%41,9), 6,7 S (%11,0), 10,0 S (%4,5), 11,2 S → 39,3 S (%42,4) + Polidispertsitatea
b. 5,0 S, 8,3 S, 12,5 S + Polidispertsitatea

12) 10,30 µM, 1,5 mM DDM, 300 mM NaCl (lagin osoko %95,0)

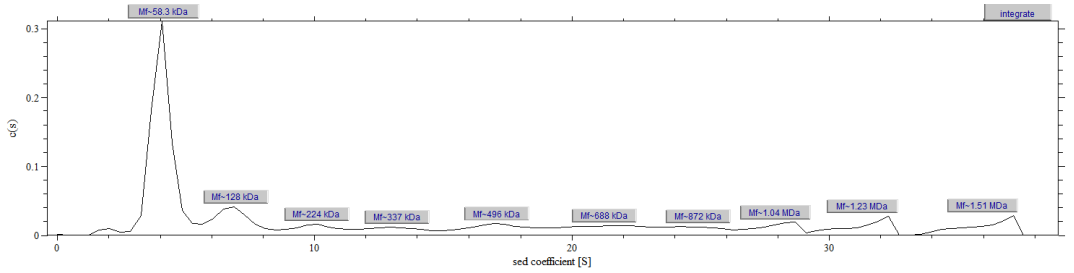

a. 1,2 S → 2,5 S (%1,1), 4,1 S (%41,9), 6,9 S (%10,0), 10,1 S (%5,0), 11,6 S → 38,0 S (%42,0)
b. 5,1 S, 8,6 S , 12,5 S + Polidispertsitatea

13) 20,60 µM, 1,5 mM DDM, 300 mm NaCl (lagin osoko 90,7%)

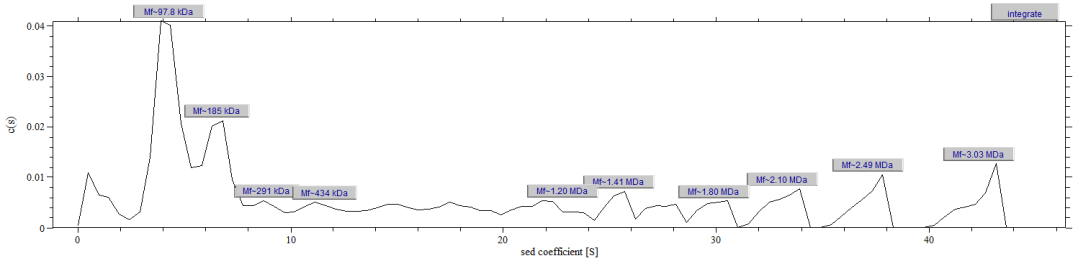

a. 4,3 S (%27,6), 6,5 S (%15,1), 8,9 S (%4,2), 10,0 S → 44,5 S (%53,1) + Polidispertsitatea
b. 5,4 S, 8,2 S, 11,0 S + Polidispertsitatea

Protein-DNA interaction assays:

Indargetzailea: 50 mM Tris-HCl (pH 7,8), 0,3 mM DDM, 0,1 mM EDTA, %5 (b/b) glizerola, 6 mM $MgCl_2$, 300 mM NaCl.

Proteina kontzentrazioa: 5,15 µM

1) pUC18 (8,84 nM DNA, 19,5 proteina:DNA (p:p) erlazioa) (lagin osoko %92,9)

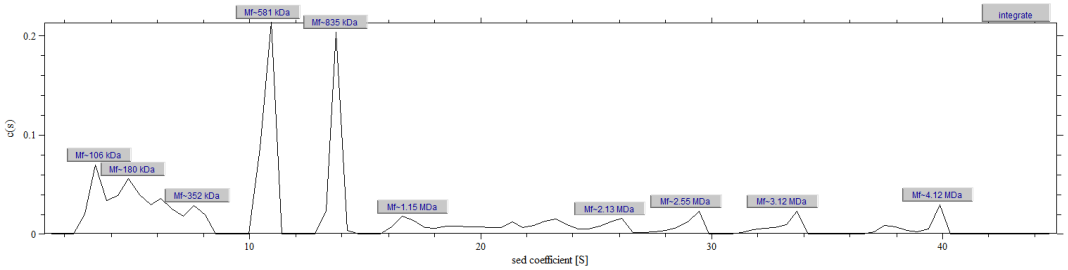

a. 3,5 S (%10,4), 4,9 S (%14,3), 5,7 S → 7,1 S (%6,2), 7,7 S (%4,2), 10,8 S (%21,7), 13,7 S (%16,8), 15,6 → 40,5 S (%26,4)
b. 4,3 S, 6,2 S, mixture of species, 9,6 S (3,9%), 13,5 S (20,2%), 17,1 S (15,6%) + Polidispertsitatea

2) pUC18 (0,14 nM DNA, 1230 proteina:DNA (p:p) erlazioa) (lagin osoko %88,3)

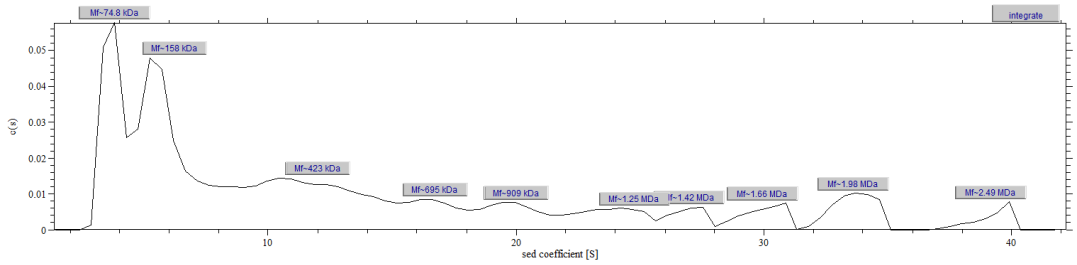

a. 3,8 S (%18,2), 6,2 S (%29,5), 12,0 S (%19,5), 16,7 (%6,1), 20,0 S (%6,4), 21,8 → 40,7 S (%20,3)
b. 4,7 S, 7,8 S, 15,0 S, 20,9 S, 25,0 S + Polidispertsitatea

$MobB_{CloDF13}$

Indargetzailea: 50 mM Tris-HCl (pH 7,8), 0,1 mM EDTA, 5% (v/v) glizerola, 300 mM NaCl.

Proteina (µM) eta DDM (mM) kontzentrazioak entseguaren arabera aldatu ziren.

1) 3,38 µM, 0,6 mM DDM (lagin osoko %95,6)

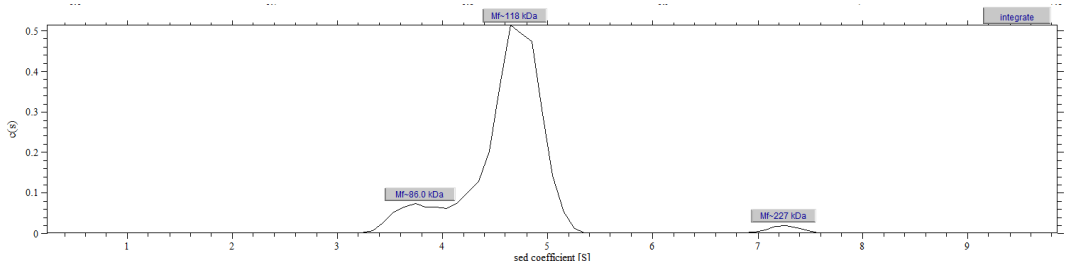

a. 3,8 S (%13,2), 4,7 S (%84,7), 7,2 S (%2,1)
b. 4,7 S, 5,8 S, 9,0 S

2) 8,12 µM, 0,6 mM (lagin osoko %72,0)

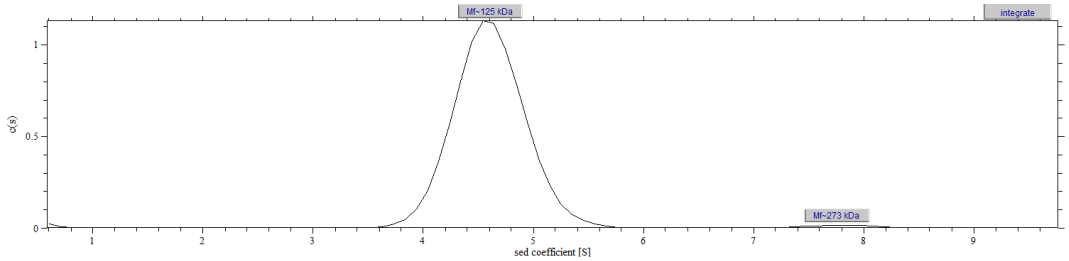

a. 4,6 S (%98,2), 7,8 S (%1,8)
b. 5,7 S, 9,6 S

3) 13,54 µM, 0,6 mM DDM (lagin osoko %96,0)

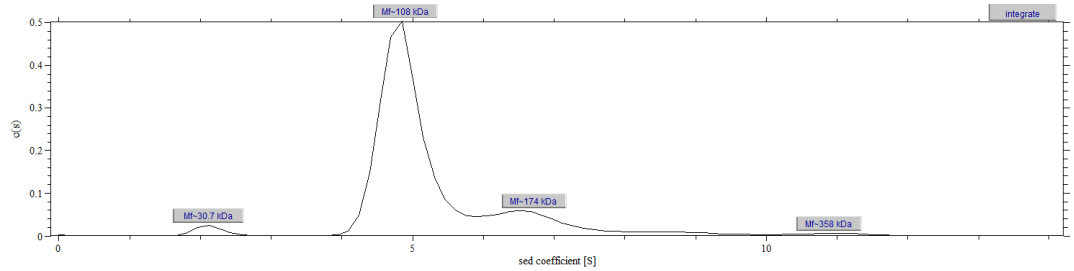

a. 2,1 S (%2,6), 4,9 S (%79,7), 6,7 S (%16,3), 10,9 S (%1,5)
b. 2,6 S , 6,1 S, 8,3 S, 13,5 S

4) 3,38 µM, 1,5 mM DDM (lagin osoko %94,8)

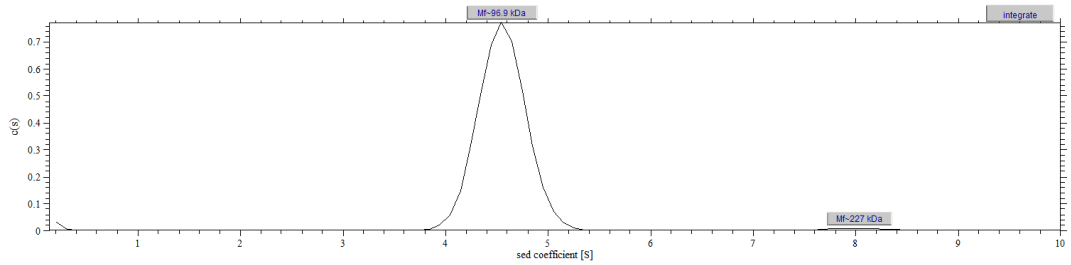

a. 4,5 S (%98,2), 8,0 S (%1,9)
b. 5,7 S, 10,0 S

5) 8,12 µM, 1,5 mM DDM (lagin osoko %97,3)

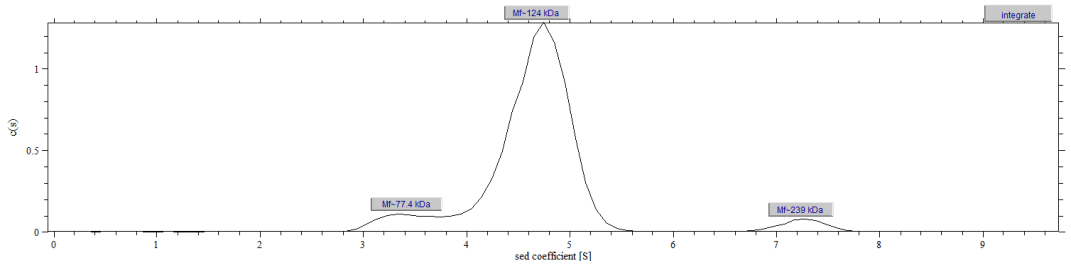

a. 3,4 S (%8,0), 4,7 S (%87,7), 7,2 S (%4,3)
b. 4,24 S, 5,81 S, 9,0 S

6) 13,54 µM, 1,5 mM DDM (lagin osoko %95,8)

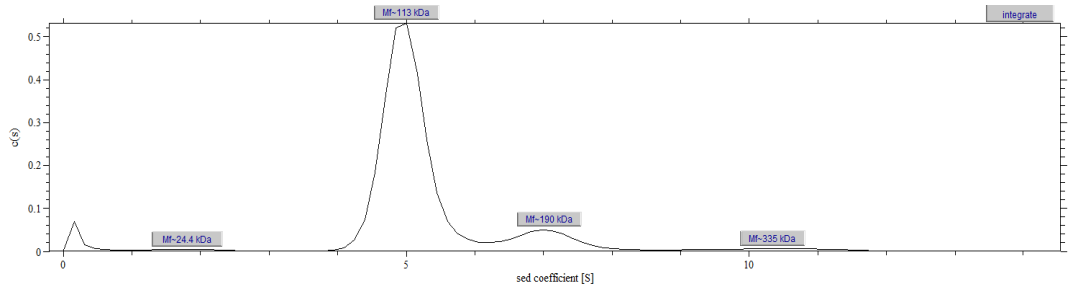

a. 1,8 S (%1,3), 5,0 S (%84,1), 7,1 S (%11,9), 10,3 S (%2,7)
b. 2,2 S, 6,2 S, 8,8 S, 12,8 S

MobBΔTMD

Indargetzailea: 50 mM Tris-HCl (pH 7,8), 0,1 mM EDTA, %5 (b/b) glizerola

Proteina honekin entsegu ugari burutu ziren, multzoka sailkatuak izan dira: (i) proteina kontzentrazioaren eragina, (ii) indar ionikoaren eragina, (iii) Cl^- ioien eragina, (iv) pHaren eragina eta (v) DNAren eragina.

<u>Proteina kontzentrazioa</u>

Indargetzailea: 50 mM Tris-HCl (pH 7,8), 0,1 mM EDTA, %5 (b/b) glizerola, 75 mM NaCl.

<u>1) 8,47 µM (lagin osoko %95,6)</u>

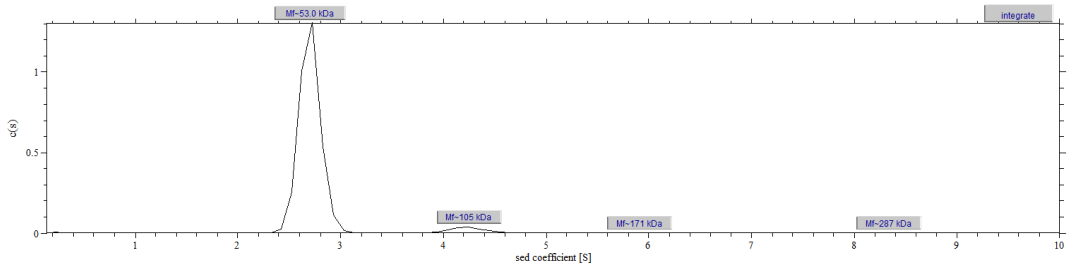

a. 2,7 S (%95,2), 4,2 S (%4,8)
b. 3,2 S , 5,0 S

<u>2) 16,94 µM (lagin osoko %99,3)</u>

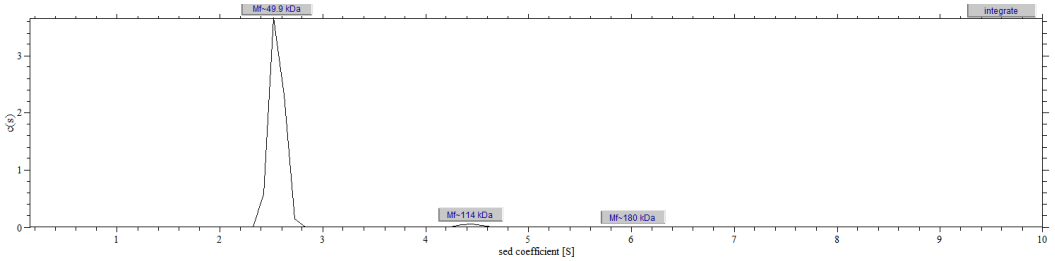

a. 2,6 S (%97,4), 4,4 S (%1,9)
b. 3,0 S, 5,3 S

<u>3) 33,89 µM (zentrifugazio zelda estua) (lagin osoko %99,5)</u>

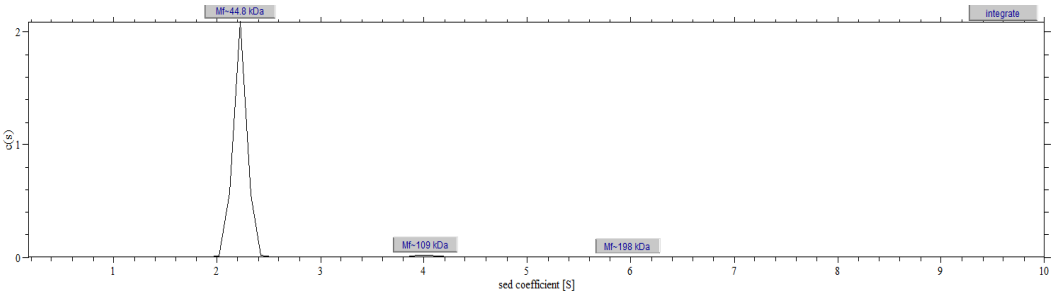

a. 2,2 S (%98,1), 4,0 S (%1,4)
b. 2,6 S, 4,8 S

Indar ionikoa

Buffer: 50 mM Tris-HCl (pH 7,8), 0,1 mM EDTA, %5 (b/b) glizerol.

Proteina kontzentrazioa: 8,47 µM

4) 20 mM NaCl (lagin osoko %90,6)

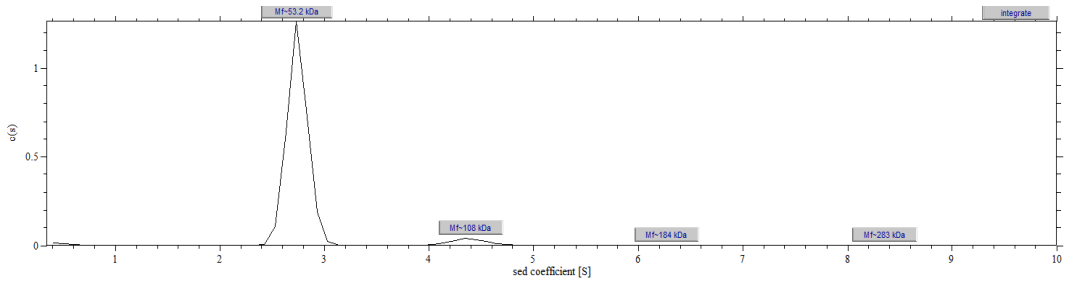

a. 2,7 S (%94,7), 4,4 S (%5,3)
b. 3,2 S, 5,2 S

5) 75 mM NaCl (lagin osoko %98,8)

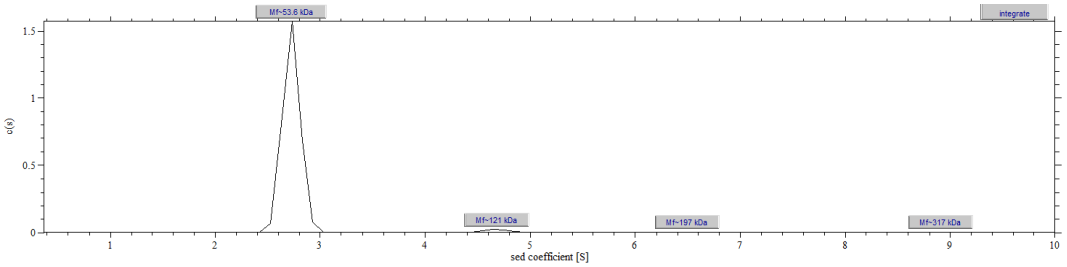

a. 2,7 S (%97,9), 4,7 S (%2,1)
b. 3,4 S, 5,9 S

6) 150 mM NaCl (lagin osoko %78,0)

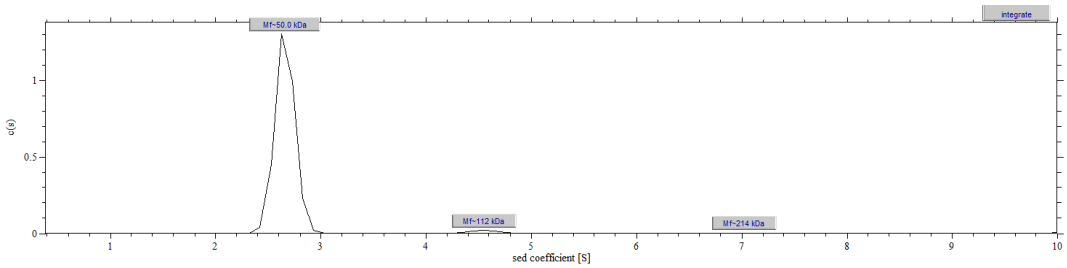

a. 2,7 S (%97,8), 4,5 S (%2,2)
b. 3,2 S, 5,5 S

7) 200 mM NaCl (lagin osoko %97,6)

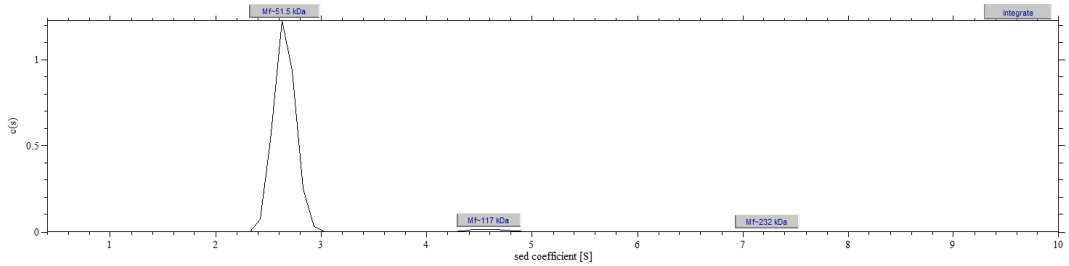

a. 2,7 S (%97,9), 4,6 S (%2,1)
b. 3,2 S, 5,5 S

Cl^- ioien eragina

Indargetzailea: 50 mM Tris-HCl (pH 7,8), 0,1 mM EDTA, 5% (b/b) glizerola.

Proteina kontzentrazioa: 8,47 µM

8) 20 mM CH_3COONa (lagin osoko %99,0)

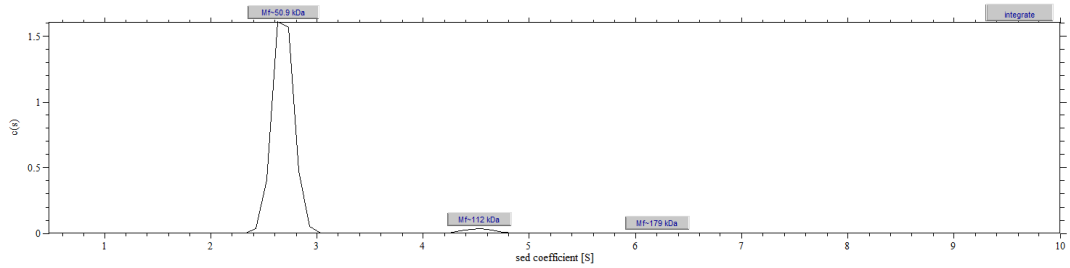

a. 2,7 S (%97,2), 4,5 S (%2,8)
b. 3,2 S, 5,4 S

9) 75 mM CH_3COONa (lagin osoko %73,5)

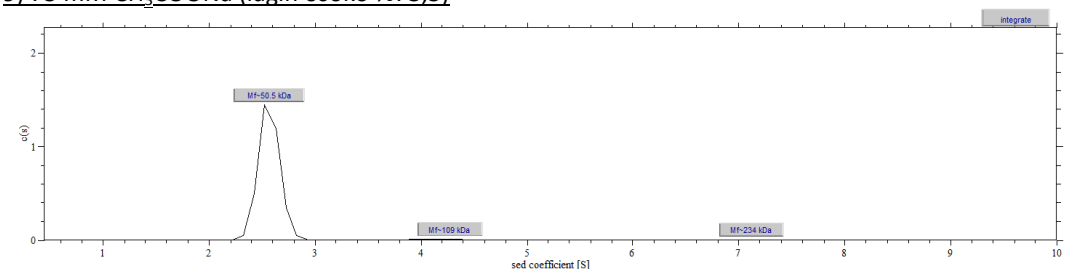

a. 2,6 S (%97,7), 4,3 S (%2,3)
b. 3,1 S, 5,1 S

10) 150 mM CH_3COONa (lagin osoko %97,1)

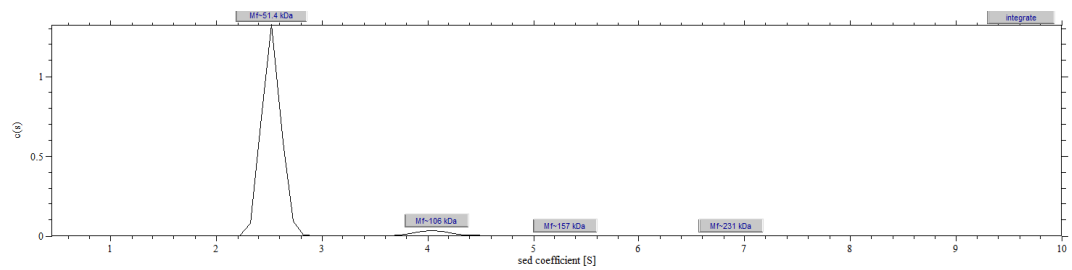

a. 2,5 S (%95,1), 4,1 S (%4,9)
b. 3,1 S, 5,0 S

pHaren eragina

Indargetzaile guztiek EDTA 0,1 mM, %5 (b/b) glizerol eta 75 mM NaCl-rekin aberasturik zeuden.

Proteina kontzentrazioa: 8,47 µM

11) 50 mM Tris-HCl (pH 7) (lagin osoko %99,5)

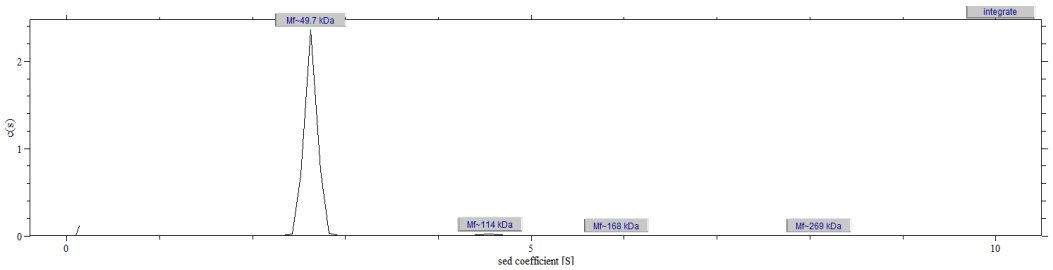

a. 2,6 S (%98,1), 4,6 S (%1,3)
b. 3,1 S, 5,4 S

12) 50 mM MES (pH 6) (lagin osoko %99,2)

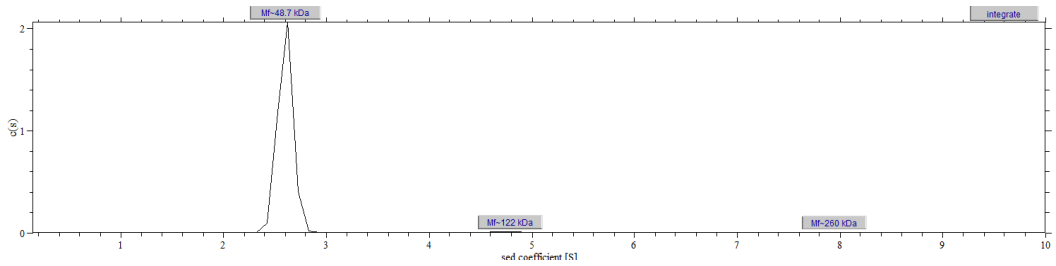

a. 2,6 S (%98,3), 4,8 S (%1,0)
b. 3,1 S, 5,7 S

13) 50 mM CH_3COOH/CH_3COONa (pH 5,6) (lagin osoko %99,6)

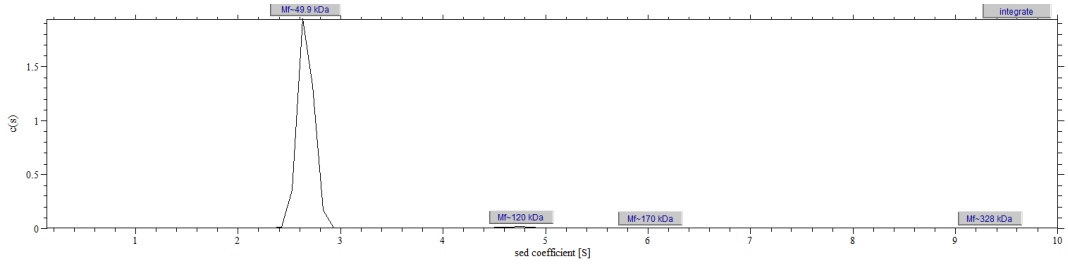

a. 2,7 S (%98,1), 4,3 S (%1,3)
b. 3,2 S, 5,7 S

APPENDIX

APPENDIX

REAGENTS, PRODUCTS, MATERIALS AND EQUIPMENT

Table A.1. Suppliers of reagents, products, materials and equipment. The equipment is represented in italics.

Supplier	Reagents, products, materials and equipment
Agencourt Biosciences (Beverley, MA, USA)	Ampure XP-PCR purification system
Agilent Technologies (Santa Clara, CAL, USA)	*PfuTurbo* DNA polimerase
Anatrace (Maumee, OH, USA)	n-Dodecyl-β-D-maltoside (DDM)
ATP Biotech Inc (Taipei, Taiwan)	Gel/PCR extraction kit
ATTO-TEC GmbH (Siegen, Germany)	ATTO 488
	ATTO 633
	ATTO 655
Avanti Polar Lipids (Alabaster, AL, USA)	Cardiolipin (CL) from bovine heart
	E. coli total lipid extract
	L-α-phosphatydilcholine (PC) from chicken egg
	L-α-phosphatidylethanolamine (PE) from *E. coli*
	L-α-phosphatidylglycerol (PG) from *E. coli*
Avestin Inc. (Ottawa, ON, Canada)	*LiposoFast-Basic*
Bandelin GmbH & Co. (Berlin, Germany)	*Sonorex digitec ultrasonic bath*
Beckman Coulter (Brea, CA, USA)	*XL-A Analytical ultracentrifuge*
Bioline (London, UK)	Hyperladder I
Biorad (Hercules, CA, USA)	Bio-Beads™ SM-2 Resin
	Bradford Protein Assay kit
	C1000TM Thermal Cycler
	ChemiDoc™
	Gel Doc™ *EZ Imager*
	Gene Pulser®/MicroPulser™ Electroporation Cuvettes, 0.2 cm gap
	Gene Pulser Xcell™ Total System
	GS-800 Calibrated Densitometer

	Precision Plus Protein™ Unstained Protein Standard
	Precision Plus Protein™ Dual Color Standard
	Prestained SDS-PAGE Standards Broad range
	Prestained SDS-PAGE Standards Low range
	Trans-blot SD
Biotek (Winooski, VT, USA)	*PowerWave™ XS*
	SinergyHT
Biotools Inc. (Wauconda, IL, USA)	*TempComp*™
Cell Biolabs, INC. (San Diego, CA, USA)	Phosphatidylcholine Assay
Clontech (Oxford, UK)	In-Fusion™ cloning enzyme
	In-Fusion™ Dry-Down 96-well plate
Constant Systems Ltd (Daventry, UK)	MC *Constant Cell Disruption system*
Corning (Corning, NY, USA)	Falcon® 96-well deep well blocks
Eppendorf (Hamburg, Germany)	*Eppendorf Thermomixer C*
Expedeon (Harston, UK)	Instant Blue
Fisher Scientific (Hampton, NH, USA)	Falcon™ 50 mL conical centrifugal tubes
	GE Healthcare HMW Native marker kit
GE Healthcare Life Sciences (Marlborough, MA, USA)	*ÄKTA FPLC UPC-900*
	Gel Filtration Cal Kit, High Molecular Weight
	Gel Filtration Cal Kit, Low Molecular Weight
	Hi Trap Chelating Sepharose FF column
	HisTrap™ FF column
	HiTrap-SP column
	PD SpinTrap G-25 column
	Sephadex G-25 in PD-10 Desalting columns
Hellma Analytics (Müllheim, Germany)	Precision cells made of Suprasil® quartz

InVitrogen (Carlsbad, CA, USA)	1 kb Plus DNA ladder
	Benchmark™ fluorescent protein standard weight marker
	Mouse anti His (C-term) monoclonal antibody
	NativePAGE™ 4-16% Bis-Tris Protein Gels, 1.0 mm, 10-well
	NativePAGE™ 5% G-250 Sample Additive
	NativePAGE™ Cathode Buffer Additive (20X)
	NativePAGE™ Running Buffer (20X)
	NativePAGE™ Sample Buffer (4X)
	Novex® Tris-Glycine gels, Sample Buffer and Running Buffer
	NuPAGE™ 4-12% Bis-Tris Protein gels
	NuPAGE™ Novex® 10% Bis-Tris Midi gels
	SYBR™ Safe stain
Jenway (Stone, Staffordshire, UK)	*6300 Spectrophotometer*
Jobin Yvon, Horiba Group (Edison, NJ, USA)	*FluoroMax®-3 spectrofluorometer*
Leica (Wetzlar, Germany)	*Leica TCS SP5*
Life Technologies (Carlsbad, CA, USA)	ProLong Gold antifade reagent
Macherey Nagel GmbH & Co. (Düren, Germany)	NucleoBond® Xtra Midi
	NucleoSpin® Gel and PCR Clean-up
	NucleoSpin® Plasmid
Malvern Instruments (Malvern, UK)	*Viscotek GPCmax (Solvent sampling module VE 2001 GPC)*
Melford Laboratories Ltd (Ipswich,UK)	5-Bromo-4-chloro-3-indolyl-β-D-galactoside (X-Gal)
	Isopropyl-β-D-thio-galactopyranoside (IPTG)
Merck (Darmstadt, Germany)	Amicon® Ultra 0,5 ml, MWCO 100 kDa
	Amicon® Ultra-15
	D-Tube™ Dyalizer Midi, MWCO 3.5 kDa
	MF membrane, pore size 0.22 µm, diam. 25 mm
	Overnight Express™ Instant TB Medium-Novagen
Molecular Dimensions (Suffolk, UK)	MemGold2™ crystallization screen

	MemGold™ crystallization screen
	MemMeso™ crystallization screen
	Power Broth
Molecular Probes (Eugene, OR, USA)	5-iodoacetamide fluorescein (5-IAF)
	Alexa Fluor goat anti-mouse antibody
MSE Ltd. (Leicestershire, UK)	*MSE Soniprep 150*
New England Biolabs (Hertfordshire, UK)	*Bam*HI-HF® enzyme
	*Dpn*I enzyme
	*Eco*RI-HF® enzyme
	M13mp18 Single-stranded DNA
	*Mfe*I-HF® enzyme
	*Nde*I enzyme
	NEB buffer 4
	*Pvu*I-HF® enzyme
	Shrimp Alcaline Phosphatase (rSAP)
	T4 DNA Ligase
	*Xho*I enzyme
Promega (Madison, WI, USA)	Wizard SV96 plasmid DNA purification system
Qiagen (Hilden, Germany)	Ni-NTA super flow
	QIAGEN Plasmid Kits
Roche (Mannheim, Germany)	Proteinase K
Santa Cruz Biotechnology (Dallas, TX, USA)	Donkey-AntiMouse IgG-HRP
Sigma-Aldrich (San Luis, MO, USA)	Choline/Acetylcholine Quantification Kit
	cOmplete™, EDTA-free Protease Inhibitor Cocktail
	DNAse Type I
	Lysozyme from chicken egg white
	Mucasol™ universal detergent
	Octyl β-D-glucopyranoside (OG)
	Pefabloc® SC
	Poly-L-lysine, 0,1% (w/v) in water

	Protease inhibitor cocktail
	SigmaMarker™ low range and high range
	Whatman® Nuclepore™ Track-Etched Membranes (0.1 µm)
Stratagene (San Diego, CA, USA)	QuikChange II Site-Directed Mutagenesis Kit
Thermo Fisher Scientific (Waltham, MA, USA)	4-Acetamido-4'-Maleimidylstilbene-2,2'-Disulfonic Acid (AmdiS)
	NanoDrop™ Lite Spectophotometer
	Nunc™ Lab-Tek™ 8-well chambered coverglass
	Pierce™ BCA Protein Assay Kit
	Pierce™ Dye Removal Columns
	PageRuler™ Plus Prestained Protein Ladder
	Thermos Nicolet Nexus
	Veriti thermocycler
Thermo Scientific (Rockford, IL, USA)	*Ava*I enzyme
	N-Ethylmaleimide (NEM)
	Phusion Flash Master Mix
	Pierce™ Bovine Serum Albumin Standard Ampules, 2 mg/mL
	Thermo Scientific Multiskan GO
Varian (Palo Alto, CA, USA)	*Cary 300 Bio*
Vivaproducts (Littleton, MA, USA)	Vivaspin® 500 Centrifugal Concentrator (MWCO 30 & 100 kDa)
Waters (Milford, MA, USA)	*CapLC capillary chromatography system*
	Q-Tof Micro mass spectrometer
Whatman Inc. (Piscataway, NJ, USA)	Grade 3MM Blotting paper
	P-11 cation exchange cellulose
	Protran nitrocellulose membrane

BUFFERS

Table A.2. Buffers and solutions.

Buffer (indargetzailea)	Composition
BIMV sucrose (BIMV sakarosa)	500 mM Tris-HCl (pH 8.0), 20 mM DTT
BIMV1	50 mM Tris-HCl (pH 8.0), 2 mM DTT, 0.1 mM PMSF
BIMV2	50 mM Tris-HCl (pH 8.0), 2 mM DTT, 20% (v/v) glycerol
Blocking solution (Blokeatze disoluzioa)	2.5% (w/v) BSA in PBS
Buffer A (A indargetzailea)	50 mM Tris-HCl (pH 7.8), 0.1 mM EDTA and 10 % (v/v) glycerol
Buffer B (B indargetzailea)	50 mM Tris-HCl (pH 7.8), 0.6 mM DDM, 0.1 mM EDTA, 10 % (v/v) glycerol and 300 mM NaCl
Cell buffer (Zelula indargetzailea)	50 mM Tris-HCl (pH 7.8), 0.1 mM EDTA, 200 mM NaCl
Dark blue buffer (Urdin ilun indargetzailea)	50 mM BisTris, 50 mM Tricine, 0,02% (w/v) Coomasie G-250
Destain (Disoluzio destindatzailea)	10% (v/v) acetic acid, 40% (v/v) methanol
Detection solution (Detekzio disoluzioa)	7.5 mL TBST, 1 mL diaminobenzidine (6 mg/mL), 1 mL %1.4 (w/v) $NiNH_4SO_4 \cdot 6H_4O$, 0.5 mL 1.8% (w/v) $CoCl_2 \cdot 6H_2O$ and 2 µl H_2O_2 100% (v/v)
DNA loading buffer (DNA karga indargetzailea)	0.25% (w/v) bromophenol-blue, 30% (v/v) glycerol/TE buffer
E. faecalis lysis buffer (*E. faecalis* lisi indargetzailea)	50 mM NaOH, 0.25% (w/v) SDS
GUV formation buffer (GUV hantura indargetzailea)	1 mM TRIS (pH 7.5), 5 mM KCl, 400 mM sucrose.
GUV fusion buffer (GUV fusio indargetzailea)	50mM Hepes (pH 7.0), 500 mM KCl, 6 mM $MgCl_2$, 300 µM TritonX100
Laemmli 6X	250 mM Tris-HCl (pH 7.0), 0.1% (w/v) bromophenol-blue, EDTA 20 mM, 50% (v/v) glycerol, 9% (v/v) 2-mercaptoethanol, 10% (w/v) SDS
Light blue buffer (Urdin argi indargetzailea)	50 mM BisTris, 50 mM Tricine, 0,002% (w/v) Coomasie G-250
Liposome buffer (Liposoma indargetzailea)	50 mM Tris-HCl (pH 7.8), 200 mM NaCl
MES	50 mM MES (pH 7.3), 50 mM Tris, 1 mM EDTA, 0.1% (w/v) SDS
MobBΔTMD crystallization buffer (MobBΔTMD kristalizazio indargetzailea)	50 mM Tris pH 7.8, 200 mM NaCl, 0.1 mM EDTA, 10% glycerol
MobB IRS (D_2O)	50 mM Tris-DCl (pD 7.8), DDM 0.6 mM, 0.1 mM EDTA, 300 mM NaCl
MobBΔTMD IRS (D_2O)	50 mM Tris-DCl (pD 7.8), 0.1 mM EDTA, 200 mM NaCl
MobBΔTMD1	50 mM Tris-HCl (pH 7.8), 0.1 mM EDTA, 50 mM imidazole, NaCl 200 mM
MobBΔTMD2	50 mM Tris-HCl (pH 7.8), 0.1 mM EDTA, 225 mM imidazole, NaCl 200 mM
MP labelling buffer (MP markaketa indargetzailea)	50 mM Tris-HCl (pH 7.4), DDM 0.3 mM, 0.1 mM EDTA, 20% (v/v) glycerol, 300 mM NaCl,

MP purification buffer (MP purifikazio indargetzailea)	50 mM Tris-HCl (pH 7.8), DDM 0.6 mM, 0.1 mM EDTA, 10% (v/v) glicerol, 300 mM NaCl
MP1	50 mM Tris-HCl (pH 7.8), 0.1 mM EDTA
MP2	50 mM Tris-HCl (pH 7.8), DDM 0.6 mM, 0.1 mM EDTA, 50 mM imidazole, 300 mM NaCl
MP3	50 mM Tris-HCl (pH 7.8), DDM 0.6 mM, 0.1 mM EDTA, 225 mM imidazole, 300 mM NaCl
MS	50% (v/v) acetonitrile, 0.25% (v/v) formic acid
Niquel solution (Nikel disoluzioa)	0,1 M $NiNH_4SO_4 \cdot 6\ H_2O$
NPI-10 Tween	50 mM NaH_2PO_4 (pH 8.0), 10 mM imidazole, 300 mM NaCl, 1% (v/v) Tween 20
NPI-20 Tween-DDM	50 mM NaH_2PO_4 (pH 8.0), 19.6 mM DDM, 20 mM imidazole, 300 mM NaCl, 1% (v/v) Tween 20
NPI-250 Tween-DDM	50 mM NaH_2PO_4 (pH 8.0), 19.6 mM DDM, 250 mM imidazole, 300 mM NaCl, 1% (v/v) Tween 20
PBS	10mM PO_4^{3-} (pH 7.4), 2.7 mM KCl, 137 mM NaCl
Permeabilization buffer (Iragazkortasun indargetzailea)	25 mM Tris–HCl (pH 7.8), 10 mM EDTA, 1.85% (w/v) glucose, 2 mg/mL lysozyme
Protein loading buffer (SAB 1X) (Proteina karga indargetzaillea (SAB 1X))	50 mM Tris-HCl (pH 6.8), 0,02% (w/v) bromophenol-blue, 100 mM DTT, 4% (w/v) glycerol, 4% (w/v) SDS
Protein loading buffer II (Proteina karga indargetzailea II)	100 mM Tris (pH 6.8), 0.2% (w/v) bromophenol-blue, 20% (v/v) glycerol, 4% (w/v) SDS
Regenerate solution (Disoluzio birsortzailea)	50 mM Tris-HCl (pH 7.8), 50 mM EDTA, 5 M Guanidine hydrochloride
SDS-PAGE buffer (SDS-PAGE indargetzailea)	25 mM Tris (pH 8.3), 200 mM glycine, 1% (w/v) SDS
SLB buffer (SLB indargetzailea)	10 mM Hepes (pH 7.4), 150 mM NaCl
Solubilization buffer (Solubilizazio indargetzailea)	50 mM Tris-HCl (pH 7.8), 19.6 mM DDM, 0.1 mM EDTA, 600 mM NaCl, 0.1 mM PMSF
Stain (Disoluzio tindatzailea)	%10 (v/v) acetic acid, 0.1% (w/v) Coomassie Brilliant Blue R-250, 40% (v/v) methanol
Super Optimal Broth with catabolite repression (SOC) (*Super Optimal Broth* katabolitoen errepresioarekin)	20 mM glucose (pH 7.0), 2.5 mM KCl, 10 mM $MgSO_4$, 10 mM $MgCl_2$, 10 mM NaCl, 2% (w/v) tryptone, 0.5% (w/v) yeast extract
SUV fusion buffer (SUV fusio indargetzailea)	50mM Hepes (pH 7.0), 500 mM KCl, 6 mM $MgCl_2$
TAE	40 mM Tris (pH 8.0), 1 mM EDTA, 1.1% (v/v) glacial acetic acid
TBE	89 mM boric acid, 2 mM EDTA, 89 mM Tris
TBST	10 mM Tris (pH 7.5), 150 mM NaCl, 0.05% (w/v) Tween 20
TBST-BSA	10 mM Tris (pH 7.5), 5% (w/v) BSA, 150 mM NaCl, 0.05% (w/v) Tween 20
TE	10 mM Tris (pH 8.0), 1 mM EDTA
$TMD_{TraJ}CD_{TrwB}$ IRS (D_2O)	50 mM Tris-DCl (pD 7.8), DDM 0.2 mM, 0.1 mM EDTA, 200 mM NaCl
Transfer buffer (Transferentzia indargetzailea)	48 mM Tris (pH 9.2), 39 mM glycine, 20% (v/v) methanol, 1.3 mM SDS
Tris0	50 mM Tris-HCl (pH 7.8), 0.1 mM EDTA, 10% (v/v) glycerol
TrwA1	100 mM Tris-HCl (pH 7.6), 2.5 mM benzamidine, 500 mM NaCl, 0.001% (w/v) PMSF
TrwA2	100 mM Tris-HCl (pH 7.6), 2.5 mM benzamidine, imidazole 20 mM, 500 mM NaCl, 0.001% (w/v) PMSF
TrwA3	100 mM Tris-HCl (pH 7.6), 2.5 mM benzamidine, imidazole 500 mM, 500 mM NaCl, 0.001% (w/v) PMSF
TrwA4	50 mM BisTris (pH 6.0), 0.1 mM EDTA, 10% (v/v)

	glycerol, 2 mM $MgCl_2$, 100 mM NaCl
TrwB C1	50 mM Tris-HCl (pH 7.8), 19.6 mM DDM, 0.1 mM EDTA, 10% (v/v) glycerol, 300 mM NaCl 300
TrwB C2	50 mM Tris-HCl (pH 7.8), 0.6 mM DDM, 0.1 mM EDTA, 10% (v/v) glycerol, 50 mM imidazole, 300 mM NaCl 300
TrwB C3	50 mM Tris-HCl (pH 7.8), 0.6 mM DDM, 0.1 mM EDTA, 10% (v/v) glycerol, 225 mM imidazole, 300 mM NaCl 300
TrwB C4	20 mM Tris-HCl (pH 7.8), 0.6 mM DDM, 0.1 mM EDTA, 10% (v/v) glycerol, 200 mM NaCl
TrwB C5	20 mM Tris-HCl (pH 7.8), 0.6 mM DDM, 0.1 mM EDTA, 10% (v/v) glycerol, 0.07% (w/v) LDAO, 200 mM NaCl
TrwB oligomers 1	50 mM Tris-HCl (pH 7.8), 1 mM DDM, 0.1 mM EDTA
TrwB oligomers 2	50 mM Tris-HCl (pH 7.8), 1 mM DDM, 0.1 mM EDTA, 200 mM NaCl
TrwB oligomers 3	50 mM Tris-HCl (pH 7.8), 0.5 mM DDM, 0.1 mM EDTA, 500 mM NaCl
TrwB oligomers 4	50 mM Tris-HCl (pH 7.8), 0.5 mM DDM, 0.1 mM EDTA, 1 M NaCl
TrwB oligomers 5	50 mM Tris-HCl (pH 7.8), 0.3 mM DDM, 0.1 mM EDTA, 50 mM imidazole, 200 mM NaCl
TrwB oligomers 6	50 mM Tris-HCl (pH 7.8), 0.3 mM DDM, 0.1 mM EDTA, 250 mM imidazole, 200 mM NaCl
TrwB oligomers 7	50 mM Tris-HCl (pH 7.8), 0.2 mM DDM, 0.1 mM EDTA, 20% (v/v) glicerol, 200 mM NaCl
TrwBΔN70 labelling buffer (TrwBΔN70 markaketa indargetzailea)	50 mM Hepes (pH 7.4), 0.1 mM EDTA, 10% (v/v) glycerol, 100 mM NaCl
TrwBΔN70-1	50 mM Tris-HCl (pH 7.6), 1 mM EDTA, 0.001% (w/v) PMSF, 10% (w/v) sucrose
TrwBΔN70-2	50 mM Tris-HCl (pH 7.6), 1 mM EDTA, 1 M NaCl, 0.001% (w/v) PMSF, 5% (w/v) Triton X-100,
TrwBΔN70-3	50 mM Tris-HCl (pH 7.6), 1 mM EDTA, 150 mM NaCl, 0.001% (w/v) PMSF
TrwBΔN70-4	50 mM Tris-HCl (pH 7.6), 1 mM EDTA, 1 M NaCl, 0.001% (w/v) PMSF

PROTEIN SEQUENCE AND INFORMATION

Sequences corresponding to restriction enzyme sites are marked in blue, while histidine-tags are marked in red. Underlined sequences are related to transmembrane helices. *Proteins related to T4CPs, but not T4CPs themselves.

WILD TYPE PROTEINS

$TrwB_{R388}$

- Wild type GenBank: 29200594
- Nucleotide sequence, as coded in pUB3 (Table 2.2):
  ATGCATCCAGACGATCAAAGAAAGGTCAGCGCCGGAATCGTTATTGTCCTGCCGCTTATCTTTTGGATTACCGCCGTT
  CAGAAAACGGAGGTACTCGGTTCGCCGAAACTTTTGGCGCTTTGGGAGCTAATGAAGCTCACCCCACAGAAGCCAA
  TTTTGTTGCTTTCTGCGCTTGGAGGTTTGGCCGTTGGAGTGTTGTTTGTCTGGCTATTGAATAGCGTCGGACAAGGC
  GAATTTGGCGGCGCTCCATTCAAGCGATTTTTGCGCGGAACTCGCATCGTCAGTGGGGGAAAACTCAAACGCATGA
  CACGCGAAAAAGCCAAGCAAGTTACCGTTGCTGGTGTACCAATGCCGCGTGATGCAGAGCCGCGCCATTTGCTGGT
  AAATGGTGCCACTGGTACGGGTAAATCGGTGTTGCTTCGTGAGCTTGCTTATACCGGACTTTTGCGCGGCGACCGCA
  TGGTAATTGTTGACCCGAATGGCGATATGTTGTCGAAATTCGGCAGGGATAAAGACATTATCTTGAACCCCTACGAT
  CAGCGTACAAAGGGTTGGTCTTTCTTCAACGAAATCCGAAATGACTACGACTGGCAGCGTTATGCGTTGTCGGTTGT
  TCCACGCGGAAAGACAGATGAGGCCGAGGAATGGGCCAGCTACGGGCGCTTGCTGTTACGTGAAACAGCTAAAAA
  ATTGGCGCTTATTGGTACGCCTTCCATGCGCGAATTGTTCCACTGGACAACCATCGCCACGTTTGACGATTTGCGGG
  GGTTTCTGGAAGGAACTTTGGCCGAATCTTTGTTTGCTGGGTCGAATGAAGCGAGCAAGGCGCTGACCTCAGCGCG
  CTTTGTTCTTTCCGACAAATTACCGGAGCATGTCACCATGCCGGACGGTGATTTCAGCATTCGTAGTTGGCTGGAAG
  ACCCGAACGGCGGCAATCTGTTCATTACGTGGCGCGAGGACATGGGGCCAGCCTTGCGTCCGTTGATCTCCGCATG
  GGTTGACGTGGTGTGCACGTCTATTCTGTCACTACCGGAAGAACCCAAGCGCCGCTTGTGGCTGTTCATCGACGAGT
  TGGCTTCGCTGGAAAAGCTGGCGAGCTTGGCCGACGCACTCACCAAAGGCCGAAAGGCAGGGCTTCGGGTTGTGG
  CGGGCCTGCAATCGACCTCGCAGCTTGATGACGTGTACGGCGTGAAAGAGGCGCAGACCCTGCGGGCCAGCTTCCG
  CTCGCTTGTTGTCCTGGGCGGCTCGCGCACCGACCCGAAAACCAATGAGGACATGAGTTTGAGCTTGGGCGAGCAT
  GAAGTCGAACGCGACCGCTACAGCAAGAACACAGGCAAACACCACAGCACCGGGCGGGCGCTTGAGCGCGTGCGC
  GAGCGCGTCGTGATGCCGGCGGAAATCGCCAACTTGCCCGACCTCACCGCCTATGTCGGCTTTGCCGGTAATCGGCC
  AATTGCCAAGGTTCCGCTTGAAATCAAGCAGTTTGCAAACCGGCAACCGGCCTTTGTTGAGGGGACTATCCTCGAGC
  ACCACCACCACCACCACTGA
- Amino acid sequence, as coded in pUB3:
  MHPDDQRKVSAGIVIVLPLIFWITAVQKTEVLGSPKLLALWELMKLTPQKPILLLSALGGLAVGVLFVWLLNSVGQGEFGG
  APFKRFLRGTRIVSGGKLKRMTREKAKQVTVAGVPMPRDAEPRHLLVNGATGTGKSVLLRELAYTGLLRGDRMVIVDPN
  GDMLSKFGRDKDIILNPYDQRTKGWSFFNEIRNDYDWQRYALSVVPRGKTDEAEEWASYGRLLLRETAKKLALIGTPSMR
  ELFHWTTIATFDDLRGFLEGTLAESLFAGSNEASKALTSARFVLSDKLPEHVTMPDGDFSIRSWLEDPNGGNLFITWREDM
  GPALRPLISAWVDVVCTSILSLPEEPKRRLWLFIDELASLEKLASLADALTKGRKAGLRVVAGLQSTSQLDDVYGVKEAQTL
  RASFRSLVVLGGSRTDPKTNEDMSLSLGEHEVERDRYSKNTGKHHSTGRALERVRERVVMPAEIANLPDLTAYVGFAGNR
  PIAKVPLEIKQFANRQP
  AFVEGTILEHHHHHH
- Protein information:
  - Number of aminoacids: 551
  - Molecular weight: 57338.07 Da
  - Theoretical pI: 9.23
  - Extinction coefficient: 72420 M^{-1} cm^{-1} (H_2O, 280 nm).
  - Predicted TM-helix positions: 9-29, 51-71

$TraJ_{PKM101}$

- Wild type GenBank: AAB58711.1
- Wild type nucleotide sequence:
  ATGGACGATAGAGAAAGAGGCTTAGCATTTTTATTTGCAATTACTTTGCCTCCAGTGATGGTATGGTTTC
  TAGTTGCAAAATTTACCTACGGTATTGATCCATCCACGGCTAAATACCTGATTCCGTATCTGGTTAAGAATACTTTTTC
  GCTATGGCCTTTATGGTCAGCTTTAATTGCAGGCTGGTTTATTGGTGTTGGCGGTCTGATCGCTTTTATCATTTATGAT
  AAATCACGCGTGTTTAAAGGCGAAAGATTCAAAAAGATTTATCGTGGTACAGAGCTTGTTCGCGCCAGAACACTCGC
  TGATAAAACACGCGAAAGAGGTGTCAACCAGTTAACCGTGGCTAATATCCCCATACCTACATACGCTGAGAACTTGC
  ATTTTTCGATTGCCGGTACAACCGGTACTGGTAAAACCACAATTTTCAATGAACTGTTATTTAAGAGCATCATTAGAG
  GCGGCAAAAATATTGCTTTAGATCCAAATGGGGGGTTCTTAAAGAATTTCTATCGTCCCGGCGATGTTATTTTAAACG
  CCTATGATAAACGCACTGAAGGTGGGTGTTTTTCAATGAAATTCGCCGTTCATATGATTACGAGCGCTTAGTGAACTC
  TATTGTTCAGGAAAGCCCTGATATGGCTACTGAAGAATGGTTCGGCTATGGCCGTCTTATTTTTAGTGAAGTTTCGAA
  AAAACTTCACAGCCTATACAGCACAGTAACTATGGAAGAAGTTATTCACTGGGCCTGTAACGTTGACCAGAAAAAAT
  TAAAAGAATTTTTAATGGGGACGCCTGCCGAAGCTATTTTTTCCGGGTCTGAAAAAGCAGTTGGAAGCGCGCGATTT
  GTTCTCAGTAAGAATCTTGCCCCACATTTGAAAATGCCGGAAGGTAATTTTTCCCTGCGTGACTGGCTTGATGATGGA
  AAGCCGGGAACCCTGTTTATCACCTGGCAGGAAGAAATGAAAAGGTCACTTAATCCGCTAATTTCCTGCTGGCTGGA
  TTCGATTTTTTCTATCGTGCTGGGTATGGGTGAAAAAGAAAGCCGCATTAATGTATTTATTGACGAGCTGGAATCACT
  CCAGTTTCTGCCAAACCTCAACGATGCACTGACCAAAGGGCGTAAAAGCGGTCTGTGTGTTTATGCTGGCTATCAAA
  CCTATTCTCAGCTGGTTAAGGTTTATGGTCGGGATATGGCTCAGACCATTCTGGCTAACATGCGTTCTAACATCGTGC
  TGGGCGGCAGCCGTCTCGGTGATGAAACGTTGGATCAAATGTCGCGCTCACTCGGTGAGATAGAAGGCGAAGTTGA
  GCGTAAAGAATCCGATCCTCAGAAGCCCTGGATTGTCCGTAAACGCCGCGACGTTAAAGTTGTTCGTGCCGTAACGC
  CTACCGAAATATCAATGTTGCCAAACCTCACCGGCTATCTGGCGTTGCCTGGTGATATGCCCGTCGCTAAGTTCAAG
  GCTAAACACGTTAAATACCATCGCAAAAACCCTGTTCCTGGCATTGAACTGAGGGAGATCTGA
- Wild type amino acid sequence:
  MDDRERGLAFLFAITLPPVMVWFLVAKFTYGIDPSTAKYLIPYLVKNTFSLWPLWSALIAGWFIGVGGLIAFIIYDKSRVFKG
  ERFKKIYRGTELVRARTLADKTRERGVNQLTVANIPIPTYAENLHFSIAGTTGTGKTTIFNELLFKS
  IIRGGKNIALDPNGGFLKNFYRPGDVILNAYDKRTEGWVFFNEIRRSYDYERLVNSIVQESPDMATEEWFGYGRLIFSEVSK
  KLHSLYSTVTMEEVIHWACNVDQKKLKEFLMGTPAEAIFSGSEKAVGSARFVLSKNLAPHLKMPEGNFSLRDWLDDGKP
  GTLFITWQEEMKRSLNPLISCWLDSIFSIVLGMGEKESRINVFIDELESLQFLPNLNDALTKGRKSGLCVYAGYQTYSQLVKV
  YGRDMAQTILANMRSNIVLGGSRLGDETLDQMSRSLGEIEGEVERKESDPQKPWIVRKRRDVKVVRAVTPTEISMLPNLT
  GYLALPGDMPVAKFKAKHVKYHRKNPVPGIELREI
- Protein information:
  - Number of amino acids: 509
  - Molecular weight: 57762.87 Da
  - Theoretical pI: 9.24
  - Extinction coefficient: 87445 M^{-1} cm^{-1} (H_2O, 280 nm).
  - Predicted TM-helix positions: 8-28, 56-76

$MobB_{ClodF13}$

- Wild type GenBank: AJ224861.1
- Nucleotide sequence, as coded in pOPINE-*mobB* (Table A3):
  ATGTTTAATACGGATTCGCTTGCCTGGCAGTGGCATATCCCGGAGCTGGCCCGGCAGATTTACCCGTGGGTCAGCTG
  GCTTTACAGGGAGTATTACGGTCTGGCCGGGGCTTTCCTGGTTATCGGCCTGTTTTTCGGTCTGGCTGAACTCTGGG
  CCGGACGGATGCGTTTTGTGGGGCTGAGTCATAAGGAGCGACGGGAGTATGCCGATCGCTATAAGCGCGATAATA
  ACCGGACTGCGCCATTTTCGGTGCTGGCCTCGCTGGATTCGCCCGGGCGGATGGTCAGGGCACGGCGGCATGTCTG
  GAACTACGCGTACTGGCTGACCGGCAGCGCCGGTCTGGCCCTTCTGGGGGGGCTGGTTGTCGCCGTGTTTATCGAG
  AGCTGGGGAGAAACCGTCCTGCGTCCGGACCTCTACGCGAACGCAGATTATTACCTGCTGCAGCCGGCTAACCTGTT
  CGGGATTGCCTGGTGCGCGGGCGGGCTGGTTGTCGGGATTGTGTTGGCGCGGCTGCTGGCGTTCCTGCTGCTTGAC
  GGTCATTTTGCGGCTGCTGACGAGGCGGTGAACGCGAAACTGAACCAGGAGAGCCGGCGCAGCAGCCAGCGGACC
  GGTGAAATGACCGACGTCCGCCACCTGCATTTCGGGGAGCCGGTACCGGTCAACGCGCTGGCCGATTTTTCCACGG
  AGCAGGCCCGGAAACAGCAGGCGGTGTTTCTGGGTAAGGATGAGCAGGGCCAGCCGGTGCTGGTCCCGCGTGATA
  CCTGGCGCAAGACCAACATTCAGATCCTCGGCCTGCCCGGGAGCGGCAAGAGCGTGATGGCCACCAACGCGCTCAT
  TCGCTGCGTACGCGATTTCGGGGACGCGGTGGTGTACTTCGACCCCAAAGGGGACGCGTGGGCGCCGCACGTCTTC
  CGGGCGCACTGCCCAAACTTCACCCTGCTGGATCTGCGGCCGGGGAAACCGGCGCAGCTGAATCTGTTCCGCGATC
  TCGACCAGTACGCCCTGAAGAATCTGCTGGTTGCCGGGTTTAACCTGAGTGAGACCGGCGACGTGGCGGACCACTA
  CCGCATCAGCGAGCAGAAAGCGGCGAAGCTGATTGCGGAGCAGTTTCCGCAGGGGGCAAACATTCAGCAGGTGCT
  GGCGGCGGCGTACGCGCTGCCGGAGGCCCTGAAAAAGGACGTGAAGGGGCTGATCACCAAGCTGGAGAACGTGG
  CCGACCTGAGCGTCCTGCAGACGGACAGCGGCATCGACGTGGCGGGGATAATCAACGGCGGCGGCTGCCTGTACG
  TCATCGGCTCGATGGACGATGAGGCGGTGATCCGGGTGCAGAAGATGCTGTTTGCCCGCTGCGCACAAATCATCAT
  TGCGCGGGATGAGTTCCGGAGGTGGCCGCACGCGAGCATCATGCTCGATGAGATTAAATACCTGCTGTCGAAGTAC
  GTGCTGAACGCGCTGGGGACGCTGCGCAGCCGGGACTGCAACCTGCTGCTCGCGCACCAGTCGCTGGGCGACTTCG
  GGCAGTGCGGCCAGGATCTGCCCGCTGATTTTGTGAAAACCACGGTGCTGGATAACACGCCGATCCGCTGGTTCTAC
  CGGGCGGCCAGCCAGGAGTCCGCGCAGTGGGCGGCGGGCCAGACCGGGGAAATCCGGGTGGACGTGGAGCGCCG
  CCGGGCCAGCCGGGAGGCGGGGAACGTGGAGCATATCAGCGGGGACAGCTTCATCCAGAAGGAGGCGCGGCCGC
  TGTTTGACGTGAACACCCTGCAACATCTGCCTGACGGGTTCGCGGTGATGACCGGGCTGGGCGTGGCGCGGCTGGC
  GTTCAGCAGCCCGCTGCGGGTTGATCGCCGGGAAATTCCGCTGAAAACCTTCCCGGTGCTGGCGAAAACGGACCCG
  CTGGCGGAGTACCAGCCGGAGGCCAGGCGGCAGCGGCCGGGTGATGATGATTTTGCGGGGCTGTACAAACATCAC
  CATCACCATCACTAA
- Amino acid sequence, as coded in pOPINE-*mobB*:
  MFNTDSLAWQWHIPELARQIYPWVSWLYREYYGLAGAFLVIGLFFGLAELWAGRMRFVGLSHKERREYADRYKRDNNR
  TAPFSVLASLDSPGRMVRARRHVWNYAYWLTGSAGLALLGGLVVAVFIESWGETVLRPDLYANADYYLLQPANLFGIAW
  CAGGLVVGIVLARLLAFLLLDGHFAAADEAVNAKLNQESRRSSQRTGEMTDVRHLHFGEPVPVNALADFSTEQARKQQA
  VFLGKDEQGQPVLVPRDTWRKTNIQILGLPGSGKSVMATNALIRCVRDFGDAVVYFDPKGDAWAPHVFRAHCPNFTLL
  DLRPGKPAQLNLFRDLDQYALKNLLVAGFNLSETGDVADHYRISEQKAAKLIAEQFPQGANIQQVLAAAYALPEALKKDV
  KGLITKLENVADLSVLQTDSGIDVAGIINGGGCLYVIGSMDDEAVIRVQKMLFARCAQIIIARDEFRRWPHASIMLDEIKYLL
  SKYVLNALGTLRSRDCNLLLAHQSLGDFGQCGQDLPADFVKTTVLDNTPIRWFYRAASQESAQWAAGQTGEIRVDVERR
  RASREAGNVEHISGDSFIQKEARPLFDVNTLQHLPDGFAVMTGLGVARLAFSSPLRVDRREIPLKTFPVLAKTDPLAEYQPE
  ARRQRPGDDDFAGLYKHHHHHH
- Protein information:
  - Number of amino acids: 660
  - Molecular weight: 73848.39 Da
  - Theoretical pI: 7.69
  - Extinction coefficient: 108290 M^{-1} cm^{-1} (H_2O, 280 nm).
  - Predicted TM-helix positions: 34-54; 105-125, 164-184

$MobC_{ClODF13}$*

- Wild type GenBank: AJ224861.1
- Nucleotide sequence, as coded in pUB49 (Table 2.2):
  ATGGCACTGGAGCGATACAACGTCAGCCACGCGAAGCGGCAGGCGCGGAACGCGGAGAAAACACGGCTGACCCTG
  CGCTGGCTGCGGGAAGAGCTGTGTTCCACGGCGGAGCTGGTTGCGCGACGGCTGGGGATTGCGGCGGTACAGCCG
  GTTTACCGCTTCCTGGACAGCCTGGTGGCGAAAGGGCTGCTGGTCCGGGCGAAATACCCGGTTGACGGCCGTCAGG
  TCAGCGTGTGGGGGCTGACGCCGCACGGGGTGGCGTTCTCGTTCGACGAGGACGAGCCGCTGACGGACATTATTCC
  GTTTCAGCCGTCGCGGGTGTCGGCGGCGCAGCTGCCGCACCGGCTGGCCGTGCAGTCCCTGCGCCTCGCCATGGAG
  GCCCGGGGGGGCCACCGGCTGGCGGTACCTGCACCGTATTGCCCTGAAAGGGATGAAGGTGCCGGACGCGCTGGCG
  GAGCTGGACGGCAGAACGGTGGCTTTTGAGGTGGAGCGCACCGTGAAGAGCCGCAGGCGCTATCAGGAGGTGGT
  GTCCGGGTATCTGTTTAACCGCCGGGCGAACGGCATCGATGAAATCTGGTACATCTGCCCGGACCGGGCGACGCAG
  GTCAGGGTGCAGCGGGCGATCCTGTCGGTGGATGAAATCGTGAATCCACAGACCGGCGAGGCCCGCAAAACGGCG
  GAGCTGGATCGTGAACGGCTGTTTGCGTGCTTTAAATTTATGACAACGGAGCTCGAGCACCACCACCACCACCACTG
  A
- Wild type amino acid sequence:
  MALERYNVSHAKRQARNAEKTRLTLRWLREELCSTAELVARRLGIAAVQPVYRFLDSLVAKGLLVRAKYPVDGRQVSVW
  GLTPHGVAFSFDEDEPLTDIIPFQPSRVSAAQLPHRLAVQSLRLAMEARGATGWRYLHRIALKGMKVPDALAELDGRTVA
  FEVERTVKSRRRYQEVVSGYLFNRRANGIDEIWYICPDRATQVRVQRAILSVDEIVNPQTGEARKTAELDRERLFACFKFM
  TTELEHHHHHH
- Protein information:
  - Number of amino acids: 251
  - Molecular weight: 28834.11 Da
  - Theoretical pI: 9.70
  - Extinction coefficient: 32555 M^{-1} cm^{-1} (H_2O, 280 nm).
  - Predicted TM-helix positions: No predicted TM-helixes.

$TraJ_{pIP501}$

- Wild type GenBank: AJ505823.1
- Nucleotide sequence, as coded in pUB48 (Table 2.2):
  ATGACTAGTTTATTAGCAGAATCAGACGGTTTAATATTGGGGAAATTTCCAAGTGGAAAAGTTGTGATCCAACCCGA
  AGATAGCAAAATAAGCAATCGAAATATTTTTGTAGTAGGTGGTCCAGGATCATTTAAAACACAAAGTTATGTTTTGC
  CTAATGTTGTAAATAATCGCAGTACGTCAATTGTTGTAACCGATCCAAAAGGGGAAATTTACGAGTTAACCAATGAA
  ATAAAAAAAGCCCAGGGCTTCAAAACGGTTGTCATAAATTTTAAAGATTTTTTACTAAGTTCTAGGTACAATCCATTA
  CTTTACATTCGCAAATCAAATGATACAAACAAGATTGCGAACGTCATAGTATCAGCAAAGAATGACCCCAAACGGAA
  AGATTTTTGGTTCAATGCACAATTAAACTTATTAAATACGTTGATTAAATATGTTTATTTTGAATATGAACCAAGCGCA
  AGAACAATTGAGGGTATTTTAGACTTTTTAGAAGAATTTGATCCACGCTATAACGAAGAAGGTGTATCAGAACTTGA
  TGAACAATTTGAGCGTTTGCCAGACGGACACGAAGCAAAACGCAGTTACTATTTAGGCTTCCGACAAGCACAAAGT
  GAAGCAAGACCAAACATTGTTATTAGTCTATTGACGACTTTACAAGATTTTGTTGATAAAGAAGTATCAGAATTTACC
  AGTACAAACGATTTTTTCTTTGAGGAATTAGGAACGTCAAAAATTTGTTTATACGTGCTAATTTCCCCATTAGATCGA
  ACTTGGGACGGCTTAGTGAATCTCTTTTTCCAACAAATGTTTACAGAGTTATATTTTTTAGGGGATAAGCACAACGCA
  AAATTGCCAGTACCTTTAGTTATGTTACTAGATGAATTTGTCAATTTGGGCTACTTTCCAACATACGAGAATTTTCTTG
  CAACGTGTCGAGGGTATCGTATTTCAGTTAGTACCATATTGCAATCTTTGCCCCAGGGCTTTGAACTTTACGGAGATA
  AGAAATTTAAAGCGATCATTGGGAATCATGCCATTAAAATATGTCTAGGTGGTGTAGAGGAAACGACCGCCGAATA
  CTTTTCAAGACAAGTAAATGATACAACAATCAAAGTATATACAGGCGGAACAAGTGAAAGTAAAACGTCCGCAAAA
  ACAACTAACCGAAGCGGAAGTAAGTCAGAAAGCTACGGTTACCAAAAAAGGCGATTGATTACCGAAGGGGAAGTT
  ATCAATTTACAACAAGAAGAAAATGGCAGAAAAAGTATTGTGTTAATTGACGGTAAACCTTACATGTTAAGAAAAAC
  GCCACAATTTGAATTGTTCGGAAATCTTCTTAAAAAGCATGAAATTTCACAGCAAGATTATATAAGCAGTCAAACGG
  AATTTGCCAAAGAATACATTGAGGAATTGGAAAAACAGCACAAACAACGAAAAGTGCAACTAGCAAGCGCCCCAAT
  TTTTCATGAGAAGAAACAAGAAGATGATTTGAATAAAAAAGAAATAAATCTACCTGAACAACCGATCGAATCAGAA
  GTAACAGAAGAAGAGGAAGAAAAAGAACTATCAATGAGTGATATTCTAAGTAGTTTTGATGAAGGTATAGAGGAA
  AACACAGCCAACAATGACAACAGCGAATTACCATTTCTCGAGCACCACCACCACCACCACTGA
- Amino acid sequence, as coded in pUB48:
  MTSLLAESDGLILGKFPSGKVVIQPEDSKISNRNIFVVGGPGSFKTQSYVLPNVVNNRSTSIVVTDPKGEIYELTNEIKKAQG
  FKTVVINFKDFLLSSRYNPLLYIRKSNDTNKIANVIVSAKNDPKRKDFWFNAQLNLLNTLIKYVYFEYEPSARTIEGILDFLEEF
  DPRYNEEGVSELDEQFERLPDGHEAKRSYYLGFRQAQSEARPNIVISLLTTLQDFVDKEVSEFTSTNDFFFEELGTSKICLYVL
  ISPLDRTWDGLVNLFFQQMFTELYFLGDKHNAKLPVPLVMLLDEFVNLGYFPTYENFLATCRGYRISVSTILQSLPQGFELY
  GDKKFKAIIGNHAIKICLGGVEETTAEYFSRQVNDTTIKVYTGGTSESKTSAKTTNRSGSKSESYGYQKRRLITEGEVINLQQE
  ENGRKSIVLIDGKPYMLRKTPQFELFGNLLKKHEISQQDYISSQTEFAKEYIEELEKQHKQRKVQLASAPIFHEKKQEDDLNK
  KEINLPEQPIESEVTEEEEEKELSMSDILSSFDEGIEENTANNDNSELPFLEHHHHHH
- Protein information:
  - Number of amino acids: 559
  - Molecular weight: 64136.24 Da
  - Theoretical pI: 5.19
  - Extinction coefficient: 45270 M^{-1} cm^{-1} (H_2O, 280 nm).
  - Predicted TM-helix positions: No predicted TM-helixes.

$TraI_{pIP501}$*

- Wild type GenBank: AJ505823.1
- Wild type nucleotide sequence:
  ATGGCGAAGAAGAAGCAAGAGCAAGTAAAATTGATTGTCTTAGTTATACTTTATCTTCTATTGTTGCCAGTAACATTG
  ATTGTGTTTAAATTATTACCTTTTATCATTGCGAATGATACAAATATTGAATTGAGTACCTTTGTTACAACTATTTTAAA
  GCACCCGATCAATACTTTTTTAGAGATCATTCAATCTAATTACATGATTCCGTTCTTCATTGTACAAATCATTGTTTTAA
  TTATTTTATTTGTCTTTCTACACCCTACCAAACGCCAACCGTTTGAGGTTGTCGGAAAAACAAACCCTGTTCATGGATC
  GGCTTATTGGGGGGAAGAATCAGAAATAAACGCACCAAAAAATGTTCATTTGATCCCTGAAAAATCAATGAAAAGC
  ATATTAGAAAAATCAATGAGGAGGGGGAAAAATGACTAG
- Wild type amino acid sequence:
  MAKKKQEQVKLIVLVILYLLLLPVTLIVFKLLPFIIANDTNIELSTFVTTILKHPINTFLEIIQSNYMIPFFIVQIIVLIILFVFLHPTKR
  QPFEVVGKTNPVHGSAYWGEESEINAPKNVHLIPEKSMKSILEKSMRRGKND
- Protein information:
  - Number of amino acids: 143
  - Molecular weight: 16452.79 Da
  - Theoretical pI: 9.52
  - Extinction coefficient: 9970 M^{-1} cm^{-1} (H_2O, 280 nm).
  - Predicted TM-helix positions: 11-31, 68-88.

MUTANT PROTEINS

$TMD_{TraJ}CD_{TrwB}$ AND $TMD_{TraJ}CD_{TrwB}$(K142T)

- Nucleotide sequence, as coded in pUBQ4 (Table 2.2):
  ATGGACGATAGAGAAAGAGGCTTAGCATTTTTATTTGCAATTACTTTGCCTCCAGTGATGGTATGGTTTCTAGTTGCA
  AAATTTACCTACGGTATTGATCCATCCACGGCTAAATACCTGATTCCGTATCTGGTTAAGAATACTTTTTCGCTATGGC
  CTTTATGGTCAGCTTTAATTGCAGGCTGGTTTATTGGTGTTGGCGGTCTGATCGCTTTTATCATTTATGATTTGAATAG
  CGTCGGACAAGGCGAATTTGGCGGCGCTCCATTCAAGCGATTTTTGCGCGGAACTCGCATCGTCAGTGGGGGAAAA
  CTCAAACGCATGACACGCGAAAAAGCCAAGCAAGTTACCGTTGCTGGTGTACCAATGCCGCGTGATGCAGAGCCGC
  GCCATTTGCTGGTAAATGGTGCCACTGGTACGGGTA***A***ATCGGTGTTGCTTCGTGAGCTTGCTTATACCGGACTTTTG
  CGCGGCGACCGCATGGTAATTGTTGACCCGAATGGCGATATGTTGTCGAAATTCGGCAGGGATAAAGACATTATCTT
  GAACCCCTACGATCAGCGTACAAAGGGTTGGTCTTTCTTCAACGAAATCCGAAATGACTACGACTGGCAGCGTTATG
  CGTTGTCGGTTGTTCCACGCGGAAAGACAGATGAGGCCGAGGAATGGGCCAGCTACGGGCGCTTGCTGTTACGTGA
  AACAGCTAAAAAATTGGCGCTTATTGGTACGCCTTCCATGCGCGAATTGTTCCACTGGACAACCATCGCCACGTTTGA
  CGATTTGCGGGGGTTTCTGGAAGGAACTTTGGCCGAATCTTTGTTTGCTGGGTCGAATGAAGCGAGCAAGGCGCTG
  ACCTCAGCGCGCTTTGTTCTTTCCGACAAATTACCGGAGCATGTCACCATGCCGGACGGTGATTTCAGCATTCGTAGT
  TGGCTGGAAGACCCGAACGGCGGCAATCTGTTCATTACGTGGCGCGAGGACATGGGGCCAGCCTTGCGTCCGTTGA
  TCTCCGCATGGGTTGACGTGGTGTGCACGTCTATTCTGTCACTACCGGAAGAACCCAAGCGCCGCTTGTGGCTGTTC
  ATCGACGAGTTGGCTTCGCTGGAAAAGCTGGCGAGCTTGGCCGACGCACTCACCAAAGGCCGAAAGGCAGGGCTTC
  GGGTTGTGGCGGGCCTGCAATCGACCTCGCAGCTTGATGACGTGTACGGCGTGAAAGAGGCGCAGACCCTGCGGG
  CCAGCTTCCGCTCGCTTGTTGTCCTGGGCGGCTCGCGCACCGACCCGAAAACCAATGAGGACATGAGTTTGAGCTTG
  GGCGAGCATGAAGTCGAACGCGACCGCTACAGCAAGAACACAGGCAAACACCACAGCACCGGGCGGGCGCTTGAG
  CGCGTGCGCGAGCGCGTCGTGATGCCGGCGGAAATCGCCAACTTGCCCGACCTCACCGCCTATGTCGGCTTTGCCG
  GTAATCGGCCAATTGCCAAGGTTCCGCTTGAAATCAAGCAGTTTGCAAACCGGCAACCGGCCTTTGTTGAGGGGACT
  ATCCTCGAGCACCACCACCACCACCACTGA
- Amino acid sequence, as coded in pUBQ4: $TraJ_{pKM101}TrwB_{R388}$
  MDDRERGLAFLFAITLPPVMVWFLVAKFTYGIDPSTAKYLIPYLVKNTFSLWPLWSALIAGWFIGVGGLIAFIIYDLNSVGQ
  GEFGGAPFKRFLRGTRIVSGGKLKRMTREKAKQVTVAGVPMPRDAEPRHLLVNGATGTG***K***SVLLRELAYTGLLRGDRMV
  IVDPNGDMLSKFGRDKDIILNPYDQRTKGWSFFNEIRNDYDWQRYALSVVPRGKTDEAEEWASYGRLLLRETAKKLALIG
  TPSMRELFHWTTIATFDDLRGFLEGTLAESLFAGSNEASKALTSARFVLSDKLPEHVTMPDGDFSIRSWLEDPNGGNLFIT
  WREDMGPALRPLISAWVDVVCTSILSLPEEPKRRLWLFIDELASLEKLASLADALTKGRKAGLRVVAGLQSTSQLDDVYGV
  KEAQTLRASFRSLVVLGGSRTDPKTNEDMSLSLGEHEVERDRYSKNTGKHHSTGRALERVRERVVMPAEIANLPDLTAYV
  GFAGNRPIAKVPLEIKQFANRQPAFVEGTILEHHHHHH
- Protein information:
  - Number of amino acids: 521
  - Molecular weight: 58282.94 Da
  - Theoretical pI: 8.99
  - Extinction coefficient: 83880 M^{-1} cm^{-1} (H_2O, 280 nm).
  - Predicted TM-helix positions: 8-28, 54-74.

In $TMD_{TraJ}CD_{TrwB}$(K142T) mutant, the $Adenine_{425}$ nucleotide (in bold and italics) was exchanged for a cytosine. This resulted in an exchange of K_{142} amino acid for a threonine.

$TMD_{TrwB}TraJ_{pIP501}$

- Nucleotide sequence, as coded in pUBQ3 (Table 2.2):
  ATGCATCCAGACGATCAAAGAAAGGTCAGCGCCGGAATCGTTATTGTCCTGCCGCTTATCTTTTGGATTACCGCCGTT
  CAGAAAACGGAGGTACTCGGTTCGCCGAAACTTTTGGCGCTTTGGGAGCTAATGAAGCTCACCCCACAGAAGCCAA
  TTTTGTTGCTTTCTGCGCTTGGAGGTTTGGCCGTTGGAGTGTTGTTTGTCTGGCTATTGAATAGCGTCGGACAAGGC
  GAACTCGAGACTAGTTTATTAGCAGAATCAGACGGTTTAATATTGGGGAAATTTCCAAGTGGAAAAGTTGTGATCCA
  ACCCGAAGATAGCAAAATAAGCAATCGAAATATTTTTGTAGTAGGTGGTCCAGGATCATTTAAAACACAAAGTTATG
  TTTTGCCTAATGTTGTAAATAATCGCAGTACGTCAATTGTTGTAACCGATCCAAAAGGGGAAATTTACGAGTTAACCA
  ATGAAATAAAAAAAGCCCAGGGCTTCAAAACGGTTGTCATAAATTTTAAAGATTTTTTACTAAGTTCTAGGTACAATC
  CATTACTTTACATTCGCAAATCAAATGATACAAACAAGATTGCGAACGTCATAGTATCAGCAAAGAATGACCCCAAA
  CGGAAAGATTTTTGGTTCAATGCACAATTAAACTTATTAAATACGTTGATTAAATATGTTTATTTTGAATATGAACCAA
  GCGCAAGAACAATTGAGGGTATTTTAGACTTTTTAGAAGAATTTGATCCACGCTATAACGAAGAAGGTGTATCAGAA
  CTTGATGAACAATTTGAGCGTTTGCCAGACGGACACGAAGCAAAACGCAGTTACTATTTAGGCTTCCGACAAGCACA
  AAGTGAAGCAAGACCAAACATTGTTATTAGTCTATTGACGACTTTACAAGATTTTGTTGATAAAGAAGTATCAGAATT
  TACCAGTACAAACGATTTTTTCTTTGAGGAATTAGGAACGTCAAAAATTTGTTTATACGTGCTAATTTCCCCATTAGAT
  CGAACTTGGGACGGCTTAGTGAATCTCTTTTTCCAACAAATGTTTACAGAGTTATATTTTTTAGGGGATAAGCACAAC
  GCAAAATTGCCAGTACCTTTAGTTATGTTACTAGATGAATTTGTCAATTTGGGCTACTTTCCAACATACGAGAATTTTC
  TTGCAACGTGTCGAGGGTATCGTATTTCAGTTAGTACCATATTGCAATCTTTGCCCCAGGGCTTTGAACTTTACGGAG
  ATAAGAAATTTAAAGCGATCATTGGGAATCATGCCATTAAAATATGTCTAGGTGGTGTAGAGGAAACGACCGCCGA
  ATACTTTTCAAGACAAGTAAATGATACAACAATCAAAGTATATACAGGCGGAACAAGTGAAAGTAAAACGTCCGCA
  AAAACAACTAACCGAAGCGGAAGTAAGTCAGAAAGCTACGGTTACCAAAAAAGGCGATTGATTACCGAAGGGGAA
  GTTATCAATTTACAACAAGAAGAAAATGGCAGAAAAAGTATTGTGTTAATTGACGGTAAACCTTACATGTTAAGAAA
  AACGCCACAATTTGAATTGTTCGGAAATCTTCTTAAAAAGCATGAAATTTCACAGCAAGATTATATAAGCAGTCAAAC
  GGAATTTGCCAAAGAATACATTGAGGAATTGGAAAAACAGCACAAACAACGAAAAGTGCAACTAGCAAGCGCCCCA
  ATTTTTCATGAGAAGAAACAAGAAGATGATTTGAATAAAAAAGAAATAAATCTACCTGAACAACCGATCGAATCAGA
  AGTAACAGAAGAAGAGGAAGAAAAAGAACTATCAATGAGTGATATTCTAAGTAGTTTTGATGAAGGTATAGAGGA
  AAACACAGCCAACAATGACAACAGCAAATTACCATTTCTCGAGCACCACCACCACCACCACTGA
- Amino acid sequence, as coded in pUBQ3: $TrwB_{R388}TraJ_{pIP501}$
  MHPDDQRKVSAGIVIVLPLIFWITAVQKTEVLGSPKLLALWELMKLTPQKPILLLSALGGLAVGVLFVWLLNSVGQGELETS
  LLAESDGLILGKFPSGKVVIQPEDSKISNRNIFVVGGPGSFKTQSYVLPNVVNNRSTSIVVTDPKGEIYELTNEIKKAQGFKTV
  VINFKDFLLSSRYNPLLYIRKSNDTNKIANVIVSAKNDPKRKDFWFNAQLNLLNTLIKYVYFEYEPSARTIEGILDFLEEFDPRY
  NEEGVSELDEQFERLPDGHEAKRSYYLGFRQAQSEARPNIVISLLTTLQDFVDKEVSEFTSTNDFFFEELGTSKICLYVLISPLD
  RTWDGLVNLFFQQMFTELYFLGDKHNAKLPVPLVMLLDEFVNLGYFPTYENFLATCRGYRISVSTILQSLPQGFELYGDKK
  FKAIIGNHAIKICLGGVEETTAEYFSRQVNDTTIKVYTGGTSESKTSAKTTNRSGSKSESYGYQKRRLITEGEVINLQQEENGR
  KSIVLIDGKPYMLRKTPQFELFGNLLKKHEISQQDYISSQTEFAKEYIEELEKQHKQRKVQLASAPIFHEKKQEDDLNKKEINL
  PEQPIESEVTEEEEEKELSMSDILSSFDEGIEENTANNDNSKLPFLEHHHHHH
- Protein information:
  - Number of amino acids: 638
  - Molecular weight: 72700.61 Da
  - Theoretical pI: 5.34
  - Extinction coefficient: 61895 M^{-1} cm^{-1} (H_2O, 280 nm).
  - Predicted TM-helix positions: 9-29, 51-71

MobBΔTMD

- Nucleotide sequence, as coded in pOPINE-*mobBΔTMD* (Table A3):
  ATGGACGAGGCGGTGAACGCGAAACTGAACCAGGAGAGCCGGCGCAGCAGCCAGCGGACCGGTGAAATGACCGA
  CGTCCGCCACCTGCATTTCGGGGAGCCGGTACCGGTCAACGCGCTGGCCGATTTTTCCACGGAGCAGGCCCGGAAA
  CAGCAGGCGGTGTTTCTGGGTAAGGATGAGCAGGGCCAGCCGGTGCTGGTCCCGCGTGATACCTGGCGCAAGACC
  AACATTCAGATCCTCGGCCTGCCCGGGAGCGGCAAGAGCGTGATGGCCACCAACGCGCTCATTCGCTGCGTACGCG
  ATTTCGGGGACGCGGTGGTGTACTTCGACCCCAAAGGGGACGCGTGGGCGCCGCACGTCTTCCGGGCGCACTGCCC
  AAACTTCACCCTGCTGGATCTGCGGCCGGGGAAACCGGCGCAGCTGAATCTGTTCCGCGATCTCGACCAGTACGCCC
  TGAAGAATCTGCTGGTTGCCGGGTTTAACCTGAGTGAGACCGGCGACGTGGCGGACCACTACCGCATCAGCGAGCA
  GAAAGCGGCGAAGCTGATTGCGGAGCAGTTTCCGCAGGGGGCAAACATTCAGCAGGTGCTGGCGGCGGCGTACGC
  GCTGCCGGAGGCCCTGAAAAAGGACGTGAAGGGGCTGATCACCAAGCTGGAGAACGTGGCCGACCTGAGCGTCCT
  GCAGACGGACAGCGGCATCGACGTGGCGGGGATAATCAACGGCGGCGGCTGCCTGTACGTCATCGGCTCGATGGA
  CGATGAGGCGGTGATCCGGGTGCAGAAGATGCTGTTTGCCCGCTGCGCACAAATCATCATTGCGCGGGATGAGTTC
  CGGAGGTGGCCGCACGCGAGCATCATGCTCGATGAGATTAAATACCTGCTGTCGAAGTACGTGCTGAACGCGCTGG
  GGACGCTGCGCAGCCGGGACTGCAACCTGCTGCTCGCGCACCAGTCGCTGGGCGACTTCGGGCAGTGCGGCCAGG
  ATCTGCCCGCTGATTTTGTGAAAACCACGGTGCTGGATAACACGCCGATCCGCTGGTTCTACCGGGCGGCCAGCCAG
  GAGTCCGCGCAGTGGGCGGCGGGCCAGACCGGGGAAATCCGGGTGGACGTGGAGCGCCGCCGGGCCAGCCGGGA
  GGCGGGGAACGTGGAGCATATCAGCGGGGACAGCTTCATCCAGAAGGAGGCGCGGCCGCTGTTTGACGTGAACAC
  CCTGCAACATCTGCCTGACGGGTTCGCGGTGATGACCGGGCTGGGCGTGGCGCGGCTGGCGTTCAGCAGCCCGCTG
  CGGGTTGATCGCCGGGAAATTCCGCTGAAAACCTTCCCGGTGCTGGCGAAAACGGACCCGCTGGCGGAGTACCAGC
  CGGAGGCCAGGCGGCAGCGGCCGGGTGATGATGATTTTGCGGGGCTGTACAAACATCACCATCACCATCACTAA
- Amino acid sequence, as coded in pOPINE-*mobBΔTMD*:
  MDEAVNAKLNQESRRSSQRTGEMTDVRHLHFGEPVPVNALADFSTEQARKQQAVFLGKDEQGQPVLVPRDTWRKTNI
  QILGLPGSGKSVMATNALIRCVRDFGDAVVYFDPKGDAWAPHVFRAHCPNFTLLDLRPGKPAQLNLFRDLDQYALKNLL
  VAGFNLSETGDVADHYRISEQKAAKLIAEQFPQGANIQQVLAAAYALPEALKKDVKGLITKLENVADLSVLQTDSGIDVAGI
  INGGGCLYVIGSMDDEAVIRVQKMLFARCAQIIIARDEFRRWPHASIMLDEIKYLLSKYVLNALGTLRSRDCNLLLAHQSLG
  DFGQCGQDLPADFVKTTVLDNTPIRWFYRAASQESAQWAAGQTGEIRVDVERRRASREAGNVEHISGDSFIQKEARPLF
  DVNTLQHLPDGFAVMTGLGVARLAFSSPLRVDRREIPLKTFPVLAKTDPLAEYQPEARRQRPGDDDFAGLYKHHHHHH
- Protein information:
  - Number of amino acids: 477
  - Molecular weight: 53118.42 Da
  - Theoretical pI: 6.74
  - Extinction coefficient: 42775 M^{-1} cm^{-1} (H_2O, 280 nm).
  - Predicted TM-helix positions: No predicted TM-helixes.

$TraI_{pIP501}TraJ_{pIP501}$

- Nucleotide sequence, as coded in pUBQ5 (Table 2.2):
  ATGGCGAAGAAGAAGCAAGAGCAAGTAAAATTGATTGTCTTAGTTATACTTTATCTTCTATTGTTGCCAGTAACATTG
  ATTGTGTTTAAATTATTACCTTTTATCATTGCGAATGATACAAATATTGAATTGAGTACCTTTGTTACAACTATTTTAAA
  GCACCCGATCAATACTTTTTTAGAGATCATTCAATCTAATTACATGATTCCGTTCTTCATTGTACAAATCATTGTTTTAA
  TTATTTTATTTGTCTTTCTACACCCTACCAAACGCCAACCGTTTGAGGTTGTCGGAAAAACAAACCCTGTTCATGGATC
  GGCTTATTGGGGGGAAGAATCAGAAATAAACGCACCAAAAAATGTTCATTTGATCCCTGAAAAATCAATGAAAAGC
  ATATTAGAAAAATCAATGAGGAGGGGGAAAAATGACGGATCCACTAGTTTATTAGCAGAATCAGACGGTTTAATAT
  TGGGGAAATTTCCAAGTGGAAAAGTTGTGATCCAACCCGAAGATAGCAAAATAAGCAATCGAAATATTTTTGTAGTA
  GGTGGTCCAGGATCATTTAAAACACAAAGTTATGTTTTGCCTAATGTTGTAAATAATCGCAGTACGTCAATTGTTGTA
  ACCGATCCAAAAGGGGAAATTTACGAGTTAACCAATGAAATAAAAAAAGCCCAGGGCTTCAAAACGGTTGTCATAA
  ATTTTAAAGATTTTTTACTAAGTTCTAGGTACAATCCATTACTTTACATTCGCAAATCAAATGATACAAACAAGATTGC
  GAACGTCATAGTATCAGCAAAGAATGACCCCAAACGGAAAGATTTTTGGTTCAATGCACAATTAAACTTATTAAATA
  CGTTGATTAAATATGTTTATTTTGAATATGAACCAAGCGCAAGAACAATTGAGGGTATTTTAGACTTTTTAGAAGAAT
  TTGATCCACGCTATAACGAAGAAGGTGTATCAGAACTTGATGAACAATTTGAGCGTTTGCCAGACGGACACGAAGC
  AAAACGCAGTTACTATTTAGGCTTCCGACAAGCACAAAGTGAAGCAAGACCAAACATTGTTATTAGTCTATTGACGA
  CTTTACAAGATTTTGTTGATAAAGAAGTATCAGAATTTACCAGTACAAACGATTTTTTCTTTGAGGAATTAGGAACGT
  CAAAAATTTGTTTATACGTGCTAATTTCCCCATTAGATCGAACTTGGGACGGCTTAGTGAATCTCTTTTTCCAACAAAT
  GTTTACAGAGTTATATTTTTTAGGGGATAAGCACAACGCAAAATTGCCAGTACCTTTAGTTATGTTACTAGATGAATT
  TGTCAATTTGGGCTACTTTCCAACATACGAGAATTTTCTTGCAACGTGTCGAGGGTATCGTATTTCAGTTAGTACCAT
  ATTGCAATCTTTGCCCCAGGGCTTTGAACTTTACGGAGATAAGAAATTTAAAGCGATCATTGGGAATCATGCCATTAA
  AATATGTCTAGGTGGTGTAGAGGAAACGACCGCCGAATACTTTTCAAGACAAGTAAATGATACAACAATCAAAGTAT
  ATACAGGCGGAACAAGTGAAAGTAAAACGTCCGCAAAAACAACTAACCGAAGCGGAAGTAAGTCAGAAAGCTACG
  GTTACCAAAAAAGGCGATTGATTACCGAAGGGGAAGTTATCAATTTACAACAAGAAGAAAATGGCAGAAAAAGTAT
  TGTGTTAATTGACGGTAAACCTTACATGTTAAGAAAAACGCCACAATTTGAATTGTTCGGAAATCTTCTTAAAAAGCA
  TGAAATTTCACAGCAAGATTATATAAGCAGTCAAACGGAATTTGCCAAAGAATACATTGAGGAATTGGAAAAACAG
  CACAAACAACGAAAAGTGCAACTAGCAAGCGCCCCAATTTTTCATGAGAAGAAACAAGAAGATGATTTGAATAAAA
  AAGAAATAAATCTACCTGAACAACCGATCGAATCAGAAGTAACAGAAGAAGAGGAAGAAAAAGAACTATCAATGA
  GTGATATTCTAAGTAGTTTTGATGAAGGTATAGAGGAAAACACAGCCAACAATGACAACAGCGAATTACCATTTCTC
  GAGCACCACCACCACCACCACTGA
- Amino acid sequence, as coded in pUBQ5: $TraI_{pIP501}TraJ_{pIP501}$
  MAKKKQEQVKLIVLVILYLLLLPVTLIVFKLLPFIIANDTNIELSTFVTTILKHPINTFLEIIQSNYMIPFFIVQIIVLIILFVFLHPTKR
  QPFEVVGKTNPVHGSAYWGEESEINAPKNVHLIPEKSMKSILEKSMRRGKNDGSTSLLAESDGLILGKFPSGKVVIQPEDS
  KISNRNIFVVGGPGSFKTQSYVLPNVVNNRSTSIVVTDPKGEIYELTNEIKKAQGFKTVVINFKDFLLSSRYNPLLYIRKSNDT
  NKIANVIVSAKNDPKRKDFWFNAQLNLLNTLIKYVYFEYEPSARTIEGILDFLEEFDPRYNEEGVSELDEQFERLPDGHEAKR
  SYYLGFRQAQSEARPNIVISLLTTLQDFVDKEVSEFTSTNDFFFEELGTSKICLYVLISPLDRTWDGLVNLFFQQMFTELYFLG
  DKHNAKLPVPLVMLLDEFVNLGYFPTYENFLATCRGYRISVSTILQSLPQGFELYGDKKFKAIIGNHAIKICLGGVEETTAEYF
  SRQVNDTTIKVYTGGTSESKTSAKTTNRSGSKSESYGYQKRRLITEGEVINLQQEENGRKSIVLIDGKPYMLRKTPQFELFGN
  LLKKHEISQQDYISSQTEFAKEYIEELEKQHKQRKVQLASAPIFHEKKQEDDLNKKEINLPEQPIESEVTEEEEEKELSMSDILS
  SFDEGIEENTANNDNSELPFLEHHHHHH
- Protein information:
  - Number of amino acids: 703
  - Molecular weight: 80583.95 Da
  - Theoretical pI: 5.63
  - Extinction coefficient: 55240 M^{-1} cm^{-1} (H_2O, 280 nm).
  - Predicted TM-helix positions: 11-31, 67-87.

BIBLIOGRAPHY

BIBLIOGRAPHY

Abajy, M.Y., Kopeć, J., Schiwon, K., Burzynski, M., Döring, M., Bohn, C., and Grohmann, E. (2007). A type IV-secretion-like system is required for conjugative DNA transport of broad-host-range plasmid pIP501 in gram-positive bacteria. J. Bacteriol. *189*, 2487–2496.

Agopian, A., Quetin, M., and Castano, S. (2016). Structure and interaction with lipid membrane models of Semliki Forest virus fusion peptide. Biochim. Biophys. Acta - Biomembr. *1858*, 2671–2680.

Aguilar, J., Zupan, J., Cameron, T.A., and Zambryski, P.C. (2010). Agrobacterium type IV secretion system and its substrates form helical arrays around the circumference of virulence-induced cells. Proc. Natl. Acad. Sci. U. S. A. *107*, 3758–3763.

Agúndez, L., Zárate-Pérez, F., Meier, A.F., Bardelli, M., Llosa, M., Escalante, C.R., Linden, R.M., and Henckaerts, E. (2018). Exchange of functional domains between a bacterial conjugative relaxase and the integrase of the human adeno-associated virus. PLoS One *13*, e0200841.

Åkesson, A., Lind, T., Ehrlich, N., Stamou, D., Wacklin, H., and Cárdenas, M. (2012). Composition and structure of mixed phospholipid supported bilayers formed by POPC and DPPC. Soft Matter *8*, 5658.

Alvarez-Martinez, C.E., and Christie, P.J. (2009). Biological diversity of prokaryotic type IV secretion systems. Microbiol. Mol. Biol. Rev. *73*, 775–808.

Andraka, N., Sánchez-Magraner, L., García-Pacios, M., Goñi, F.M., and Arrondo, J.L.R. (2017). The conformation of human phospholipid scramblase 1, as studied by infrared spectroscopy. Effects of calcium and detergent. Biochim. Biophys. Acta - Biomembr. *1859*, 1019–1028.

Angelova, M.I., and Dimitrov, D.S. (1986). Liposome electroformation. Faraday Discuss. Chem. Soc. *81*, 303.

Angelova, M.I., Soléau, S., Méléard, P., Faucon, F., and Bothorel, P. (1992). Preparation of giant vesicles by external AC electric fields. Kinetics and applications. In Trends in Colloid and Interface Science VI, (Darmstadt: Steinkopff), pp. 127–131.

Angius, F., Ilioaia, O., Uzan, M., and Miroux, B. (2016). Membrane Protein Production in Escherichia coli: Protocols and Rules. In Methods in Molecular Biology (Clifton, N.J.), pp. 37–52.

Arechaga, I., Miroux, B., Runswick, M.J., and Walker, J.E. (2003). Over-expression of Escherichia coli F1F(o)-ATPase subunit a is inhibited by instability of the uncB gene transcript. FEBS Lett. *547*, 97–100.

Arechaga, I., Peña, A., Zunzunegui, S., del Carmen Fernández-Alonso, M., Rivas, G., and de la Cruz, F. (2008). ATPase activity and oligomeric state of TrwK, the VirB4 homologue of the plasmid R388 type IV secretion system. J. Bacteriol. *190*, 5472–5479.

Arends, K., Celik, E.-K., Probst, I., Goessweiner-Mohr, N., Fercher, C., Grumet, L., Soellue, C., Abajy, M.Y., Sakinc, T., Broszat, M., et al. (2013). TraG encoded by the pIP501 type IV secretion system is a two-domain peptidoglycan-degrading enzyme essential for conjugative transfer. J. Bacteriol. *195*, 4436–4444.

Arrondo, J.L., and Goñi, F.M. (1999). Structure and dynamics of membrane proteins as studied by infrared spectroscopy. Prog. Biophys. Mol. Biol. *72*, 367–405.

Arrondo, J.L., Muga, A., Castresana, J., and Goñi, F.M. (1993). Quantitative studies of the structure of proteins in solution by Fourier-transform infrared spectroscopy. Prog. Biophys. Mol. Biol. *59*, 23–56.

Atmakuri, K., Cascales, E., and Christie, P.J. (2004). Energetic components VirD4, VirB11 and VirB4 mediate early DNA transfer reactions required for bacterial type IV secretion. Mol. Microbiol. *54*, 1199–1211.

Aussel, L., Barre, F.X., Aroyo, M., Stasiak, A., Stasiak, A.Z., and Sherratt, D. (2002). FtsK is a DNA motor protein that activates chromosome dimer resolution by switching the catalytic state of the XerC and XerD recombinases. Cell *108*, 195–205.

Avila, P., and de la Cruz, F. (1988). Physical and genetic map of the IncW plasmid R388. Plasmid *20*, 155–157.

Bachman, J. (2013). Site-Directed Mutagenesis. In Methods in Enzymology, pp. 241–248.

Bagatolli, L.A., and Needham, D. (2014). Quantitative optical microscopy and micromanipulation studies on the lipid bilayer membranes of giant unilamellar vesicles. Chem. Phys. Lipids *181*, 99–120.

Bangham, A.D., Standish, M.M., and Miller, N. (1965). Cation Permeability of Phospholipid Model Membranes: Effect of Narcotics. Nature *208*, 1295–1297.

Basu, U., Lee, S.-W., Deshpande, A., Shen, J., Sohn, B.-K., Cho, H., Kim, H., and Patel, S.S. (2020). The C-terminal tail of the yeast mitochondrial transcription factor Mtf1 coordinates template strand alignment, DNA scrunching and timely transition into elongation. Nucleic Acids Res. *48*.

Bauer, T., Rösch, T., Itaya, M., and Graumann, P.L. (2011). Localization Pattern of Conjugation Machinery in a Gram-Positive Bacterium. J. Bacteriol. *193*, 6244–6256.

Bellanger, X., Payot, S., Leblond-Bourget, N., and Guédon, G. (2014). Conjugative and mobilizable genomic islands in bacteria: evolution and diversity. FEMS Microbiol. Rev. *38*, 720–760.

Bello-López, J.M., Cabrero-Martínez, O.A., Ibáñez-Cervantes, G., Hernández-Cortez, C., Pelcastre-Rodríguez, L.I., Gonzalez-Avila, L.U., and Castro-Escarpulli, G. (2019). Horizontal gene transfer and its association with antibiotic resistance in the genus aeromonas spp. Microorganisms *7*.

Berrow, N.S., Alderton, D., Sainsbury, S., Nettleship, J., Assenberg, R., Rahman, N., Stuart, D.I., and Owens, R.J. (2007). A versatile ligation-independent cloning method suitable for high-throughput expression screening applications. Nucleic Acids Res. *35*, e45.

Bhatty, M., Gomez, J.A.L., and Christie, P.J. (2013). The Expanding Bacterial Type IV Secretion Lexicon. Res. Microbiol. *164*, 620–639.

Biner, O., Schick, T., Müller, Y., and von Ballmoos, C. (2016). Delivery of membrane proteins into small and giant unilamellar vesicles by charge-mediated fusion. FEBS Lett. *590*, 2051–2062.

Birch, J., Axford, D., Foadi, J., Meyer, A., Eckhardt, A., Thielmann, Y., and Moraes, I. (2018). The fine art of integral membrane protein crystallisation. Methods *147*, 150–162.

Bird, L.E. (2011). High throughput construction and small scale expression screening of multi-tag vectors in Escherichia coli. Methods *55*, 29–37.

Bleicken, S., Wagner, C., and García-Sáez, A.J. (2013). Mechanistic differences in the membrane activity of Bax and Bcl-xL correlate with their opposing roles in apoptosis. Biophys. J. *104*, 421–431.

Bleicken, S., Hofhaus, G., Ugarte-Uribe, B., Schröder, R., and García-Sáez, A.J. (2016). cBid, Bax and Bcl-xL exhibit opposite membrane remodeling activities. Cell Death Dis. *7*, e2121.

Bolland, S., Llosa, M., Avila, P., and de la Cruz, F. (1990). General organization of the conjugal transfer genes of the IncW plasmid R388 and interactions between R388 and IncN and IncP plasmids. J. Bacteriol. *172*, 5795–5802.

Booth, P.J., Templer, R.H., Meijberg, W., Allen, S.J., Curran, A.R., and Lorch, M. (2001). *In Vitro* Studies of Membrane Protein Folding. Crit. Rev. Biochem. Mol. Biol. *36*, 501–603.

Boudaher, E., and Shaffer, C.L. (2019). Inhibiting bacterial secretion systems in the fight against antibiotic resistance. Medchemcomm *10*, 682–692.

Bourg, G., Sube, R., O'Callaghan, D., and Patey, G. (2009). Interactions between Brucella suis VirB8 and its homolog TraJ from the plasmid pSB102 underline the dynamic nature of type IV secretion systems. J. Bacteriol. *191*, 2985–2992.

Bradford, M.M. (1976). A rapid and sensitive method for the quantitation of microgram quantities of protein utilizing the principle of protein-dye binding. Anal. Biochem. *72*, 248–254.

Cabezon, E., and de la Cruz, F. (2006). TrwB: An F1-ATPase-like molecular motor involved in DNA transport during bacterial conjugation. Res. Microbiol. *157*, 299–305.

Cabezón, E. (1996). Función de las proteínas de la familia de trag en la conjugación bacteriana. Caracterización de trwb de r388. Universidad de Cantabria.

Cabezón, E., and Arechaga, I. (2020). Spectrophotometric Assays to Quantify the Activity of T4SS ATPases. In Methods in Molecular Biology, (Humana Press Inc.), pp. 135–143.

Cabezón, E., Lanka, E., and de la Cruz, F. (1994). Requirements for mobilization of plasmids RSF1010 and ColE1 by the IncW plasmid R388: trwB and RP4 traG are interchangeable. J. Bacteriol. *176*, 4455–4458.

Cabezón, E., Sastre, J.I., and de la Cruz, F. (1997). Genetic evidence of a coupling role for the TraG protein family in bacterial conjugation. Mol. Gen. Genet. *254*, 400–406.

Cascales, E., and Christie, P.J. (2004a). Agrobacterium VirB10, an ATP energy sensor required for type IV secretion. Proc. Natl. Acad. Sci. *101*, 17228–17233.

Cascales, E., and Christie, P.J. (2004b). Definition of a Bacterial Type IV Secretion Pathway for a DNA Substrate. Science (80-.). *304*, 1170–1173.

Cascales, E., Atmakuri, K., Sarkar, M.K., and Christie, P.J. (2013). DNA Substrate-Induced Activation of the Agrobacterium VirB/VirD4 Type IV Secretion System. J. Bacteriol. *195*, 2691–2704.

Cassini, A., Högberg, L.D., Plachouras, D., Quattrocchi, A., Hoxha, A., Simonsen, G.S., Colomb-Cotinat, M., Kretzschmar, M.E., Devleesschauwer, B., Cecchini, M., et al. (2019). Attributable deaths and disability-adjusted life-years caused by infections with antibiotic-resistant bacteria in the EU and the European Economic Area in 2015: a population-level modelling analysis. Lancet Infect. Dis. *19*, 56–66.

Castellana, E.T., and Cremer, P.S. (2007). Imaging large arrays of supported lipid bilayers with a macroscope. Biointerphases *2*, 57–63.

Casu, B., Smart, J., Hancock, M.A., Smith, M., Sygusch, J., and Baron, C. (2016). Structural Analysis and Inhibition of TraE from the pKM101 Type IV Secretion System. J. Biol. Chem. *291*, 23817–23829.

Casu, B., Arya, T., Bessette, B., and Baron, C. (2017). Fragment-based screening identifies novel targets for inhibitors of conjugative transfer of antimicrobial resistance by plasmid pKM101. Sci. Rep. *7*, 14907.

Casu, B., Mary, C., Sverzhinsky, A., Fouillen, A., Nanci, A., and Baron, C. (2018). VirB8 homolog TraE from plasmid pKM101 forms a hexameric ring structure and interacts with the VirB6 homolog TraD. Proc. Natl. Acad. Sci. U. S. A. *115*, 5950–5955.

Cattoni, D.I., Flecha, F.L.G., and Argüello, J.M. (2008). Thermal stability of CopA, a polytopic membrane protein from the hyperthermophile Archaeoglobus fulgidus. Arch. Biochem. Biophys. *471*, 198–206.

Celaya, G., Perales-Calvo, J., Muga, A., Moro, F., and Rodriguez-Larrea, D. (2017). Label-Free, Multiplexed, Single-Molecule Analysis of Protein-DNA Complexes with Nanopores. ACS Nano *11*, 5815–5825.

Chan, M. (2015). WHO Library Cataloguing-in-Publication Data Global Action Plan on Antimicrobial Resistance.

Chandradoss, S.D., Haagsma, A.C., Lee, Y.K., Hwang, J.-H., Nam, J.-M., and Joo, C. (2014). Surface

passivation for single-molecule protein studies. J. Vis. Exp.

Chandran Darbari, V., and Waksman, G. (2015). Structural Biology of Bacterial Type IV Secretion Systems. Annu. Rev. Biochem. *84*, 603–629.

Chang, Y.-W., Shaffer, C.L., Rettberg, L.A., Ghosal, D., and Jensen, G.J. (2018). In Vivo Structures of the Helicobacter pylori cag Type IV Secretion System. Cell Rep. *23*, 673–681.

Chaton, C.T., and Herr, A.B. (2015). Elucidating Complicated Assembling Systems in Biology Using Size-and-Shape Analysis of Sedimentation Velocity Data. In Methods in Enzymology, (Academic Press Inc.), pp. 187–204.

Chen, Y., Zhang, X., Manias, D., Yeo, H.-J., Dunny, G.M., and Christie, P.J. (2008). Enterococcus faecalis PcfC, a Spatially Localized Substrate Receptor for Type IV Secretion of the pCF10 Transfer Intermediate. J. Bacteriol. *190*, 3632–3645.

Cheng, Y. (2018). Membrane protein structural biology in the era of single particle cryo-EM. Curr. Opin. Struct. Biol. *52*, 58–63.

Chetrit, D., Hu, B., Christie, P.J., Roy, C.R., and Liu, J. (2018). A unique cytoplasmic ATPase complex defines the Legionella pneumophila type IV secretion channel. Nat. Microbiol. *3*, 678–686.

Christie, P.J. (2004). Type IV secretion: the Agrobacterium VirB/D4 and related conjugation systems. Biochim. Biophys. Acta - Mol. Cell Res. *1694*, 219–234.

Christie, P.J. (2016). The Mosaic Type IV Secretion Systems. EcoSal Plus *7*.

Christie, P.J., Atmakuri, K., Krishnamoorthy, V., Jakubowski, S., and Cascales, E. (2005). Biogenesis, architecture, and function of bacterial Type IV Secretion Systems. Annu. Rev. Microbiol. *59*, 451–485.

Christie, P.J., Whitaker, N., and González-Rivera, C. (2014). Mechanism and structure of the bacterial type IV secretion systems. Biochim. Biophys. Acta - Mol. Cell Res. *1843*, 1578–1591.

Christie, P.J., Gomez Valero, L., and Buchrieser, C. (2017). Biological Diversity and Evolution of Type IV Secretion Systems. In Current Topics in Microbiology and Immunology, pp. 1–30.

Cohen, S.N., Chang, A.C., and Hsu, L. (1972). Nonchromosomal antibiotic resistance in bacteria: genetic transformation of Escherichia coli by R-factor DNA. Proc. Natl. Acad. Sci. U. S. A. *69*, 2110–2114.

Cornish-Bowden, A. (1979). Fundamentals of Enzyme Kinetics (Butterworth-Heinemann).

Correia, J.J., and Stafford, W.F. (2015). Sedimentation Velocity. pp. 49–80.

Crane, J.M., and Tamm, L.K. (2007). Fluorescence microscopy to study domains in supported lipid bilayers. Methods Mol. Biol. *400*, 481–488.

Daghastanli, K.R.P., Ferreira, R.B., Thedei, G., Maggio, B., and Ciancaglini, P. (2004). Lipid composition-dependent incorporation of multiple membrane proteins into liposomes. Colloids Surfaces B Biointerfaces *36*, 127–137.

Datta, N., and Hedges, R.W. (1972). Trimethoprim Resistance Conferred by W Plasmids in Enterobacteriaceae. J. Gen. Microbiol. *72*, 349–355.

Deamer, D., and Bangham, A.D. (1976). Large volume liposomes by an ether vaporization method. Biochim. Biophys. Acta *443*, 629–634.

Denisov, I.G., and Sligar, S.G. (2017). Nanodiscs in Membrane Biochemistry and Biophysics. Chem. Rev. *117*, 4669–4713.

Dey, B., Thukral, S., Krishnan, S., Chakrobarty, M., Gupta, S., Manghani, C., and Rani, V. (2012). DNA-

protein interactions: methods for detection and analysis. Mol. Cell. Biochem. *365*, 279–299.

Dezi, M., Di Cicco, A., Bassereau, P., and Lévy, D. (2013). Detergent-mediated incorporation of transmembrane proteins in giant unilamellar vesicles with controlled physiological contents. Proc. Natl. Acad. Sci. U. S. A. *110*, 7276–7281.

Dodd, C.E., Johnson, B.R.G., Jeuken, L.J.C., Bugg, T.D.H., Bushby, R.J., and Evans, S.D. (2008a). Native *E. coli* inner membrane incorporation in solid-supported lipid bilayer membranes. Biointerphases *3*, FA59–FA67.

Dodd, C.E., Johnson, B.R.G., Jeuken, L.J.C., Bugg, T.D.H., Bushby, R.J., and Evans, S.D. (2008b). Native E. coli inner membrane incorporation in solid-supported lipid bilayer membranes. Biointerphases *3*, FA59.

Dong, H., Nilsson, L., and Kurland, C.G. (1995). Gratuitous overexpression of genes in Escherichia coli leads to growth inhibition and ribosome destruction. J. Bacteriol. *177*, 1497–1504.

Dower, W.J., Miller, J.F., and Ragsdale, C.W. (1988). High efficiency transformation of E.coli by high voltage electroporation. Nucleic Acids Res. *16*, 6127–6145.

Draper, O., César, C.E., Machón, C., de la Cruz, F., and Llosa, M. (2005). Site-specific recombinase and integrase activities of a conjugative relaxase in recipient cells. Proc. Natl. Acad. Sci. U. S. A. *102*, 16385–16390.

Drew, D., Slotboom, D.-J., Friso, G., Reda, T., Genevaux, P., Rapp, M., Meindl-Beinker, N.M., Lambert, W., Lerch, M., Daley, D.O., et al. (2005). A scalable, GFP-based pipeline for membrane protein overexpression screening and purification. Protein Sci. *14*, 2011–2017.

Drew, D., Lerch, M., Kunji, E., Slotboom, D.-J., and de Gier, J.-W. (2006). Optimization of membrane protein overexpression and purification using GFP fusions. Nat. Methods *3*, 303–313.

Drew, D., Newstead, S., Sonoda, Y., Kim, H., von Heijne, G., and Iwata, S. (2008). GFP-based optimization scheme for the overexpression and purification of eukaryotic membrane proteins in Saccharomyces cerevisiae. Nat. Protoc. *3*, 784–798.

Drew, D.E., von Heijne, G., Nordlund, P., and de Gier, J.W. (2001). Green fluorescent protein as an indicator to monitor membrane protein overexpression in Escherichia coli. FEBS Lett. *507*, 220–224.

Durand, E., Waksman, G., and Receveur-Brechot, V. (2011). Structural insights into the membrane-extracted dimeric form of the ATPase TraB from the Escherichia coli pKM101 conjugation system. BMC Struct. Biol. *11*, 4.

Ebel, C. (2011). Sedimentation velocity to characterize surfactants and solubilized membrane proteins. Methods *54*, 56–66.

Echabe, I., Prado, A., Goñi, F.L.M., Arondo, J.L.R., and Dornberger, U. (1998). Topology of sarcoplasmic reticulum Ca^{2+} -ATPase: An infrared study of thermal denaturation and limited proteolysis. Protein Sci. *7*, 1172–1179.

van den Elzen, P.J., Konings, R.N., Veltkamp, E., and Nijkamp, H.J. (1980). Transcription of bacteriocinogenic plasmid CloDF13 in vivo and in vitro: structure of the cloacin immunity operon. J. Bacteriol. *144*, 579–591.

Endo, S., Nagayama, K., and Wada, A. (1985). Probing Stability and Dynamics of Proteins by Protease Digestion I: Comparison of Protease Susceptibility and Thermal Stability of Cytochromes c. J. Biomol. Struct. Dyn. *3*, 409–421.

Enterina, J.R., Wu, L., and Campbell, R.E. (2015). Emerging fluorescent protein technologies. Curr. Opin. Chem. Biol. *27*, 10–17.

Escudero, J., Den Dulk-Ras, A., Regensburg-Tuïnk, T.J.G., and Hooykaas, P.J.J. (2003). VirD4-independent

transformation by CloDF13 evidences an unknown factor required for the genetic colonization of plants via Agrobacterium. Mol. Microbiol. *47*, 891–901.

Evans, R.P., and Macrina, F.L. (1983). Streptococcal R plasmid pIP501: endonuclease site map, resistance determinant location, and construction of novel derivatives. J. Bacteriol. *154*, 1347–1355.

Fercher, C., Probst, I., Kohler, V., Goessweiner-Mohr, N., Arends, K., Grohmann, E., Zangger, K., Meyer, N.H., and Keller, W. (2016). VirB8-like protein TraH is crucial for DNA transfer in Enterococcus faecalis. Sci. Rep. *6*, 24643.

Fernández-González, E., de Paz, H.D., Alperi, A., Agúndez, L., Faustmann, M., Sangari, F.J., Dehio, C., and Llosa, M. (2011). Transfer of R388 derivatives by a pathogenesis-associated type IV secretion system into both bacteria and human cells. J. Bacteriol. *193*, 6257–6265.

Fernández-González, E., Bakioui, S., Gomes, M.C., O'Callaghan, D., Vergunst, A.C., Sangari, F.J., and Llosa, M. (2016). A Functional oriT in the Ptw Plasmid of Burkholderia cenocepacia Can Be Recognized by the R388 Relaxase TrwC. Front. Mol. Biosci. *3*, 16.

Fronzes, R., Schafer, E., Wang, L., Saibil, H.R., Orlova, E. V., and Waksman, G. (2009). Structure of a Type IV Secretion System Core Complex. Science (80-.). *323*, 266–268.

Frost, L.S., Leplae, R., Summers, A.O., and Toussaint, A. (2005). Mobile genetic elements: The agents of open source evolution. Nat. Rev. Microbiol. *3*, 722–732.

García-Cazorla, Y., Getino, M., Sanabria-Ríos, D.J., Carballeira, N.M., de la Cruz, F., Arechaga, I., and Cabezón, E. (2018). Conjugation inhibitors compete with palmitic acid for binding to the conjugative traffic ATPase TrwD, providing a mechanism to inhibit bacterial conjugation. J. Biol. Chem. *293*, 16923–16930.

García-Sáez, A.J., Carrer, D.C., and Schwille, P. (2010). Fluorescence Correlation Spectroscopy for the Study of Membrane Dynamics and Organization in Giant Unilamellar Vesicles. (Humana Press), pp. 493–508.

Garcillán-Barcia, M.P., Francia, M.V., and de La Cruz, F. (2009). The diversity of conjugative relaxases and its application in plasmid classification. FEMS Microbiol. Rev. *33*, 657–687.

Garten, M., Aimon, S., Bassereau, P., and Toombes, G.E.S. (2015). Reconstitution of a transmembrane protein, the voltage-gated ion channel, KvAP, into giant unilamellar vesicles for microscopy and patch clamp studies. J. Vis. Exp. 52281.

GE Healthcare (2007). Purifying Challenging Proteins Principles and Methods.

Geertsma, E.R., Nik Mahmood, N.A.B., Schuurman-Wolters, G.K., and Poolman, B. (2008). Membrane reconstitution of ABC transporters and assays of translocator function. Nat. Protoc. *3*, 256–266.

Gennis, R.B. (1989). Biomembranes (New York, NY: Springer New York).

Geourjon, C., Orelle, C., Steinfels, E., Blanchet, C., Deléage, G., Di Pietro, A., and Jault, J.M. (2001). A common mechanism for ATP hydrolysis in ABC transporter and helicase superfamilies. Trends Biochem. Sci. *26*, 539–544.

Ghisaidoobe, A., and Chung, S. (2014). Intrinsic Tryptophan Fluorescence in the Detection and Analysis of Proteins: A Focus on Förster Resonance Energy Transfer Techniques. Int. J. Mol. Sci. *15*, 22518–22538.

Giepmans, B.N.G., Adams, S.R., Ellisman, M.H., and Tsien, R.Y. (2006). The fluorescent toolbox for assessing protein location and function. Science *312*, 217–224.

Gillings, M., Boucher, Y., Labbate, M., Holmes, A., Krishnan, S., Holley, M., and Stokes, H.W. (2008). The evolution of class 1 integrons and the rise of antibiotic resistance. J. Bacteriol. *190*, 5095–5100.

Girard, P., Pécréaux, J., Lenoir, G., Falson, P., Rigaud, J.-L., and Bassereau, P. (2004). A new method for the reconstitution of membrane proteins into giant unilamellar vesicles. Biophys. J. *87*, 419–429.

Goessweiner-Mohr, N., Eder, M., Hofer, G., Fercher, C., Arends, K., Birner-Gruenberger, R., Grohmann, E., and Keller, W. (2014a). Structure of the double-stranded DNA-binding type IV secretion protein TraN from *Enterococcus*. Acta Crystallogr. Sect. D Biol. Crystallogr. *70*, 2376–2389.

Goessweiner-Mohr, N., Fercher, C., Arends, K., Birner-Gruenberger, R., Laverde-Gomez, D., Huebner, J., Grohmann, E., and Keller, W. (2014b). The type IV secretion protein TraK from the Enterococcus conjugative plasmid pIP501 exhibits a novel fold. Acta Crystallogr. D. Biol. Crystallogr. *70*, 1124–1135.

Goméz-Moreno Caleras, C., and Sanz, J.S. (2003). Estructura de proteínas. (Editorial Ariel).

Gomis-Ruth, F., Sola, M., Cruz, F., and Coll, M. (2005). Coupling Factors in Macromolecular Type-IV Secretion Machineries. Curr. Pharm. Des. *10*, 1551–1565.

Gomis-Rüth, F.X., and Coll, M. (2006). Cut and move: protein machinery for DNA processing in bacterial conjugation. Curr. Opin. Struct. Biol. *16*, 744–752.

Gomis-Rüth, F.X., Moncalián, G., Pérez-Luque, R., González, A., Cabezón, E., de la Cruz, F., and Coll, M. (2001). The bacterial conjugation protein TrwB resembles ring helicases and F1-ATPase. Nature *409*, 637–641.

Gomis-Rüth, F.X., Moncalián, G., de la Cruz, F., and Coll, M. (2002a). Conjugative Plasmid Protein TrwB, an Integral Membrane Type IV Secretion System Coupling Protein. J. Biol. Chem. *277*, 7556–7566.

Gomis-Rüth, F.X., de la Cruz, F., and Coll, M. (2002b). Structure and role of coupling proteins in conjugal DNA transfer. Res. Microbiol. *153*, 199–204.

Goñi, F.M., and Alonso, A. (2000). Spectroscopic techniques in the study of membrane solubilization, reconstitution and permeabilization by detergents. Biochim. Biophys. Acta *1508*, 51–68.

González-Prieto, C., Gabriel, R., Dehio, C., Schmidt, M., and Llosa, M. (2017). The Conjugative Relaxase TrwC Promotes Integration of Foreign DNA in the Human Genome. Appl. Environ. Microbiol. *83*.

González-Rivera, C., Khara, P., Awad, D., Patel, R., Li, Y.G., Bogisch, M., and Christie, P.J. (2019). Two pKM101-encoded proteins, the pilus-tip protein TraC and Pep, assemble on the *Escherichia coli* cell surface as adhesins required for efficient conjugative DNA transfer. Mol. Microbiol. *111*, 96–117.

González Flecha, F.L. (2017). Kinetic stability of membrane proteins. Biophys. Rev. *9*, 563–572.

Gordon, J.E., Costa, T.R.D., Patel, R.S., Gonzalez-Rivera, C., Sarkar, M.K., Orlova, E. V., Waksman, G., and Christie, P.J. (2017). Use of chimeric type IV secretion systems to define contributions of outer membrane subassemblies for contact-dependent translocation. Mol. Microbiol. *105*, 273–293.

Grant, S.G., Jessee, J., Bloom, F.R., and Hanahan, D. (1990). Differential plasmid rescue from transgenic mouse DNAs into Escherichia coli methylation-restriction mutants. Proc. Natl. Acad. Sci. U. S. A. *87*, 4645–4649.

Greene, R.F., and Pace, C.N. (1974). Urea and guanidine hydrochloride denaturation of ribonuclease, lysozyme, alpha-chymotrypsin, and beta-lactoglobulin. J. Biol. Chem. *249*, 5388–5393.

Grohmann, E., Goessweiner-Mohr, N., and Brantl, S. (2016). DNA-Binding Proteins Regulating pIP501 Transfer and Replication. Front. Mol. Biosci. *3*, 42.

Grohmann, E., Keller, W., and Muth, G. (2017). Mechanisms of Conjugative Transfer and Type IV Secretion-Mediated Effector Transport in Gram-Positive Bacteria. In Current Topics in Microbiology and Immunology, pp. 115–141.

Grohmann, E., Christie, P.J., Waksman, G., and Backert, S. (2018). Type IV secretion in Gram-negative

and Gram-positive bacteria. Mol. Microbiol. *107*, 455–471.

Guédon, G., Libante, V., Coluzzi, C., Payot, S., and Leblond-Bourget, N. (2017). The obscure world of integrative and mobilizable elements, highly widespread elements that pirate bacterial conjugative systems. Genes (Basel). *8*, 337.

Guglielmini, J., de la Cruz, F., and Rocha, E.P.C. (2013). Evolution of Conjugation and Type IV Secretion Systems. Mol. Biol. Evol. *30*, 315–331.

Gunton, J.E., Gilmour, M.W., Alonso, G., and Taylor, D.E. (2005). Subcellular localization and functional domains of the coupling protein, TraG, from IncHI1 plasmid R27. Microbiology *151*, 3549–3561.

Gunton, J.E., Gilmour, M.W., Baptista, K.P., Lawley, T.D., and Taylor, D.E. (2007). Interaction between the co-inherited TraG coupling protein and the TraJ membrane-associated protein of the H-plasmid conjugative DNA transfer system resembles chromosomal DNA translocases. Microbiology *153*, 428–441.

Guo, M., Gorman, P.M., Rico, M., Chakrabartty, A., and Laurents, D. V. (2005). Charge substitution shows that repulsive electrostatic interactions impede the oligomerization of Alzheimer amyloid peptides. FEBS Lett. *579*, 3574–3578.

Gupta, K., Donlan, J.A.C., Hopper, J.T.S., Uzdavinys, P., Landreh, M., Struwe, W.B., Drew, D., Baldwin, A.J., Stansfeld, P.J., and Robinson, C. V. (2017). The role of interfacial lipids in stabilizing membrane protein oligomers. Nature *541*, 421–424.

Guynet, C., Cuevas, A., Moncalián, G., and de la Cruz, F. (2011). The stb operon balances the requirements for vegetative stability and conjugative transfer of plasmid R388. PLoS Genet. *7*, e1002073.

Guzmán-Herrador, D.L., Steiner, S., Alperi, A., González-Prieto, C., Roy, C.R., and Llosa, M. (2017). DNA Delivery and Genomic Integration into Mammalian Target Cells through Type IV A and B Secretion Systems of Human Pathogens. Front. Microbiol. *8*, 1503.

Haft, R.J.F., Gachelet, E.G., Nguyen, T., Toussaint, L., Chivian, D., and Traxler, B. (2007). In vivo oligomerization of the F conjugative coupling protein TraD. J. Bacteriol. *189*, 6626–6634.

Hamilton, C.M., Lee, H., Li, P.-L., Cook, D.M., Piper, K.R., von Bodman, S.B., Lanka, E., Ream, W., and Farrand, S.K. (2000). TraG from RP4 and TraG and VirD4 from Ti Plasmids Confer Relaxosome Specificity to the Conjugal Transfer System of pTiC58. J. Bacteriol. *182*, 1541–1548.

Hanson, P.I., and Whiteheart, S.W. (2005). AAA+ proteins: have engine, will work. Nat. Rev. Mol. Cell Biol. *6*, 519–529.

Hardy, D., Desuzinges Mandon, E., Rothnie, A.J., and Jawhari, A. (2018). The yin and yang of solubilization and stabilization for wild-type and full-length membrane protein. Methods *147*, 118–125.

Harrison, M.L., Desaulniers, M.A., Noyce, R.S., and Evans, D.H. (2016). The acidic C-terminus of vaccinia virus I3 single-strand binding protein promotes proper assembly of DNA-protein complexes. Virology *489*, 212–222.

Heim, R., and Tsien, R.Y. (1996). Engineering green fluorescent protein for improved brightness, longer wavelengths and fluorescence resonance energy transfer. Curr. Biol. *6*, 178–182.

Helenius, A., and Simons, K. (1975). Solubilization of membranes by detergents. Biochim. Biophys. Acta - Rev. Biomembr. *415*, 29–79.

Hellman, L.M., and Fried, M.G. (2007). Electrophoretic mobility shift assay (EMSA) for detecting protein-nucleic acid interactions. Nat. Protoc. *2*, 1849–1861.

Hellmann, N., and Schneider, D. (2019). Hands On: Using Tryptophan Fluorescence Spectroscopy to

Study Protein Structure. (Humana Press, New York, NY), pp. 379–401.

Hill, J.L., Hammudi, M.B., and Tien, M. (2014). The Arabidopsis cellulose synthase complex: a proposed hexamer of CESA trimers in an equimolar stoichiometry. Plant Cell *26*, 4834–4842.

Högberg, L.D., Heddini, A., and Cars, O. (2010). The global need for effective antibiotics: challenges and recent advances. Trends Pharmacol. Sci. *31*, 509–515.

Holloway, P.W. (1973). A simple procedure for removal of Triton X-100 from protein samples. Anal. Biochem. *53*, 304–308.

Hopkins, A.L., Mason, J.S., and Overington, J.P. (2006). Can we rationally design promiscuous drugs? Curr. Opin. Struct. Biol. *16*, 127–136.

Horger, K.S., Estes, D.J., Capone, R., and Mayer, M. (2009). Films of Agarose Enable Rapid Formation of Giant Liposomes in Solutions of Physiologic Ionic Strength. J. Am. Chem. Soc. *131*, 1810–1819.

Hormaeche, I. (2003). Purificación de la proteína acopladora trwb. El papel del dominio transmembrana en el mecanismo de conjugación de r388. Universidad del País Vasco - Euskal Herriko Unibertsitatea.

Hormaeche, I., Alkorta, I., Moro, F., Valpuesta, J.M., Goni, F.M., and De La Cruz, F. (2002). Purification and properties of TrwB, a hexameric, ATP-binding integral membrane protein essential for R388 plasmid conjugation. J. Biol. Chem. *277*, 46456–46462.

Hormaeche, I., Iloro, I., Arrondo, J.L.R., Goñi, F.M., De La Cruz, F., and Alkorta, I. (2004). Role of the Transmembrane Domain in the Stability of TrwB, an Integral Protein Involved in Bacterial Conjugation. J. Biol. Chem. *279*, 10955–10961.

Hormaeche, I., Segura, R.L., Vecino, A.J., Goñi, F.M., de la Cruz, F., and Alkorta, I. (2006). The transmembrane domain provides nucleotide binding specificity to the bacterial conjugation protein TrwB. FEBS Lett. *580*, 3075–3082.

Horodniceanu, T., Bouanchaud, D.H., Bieth, G., and Chabbert, Y.A. (1976). R plasmids in Streptococcus agalactiae (group B). Antimicrob. Agents Chemother. *10*, 795–801.

Howard, M. (2004). A mechanism for polar protein localization in bacteria. J. Mol. Biol. *335*, 655–663.

Hu, B., Khara, P., Song, L., Lin, A.S., Frick-Cheng, A.E., Harvey, M.L., Cover, T.L., and Christie, P.J. (2019). In situ molecular architecture of the helicobacter pylori cag type IV secretion system. MBio *10*.

Itaya, M., Sakaya, N., Matsunaga, S., Fujita, K., and Kaneko, S. (2006). Conjugational transfer kinetics of pLS20 between Bacillus subtilis in liquid medium. Biosci. Biotechnol. Biochem. *70*, 740–742.

Jakubowski, S.J., Krishnamoorthy, V., Cascales, E., and Christie, P.J. (2004). Agrobacterium tumefaciens VirB6 domains direct the ordered export of a DNA substrate through a type IV secretion System. J. Mol. Biol. *341*, 961–977.

Jiménez, M., Martos, A., Vicente, M., and Rivas, G. (2011). Reconstitution and Organization of *Escherichia coli* Proto-ring Elements (FtsZ and FtsA) inside Giant Unilamellar Vesicles Obtained from Bacterial Inner Membranes. J. Biol. Chem. *286*, 11236–11241.

Johnsborg, O., Eldholm, V., and Håvarstein, L.S. (2007). Natural genetic transformation: prevalence, mechanisms and function. Res. Microbiol. *158*, 767–778.

Johnson, C.M., and Grossman, A.D. (2015). Integrative and Conjugative Elements (ICEs): What They Do and How They Work. Annu. Rev. Genet. *49*, 577–601.

Jørgensen, I.L., Kemmer, G.C., and Pomorski, T.G. (2017). Membrane protein reconstitution into giant unilamellar vesicles: a review on current techniques. Eur. Biophys. J. *46*, 103–119.

Kelly, S.M., and Price, N.C. (2000). The use of circular dichroism in the investigation of protein structure and function. Curr. Protein Pept. Sci. *1*, 349–384.

Kittell, B.L., and Helinski, D.R. (1993). Plasmid Incompatibility and Replication Control. In Bacterial Conjugation, (Boston, MA: Springer US), pp. 223–242.

Kohler, V., Goessweiner-Mohr, N., Aufschnaiter, A., Fercher, C., Probst, I., Pavkov-Keller, T., Hunger, K., Wolinski, H., Büttner, S., Grohmann, E., et al. (2018). TraN: A novel repressor of an Enterococcus conjugative type IV secretion system. Nucleic Acids Res. *46*, 9201–9219.

Kreuzer, K.N., and Jongeneel, C. V (1983). Escherichia coli phage T4 topoisomerase. Methods Enzymol. *100*, 144–160.

Kudalkar, E.M., Deng, Y., Davis, T.N., and Asbury, C.L. (2016). Coverslip Cleaning and Functionalization for Total Internal Reflection Fluorescence Microscopy. Cold Spring Harb. Protoc. *2016*, pdb.prot085548.

Kumar, R.B., and Das, A. (2002). Polar location and functional domains of the Agrobacterium tumefaciens DNA transfer protein VirD4. Mol. Microbiol. *43*, 1523–1532.

Kumar, R.B., Xie, Y.H., and Das, A. (2000). Subcellular localization of the Agrobacterium tumefaciens T-DNA transport pore proteins: VirB8 is essential for the assembly of the transport pore. Mol. Microbiol. *36*, 608–617.

Kurczy, M.E., Mellander, L.J., Najafinobar, N., and Cans, A.-S. (2014). Composition based strategies for controlling radii in lipid nanotubes. PLoS One *9*, e81293.

Kurenbach, B., Grothe, D., Farias, M.E., Szewzyk, U., and Grohmann, E. (2002). The tra Region of the Conjugative Plasmid pIP501 Is Organized in an Operon with the First Gene Encoding the Relaxase. J. Bacteriol. *184*, 1801–1805.

Kurenbach, B., Bohn, C., Prabhu, J., Abudukerim, M., Szewzyk, U., and Grohmann, E. (2003). Intergeneric transfer of the Enterococcus faecalis plasmid pIP501 to Escherichia coli and Streptomyces lividans and sequence analysis of its tra region. Plasmid *50*, 86–93.

Kurenbach, B., Kopeć, J., Mägdefrau, M., Andreas, K., Keller, W., Bohn, C., Abajy, M.Y., and Grohmann, E. (2006). The TraA relaxase autoregulates the putative type IV secretion-like system encoded by the broad-host-range Streptococcus agalactiae plasmid pIP501. Microbiology *152*, 637–645.

Kwak, M.-J., Kim, J.D., Kim, H., Kim, C., Bowman, J.W., Kim, S., Joo, K., Lee, J., Jin, K.S., Kim, Y.-G., et al. (2017). Architecture of the type IV coupling protein complex of Legionella pneumophila. Nat. Microbiol. *2*, 17114.

Kwon, C.W., Park, K.-M., Kang, B.-C., Kweon, D.-H., Kim, M.-D., Shin, S.W., Je, Y.H., and Chang, P.-S. (2015). Cysteine Protease Profiles of the Medicinal Plant Calotropis procera R. Br. revealed by de novo transcriptome analysis. PLoS One *10*, e0119328.

Kyne, C., Jordon, K., Filoti, D.I., Laue, T.M., and Crowley, P.B. (2017). Protein charge determination and implications for interactions in cell extracts. Protein Sci. *26*, 258–267.

de la Cruz, F., and Grinsted, J. (1982). Genetic and molecular characterization of Tn21, a multiple resistance transposon from R100.1. J. Bacteriol. *151*, 222–228.

Laemmli, U.K. (1970). Cleavage of Structural Proteins during the Assembly of the Head of Bacteriophage T4. Nature *227*, 680–685.

Lakowicz, J.R. (2006). Principles of fluorescence spectroscopy (Springer).

Lamichhane, N., Udayakumar, T., D'Souza, W., Simone II, C., Raghavan, S., Polf, J., and Mahmood, J. (2018). Liposomes: Clinical Applications and Potential for Image-Guided Drug Delivery. Molecules *23*, 288.

Lang, S., and Zechner, E.L. (2012). General requirements for protein secretion by the F-like conjugation system R1. Plasmid *67*, 128–138.

Lang, S., Gruber, C.J., Raffl, S., Reisner, A., and Zechner, E.L. (2014). Common requirement for the relaxosome of plasmid R1 in multiple activities of the conjugative type IV secretion system. J. Bacteriol. *196*, 2108–2121.

Langer, P.J., and Walker, G.C. (1981). Restriction endonuclease cleavage map of pKM101: relationship to parental plasmid R46. Mol. Gen. Genet. *182*, 268–272.

Langer, P.J., Shanabruch, W.G., and Walker, G.C. (1981). Functional organization of plasmid pKM101. J. Bacteriol. *145*, 1310–1316.

Larrea, D., de Paz, H.D., Arechaga, I., de la Cruz, F., and Llosa, M. (2013). Structural independence of conjugative coupling protein TrwB from its Type IV secretion machinery. Plasmid *70*, 146–153.

Larrea, D., de Paz, H.D., Matilla, I., Guzmán-Herrador, D.L., Lasso, G., de la Cruz, F., Cabezón, E., and Llosa, M. (2017). Substrate translocation involves specific lysine residues of the central channel of the conjugative coupling protein TrwB. Mol. Genet. Genomics *292*, 1037–1049.

Lawley, T.., Klimke, W.., Gubbins, M.., and Frost, L.. (2003). F factor conjugation is a true type IV secretion system. FEMS Microbiol. Lett. *224*, 1–15.

Leake, M.C., Chandler, J.H., Wadhams, G.H., Bai, F., Berry, R.M., and Armitage, J.P. (2006). Stoichiometry and turnover in single, functioning membrane protein complexes. Nature *443*, 355–358.

Lebowitz, J., Lewis, M.S., and Schuck, P. (2002). Modern analytical ultracentrifugation in protein science: a tutorial review. Protein Sci. *11*, 2067–2079.

Lederberg, J., and Tatum, E.L. (1946). Gene recombination in Escherichia coli. Nature *158*, 558.

Lee, K.B., and Thomas, J.O. (2000). The effect of the acidic tail on the DNA-binding properties of the HMG1,2 class of proteins: Insights from tail switching and tail removal. J. Mol. Biol. *304*, 135–149.

Lee, C.A., Thomas, J., and Grossman, A.D. (2012). The Bacillus subtilis Conjugative Transposon ICEBs1 Mobilizes Plasmids Lacking Dedicated Mobilization Functions. J. Bacteriol. *194*, 3165–3172.

Leonetti, C.T., Hamada, M.A., Laurer, S.J., Broulidakis, M.P., Swerdlow, K.J., Lee, C.A., Grossman, A.D., and Berkmen, M.B. (2015). Critical Components of the Conjugation Machinery of the Integrative and Conjugative Element ICEBs1 of Bacillus subtilis. J. Bacteriol. *197*, 2558–2567.

Li, Y.G., and Christie, P.J. (2018). The Agrobacterium VirB/VirD4 T4SS: Mechanism and Architecture Defined Through In Vivo Mutagenesis and Chimeric Systems. In Current Topics in Microbiology and Immunology, pp. 233–260.

Li, Y.G., Hu, B., and Christie, P.J. (2019). Biological and Structural Diversity of Type IV Secretion Systems. Microbiol. Spectr. *7*.

Lira, R.B., Dimova, R., and Riske, K.A. (2014). Giant unilamellar vesicles formed by hybrid films of agarose and lipids display altered mechanical properties. Biophys. J. *107*, 1609–1619.

Llosa, M., and Alkorta, I. (2017). Coupling Proteins in Type IV Secretion. In Current Topics in Microbiology and Immunology, pp. 143–168.

Llosa, M., Bolland, S., and de la Cruz, F. (1994). Genetic organization of the conjugal DNA processing region of the IncW plasmid R388. J. Mol. Biol. *235*, 448–464.

Llosa, M., Gomis-Rüth, F.X., Coll, M., and de la Cruz Fd, F. (2002). Bacterial conjugation: a two-step mechanism for DNA transport. Mol. Microbiol. *45*, 1–8.

Llosa, M., Zunzunegui, S., and de la Cruz, F. (2003). Conjugative coupling proteins interact with cognate and heterologous VirB10-like proteins while exhibiting specificity for cognate relaxosomes. Proc. Natl. Acad. Sci. *100*, 10465–10470.

López-Lorente, Á.I., and Mizaikoff, B. (2016). Mid-infrared spectroscopy for protein analysis: Potential and challenges. Anal. Bioanal. Chem. *408*, 2875–2889.

López-Montero, I., López-Navajas, P., Mingorance, J., Vélez, M., Vicente, M., and Monroy, F. (2013). Membrane reconstitution of FtsZ-ZipA complex inside giant spherical vesicles made of E. coli lipids: large membrane dilation and analysis of membrane plasticity. Biochim. Biophys. Acta *1828*, 687–698.

Low, H.H., Gubellini, F., Rivera-Calzada, A., Braun, N., Connery, S., Dujeancourt, A., Lu, F., Redzej, A., Fronzes, R., Orlova, E. V, et al. (2014). Structure of a type IV secretion system. Nature *508*, 550–553.

Lu, J., and Frost, L.S. (2005). Mutations in the C-terminal region of TraM provide evidence for in vivo TraM-TraD interactions during F-plasmid conjugation. J. Bacteriol. *187*, 4767–4773.

Lu, J., Wong, J.J.W., Edwards, R.A., Manchak, J., Frost, L.S., and Glover, J.N.M. (2008). Structural basis of specific TraD-TraM recognition during F plasmid-mediated bacterial conjugation. Mol. Microbiol. *70*, 89–99.

Luirink, J., van der Sande, C., Tommassen, J., Veltkamp, E., De Graaf, F.K., and Oudega, B. (1986). Effects of divalent cations and of phospholipase A activity on excretion of cloacin DF13 and lysis of host cells. J. Gen. Microbiol. *132*, 825–834.

Lukaszczyk, M., Pradhan, B., and Remaut, H. (2019). The Biosynthesis and Structures of Bacterial Pili. In Subcellular Biochemistry, (Springer New York), pp. 369–413.

Machon, C., Rivas, S., Albert, A., Goni, F.M., and de la Cruz, F. (2002). TrwD, the Hexameric Traffic ATPase Encoded by Plasmid R388, Induces Membrane Destabilization and Hemifusion of Lipid Vesicles. J. Bacteriol. *184*, 1661–1668.

Marsh, D. (1996). Components of the lateral pressure in lipid bilayers deduced from HII phase dimensions. Biochim. Biophys. Acta *1279*, 119–123.

Matilla, I., Alfonso, C., Rivas, G., Bolt, E.L., de la Cruz, F., and Cabezon, E. (2010). The Conjugative DNA Translocase TrwB Is a Structure-specific DNA-binding Protein. J. Biol. Chem. *285*, 17537–17544.

Mazur, J., Roy, K., and Kanwar, J.R. (2018). Recent advances in nanomedicine and survivin targeting in brain cancers. Nanomedicine (Lond). *13*, 105–137.

Meir, A., Chetrit, D., Liu, L., Roy, C.R., and Waksman, G. (2018). Legionella DotM structure reveals a role in effector recruiting to the Type 4B secretion system. Nat. Commun. *9*, 507.

Méléard, P., Bagatolli, L.A., and Pott, T. (2009). Giant unilamellar vesicle electroformation from lipid mixtures to native membranes under physiological conditions. Methods Enzymol. *465*, 161–176.

Metola, A. (2017). Interaction between colicin A pore-forming domain and its cognate immunity protein. Universidad del País Vasco UPV/EHU.

Mihajlovic, S., Lang, S., Sut, M. V., Strohmaier, H., Gruber, C.J., Koraimann, G., Cabezon, E., Moncalian, G., de la Cruz, F., and Zechner, E.L. (2009). Plasmid R1 Conjugative DNA Processing Is Regulated at the Coupling Protein Interface. J. Bacteriol. *191*, 6877–6887.

Milcovich, G., Lettieri, S., Antunes, F.E., Medronho, B., Fonseca, A.C., Coelho, J.F.J., Marizza, P., Perrone, F., Farra, R., Dapas, B., et al. (2017). Recent advances in smart biotechnology: Hydrogels and nanocarriers for tailored bioactive molecules depot. Adv. Colloid Interface Sci. *249*, 163–180.

Miles, A.J., and Wallace, B.A. (2016). Circular dichroism spectroscopy of membrane proteins. Chem. Soc. Rev. *45*, 4859–4872.

Mileykovskaya, E., and Dowhan, W. (2009). Cardiolipin membrane domains in prokaryotes and eukaryotes. Biochim. Biophys. Acta - Biomembr. *1788*, 2084–2091.

Miroux, B., and Walker, J.E. (1996). Over-production of Proteins inEscherichia coli: Mutant Hosts that Allow Synthesis of some Membrane Proteins and Globular Proteins at High Levels. J. Mol. Biol. *260*, 289–298.

Mizuguchi, K., and Ahmad, S. (2014). Conformational changes in DNA-binding proteins: Relationships with precomplex features and contributions to specificity and stability. Proteins Struct. Funct. Bioinforma. *82*, 841–857.

Moffatt, B.A., and Studier, F.W. (1987). T7 lysozyme inhibits transcription by T7 RNA polymerase. Cell *49*, 221–227.

Moncalián, G., and de la Cruz, F. (2004). DNA binding properties of protein TrwA, a possible structural variant of the Arc repressor superfamily. Biochim. Biophys. Acta - Proteins Proteomics *1701*, 15–23.

Moncalián, G., Grandoso, G., Llosa, M., and de la Cruz, F. (1997). oriT-processing and regulatory roles of TrwA protein in plasmid R388 conjugation. J. Mol. Biol. *270*, 188–200.

Moncalián, G., Cabezón, E., Alkorta, I., Valle, M., Moro, F., Valpuesta, J.M., Goñi, F.M., and de la Cruz, F. (1999). Characterization of ATP and DNA Binding Activities of TrwB, the Coupling Protein Essential in Plasmid R388 Conjugation. J. Biol. Chem. *274*, 36117–36124.

Moon, C.P., and Fleming, K.G. (2011). Using Tryptophan Fluorescence to Measure the Stability of Membrane Proteins Folded in Liposomes. In Methods in Enzymology, pp. 189–211.

Mortelmans, K.E., and Stocker, B.A. (1979). Segregation of the mutator property of plasmid R46 from its ultraviolet-protecting property. Mol. Gen. Genet. *167*, 317–327.

Mossey, P., Hudacek, A., and Das, A. (2010). Agrobacterium tumefaciens type IV secretion protein VirB3 is an inner membrane protein and requires VirB4, VirB7, and VirB8 for stabilization. J. Bacteriol. *192*, 2830–2838.

Nijkamp, H.J., de Lang, R., Stuitje, A.R., van den Elzen, P.J., Veltkamp, E., and van Putten, A.J. (1986). The complete nucleotide sequence of the bacteriocinogenic plasmid CloDF13. Plasmid *16*, 135–160.

Núñez, B., and De La Cruz, F. (2001). Two atypical mobilization proteins are involved in plasmid CloDF13 relaxation. Mol. Microbiol. *39*, 1088–1099.

Ó'Fágáin, C. (2017). Protein stability: Enhancement and measurement. In Methods in Molecular Biology, p.

Oikonomou, C.M., and Jensen, G.J. (2019). Electron Cryotomography of Bacterial Secretion Systems. In Protein Secretion in Bacteria, (American Society of Microbiology), pp. 1–12.

Opekarová, M., and Tanner, W. (2003). Specific lipid requirements of membrane proteins--a putative bottleneck in heterologous expression. Biochim. Biophys. Acta *1610*, 11–22.

Oudega, B., Stegehuis, F., van Tiel-Menkveld, G.J., and de Graaf, F.K. (1982). Protein H encoded by plasmid CloDF13 is involved in excretion of cloacin DF13. J. Bacteriol. *150*, 1115–1121.

Pace, H., Simonsson Nyström, L., Gunnarsson, A., Eck, E., Monson, C., Geschwindner, S., Snijder, A., and Höök, F. (2015). Preserved transmembrane protein mobility in polymer-supported lipid bilayers derived from cell membranes. Anal. Chem. *87*, 9194–9203.

Pace, H.P., Hannestad, J.K., Armonious, A., Adamo, M., Agnarsson, B., Gunnarsson, A., Micciulla, S., Sjövall, P., Gerelli, Y., and Höök, F. (2018). Structure and Composition of Native Membrane Derived Polymer-Supported Lipid Bilayers. Anal. Chem. *90*, 13065–13072.

Parsons, J.A., Bannam, T.L., Devenish, R.J., and Rood, J.I. (2007). TcpA, an FtsK/SpoIIIE homolog, is essential for transfer of the conjugative plasmid pCW3 in Clostridium perfringens. J. Bacteriol. *189*, 7782–7790.

Paterson, E.S., Moré, M.I., Pillay, G., Cellini, C., Woodgate, R., Walker, G.C., Iyer, V.N., and Winans, S.C. (1999). Genetic analysis of the mobilization and leading regions of the IncN plasmids pKM101 and pCU1. J. Bacteriol. *181*, 2572–2583.

de Paz, H.D., Sangari, F.J., Bolland, S., García-Lobo, J.M., Dehio, C., de la Cruz, F., and Llosa, M. (2005). Functional interactions between type IV secretion systems involved in DNA transfer and virulence. Microbiology *151*, 3505–3516.

De Paz, H.D., Larrea, D., Zunzunegui, S., Dehio, C., De La Cruz, F., and Llosa, M. (2010). Functional dissection of the conjugative coupling protein TrwB. J. Bacteriol. *192*, 2655–2669.

Pedro, A.Q., Queiroz, J.A., and Passarinha, L.A. (2019). Smoothing membrane protein structure determination by initial upstream stage improvements. Appl. Microbiol. Biotechnol. *103*, 5483–5500.

Phillips, R., Ursell, T., Wiggins, P., and Sens, P. (2009). Emerging roles for lipids in shaping membrane-protein function. Nature *459*, 379–385.

Pohlman, R.F., Genetti, H.D., and Winans, S.C. (1994). Entry exclusion of the IncN plasmid pKM101 is mediated by a single hydrophilic protein containing a lipid attachment motif. Plasmid *31*, 158–165.

Poolman, B., Doeven, M.K., Geertsma, E.R., Biemans-Oldehinkel, E., Konings, W.N., and Rees, D.C. (2005). Functional Analysis of Detergent-Solubilized and Membrane-Reconstituted ATP-Binding Cassette Transporters. In Methods in Enzymology, pp. 429–459.

Pott, T., Bouvrais, H., and Méléard, P. (2008). Giant unilamellar vesicle formation under physiologically relevant conditions. Chem. Phys. Lipids *154*, 115–119.

van Putten, A.J., Jochems, G.J., de Lang, R., and Nijkamp, H.J. (1987). Structure and nucleotide sequence of the region encoding the mobilization proteins of plasmid CloDF13. Gene *51*, 171–178.

Racker, E. (1979). Reconstitution of membrane processes. Methods Enzymol. *55*, 699–711.

Rath, A., Glibowicka, M., Nadeau, V.G., Chen, G., and Deber, C.M. (2009). Detergent binding explains anomalous SDS-PAGE migration of membrane proteins. Proc. Natl. Acad. Sci. *106*, 1760–1765.

Redzej, A., Ukleja, M., Connery, S., Trokter, M., Felisberto-Rodrigues, C., Cryar, A., Thalassinos, K., Hayward, R.D., Orlova, E. V, and Waksman, G. (2017). Structure of a VirD4 coupling protein bound to a VirB type IV secretion machinery. EMBO J. *36*, 3080–3095.

Reeves, J.P., and Dowben, R.M. (1969). Formation and properties of thin-walled phospholipid vesicles. J. Cell. Physiol. *73*, 49–60.

Richmond, D.L., Schmid, E.M., Martens, S., Stachowiak, J.C., Liska, N., and Fletcher, D.A. (2011). Forming giant vesicles with controlled membrane composition, asymmetry, and contents. Proc. Natl. Acad. Sci. U. S. A. *108*, 9431–9436.

Rigaud, J.-L., and Lévy, D. (2003). Reconstitution of membrane proteins into liposomes. Methods Enzymol. *372*, 65–86.

Rigaud, J.L., Pitard, B., and Levy, D. (1995). Reconstitution of membrane proteins into liposomes: application to energy-transducing membrane proteins. Biochim. Biophys. Acta *1231*, 223–246.

Ripoll-Rozada, J., Zunzunegui, S., de la Cruz, F., Arechaga, I., and Cabezón, E. (2013). Functional interactions of VirB11 traffic ATPases with VirB4 and VirD4 molecular motors in type IV secretion systems. J. Bacteriol. *195*, 4195–4201.

Saliba, A.-E., Vonkova, I., Ceschia, S., Findlay, G.M., Maeda, K., Tischer, C., Deghou, S., van Noort, V., Bork, P., Pawson, T., et al. (2014). A quantitative liposome microarray to systematically characterize protein-lipid interactions. Nat. Methods *11*, 47–50.

Sambrook, J., and Russell, D.W. (David W. (2001). Molecular cloning : a laboratory manual (Cold Spring Harbor Laboratory Press).

Sanowar, S., and Le Moual, H. (2005). Functional reconstitution of the Salmonella typhimurium PhoQ histidine kinase sensor in proteoliposomes. Biochem. J. *390*, 769–776.

Sastre, J.I., Cabezón, E., and de la Cruz, F. (1998). The carboxyl terminus of protein TraD adds specificity and efficiency to F-plasmid conjugative transfer. J. Bacteriol. *180*, 6039–6042.

Schagger, H., Cramer, W.A., and Vonjagow, G. (1994). Analysis of Molecular Masses and Oligomeric States of Protein Complexes by Blue Native Electrophoresis and Isolation of Membrane Protein Complexes by Two-Dimensional Native Electrophoresis. Anal. Biochem. *217*, 220–230.

Schellman, J.A. (2002). Fifty years of solvent denaturation. Biophys. Chem. *96*, 91–101.

Schlegel, S., Löfblom, J., Lee, C., Hjelm, A., Klepsch, M., Strous, M., Drew, D., Slotboom, D.J., and de Gier, J.-W. (2012). Optimizing membrane protein overexpression in the Escherichia coli strain Lemo21(DE3). J. Mol. Biol. *423*, 648–659.

Schroder, G., and Lanka, E. (2003). TraG-Like Proteins of Type IV Secretion Systems: Functional Dissection of the Multiple Activities of TraG (RP4) and TrwB (R388). J. Bacteriol. *185*, 4371–4381.

Schroder, G., Krause, S., Zechner, E.L., Traxler, B., Yeo, H.-J., Lurz, R., Waksman, G., and Lanka, E. (2002). TraG-Like Proteins of DNA Transfer Systems and of the Helicobacter pylori Type IV Secretion System: Inner Membrane Gate for Exported Substrates? J. Bacteriol. *184*, 2767–2779.

Schröder, G., and Lanka, E. (2005). The mating pair formation system of conjugative plasmids-A versatile secretion machinery for transfer of proteins and DNA. Plasmid *54*, 1–25.

Schuck, P., Perugini, M.A., Gonzales, N.R., Howlett, G.J., and Schubert, D. (2002). Size-Distribution Analysis of Proteins by Analytical Ultracentrifugation: Strategies and Application to Model Systems. Biophys. J. *82*, 1096–1111.

Scotto, A.W., and Zakim, D. (1986). Reconstitution of membrane proteins: catalysis by cholesterol of insertion of integral membrane proteins into preformed lipid bilayers. Biochemistry *25*, 1555–1561.

Seddon, A.M., Curnow, P., and Booth, P.J. (2004). Membrane proteins, lipids and detergents: not just a soap opera. Biochim. Biophys. Acta *1666*, 105–117.

Segura, R.L., Águila-Arcos, S., Ugarte-Uribe, B., Vecino, A.J., De La Cruz, F., Goñi, F.M., and Alkorta, I. (2013). The transmembrane domain of the T4SS coupling protein TrwB and its role in protein-protein interactions. Biochim. Biophys. Acta - Biomembr. *1828*, 2015–2025.

Segura, R.L., Águila-Arcos, S., Ugarte-Uribe, B., Vecino, A.J., de la Cruz, F., Goñi, F.M., and Alkorta, I. (2014). Subcellular location of the coupling protein TrwB and the role of its transmembrane domain. Biochim. Biophys. Acta - Biomembr. *1838*, 223–230.

Seo, M., Lei, L., and Egli, M. (2019). Label-Free Electrophoretic Mobility Shift Assay (EMSA) for Measuring Dissociation Constants of Protein-RNA Complexes. Curr. Protoc. Nucleic Acid Chem.

Shaffer, C.L., Good, J.A.D., Kumar, S., Krishnan, K.S., Gaddy, J.A., Loh, J.T., Chappell, J., Almqvist, F., Cover, T.L., and Hadjifrangiskou, M. (2016). Peptidomimetic Small Molecules Disrupt Type IV Secretion System Activity in Diverse Bacterial Pathogens. MBio *7*, e00221-16.

Shaklee, P.M., Semrau, S., Malkus, M., Kubick, S., Dogterom, M., and Schmidt, T. (2010). Protein Incorporation in Giant Lipid Vesicles under Physiological Conditions. ChemBioChem *11*, 175–179.

Shapiro, L., McAdams, H.H., and Losick, R. (2002). Generating and Exploiting Polarity in Bacteria. Science (80-.). *298*, 1942–1946.

Shevchenko, A., Wilm, M., Vorm, O., and Mann, M. (1996). Mass spectrometric sequencing of proteins silver-stained polyacrylamide gels. Anal. Chem. *68*, 850–858.

Sidorova, N.Y., Hung, S., and Rau, D.C. (2010). Stabilizing labile DNA-protein complexes in polyacrylamide gels. Electrophoresis *31*, 648–653.

Siguier, P., Gourbeyre, E., and Chandler, M. (2014). Bacterial insertion sequences: Their genomic impact and diversity. FEMS Microbiol. Rev. *38*, 865–891.

Simeonov, P., Werner, S., Haupt, C., Tanabe, M., and Bacia, K. (2013). Membrane protein reconstitution into liposomes guided by dual-color fluorescence cross-correlation spectroscopy. Biophys. Chem. *184*, 37–43.

Sjöstrand, D., Diamanti, R., Lundgren, C.A.K., Wiseman, B., and Högbom, M. (2017). A rapid expression and purification condition screening protocol for membrane protein structural biology. Protein Sci. *26*, 1653–1666.

Skrzypek, R., Iqbal, S., and Callaghan, R. (2018). Methods of reconstitution to investigate membrane protein function. Methods *147*, 126–141.

Slotboom, D.J., Duurkens, R.H., Olieman, K., and Erkens, G.B. (2008). Static light scattering to characterize membrane proteins in detergent solution. Methods *46*, 73–82.

Smeekens, S.P., and Romano, L.J. (1986). Promoter and nonspecific DNA binding by the T7 RNA polymerase. Nucleic Acids Res. *14*, 2811–2827.

Smillie, C., Garcillán-Barcia, M.P., Francia, M.V., Rocha, E.P.C., and de la Cruz, F. (2010). Mobility of plasmids. Microbiol. Mol. Biol. Rev. *74*, 434–452.

Smith, P.K., Krohn, R.I., Hermanson, G.T., Mallia, A.K., Gartner, F.H., Provenzano, M.D., Fujimoto, E.K., Goeke, N.M., Olson, B.J., and Klenk, D.C. (1985). Measurement of protein using bicinchoninic acid. Anal. Biochem. *150*, 76–85.

Steen, J.A., Bannam, T.L., Teng, W.L., Devenish, R.J., and Rood, J.I. (2009). The putative coupling protein TcpA interacts with other pCW3-encoded proteins to form an essential part of the conjugation complex. J. Bacteriol. *191*, 2926–2933.

Strop, P., and Brunger, A.T. (2005). Refractive index-based determination of detergent concentration and its application to the study of membrane proteins. Protein Sci. *14*, 2207–2211.

Stroud, Z., Hall, S.C.L., and Dafforn, T.R. (2018). Purification of membrane proteins free from conventional detergents: SMA, new polymers, new opportunities and new insights. Methods *147*, 106–117.

Studier, F.W., and Moffatt, B.A. (1986). Use of bacteriophage T7 RNA polymerase to direct selective high-level expression of cloned genes. J. Mol. Biol. *189*, 113–130.

Subburaj, S., Luo, N., Lu, X., Li, X., Cao, H., Hu, Y., Li, J., and Yan, Y. (2016). Molecular characterization and evolutionary origins of farinin genes in Brachypodium distachyon L. J. Appl. Genet. *57*, 287–303.

Subburaj, Y., Cosentino, K., Axmann, M., Pedrueza-Villalmanzo, E., Hermann, E., Bleicken, S., Spatz, J., and García-Sáez, A.J. (2015). Bax monomers form dimer units in the membrane that further self-assemble into multiple oligomeric species. Nat. Commun. *6*, 8042.

Sutherland, M.C., Nguyen, T.L., Tseng, V., and Vogel, J.P. (2012). The Legionella IcmSW complex directly interacts with DotL to mediate translocation of adaptor-dependent substrates. PLoS Pathog. *8*, e1002910.

Szoka, F., and Papahadjopoulos, D. (1980). Comparative properties and methods of preparation of lipid vesicles (liposomes). Annu. Rev. Biophys. Bioeng. *9*, 467–508.

Tacconelli, E., Carrara, E., Savoldi, A., Kattula, D., and Burkert, F. GLOBAL PRIORITY LIST OF ANTIBIOTIC-RESISTANT BACTERIA TO GUIDE RESEARCH, DISCOVERY, AND DEVELOPMENT OF NEW ANTIBIOTICS.

Tato, I., Zunzunegui, S., de la Cruz, F., and Cabezon, E. (2005). TrwB, the coupling protein involved in DNA transport during bacterial conjugation, is a DNA-dependent ATPase. Proc. Natl. Acad. Sci. U. S. A. *102*, 8156–8161.

Tato, I., Matilla, I., Arechaga, I., Zunzunegui, S., de la Cruz, F., and Cabezon, E. (2007). The ATPase activity of the DNA transporter TrwB is modulated by protein TrwA: implications for a common assembly mechanism of DNA translocating motors. J. Biol. Chem. *282*, 25569–25576.

Teese, M.G., and Langosch, D. (2015). Role of GxxxG Motifs in Transmembrane Domain Interactions. Biochemistry *54*, 5125–5135.

Thermo Scientific Pierce (2010). Protein : Nucleic Acid Interaction Technical Handbook.

Thoma, J., Manioglu, S., Kalbermatter, D., Bosshart, P.D., Fotiadis, D., and Müller, D.J. (2018). Protein-enriched outer membrane vesicles as a native platform for outer membrane protein studies. Commun. Biol. *1*, 23.

Thomas, C.M., and Nielsen, K.M. (2005). Mechanisms of, and Barriers to, Horizontal Gene Transfer between Bacteria. Nat. Rev. Microbiol. *3*, 711–721.

Thomas, C.M., Thomson, N.R., Cerdeño-Tárraga, A.M., Brown, C.J., Top, E.M., and Frost, L.S. (2017). Annotation of plasmid genes. Plasmid *91*, 61–67.

Van Tiel-Menkvled, G.J., Rezee, A., and De Graaf, F.K. (1979). Production and excretion of cloacin DF13 by Escherichia coli harboring plasmid CloDF13. J. Bacteriol. *140*, 415–423.

Tong, J., and McIntosh, T.J. (2004). Structure of supported bilayers composed of lipopolysaccharides and bacterial phospholipids: raft formation and implications for bacterial resistance. Biophys. J. *86*, 3759–3771.

Toseland, C.P. (2013). Fluorescent labeling and modification of proteins. J. Chem. Biol. *6*, 85–95.

Tsirigos, K.D., Peters, C., Shu, N., Käll, L., and Elofsson, A. (2015). The TOPCONS web server for consensus prediction of membrane protein topology and signal peptides. Nucleic Acids Res. *43*, W401-7.

Tsumoto, K., Matsuo, H., Tomita, M., and Yoshimura, T. (2009). Efficient formation of giant liposomes through the gentle hydration of phosphatidylcholine films doped with sugar. Colloids Surfaces B Biointerfaces *68*, 98–105.

Varnier, A., Kermarrec, F., Blesneac, I., Moreau, C., Liguori, L., Lenormand, J.L., and Picollet-D'hahan, N. (2010). A Simple Method for the Reconstitution of Membrane Proteins into Giant Unilamellar Vesicles. J. Membr. Biol. *233*, 85–92.

Vecino, A.J. (2009). La reconstitución en liposomas de TrwB, un nanomotor que transporta DNA, revela la importancia del dominio transmembrana de la proteína.

Vecino, A.J., Segura, R.L., Ugarte-Uribe, B., Aguila, S., Hormaeche, I., de la Cruz, F., Goñi, F.M., and Alkorta, I. (2010). Reconstitution in liposome bilayers enhances nucleotide binding affinity and ATP-specificity of TrwB conjugative coupling protein. Biochim. Biophys. Acta *1798*, 2160–2169.

Vecino, A.J., de la Arada, I., Segura, R.L., Goñi, F.M., de la Cruz, F., Arrondo, J.L.R., and Alkorta, I. (2011). Membrane insertion stabilizes the structure of TrwB, the R388 conjugative plasmid coupling protein. Biochim. Biophys. Acta *1808*, 1032–1039.

Vecino, A.J., Segura, R. de L., de la Arada, I., de la Cruz, F., Goñi, F.M., Arrondo, J.L., and Alkorta, I. (2012). Deletion of a single helix from the transmembrane domain causes large changes in membrane insertion properties and secondary structure of the bacterial conjugation protein TrwB. Biochim. Biophys. Acta - Biomembr. *1818*, 3158–3166.

Veltkamp, E., and Nijkamp, H.J.J. (1973). The role of DNA polymerase I, II and III in the replication of the bacteriocinogenic factor Clo DF13. MGG Mol. Gen. Genet. *125*, 329–340.

Vogel, R., Fan, G.B., Sheves, M., and Siebert, F. (2001). Salt dependence of the formation and stability of the signaling state in G protein-coupled receptors: Evidence for the involvement of the Hofmeister effect. Biochemistry.

Voth, D.E., Broederdorf, L.J., and Graham, J.G. (2012). Bacterial Type IV secretion systems: versatile virulence machines. Future Microbiol. *7*, 241–257.

De Vrije, T., Tommassen, J., and De Kruijff, B. (1987). Optimal posttranslational translocation of the precursor of PhoE protein across Escherichia coli membrane vesicles requires both ATP and the protonmotive force. Biochim. Biophys. Acta *900*, 63–72.

Wagner, S., Bader, M.L., Drew, D., and de Gier, J.-W. (2006). Rationalizing membrane protein overexpression. Trends Biotechnol. *24*, 364–371.

Wagner, S., Klepsch, M.M., Schlegel, S., Appel, A., Draheim, R., Tarry, M., Högbom, M., van Wijk, K.J., Slotboom, D.J., Persson, J.O., et al. (2008). Tuning Escherichia coli for membrane protein overexpression. Proc. Natl. Acad. Sci. U. S. A. *105*, 14371–14376.

Waksman, G. (2019). From conjugation to T4S systems in Gram-negative bacteria: a mechanistic biology perspective. EMBO Rep. *20*, e47012.

Walde, P., Cosentino, K., Engel, H., and Stano, P. (2010). Giant Vesicles: Preparations and Applications. ChemBioChem *11*, 848–865.

Walker, J.E., Saraste, M., Runswick, M.J., and Gay, N.J. (1982). Distantly related sequences in the alpha- and beta-subunits of ATP synthase, myosin, kinases and other ATP-requiring enzymes and a common nucleotide binding fold. EMBO J. *1*, 945–951.

Walldén, K., Williams, R., Yan, J., Lian, P.W., Wang, L., Thalassinos, K., Orlova, E. V, and Waksman, G. (2012). Structure of the VirB4 ATPase, alone and bound to the core complex of a type IV secretion system. Proc. Natl. Acad. Sci. U. S. A. *109*, 11348–11353.

Wallin, E., and von Heijne, G. (1998). Genome-wide analysis of integral membrane proteins from eubacterial, archaean, and eukaryotic organisms. Protein Sci. *7*, 1029–1038.

Wang, A., and Macrina, F.L. (1995). Streptococcal plasmid pIP501 has a functional oriT site. J. Bacteriol. *177*, 4199–4206.

Wang, Q., Zeng, M., Wang, W., and Tang, J. (2007). The HMGB1 acidic tail regulates HMGB1 DNA binding specificity by a unique mechanism. Biochem. Biophys. Res. Commun. *360*, 14–19.

Weinberger, A., Tsai, F.-C., Koenderink, G.H., Schmidt, T.F., Itri, R., Meier, W., Schmatko, T., Schröder, A., and Marques, C. (2013). Gel-assisted formation of giant unilamellar vesicles. Biophys. J. 105, 154–164.Weinberger, A., Tsai, F.-C., Koenderink, G.H., Schmidt, T.F., Itri, R., Meier, W., Schmatko, T., Schröder, A., and Marques, C. (2013). Gel-assisted formation of giant unilamellar vesicles. Biophys. J. *105*, 154–164.

Whitaker, N., Chen, Y., Jakubowski, S.J., Sarkar, M.K., Li, F., and Christie, P.J. (2015). The All-Alpha Domains of Coupling Proteins from the Agrobacterium tumefaciens VirB/VirD4 and Enterococcus faecalis pCF10-Encoded Type IV Secretion Systems Confer Specificity to Binding of Cognate DNA Substrates. J. Bacteriol. *197*, 2335–2349.

Whitaker, N., Berry, T.M., Rosenthal, N., Gordon, J.E., Gonzalez-Rivera, C., Sheehan, K.B., Truchan, H.K., VieBrock, L., Newton, I.L.G., Carlyon, J.A., et al. (2016). Chimeric Coupling Proteins Mediate Transfer of Heterologous Type IV Effectors through the Escherichia coli pKM101-Encoded Conjugation Machine. J. Bacteriol. *198*, 2701–2718.

Winans, S.C., and Walker, G.C. (1985). Conjugal transfer system of the IncN plasmid pKM101. J. Bacteriol. *161*, 402–410.

Witkowska, A., Jablonski, L., and Jahn, R. (2018). A convenient protocol for generating giant unilamellar vesicles containing SNARE proteins using electroformation. Sci. Rep. *8*, 9422.

World Health Organization (2015). Global action plan on antimicrobial resistance (World Health Organization).

World Health Organization (2019). Thirteenth general programme of work 2019-2023.

Yamamoto, K., Tamai, R., Yamazaki, M., Inaba, T., Sowa, Y., and Kawagishi, I. (2016). Substrate-dependent dynamics of the multidrug efflux transporter AcrB of Escherichia coli. Sci. Rep. *6*, 21909.

Yanagida, K., Sakuda, A., Suzuki-Minakuchi, C., Shintani, M., Matsui, K., Okada, K., and Nojiri, H. (2016). Comparisons of the transferability of plasmids pCAR1, pB10, R388, and NAH7 among Pseudomonas putida at different cell densities. Biosci. Biotechnol. Biochem. *80*, 1020–1023.

Yang, P.-C., and Mahmood, T. (2012). Western blot: Technique, theory, and trouble shooting. N. Am. J. Med. Sci. *4*, 429.

Yanisch-Perron, C., Vieira, J., and Messing, J. (1985). Improved M13 phage cloning vectors and host strains: nucleotide sequences of the M13mp18 and pUC19 vectors. Gene *33*, 103–119.

Ye, J., Osborne, A.R., Groll, M., and Rapoport, T.A. (2004). RecA-like motor ATPases--lessons from structures. Biochim. Biophys. Acta *1659*, 1–18.

Yokogawa, M., Fukuda, M., and Osawa, M. (2019). Nanodiscs for Structural Biology in a Membranous Environment. Chem. Pharm. Bull. *67*, 321–326.

Zechner, E.L., Lang, S., and Schildbach, J.F. (2012). Assembly and mechanisms of bacterial type IV secretion machines. Philos. Trans. R. Soc. B Biol. Sci. *367*, 1073–1087.